Understanding the biological significance of L-selectin shedding during leukocyte transendothelial migration

Rzeniewicz, Karolina Anna

Awarding institution:
King's College London

UNDERSTANDING THE BIOLOGICAL SIGNIFICANCE OF L-SELECTIN SHEDDING DURING LEUKOCYTE TRANSENDOTHELIAL MIGRATION

Karolina Rzeniewicz

This thesis is submitted for the degree of

Doctor of Philosophy

(PhD)

from

King's College London, School of Medicine

University of London

September 2013

King's College London,

School of Medicine,

Cardiovascular Division,

Denmark Hill Campus,

London, U.K.

First supervisor: Dr Aleksandar Ivetic

Second supervisor: Dr Maddy Parsons

ABSTRACT

Inflammation is a response of the immune and vascular systems to the stimuli perceived as harmful to the host. Inflammation can be acute or chronic, and the recruitment of leukocytes to the affected tissues is a fundamental process during the course of both these events. Leukocytes are recruited in a process known as the multi-step adhesion cascade, which is a highly co-ordinated series of adhesive events mediated by the cell adhesion molecules (CAMs) on both leukocytes and endothelial cells. L-selectin is a CAM involved in the initial stages of the cascade, i.e. tethering and rolling, although there is a mounting body of evidence that points towards its role at later stages of the cascade, such as chemotaxis beyond transendothelial migration (TEM). The work outlined in this thesis explores the possibility that L-selectin actively contributes to TEM in monocytes. There are two important and measurable properties of L-selectin: (i) its rapid proteolysis (or "shedding") upon cell activation, and (ii) its transition from being monomeric in the plasma membrane to being clustered, following ligand binding, which is a hallmark of downstream signalling. By expressing C-terminally green fluorescent protein (GFP)-tagged L-selectin in THP-1 monocytes, it was possible for the first time to monitor and analyse the spatio-temporal distribution of L-selectin and its shedding during TEM. In addition, co-expressing L-selectin-GFP with L-selectin tagged to red fluorescent protein (RFP) enabled measurement of L-selectin clustering during TEM via the use of fluorescence lifetime imaging microscopy (FLIM) to monitor Forster resonance energy transfer (FRET) between the GFP and RFP-tags. Interestingly, the majority of L-selectin was found to be clustered exclusively in pseudopods protruding beneath the endothelial monolayer, where L-selectin ligands are known to exist. L-selectin clustering was also found to occur following cross-linking of either CD43 or PECAM-1, suggesting inside-out signalling is an important factor in modulating L-selectin function. Moreover, both the extracellular cleavage domain and two cytoplasmic tail serine residues were involved in fundamentally regulating L-selectin clustering. Finally, the sub-cellular distribution of L-selectin clustering correlated tightly with the dynamics of the pseudopods that protruded beneath the endothelial monolayer during TEM. This thesis aims to understand the contribution that L-selectin has during the later stages of the adhesion cascade, and will re-shape the currently held perspective that this cell adhesion molecule's role is solely restricted to just tethering and rolling.

CONTENTS

LIST OF FIGURES

LIST OF TABLES

ACKNOWLEDGEMENTS

First of all I would like to thank my supervisor Dr Aleksandar Ivetic for the excellent guidance he has provided throughout the course of my PhD project. On many occasions it was his passion for science, outstanding knowledge and hands-on assistance in the lab that have helped me to overcome the hurdles I encountered during this project.

Secondly, I am grateful to my second supervisor Dr Maddy Parsons, who has helped so much with the FRET experiments and has always had a good piece of handy advice.

I would also like to thank all the friends that I have made during my PhD, for making my day-to-day life at the JBC so enjoyable. I would especially like to thank Lauren Jade Porter, who has been my lab-mate and flat-mate and whom I shared a lot of ups and downs with, both work- and life-related. I also give my special thanks to Rajesh Mistry who has always laughed with me at things no one else finds funny. Moreover, I would like to thank Thomas Murray, Iain Sawyer, Dan Martin, Gosia Furmanik, Russell Simpson, Hannah Tomlins, Dipen Rajgor, Angela Rey-Gallardo, Daniel J Brayson and Anne Jacob for all the great times we shared in and out of the lab.

I must express that I owe my deepest gratitude to my amazing family that has always helped me to pursue my dreams. I am so lucky to have their unconditional love and support.

Lastly, I would like to thank my boyfriend Matt Hancock, who has made the toughest times so much easier.

It would have been so much more difficult without all of you.

Thank you all so very much!

DECLARATION OF INDEPENDENT WORK

I, the author of this thesis, declare that the work presented in this thesis was conducted by myself, except where indicated in the text.

……...

Karolina Rzeniewicz

ABBREVIATIONS

2D	Two-dimensional
3D	Three-dimensional
A	Alanine
ACLB	Albumin-coated latex beads
ADAM	A disintegrin and metalloprotease
AJs	Adherens junctions
apoE	Apolipoprotein E
ARDS	Adult respiratory distress syndrome
ATCC	American tissue culture collection
ATP	Adenosine triphosphate
BAEC	Bovine aortic endothelial cells
BCR	B cell receptor
BKMGEC	Bovine kidney microvascular glomerular endothelial cells
BM	Basement membrane
BMEC	Brain microvascular endothelial cells
BSA	Bovine serum albumin
Btk	Burton's tyrosine kinase
C-Abl	Abelson murine leukemia viral oncogene homolog-1
CalDAG-GEF 1	Calcium and diacylglycerol-regulated GEF I
CaM	Calmodulin
CAM	Cell adhesion molecule
CCD	Charge-coupled device
CCL2	C-C motif chemokine 2
CCL7	C-C motif chemokine 7
CCR2	C-C motif chemokine receptor 2
CCR7	C-C motif chemokine receptor 7
CD"X"	Cluster of differentiation, where "X" denotes a number
CD44v	CD44 variant
Cdc42	Cell division cycle 42
cDNA	Complementary DNA
CEA	Carcinoembryonic antigen
CFP	Cyan fluorescent protein
CID	Chemically induced dimerization
CIP	Calf intestinal alkaline phosphatase
CLS	C-terminal portion of human L-selectin
CNV	Copy number variations

COX	Cyclooxygenase
CS	Chondroitin sulfate
CSPG	Chondroitin sulfate proteoglycan
C-terminal	Carboxy-terminal
CVD	Cardiovascular disease
CX3CR1	C-X3-C motif chemokine receptor 1
CXCR4	C-X-C motif chemokine receptor type 4
D	Aspartate
DCs	Dendritic cells
dd$H_2$0	Double-distilled H_2O
DMSO	Dimethyl-sulphoxide
DNA	Deoxyribonucleic acid
DRM	Detergent resistant membrane
DS	Dermatan sulfate
DSPG	Dermatan sulgate proteoglycan
DTT	1,4-dithiolthreitol
EAPs	Endothelial adhesion platforms
EC	Endothelial cell
ECM	Extracellular matrix
EDTA	Ethylene Diamine-tetraacetic acid
EEA1	Early endosome antigen 1
EF-1α	Elongation factor 1α
EGF	Epidermal growth factor
eGFP	Enhanced green fluorescent protein
ELAM-1	Endothelial leukocyte adhesion molecule-1
ELC	EBV –induced molecule 1 ligand chemokine
Elf4	Ets-related transcription factor 4
ERK	Extracellular signal-regulated kinase
ERM	Ezrin/radixin/moesin
ESAM	Endothelial cell selective adhesion molecule
ESL-1	E-selectin ligand 1
Ets1	E26 Transformation-specific Sequence 1
F	Phenylalanine
FA	Focal adhesion
FACS	Fluorescence activated cell sorting
F-actin	Filamentous actin
FCS	Foetal calf serum
FERM	Band 4.1/ezrin/radixin/moesin

FITC	Fluorescein isothiocyanate
FLIM	Fluorescence lifetime imaging microscopy
fMLP	Formyl-methionine-leucine-phenylalanine
FOXM-1	Forkhead Box M1
FOXO-1	Forkhead box O1
FPR	*N*-formyl peptide receptor
FRET	Fluorescence resonance energy transfer
G	Glycine
Gag	Gene encoding group specific antigen
GAG	Glycosaminoglycan
G-CSF	Granulocyte colony stimulating factor
GDI	GDP dissociation inhibitor
GDP	Guanosine diphosphate
GEF	Guanine nucleotide exchange factor
GFP	Green fluorescent protein
GlyCAM-1	Glycosylation-dependent cell adhesion molecule-1
GPCR	G protein-coupled receptor
Grb2	Growth factor receptor-bound protein 2
GST	Glutathione S-transferase
GTP	Guanosine triphosphate
HBSS	Hank's buffered saline solution
HEK 293T	Human embryonic kidney-293 cell line
HEPES	4-(2-hydroxyethyl)-1-piperazineethanesulfonic acid
HEV	High endothelial venule
HIV	Human immunodeficiency virus
HMGB-1	High mobility group 1
HRP	Horseradish peroxidase
HS	Heparan sulfate
HSPG	Heparan sulfate proteoglycan
HUVEC	Human umbilical cord endothelial cells
ICAM-1	Inter-cellular adhesion molecule 1
Ig	Immunoglobulin
IgA	Immunoglobulin with A class heavy chains
IgE	Immunoglobulin with E class heavy chains
IgG	Immunoglobulin with G class heavy chains
IL	Interleukin
IP	Immuno-precipitation
IPTG	Isopropyl β-D-1-thiogalactopyranoside

Irf1	Interferon regulatory transcription factor 1
JAM	Junctional adhesion molecule
JNK	c-Jun N-terminal kinase
K	Lysine
KC	Keratinocyte chemoattractant
Klf2	Kruppel-like factor 2
L	Leucine
LAD	Leukocyte adhesion deficiency
LAM-1	Leukocyte adhesion molecule -1
LB	Luria Bertani
LBRC	Lateral border recycling compartment
Lck	Leukocyte-specific protein tyrosine kinase
LDL	Low density lipoprotein
LECAM-1	Lectin adhesion molecule-1
LER	Low expression regions
LFA-1	Lymphocyte function-associated antigen 1
LPS	Lipopolysaccharide
M	Methionine
mAb	Monoclonal antibody
MAC-1	Macrophage-1 antigen
MadCAM-1	Mucosal addressin cell adhesion molecule 1
MAPK	Mitogen activated protein kinase
mCherryFP	Monomeric cherry fluorescent protein
MCP-1	Monocyte chemoattractant protein 1
M-CSF-1	Macrophage colony stimulating factor-1
MES	2-morpholinoethanesulfonic acid, monohydrate
MFI	Mean fluorescence intensity
MI	Myocardial infarction
MIG	Monokine induced by gamma interferon
MLN	Mesenteric lymph node
Moesin	Membrane-organising extension spike protein
MOI	Multiplicity of infection
mRNA	Messenger RNA
MS	Multiple sclerosis
mTOR	Mammalian target of Rapamycin
MW	Molecular weight
Mzf1	Myeloid zinc finger 1
N	Asparagine

Naf-1	Nef-associated factor 1
NEB	New England Biolabs
NK	Natural killer
NP-40	Nonidet P-40 substitute
NSAID	Non-steroid anti-inflammatory drugs
N-terminal	Amino-terminal
O_2^-	Superoxide anion
oxLDL	Oxidised LDL
P	Proline
PAF	Platelet activating factor
PAGE	Polyacrylamide gel electrophoresis
PAK-PBD	p21-binding domain of PAK
PBL	Peripheral blood lymphocyte
PBMC	Peripheral blood mononuclear cell
PBS	Phosphate buffer saline
PC	Phosphatidylcholine
PCR	Polymerase chain reaction
PECAM-1	Platelet endothelial cell adhesion molecule 1
PFA	Paraformaldehyde
PG	Proteoglycan
PGE	Prostaglandin
Phospho-	Phosphorylated
PI3K	Phosphoinositide 3-kinase
PKC	Protein kinase C
PLB	Protein loading buffer
PLC	Phospholipase C
PLL	Poly-L-lysine
PLN	Peripheral lymph node
PMA	Phorbol-12'-myristate-13'-acetate
PMN	Polymorphonuclear cells
PMSF	Phenyl-methyl-sulfonyl-fluoride
PNAd	Peripheral lymph node addressins
Pol	Viral polymerase
PPME	Polyphosphomonoester core polysaccharide
PS	Phosphatidylserine
PSGL-1	P-selectin glycoprotein ligand-1
PVDF	Polyvinylidene fluoride
R	Arginine

Rac	Ras-related C3 botulinum toxin substrate
Rev	Regulator of expression of virion proteins
RFP	Red fluorescent protein
Rho	Ras homolog
Rhotekin-C21	Rho-binding domain of Rhotekin
RNA	Ribonucleic acid
ROCK	Rho-associated coiled coil-containing protein kinase
RPE	Red phycoeyrthrin
rpm	Revolutions per minute
RPMI-1640	Roswell Park Memorial Institute-1640
S	Serine
S.E.M.	Standard error of the mean
SCR	Sequence consensus repeat
SDF-1	Stromal cell-derived factor 1
SDS	Sodium dodecyl sulphate
SDS-PAGE	Sodium dodecyl sulphate-Polyacrylamide gel electrophoresis
SEM	Scanning electron microscopy
SFK	Src family kinases
SGPG	Sulfoglucuronosyl paragloboside
SLC	Secondary lymphoid tissue chemokine
SLE	Systemic Lupus Erythematosus
sLe^x	Sialyl Lewis X
sL-selectin	Soluble L-selectin
SNP	Small nucleotide polymorphism
SOS	Son of sevenless
Sp1	Specificity protein 1
Src	Sarcoma
STE	Sodium Chloride-Tris-EDTA
Syk	Spleen tyrosine kinase
TACE	TNF-α converting enzyme (also known as ADAM17)
TAE	Tris-acetate-EDTA
TBS	Tris-buffered saline
TCR	T cell receptor
TEM	Transendothelial migration
TF	Transcription factor
TJs	Tight junctions
TMD	Transmembrane domain
TNF-α	Tumour necrosis factor α

TRITC	Tetra-methyl-rhodamine-5-(and-6)-isothiocyanate
U.K.	United Kingdom
U.S.A.	United States of America
UUO	Unilateral ureteral obstruction
VCAM-1	Vascular cell adhesion molecule 1
VLA-4	Very late antigen 4
VSV-G	The vesicular stomatitis virus G protein
VVO	Vesiculo-vacuolar organelle
WASP-CRIB-C	Cdc42/Rac interacting domain of (cassette) of the Wiskott-Aldrich syndrome protein
WT	Wild type
Y	Tyrosine
YFP	Yellow fluorescent protein
ZAP-70	Zeta-chain-associated protein kinase 70
α	Alpha
β	Beta
Δ	Delta
θ	Theta
ι	Iota

CHAPTER 1. INTRODUCTION

1.1 INFLAMMATION

Inflammation is believed to have evolved as an adaptive response of the immune system to homeostatic imbalance. The most common causes of such imbalances are infections and tissue injuries. A pathogen or injury triggers an acute inflammatory response, which is a controlled physiological reaction of a healthy organism that serves to protect the host. However, inflammation underlies not only physiological, but also a variety of pathological processes. The majority of cases where inflammation is detrimental to the host are the chronic inflammation states that ensue when the acute phase is not resolved.

Inflammation was first described in the 1st century A.D. by a Roman medical writer Celsius, who identified its four cardinal signs: redness, swelling, fever and pain. Two hundred years later another accomplished medical researcher of antiquity, Galen of Pergamon, added the fifth sign to the list – loss of function. In other words, any organ/tissue afflicted with inflammation loses it's ability to function normally. Inflammation of a certain organ/tissue is denoted by the addition of the suffix "-itis" (from ancient Greek, initially meaning "pertaining to", now has come to mean "inflammation of"), e.g. inflammation of peritoneum is known as peritonitis, inflammation of the tonsils is called tonsillitis, etc. There are two components of an inflammatory response: the vascular arm and the cellular arm. The vascular arm is the vascular tissue that reacts immediately to the harmful stimuli by vasodilation (widening of the blood vessels) and an increase in the vascular permeability. The vascular arm is especially important for acute inflammation. The cellular arm is composed of the cells of the immune system – leukocytes. There are several subsets of leukocytes: lymphocytes (T cells, B cells, NK cells), monocytes, dendritic cells, mast cells and "granulocytes" – neutrophils, basophils and eosinophils, (also collectively known as polymorphonuclear leukocytes, PMN). Majority of leukocytes originate in the bone marrow, however yolk sac-derived macrophages have been recently identified [1], suggesting a greater complexity of leukocyte origin than previously anticipated. Leukocytes guard the peripheral tissues through circulation in the blood and the lymphatic system. All leukocytes contribute to a successful outcome of an inflammatory response through integration of innate and adaptive immune responses. In broad terms, innate responses (killing and engulfing of the pathogens) are mediated by granulocytes and monocytes, whereas the adaptive responses (production of antigen-specific antibodies) depend on lymphocytes.

1.1.1 Acute inflammation

Acute inflammation is initiated by the vascular arm, which also involve the contribution of tissue-resident macrophages and mast cells of the cellular arm that respond directly to the pathogen/injury. Various inflammatory mediators are responsible for different aspects of a successful inflammatory response. Platelet activating factor (PAF), prostaglandins (PGEs) as well as vasoactive amines and peptides cause vasodilation and increased endothelial permeability of the capillaries. Additionally, PAF and various cytokines mediate leukocyte recruitment to the sites of inflammation. As a result leukocytes, predominantly neutrophils, extravasate from the blood vessels and in to the affected tissues. Hence, vasodilation and leukocyte emigration in to the tissues are responsible for heat (because the blood core temperature is brought more readily to the skin surface), redness and swelling. Pain is mainly a result of the activity of bradykinin and prostaglandin 2 (PGE2), and the latter is also pyrogenic (causes fever) [2, 3].
A successful acute inflammatory response results in the elimination of the infectious agent and is followed by a tissue healing phase. If the immune system fails to eliminate the pathogen, inflammation persists and develops into a "chronic inflammation" (**section 1.1.2**).

1.1.2 Chronic inflammation

A hallmark of acute-to-chronic inflammation transition is a decrease in infiltrating neutrophils and a profound increase in the influx of mononuclear cells (monocytes and lymphocytes). Trafficking of monocytes in both acute and chronic inflammation is discussed in more detail in **section 1.6** of this thesis.
Apart from persistent pathogens, chronic inflammation can result from other causes of tissue damage like undegradable foreign objects, e.g. silica [4] or asbestos [5] particles, or autoimmune responses (due to persistence of self-antigens), e.g. multiple sclerosis (MS) or systemic lupus erythematosus (SLE). Perhaps the most notorious example of chronic inflammation is atherosclerosis, the main driver of cardiovascular disease (CVD). CVD includes myocardial infarction, heart failure and stroke, and is a leading cause of death worldwide. Monocyte-driven mechanisms underlying atherosclerosis are described in more detail in **section 1.6.2**. The involvement of L-selectin in atherosclerosis is discussed in **section 1.13.1**.

1.2 THE LEUKOCYTE ADHESION CASCADE

Migration of leukocytes out of the blood vessels and into the inflamed tissues depends on a highly co-ordinated, multistep process termed the "Multi-step leukocyte adhesion cascade". The leukocyte adhesion cascade is also utilised by naïve lymphocytes during

their recirculation (homing) to the peripheral lymph nodes (PLNs). This is a dynamic process that requires the synchronised activity of various cell adhesion molecules (CAMs) on both the leukocyte and the endothelium. In general, leukocyte recruitment is initiated by tethering and rolling of leukocytes on inflamed endothelium due to the interaction between the selectin family of glycoproteins and their ligands [6] (**figure 1.1**). Next, activation and arrest of leukocytes takes place as a result of chemokine-induced integrin activity, which leads to arrest of leukocytes on the endothelium. This step is followed by intravascular crawling and transmigration of leukocytes through the endothelium, via the paracellular or transcellular route [6]. The stages of the cascade and the CAMs involved are discussed more thoroughly in the following sections.

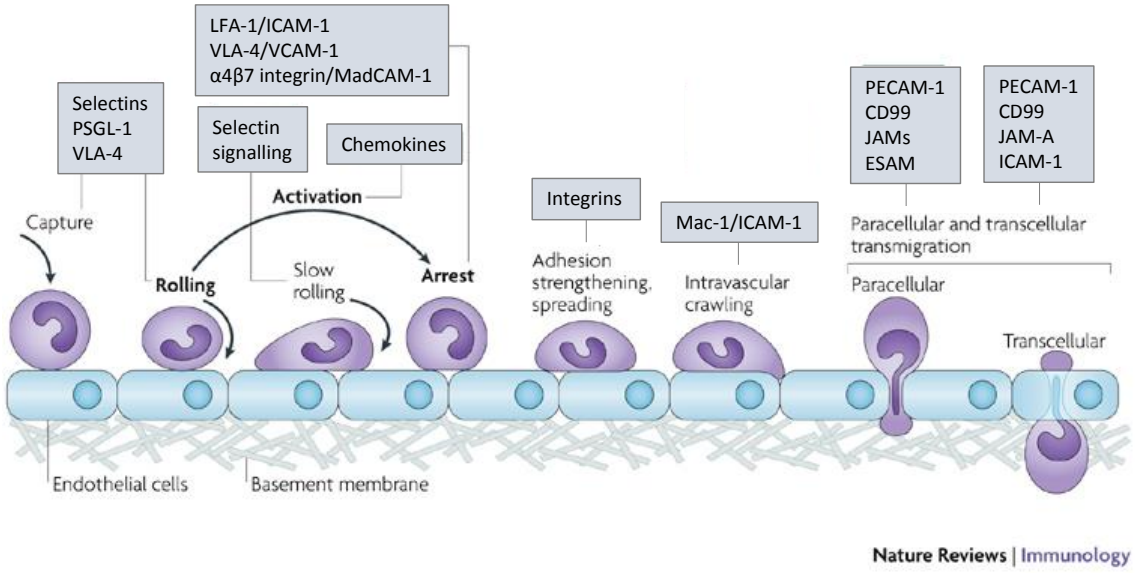

Figure 1.1 The leukocyte adhesion cascade. Homing of naïve lymphocytes to LN or recruitment of leukocytes to sites of inflammation is a strictly defined and dynamic process, which requires the co-ordinated activity of both leukocyte and endothelial cell adhesion molecules. Initially, capture of leukocytes (tethering) from free blood flow occurs through interaction between the selectins and their ligands, e.g. PSGL-1. Subsequent tethering, rolling and slow rolling is also selectin-mediated, however, LFA-1, VLA-4 and α4β7 integrins and their counter-receptors contribute to these steps as well. Chemokine-mediated inside-out activation of integrins and resultant outside-in integrin signalling leads to leukocyte arrest and firm adhesion onto ECs. Next, integrin-mediated adhesion strengthening and leukocyte spreading as well as MAC-1/ICAM-1-dependent intravascular crawling act collectively as prerequisites to promote transendothelial migration (TEM). TEM can occur through a paracellular or a transcellular route. Both transcellular and paracellular routes are dependent on PECAM-1, CD99 and JAMs. Additionally, paracellular route utilises ESAM and transcellular route employs ICAM-1. For abbreviations used see **Abbreviations section**. Image modified from Ley et al., *Nat Rev Immunol*, 2007 [6].

1.2.1. Leukocyte tethering

In the absence of inflammation, leukocytes in flowing blood pass over the endothelium. The wall shear stress, which is a parallel force applied to the endothelium by the shear force of the flowing blood, ensures that no inappropriate contacts between the leukocytes and the endothelium can be made. However, vasodilation of blood vessels at sites of inflammation (**section 1.1.1**) slows the blood flow, thereby reducing the shear stress. Additionally, the red blood cells that are more flexible and flow faster than the leukocytes, displace the leukocytes towards the walls of the venules [7, 8]. Collectively, this allows the leukocytes to form contacts with the endothelium. The initial contact between the flowing leukocytes and the endothelium is established through the formation of transient "tethers". Tethering (also known as leukocyte capture) is facilitated by the microvilli – thin actin-rich projections that protrude from the leukocyte body. A tether is formed when parts of microvillar plasma membrane are taken apart from the underlying cytoskeleton and are stretched into a less rigid structure [9]. Tethers act like "elastic bands" that help to decrease the pulling force of the blood flow imposed on the bonds forming between the leukocyte and endothelium [9, 10]. Tethering of leukocytes is mediated by the selectins (**section 1.7**) and their ligands, most important being P-selectin glycoprotein ligand 1 (PSGL-1) (**figure 1.2**). Whilst all members of the selectin family recruit leukocytes at sites of inflammation, L-selectin is almost single-handedly responsible for the recirculation of naïve lymphocytes to the PLNs [11-13]. Leukocyte α4 integrins, namely α4β1 (very late antigen 4, VLA-4) [14] and α4β7 [15], have also been reported to mediate tethering (**figure 1.2**). Leukocyte CAMs involved in the formation of tethers are localised to the tips of leukocyte microvilli [15-18]. Microvillar localisation of these CAMs provides a spatial advantage over the cell body localisation, and is ideal for the initiation of contacts with the endothelium.

The significance of L-selectin-mediated tethering for leukocyte recruitment *in vivo* has been demonstrated by Stein et al. (1999) [19] and Eriksson et al. (2001) [20]. These studies showed that vessel diameter plays a key role in this particular phase of the adhesion cascade. Specifically, tethering is important for recruitment of leukocytes in the vessels that are larger than 20 μm in diameter, [19]. In contrast, the recruitment of leukocytes in venules with diameters less than 20 μM commences by initiation of rolling, and tethering is not required [19]. It was postulated that his is because in such narrow venules (<20 μm), the leukocytes are already in close contact with the vessel walls, and the initial capture is not needed [19]. Additionally, in vessels that have a diameter of more than 45 μm, L-selectin plays a prominent role in the initiation of secondary tethers, in the process known as "secondary leukocyte capture" (**section 1.2.3**) [20].

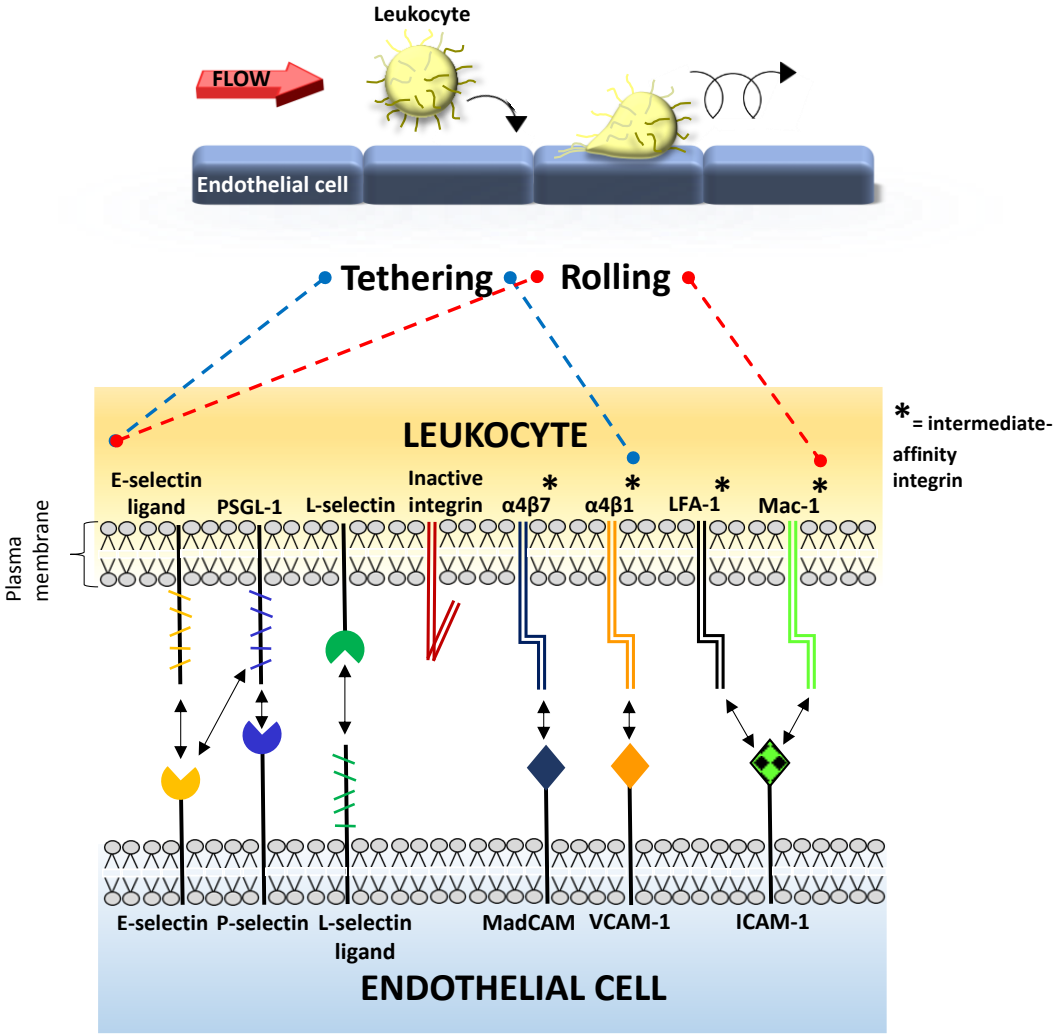

Figure 1.2 Cell adhesion molecules mediating tethering and rolling. The leukocyte adhesion cascade is a multistep process that involves synchronised interactions of CAMs on both the leukocyte and the endothelium. This schematic depicts CAMs involved in the first two stages of the cascade: leukocyte tethering and leukocyte rolling. Full names of the CAMs can be found in the **Abbreviations section**.

1.2.2 Leukocyte rolling

After the initial tethering is established, if there is sufficient ligand presented on the surface of the endothelium, then leukocytes will begin to "roll". Rolling of lymphocytes on non-inflamed high endothelial venules (HEV) in PLN occurs constitutively [11, 21, 22]. However, rolling of leukocytes on other vascular beds is only triggered when the endothelium becomes inflamed. Rolling of leukocytes from P-, E- and L-selectin null mice [11, 23-25] or upon antibody-mediated blocking of selectins [26-31] is dramatically reduced. Thus, the selectins are the primary mediators of the leukocyte rolling. Additionally, leukocyte integrins VLA-4, lymphocyte function-associated antigen 1 (LFA-1), macrophage adhesion ligand-1 (Mac-1) and α4β7 integrin have been found to support

this process [14, 15, 32-35] (**figure 1.2**). Integrins that mediate rolling are thought to be in their "intermediate" state of activation (intermediate-affinity), which unlike the "high" activation state (high-affinity) does not promote adhesion [36, 37].

Rolling is a continuous movement of the leukocytes along the endothelial cells (ECs) that lasts from seconds to minutes, depending on the vascular bed [38-40]. This movement depends on the formation and breakage of bonds formed between CAMs and their respective ligands on both leukocytes and the endothelial cells. The forces exerted on the leukocyte by the flowing blood, collectively known as the hydrodynamic drag, and the bonds formed between the selectins and their ligands counter-balance each other and result in leukocyte rolling [10, 41-43]. The hydrodynamic drag increases with the increasing wall shear stress [41]. In fact, selectin-mediated rolling requires a minimum shear stress for the formation of the so-called "catch-slip" bonds, and the cells do not adhere below the critical shear stress of 0.1 dynes/cm^2 [44-48]. The bonds formed by the selectins are called "catch-slip" bonds due to their biphasic responses to the applied force [49]. The strength of those bonds increases with the increasing force (catch), but then deceases when further force is applied (slip) [49, 50]. During rolling, shear stress acting on the rear of the cell is stronger than that acting at its front. Hence, the catch-slip bond phenomenon allows formation of new bonds at the front edge and dissociation of the preexisting bonds at the rear edge, promoting the cell to roll in the general direction of blood flow [48].

The three selectins have both overlapping and distinctive functions and each of the selectins mediates rolling at an individual velocity [24, 51, 52]. It has been suggested that L-selectin is most efficient in capturing leukocytes from flow [53, 54], and mediates the fastest type of rolling [52, 55]. P-selectin can both initiate [56] and maintain [27] rolling, whereas E-selectin mediates stable rolling that has the lowest velocity [51]. As rolling progresses, the strength of the catch bonds increase and the selectins and integrins mediate rolling at progressively lower velocities [24, 57]. This "slow rolling" enables the leukocytes to sample for chemokines presented by the inflamed endothelium [51, 58, 59]. Eventually, the transition from leukocyte rolling to arrest takes place as a result of leukocyte activation (**section 1.2.4**). Therefore, the role of leukocyte rolling appears to be to slow the leukocytes down and prolong their passage through the venules. This allows the leukocytes to survey the endothelium for chemoattractants and gives them time to become activated and employ the integrin-based adhesion machinery.

1.2.3 Secondary leukocyte capture

Leukocyte tethering and rolling can be augmented by a phenomenon known as "secondary capture". Secondary capture takes place when free flowing leukocytes tether

to and roll on the adherent leukocytes and it has been observed both *in vitro* and *in vivo* [20, 54, 60, 61]. Additionally, adherent leukocyte fragments have been proposed to participate in the capture of circulating leukocytes [62]. Secondary leukocyte capture is mediated by L-selectin on free-flowing leukocytes [60], and freely available PSGL-1, belonging to the leukocytes already interacting with the endothelium [62]. Depending on the vessel size and flow rate, the homotypic leukocyte-leukocyte interactions can account for 25-70% of the total leukocyte accumulation [20, 54]. This demonstrates the importance of the secondary capture for amplification of the leukocyte accumulation at sites of inflammation. Leukocytes engage secondary capture mechanisms more as vessel size increases, raising the possibility that secondary capture may play a role during inflammation of large blood vessels, and in diseases such as atherosclerosis [20]. It has been reported that secondary capture of leukocytes can be seen as formation of characteristic “strings” or grape-shaped “clusters” (both hereafter referred to as strings) [20, 53, 54, 63, 64]. The formation of the strings occurs when a newly captured leukocyte binds upstream of the already adherent one. However, it has been reported that strings can form in the absence of L-selectin – the primary secondary capture mediator [65]. Additionally, it has also been shown that formation of the strings can occur without the initial leukocyte-leukocyte interactions in a process called “hydrodynamic recruitment” [66]. Hydrodynamic recruitment theory postulates that the perturbations in the fluid surrounding an adherent leukocyte may play a critical role in bringing the apposing leukocytes within binding distance [66]. It has been suggested that formation of these strings could be a result of a synergistic action of L-selectin-mediated secondary capture and random leukocyte collisions resulting from the hydrodynamic recruitment [64].

1.2.4 Transition from leukocyte rolling to arrest

The transition from leukocyte rolling to firm adhesion (arrest) is a key element of the inflammatory response. During decelerated rolling, when leukocytes are able to survey the endothelium for the inflammatory cues [59, 67], the cells need to “decide” whether to arrest or to detach and leave the site. This “decision-making” process involves at least two main mechanisms: the chemokine-mediated “inside-out” integrin activation and the “outside-in” signalling evoked by CAMs binding to their respective ligands during rolling. If signalling triggered by the chemokines and CAMs reach a certain threshold, then the rolling leukocyte becomes “activated”. Activated leukocytes arrest on the ECs.

Chemokines are important for both homing of naïve lymphocytes to PLNs and for the recruitment of leukocytes to the sites of inflammation. However, specific expression and regulation of each chemokine, as well as chemokine receptor expression patterns on the leukocytes, create a functional diversity that allows the chemokines to direct different leukocyte subsets to different vascular beds. Chemokines bind to seven-pass

transmembrane G-protein coupled receptors (GPCRs) on leukocytes, which triggers complex signalling pathways inside the cell that eventually lead to integrin activation [59, 68-74]. This is known as 'inside-out' signalling because signals generated intracellularly are transmitted out to the extracellular domain of the integrin. Integrin activation occurs through their transition from a bent low-affinity form to a high-affinity (extended) form [68, 75-77]. High-affinity integrins mediate firm leukocyte adhesion through binding to their endothelial ligands, such as ICAM-1 and VCAM-1 (**section 1.2.5**) [75, 78-80]. Additionally, chemokines promote lateral mobility of the integrins, which results in formation of integrin clusters that enhance the integrin/ligand encounter frequency [80]. Irrespective of their ability to activate the integrins, chemokines have also been shown to cause microvillar collapse [81]. Loss of microvilli is beneficial during the transition from rolling to arrest as it enlarges the region of contact between the leukocyte and the ECs.

Apart from the chemokines, transition from leukocyte rolling to arrest is also mediated by CAMs. Binding to E-selectin [82] or P-selectin [83], or engagement of L-selectin [84-89], is known to cause upregulation and activation of leukocyte integrins, and thus promote leukocyte adhesion. Additionally, extensive studies of L-selectin-mediated signalling have shown that its ligation triggers leukocyte activation resulting in variety of cellular responses, including upregulation of chemokine receptors (**section 1.11.3**) [85, 86, 90]. Furthermore, it has been shown that L-selectin cross-linking enhances cytokine- or chemokine-induced adhesion through β2 integrins [85, 91], and Spertini et al. (1991) showed that activation of lymphocytes with physiological stimuli enhanced L-selectin-dependent binding to HEV [92]. This suggests that an overlap and/or synergy between chemokine-mediated inside-out signalling and CAMs mediated outside-in signalling is likely to exist for successful transition from leukocyte rolling to arrest to occur (**figure 1.3**). More than one "input" needed to activate and arrest the rolling leukocyte might be necessary to provide a few "safety levels" of activation. This would be particularly true for neutrophils, the first mediators of an acute inflammatory response, whose inappropriate activation in the bloodstream could be detrimental to the host.

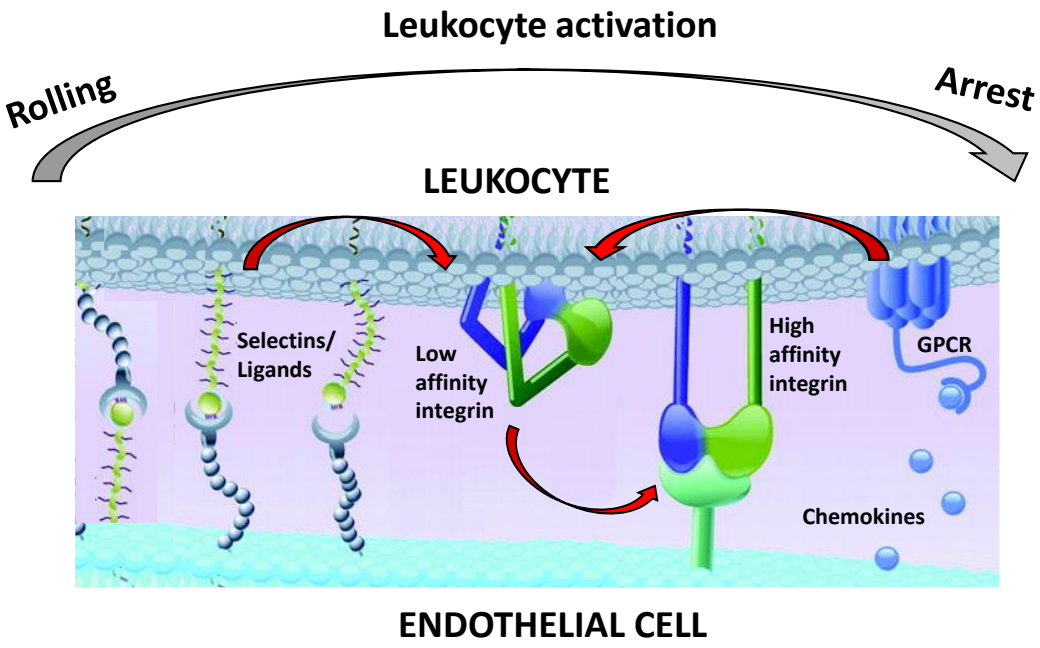

Figure 1.3 Transition from leukocyte rolling to arrest. To convert reversible rolling interactions into stable adhesion, the leukocyte must first become activated. Two main mechanisms contribute to leukocyte activation are depicted in this figure. The first one involves inside-out activation of the integrins in response to GPCR/chemokine binding. The second mechanism is initiated by ligation of selectins and their ligands. This leads to a variety of cellular responses, including upregulation, activation and adhesion through integrins as well as expression of chemokine receptors (not shown in the figure). Image adapted from Totani and Evangelista, *Arterioscler Thromb Vasc Biol*, 2010 [93].

1.2.5 Leukocyte arrest

Progressively slower leukocyte rolling and leukocyte activation described in the sections above result in the firm adhesion of the leukocyte on the endothelium (arrest). Leukocyte arrest is a result of a solid attachment through integrins and their ligands (**figure 1.4**). The integrins, therefore, are involved in mediating tethering, rolling (**figure 1.2**) and firm adhesion. This is a result of their ability to exist in multiple affinity states. As mentioned before, rolling interactions are mediated by the integrins activated to their intermediate-affinity states [36]. During leukocyte activation, integrins acquire high-affinity conformations and thus can mediate firm adhesion [77, 94]. Activation of the integrins to certain affinity states is differently regulated in various leukocyte subsets by cytoplasmic proteins talin and kindlins1-3 [95-99]. Mutations in the kindlin-3 gene result in leukocyte adhesion deficiency III (LADIII) [96, 100, 101] (**section 1.2.9**). Integrin deactivation has been recently shown to occur as a result of binding of a cytosolic protein SHARPIN [102]. Interestingly, activation of integrins was found to be counter-balanced by an anti-inflammatory cytokine growth differentiation factor (GDF) 15 released by the tissue damaged upon MI [103]. GDF15 null mice suffered from increased mortality due to the

excessive recruitment of leukocytes to the infarcted area [103]. This suggests that regulation of integrin activation plays an important role in the modulation and extent of the inflammatory response.

The most studied β2 integrins are LFA-1 (CD11a/CD18 or αLβ2) and Mac-1 (CD11b/CD18 or αMβ2). Both LFA-1 and Mac-1 bind to the immunoglobulin (Ig) superfamily members ICAMs (inter-cellular adhesion molecules), but whilst LFA-1 binds both ICAM-1 [104-106] and ICAM-2 [107], Mac-1 binds ICAM-1 [108]. Additionally, binding of Mac-1 to the endothelial receptor for advanced glycation endoproducts (RAGE) has also been reported [109]. Apart from β2 integrins, β1 integrin VLA-4 (α4β1) mediates adhesion through binding to another Ig superfamily member VCAM-1 [110], and α4β7 contributes to leukocyte arrest through its interaction with mucosal addressin cell adhesion molecule 1 (MadCAM) [111].

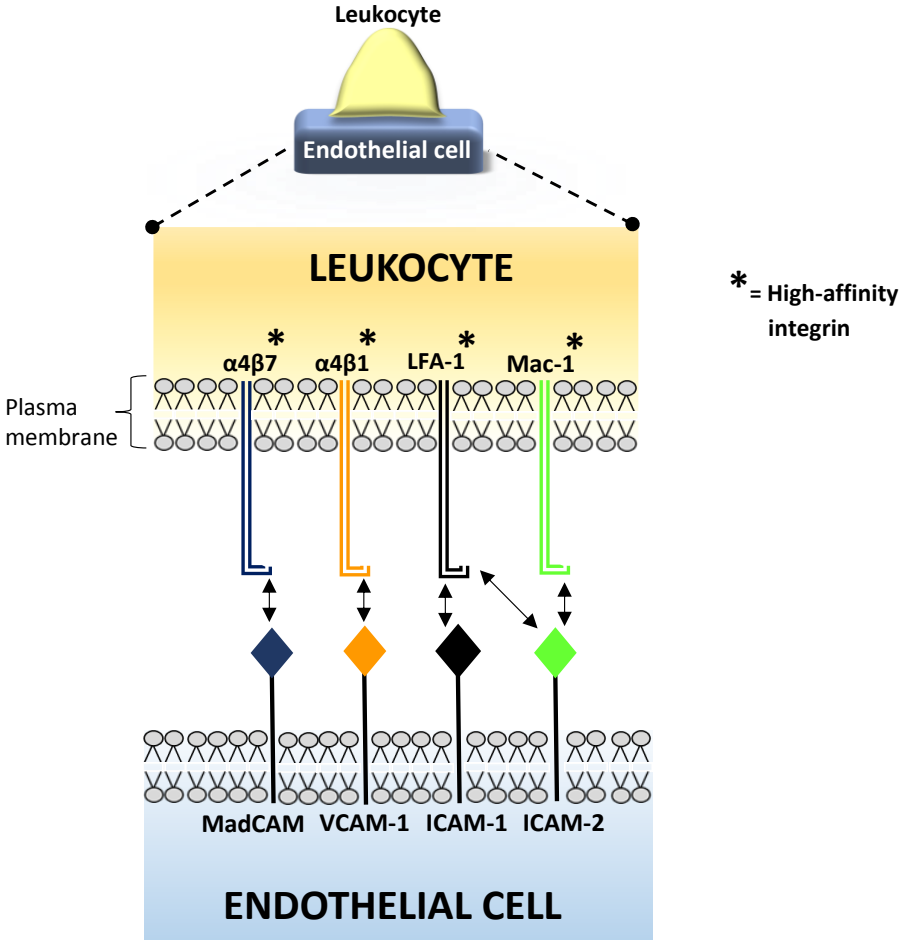

Figure 1.4 CAMs involved in leukocyte arrest. This diagram shows cell surface receptors on both leukocyte and the endothelium that participate in the firm leukocyte adhesion (arrest). The leukocyte arrests through its β2 and α4 integrins that bind to their respective ligands on the endothelium. Full names of the CAMs can be found in the **Abbreviations section**.

1.2.6 Adhesion stabilisation and leukocyte spreading

Adhesion stabilisation (strengthening) and leukocyte spreading were designated as separate to the adhesion phases of the leukocyte adhesion cascade, as they are driven by different mechanisms. Described above, chemokine-mediated inside-out signalling leads to integrin activation and firm leukocyte adhesion. Further interaction of the active integrins with their ligands generates outside-in signalling that drives adhesion stabilisation, strengthening and spreading of the already arrested leukocytes [110, 112, 113]. Ligand-induced integrin clusters form “signalosomes”, which are clusters of signalling molecules that generate intracellular signals [110].

Inside-out and outside-in signalling define a dual regulation of the integrins in the adhesion of leukocytes. First of all, the integrins are responsible for leukocyte arrest and initial adhesion through the chemokine-mediated inside-out signalling. Secondly, they are important for adhesion maintenance and leukocyte spreading through the ligand engagement and resulting outside-in signalling.

1.2.7 Pre-requisite steps for the leukocyte transendothelial migration

1.2.7.1 Intraluminal crawling

Transendothelial migration (TEM), also known as diapedesis, is the last step in the leukocyte adhesion cascade. Upon arrest of the rolling leukocytes, TEM is not initiated immediately, but is preceded by the locomotion of leukocytes on the luminal endothelial surface. This is known as “intraluminal crawling”, whereby leukocytes crawl on ECs seeking optimal transmigration sites [114, 115]. Crawling is dependent on β2 integrins and their ligands, and Mac-1/ICAM-1 interaction controls this process *in vivo* [114, 116], and both Mac-1/ICAM-1 and LFA-1/ICAM-2 binding have been shown to mediate crawling *in vitro* [117]. Blockade of β2 integrins results in increased rate of transcellular migration [114], reflecting impairment in locomotion to the EC junctions. Efficient crawling, TEM and subsequent migration through the ECM is dependent on the correct polarisation of leukocytes, which have a leading edge at the front and a single trailing end (or uropod) at the rear [118, 119]. Polarisation of leukocytes depends on Rho GTPases [118] (**section 1.5**), and on surface CD44 glycoprotein [120]. Additionally, another surface protein, namely inhibitory Ly49Q receptor, has been proposed to regulate neutrophil polarization and migration upon inflammation [121].

1.2.7.2 Endothelial adhesive platforms and docking structures

The endothelium facilitates leukocyte TEM through formation of specialised clusters containing integrin ligands ICAM-1 and VCAM-1. One example of such clusters are the endothelial adhesion platforms (EAPs) that contain ICAM-1, VCAM-1, and the

tetraspanin members, CD9 and CD151. [122]. EAPs exist in the membranes of the ECs as pre-formed pro-adhesive microdomains, thereby promoting leukocyte adhesion and TEM [122]. The importance of the tetraspanin-based adhesive platforms for leukocyte recruitment is highlighted by a study by Rohlena et al. (2009), who suggest that pathologically elevated levels of CD81 tetraspanin facilitate monocyte adhesion and promote atherosclerosis in humans [123]. Another form of endothelial pro-transmigratory clusters are the "docking structures" or "transmigratory cups" that form only upon leukocyte/endothelium engagement, and are actin-rich projections that "embrace" the adherent leukocyte [124-126]. These structures are rich in F-actin, actin-binding proteins, ICAM-1, VCAM-1, active ezrin/radixin/moesin (ERM) proteins [124, 127], and can be observed *in vitro* and *in vivo* during both paracellular and transcellular TEM (**section 1.2.8**) [125, 128]. The existence and formation of the docking structures is however not completely understood, as some reports show the enrichment of ICAM-1 around the transmigrating leukocytes without the actin-rich projections [126, 129, 130]. It has been suggested that formation of the docking structures *in vitro* might be seen under certain experimental conditions, where levels of integrin activation are high [131]. On the other hand, it has been shown that during TEM *in vivo* the docking structures develop into "endothelial domes" that fully encapsulate transmigrating neutrophils preventing excessive endothelial permeability [128].

1.2.8 Leukocyte transendothelial migration

Leukocytes can cross the endothelium monolayer either through the junctions between the adjacent ECs (paracellular route, **section 1.2.8.1**) or by migrating directly through an EC (transcellular route, **section 1.2.8.2**). Both routes have been documented *in vitro* and *in vivo*, however the studies yield contradictory results, and transmigration exclusively through either the paracellular [132-134] or the transcellular [135-138] route has been reported. The contribution of the transcellular route to the total leukocyte transmigration ranges from 5-30% *in vitro*, which is dependent on the type of the ECs used and the presence or absence of a chemoattractant [125, 139, 140]. It has been proposed that leukocytes choose the route of the least resistance [141], which would differ depending on the vascular bed. In majority of cases this would be the "leaky" junctions of the permeable endothelium, but for example very tight junctions of brain/blood barrier would facilitate transcellular migration at sites of cerebral inflammation [142, 143]. Additionally, transcellular migration might be a route of choice when leukocytes are defective in locomotion and cannot reach the junctions [114, 144]. Interestingly, it has been shown that rendering of the endothelial junctions resistant to permeability through genetic replacement of VE-cadherin with the VE-cadherin/α-catenin fusion protein, abolished the majority of the neutrophil recruitment to sites of inflammation, but did not affect

lymphocyte trafficking to LNs [145]. This suggests that TEM of lymphocytes through HEV and leukocytes across the inflamed ECs might be fundamentally different.

1.2.8.1 The paracellular route

In the absence of inflammation, endothelial integrity is maintained by various endothelial junctional molecules (**section 1.3**). However, upon inflammatory challenge, this integrity is disrupted and the endothelium becomes permeable or "leaky" (**section 1.1**). Leukocytes play an important role in promoting endothelial permeability, and it has been shown that leukocyte binding triggers ICAM-1-dependent signalling in the ECs that results in phosphorylation of vascular endothelial cell–specific cadherin (VE-cadherin), catenin disassociation and junction disruption [146, 147]. A number of endothelial junctional and leukocyte CAMs are then engaged to mediate TEM (**figure 1.5**). Endothelial junctional molecules known to actively facilitate TEM include: ICAM-1, ICAM-2, junction adhesion molecule (JAM)-A, JAM-B, JAM-C, platelet/endothelial cell adhesion molecule 1 (PECAM-1, CD31), CD99 and endothelial cell selective adhesion molecule (ESAM) [148-152]. These molecules reside at the endothelial junctional membrane, however, PECAM-1 has also been shown to constitutively recycle from the membrane network just below the cell border, termed the lateral border recycling compartment (LBRC) [153]. During TEM, delivery of PECAM-1 from the LBRC is targeted at the sections of the junction at which the diapedesis is occurring [153], which is a kinesin-mediated, microtubule-dependent process [154]. The LBRC is believed to facilitate TEM by providing a membrane surface area that is rich in the unengaged PECAM-1, and that physically displaces zones of VE-cadherin [153, 154]. In addition to PECAM-1, JAM-A and CD99, but not VE-cadherin, have also been found in the LBRC [139]. During a paracellular TEM event, PECAM-1 and CD99 molecules are engaged in homophilic interactions, ICAM-1 and -2 interact with integrins and JAMs either bind integrins or are involved in homophilic interactions [148, 155, 156]. The sequence in which the endothelial CAMs become engaged during the paracellular TEM event is proposed to be as follows: (1) ICAM-2 binds to leukocyte integrins and guide the leukocytes in to the junctions (very early penetration step), (2) endothelial JAM-A binds ligands on the leukocytes (possibly JAM-A or LFA-1) facilitating further passage, (3) endothelial and leukocyte PECAM-1 engage in homophilic interactions mediating subsequent leukocyte transit between the ECs [156-159]. Additionally, homophilic interaction between endothelial and leukocyte CD99 has been shown to mediate the transmigration at a stage distant and subsequent to PECAM-1 [150, 151]. Ligation of PECAM-1 during the transmigration leads to expression of the leukocyte α6β1 integrin, which facilitate subsequent passage through the basement membrane (BM) [148, 160].

As leukocytes migrate past the endothelial barrier, the homotypic interactions between VE-cadherin, JAMs, CD99 and PECAM-1 ensure to re-seal the junction.

Interestingly, reverse TEM (rTEM) was recently observed during mouse ischemia-reperfusion injury in vivo, whereby neutrophils were seen crossing the EC junction in an abluminal to luminal direction [161]. The process of rTEM is strongly dependent on JAM-C and is thought to contribute to dissemination of systemic inflammation [161].

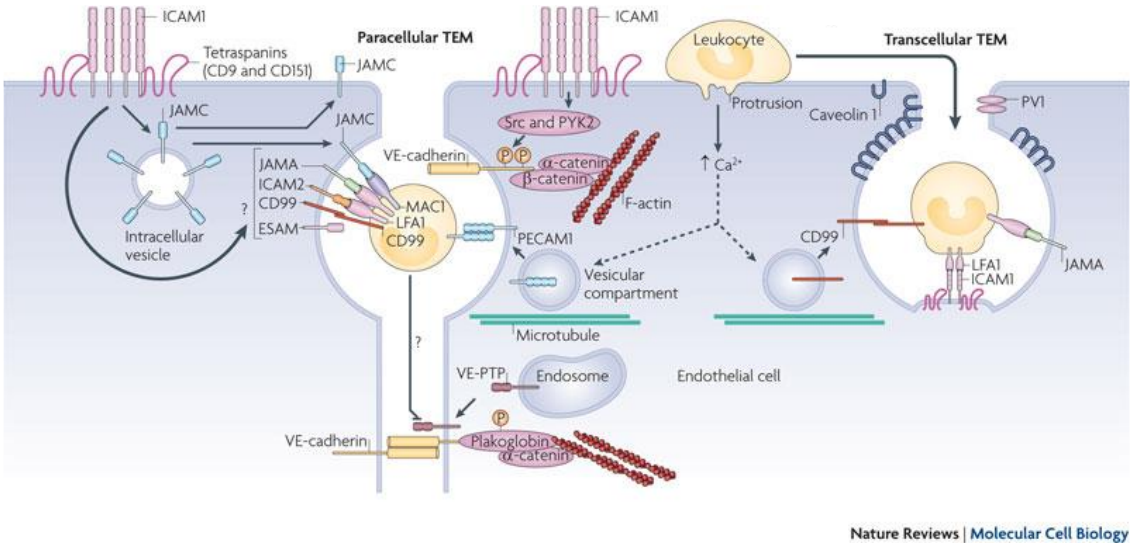

Figure 1.5 Paracellular and transcellular transendothelial migration. Schematic image of leukocytes transmigrating via paracellular or transcelular routes. Leukocyte activated β1- and β2-integrins bind to their endothelial ligands: ICAMs, VCAM1 or JAMs as well as to the ECM upon eventual contact between leukocyte and basement membrane (not shown in the schematic). During paracellular migration, engagement of ICAM-1 modifies VE-cadherin function leading to catenin disassociation and junction opening. PECAM-1 and CD99 form homophilic interactions between extravasating leukocytes and the ECs. PECAM-1, JAM-A and CD99 are recruited to sites of transmigration from the LBRC. During transcellular migration endothelial vesicles form around the leukocyte creating a transcellular pore and importance of LBRC, VVO and caveolin 1 has been shown for this process. For the full names of the CAMs see the **Abbreviations section**. Image taken from Nourshargh et al., *Nat Rev Mol Cell Biol*, 2010 [162].

1.2.8.2 The transcellular route

The transcellular route of leukocyte transmigration is still not well understood, however, certain mechanisms and main players have been proposed (**figure 1.5**). Leukocytes are believed to commence transcellular migration by using actin-rich protrusions, termed “invasive podosomes” to probe the ECs for areas of low resistance [140]. The ECs facilitate subsequent transmigration through the accumulation of membrane vesicles around the passing leukocyte that form a channel through the EC. A number of vesicle types have been shown to surround the transmigrating leukocyte: caveolin 1 containing caveolae [129], vesiculo-vacuolar organelle (VVO) [140] and, recently, the LBRC [139].

Apart from the LBRC-derived PECAM-1, CD99 and JAM-A that have the same role in mediating leukocyte passage as in the paracellular TEM [139] (**section 1.2.8.1**), ICAM-1 has also been shown to actively facilitate transcellular migration [126, 129]. Following ligation, ICAM-1 redistributes to the site of transcellular diapedesis and is enriched in the vesicles surrounding the leukocyte, where it can interact with its ligands on the passing leukocyte [126, 129, 139].

1.2.9 Human leukocyte adhesion deficiencies

Three autosomal recessive immunodeficiency disorders have been identified in humans that result in defective leukocyte recruitment [163]. These disorders have a collective name of leukocyte adhesion deficiencies (LADs) and are hereditary diseases that manifest themselves by recurrent infections [163]. Amongst patients with LADs, following abnormalities have been described: high blood leukocyte counts, recurrent skin and ear infections, severe bleeding, pneumonia, fungal infections and no delayed-type hypersensitivity reaction upon skin testing [164-167]. LADs were named LAD-I, LAD-II and LAD-III, which represents order in which they were discovered, as well as their prevalence [167].

LAD-I was first reported in 1980 when it was found to be an X-linked disease severely affecting neutrophil attachment [165]. It was later identified that LAD-I is a consequence of various mutations in the common β2 (CD18) integrin subunit that result in a truncated or absent protein [163, 168]. Neutrophils isolated from LAD-I patients roll normally on inflamed endothelium suggesting that deficiency exclusively limits the adhesion stage of the leukocyte recruitment cascade, and has no influence on initial selectin-mediated contacts [169].

LAD-II was described for the first time in 1992 when neutrophils isolated from two patients were found to be unable to interact with E-selectin due to their lack of sialyl Lewis X (sLe^x) moieties [164]. The pathology underlying LAD-II is the loss-of-function mutations in *SLC35C1* gene, which encodes the Golgi-localised GDP-fucose transporter [170, 171]. Thus, LAD-II is sometimes referred to as congenital deficiency of glycosylation–IIc (CDG-IIc). GDP-fucose transporter is essential for posttranslational fucosylation of glycoproteins. Therefore, its loss affects synthesis of functional selectin ligands that are known to require fucosylation for successful selectin binding [172] (**section 1.7.2**). Rolling of neutrophils isolated from LAD-II patients was dramatically impaired, further suggesting that selectin/ligand-mediated initial contacts between the leukocytes and the endothelium are abolished in this immunodeficiency disorder [169].

Most rare of all, LAD-III (also known as LAD-I/variant) was first reported in 1997 [166]. It was shown that, whilst normal surface expression of integrins was found on leukocytes from LAD-III patients, the integrins were unable to become activated upon cellular

activation [166]. This was initially attributed to the loss of CalDAG-GEF1, an upstream regulator of small GTPase Rap1 [173, 174]. However, controversies arose, when patients with LAD-III were identified that had both normal CalDAG-GEF1 expression and Rap1 activation [96, 100]. It has now been discovered that LAD-III is caused by mutations in kindlin-3 [96, 100, 101], an adaptor protein that upregulates integrin affinity [95].

1.3 THE ENDOTHELIUM

Endothelial cells play an important role in many vascular functions, e.g. regulation of vascular permeability or vascular wall remodelling. However, the nature of the endothelium, for example its shape and range of adhesion molecules it expresses, is also an important determinant in promoting efficient recruitment of leukocytes to sites of inflammation. It is the leukocyte/endothelial interactions that are of special interest for this thesis. The vascular endothelium is comprised of a monolayer of ECs, which form a barrier between the vessel lumen and the surrounding tissue [175]. Adhesion of adjacent ECs is formed by various adhesion molecules that mediate cell-cell junctions of ranging affinities [175]. Endothelial junctions are multifaceted arrangements formed by transmembrane adhesive molecules attached to a network of cytoplasmic/cytoskeletal proteins. There are at least four diverse types of endothelial junctions: tight junctions, gap junctions, adherens junctions and discontinuous adherens junctions [176, 177]. Endothelial junctions control the passage of various nutrients and macromolecules out of the blood flow as well as regulate the extravasation of leukocytes during inflammation [175, 177].

1.3.1 Tight junctions

Tight junctions (TJs) form a very close contact between neighbouring cells [177]. They are the most apical constituent of the junctional complex in vertebrates and are described as focal contacts between the plasma membranes of bordering cells in ultrathin section electron microscopy [178, 179]. TJs do not form an incessant seal around the cells but are made of discontinuities or aqueous pores that are selectively permeable to small molecules, such as inorganic ions, with selectivity based on the size and charge [177, 179]. The main components of TJs as well as permeability regulators are tetraspan transmembrane proteins termed claudins, which co-polymerize in individual TJ strands, associating between adjacent cells in both a heterotypic and homotypic manner [180-187]. Other TJ proteins include occludins [188], junctional adhesion molecules (JAMs) [189], ESAM [190] and Coxsackievirus and Adenovirus Receptor (CAR) [191]. JAMs are the only described TJ proteins active in TEM [148, 192, 193].

1.3.2. Gap junctions

Gap junctions are essentially transmembrane hydrophilic channels, composed of the connexin family of proteins, and they permit direct exchange of ions and small molecules between neighbouring cells [194, 195]. Gap junctions allow establishment of homotypic (endothehial to endothelial) or heterotypic (e.g. endothelial-smooth muscle cells) interactions between cells. *In vivo*, the occurrence of gap junctions is related to that of TJs and, typically, gap junctions and TJs are intercalated [177]. As connexin proteins are also found on leukocytes [196-198], it has been proposed that leukocytes and ECs can communicate through gap junctions during the inflammatory events ("gap junction coupling") [198]. Leukocyte/endothelium gap junction coupling could serve to prevent endothelium leaking during TEM [198].

1.3.3. Adherens junctions

Adherens junctions (AJs), also termed *zonula adherens*, form intercellular connections that join cytoskeletal elements, such as intermediate filaments and actin filaments of adjacent cells, therefore providing tissue strength [199]. Research on epithelial and ECs revealed that adherens junctions use cadherin-catenin complexes in order to connect to cortical actin filaments that lie parallel to the cell surface, and they appear linear in morphology along the borders between neighbouring cells [148, 176, 200]. In the endothelium, the major cadherin is it the vascular endothelial cadherin (VE-cadherin), which forms homophilic interactions with VE-cadherin expressed on adjacent EC [201-203]. VE-cadherin/catenin interaction is disrupted during leukocyte emigration to allow endothelial permeability (**section 1.2.8.1**) [203, 204].

1.3.4. Discontinuous adherens junctions

Discontinuous adherens junction is the most recently identified novel type of endothelial cell-cell junction [176]. As the name suggests, discontinuous AJs are not linear in sub-cellular distribution along cell borders, but are localised at the end of stress fibers, at points where stress fibers appear to join between adjacent cells to form stellate-like arrangements [176]. These have been recently characterised, and their role during the inflammatory response was speculated to be the resistance of the mechanical stress imposed by the transmigrating leukocytes [176].

1.3.5. Focal adhesions

Focal adhesions (FAs) are specialized points of adhesion produced by different cell types grown in culture. FAs are composed of integrins that span the plasma membrane, interacting on the outside with constituents of the ECM, and on the inside with the actin

cytoskeleton. FAs are made up of many proteins, which have primarily a structural role, although some engage in transducing signals [205]. FAs, just like discontinuous AJs, anchor stress fibers in ECs, but whereas discontinuous AJs play role in attaching stress fibers in confluency – especially after TNF-α stimulation, FA are important for anchoring cells to substrate in subconufluency, for example during migration [176]. Note that leukocytes do not possess stress fibres, although focal adhesion-like structures have been observed [206].

1.4 MIGRATION OF LEUKOCYTES BEYOND THE ENDOTHELIUM

Once the leukocytes cross the endothelium they must overcome the basement membrane (BM) and the pericyte sheath, and then migrate through the interstitium towards the source of inflammation. BM is an extracellular matrix (ECM)-like material, composed of collagens, laminins and heparan sulfate proteoglycans (HSPG) [207]. Pericytes are embedded in the BM forming a discontinuous cellular layer within the vessel wall [208]. Leukocytes cross the BMs using β1 and β2 integrins that act as receptors for BM components [209, 210], e.g. integrin α6β1 is a receptor for BM laminin [160, 211, 212]. Additionally, leukocytes utilise proteases to degrade the BMs to aid their way through, for example neutrophils use elastase [213-215] and lymphocytes employ gelatinases [216]. Furthermore, it is known that BMs contain areas of low resistance, termed low expression regions (LER), which contain ≤ 60% protein deposition as compared to other BM sites, and are the preferred points of leukocyte emigration [217]. It has been shown that whilst neutrophils enlarge the LER size during passage – most probably a result of proteolysis - monocytes do not modify LERs, possibly due to their higher degree of flexibility that allows them to squeeze through the pre-existing areas [218]. Pericytes actively support leukocyte emigration in the process of “abluminal crawling”, whereby neutrophils crawl along pericyte processes for relatively long time and distance (~30 minutes, ~54 μm), until they reach gaps between adjacent pericytes [219]. Abluminal crawling is mediated by interactions between pericyte ICAM-1 and neutrophil LFA-1 and Mac-1 [219]. Gaps between pericytes co-localise with LERs, and so the leukocytes preferably migrate between the pericytes [220], however, migration directly through the pericytes (transcellular route) has also been reported [137].

Heparan sulfates form a fundamental part of BMs, are deposited within the interstitium, are known to bind chemokines, and thus can form stable chemokine gradients that guide leukocyte emigration [221, 222]. Migration through the interstitium follows a chemoattractant (cytokines, chemokines, hydrogen peroxide) gradient and towards the source of the inflammation, and is known as chemotaxis or directed cell migration. Chemotaxis requires engagement of chemokine receptors on leukocytes, and interestingly, L-selectin ligation has been shown to result in chemokine receptor

upregulation and enhanced chemotaxis *in vitro* (see **section 1.11.3**). Furthermore, establishment of cell polarity (extended leading edge at the cell front and rounded back), gradient-sensing and motility are crucial for successful chemotaxis and are mainly controlled by small Rho GTPases (for the role of the Rho GTPases in leukocyte migration see **section 1.5** below). In contrast to migration on two-dimensional (2D) substrates, i.e. endothelial monolayers, pericytes or ligand-coated surfaces, leukocyte migration through the interstitium or in three-dimensional (3D) composites can occur without integrins [223, 224]. This opens up the possibility that other cell adhesion molecules (non-integrin receptors) may play a role in facilitating leukocyte locomotion in 3D environments. In fact, leukocyte chemotaxis *in vivo* has been shown to be dependent on L-selectin and this is discussed in more detail in **section 1.7.5.1.2** of this thesis. Leukocytes arrest locally when they reach the source of inflammation, which confines their motility to the areas, in which their function is needed. It has been reported that the interstitial arrest is an active process that depends on specific chemokines and calcium signalling [225, 226].

1.5 REGULATION OF LEUKOCYTE MIGRATION BY SMALL RHO GTPASES

The Rho family of small (~21 kDa) GTPases regulate cytoskeletal dynamics, thereby affecting multiple cellular functions including cell shape, polarity and motility [227, 228]. The Rho GTPases are GTP hydrolases that act as molecular binary switches that cycle between GTP-bound (active) and GDP-bound (inactive) forms [229]. The activity of Rho GTPases is modulated by guanine nucleotide exchange factors (GEFs), GTPase activating proteins (GAPs) and GDP dissociation inhibitors (GDIs). GEFs catalyse the exchange of GDP into GTP, thereby activating the GTPases [230], whereas GAPs stimulate intrinsic GTPase activity, which leads to hydrolysis of GTP to GDP and inactivation [231]. GDIs maintain the Rho GTPases in a GDP-bound, inactive state [232]. The active Rho GTPases interact with a variety of downstream targets to induce cellular responses [233]. The most extensively studied family members are RhoA, Rac1, Rac2 and Cdc42, which have all been shown to control leukocyte migration (see summary in **table 1.1**). Ectopic expression of either dominant negative or dominant constitutively active forms of RhoA, Rac1 or Cdc42 have all been found to impair leukocyte polarisation and migration [118, 234-239]. This suggests that a tightly regulated, fine balance must exist between activation and deactivation of the Rho GTPases for successful leukocyte locomotion.

The significance of RhoA activity for leukocyte migration has been shown by expression of dominant constitutively active RhoA or expression of dominant negative RhoA or inhibition of RhoA signalling, which affects migration on 2D substrates and across filters, crawling on HUVEC, TEM and chemotaxis [118, 234, 236, 240]. RhoA has been shown to be responsible for tail retraction in migrating monocytes, neutrophils and lymphocytes

[118, 238, 241]. Lack of RhoA activity does not impair gradient sensing but leads to formation of multiple competing lamellipodia, whereas expression of its dominant active form results in a rounded cell that does not protrude [238, 240, 241]. Hence, it has been proposed that RhoA must be actively inhibited at the leading edge to allow lamellipodial protrusions but must be active at the rear to confer rounded "backness" [240, 241]. However, a recent study by Heasman et al. (2010) has demonstrated that RhoA activity is also important at the front of migrating lymphocytes (2D substrates and TEM), where it controls both membrane protrusion and retraction, thereby contributing to the formation of a leading edge [118]. RhoA exerts its activity through activating RhoA kinase (ROCK) [236, 240], and ROCK has been shown to mediate monocyte tail retraction during diapedesis through negatively regulating integrin adhesion at the back [241]. Additionally, RhoA/ROCK signalling pathway is known to control myosin phosphorylation, and myosin-based contractility has previously been implicated in the tail retraction of migrating neutrophils [242].

Ectopic expression of either dominant negative Rac1 or dominant constitutively active Rac1 have both been found to impair chemotaxis of mouse macrophage-like cell line and both human and mouse neutrophils [234, 238]. This was due to a polarisation defect that took the neutrophil migration speed down to basal levels (as seen with no chemoattractant present) [234]. In keeping with this, it has been found that Rac1 plays an essential role in stimulating actin polymerization at the leading edge, and controls pseudopod formation in migrating neutrophils [237]. Interestingly, it has also been reported that neutrophils lacking Rac1 activity were still able to develop oriented leading edge and sense the chemoattractant gradient, but much like RhoA deficient leukocytes, presented with a uropod retraction defect [238]. This was found to be a result of a positive role of Rac1 in stimulating uropod-localized Rho activity [238]. Further investigations found that migrating neutrophils establish dual communication from front to back with Rac1 and/or Rac2 locally inhibiting, and Rac1 globally activating, Rho-mediated backness [238]. Rac2 deficiency results in reduced actin polymerisation, impaired cell polarisation and overall decrease in chemotaxis in mouse neutrophils and T cells [243, 244]. Interestingly Rac2 null neutrophils have reduced emigration in to the inflamed peritoneum as well as decreased rolling on GlyCAM-1, but not on P-selectin [243]. As GlyCAM-1 is a ligand for L-selectin during rolling, this suggests that Rac2 might act downstream of L-selectin to facilitate leukocyte emigration. In line with this, activation of Rac2 upon L-selectin ligation has been previously reported (**section 1.11.4**) [245, 246].

Transmigration of monocytic cell lines across bare filters and HUVEC monolayers is impaired when dominant negative or dominant constitutively active Cdc42 constructs are expressed [235, 236]. Interestingly, neutrophils expressing dominant negative Cdc42 are able to retract their tails and migrate at a speed seen in WT cells [247]. However, the

cells do not establish polarity and migrate only short distances in a disorganised, vacillating manner [234, 237]. Cdc42 has been shown to control the number, stability and directionality of pseudopods but, unlike Rac, is neither necessary nor sufficient for actin polymerization [237]. Additionally, Cdc42 was shown to regulate CD11b distribution and functioning and it was proposed that in turn CD11b is required for proper MLC-based contractility to suppress inappropriate protrusions [247]. Therefore, Cdc42 is primarily responsible for maintaining proper cell polarity to enable directed cell migration.

Rho GTPase	*Leukocyte type*	*Role*	*Citation*
RhoA	Monocytes and monocytic cell lines, lymphocytes and lymphocytic cell lines, primary human neutrophils	Active mainly at the back but activity at the front has been reported, promotes migration through limiting membrane protrusions and retraction of the leukocyte tail (via p160ROCK, during TEM this allows to complete diapedesis) *Constitutively active*: promotes TEM (via p160ROCK), impairs chemotaxis *Constitutively inactive or inhibited*: reduced and slower TEM, responds to chemotactic gradient but does not withdraw the tail, accumulation of beta2 integrin in unretracted tails, rounded cell (global "backness")	[118, 234, 236, 238, 240, 241]
Rac1	Monocytic cell lines, neutrophils and neutrophil-like cell lines	Controls actin polymerisation at the front, responsible for extension of the protrusions, regulates local and global RhoA activity *Constitutively active*: impaired chemotaxis *Constitutively inactive*: able to sense the chemoattractant gradient but decrease in chemotaxis due to polarisation defect, fails to retract uropod due to the lack of RhoA stimulation at the back	[234, 236-238]
Rac2	Mouse neutrophils and T cells	Plays a role in actin polymerisation, cell polarisation and chemotaxis *Deficiency*: decreased neutrophil numbers in peritoneal exudate upon peritonitis, reduced tethering on GlyCAM-1 under flow, impaired polarisation, loss of directional movement, decreased chemotaxis	[243, 244]
Cdc42	Monocytic cell lines, neutrophils and neutrophil-like cell lines	Controls the stability, number, and directionality of the protrusions, role in regulating CD11b activity reported *Constitutively active*: impaired chemotaxis and TEM (across stimulated ECs or towards MCP-1), does not stimulate formation of actin-rich filopodia *Constitutively inactive or inhibited*: decreased TEM towards MCP-1, unable to polarise and loss of directional migration, hesitant migration for short distances, speed of migration and tail retraction unaffected	[234-237, 247]

Table 1.1 Role of the Rho GTPases in leukocyte migration. This table shows summary information about the role of RhoA, Rac1/2 and Cdc42 in the migration of leukocytes. The role of each GTPase is accompanied by the information about effects of its inactivation (expression of constitutively inactive construct or GTPase inhibition) or over-activation (expression of constitutively active construct).

1.6 MIGRATION OF MONOCYTES

Monocytes are important players in both acute and chronic inflammation as well as in immune surveillance. Monocytes originate in bone marrow, where they derive from a common myeloid progenitor that they share with granulocytes [248]. Circulating monocytes have a half-life of 1 and 3 days in mice and humans, respectively [249, 250], comprise from 4% (mice) to 10% (humans) of all circulating leukocytes and can differentiate into macrophages or dendritic cells (DCs) once in tissues [251-254]. A large reservoir of monocytes have also been discovered in the spleen in mice, and these monocytes can be rapidly mobilised upon myocardial infarction (MI) [255]. In broad terms, monocyte subsets are known as "classical" (or "inflammatory") and "non-classical" (also known as "patrolling" or "resident"), and the two subsets can be distinguished by their cell surface receptors (markers). Classical monocytes in humans express high levels of CD14, C-C chemokine receptor 2 (CCR2) and L-selectin (CD62), low levels of CX3C chemokine receptor 1 (CX3CR1) and do not express CD16 ($CD14^{Hi}CD16^{-}CCR2^{+}CX3CR1^{Low}CD62^{+}$); in mice classical monocytes express high levels of lymphocyte antigen Ly6C (Ly6C), CCR2 and L-selectin, and low levels of CXC3R1 ($Ly6C^{Hi}CCR2^{+}CX3CR1^{Low}CD62^{+}$); non-classical monocytes are known as $CD14^{Dim}CD16^{+}CCR2^{-}CX3CR1^{Hi}CD62^{-}$ in humans and $Ly6C^{Low}CCR2^{-}CX3CR1^{Hi}CD62^{-}$ in mouse [254, 256-259]. Because monocyte subsets are defined by the expression of surface markers, it is currently unclear whether they can interconvert [253, 254]. However, it is known that classical monocytes specialise in phagocytosis and reactive oxygen species (ROS) production, whereas non-classical monocytes are weak phagocytes, do not generate ROS and, following activation, produce a different set of cytokines to classical monocytes [260]. Both classical and non-classical monocytes maintain tissue homeostasis in health (**section 1.6.1**), but can also drive disease (**section 1.6.2**).

1.6.1 Migration of monocytes in health

In a healthy organism, monocytes are important components of an acute inflammatory response (**section 1.1.1**), where their infiltration at sites of inflammation follows that of the neutrophils, and can sustain for days. The majority of studies have shown that it is the classical monocyte subset that dominates early on during monocyte infiltration, however, non-classical monocytes have also been reported to be the first ones to arrive at the sites of the tissue insult (see below). Monocyte behaviour, in the context of acute inflammation, is best characterised in a model of *Listeria monocytogenes* infection, and elevated numbers of monocytes in tissues of rabbits infected with this pathogen were first reported in 1926, hence the current species name "*monocytogenes*" [261]. During a

challenge with *L. monocytogenes*, infiltration of monocytes is dependent on the CCR2 receptor and its ligands (C-C motif) ligand 2 (CCL2, also known as MCP-1, monocyte chemoattractant protein-1) and CCL7, and absence of either CCR2 or CCL2/7 results in profound reduction in the numbers of recruited monocytes and increased bacterial burden [262-264]. Monocyte egress from bone marrow during infection is dependent on CCR2-mediated signalling [265], and it has been shown that inflammation evoked by *L. monocytogenes* infection specifically promotes monopoiesis in bone marrow to sustain delivery of monocytes to peripheral sites of infection [266]. CCR2/CCL2-mediated recruitment of monocytes have also been shown to drive monocyte migration to lung during *Mycobacterium tuberculosis* infection [267, 268], to the small intestine during *Toxoplasma gondii* infection [269] and during an acute ischemic-reperfusion injury in kidney [270]. Once at the site of inflammation, monocytes differentiate into scavenging macrophages or DCs depending on the cytokines present in the local environment [271, 272], and antigen-loaded monocyte-derived DCs subsequently travel to PLNs via afferent lymphatics [273]. Interestingly, direct entry of monocytes through HEV of PLNs that drain the local site of inflammation has also been reported to occur in an MCP-1 and MIG (monokine induced by gamma interferon, CXCL9) dependent manner [274, 275].

Non-classical monocytes constitutively migrate into non-inflamed tissues in a CX3CR1-dependent manner, and give rise to resident tissue macrophages and dendritic cells [254]. Non-classical monocytes also scan the resting endothelium in a long-range crawling manner in a search of infected or damaged cells, and their activity has been so far detected in the skin, mesentery, central nervous system and heart in mice [276-278]. Additionally, human non-classical monocytes adoptively transferred into mice were shown to crawl in the skin microvasculature in the same manner [260]. Due to their patrolling behaviour, these monocytes are also known as “patrolling monocytes” and, upon MI or detection of infection or an injury, they can rapidly infiltrate affected tissues, well before the arrival of the classical monocytes or even neutrophils [276, 278]. During this early infiltration stage, patrolling monocytes produce pro-inflammatory cytokines that serve to induce the inflammatory response [254, 276].

A co-ordination in homeostasis maintenance between the classical and non-classical monocytes has been elegantly demonstrated in a study by Nahrendorf et al. (2007), who showed that upon MI, sequential recruitment of classical and non-classical monocytes is responsible for digestion of damaged tissue and tissue healing phase, respectively [258].

1.6.2 Migration of monocytes in disease

Monocyte trafficking in chronic inflammation (**section 1.1.2**) has been mainly studied in atherosclerosis, a chronic inflammatory disease of the arterial wall, characterised by the formation of lipid-laden lesions. Heart attack and stroke induced by atherosclerosis

accounts for nearly three quaters of all deaths from CVD worldwide, and hence recognition of the detailed pathological processes underlying atherosclerosis is needed to improve existing therapeutic strategies. Murine models of atherosclerosis have been established, whereby apolipoprotein E (apoE) deficient mice develop atherosclerotic lesions when placed on high fat diet. Those mice have an altered plasma lipid profile and marked monocytosis [279-282]. The number of circulating monocytes directly correlates with the atherosclerotic plaque size in mice and also is thought to be a CVD risk factor in humans [281]. Atherosclerotic lesions first develop when low-density lipoprotein (LDL) starts to accumulate in the arterial walls. LDL accumulation occurs preferentially in the areas of disturbed laminar flow, such as the branching points of the arterial tree [283-285]. Once trapped in the vessel wall, LDL can undergo oxidation (giving rise to oxidised LDL, oxLDL) [286]. It has been shown that exposure of human ECs to oxLDL induces them to express a plethora of genes, many of them associated with cell adhesion [287]. In line with this, endothelial adhesion molecules P-selectin, VCAM-1 and ICAM-1 have been shown to be involved in atherosclerotic lesion development [288-291], and leukocyte recruitment in atherosclerosis has been also reported [292, 293]. Interestingly, L-selectin has been implicated in the recruitment of leukocytes at sites of atherosclerotic lesion formation, and this is discussed in more detail in **section 1.13.1**. Multiple reports have shown that monocytes are involved in the early steps atherosclerogenesis [294-297]. Monocytes have been mainly observed to be recruited from the arterial lumen [294, 298], however, infiltration from vasa-vasorum has been reported at later stages of the atherosclerotic plaque development [299]. Although the majority of reports describing atherosclerosis formation in mice point towards the recruitment of classical monocytes [279, 280, 300], recruitment of non-classical monocytes has also been shown to contribute to plaque formation [301]. It is possible that the contribution of the two monocyte subsets varies accordingly to the anatomical location of the plaque, i.e. arterial arch versus arterial sinuses [302]. During the development of atherosclerosis monocytes undergo so-called “vicious cycle” of recruitment, whereby monocyte-derived macrophages at sites of the lesion produce cytokines and chemokines, which in turn serve to recruit more monocytes. Monocyte-derived macrophages can take up LDL, oxLDL and other lipids and become lipid-loaded “foam cells” [303-305]. Aggregations of foam cells form the atheromatous core and as this process progresses, the atheromatous core of the plaque converts into a necrotic one, which consists of lipids, cholesterol crystals and cell debris [306]. Plaques having necrotic cores are vulnerable and prone to rupture [307]. Ruptured plaques invariably occlude the blood vessels that supply oxygen-rich blood to the heart or brain, which ultimately leads to MI or stroke.

As this thesis is dedicated to the adhesive and signalling function of L-selectin, the following sections are dedicated to molecular details surrounding this cell adhesion molecule.

1.7 THE SELECTINS

The selectins are a family of cell adhesion molecules that mediate many critical interactions within the vasculature. The selectins and their carbohydrate ligands are expressed on ECs, platelets and leukocytes (**figure 1.6**). Therefore, they can facilitate the contact between the blood and vascular cells, whenever such contact is needed. The family of selectin proteins consists of three members, P-selectin, E-selectin and L-selectin, which were all discovered in the 1980s. All three members were discovered as part of a concerted effort to identify all possible epitopes that existed in the mouse circulation through the generation of monoclonal antibodies. The approach was to identify all the "clusters of differentiation" recognised by mAbs raised against the unknown epitopes on the surface of the leukocytes, and hence the identified epitopes were given the CD name followed by a number. P-selectin (CD62P) (**section 1.7.3**) was identified, when in 1986 its expression was found on human activated platelets (hence P- for platelet) [308] and human ECs [309]. In resting cells, P-selectin is stored in α-granules of platelets and Weibel-Palade bodies of ECs, and is translocated to the platelet/EC surface upon activation [308-310]. The discovery of E-selectin (CD62E, **section 1.7.4**) followed a year later, where it was identified as a cell surface adhesion molecule expressed on activated ECs (hence E- for endothelium) [311]. L-selectin (CD62L, **section 1.7.5**) was first observed in 1983 as a cell surface protein responsible for murine lymphocyte (L- for lymphocyte) recirculation to the LNs [12], and is thus also known as the "lymphocyte homing receptor".

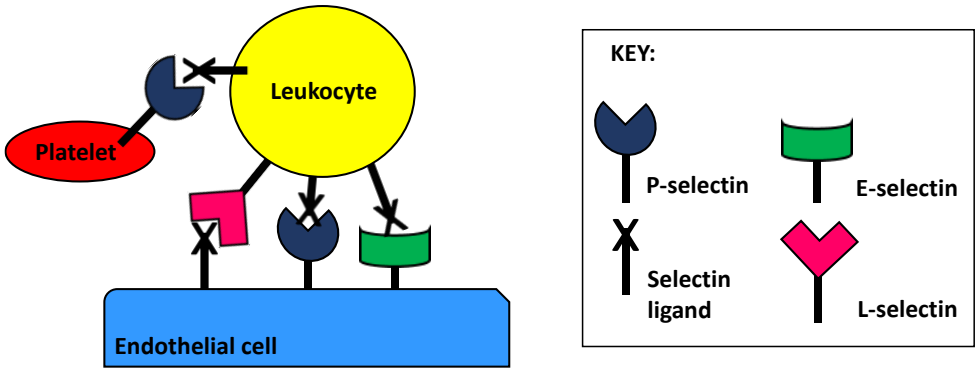

Figure 1.6 Location of the selectins and their ligands. The selectin family comprises three members: E-selectin, P-selectin and L-selectin. Upon cell activation, P-selectin is translocated to the surface of platelets and ECs, and E-selectin is expressed on ECs. L-selectin is constitutively expressed on virtually all circulating leukocytes. Selectins recognise carbohydrate ligands decorated with sulphated, sialylated and fucosylated moieties.

1.7.1 Selectin structure and function

All selectins are highly related type I, single-pass transmembrane glycoproteins [312]. Each selectin is composed of: (i) an amino (N)-terminal calcium-dependent (C-type) lectin ectodomain that interacts with carbohydrate motifs presented by selectin counter-receptors, (ii) a single epidermal growth factor (EGF)-like domain, (iii) two to nine sequence consensus repeat (SCR) domains, (iv) a single transmembrane region and (v) a C-terminal cytoplasmic tail [16, 313, 314] (**figure 1.7**).

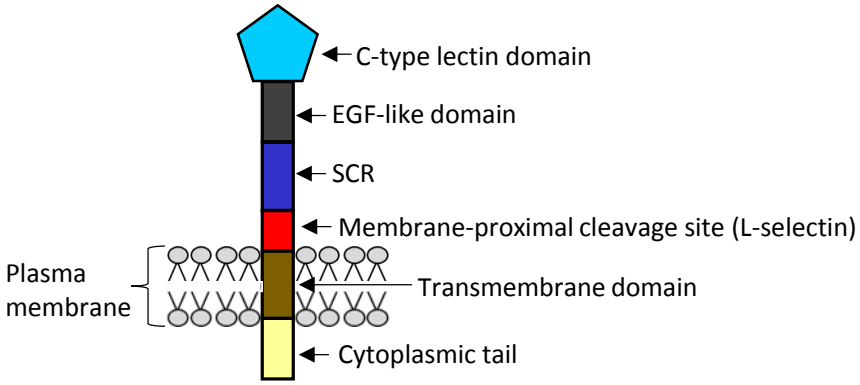

Figure 1.7 The protein structure of the selectins. The selectin proteins have conserved protein structure within their extracellular domain. The common structure is comprised of an N-terminal calcium-dependent C-type lectin, which binds to carbohydrate-bearing ligands. Lectin domain is followed by the epidermal growth factor (EGF)-like domain and several sequence consensus repeats (SCR), that share homology with complement proteins. Nine, six and two SCRs are present in P-, E- and L-selectin respectively. SCRs in L-selectin proteins are followed by a membrane-proximal extracellular cleavage site, which has not been identified in the other two family members. Each selectin has a single-pass transmembrane domain and a COOH-terminal cytoplasmic tail. The tails are not conserved between the selectins, which allows for their unique regulation and signalling.

The homology of the lectin domain differs between selectin members within the same species is around 52%, however, this increases to around 72% between the same selectins from different species [16]. Such high homology represents the importance of the lectin domain. The lectin domain possesses two high affinity binding sites for calcium ions and interacts with its ligands in a Ca^{2+}-dependent manner [315, 316]. It has been shown that upon calcium binding, the L-selectin lectin domain undergoes a conformational change, which leads to the exposure of an epitope responsible for interacting with the ligand [316]. It is this property that signifies the C-type lectin domain. The sequence identity of the EGF-like domains of one selectin between different species is around 60% [16]. This sequence conservation suggests a significant role for the EGF-like domain in the function of the selectins. Indeed, it has been shown that both lectin

and EGF-like domains are needed for optimal ligand recognition and binding of P-selectin [317, 318]. The L-selectin EGF-like domain was also found to regulate binding of the lectin domain to its ligand [319, 320]. Resolution of the crystal structures of E- and P-selectin lectin and EGF domains co-complexed with their ligands revealed existence of extended and bent conformations of the EGF-like domain [321]. It was subsequently shown that the region at the junction of the lectin and EGF-like domains of L-selectin acts like a hinge allowing closed- and open-angle protein conformations, thereby regulating bond formation between the lectin domain and its ligands [47]. Open-angle (extended) conformation was further shown to have greater affinity for ligand and mediated rolling with increased efficiency [322]. The hinge is likely to explain the "catch-slip" bond phenomenon that occurs during selectin-dependent rolling (**section 1.2.2**). Additionally, EGF-like domain has been shown to regulate cleavage of L-selectin ectodomain in a proteolytic process termed "shedding" (**section 1.9.2**) [323].

SCRs show a lower degree of sequence conservation than the lectin and EGF-like domains [16]. Human E- and P-selectin contain 6 [324] and 9 [325] SCRs, respectively, but their number can vary from 4 to 9 in other species [16]. Human L-selectin has two SCRs, the number of which is conserved across species [16]. The variable number of SCRs between the selectins may be explained by their different cellular locations. Although L-selectin possesses only two SCRs, it is expressed at the tips of the leukocyte microvilli [18], therefore its exposure to the potential ligands is relatively high during tethering. Nine and six SCRs in P- and E-selectin, respectively suggest that P-selectin would be more exposed to the leukocyte ligands than E-selectin. This corresponds to the timeline of when these two molecules become engaged during rolling (**sections 1.2.2**, **1.7.3** and **1.7.4**).

Unlike E- and P-selectin, SCRs in L-selectin are followed by a membrane proximal cleavage site [326]. This site allows L-selectin shedding [327] (see **section 1.9.2**), which is associated with cell activation [328]. Although soluble forms of E- [329] and P-selectin [330] have been found in the sera of patients suffering from chronic inflammatory diseases, no discernable cleavage site has been identified.

The transmembrane and cytoplasmic domains of the selectins do not show any sequence conservations between family members, although the sequence conservation of one selectin member across different species is considerably high [16]. The sequence conservation across various species is logical as the selectins are expected to perform the same functions in all species. The lack of sequence conservation between the selectins of one species is likely to reflect the specific functions each of the selectin has. Varied amino acid sequences within the cytoplasmic tails of the selectins are understood to provide binding motifs for different cytoplasmic proteins. This in turn would control the unique signalling generated downstream of each of the selectins and explain their

functional differences. The cytoplasmic tail of L-selectin and its binding partners are described in more detail in **section 1.10**.

1.7.2 Common selectin ligands

The selectins recognise ligands that are glycosylated [314, 331-336]. Modifications include sulfation, fucosylation and sialylation [337] and a minimal recognition motif for P-, E- and L-selectin is the sialyl-Lewis X (sLe^x) tetrasaccharide that is built of sialic acid α2-3-linked to galactose, which is further β1-4-connected to N-acetylglucosoamine, and α1-3-links to fucose [334, 335, 338] (**figure 1.8 A**). Glycosylation modifications are performed by the enzyme fucosyltransferase VII [339], sialyltransferases such as ST3Gal-IV [340, 341], and sulfotransferases such as HEC-GlcNAc6ST [342] or GlcNAc6ST-1 [343]. The absolute requirement for glycosylation of selectin ligands is demonstrated by the loss of leukocyte rolling in mouse models lacking certain glycosylation enzymes, e.g. ST3Gal-IV or HEC-GlcNAc6ST [341, 342], and in LAD-II immunodeficiency syndrome in humans, where fucosylation is abolished (**section 1.2.9**). The sulfated/sialylated/fucosylated structures are found on the non-reducing termini of both O- and N-linked glycoconjugates [344-347], with an exception of PSGL-1 – a ligand for all three selectins – which is sulfated on a tyrosine residue within its protein backbone [348]. O-linked glycans are sugar moieties linked to the proteins via oxygen molecule of either serine or threonine side chains [349]. N-glycans represent another type of linkage, where the sugar moieties are connected to the proteins via a nitrogen atom of the amine group in the asparagine side chain [349]. Anchorage mode of the canonical selectin ligand sLe^x to both O- and N-linked glycans is shown in **figure 1.8 B**.

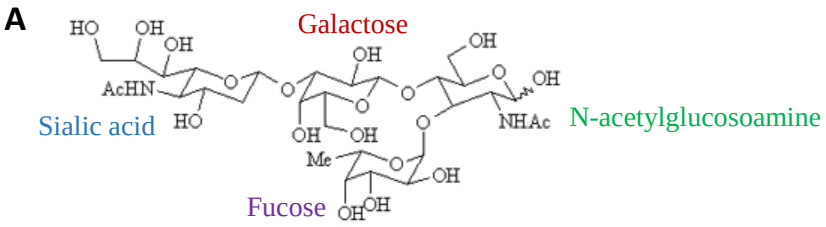

Sialyl Lewis X (sLe^x) tetrasaccharide

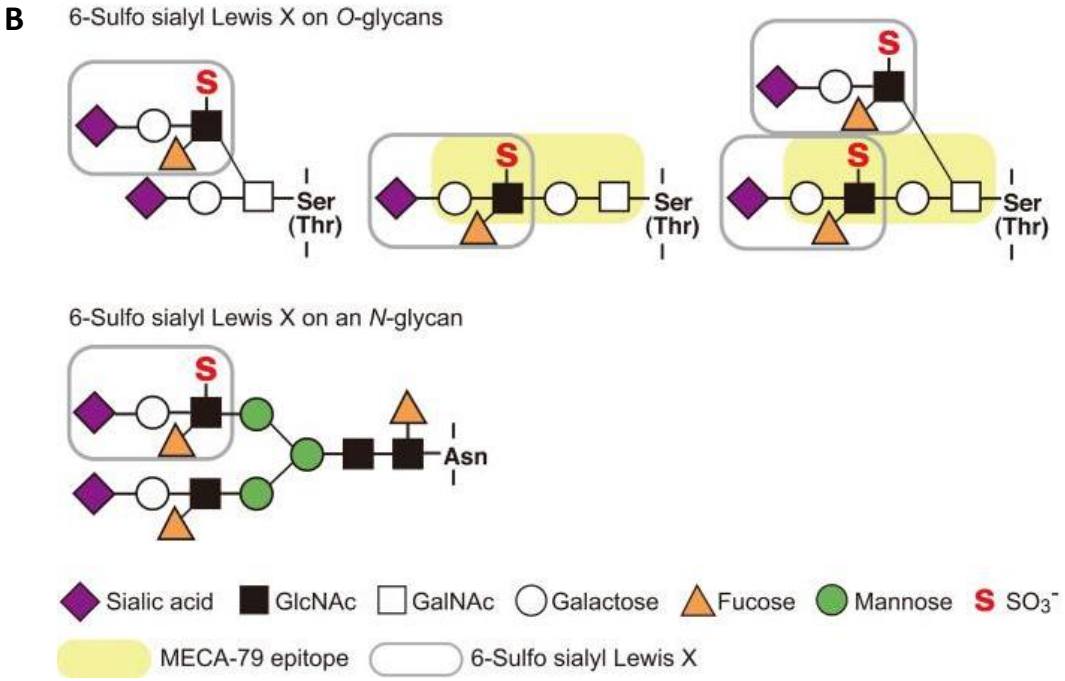

Figure 1.8 Presentation of sialyl-Lewis^x on O- and N-glycans. Canonical selectin ligand sLe^x (**A**) can be presented to the selectins by both O- and N-linked glycans (**B**). Note that the sulfation (red S) on PSGL-1 is not present on the carbohydrate motif but occurs on the tyrosine residue within the protein. Meca-79 is a mAb reactive with PNAd L-selectin ligands (**section 1.8.1**). Image in B taken from Hirakawa et al., *Journal of Biological Chemistry*, 2010 [345].

Although sLe^x binds to all three selectins, the affinity of such binding is relatively low and it is likely that selectins recognise multiple motifs presented by their ligands [16]. Furthermore, differences exist in the requirements for sugar modifications between the selectins, for example ligand sulfation is needed for P- and L-selectin, but not E-selectin binding [350]. To this date, multiple ligands for the selectins have been identified. P-selectin can bind to PSGL-1 [351], variant of CD44 (CD44v) [352], endoglycan [353] and versican [354]. E-selectin binds to PSGL-1 [351], L-selectin [355], CD43 [356, 357], CD44 [358-360], CD44v [361], E-selectin ligand-1 (ESL-1) [362, 363], carcinoembryonic antigen (CEA) [361], podocalyxin [364] and endoglycan [353]. L-selectin binds to a variety of ligands expressed both inside and outside of the vasculature. L-selectin ligands are described in more detail in **section 1.8** (see summary in **table 1.2**).

1.7.3 P-selectin and its role in the leukocyte adhesion cascade

P-selectin (CD62P, GMP-140, PADGEM) is expressed by activated platelets and ECs [308, 309]. P-selectin null mice have elevated counts of circulating granulocytes, which reflects a defect in leukocyte extravasation [25]. Additionally, baseline leukocyte rolling in mouse mesentery microcirculation is completely abolished, and leukocyte recruitment is delayed in both trauma and thioglycollate-induced models of inflammation [25, 365]. Upon inflammatory challenge, endothelial P-selectin, which is synthesised constitutively and stored in intracellular vesicles of endothelial Weibel-Palade bodies, is translocated to the plasma membrane, where it can bind to its leukocyte ligand PSGL-1 [310, 366, 367]. In murine, but not primate ECs, stimulation with TNF-α additionally induces P-selectin gene expression [368]. Owing to its rapid translocation from the intracellular pool, P-selectin mediates most leukocyte rolling during the first phase (<2 hours) after the inflammatory challenge [25, 365]. This explains the delays in leukocyte recruitment seen in P-selectin deficient mice. It is possible that E-selectin can mediate rolling in the absence of P-selectin [369], however E-selectin cannot mediate tethering [24]. On the other hand, in the absence of P-selectin, it appears that tethering can be compensated for by L-selectin [24]. However, L-selectin mediates much more rapid rolling (above 100 μm/s) than P-selectin (below 50 μm/s), and also it cannot compensate for the initial (<1 hour) rolling absent in P-selectin deficient mice during trauma-induced model of inflammation [52, 365]. Thus, it seems that P-selectin co-operates with L-selectin to maintain the rolling at a speed of 20-70 μm/s [52], however, under certain inflammatory conditions (trauma), the very initial rolling is unique to P-selectin [52, 365].

As described in **section 1.2.4**, engagement of the selectins leads to the activation of integrins, which contributes to leukocyte activation and arrest. *In vitro* and *in vivo* experiments with mouse and *in vitro* experiments with human neutrophils as well as precipitation studies of transfected HEK 293T cell line revealed that engagement of P-selectin by PSGL-1 leads to activation of Src kinases which phosphorylate Nef associated factor 1 (Naf-1) at Tyr552 [366]. Subsequently, activated Naf-1 recruits phosphoinositide 3-kinase (PI3K) (p85-p110δ heterodimer) to this complex, which eventually triggers activation of β2 integrins Mac-1 and LFA-1 [366].

Apart from its role in the recruitment of leukocytes to the activated endothelium, P-selectin also mediates certain platelet interactions. Upon activation, platelet P-selectin is translocated from the intracellular α-granules to the platelet surface [308], where it mediates contacts with leukocytes [370] through interaction with leukocyte PSGL-1 [371]. Platelet-leukocyte aggregates have been reported to circulate in bloodstream of patients with coronary artery disease [372] and *Helicobacter pylori* infection [373], and have been suggested to contribute to atherosclerosis development in a mouse model

[374]. Additionally, P-selectin facilitates platelet-platelet interactions and formation of platelet aggregates [375]. Formation of platelet aggregates is an important step during blood coagulation at the site of an injury.

1.7.4 E-selectin and its role in the leukocyte adhesion cascade

E-selectin (CD62E, ELAM-1) expression is induced upon stimulation with TNF-α, LPS or interleukin-1β (IL-1β), and is a result of *de novo* protein production [51, 368, 376, 377]. E-selectin expression on the surface of the endothelium can be seen 2 hours after stimulation with a pro-inflammatory agent and peaks after 4 hours [378]. Upon its expression on the endothelial surface, E-selectin joins P-selectin in mediating leukocyte rolling. E-selectin is different to the other two family members in that it is not able to mediate tethering [24, 53, 56]. After some time, the co-operation between E- and P-selectin in rolling maintenance is discontinued and rolling becomes dependent only on E-selectin and its ligands [379]. E-selectin is known as a mediator of "slow rolling" (3-5 μm/s), and its absence significantly increases rolling velocities of leukocytes as well as promotes their 'skipping' behaviour [51, 379, 380]. Skipping behaviour of leukocytes in the absence of E-selectin is characterised by cycles of short steady rolling episodes followed by detachment and re-tethering further downstream [379]. This results in sharp and transient changes in velocity and leukocytes moving in this manner fail to engage in steady rolling [379]. It was established that E-selectin mediates slow and stable rolling through interaction with CD44 and ESL-1, respectively [379].

It should be noted that human L-selectin from neutrophils can interact with E-selectin [355, 381]. This is because neutrophil L-selectin is modified with sLe^x moieties and thus becomes a ligand for E-selectin [355]. This is neutrophil specific as L-selectin from lymphocytes does not bear sLe^x epitopes [355]. This represents glycosylation-dependent specificity of selectins and their ligands, which in this case allows trafficking of naïve lymphocytes to LNs and neutrophils to the sites of inflammation. However, L-selectin from mouse neutrophils cannot bind E-selectin [381], revealing a species-specific interaction. It should therefore be made clear that much of our current understanding of how L-selectin contributes to leukocyte rolling comes from studying murine models, and little is known how this may reflect the human system where E-selectin/L-selectin interaction can occur.

Much like P-selectin, binding of E-selectin to its counter-receptors leads to integrin activation, which supports transition from leukocyte rolling to arrest (**section 1.2.4**). Both *in vitro* and *in vivo* experiments on murine neutrophils revealed that interaction of PSGL-1 or CD44 with endothelial E-selectin triggers a signalling pathway in leukocytes that starts with Src family kinases (SFKs) [382, 383]. This is followed by activation of spleen tyrosine kinase (Syk) and Burton's tyrosine kinase (Btk), which in turn leads, through

phospholipase C (PLC) γ2, to the activation of p38 mitogen-activated protein kinase (MAPK); this pathway triggers the β2 integrin-mediated slow rolling of leukocytes [382, 383]. Additionally, Mueller et al. (2010) reports the involvement of PI3K gamma (PI3Kγ) in this signalling pathway [383] and Yago et al. (2010) stress the importance of lipid rafts for efficient PSGL-1 and CD44 signalling (2010) [382]. The cytoplasmic domain of PSGL-1 is crucial for signalling to downstream components of this particular signalling pathway as deletion of this domain in PSGL-1 prevents phosphorylation of Src family kinases (SFKs) and reduces E-selectin-triggered neutrophil slow rolling on immobilised ICAM-1 [382]. Conversely, Hidalgo et al. (2007) claim that in murine leukocytes transition from rolling to arrest *in vivo* is mediated by E-selectin interacting with CD44 and ESL-1, whereas there is no role for PSGL-1 in this process [379]. The controversies described could be due to the experimental techniques and/or the inflammatory models used in the respective studies.

1.7.5 L-selectin

L-selectin (CD62L, TQ1, Leu-8, LAM-1, LECAM-1) is expressed on all circulating leukocytes, with an exception of activated T and B cells [384-386] and a subset of memory T cells [387]. As mentioned earlier, L-selectin was discovered through screening of leukocytes with antibodies raised against unknown antigens. The antigen on mouse lymphocytes was recognised by MEL-14 mAb [12] and its human homolog was identified in 1990 by raising mAbs against molecules shed from human leukocytes following their activation [388]. There were 5 mAbs raised: DREG-55, -56, -110, -152 and -200, out of which DREG-56 showed specific >90% inhibition of binding of human lymphocytes to PLN HEV [388]. L-selectin was established to be responsible for the migration of lymphocytes to PLN, Peyer's patches (specialised lymph nodes in the gut), mesenteric lymph nodes (MLNs) and spleen as well as for leukocyte recruitment to sites of inflammation [11, 12, 389-398]. L-selectin was found to play a prominent role in skin inflammation, and its absence or blocking results in decreased leukocyte recruitment, reduced delayed-type and immediate-type hypersensitivity responses and delayed allograft rejection [391, 392, 399-401]. Its predicted molecular weight (MW) is 30 kDa but the actual MWs have been reported to be 74 kDa for lymphocytes [402] and 90-120 kDa for neutrophils [381]. This increase in the MW is a result of L-selectin protein glycosylation, which is thought to occur differently in various leukocyte subsets [313].

1.7.5.1 The role of L-selectin during leukocyte recruitment

1.7.5.1.1 Roles for L-selectin within the vasculature

Although mainly known for its ability to mediate tethering and rolling, L-selectin takes part in other stages of the leukocyte adhesion cascade (**figure 1.9**).

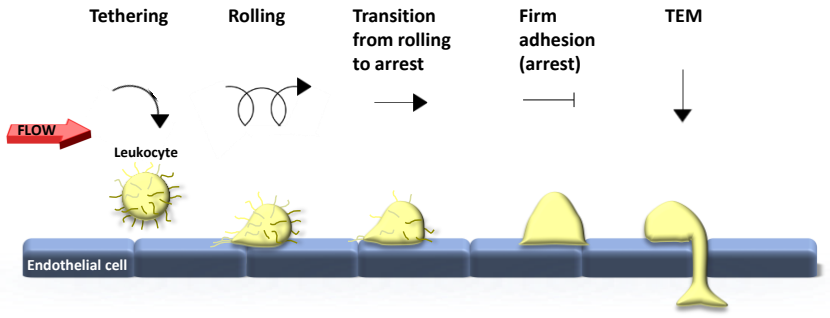

Phase of the adhesion cascade	Tethering	Rolling	Transition from rolling to arrest	Firm adhesion (arrest)	TEM
Role of L-selectin	Initiates and mediates capture through binding of endothelial ligands and leukocyte PSGL-1	Mediates rolling at velocities higher than P-selectin and E-selectin	Ligation induces signalling contributing to leukocyte activation	Supports firm adhesion through β integrins	Shedding regulates lymphocyte TEM across HEV; Increased TEM seen upon cross-linking but the mechanism is unknown

Figure 1.9 The role of L-selectin during the leukocyte adhesion cascade. L-selectin is best known for its ability to mediate leukocyte tethering and rolling. In addition, L-selectin also mediates leukocyte activation and transition from rolling to arrest as well as modulates adhesion through β integrins. L-selectin has been shown to regulate TEM during lymphocyte homing to PLN, and there are some indications pointing at its possible role during TEM at sites of inflammation. For abbreviations used see the **Abbreviations section**.

L-selectin mediates leukocyte recruitment through both its adhesive and signalling properties. The adhesive interactions are important for mediating tethering and rolling. L-selectin-mediated tethering is facilitated by its microvillar localisation [18, 19, 403] and the unique kinetic properties of L-selectin/ligand bonds that allow shear-dependent tethering [46, 404, 405]. Out of the three selectins L-selectin mediates the fastest type of rolling (>100 μm/s) [52, 405, 406], and is the only selectin that can mediate secondary capture of free flowing leukocytes (**section 1.2.3**). L-selectin co-operates with P-selectin in mediating rolling (**section 1.7.3**), however its distinct contribution can be seen at later time-points (>1-2 hours) in cytokine-stimulated venules [365, 398, 407]. L-selectin-deficient mice have been shown to have a dramatic reduction in lymphocyte rolling and/or accumulation on PLN HEV, which resulted in 70-90% decrease of lymphocyte numbers in PLNs and corresponding elevated numbers of lymphocytes in circulation and spleen [11, 389-391, 395, 408]. L-selectin has also been reported to mediate leukocyte

rolling in exteriorised mesenteric [11, 28, 29, 409] and cremasteric muscle venules [52, 365], and L-selectin deficient mice present with monocytosis (elevated levels of circulating monocytes), suggesting impaired monocyte emigration [389]. The importance of L-selectin-dependent recruitment at sites of inflammation was demonstrated through thioglycollate-induced peritonitis model, where 40-80% reduction of leukocyte (lymphocyte, neutrophil and monocyte) emigration in to the inflamed peritoneum was seen [11, 392]. L-selectin has also been shown to mediate rolling on activated ECs *in vitro* [410]. Vascular ligands for L-selectin are induced on activated endothelium (**section 1.8.2**) and presumably are important for mediating rolling. L-selectin was shown to mediate rolling (together with α4 integrin) in rat mesenteric venules 12 days after immunisation with *Mycobacterium butyricum*, suggesting a role for L-selectin in chronic inflammation [411]. The role of L-selectin in atherosclerosis, the chronic inflammation of the arteries, is discussed in more detail in **section 1.13.1**. Furthermore, L-selectin was shown to mediate neutrophil recruitment in myocardial ischemia/reperfusion model in cats, where anti-L-selectin mAb significantly decreased neutrophil accumulation on ischemic/reperfused coronary endothelium [412].

Apart from mediating tethering and rolling through the virtue of its lectin domain and catch-slip bond phenomenon, L-selectin generates intracellular signalling that results in leukocyte adhesion. As described in **section 1.2.4**, one of the prominent events driving the transition from leukocyte rolling to arrest is outside-in signalling triggered by L-selectin engagement, which results in integrin activation. Rolling of neutrophils on L-cells transfected with E-selectin and ICAM-1 have been shown to induce co-clustering of L-selectin and PSGL-1, which is necessary for the rolling cells to adhere (arrest) [413]. Furthermore, cross-linking of L-selectin has been shown to induce the transition from neutrophil rolling to LFA-1- and Mac-1-dependent arrest during perfusion of cells over monolayers of E-selectin and ICAM-1 [414]. A number of studies have now established the role of outside-in L-selectin signalling in mediating leukocyte adhesion through β1 and β2 integrins, and these reports are discussed in more detail in **section 1.11.2**. In addition to its direct role in the integrin-mediated arrest, L-selectin engagement has also been shown to act in synergy with various chemokines and cytokines to enhance adhesion (**section 1.2.4**). In concert with its role in synergising outside-in signalling and chemokine-mediated adhesion, engagement of L-selectin has been shown to regulate expression levels of the chemokine receptors present on the leukocyte surface (**section 1.11.3**).

L-selectin, and specifically its shedding, regulates TEM across HEV during lymphocyte homing to PLN (**section 1.9.2**). It is thus possible that L-selectin might also be involved in leukocyte TEM at sites of inflammation. This is currently unclear, although stimulation through L-selectin was found to enhance leukocyte transmigration to various

chemokines (e.g. SDF-1, IL-8, SLC) *in vitro* [85, 91, 415]. L-selectin has been shown to mediate leukocyte chemotaxis in extravascular tissues *in vivo* (**section 1.7.5.1.2**), and perhaps it is the relationship between L-selectin and certain chemokines that drives leukocyte emigration and influence TEM in inflammation.

1.7.5.1.2 Roles for L-selectin outside the vasculature

Much of the current literature on L-selectin is centred mainly on its role in tethering and rolling during the leukocyte adhesion cascade. Interestingly however, reports can be found that point towards a prominent role L-selectin might play in leukocyte migration beyond the vasculature both during homing of lymphocytes to PLNs and during inflammation. There is a number of reports suggesting that engagement of L-selectin enhances leukocyte chemotaxis *in vitro* (**section 1.11.3**), and a role for L-selectin in directed cell migration *in vivo* has also been proposed. For example, in L-selectin deficient mice defects were seen in the interstitial migration away from the venules, both during trafficking of lymphocytes to MLN [415], and during the antigen-induced leukocyte recruitment in the cremasteric muscle model of inflammation [416]. Likewise, in a mouse model of multiple sclerosis (MS), emigrated L-selectin deficient leukocytes were found to be located perivascularly and did not infiltrate the brain tissue, which in turn limited the demyelinating pathology [417]. Interestingly, screening with L-selectin-IgG chimera showed that L-selectin ligands are present on myelin sheaths of axons [418], suggesting L-selectin dependent leukocyte infiltration results in myelin destruction during MS progression. In all of the above-described studies, the emigrated leukocytes were not able to disseminate in to the surrounding tissues and remained closely associated with the venules. This would suggest an impairment in chemotaxis that was caused by L-selectin knock-out. Interestingly, another report demonstrated that chemotaxis *in vivo* was indeed abolished in L-selectin null mice [398]. Hickey et al. (2000) found that 50% of the emigrated leukocytes had a profound decrease in their ability to migrate towards a KC (keratinocyte chemokine)-soaked agarose block and remained closely associated with the cremasteric microvessels [398]. Similarly, the path length of extravascular locomotion was 40-50% decreased in L-selectin null leukocytes as compared to WT ones during emigration upon cremaster superfusion with PAF or KC [398]. Interestingly, leukocytes from mice expressing a sheddase-resistant form of L-selectin (i.e. a mutant resistant to shedding) were also found to have impaired chemotaxis as measured by the distance they travelled away from the KC-perfused cremaster microvessel [419]. These two different scenarios, first, where L-selectin is lacking and second, where it is constitutively expressed in its non-cleavable form on the leukocyte surface, seem to exert the same effect on chemotaxis. Therefore, it can be speculated that the L-selectin's involvement in migration through the ECM may rely on its ability to undergo shedding

and subsequent re-expression. Alternatively signalling involving the cleaved L-selectin ("stump") may be possible. Furthermore, the migration defect of leukocytes expressing sheddase-resistant L-selectin was true for KC, but not TNF-α superfusion [419], suggesting that L-selectin dependent chemotaxis has preference towards certain chemokines and is insensitive to or overridden by others. In keeping with this, it has been shown *in vitro* that engagement of L-selectin on murine T and B cells enhanced their chemotaxis to secondary lymphoid tissue chemokine (SLC), but not to SDF-1 or EBV-induced molecule 1 ligand chemokine (ELC) [415].

In addition to a defect in chemotaxis, L-selectin-null mice have been shown to have greatly (50-60%) reduced total number of emigrated leukocytes at various sites of inflammation [11, 392, 398, 420]. Interestingly, Hickey et al. (2000) saw no gross defects in leukocyte rolling, suggesting that at least in certain cases reduced emigration was not due to a decrease in L-selectin-dependent rolling [398]. As all of these studies were performed *in vivo*, it can be assumed that a great abundance of cytokines and chemokines were present to elicit L-selectin-dependent cellular responses. Perhaps it is the chemokines and the ECM environment that synergise to drive L-selectin dependent migration beyond the vessel lumen. The nature of L-selectin signalling occurring outside the vasculature is expected to be different from the signalling that takes place during the leukocyte recruitment inside the venules. During tethering and rolling, L-selectin engages transiently with its ligands, which is a result of the disruptive forces imposed by blood flow. However, it can be assumed that once the leukocyte is in the ECM, much slower movement of the cell will prolong L-selectin/ligand interactions and therefore enhance and/or modify L-selectin signalling. In line with this, the capability of L-selectin to bind components of the ECM has been reported on numerous occasions (**section 1.8.3**).

Taken together, L-selectin plays a vital role in leukocyte trafficking both during interactions of leukocytes with ECs and during interstitial migration outside the vessel wall (and in the absence of shear stress). It is currently unknown how inta- and extra-vascular activity of L-selectin is linked, although shedding of the extracellular domain is likely to play a role (for the physiological relevance of L-selectin shedding see **section 1.9.2**).

1.7.5.2 Current methods used to study L-selectin-dependent phenomena

Current *in vivo* and *in vitro* methods used to study the role of L-selectin in the leukocyte adhesion cascade involve intravital microscopy of various tissues and organs, analysis of cell exudates following thiglycollate-induced peritonitis, parallel plate flow chamber assays and transwell assays. The majority of these studies concentrate on the effects of L-selectin on total numbers of recruited leukocytes and do not investigate the sub-cellular distribution of L-selectin. In the studies where visualisation of cell-associated L-selectin

was performed, the leukocytes were first labelled using an anti-L-selectin mAb, and then perfused over immobilised ligand [379, 421]. Such reports ignore the fact that using antibodies causes, firstly, L-selectin clustering and signalling in an "outside-in" manner (**section 1.11**), and secondly, blocks the lectin (ligand binding) domain. Hence, treatment of leukocytes with anti-L-selectin antibodies prior to the flow experiments might pose serious risks to correct data interpretation. Therefore, the current methods of visualising L-selectin cannot be classified as "non-invasive", and other approaches are needed for reliable tracking of L-selectin's fate during the leukocyte adhesion cascade. For example, tagging of L-selectin with a fluorescent protein would help to address the aforementioned visualisation issues, providing a non-invasive way of monitoring L-selectin by not interfering with its function (i.e. provided the tag itself would not affect L-selectin's form and function).

1.8 LIGANDS FOR L-SELECTIN

L-selectin was firstly recognised to bind carbohydrate ligands on PLN HEV (**section 1.8.1**), however it is now known that many other L-selectin ligands, distinct from the "classical" HEV ligands exist. For example, numerous L-selectin ligands have been reported at sites of inflammation (**section 1.8.2**), in the ECM (**section 1.8.3**) and on a variety of other cells and tissues (**section 1.8.4**). A summary of all L-selectin ligands identified to date is shown in **table 1.2** and the ligands are discussed in more detail in the sections below.

1.8.1 L-selectin ligands on high endothelial venules (HEV)

Initial work showed that L-selectin recognises carbohydrate ligands on PLN HEV in a calcium dependent manner [11, 422-424]. Early attempts on identifying carbohydrate-based ligands for L-selectin suggested that sugar moieties were mainly O-linked glycans [337], and despite their prevalence, L-selectin-dependent rolling can also occur on N-linked glycans [346, 347]. L-selectin recognises mucin (glycoprotein with multiple O-linked glycans) ligands on HEV that have a collective term of peripheral lymph node addressins (PNAd) and are reactive with MECA-79 mAb [425]. MECA-79 is routinely used to detect L-selectin reactive vessels and it has been shown to block lymphocyte tethering and rolling on HEV [426], as well as immunoprecipitate the same set of proteins from mouse PLNs and human tonsils as the L-selectin-IgG chimera [427]. The reason for this is that MECA-79 mAb recognises an epitope that overlaps with the basic L-selectin recognition determinant – the 6-sulpho-sLe^x motif (**figure 1.8**). Sulfation of the sLe^x moiety is necessary for efficient interaction with L-selectin, as sulfation greatly enhances L-selectin binding in cell-free assays and during binding of L-selectin-IgG chimera or L-selectin expressing cells to ECs transfected with relevant sulfotransferases

[428-431]. A number of 6-sulpho-sLe^x-bearing PNAd sialomucins have been identified to date. The first ones to be recognised were glycosylation-dependent cell adhesion molecule 1 (GlyCAM-1) [337, 432, 433], CD34 [434, 435] and a CD34 family member podocalyxin-like protein [436]. Subsequent studies identified further L-selectin ligands expressed on PLN HEV: sgp200 protein [427], endomucin [437], nepmucin (not expressed on Peyer's patches HEV) [438] and mucosal vascular addressin cell adhesion molecule 1 (MadCAM-1) (expressed only on MLN HEV) [439]. Interestingly, CD34 [440] or GlyCAM-1 [428] null mice did not present with any abnormalities in lymphocyte homing to PLNs, suggesting that HEV mucins might be functionally redundant, and can compensate for each other to mediate all rolling. On the other hand, HEC-GlcNAc6ST sulfotransferase deficiency resulted in greatly diminished lymphocyte recirculation to LNs [342]. It is therefore the specific post-translational modifications of L-selectin ligands rather that than the ligand protein backbone that are crucial for L-selectin mediated lymphocyte homing.

Apart from the well-known mucins, non-mucin (as defined be their resistance to O-sialoglycoprotease treatment) ligands for L-selectin have been identified on HEV in human PLN cryosections [441]. These ligands bear sLe^x and L-selectin ligand activity but lack MECA-79 antigen, and are capable of mediating lymphocyte binding [441]. It is hard to say whether similar ligands are present on HEV in mice, however it is plausible as blocking with MECA-79 mAb was shown to result in significant but not total inhibition of lymphocyte homing to PLN [442, 443]. Alternatively, differences in L-selectin HEV ligands might exist between species, as it has been shown that e.g. MECA-79 mAb weakly stains Peyer's patches HEV in mice but strongly in sheep, rabbit and pig [443, 444]. Therefore, the complexity of L-selectin HEV ligands is likely to be higher than currently anticipated. Additionally, it is noteworthy that MECA-79-reactive HEV-like venules are commonly found at sites of chronic inflammation, implying the role of the "classical" L-selectin HEV ligands in inflammation (**section 1.8.2**).

1.8.2 Ligands for L-selectin on the endothelium at sites of inflammation

As mentioned at the end of the section above, venules resembeling HEV are often found at sites of chronic inflammation. MECA-79-reactive HEV-like vessels together with dendritic cells and zones of B and T cells populate tissues at sites of persistent inflammation in a process known as lymphoid organ neogenesis [445, 446]. PNAd, MadCAM and/or CD34 expressing HEV-like venules have been identified in various inflammatory diseases (the diseases are listed in **table 1.2**) [442, 447-453]. Additionally, HEV-like structures have also been identified in gastric lymphoma that lacked MECA-79 reactivity, but nevertheless could bind L-selectin through 6-sulfo-sLe^x [454]. This

suggests that much like in the case of PLN HEV, other ligands than PNAd are involved in binding L-selectin at sites of chronic inflammation.

MECA-79 staining of acutely inflamed vessels has not been reported to date, and the existence of other L-selectin ligands at sites of inflammation *in vivo* is controversial. For example, no L-selectin ligand activity during leukocyte recruitment in the exteriorised cremaster muscle venules was found by Eriksson (2008) [455]. On the other hand, an unidentified ligand has been observed during neutrophil recruitment to the inflamed peritoneum and in the cremaster muscle model of inflammation in a different study [456]. *In vitro*, the situation seems to be clearer as several studies found L-selectin ligand activity on activated ECs. As mentioned in **section 1.7.4**, human but not mouse L-selectin from neutrophils binds E-selectin, as identified by cell-free binding experiments and neutrophil recruitment in parallel-plate flow chamber assay [355, 381]. Sulfoglucuronosyl paragloboside (SGPG) has been identified as L-selectin ligand during interaction of PBL with IL-1β stimulated bovine brain microvascular endothelial cells (BMEC) in a static binding assay [457]. Additionally, unidentified ligands were seen during leukocyte recruitment to TNF-α activated bovine kidney microvascular glomerular endothelial cells (BKMGEC) or human cardiac microvascular ECs (HCMEC) in static and non-static (rotation or flow) *in vitro* [458, 459]. These ligands were synthetized *de novo*, required sialylation or sulfation and mediated interaction for prolonged period of time (24-48 hours) [458, 459]. Furthermore, inducible L-selectin ligand has been seen on IL-4 stimulated HUVEC, and this ligand supported L-selectin-mediated monocyte recruitment for at least 48 hours under rotating conditions [410]. Given that rolling has been observed to be dependent on L-selectin at later time-points (> 1-2 h) [52, 365, 411], it is plausible that it is these unidentified ligands, which persist on the endothelium for long periods of time that bind L-selectin to support leukocyte rolling at later stages of the recruitment. Additionally, it seems that the vascular bed specificity for these ligands exists as demonstrated by the study by Zakrzewicz et al. (1997), who observed L-selectin ligands on HCMEC but not on the ECs derived from the macrovessels [459].

Interestigly, L-selectin ligand(s) were also detected on resting bovine aortic endothelial cells (BAEC), and their expression increased after TNF-α stimulation [460]. These ligands supported monocyte recruitment to BAEC under rotating conditions [460], suggesting a role for L-selectin/ligand binding in the recruitment of monocytes to the aortic endothelium and in development of atherosclerosis. The role of monocytes and L-selectin in the pathogenesis of atherosclerosis is described in **sections 1.6.2** and **1 .13.1**, respectively.

1.8.3 L-selectin ligands in the extravascular tissues

A substantial number of reports have identified components of the extracellular matrix (ECM) as ligands for L-selectin. The majority of these ligands belong to the family of sulfated proteoglycans (PGs), and binding of heparan sulfate (HS), dermatan sulfate (DS) and chondroitin sulfate (CS) PGs derived from rodent and human tissues to L-selectin has been shown [461-463]. The proteoglycans involved in L-selectin binding have been identified as HSPG collagen XVIII, CS/DS PG versican and DSPG biglycan, and all bind L-selectin via their sulfated glycosamicoglycan (GAG) chains [221, 354, 463-466]. PGs are well-known for their involvement in tissue architecture maintenance, however emerging body of evidence suggests that they also act as signalling molecules actively participating in the inflammatory response [467]. In keeping with this, accumulation of versican and biglycan is associated with development of atherosclerotic lesions in humans and mice [468-475], and loss of collagen XVIII has been shown to promote atherosclerosis in mice [476]. Interestingly, lubricin, a mucin-like protein isolated from the synovial fluid of patients with rheumatoid arthritis, has also been shown to bind L-selectin via its sialylated and sulfated oligosaccharides [477]. These reports suggest that L-selectin and its ECM ligands could mediate leukocyte emigration during chronic inflammatory diseases. A role for ECM components in leukocyte tissue infiltration has been suggested by Ogawa et al. (2004), who found that monocytes from L-selectin null mice and sulfatide null mice display the same extent of emigration defect in murine unilateral ureteral obstruction (UUO) model [420]. Sulfatide is an ECM glycolipid, which also has been shown to bind L-selectin via its long sulfated sugar chains [478]. Notably, distribution of sulfatide and L-selectin ligands in both normal and ureteric obstructed kidneys is very similar, and 24 hours after UUO both relocate from distal renal tubules to vascular bundles, where subsequent infiltration of monocytes is seen [420, 479]. The same staining pattern has been observed for versican, although examination of leukocyte emigration was not performed in this study [465]. Interestingly, interstitial infiltration of L-selectin-positive cells has been seen in kidney biopsy sections from patients with immunoglobulin A (IgA) nephropathy [480], suggesting a role for L-selectin in pathogenesis of kidney disease in humans.

Heparan sulfates are commonly present on the luminal surface of ECs, where they are involved in chemokine presentation [481, 482]. Interestingly however it is unlikely that these heparan sulfate moieties mediate L-selectin binding. L-selectin has been shown to have a pH-dependent preference for its ligands, and whilst 6-sulfo-sLe^x binding occurs at the blood pH of 7.4, binding of HS and CS chains was observed at pH of 5.6 [483]. In line with this, L-selectin dependent rolling was seen at the pH range between 6.8 and 7.4 and no rolling was detected below pH 5.6 [483]. A very recent report found that in

acidic conditions, the carbohydrate binding domain of L-selectin becomes protonated and shares more bonds with sulfated GAG chains, which increases binding affinity [484]. Acidic pH is often found at sites of inflammation [485, 486] and perhaps it is an important factor in modulating L-selectin's affinity for its intra- versus- extravascular ligands.

1.8.4 Various L-selectin ligands on other cells

Apart from ECs and ECM components L-selectin can bind variety other cells. The best known non-vascular ligand for L-selectin is PSGL-1, which binds L-selectin through a sLe^x moiety and sulfated tyrosine residues within its protein backbone [62]. L-selectin/PSGL-1 interactions are responsible for secondary capture of leukocytes at sites of inflammation (**section 1.2.3**). Interestingly PSGL-1 has been discovered on the endothelium of microvessels induced in advanced atherosclerotic plaques, where it supports leukocyte infiltration [299]. This yet again points towards a role for L-selectin in atherosclerosis (**section 1.13.1**). Another cell surface leukocyte protein endoglycan has been reported to bind L-selectin [487]. Like podocalyxin and CD34, endoglycan is a member of the CD34 family and is also expressed on the vascular endothelium, smooth muscle cells and hematopoietic precursor populations [487]. Despite being a mucin, endoglycan shows similarities to PSGL-1 in that it binds L-selectin via sLe^x and sulfated tyrosine residues [487]. However, a relevant contribution of endoglycan to L-selectin-dependent recruitment has not yet been established. L-selectin has been shown to bind a variety of ligands on cancer cells (**table 1.2**) [352, 361, 488], suggesting a role for L-selectin in cancer metastasis. Indeed, it has been shown that L-selectin-dependent interactions of leukocytes at the sites of tumour cells embolization facilitate initiation of tumour cell extravasation [489]. MECA-79 reactive ligands for L-selectin have also been found on human endometrium during the window of implantation [490]. In agreement with this, a role for L-selectin in trophoblast implantation has been reported [491].

Taken together L-selectin has the ability to bind a variety of ligands, in both health and disease. This in turn opens up multiple possibilities for L-selectin-dependent therapies (**section 1.13.2**).

Localisation	*L-selectin ligand*	*Notes*	*Citation*
PLN HEV	• GlyCAM-1 • CD34 • Podocalyxin-likeprotein[1] • Sgp200 • Endomucin • Nepmucin[2] • MadCAM-1[3] (PNAd mucins (MECA-79 reactive) Bind L-selectin through 6-sulfo-sLe^x) • Unidentified[4]	[1]Belongs to CD43 family [2]Not expressed in PP HEV [3]Not expressed in PLN (Mesenteric LN only) [4]O-glycoprotease resistant (non-mucin)	[337, 427, 432-439, 441]
ECs at sites of inflammation	• MECA-79 reactive antigens[1] • E-selectin[2] • Unidentified, seen *in vivo* • Unidentified, induced on HUVEC by IL-4 • Sulfoglucuronosyl paragloboside (SGPG), induced on BMEC by IL-1β • Unidentified, induced by TNF-α on HCMEC[3], BKMGEC[4] and BAEC	[1]Expressed on HEV-like vessels induced in certain chronic inflammatory diseases: ulcerative colitis, Crohn's disease, asthma, diabetis, cutaneous inflammation and lymphoma, Grave's disease, rheumatoid arthritis [2]On human, but not mouse neutrophils [3]Sulfation but not sialylation required [4] Sialylated, *de novo* synthesised	[381, 410, 442, 447-453, 456-460]
ECM	• Versican (CS/DS PG)[1] • Biglycan(DSPG)[1] • Collagen VXIII(HSPG)[1] • Sulfatide (sulphated glycolipid)[2] • Lubricin (mucin-like glycoprotein)[1]	[1]Bind L-selectin through long sulfatated GAGs [2]Binds L-selectin via cluster of sialylated and sulphated sugars	[221, 354, 420, 461-466, 477, 479]
Various	• PSGL-1[1] • Endoglycan[1] • Podocalyxin-like protein (Non-MECA-79 reactive)[2] • MECA-79 reactive[3] • Carcinoembryonic antigen (CEA)[4] • CD44[5] and CD44v[6] • Human complement factor H • Nucleolin	[1]Binding through sLe^x and Tyr-SO_3 [2]On colon carcinoma cells [3]On human endometrium during the window of implantation [4]Expressed by CLS174T colon carcinoma cell line [5]Expressed by hematopoietic-progenitor cells [6]Various isoforms Isolated from CLS174T colon carcinoma	[62, 352, 361, 487, 488, 490, 492-494]

Table 1.2 L-selectin ligands. This is a current list of identified L-selectin ligands. This table shows known L-selectin ligands alongside the details about the location of their expression and ligand nature. Note that the list may not be exhaustive. For the abbreviations used see **Abbreviations section**.

1.9 REGULATION OF L-SELECTIN EXPRESSION

L-selectin levels on circulating leukocytes are fairly constant, however, under certain cell activating conditions, cell surface L-selectin is rapidly downregulated in a process known as “shedding” (**section 1.9.2**) [495, 496]. Additionally, upon T cell activation, L-selectin shedding is accompanied by modulations in L-selectin messenger RNA (mRNA) levels and stability [386, 497]. Certain T cell subsets (central memory T cells) subsequently upregulate surface L-selectin expression, which enables recirculation to PLN [387, 498]. Furthermore, human leukemic cells freshly isolated from patients were shown to sustain high L-selectin mRNA levels, which was associated with increased leukocyte infiltration into various organs [499]. Thus, L-selectin expression levels can be actively regulated both transcriptionally (**section 1.9.1**) and post-translationally (through shedding), and deviations in these balances are often seen in disease.

1.9.1 Transcriptional regulation of L-selectin expression

Human L-selectin from all leukocyte subsets is encoded by the *lam-1* gene (Chromosome 1) containing at least 10 exons that produce single L-selectin mRNA, and 9 of these exons are translated in to L-selectin protein [313]. Post-translational glycosylation accounts for differences in L-selectin MW seen between the leukocyte subsets [381, 402]. No reports exist about alternative L-selectin protein variants, however, three different L-selectin isoforms were discovered in mice (L-selectin-v1-3) [500]. Mouse L-selectin-v1-3 comprise only 3-5% of the total L-selectin protein [500], and it is currently unclear how these splice variants may affect L-selectin-dependent recruitment.

The positioning of the L-selectin gene promoter is located immediately upstream (-288/-1 bp) of the START codon, and can be activated by a number of transcription factors (TFs), e.g. Krupper-like factor 2(Klf2), Forkhead box protein O1 (FOXO-1), E-twenty six (Ets1), myeloid zinc finger 1 (Mzf1), specificity protein 1 (Sp1), and to a lesser extent, interferon regulatory TF (Irf1) [501-504]. It has been shown that FOXO-1 and another TF – Elf4 (Ets-related transcription factor) – regulate the expression of Klf2 [505-507]. Therefore, FOXO-1 appears to regulate L-selectin expression by at least two mechanisms: by activating Klf2 and by directly binding to the FOXO-1 motif identified within the L-selectin promoter region [503]. Deficiency in FOXO-1, Klf2 or Elf1 result in decreased L-selectin expression, reduced lymphocyte homing to PLNs and increased T cell accumulation in non-lymphoid tissues [504-510]. In line with this, Klf2 over-expression leads to increased L-selectin expression and augments lymphocyte recruitment to PLN [501]. It has been shown that upon T cell receptor (TCR) ligation, Klf2 mRNA levels are reduced, which results in decreased L-selectin gene transcription [511].

Klf2 expression was shown to be downregulated by the phosphatidylinositol-3-OH kinase (PI(3)K) that mediated its effects through the mammalian target of Rapamycin (mTOR) [511]. This signalling pathway is not active in naïve T cells and thus L-selectin transcription is maintained on T cells that home to PLN and becomes quenched in activated T cells [511]. Interestingly, another TF, Forkhead Box M1 (FOXM-1) was recently shown to control L-selectin levels on monocytes but not neutrophils [512]. FOXM-1 deficient mice showed impaired accumulation of monocytes during acute liver injury [512], implying a role for this TF in the L-selectin-dependent monocyte homing to sites of inflammation. Hence, it seems that transcriptional regulation of L-selectin expression depends on both leukocyte subset and the cell activation status. Interestingly, genetic variations in the proximal 5´ flanking region of the L-selectin promoter have been identified in Chinese and Japanese populations, and have been proposed to be the risk factors for Grave's autoimmune disease and the immunoglobulin A nephropathy [480, 513]. One of the variations (–642A>G substitution) was subsequently shown to impair the transcription efficiency of the L-selectin gene [514].

1.9.2 Regulation of L-selectin expression by proteolytic cleavage (shedding)

Endoproteolytic cleavage of L-selectin, termed "shedding", occurs at an extracellular site proximal to the cell membrane (**figure 1.7**) and results in the formation of a 68 kDa soluble form of L-selectin (sL-selectin) and retention of a 6 kDa transmembrane fragment (and will be referred to interchangably as "stump") [326, 515]. The proteolytic activity is membrane-associated [516, 517] and can be inhibited by hydroxamic acid-based metalloprotease inhibitors, which are often employed to study L-selectin shedding [313, 517-520]. Upon cell activation, L-selectin is cleaved between lysine-283 and serine-284 by A Disintegrin and Metalproteinase 17 (ADAM17) (also known as TNF-α converting enzyme, TACE) [326, 521-523]. Additionally, ADAM8 and ADAM10 have been reported to have the ability to shed L-selectin [524, 525]. ADAM10 is most closely related to ADAM17 [526], and *in vitro* studies showed that it can be activated to cleave L-selectin, when ADAM17 is chronically absent [525]. Notably, emigrated ADAM17 null neutrophils were shown to be able to shed their L-selectin in the model of murine peritonitis [527]. It is possible that this was due to ADAM8 activity, as ADAM8 has been shown to be upregulated on human neutrophils upon adhesion to ECs [524]. Additionally, ADAM8 has also been implicated in L-selectin cleavage during chronic inflammatory disease, i.e. rheumatoid arthritis [524]. Interestingly, neither point mutations nor mutations of multiple conserved amino acids within the cleavage site were found to affect L-selectin shedding [522, 528]. However, deletions of several amino acids within the L-selectin cleavage domain – which brought the cleavage site closer to the plasma membrane – abolished L-selectin shedding [323, 522, 528]. Therefore, metalloproteases that cleave L-selectin

seem to target a “relaxed” sequence specificity, but are more sensitive to the physical distance of the cleavage site from the plasma membrane, and possibly other structural features of the cleavage site.

L-selectin is shed upon stimulation with various cell activating factors, e.g. phorbol 12-myristate 13-acetate (PMA), N-formyl-methionyl-leucyl-phenylalanine (fMLP), thrombin, IgE receptor agonists, a peptide component of complement activation (C5a), IL-8, lipopolysaccharide (LPS), TNF-α, PAF, H_2O_2, phosphatase inhibitors, as a result of mechanical force imposed during rolling, upon B- or T cell receptor (BCR and TCR, respectively) engagement, or upon ectodomain cross-linking [419, 421, 495, 496, 529-538]. Protein kinase C (PKC) and various mitogen activated protein kinases (MAPK) have been implicated in mediating L-selectin shedding [495, 496, 511, 531, 539-541]. The interaction between PKC, L-selectin, and contribution of sequences within the tail to shedding are discussed in more detail in **section 1.10.2**.

The shed extracellular domain of L-selectin remains functionally active and can prevent leukocyte attachment to ECs *in vitro* [542] and in vivo [543], possibly acting like an “adhesion buffer” limiting excess leukocyte recruitment at sites of inflammation. In addition to cell-activation induced shedding, L-selectin is constitutively cleaved from the cell surface, which is known as “basal shedding” [521, 544]. The plasma of healthy humans contains 1.6±0.8 μg/mL of sL-selectin [542, 545], and such high concentration suggests that basal shedding is a physiologically relevant process. In keeping with this, plasma sL-selectin levels are affected in certain inflammatory diseases, e.g. elevated sL-selectin is seen in patients with SLE [546, 547] or type I diabetes [548], and low levels were observed in patients suffering from adult respiratory distress syndrome (ARDS) [549]. Not much is currently known about basal shedding. It is dependent on metalloprotease activity and utilizes the same cleavage site as the activation-induced shedding, however the exact metalloprotease has not been identified [521, 544]. ADAM17 null mice have been reported to produce sL-selectin and “stump”, implying that other than ADAM17 metalloprotease mediates basal shedding [521, 544]. At the same time, increased surface levels of L-selectin were seen on neutrophils from ADAM17 null mice, suggesting that this enzyme does control L-selectin surface density under resting conditions [521, 527]. It is possible that two mechanisms of basal L-selectin turnover exist, one that is independent and the other that is dependent on ADAM17. The first one controls homeostatic sL-selectin plasma levels and the latter controls L-selectin surface density. Interestingly, in 1996 it was shown that a protease-independent mechanism of L-selectin shedding could also occur [529]. Seven years later, generation of mice expressing sheddase-resistant mutant of L-selectin showed that very low (<5% of wild type) sL-selectin levels were present in plasma of these mice, suggesting that the protease-independent mechanism could contribute to basal L-selectin shedding [22]. Of

note, L-selectin shedding during neutrophil apoptosis has been shown to be dependent and independent on ADAM17 at early and later stages, respectively [550].

Although the physiological significance of L-selectin shedding is not entirely understood, a few definite and putative roles have been identified. As mentioned above, shedding maintains physiological sL-selectin levels in plasma. Several studies using hydroxamic acid-based metalloprotease inhibitors or mice expressing sheddase-resistant L-selectin suggested a role of shedding at various stages of the leukocyte adhesion cascade. Some reports implicate shedding as a mechanism limiting leukocyte rolling at sites of inflammation [519, 551, 552], however others find no influence of L-selectin cleavage on leukocyte rolling velocity or flux [419, 520]. Shedding was found to play an important role during T cell recirculation to PLN. It has been shown that during TEM across PLN HEV naïve T cells downregulate their surface L-selectin to 30% of the blood levels, and then re-express the protein upon the exit [553]. In line with this, blocking L-selectin shedding results in reduced TEM of naïve T cells across HEV [22, 518]. Furthermore, L-selectin shedding occurs in activated T lymphocytes and this prevents them from re-entering the PLNs [22, 419]. Shedding is also thought to occur during TEM at sites of inflammation as surface levels of L-selectin on emigrated leukocytes are low compared to “resting” levels seen on cells in the circulation or in culture [520, 554-556]. However, the exact timing or spatial distribution of L-selectin shedding on transmigrating leukocytes has not been investigated so far. Interestingly, L-selectin shedding has also been proposed to be important in leukocyte migration beyond vessel walls and possibly controls chemotaxis *in vivo* (**section 1.7.5.1.2**) [419]. Finally, it is likely that L-selectin shedding is regulated differently depending on the leukocyte subset. ADAM17 null mice showed increased adhesion and early emigration of neutrophils but not monocytes at sites of inflammation [527]. Additionally, ADAM17 null neutrophils did, and monocytes did not shed their L-selectin upon emigration in the thioglycollate-induced peritonitis mouse model of inflammation [527].

1.10 THE CYTOPLASMIC TAIL OF L-SELECTIN

The cytoplasmic tail of L-selectin is only 17 amino acid-long, however it is known to interact with a number of cytoplasmic proteins. These interactions are important for L-selectin function, sub-cellular distribution and signalling [90, 496, 515, 557-561]. The main players involved in the interactions at the tail of L-selectin are the actin binding proteins α-actinin and the ERM proteins, ezrin and moesin, as well as the calcium-sensing protein calmodulin. Another important feature of the L-selectin tail are the two serine residues, of which phosphorylation is likely to regulate L-selectin shedding amongst other aspects of L-selectin [495, 496]. **Figure 1.10** shows a schematic summary of the interactions between the L-selectin tail and its main cytosolic binding partners, and

these interactions are described in more detail in the following sections. Of note, L-selectin has also been shown to bind the p56^{Lck} kinase, SOS/Grb2 [245], c-Abl [562] and high mobility group 1 (HMG1) [563]. No information is currently available about the functional implications of L-selectin interaction with HMG1. The involvement of p56^{Lck} and c-Abl is described in the subsequent sections with respect to signalling downstream of the L-selectin tail (**section 1.11.4**).

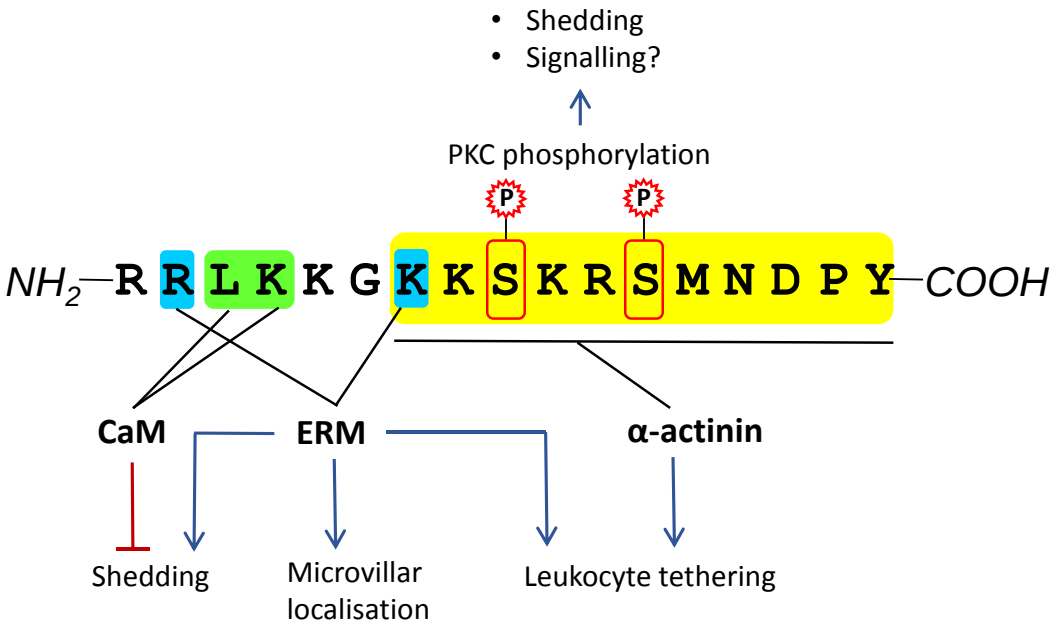

Figure 1.10 The cytoplasmic tail of L-selectin. The short, 17 amino acid cytoplasmic tail of L-selectin interacts simultaneously with CaM (L358 and K359), ERM proteins (R357 and K362) and α-actinin (K363 to Y372). Phosphorylation of the L-selectin tail occurs at S364 and S367. The outcomes of each of the interaction as well as the results of the phosphorylation are depicted on the diagram and discussed in the text. For abbreviations used see **Abbreviations section**. Image adapted from Ivetic and Ridley, *Biochem. Soc. Trans*., 2004 [564].

1.10.1 Interaction with α-actinin

The first molecule identified to bind to the cytoplasmic tail of L-selectin was the cytoplasmic actin-binding protein α-actinin [565]. L-selectin/α-actinin interaction was shown through a solid-phase binding assay and co-immunoprecipitation studies in L-selectin transfectants and Jurkat T lymphocytes [565, 566]. Interaction with α-actinin is mediated by the 11 amino acid COOH-terminal domain of the L-selectin tail [565] (**figure 1.10**). Deletion of this sequence was earlier reported to abolish *in vitro* binding of lymphocytes to HEV in frozen LN sections as well as *in vivo* rolling of leukocytes in exteriorized rat mesenteric venules [557]. Therefore, α-actinin-mediated linkage of L-selectin to the actin cytoskeleton is critical for the L-selectin-dependent adhesion of leukocytes to the endothelium. On the other hand, L-selectin lacking the 11 terminal amino acids correctly localised to microvilli, suggesting that α-actinin is not important for

L-selectin microvillar positioning [565]. Two other cytoskeletal proteins, vinculin and talin, are also thought to associate with the L-selectin/α-actinin complex [565].

1.10.2 Cytoplasmic serine residues and interaction with PKC isoforms

Two serine residues at position 364 (S364) and 367 (S367) of L-selectin have been shown to be important for ectodomain shedding (**figure 1.10**). Phosphorylation of S364 and S367 within the L-selectin cytoplasmic tail mediates PKC-dependent shedding in response to PMA, IL-8, thrombin, IgE agonists, C5a, PAF and fMLP [495]. In line with this, mutation of S364 or S367 into non-phosphorylatable alanines desensitizes L-selectin to PKC-dependent shedding, and mutation of S367 into a phospho-mimicking aspartate sensitizes shedding [534]. Strangely, mutation of S364 into aspartate was found to reduce rather that promote shedding [496]. It is possible that this substitution is not a successful phosphomimic or perhaps a complex relationship between the two serines exist, where S364 needs not to be phosphorylated to drive S367 phosphorylation and shedding. Studies by Kilian et al. (2004) showed that PKC isozymes θ and ι transiently interact with the cytoplasmic tail of L-selectin and are involved in the phosphorylation of S364 and S367, with a preference to the former [567]. Once phosphorylated, the cytoplasmic domain of L-selectin increases binding of PKCθ and promotes binding of PKCα [567]. This suggests that serine phosphorylation and L-selectin shedding could promote formation of a signalling complex at the tail of L-selectin. However, it is currently unknown which event occurs first, serine phosphorylation or shedding, and it is possible that the PKC isoforms could bind the L-selectin “stump”. Shedding is linked to the disassociation of calmodulin (CaM, **section 1.10.4**) from the L-selectin tail, and CaM does not co-immunoprecipitate with the “stump” [559]. Perhaps a change-over of binding partners – from CaM to PKC isoenzymes – is involved in signalling downstream of L-selectin tail upon PKC-mediated shedding. In support of this theory, L-selectin is a well-known signalling molecule and phosphorylation of its single cytoplasmic tyrosine residue has been associated with intracellular signalling events (**section 1.11.4**). On the other hand, shedding induced by the phosphatase inhibitors (cantharidin and calyculin A, the PP2A-type phosphatase inhibitors) is independent of both PKC and phosphorylation of the L-selectin serine residues, but is driven by p38 MAPK, phosphorylation of ADAM17 cytoplasmic tail and upregulation of surface ADAM17 levels [496]. Further differences between PKC- and p38 MAPK-dependent shedding is demonstrated by the fact that the PKC-mediated shedding requires interaction of the L-selectin tail with the ERM proteins, whereas p38 MAPK-mediated shedding occurs independently of the ERMs (**section 1.10.3**) [496]. In conclusion, protease-sensitive site-dependent L-selectin shedding can be regulated by PKC, ERM

and modulation of L-selectin cytoplasmic tail, or by p38 MAPK and regulation of ADAM17 phosphorylation and surface expression.

1.10.3 Interaction with the exrin/radixin/moesin (ERM) family members

The family of ERM proteins consists of three members, exrin, radixin and moesin, which have an approximate MW of 75-82 kDa. Inactive ERM proteins reside in the cytosol in an auto-inhibited conformation, where N- and C-termini interact with each other [568]. Upon activation, the ERM proteins switch into an extended form, where the N-terminal FERM (band Four point one Ezrin Radixin Moesin) domain binds the integral transmembrane proteins and the C-terminal domain binds F-actin [569, 570]. Thus, the active ERM proteins serve to link the transmembrane proteins to the actin cytoskeleton. Apart from their structural purpose, the ERM proteins can modulate leukocyte function, and especially motility, by acting both upstream and downstream of the Rho GTPases [571]. In murine lymphocytes, the cytoplasmic tail of L-selectin was shown to bind ezrin and moesin as radixin expression is absent in leukocytes [563]. L-selectin arginine-357 (R357) and lysine-362 (K362) were shown to contribute to binding ERM (R357 having a predominant role), and both are located within a 6 amino acid, membrane proximal cytoplasmic tail domain [558] (**figure 1.10**). Cell lines expressing alanine swap mutations of L-selectin at positions R357 or K362, which abrogate ERM binding, showed impaired microvillar positioning, reduced PMA-induced shedding, as well as decreased tethering efficiency [496, 558]. Interestingly, L-selectin/ERM interaction was shown to be dispensable for the phosphatase inhibitor-mediated shedding [496]. Thus, L-selectin/ERM interaction is important for PKC-mediated shedding and localisation of L-selectin to leukocyte microvilli, which in turn is likely to positively influence tethering. Both R357 and K362 are juxtaposed to L358 and K359, which are amino acid residues responsible for calmodulin (CaM) binding (**section 1.10.4**) [559]. A detailed study by Killock et al. (2009), involving molecular modelling*, in vitro* binding assays and *in vivo* protein-protein interaction studies showed that, despite close proximity of their putative binding sites, CaM and ERM interact with the L-selectin tail in a non-competitive way [572]. Moreover, the same report predicted that ERM, L-selectin and CaM can form a 1:1:1 ternary complex in resting leukocytes, which was confirmed by other recent studies (see **section 1.10.4** below) [573, 574]. Additionally, it has been proposed that CaM and ERM derived from adjacent L-selectin molecules interact in *cis* upon L-selectin clustering, which is likely to promote intracellular signalling, possibly involving Rap1A mobilisation via Ras/SOS pathway [496]. Signalling triggered by ligation of L-selectin domain is discussed in more detail in **section 1.11** of this thesis.

1.10.4 Interaction with calmodulin (CaM)

Calmodulin (CaM) is an ubiquitous 17 kDa calcium regulatory protein that associates with the tail of L-selectin in resting transfected cell lines and primary leukocytes [515, 559, 572]. The amino acid residues in the L-selectin cytoplasmic tail that contribute to interaction with CaM are leucine-358 (L358) and lysine-359 (K359) (**figure 1.10**) [515, 559]. Inhibition of CaM promotes protease-dependent shedding of the L-selectin ectodomain (**section 1.9.2**) in human neutrophils, and significantly reduces adhesion of pre-B lymphocytic cells to HEV as well as their rolling on MECA-79 antigen [515]. Direct proof for the involvement of CaM in the ectodomain shedding was provided by Matala et al. (2001) who showed, through L-selectin tail mutational analysis, that disassociation of CaM from L-selectin increases shedding [559]. Through biophysical studies it has been suggested that CaM binds L-selectin via interaction with both its cytoplasmic tail and the transmembrane domain (TMD) [575]. A mechanism was proposed, whereby CaM, in a compact conformation, wraps around L-selectin tail and reaches into the TMD [575]. This in turn pulls the L-selectin molecule down, thereby burying the extracellular cleavage site in the plasma membrane [575] (**figure 1.11 A**). However, it is hard to envisage the hydrophilic amino acids of the L-selectin membrane proximal cleavage site being inserted in to the hydrophobic plasma membrane. Interestingly, recent studies using CLS (C-terminal portion of human L-selectin, comprising the entire tail and TMD) reconstituted in liposomes showed that CaM assumes an extended conformation when binding to the L-selectin tail, where only single lobe of CaM is involved in this interaction [574, 576] (**figure 1.11 B**). When the liposomes contain negatively charged lipids (i.e. phosphatidylserine, PS) that mimic the inner leaflet of the plasma membrane, this interaction is abolished [576]. This is because the basic-rich L-selectin tail interacts with the anionic lipid bilayer instead [576] (**figure 1.11 C**). Most interestingly, the FERM domain of moesin was shown to desorb the L-selectin tail from the anionic membrane surface and facilitate L-selectin/CaM interaction [573] (**figure 1.11 D**). These results are in agreement with a ternary model of L-selectin/CaM/ERM binding proposed earlier by Killock et al. (2009) [572], and suggest that plasma membrane environment is crucial for the interaction of L-selectin with its cytosolic binding partners.

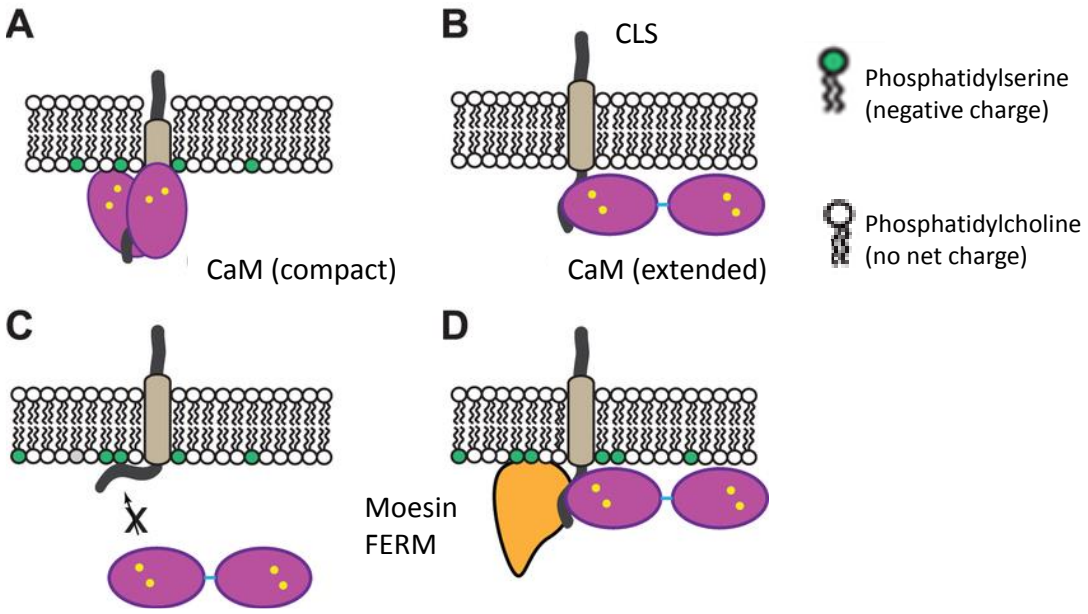

Figure 1.11 Models of association between L-selectin and calmodulin. Schematic illustration of L-selectin/CaM interaction modes that have been proposed most recently. **A)** CaM has a compact conformation and wraps around L-selectin tail and TMD, pulling the L-selectin molecule down, thereby burying the extracellular cleavage site in the plasma membrane. **B)** CaM has an extended conformation, where only one lobe interacts with the L-selectin tail (in neutral charge liposome environment). **C)** In the presence of PS, L-selectin tail has a preference for the inner leaflet of the plasma membrane and does not bind CaM. **D)** FERM domain of moesin desorbs the L-selectin tail from the negatively charged membrane and facilitates CaM binding. This leads to the formation of a ternary L-selectin/ERM/CaM complex. For abbreviations used see the **Abbreviations section**. Image adapted from Deng et al. , *PLoS One*, 2013 [574].

Since in many proteins phosphorylation of critical serine residues can abolish CaM binding [577, 578], it was proposed that serine phosphorylation of L-selectin would disrupt L-selectin/CaM interaction, leading to L-selectin shedding [515]. As described earlier, the cytoplasmic tail of L-selectin was found to associate with protein kinase C (PKC) isoforms [567], and serine phosphorylation shown to be involved in the PKC-mediated shedding of L-selectin [495, 496]. It is thus plausible that upon cell activation sequential changes in binding of CaM, ERM and PKC isoforms as well as modulation of the plasma membrane composition regulate L-selectin phosphorylation and shedding.

1.11 L-SELECTIN OUTSIDE-IN SIGNALLING

Outside-in signalling downstream of L-selectin has been studied through ligation of the ectodomain with various compounds, from primary anti-L-selectin mAb, through primary mAbs followed by secondary antibodies (cross-linking) to physiological and synthetic L-selectin ligands. Various cellular responses resulting from L-selectin ectodomain ligation are summarised in **table 1.3**, and are discussed in more detail in the sections below.

1.11.1 Changes in lateral mobility of L-selectin in the plasma membrane

Through the generation of CLS L-selectin it has been shown that L-selectin is monomeric in the dodecylphosphocholine detergent micelles [579]. In other words, in resting state the cytoplasmic and transmembrane domains of L-selectin do not have the ability to self-assemble, and no spontaneous oligomerisation can occur [579]. This finding has been confirmed in a very recent report, where the micropipette adhesion frequency assay was used to show that L-selectin is monomeric in the neutrophil membrane [580]. In contrast, PSGL-1 and P-selectin, two other CAMs actively mediating leukocyte recruitment, have been shown to exist in plasma membranes as homodimers [581, 582]. Expression of transgenic PSGL-1 and P-selectin that existed as monomers resulted in destabilised neutrophil rolling [583], suggesting that receptor oligomerisation is a functionally important process for successful leukocyte recruitment. Interestingly, dimerization of L-selectin molecules by labelling with mAb (LAM1-118, non-function blocking antibody) increased L-selectin's avidity for its ligands and enhanced tether formation under flow [584]. Similarly, chemically induced dimerization (CID), where two adjacent L-selectin molecules are artificially brought together without ectodomain engagement, resulted in enhanced ligand binding as well as increased rolling flux and decreased rolling velocity of 300.19 cells on transformed HUVEC that expressed L-selectin ligands [585]. This implies that upon stimulation, adjacent monomeric L-selectin molecules do come together, which leads to signal propagation and results in the cellular responses. An obvious stimulus that could elicit L-selectin oligomerisation (hereafter referred to as "clustering") would be the engagement of ectodomain that could physically bring the adjacent molecules together. Indeed, L-selectin "patching" (a distinct strong immunofluorescence signal belonging to the fluorescently-conjugated secondary antibody used for cross-linking) has been observed upon L-selectin cross-linking or binding of E-selectin-IgG chimera [87, 91, 586]. In these experiments L-selectin clustering coincided with upregulation of and adhesion through Mac-1 (for L-selectin mediated integrin-dependent adhesion see **section 1.11.2**). In U937 monocytic cells triple-expressing L-selectin, ezrin-GFP and CaM-mCherry, labelling of L-selectin with mAb has been shown to induce CaM/ERM interaction in *cis* (as measured by FRET between ezrin-GFP and CaM-mCherry), which was potentiated after cross-linking with secondary antibody [572]. This suggests that a degree of L-selectin clustering regulates the lateral mobility of its cytosolic binding partners and could lead to the assembly of signalling platforms associated with two adjacent L-selectin tails [572]. Additionally, L-selectin cross-linking, sequential stimulation of L-selectin with two mAb or ligation of L-selectin ectodomain with GlyCAM-1 has been shown to redistribute L-selectin into cholesterol-rich detergent resistant membranes (DRM) [560, 587]. Movement to DRM

was dependent on the 11 terminal amino acids of L-selectin tail, as mutant L-selectin lacking this sequence failed to translocate to DRM [560]. Cholesterol-rich membrane microdomains, termed lipid rafts, are known to mediate immune cell signalling [382, 588], and hence it is plausible that upon ligand binding L-selectin clusters and translocates to DRMs, where it can interact with its signling partners.

1.11.2 Activation and upregulation of the integrins

As described in **sections 1.2.4** and **1.7.5.1.1** outside-in signalling triggered by L-selectin ectodomain ligation is vital for the arrest of the rolling leukocytes. Antibody-mediated cross-linking of L-selectin, ligation with GlyCAM-1 or E-selectin-IgG chimera result in leukocyte adhesion through β1 and β2 integrins [86, 88, 589, 590]. Interestingly, binding of soluble fibronectin – which is a β1 integrin dependant process – occurred in naïve, but not memory, T cells upon ligation with fucoidan (a known polyvalent mimic of natural occurring L-selectin ligands, it is found in brown sea weed) [88]. Similarly, L-selectin cross-linking or GlyCAM-1 binding led to increased adhesion through or activation of β2 integrins, respectively, that occurred in naïve but not memory T cells [86]. This suggests that L-selectin on certain lymphocyte subsets might transduce signalling in a functionally different manner to promote adhesion. Stimulation with primary antibodies was shown to increase activity, as measured by the expression levels of active epitopes, of β1 and β2 integrins on neutrophil surface in the absence of increased integrin expression [591]. However, upregulation of Mac-1 (CD11bCD18) integrin levels on neutrophils are seen upon L-selectin cross-linking as well as upon simultaneous stimulation of L-selectin with two primary antibodies [87, 89, 91]. Perhaps L-selectin-mediated regulation of integrin-dependent adhesion is governed by the magnitude of clustering, where initial engagement (i.e. elicited by single primary antibodies) causes activation of cell surface integrins, and further clustering (i.e. cross-linking or stimulation with two antibodies at once) leads to expression of new integrin molecules on the cell surface. As far as the signalling pathways are concerned, it has been reported that L-selectin-dependent adhesion through Mac-1 is a result of p38 and p42/44 MAPK (ERK1/2) phosphorylation [413, 589]. Interestingly, phosphorylation of p38 MAPK was seen as soon as 1 minute upon cross-linking, it then dropped at 2 minutes and then rose again at 3-5 minutes upon L-selectin cross-linking [589]. Phosphorylation of ERK1/2 had delayed kinetics with phosphorylation peaking at 3-5 minutes, suggesting that p38 MAPK might be the primary kinase responsible for L-selectin mediated Mac-1-dependent adhesion [589]. In fact, inhibition of p38 MAPK completely abolished L-selectin-dependent neutrophil adhesion to the albumin-coated latex beads (ACLB, used to test for Mac-1 dependent adhesiveness) [589]. However, the influence of ERK1/2 inhibitor on ACLB binding was not tested in this study [589], and hence the relative ERK1/2 contribution to Mac-1-

dependent L-selectin-mediated adhesion in this system is not known. Another report has shown that inhibition of ERK1/2 blocks 80% of β2 integrin upregulation induced by L-selectin cross-linking, highlighting the importance of this kinase [91]. Whether L-selectin signals to the integrins through co-clustering in specific membrane domains is currently unclear. Co-localisation of L-selectin and CD18 integrin has been reported upon L-selectin cross-linking [87], however, such an event might be ligand-specific, as no co-localisation was found after L-selectin/E-selectin-IgG binding [413].

1.11.3 Regulation of chemokine receptor expression and chemotaxis

L-selectin cross-linking or ligation with sulfatides or fucoidan have been shown to upregulate CXCR4 receptor on the surface of human peripheral blood lymphocytes (PBL), granulocytes and monocytes, murine T cells and K562 myeloid cell line transfected with L-selectin [85, 90]. Notably, sulfatide-triggered CXCR4 upregulation occurred in CD4+, but not CD8+ T cells or B cells [90], suggesting that L-selectin signalling might be specific to leukocyte subtype. Enhanced surface CXCR4 expression was a result of pre-formed intracellular stores mobilisation, as verified by flow cytometry and measurement of total protein content in permeabilized cells [85]. Furthermore, L-selectin dependent CXCR4 upregulation was selective and specific, as no enhanced expression of other CCR receptors, CCR5 and CCR7, was seen upon ligation with fucoidan or sulfatides [85]. L-selectin cytoplasmic tail was found to be important for signal transduction leading to CXCR4 expression, as K562 cells expressing truncated L-selectin mutant (lacking 16 of total 17 cytoplasmic amino-acids) failed to upregulate the receptor as seen with L-selectin null cells [90]. Additionally, L-selectin-induced CXCR4 upregulation was shown to be dependent on tyrosine phosphorylation, as pre-treatment of T cells with tyrosine kinase inhibitors prior to sulfatide stimulation resulted in decreased receptor expression [90]. Kinase shown to play a predominant role in CXCR4 upregulation were shown to be the Src family kinases [90], and activation of Src kinases downstream of L-selectin has been repeatedly reported (**section 1.11.4**).

CXCR4 is a receptor for stromal-derived factor 1 (SDF-1), a potent leukocyte chemoattractant and this receptor/ligand pair is known to be crucial for lymphocyte homing as well as recruitment to the inflammatory sites [592-595]. It is interesting that in addition to induction of CXCR4 surface expression, L-selectin ligation selectively inhibited CXCR4 internalisation induced by SDF-1, and this persistent CXCR4 expression resulted in enhanced F-actin polymerisation [85]. CXCR4/SDF-1 binding leads to firm adhesion of rolling leukocytes [59, 80], which is in keeping with a role for L-selectin inside the vasculature during the transition from leukocyte rolling to arrest (**sections 1.2.4** and **1.5.7.1.1**). It therefore makes sense that stimulation via L-selectin was shown to enhance SDF-1 induced adhesion to HUVEC monolayers [85]. However,

it has to be noted that CXCR4 upregulation occurred two [90] or even ten [85] minutes after stimulation with ligands, and leukocytes arrest in seconds *in vivo*. This suggests that L-selectin-dependent CXCR4 signalling might be required in the later stages of the recruitment, i.e. TEM or chemotaxis. Indeed, L-selectin cross-linking or sulfatide binding has been shown to enhance PBL migration towards SDF-1 across both naked filters and HUVEC monolayers [85, 90]. L-selectin has been also shown to mediate leukocyte chemotaxis *in vivo* (see **section 1.7.5.1.2**). Interestingly, when primary mAb alone (no cross-linking) was used to cluster L-selectin, slightly decreased chemotaxis towards SDF-1 was observed as compared to baseline [85]. This suggests that the magnitude of L-selectin clustering is an important factor affecting signalling downstream of the L-selectin tail. Furthermore, L-selectin ligation with mAb or EC-expressed ligand enhanced mouse T and B chemotaxis towards SLC [415]. This was not associated with CCR7 (SLC receptor) upregulation, but was strongly dependent on L-selectin expression levels and was mediated by PKC, MAPK, and Syk family kinases [415]. This suggests that L-selectin-mediated chemotaxis occurs through more than one signalling pathway, dependent on the ligand, magnitude of L-selectin clustering and the type of chemokine involved.

1.11.4 Activation of protein kinases, Rho GTPases, and production of secondary messengers

Protein phosphorylation is a reversible post-translational modification of proteins that occurs through phosphate group addition by a protein kinase. The human genome contains 518 putative protein kinase genes, and kinases mediate majority of cellular signalling in eukaryotic cells by altering the activity of their substrates [596]. Mitogen-activated protein kinases (MAPK) are serine-threonine protein kinases that become activated by various stimuli, and the best studied MAPKs are the p38 MAPK, extracellular signal-regulated kinases (ERK) and c-Jun N-terminal kinase (JNK) [597, 598]. Another well-known kinases are the Src family kinases (SFK) [599] and the c-Abl (Abelson murine leukemia viral oncogene homolog-1) kinases [600] that phosphorylate tyrosine residues within proteins.

Active MAPK is itself tyrosine phosphorylated, and such phosphorylation was seen in human neutrophils, PBL and Jurkat T cells upon stimulation of L-selectin with sulfatides, fucoidan, sLe^x, E-selectin-IgG chimera, mAb or Fab fragments or after L-selectin cross-linking [88, 245, 413, 589, 601]. Additionally, some of these studies found that ectodomain ligation resulted in tyrosine phosphorylation of L-selectin itself [88, 245]. Interestingly, MAP kinases (p38 and ERK) have been shown to mediate L-selectin shedding [511, 531, 539-541]. In the light of the fact that L-selectin ligation leads to MAPK activation, it can be speculated that engagement of the L-selectin ectodomain regulates

its own shedding through a signalling pathway involving MAPK. In support of this theory, multiple studies have shown that L-selectin cross-linking induces shedding [529, 533-536]. Both MAPK and L-selectin tyrosine phosphorylation is dependent on $p56^{lck}$, which is a member of the Src family kinases [88, 245, 598]. The involvement of MAPK, Src and other kinases in L-selectin-mediated integrin-dependent adhesion and chemokine receptor expression and chemotaxis were discussed in more detail in **sections 1.11.2** and **1.11.3** of this thesis, respectively. The kinase $p56^{lck}$ has been found to become activated (tyrosine phosphorylated) upon L-selectin stimulation in Jurkat T cells [245, 602], and has been shown to directly associate with L-selectin tail upon stimulation with sulfatides, where it forms a signalling complex involving c-Abl and ZAP-70 kinases [602]. It has also been shown that $p56^{lck}$-dependent tyrosine phosphorylation of L-selectin tail upon mAb binding was associated with formation of L-selectin/Grb2/SOS complex and activation of Rac2 activity via Ras in Jurkat T cells [245]. That the two groups found different $p56^{lck}$-dependent signalling complexes associated with L-selectin tail suggests either that the signalling pathways downstream of L-selectin tail are ligand-dependent (i.e. mAb versus sulfatides), or that ligation can activate multiple signalling pathways simultaneously. Furthermore, $p56^{lck}$-dependent Ras activation was also found after L-selectin ligation with sLe^x or fucoidan [88, 245, 246], and L-selectin-mediated activation of Ras and Rac2 results in actin polymerisation [246]. In Jurkat T lymphocytes, L-selectin clustering with mAb or fucoidan leads to marked increase in the activity of another protein kinase – JNK – and this is dependent on $p56^{lck}$ and Rac1 [603]. Upregulation of Rac1 activity upon L-selectin/fucoidan ligation was independently shown in another report, where active Rac1 was seen as soon as 1 minute after binding [566].

Oxidative burst (superoxide, O_2^-, synthesis) or potentiation of TNF-α- or fMLP-induced oxidative burst was shown following cross-linking of L-selectin [89, 604] or upon mAb binding [245]. Superoxide is not the only secondary messenger produced upon ligation of L-selectin ectodomain. Increase in “calcium flux”, a transient increase in free cytosolic Ca2+, which is known to elicit various cellular responses has also been reported. Specifically, L-selectin cross-linking has been shown to induce calcium flux in human primary neutrophils [89, 601, 604], however, binding of sulfatides also lead to transient increase in free Ca2+ in murine CD4+ T cells [90]. Both O_2^- synthesis and calcium flux required activation of tyrosine kinases or MAPK [245, 601], which is in agreement with the above-described L-selectin-mediated signalling pathways. However, a distinct tyrosine/MAP kinase-independent signalling pathway has also been shown to be triggered downstream of L-selectin. Cross-linking of L-selectin has been observed to activate neutral sphingomyelinase in Jurkat T cells, which resulted in hydrolysis of cellular sphingomyelin and in release of ceramide [605]. Ceramide is a known secondary messenger regulating various cellular functions, including inflammatory responses [606,

607]. This demonstrates that signalling downstream of L-selectin is a complex process that branches out into multiple signalling pathways both dependent and independent on tyrosine kinase or MAPK activity.

In addition to the effects L-selectin outside-in signalling has on the leukocytes on which it is expressed, signalling through L-selectin might be involved in mediating the inflammatory response in a much broader manner. Induced expression of mRNA for IL-8 and TNF-α has been seen in human neutrophils upon sulfatide binding [88], and an increase in c-Abl-dependent expression of macrophage colony stimulating factor (M-CSF)-1 was observed upon stimulation of L-selectin with mAb in Jurkat T cells and neutrophils [608]. It is thus plausible that secretion of these cytokines could augment the inflammatory response via the autocrine and paracrine signalling to the secreting and adjacent cells, respectively.

Ligand	*Cell type*	*Consequence of binding*	*Notes*	*Citation*
X-linking	Human neutrophils, PBL, Jurkat T lymphocytes, 300.19 pre-B cells, U937 monocytic cell line	• Patching • Redistribution of L-selectin to DRM that was dependent on L-selectin tail • Calcium flux, oxidative burst (O_2- generation), potentiation of oxidative burst caused by fMLP and TNF-α , • Increased adhesion through β2 integrins[1] • Co-localisation with active CD18 • Upregulation of Mac-1, adhesion via MAC-1 that was dependant on MAPK phosphorylation[2] • Potentiation of IL-8 or PAF induced Mac-1 dependant adhesion • Potentiation of SDF-1-induced adhesion to HUVEC • Increased transmigration through cytokine stimulated HUVEC, and towards SDF-1 • Activation of neutral sphingomyelinase resulting in consumption of sphingomyelin and production of ceramide • Upregulation of CXCR4 • CaM/ERM interaction in *cis* • L-selectin shedding	[1]Occured in neutrophils and naïve, but not memory T cells [2]Phosphorylation of p38 increased at 1 minute and 3 minutes, phosphorylation of p42/44 MAPK increased at 1 minute but decreased at 3 minutes after X-linking	[85-87, 89, 91, 413, 529, 533-536, 560, 572, 587, 589, 604, 605, 609]
GlyCAM-1	Human neutrophils, PBL, Jurkat T lymphocytes	• Redistribution of L-selectin to DRM (dependent on L-selectin tail) • Adhesion through β1 integrins • Activation of β2 integrins[1]	[1]Naïve, but not memory T cells	[86, 88, 560]
Primary antibody	Human neutrophils, Jurkat T lymphocytes, Human leukemic CEM cells, Jurkat T lymphocytes, Murine lymphocytes U937 monocytic cell line	• MAPK phosphorylation[1] • $p56^{lck}$ dependent tyrosine phosphorylation of L-selectin tail and MAPK, formation of L-selectin/Grb2/SOS complex and activation of Rac2 and O_2^- synthesis via Ras • Actin filament polymerisation that was dependent on activation of Ras and Rac2 • Upregulation of JNK activity that was dependent on p56lck and Rac1 • Expression of M-CSF-1 that was dependent on c-Abl kinase • CaM/ERM interaction in *cis*[2]	[1]Also Fab fragments to a lesser extent [2]As measured by FRET efficiency between ezrin-GFP and CaM-mChery, this interaction was weaker than that observed for cross-linking	[245, 246, 415, 572, 601, 603, 608]

		• Enhanced chemotaxis towards SLC that was dependent on L-selectin levels and was mediated by PKC, MAPK and Syk family kinases[3]	[3]Also observed upon engagement with EC ligands	
Two primary antibodies	Human neutrophils, 300.19 pre-B cells	• Upregulation of Mac-1 • Association with cytoskeleton in DRM		[87, 587]
E-selectin	Human neutrophils	• Patching • MAPK-dependent rapid co-localization and capping of L-selectin and PSGL-1 on neutrophils in suspension which was critical for boosting CD11b/CD18 activity[1] • Co-clustering of L-selectin and PSGL-1 results in transition from rolling to arrest	[1]CD18 clustering did not co-localise with areas of L-selectin clustering	[413, 586]
Sulfatides	Human neutrophils, Murine $CD4^+$ T cells, K562 myeloid cell line, human monocytes, granulocytes and PBL, Jurkat T lymphocytes	• MAPK phosphorylation, • Calcium flux dependent on tyrosine kinases and MAPK • Enhanced expression of mRNAs for IL-8 and TNF-α • Upregulation of CXCR4[1] • Tyrosine phosphorylation of $p56^{lck}$ itself and $p56^{lck}$ dependent tyrosine phosphorylation of L-selectin tail, formation of L-selectin/ZAP-70/c-Abl complex	[1]Murine CXCR4 upregulation was not L-selectin dependent in $CD8^+$ T cells and B cells	[85, 88, 90, 601, 602]
sLe^x	Jurkat T lymphocytes, PBL	• Tyrosine phosphorylation of L-selectin and MAPK and activation of Ras that was p56lck dependent		[245]
Fucoidan	Jurkat T lymphocytes, PBL	• $p56^{lck}$ dependent tyrosine phosphorylation of L-selectin and MAPK and activation of Ras • Soluble fibronectin binding[1] • Upregulation of JNK • Upregulation of CXCR4 • Upregulation of Rac1	[1]Soluble fibronectin was bound by Jurkat T lymphocytes and naïve T cells but not memory T cells	[85, 88, 566, 603]

Table 1.3 Inside-out signalling evoked by L-selectin ectodomain ligation. Ligation of L-selectin ectodomain triggers clustering and signalling downstream of L-selectin tail. Clustering can be caused by antibodies or ligands. L-selectin-dependent signalling has been shown to affect multiple cellular functions. Consequences of L-selectin ligation are summarised in this table alongside the factors used for the ectodomain engagement "X-linking" indicates treatment with anti-L-selectin monoclonal antibody followed by cross-linking with secondary antibody. "Patching" indicates formation of large L-selectin clusters at the cell surface. For abbreviations used see **Abbreviations section**.

1.12 REGULATION OF L-SELECTIN FUNCTION BY INSIDE-OUT SIGNALLING

Although the majority of the current literature describes the outside-in signalling that follows the ligation of L-selectin ectodomain (**section 1.11** above), reports can be found where L-selectin's activity is modified by signals generated intracellularly (inside-out signalling). At this point, it has to be made clear that this section addresses changes in L-selectin activity other than ectodomain shedding (**section 1.9.2**), which occurs upon cell activation and is a result of intracellular signalling events. Neutrophil activation with granulocyte colony stimulating factor (G-CSF) or macrophage CSF (M-CSF) or T cell activation through CD2 or CD3 markedly enhanced the ability of these cells to bind PPME (polyphosphomonoester core derived from yeast, a known physiological L-selectin ligand mimic) [92]. The stimuli did not alter surface L-selectin levels as measured by flow cytometry [92], suggesting that the observed effects were due to modification of L-selectin's affinity for ligand. Additionally, pre-incubation of lymphocytes with lineage specific stimuli resulted in increased adhesion to HEV, which occurred in an L-selectin dependent manner [92]. Furthermore, it has been shown that exposure of PBL and 300.19 cells expressing L-selectin to fever-range hyperthermia (40°C) caused a significant increase in the association of L-selectin with DRM as measured by flow cytometry [560]. Additionally heat-treated PBL showed 1.6- to 2-fold increase in the L-selectin-dependent adhesion to HEV in PLN cryosections *in vitro* and in homing to PLN and Peyer's patches *in vivo* [560, 610]. The hyperthermia-induced L-selectin-mediated effects were dependent on the cytoplasmic tail as the LDcyto L-selectin mutant (lacking 11 terminal amino acids) did not translocate to DRM and 300.19 cells expressing LDcyto did not have increased adhesion to HEV *in vitro* [560]. Increased adhesion was subsequently attributed to the soluble factors secreted by heat-treated leukocytes, as when PBLs maintained at 37°C were incubated with supernatants from PBLs cultured at 40°C, similar extent of increased adhesion was observed [610]. The possible mechanisms by which these factors could increase adhesion in L-selectin dependent manner were not investigated, and the factors themselves are unknown. Interestingly, febrile temperatures did not alter total L-selectin protein levels or surface levels, as analysed by Western blotting or flow cytometry, respectively, and did not increase L-selectin's affinity for carbohydrate ligands as measured by PPME binding [610]. However, PBLs cultured in 40°C showed increased immunogold labelling of L-selectin molecules on microvilli, without any changes in overall microvilli morphology or number [610]. This raises the possibility that fever-range hyperthermia causes alterations in L-selectin's conformation that expose epitopes for gold-labelled mAbs [610]. As high

temperatures are known to increase membrane fluidity [611], this could be a pre-requisite to or a result of L-selectin translocation to DRM.

The studies discussed above demonstrate that, much like outside-in signalling, inside-in signalling can modify L-selectin function in a number of ways. Hence, L-selectin outside-in and inside-out signalling together are likely to form a multifaceted signalling network that regulate numerous cellular functions during the leukocyte adhesion cascade.

1.13 L-SELECTIN AND DISEASE

Genetic variations are known to cause or contribute to many diseases and a number of genetic variations in the L-selectin gene have been identified. They are defined as single-nucleotide polymorphisms (SNPs), where differences in single nucleotides result in the existence of two alternate alleles. Allele frequency, and hence genotype distribution, often differ between patients and controls, implying that certain alleles associate with disease susceptibility. SNPs within the coding sequence of L-selectin result in amino acid substitution and have been identified as T49S (threonine or serine at position 49 within the lectin domain), F206L (phenyloalanine or leucine at position 206 within the EGF domain), P213S (proline or serine at position 213 within the SCR domain) and S238P (serine or proline at position 238, SCR domain). No SNPs have been found in the transmembrane or cytosolic domains, and T49S has not been linked to any disease so far. An increase in the allele frequencies of F206L SNP of the L-selectin gene, and the associated F/L genotype was observed in Tunisian patients with inflammatory bowel disease as compared to controls [612]. Additionally, the L allele in F206L SNP was linked to higher risk for development of brucellosis in patients of Iranian Caucasian origin [613], but proved protective in development of Type 1 diabetes in subjects of Polish Caucasian origin [614]. P213S polymorphism is thought to contribute to susceptibility to Type 2 diabetes (T2D), insulin resistance, Grave's disease and coronary artery disease in the Chinese population, and the P allele appears to be the risk factor [513, 615-617]. Genotype 213PP is also a genetic risk factor for the development of nephropathy during T2D in Japanese patients [618]. No association between P213S polymorphism and T2D has been found in the study on Romanian population [619], suggesting that L-selectin gene polymorphism is influenced by ethnicity. Interestingly, in European and North American white population the P213S donor-recipient incompatibility could possibly be associated with kidney transplant survival [620]. Generation of L-selectin constructs harbouring the relevant SNPs could help to understand the described above pathological and protective mechanisms, which in turn could fuel new therapeutic approaches. One such study was indeed performed, where cells transfected with 238S variant of L-selectin showed marked reduction in rolling on and adhesion to IL-1β-stimulated HUVEC *in vitro* [514]. The reduction in L-selectin-dependent adhesion was proposed to play a role in the

pathogenesis of immunoglobulin A nephropathy in patients with S238P SNP, observed earlier by the same group [480]. Of note, recent availability in genome wide sequencing resulted in great number of Ensembl (on-line genome database for vertebrates and other eukaryotic species) submissions, reporting other variations found in *lam-1* gene. Identified variations include copy-number variations (CNV), duplications, inversions, insertions and deletions [621]. Although links between these variations and disease have not been identified yet, it can be expected that some, if not all, of these alterations would have a profound effect on L-selectin protein function. For example, CNV and duplications could result in elevation of L-selectin protein levels, altered leukocyte trafficking and disease.

From the L-selectin SNP/disease associations and various reports mentioned in this chapter, it can be seen that L-selectin plays a role in the pathogenesis of the chronic inflammatory diseases. The most notorious of all chronic inflammatory diseases is atherosclerosis – the main cause of CVD and death worldwide. Recruitment of L-selectin-positive classical monocytes during atherosclerosis progression (**section 1.6.2**) [279, 280, 300], as well as the accumulation of L-selectin ligands in the atherosclerotic plaques (**section 1.8.3**) [468-476] suggest the involvement of L-selectin in the pathology of this disease. In keeping with this, a role for L-selectin in atherosclerosis has been reported. These studies are descried in more detail in **section 1.13.1** below.

1.13.1 L-selectin and atherosclerosis

The first report to imply L-selectin's involvement in pathogenesis of atherosclerosis was published by Eriksson et al. (2001), who showed that L-selectin-mediated secondary capture accounts for 20-50% of all leukocyte capture on atherosclerotic lesions [20]. Subsequently, existence of MECA-79-nonreactive ligands on the aortic ECs and L-selectin-dependent primary capture in atherosclerosis was proposed by Galikna et al. (2006) [622]. These ligands were thought to mediate 50-57% of total T and B cell homing to the aortic endothelium before and during development of atherosclerosis as established through studies on L-selectin deficient mice [622]. In line with this hypothesis, MECA-79-nonreactive L-selectin ligands were found on both resting and cytokine-stimulated aortic endothelium, and supported monocyte adhesion *in vitro* [460]. Interestingly, a recent study stresses the importance of neovessels for leukocyte recruitment during later stages of atherosclerosis [299]. Eriksson (2011) showed that a network of microvessels that penetrate the advanced plaques serve as entry points for extravasating leukocytes [299]. Surprisingly, PSGL-1, a known leukocyte CAM, was found to be expressed by microvessel endothelium [299]. Primary interactions between the endothelial PSGL-1 and leukocyte L-selectin were established to mediate virtually all leukocyte recruitment that occurred via the microvessels [299]. Hence, it appears that L-

selectin plays a dual role in the leukocyte recruitment during atherosclerosis development. L-selectin recruits leukocytes to the aortic ECs through both primary and secondary capture mechanisms, and facilitates leukocyte entry to the advanced lesions from the microvessels through direct binding of endothelial PSGL-1. On the other hand, a contradictory report showed that L-selectin null mice had a two-fold increase in the plaque area during the early stages of atherosclerosis progression [623]. The same report found no differences in the atherosclerotic burden between L-selectin null and WT mice during later stages of the disease, and no changes in the plaque cellular composition between the two mouse strains at neither of the stages [623]. This report suggests that L-selectin does not promote atherosclerosis, but rather has a protective role in the early development stages. However, this study investigated lesion formation through the assessment of plaques in the descending aorta, but the cellular composition was examined in the plaques derived from aortic sinuses [623]. Therefore it cannot be excluded that L-selectin-dependent recruitment contributed to the formation of lesions in the descending aorta. Taken together, a strong link between L-selectin and atherosclerosis exists, however more research is required to explain current controversies. For example, the generation of transgenic mice expressing L-selectin-GFP chimera could help to directly visualise trafficking and distribution of L-selectin-positive leukocytes during development of atherosclerosis.

1.13.2 Therapeutic implications of L-selectin

Due to its prominent role in mediating the inflammatory response in both acute and chronic inflammation, as well as its association with many chronic diseases, L-selectin is an attractive target for therapy. L-selectin has been shown to be modulated by non-steroidal anti-inflammatory drugs (NSAIDs). NSAIDs are commonly known to exert their action through inhibition of cyclooxygenase (COX), however it now becomes clear that a group of NSAID also stimulate cell surface NADPH-oxidase to generate superoxide anion, which in turns activate ADAM17 on neutrophils [624]. This causes L-selectin shedding and thus prevents neutrophil attachment to ECs *in vitro* [624-626]. Anti-L-selectin compounds are continually being tested at various stages of pre-clinical and clinical trials. For example, aselizumab, a humanised anti-L-selectin antibody, was tested for its ability to decrease posttraumatic inflammatory response in the multiple injured patients [627]. However, despite being well tolerated by the study subjects, it did not outperform the placebo [627]. Some hopes are presently attached with the L- and P-selectin ligand PSGL-1-IgG chimera (drug name YSPSL) that has shown no adverse effects in Phase II trial, and is currently undergoing further tests in trials on renal allograft rejection [628].

Academic research plays a central role in discoveries that drive novel therapeutic ideas. An exciting report, published last year by Bernal et al. (2012), demonstrates that transient transfection of cardiac mesoangioblasts with L-selectin greatly improves the ability of these cells to home to the damaged heart tissue in a mouse model of myocardial infarction [629]. Cardiac mesoangioblasts are mesenchymal stem cells that can differentiate into cardiomyocytes [630]. Augmented recruitment of L-selectin transfectants resulted in much better heart tissue regeneration as compared to unmodified cardiac mesoangioblasts [629]. This report opens up a new opportunity for L-selectin-based stem cell therapy in the cardiovascular disease.

1.14 ORIGINAL HYPOTHESIS

The role of L-selectin in leukocyte tissue infiltration has been currently allocated mainly to mediating leukocyte tethering and rolling as well as to the activation of integrin-dependent adhesion. However, an emerging body of evidence suggests that L-selectin plays a prominent role during migration of leukocytes beyond the vessel wall. The event of transendothelial migration links intra- and extra-vascular locomotion of leukocytes. It is therefore proposed that L-selectin might be directly involved in the exit of leukocytes from the vasculature and in to the surrounding space. Furthermore, it is postulated that shedding of L-selectin is likely to play a role in regulating TEM. L-selectin-dependent migration of monocytes is of particular interest given the strong association of both L-selectin and monocytes with chronic inflammatory disease. Hence, the ultimate goal of this PhD project is to establish the role that L-selectin and its shedding may play during monocyte TEM.

1.15 AIMS OF THE PROJECT

To test the hypothesis produced in **section 1.14**, a number of aims were established for this project:

1. To generate and characterise monocytic cell line expressing WT L-selectin-GFP to visualise the sub-cellular distribution of L-selectin without the use of monoclonal antibody.
2. With the use of sheddase-resistant and cytoplasmic serine mutants of L-selectin, determine its spatio-temporal distribution during TEM, which would provide clues to:
   a) When and where in the cell shedding of L-selectin occurs.
   b) What the relative contribution of the intracellular and extracellular domains are in this process.
3. To investigate whether other molecules known to act during the adhesion cascade have an effect on L-selectin clustering, which would give insight in to outside-in and inside-out signalling mechanisms.
4. To determine how L-selectin shedding and clustering may influence monocyte responses, with particular consideration to cell morphology and chemotaxis.

CHAPTER 2. MATERIALS AND METHODS

2.1 CELL CULTURE REAGENTS, CHEMICALS, BUFFERS AND SOLUTIONS

Tabulated list of cell culture media, reagents, buffers and solutions used in this thesis is presented in **table 2.1**.

	Product/Material	**Supplier**	**Ingredients (Recipe)/Stock**	**Storage**
Cell Culture	RPMI (Roswell Park Memorial Institute)-1640 + 5 mM L-glutamine	Gibco® Invitrogen, U.K.	Manufacturers Recipe	+4°C
	Foetal Calf Serum	Gibco® Invitrogen, U.K.	N/A	-20°C
	EGM-2 Media BulletKit	Lonza	Walkersville Endothelial Growth Medium supplemented with hEGF, Hydrocortisone, FBS (Fetal Bovine Serum), GA-1000 (Gentamicin, Amphotericin-B),VEGF, hFGF-B, R3-IGF-1, Ascorbic Acid, Heparin	+4°C
	Fibronectin	Sigma-Aldrich®, Germany	1 mg/mL	
	HBSS (Hank's Buffered Saline Solution)	Gibco® Invitrogen, U.K.	1.26 mM Calcium-, 0.493 mM magnesium-, 5.33 mM potassium- and 137.93 mM sodim chloride, 0.407 mM magnesium sulfate, 0.441 mM potassium phosphate monobasic, 4.17 mM sodium bicarbonate, 0.338 mM sodium phosphate dibasic (Na2HPO4) anhydrous, 5.56 mM D-Glucose, 0.026 mM phenol red	+4°C
	OPTIMEM®	Gibco® Invitrogen, U.K.	Manufacturers Recipe (complete formulation is confidential)	+4°C
	Penicillin/Streptomycin	Sigma-Aldrich®, Germany	10,000 Unit penicillin and 10,000 µg/mL streptomycin	-20°C

	Luria Bertani (LB) media	Sigma-Aldrich®, Germany	20 g in 1 litre ddH_20	RT
	LB Agar	Sigma-Aldrich®, Germany	35 g in 1 litre ddH_20	RT (plates at +4°C)
Buffers and Solutions	Cytobuster™ Protein Extraction Reagent	Novagen®, Germany	N/A	RT
	Poly-L-lysine (PLL)	Sigma-Aldrich®, Germany	0.1% (w/v) manufacturers solution	+4°C
	STE buffer	Made in house	10 mM Tris-HCl, pH 8.0, 150 mM NaCl, 1 mM EDTA	On ice upon preparation
	GFP-Trap® Wash/Dilution Buffer	Made in house	10 mM Tris/Cl pH 7.5, 150 mM NaCl, o.5 mM EDTA, 25 nM calyculin A, 5 µM bisindolylmaleimide	On ice upon preparation
	GFP-Trap® Lysis Buffer	Made in house	10 mM Tris/Cl pH 7.5, 150 mM NaCl, o.5 mM EDTA, 0,5% NP-40, 25 nM calyculin A, 5 µM bisindolylmaleimide	On ice upon preparation
	HEPES (4-(2-hydroxyethyl)-1-piperazineethanesulfonic acid)	Sigma-Aldrich®, Germany	1M	+4°C
	PBS (Phosphate Buffered Saline), pH 7.4	Severn Biotech® Ltd, U.K.	0.8% sodium chloride (w/v), <0.1 % potassium chloride (w/v), <0.2% monosodium phosphate (w/v), <0.1% potassium phosphate (w/v), 0.1% sodium azide (w/v)	RT
	Coomassie Blue R350 Staining Solution	Fluka®, Sigma-Aldrich, Germany	0.25 g of powder in 500 mL, 50% methanol, 40% ddH20, 10% acetic acid (v/v)	RT
	Coomassie Blue De-stain solution	Made in house	50% methanol, 40% ddH20, 10% acetic acid (v/v)	RT
	GelCode™ Blue Stain reagent	Thermo Scientific, U.K.	N/A	RT
	6x DNA loading buffer	Made in house	30% glycerol (v/v), 0.25% (w/v) bromophenol blue (w/v), 0.25% xylene cyanol FF (w/v)	RT

	4x Protein Loading Buffer	Made in house	200 mM Tris-HCl pH 6.8, 8 % SDS (v/v), 20% glycerol (v/v), 0.4 bromphenol-blue % (w/v), 3.6% β-mercaptoethanol (v/v)	RT
	2x Protein Loading Buffer	Made in house	100 mM Tris-HCl pH 6.8, 4 % SDS (v/v), 10% glycerol (v/v), 0.2 bromphenol-blue % (w/v), 1.8% β-mercaptoethanol (v/v)	RT
	30% bovine serum albumin (BSA) (sterile filtered)	Sigma-Aldrich®, Germany	N/A	+4°C
	Tris-buffered saline (TBS) solution	Made in house	150 mM NaCl/15 mM Tris-HCl, pH 7.4 in ddH_20	RT
	10x TAE (400 mM Tris-Acetate and 10 mM EDTA) buffer	Invitrogen®, U.K.	N/A	RT
	20x MES (2-morpholinoethanesulfonic acid, monohydrate)-SDS Buffer (Running Buffer)	Invitrogen®, U.K.	N/A	RT
	20x Novex® NuPAGE® transfer buffer	Invitrogen®, U.K.	N/A	RT
	Novex® NuPAGE® Sharp® Ladder protein standard solution	Invitrogen®, U.K.	N/A	-20°C
	1 kB DNA standard solution	New England Biolabs®	500 µg/mL	-20°C
	Western Lightning™ Chemiluminescence Reagent	Perkin-Elmer LAS, inc. U.S.A.	N/A	+4°C
	Milk buffer	High Street Supermarket	5% dry milk powder, w/v in TBS with 0.1% NP-40 substitute	+4°C
	Western blotting “stripping buffer”	Made in house	62.5 mM Tris-HCl pH 6.7, 2% SDS (v/v), 100 mM β-mercaptoethanol	RT
Chemicals	QIAprep® Miniprep DNA isolation kit	Qiagen, U.K.	As per manufacturer’s instructions	RT, upon RNAse A

				addition Buffer P1 at +4°C
	QIAprep® Maxiprep DNA isolation kit	Qiagen, U.K.	As per manufacturer's instructions	RT, upon RNAse A addition Buffer P1 at +4°C
	QIAquick Gel Extraction Kit	Qiagen, U.K.	As per manufacturer's instructions	RT
	Ampicillin	Sigma-Aldrich®, Germany	100 mg/mL	-20°C
	Methanol	Fisher Scientific, U.S.A.	N/A	RT
	Isopropanol	Fisher Scientific, U.S.A.	N/A	RT
	Glutaraldehyde	GPR™	N/A	+4°C
	β-mercaptoethanol	Sigma-Aldrich®, Germany	N/A	RT
	Di-methyl-sulphoxide (DMSO; cell culture tested)	Sigma-Aldrich®, Germany	N/A	RT
	TRIZMA® base	Sigma-Aldrich®, Germany	Used to make 1 M Tris.HCl (pH 6.8, 7.4 or 8,0) in ddH_20	RT
	Sodium Chloride (NaCl)	Sigma-Aldrich®, Germany	1 M in ddH_20	RT
	Glycerol	Sigma-Aldrich®, Germany	N/A	RT
	Triton-X100	Sigma-Aldrich®, Germany	N/A	RT
	Nonidet P-40 substitute (NP-40)	Fluka®, Sigma-Aldrich, Germany	N/A	RT
	Tween-20	Sigma-Aldrich®, Germany	N/A	RT
	SDS	Sigma-Aldrich®, Germany	20% in H_2O manufacturer's solution	RT
	Glutathione Sepharose 4B® beads	GE Healthcare®, U.K.	50% ethanol/beads slurry	+4°C
	GFP-Trap® A	Chromotek, Germany	Small GFP-binding protein coupled to agarose beads (Manufacturers composition)	+4°C
	Ethylene Diamine-tetraacetic acid (EDTA)	Sigma-Aldrich®, Germany	0.5 M, pH 8.0, in ddH_20	RT

	Solution			
	Magnesium Chloride ($MgCl_2$)	Sigma-Aldrich®, Germany	0.1M, in ddH_20	RT
	Isopropyl-ß-Dthiogalactopyranosid (IPTG)	Sigma-Aldrich®, Germany	0.1 M in ddH_20	-20°C
	Phenyl-methyl-sulfonylfluoride (PMSF)	BioChemica, Germany	200 mM in methanol	-20°C
	1,4-Dithio-DL-threitol (DTT)	Sigma-Aldrich®, Germany	0.1 M in ddH_20	Used upon preparation
	Lysozyme	Sigma-Aldrich®, Germany	powder	-20°C
	Calyculin A	Sigma-Aldrich®, Germany	20 µM in DMSO	-80°C
	Bisindolylmaleimide	Calbiochem®	1mM	-20°C
	Protease Inhibitor Cocktail	Sigma-Aldrich®, Germany	N/A	-20°C
	Novex® NuPAGE® Bis-Tris 4-12 % gradient gels, 10 wells, thickness: 1.0 or 1.5 mm	Invitrogen®, U.K.	Manufacturers composition	RT
	Phorbol-12'-myristate-13'-acetate (PMA)	Sigma-Aldrich®, Germany	32.5 µM in ethanol	-20°C
	Sodium Fluoride (NaF)	Sigma-Aldrich®, Germany	powder	RT
	Sodium ortho-vanadate (Na_3VO_4)	Sigma-Aldrich®, Germany	0.5 M in ddH_20	RT
	Recombinant Human Tumor Necrosis Factor alpha (TNF-α)	R&D systems	100 µg/mL	-80°C
	Recombinant Human Monocyte Chemoattractant protein 1 (MCP-1)/CCL2/JE	R&D systems	100 µg/mL	-20°C
	Recombinant Human CXCL1/GRO alpha	R&D systems	100 µg/mL	-20°C
	Ro-31-9790	Kind Gift from Ann Ager,	30 mM in DMSO	-20°C

		University of Cardiff, Cardiff, U.K.		
	LY-374973, N-[N-(3,5-Difluorophenacetyl)-L-alanyl]-S-phenylglycine t-butyl ester (DAPT)	Sigma-Aldrich®, Germany	18 mg/mL in DMSO	-20°C
	Ro-31-8220	Calbiochem®, Merck KGaA, Germany	500 µM in ddH_20	-20°C
	Paraformaldehyde (PFA)	BDH Laboratory Supplies, U.K.	8% in PBS (w/v)	-20°C
	Tetra-methyl-rhodamine-5-(and-6)-isothiocyanate (TRITC)-conjugated phalloidin	Sigma-Aldrich®, Germany	0.2 mg/mL in methanol	-20°C

Table 2.1 Reagents used during this research project. Other chemical/reagents used may be noted in the text, and the supplier was Sigma-Aldrich®, Germany, unless otherwise stated. See **Abbreviations section** for abbreviations used.

2.2 ANTIBODIES

Tabulated list of primary antibodies used in this thesis is presented in **table 2.2.**, and secondary antibodies in **table 2.3**.

Antibody	Antigen	Origin	Mono/ Polyclonal	Isotope	Stock conc. (µg/mL)	Source
DREG56	L-selectin	Mouse	Monoclonal	IgG_1	200	ATCC (HB- 300 hybridoma)
Anti-GFP (FL)	GFP	Rabbit	Polyclonal	IgG	200	Santa Cruz Biotechnology
Anti-CaM	Calmodulin	Mouse	Monoclonal	IgG_1	1000	Upstate/ Millipore
Anti-biglycan	Biglycan	Rabbit	Polyclonal	IgG	400	Abcam
Anti-collagen XVIII	Collagen XVIII	Rat	Monoclonal	IgG_{2B}	100	Santa Cruz Biotechnology
Anti-CD43	CD43	Mouse	Monoclonal	IgG_1	200	Santa Cruz Biotechnology
Anti-CD44	CD44	Rabbit	Polyclonal	IgG	200	Santa Cruz Biotechnology
Anti-JAM-A	JAM-A	Mouse	Monoclonal	IgG_1	200	Santa Cruz Biotechnology
Anti-PSGL-1	PSGL-1	Mouse	Monoclonal	IgG_1	200	Santa Cruz Biotechnology
Anti-PECAM-1	PECAM-1	Mouse	Monoclonal	IgG_1	205	Dako
Anti-EEA1	EEA1	Mouse	Monoclonal	IgG_1	250	BD Transduction Laboratories™
Anti-ERM	ERM	Rabbit	Polyclonal	?	?	Cell Signaling Technology®
Anti-phospho-ERM	Phospho-ERM (Thr 567 (E), 564 (R) and 558 (M)	Rabbit	Polyclonal	?	?	Cell Signaling Technology®
Anti-RhoA	RhoA	Mouse	Monoclonal	IgG_1	200	Santa Cruz Biotechnology
Anti-Rac1	Rac1	Mouse	Monoclonal	IgG_{2b}	1000	Merck Millipore
Anti-Cdc42	Cdc42	Mouse	Monoclonal	IgG1	1000	Abcam
Anti-actin	Beta-actin	Goat	Polyclonal	IgG	200	Santa Cruz Biotechnology
Anti-CCR2	CCR2	Rabbit	Monoclonal	IgG	1000	Abcam
IgG_1	N/A	Mouse	Monoclonal	IgG_1	200	Santa Cruz Biotechnology
IgG	N/A	Rabbit	Polyclonal	IgG	200	Abcam

Table 2.2 List of primary antibodies used in this thesis. Dilutions at which the antibodies were used are described in specific sections of **"Materials and Methods"** or within results chapters. All antibodies were purchased from the indicated supplier, apart from DREG56, which was purified from hybridomas in house. '?' indicates unavailable information. See **Abbreviations section** for description of abbreviations.

Antibody	Antigen	Origin	Stock conc. (µg/mL)	Source
Rabbit anti-mouse-FITC	Mouse Immunoglobulins	Rabbit	970	Dako
Goat anti-mouse-RPE	Mouse Immunoglobulins	Goat	1000	Dako
Goat anti-mouse-HRP	Mouse Immunoglobulins	Goat	1000	Dako
Goat anti-rabbit-HRP	Rabbit Immunoglobulins	Goat	250	Dako
Rabbit anti-goat-HRP	Goat Immunoglobulins	Rabbit	650	Dako
Goat anti-mouse-AlexaFluor®633	Mouse Immunoglobulins	Goat	2000	Molecular Probes® Invitrogen®
Goat anti-rabbit-AlexaFluor®633	Rabbit Immunoglobulins	Goat	2000	Molecular Probes® Invitrogen®
Donkey anti-goat-AlexaFluor®633	Goat Immunoglobulins	Donkey	2000	Molecular Probes® Invitrogen®

Table 2.3 List of secondary antibodies used in this thesis. Dilutions at which the antibodies were used are described in specific sections of **"Materials and Methods"** or within results chapters. See **Abbreviations section** for description of abbreviations.

2.3 CLONING

Human L-selectin cDNA was amplified by PCR (see **section 2.4**) from pCMV6-AC-GFP vector (OriGene). PCR primers were designed with BamHI and XhoI restriction sites engineered at 5' and 3' ends, respectively (forward primer: 5'-GAGAGAGGATCCGGTACCGAGGAGA-3'; reverse primer 5'-GAGAGACTCGAGATATGGGTCATTCATACTTCTC-3'). PCR products amplified by Pfu DNA polymerase (Stratagene) were excised from 0.8 % agarose gels and purified using QIAquick Gel Extraction kit (Qiagen) according to manufacturer's protocol. The pHR'SIN-SEW lentiviral backbone vectors were provided by Prof. Adrian Thrasher (Institute of Child Health, UCL) and were carrying either enhanced green fluorescent protein (eGFP, from now on referred to as GFP) or red fluorescent protein (RFP) C-terminal tags. The vectors were named pHR'SIN-SEW-GFP or pHR'SIN-SEW-RFP according to the fluorescent tag they were bearing. The vectors were linearised by double digestion with BamHI and XhoI restriction enzymes (New England Biolabs, NEB) according to manufacturer's protocol (NEB). Digests were resolved on a 0.8% agarose gel and the vector was purified with a QIAquick Gel Extraction kit according to manufacturer's protocol. Purified vectors were dephosphorylated with calf intestinal alkaline phosphatase (CIP, from NEB) for 1 hour at 37ºC and cleaned from the reaction mixture using QIAquick Gel Extraction Kit according to manufacturer's protocol. The

vectors were then ligated with the insert with a molar vector to insert ratio of 1:3. Ligation was performed by T4 DNA ligase (Promega) in a 10 µL reaction at 4ºC overnight prior to transformation (see **section 2.7**). Colonies were selected and grown overnight to generate plasmid preps using a QIAprep® Miniprep DNA isolation kit (Qiagen, U.K.) and following manufacturer's protocol. The open reading frames were subsequently sequenced by Geneservice using primers targeting sequences approximately 100 bp upstream of the L-selectin start codon (primer Frd1: 5'-GCGCTTCTGCTTCCCGAGCTCTAT-3'), approximately 300 bp into the ORF (primer Frd2: 5'- GACGTGGGTGGGAACCAACAAATCT-3') and approximately 700 bp into the ORF (primer Frd3: 5' CCACCTGTGGACCATTTGGAAACTG-3'). Collectively, the design of these primers ensured that the entire open reading frame was sequenced.

2.4 POLYMERASE CHAIN REACTION (PCR)

PCR amplifications were performed using 1 µL (10 µM) of each primer (synthetized by Sigma-Aldrich) and 100 ng of DNA template. PCR reactions were performed in a 50 µL reaction volume, using thin walled PCR tubes in a thermo cycler (Perkin Elmer, GeneAmp PCR System 2400) using the following conditions: hot-start denaturation 95°C 5 min, denaturation 95°C 30 seconds*, annealing 55°C 40 seconds*, elongation 72°C (30 seconds per 500 bp)*, end 72°C 2 min. (*Repeated for 25 cycles).
PCR reactions were mixed with 6x DNA loading buffer (**table 2.1**) and separated by gel electrophoresis on agarose gels supplemented with ethidium bromide or SafeView™ dye as described in **section 2.6**. PCR products were visualized using UV detection of before being purified, cloned and dispatched for sequencing.

2.5 *IN VITRO* PCR MUTAGENESIS AND SEQUENCING OF THE MUTANTS

The pHR'SIN-SEW plasmid containing the cDNA of human WT L-selectin fused with GFP or RFP (pHR'SIN-SEW-L-selectin^{WT}-GFP or pHR'SIN-SEW-L-selectin^{WT}-RFP (for cloning method see **section 2.3**) was used as a template for generating mutations. A QuickChange™ (Stratagene) PCR *in vitro* mutagenesis protocol was employed in order to generate the S364A, S367A, SSAA, ΔM-N, ΔM-N SSAA S364D, S367D, SSDD and R357A mutants (single amino acid names for Serine [S], Aspartate [D] and Arginine [R]) using the pHR'SIN-SEW-L-selectin^{WT}-GFP plasmid and SSAA, ΔM-N and ΔM-N SSAA using the pHR'SIN-SEW-L-selectin^{WT}-RFP plasmid. Briefly, polymerase chain reaction (PCR) mutagenesis reaction was followed by 1 hour digestion with DpnI restriction enzyme (NEB). This step involves the cleavage of methylated, but not unmethylated DNA. Note that methylated DNA is derived from bacterially synthesised DNA, and not PCR synthesised DNA (where the mutation has been generated). DpnI restriction enzyme (1 µL) was added to 50 µL PCR mutagenesis reaction at 37ºC, and then 1 µL of

the mixture was used to transform competent bacteria (**section 2.7**). The open reading frames of all the mutants were subsequently sequenced by Geneservice using primer Frd3 (see **section 2.3**) to ensure insertion of the desired mutations into the L-selectin tail and once this was confirmed, the ORFs were sequenced with primers Frd1 and Frd2 to ensure no spontaneous mutations appeared within the insert during the mutagenesis procedure. Two-step mutagenesis was applied when obtaining ΔM-N mutant as deletion of eight amino acid codons in single PCR reaction was not considered likely. Therefore two sets of primers were designed: ΔMIKE and ΔMIKEGDYN. Once the ΔMIKE pair of primers was successfully used – as confirmed by sequencing – to delete MIKE amino acid sequence, ΔMIKEGDYN pair of primers was used to further delete GDYN amino acid sequence. When generating ΔM-N SSAA mutants, pHR'SIN-SEW-L-selectin$^{\Delta M\text{-}N}$-GFP/RFP plasmid was used as a template for the SSAA primers. All the primers used for *in vitro* PCR mutagenesis during this thesis are shown in **table 2.4**.

Mutation	Primer	Sequence
S364A	Frd	GATTAAAAAAAGGCAAGAAAGCCAAGAGAAGTATGAATGACC
	Rev	GGTCATTCATACTTCTCTTGGCTTTCTTGCCTTTTTTTAATC
S367A	Frd	GGCAAGAAATCCAAGAGAGCTATGAATGACCCATATCAC
	Rev	GTGATATGGGTCATTCATAGCTCTCTTGGATTTCTTGCC
SSAA	Frd	GGCAAGAAAGCCAAGAGAGCTATGAATGACCCATATCAC
	Rev	GTGATATGGGTCATTCATAGCTCTCTTGGCTTTCTTGCC
ΔMIKE	Frd	CAAAAGTTTCTCACCCCTCTTCATTC
	Rev	GAATGAAGAGGGGTGAGAAACTTTTG
ΔMIKEGDYN	Frd	GACAAAAGTTTCTCAGGTGATTATAACCCC
	Rev	GGGGTTATAATCACCTGAGAAACTTTTGTC
S364D	Frd	GGCAAGGAGATTAAAAAAAGGCAAGAAAGACAAGAGAAGTATGAATGACCCATATCAC
	Rev	GTGATATGGGTCATTCATACTTCTCTTGTCTTTCTTGCCTTTTTTTAATCTCCTTGCC
S367D	Frd	GGCAAGAAATCCAAGAGAGATATGAATGACCCATATCAC
	Rev	GTGATATGGGTCATTCATATCTCTCTTGGATTTCTTGCC
SSDD	Frd	GGCAAGAAAGACAAGAGAGATATGAATGACCCATATCAC
	Rev	GTGATATGGGTCATTCATATCTCTCTTGTCTTTCTTGCC
R357A	Frd	GGCATTTATCATTTGGCTGGCAAGGGCATTAAAAAAAGGCAAGAAATCCAAG
	Rev	CTTGGATTTCTTGCCTTTTTTTAATGCCCTTGCCAGCCAAATGATAAATGCC

Table 2.4 Sequences of the mutagenesis primers. This table outlines all the mutagenesis primers that were used during this project. The primers are all written in the direction of 5' to 3'.Frd, forward primer; Rev, reverse primer.

2.6 AGAROSE GEL ELECTROPHORESIS

PCR products were mixed with 6x gel loading buffer (**table 2.1**) and resolved by electrophoresis on a 0.8% 1x tris-acetate-EDTA (TAE) (Invitrogen) agarose gels with ethidium bromide (1:10 000) or SafeView™ (1:500). Gels were resolved at 120V until the bands had been adequately separated (normally, when the dye front had reached the bottom of the gel. Gels were visualized by UV transillumination and digital images were acquired. Product sizes were determined by using DNA ladders (GeneRuler™ or NEB).

2.7 TRANSFORMATION OF *ESCHERICHIA COLI* BL-21 AND PLASMID PURIFICATION

For every transformation, 50 μl of competent BL-21 *Escherichia coli* (*E. coli*) (kindly provided by Alison Brewer) were slowly thawed on ice and allowed to mix with 200-1000 ng of plasmid or 1 μl of PCR mutagenesis reaction for 1 hour on ice. Alternatively, 2 μl of ligation reaction were added to 50 μl One Shot® TOP10 Chemically Competent *E. coli* (Invitrogen). The genotype of TOP10 cell is similar to DH10B™ strain. Following 30 minute-long incubation on ice, bacteria were heat-shocked by submerging tubes into a water bath pre-heated at 42°C for 45 seconds, and then rapidly cooled on ice for a further 10 minutes. LB (200 μl) was added to each transformation reaction and incubated shaking in a 37°C for 1 hour. The transformation (200 μL) was plated out onto a pre-warmed appropriate antibiotic treated LB agar plates and allowed to culture at 37°C overnight for colony formation. The following morning colonies were picked and cultured in 3 mL of LB supplemented with the appropriate antibiotic for around 8 hours. Bacteria were subsequently harvested for plasmid isolation using QIAprep® Miniprep DNA isolation kit (Qiagen, U.K.) according to manufacturer's protocol (see below). Alternatively 1 mL was inoculated in to 100 mL of LB supplemented with the appropriate antibiotic and bacteria were cultured overnight. Following day bacteria were harvested by centrifugation at 4,000 rpm (SORVALL® Legend RT, U.K.) for 45 minutes at 4°C and plasmid isolation was performed using QIAprep® Maxiprep DNA isolation kit (Qiagen, U.K.) according to manufacturer's protocol. Briefly, both QIAprep® Mini- and Maxiprep DNA isolation kits are based on alkaline lysis of bacterial cells. The lysis if followed lysate preparation, clearing and immobilisation of liberated DNA onto silica membranes within a spin column under high salt conditions. The DNA pellets obtained after washing and

elution from the spin column were dissolved in ddH2O and the concentration determined by measuring the OD260 using NanoDrop spectrophotometer (Thermo Scientific, U.K.). The quality of the DNA was assessed by monitoring OD260/OD280 ratio and was deemed acceptable if determined to be close to the value of 1.8 absorbance units.

2.8 PROTEIN ANALYSIS

2.8.1 SDS-Polyacrylamide Gel Electrophoresis (SDS-PAGE) of extracts derived from THP-1 cells and HUVEC.

Cells were harvested by centrifugation at 1200 rpm (SORVALL® Legend RT, U.K.), samples were lysed in appropriate volume of CytoBuster™ Protein Extraction Reagent (Novagen, U.K.) supplemented with 1x protease inhibitor cocktail (Sigma-Aldrich®, Germany) and four times concentrated protein loading buffer (PLB) was added. Samples were incubated at 95 ºC for 5 minutes and the denatured proteins were then resolved by polyacrylamide gel electrophoresis on pre-cast Novex® NuPAGE® 4-12% Bis-Tris gradient gels (Invitrogen®, U.K.) in MES-SDS buffer at constant 100-200 V until the dye front left the gel. Novex® sharp pre-stained protein standard molecular weight markers (Invitrogen) were used for all gels.

2.8.2 Protein gel staining

Proteins resolved on polyacrylamide gels as described in **section 2.8.1** were often directly stained using Coomassie Blue R350® staining solution or GelCode® Blue Safe Protein Stain (Thermo Scientific, US) (**table 2.1**). For the Coomassie Blue staining, the gels were incubated with 20-30 mL of Coomassie staining solution for 15-30 min in a plastic 14-cm diameter dish. Gels were subsequently incubated with Coomassie destain solution (**table 2.1**) (until the protein bands were clearly visible over the background staining. For GelCode® staining, the gels were first prefixed with a 50% methanol (v/v) and 7% acetic acid (v/v) solution for 15 minutes at room temperature (RT) and then washed three times for five minutes with approximately 100 ml of ultrapure water. Further incubation with ultrapure water was continued until the protein bands became clearly visible. Gels were stored in sterile water at 4 °C and scanned in with a commercially available scanner (LI-COR®).

2.8.3 Immunoblotting (Western blotting)

Polyacrylamide gels were transferred to polyvinylidene fluoride (PVDF) Immobilon-P® (Millipore®, U.K.) transfer membranes that had been pre-wetted with 100% methanol and then equilibrated in transfer buffer, using the NuPAGE® transfer module (Invitrogen, U.K.). Transfer was carried out at 25 V for two hours. Subsequently, membranes were

blocked in 5% milk in TBS (Tris-buffered saline) supplemented with 0.1% NP40 (TBS_N) for 1 h at RT. Immunodetection of proteins of interest was performed with the use of appropriate primary antibody at a dilution of 1:500 in blocking solution at 4ºC with continuous agitation overnight. The next day, membranes were washed in TBS for five minutes, then in TBS_N for ten minutes, then in TBS for 5 minutes and finally blocked in 5% milk in TBS_N for 60 min at RT. Subsequently, horseradish peroxidase (HRP)-conjugated secondary antibody was added at a dilution of 1:3,000 for another hour and then membranes were washed again as described above. For detection of CaM, the PVDF membranes were rinsed with PBS once for 5 minutes, incubated for 15 minutes at RT in 20 mL of 0.25% glutaraldehyde in PBS and washed with TBS before the first blocking step. The TBS wash step serves to quench any excess reactive glutaraldehyde carried over from the initial fixation step. Treatment with glutaraldehyde prevented CaM protein from being washed from the membrane during the labelling procedure. After thorough washing in TBS, the membrane was blocked, and labelled as described above. Protein detection was performed using Western Lightning™ chemiluminescent reagent (Perkin Elmer®, U.S.A) as directed by manufacturer, followed by exposure of membranes to SuperRX X-ray films (Fuji®, Japan). Films were developed using a Compact X4 automatic X-ray film developer (X-ograph imaging Systems, U.K.). When detectin MCP-1 whose molecular weight was similar to the MW of beta-actin used as a loading control, the primary and secondary antibodies used to detect MCP-1 were removed and membrane re-probed with anti-actin antibody. This was achieved by incubation of the membrane with “stripping buffer” (**Table 2.1**) at 60°C for 30 minutes. The membrane was then washed in TBS_N for 10 min at RT and probed with the secondary antibody to confirm the removal of the previous signal. Once this was verified, the membrane was blocked with 5% milk in TBS_N for 60 min at RT and detection of actin was performed according to the protocol described above.

2.8.4 GFP-Trap® Immunoprecipitation

Immunoprecipitation of wild type and mutant forms of L-selectin-GFP fusion protein and GFP protein were performed using commercially available GFP-binding protein covalently conjugated to agarose beads (GFP-Trap®_A, Chromotek, Germany).In brief, GFP-Trap® is a high quality GFP-binding protein coupled to agarose beads. The manufacturer’s protocol was used with minor adjustments. Briefly, 30 million THP-1 cells expressing wild type or mutant forms of L-selectin-GFP fusion protein or just GFP protein were harvested and washed with 10 mL PBS (to remove any traces of albumin from tissue culture). Each cell pellet was then resuspended in 200 µL of lysis buffer (10 mM Tris/Cl pH 7.5, 150 mM NaCl, 0.5 mM EDTA, 0.5% NP40, 25 nM calyculin A, 5 µM bisindolylmaleimide) supplemented with 1x protease inhibitor cocktail (Sigma-Aldrich®,

Germany) and the samples were incubated on ice for 30 minutes with extensive pipetting performed every 10 minutes. Phosphatase inhibitor calyculin A and kinase inhibitor bisindolylmaleimide were added to ensure that protein phosphorylation status was preserved in the immunoprecipitation assay. The lysates were centrifuged at 20,000 x g (eppendorf centrifuge 5417R, Eppendorf®, Hannover, Germany) for 10 minutes at 4 °C and obtained supernatant was transferred to a fresh pre-cooled eppendorf tube and 550 µL of dilution/wash buffer (10 mM Tris/Cl pH 7.5, 150 mM NaCl, 0.5 mM EDTA, 25 nM calyculin A, 5 µM bisindolylmaleimide) was added per sample. The lysate (50 µL) was then mixed with 50 µL of 2x protein loading buffer (PLB) and the samples were boiled at 95 °C for 5 min. These were later used to determine the total levels of protein within a given cell lysate (input). The remaining cell lysate was then added to 25 µL of GFP-Trap® beads that had been pre-equilibrated with the dilution/wash buffer (three washes), and beads/lysate mixture was incubated overnight at 4 °C under rotation. The bead pellets were subsequently washed three times with dilution/wash buffer and then 100 µL 2x PLB was added per sample. Finally, the resuspended beads were boiled at 95 °C for 10 min in order to free the immunocomplexes from the beads. The beads were collected by centrifugation at 2,700 x g (eppendorf centrifuge 5417R, Eppendorf®, Hannover, Germany) for 2 minutes at 4 °C, and the supernatant loaded and resolved on polyacrylamide gels (see **section 2.8.1**).

2.8.5 Densitometry analysis

Conventional scanner (EPSON® Perfection 2400) was used to scan developed X-ray films. Scanned images were quantified by using ImageJ® software version 1.43 (National Institutes of Health, U.S.A.). Fold-changes were determined on the basis of the signal intensities amongst all the selected bands. These intensities were then normalised against the signal intensity of a protein deemed as “loading control”, for example, actin. The results were expressed as a “fold change” against the control in any given experiment.

2.9 PURIFICATION OF GST FUSION PROTEINS

Glutathione-S-transferase (GST)-fusion proteins of Rho GTPase effector domains were kindly provided by John G. Collard, Netherlands Cancer Institute, Amsterdam, the Netherlands. Three different GST-fusion proteins were used: p21-binding domain of PAK (PAK-PBD), Cdc42/Rac interacting domain (cassette) of the Wiskott-Aldrich syndrome protein (WASP-CRIB-C) and the Rho-binding domain of Rhotekin (Rhotekin-C21). All GST-fusion proteins were expressed in *E. coli* BL-21, which were grown in LB-medium containing 0.1 mg/mL ampicillin over night at 37 °C under aerobic agitation. On the following day, cultures were diluted 1:20 in fresh LB-medium and incubated at 37 °C

under agitation. Once the approximate OD600 of 0.8 was reached, expression of GST-fusion proteins was induced with 0.5 mM IPTG (**table 2.1**) for 2.5 hours at 30 °C. Cultures were subsequently centrifuged for 45 min at 3,000 rpm at 4 °C (SORVALL® Legend RT, U.K.) and the bacterial cell pellets frozen at -80 °C. The frozen pellet from a 150-mL-culture was thawed on ice and resuspended in 2.25 mL of ice-cold STE buffer (10 mM Tris-HCl, pH 8.0, 150 mM NaCl, 1 mM EDTA) supplemented with 1 mM PMSF (**table 2.1**). The suspension was then homogenised finally with a 19G hyperdermic needle (Kendall, U.K.). Subsequently, 100 µg/mL of lysozyme (Sigma-Aldrich®, Germany) was added to the suspension and the mixture incubated on ice for 15 minutes. Consequent addition of 5 mM DTT, 1% Tween-20 (v/v) and 0.03% SDS (v/v) led to a change in viscosity upon mixing, which indicated that lysis of the bacteria had occurred. The lysate was then centrifuged (eppendorf centrifuge 5417R, Eppendorf®, Hannover, Germany) for 20 min at 14,000 rpm at 4 °C. The supernatant was then added to 100 µL of glutathione Sepharose 4B® beads (GE Healthcare®, U.K.), which had been pre-equilibrated in STE buffer (three washes), and incubated for 1 h at 4 °C under rotating conditions. After the binding of the purified GST-proteins to the beads had occurred, beads were centrifuged and washed three times with STE buffer for three minutes at 1,200 rpm (eppendorf centrifuge 5417R, Eppendorf®, Hannover, Germany) at 4 °C. The yield was determined by comparison to a linear BSA calibration standard by protein electrophoresis. Representative Commassie-stained gel is shown in **figure 2.1**. Beads were best used within 24 h of production.

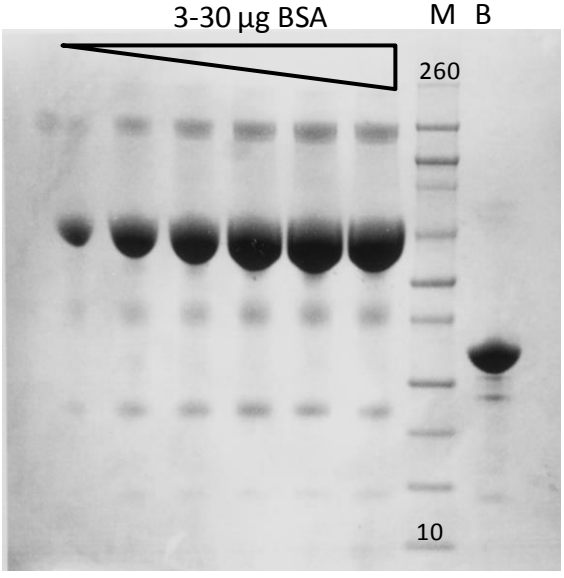

Figure 2.1 Determining protein concentration of GST-fused effector domain bound to glutathione sepharose beads. Increasing amounts of BSA (3, 12, 18, 24, 27 and 30 µg) are resolved in the first six lanes of the polyacrylamide gel. The concentration range normally loaded is between 3- and 30-µg BSA. M = molecular weight standards (from bottom to top: 10, 15, 20, 30, 40, 50, 60, 80, 110, 160 and 260 kDa). B = 5 µL of glutathione beads boiled and loaded onto the last lane of the gel. Coomassie staining of the polyacrylamide gel reveals that 5 µL of beads

prepared in this example carries the equivalent of approximately 10 µg of protein. This particular example shows yield of PAK-PBD.

2.10 RHO GTPASE ACTIVATION ASSAYS

Ten million THP-1 cells expressing wild type or mutant forms of L-selectin-GFP or just GFP were harvested from cell suspension, washed with 5 mL PBS and resuspended in 1 mL of ice cold lysis buffer (10 mM $MgCl_2$, 1 mM EDTA, pH 8.0, 25 mM HEPES pH 7.0, 150 mM NaCl, 2% glycerol (v/v), 1% Triton X-100 (v/v), 1 mM Na_3VO_4, 50 nM NaF, 25 nM calyculin A) supplemented with 1x protease inhibitor cocktail (Sigma-Aldrich®, Germany). Immediately after resuspension, the samples were span down at 14,000 rpm (eppendorf centrifuge 5417R, Eppendorf®, Hannover, Germany) for 10 min, which incorporated both lysis and centrifugation. The lysate (50 µL) was then mixed with 50 µL of 2x protein loading buffer (PLB) and the samples were boiled at 95 °C for 5 min. These were later used to determine the total levels of RhoGTPase within a given cell lysate. The remaining part of the lysate was mixed with approximately 40 µg of GST-fusion RhoGTPase bait protein conjugated to the glutathione sepharose beads (see **section 2.9**) and the beads/lysate mixture was incubated for 1 hour at 4 °C under rotation. After the incubation step was completed, the beads were washed three times with 1 mL of the cell lysis buffer and then 20 µL of 2x PLB was added per sample. The samples were boiled at 95 °C for 10 min and allowed to cool down. Finally, the samples were loaded and resolved on polyacrylamide gels (see **section 2.8.1**).

2.11 LENTIVIRAL GENE DELIVERY AND GENERATION OF STABLE CELL LINES

2.11.1 Lentiviral production in HEK 293T packaging cell line

Lentiviral particles carrying C-terminally GFP- or RFP-tagged L-selectin were produced using HEK 293T packaging cell line and pCMVΔR8.91 or psPAX2 (envelope) and pMD.G (packaging) helper vectors. HEK 293T cells were plated one day prior to transfection at a density of 10 - 15 x 10^6 cells per dish (diameter of 14 cm). On the day of transfection 30 µg pCMVΔR8.91 or psPAX2, 10 µg pMD and 40 µg pHR'SIN-SEW-L-selectin-GFP (or –RFP) or pLenti CMV Puro DEST (w118-1) carrying sequences for Rho GTPase Raichu probes, were added to 4 mL OPTIMEM (GIBCO®, Invitrogen) in one tube and 1 µL of 10 mM polyethylene imine (PEI) was added to 4 mL of OPTIMEM in a second tube (the amounts of DNA and volumes of OPTIMEM and PEI described were for 1 dish of HEK 293T cells, and if more dishes were used, the reagents were adjusted accordingly). The tubes were mixed together and incubated in RT for 15 minutes. Culture media was aspirated off HEK 293T cells and the transfection mixture was added onto

the packaging cells in a dropwise manner (8 mL per dish). After 4 hours of incubation transfection media was aspirated and fresh media was added. Cell supernatants containing lentivirus particles were collected 48 hours after transfection (1st harvest), new media was added and then supernatant was collected again after 72 hours post-transfection (2nd harvest). Supernatants form both harvests were pooled and subsequently filtered with 0.45 µm filter (MILLEX® GP) and either frozen in -80ºC or concentrated by ultracentrifugation.

2.11.2 Lentivirus concentration

Lentiviral particles produced as described in **section 2.11.1** were concentrated by ultracentrifugation. Ultracentrifugation was performed in 11.5 mL tubes in TH641 rotor at 50, 000 xg (SORVALL® Discovery ultracentrifuge) for two hours at 4ºC. After ultracentrifugation, supernatant was decanted and 50 µL of RPMI (supplemented with 10% FCS (v/v) and 1% penicillin/streptomycin (v/v)) was added to a small yellowish pellet residing at the bottom of each tube and incubated on ice for 40 minutes. The pellets were then resuspended in the added volume, the volumes pooled together, aliquoted in 50 µL and stored in -80ºC until used. Concentrated virus was subsequently titrated before transduction of THP-1 cells took place.

2.11.3 Measuring lentiviral titres

In order to establish lentiviral titres, HEK 293T cells were plated in 24-well plates, at a density of 1 x 10^5 cells/well (day 0). On the day of transduction, HEK 293T cells were counted and serial dilutions of the concentrated lentivirus (10^{-6} to 10^{-1}) were added onto the cells (day 1). On day 2, media was changed and on the day 4 media was removed, cells taken off with trypsin/EDTA, resuspended in PBS and analysed in duplicates by flow cytometry. When lentiviral particles carrying L-selectin-GFP or Raichu CFP/YFP construct were titrated, percentage of positive cells was determined by obtaining direct FACS data of either GFP or YFP expression levels, respectively. When lentiviral particles carrying L-selectin-RFP were titrated, cells were first stained with mouse anti-L-selectin DREG56 antibody and then α-mouse secondary RPE-conjugated antibody and L-selectin expression was determined by obtaining flow cytometry data of the RPE fluorescence. Virus titre was established from cells that were ideally 1-30% transduced to ensure that multiple integrations were avoided and calculations were done within the linear range. Titres were calculated according to the following equation: T= PxN/DxV, where T = titre, P = GFP/YFP/RFP positive cells, D = dilution and V = volume. Titres for all the lentiviral particles generated throughout this project are shown in **Table 2.5**.

Lentiviral vector plasmid	Gene of interest	Titre (x 10^8 i.u./mL)

pHR´SIN-SEW	WT L-selectin-GFP	2.128
pHR´SIN-SEW	GFP	2.56
pHR´SIN-SEW	S364A L-selectin-GFP	2.18
pHR´SIN-SEW	S367A L-selectin-GFP	2.56
pHR´SIN-SEW	SSAA L-selectin-GFP	6.3
pHR´SIN-SEW	ΔM-N L-selectin-GFP	2.84
pHR´SIN-SEW	ΔM-N SSAA L-selectin-GFP	13.3
pHR´SIN-SEW	WT L-selectin-RFP	12.56
pHR´SIN-SEW	SSAA L-selectin-RFP	2.71
pHR´SIN-SEW	ΔM-N L-selectin-RFP	1.87
pHR´SIN-SEW	ΔM-N SSAA L-selectin-RFP	4.4
pLenti CMV Puro DEST (w118-1)	CFP/YFP RhoA Raichu probe	10.56
pLenti CMV Puro DEST (w118-1)	CFP/YFP Rac1 Raichu probe	9.2
pLenti CMV Puro DEST (w118-1)	CFP/YFP Cdc42 Raichu probe	9.1

Table 2.5 Lentivirus titres. The table shows titres in infection units (i.u.) per mL of all concentrated lentivirus suspensions generated throughout this research project. See **Abbreviations section** for abbreviations used.

2.11.4 Transduction of THP-1 cells

THP-1 cells were resuspended at the density of 0.4 x 10^6 cells/mL on a day prior to the transductions. The next day, 1 x 10^6 cells were harvested, centrifuged and resuspended in fresh media into which lentivirus suspension was added (total volume of media and lentivirus suspension was 1 mL). Volume of concentrated virus that was added per transduction was found on the basis of the titre and desired multiplicity of infection (MOI) accordingly to the following equation: (Number of cells transduced) x (MOI)/(Titre) = (mL of virus). The MOIs used were that of 5, 7 or 20. The cells were then placed in the CO_2 incubator at 37 °C and fed fresh media two days after the transduction. Four days after the transduction the entire media was replaced with fresh media.

2.12 CELLS AND CELL CULTURE

All cells were cultured in a 5% CO_2 incubator at 37°C.

2.12.1 THP-1 cells (Acute Monocytic Leukemia, human)

THP-1 cell line was purchased from American Type Culture Collection (ATCC). Cells were maintained in RPMI-1640 (GIBCO®, Invitrogen) medium supplemented with 10% FCS, 1% antibiotics (penicillin/streptomycin) and 0.05 mM β-mercaptoethanol (BME), referred to as “THP-1 media”. For cell line maintenance, cells were seeded at a density

of 0.3-0.5 x 10^6 cells/mL and split every 2-3 days when the density reached 0.7-0.9 x $10x^6$ cells/mL. Cells were seeded at 0.4 x 10^6 cells/mL one day prior to any given experiment.

2.12.2 HEK 293T cells (Human Epithelial Kidney cells)

HEK 293T cells were a kind gift from Dr Yolanda Calle (Cancer Division, King's College London). Cells were maintained in RPMI-1640 medium supplemented with 10% FCS and 1% antibiotics (penicillin/streptomycin). Medium was renewed every 2-3 days and cells were passaged with a subcultivation ratio of 1:3 to 1:6.

2.12.3 Human umbilical vein endothelial cells (HUVEC)

HUVEC were purchased from Lonza and were maintained in EGM-2 growth media supplemented with appropriate growth factors (Lonza) (**Table 2.1**), 10% FCS and 1% antibiotics (penicillin/streptomycin) in fibronectin-coated (10 µg/mL) tissue culture dishes (14 cm diameter). Cells were initially expanded for 6 passages. For passaging, media was aspirated and cells washed once with sterile PBS. Two millilitres of trypsin-EDTA (Sigma-Aldrich®, Germany) was added on to cells and the cells were incubated in a 5% CO_2 incubator at 37°C until all HUVEC cells detached from the plates. EGM-2 media was then added (8 mL) to neutralise the action of trypsin and the cells were centrifuged (SORVALL® Legend RT, U.K.) for 5 minutes at RT. Cell pellets were then resuspended in fresh EGM-2 media and seeded in to plastic tissue culture dishes. After 6 passages, HUVEC were cryopreserved (**section 2.12.4**) and were again re-cultured prior to the experiments. Media was changed in to fresh every second day, and cultures were used for experiments when reached confluence (3–5 days).

2.12.4 Cryopreservation of cells

Cells destined for cryopreservation were grown in log phase for a couple of days before freezing. Approximately 10 million cells were harvested, and the cell pellet was resuspended in 10% DMSO and 90% FCS (v/v) and placed in a single pre-cooled Corning® freezing vial. The vials were immediately placed on ice and transferred to -80 °C freezer. After 24 hours, vials were transferred to liquid nitrogen for long-term storage. For re-culturing, frozen cells were rapidly thawed in a water-bath at 37 °C and thawed suspension added to 9 mL of fresh cultivation media. After 5 minutes of centrifugation (SORVALL® Legend RT, U.K.), the cell pellets were resuspended in fresh media, placed into tissue culture flasks and flasks placed in the incubator for culturing.

2.13 FLOW CYTOMETRY

2.13.1 Technical equipment

All samples were analysed on a FACSCalibur flow cytometer (BD Biosciences). All fluorophores were excited at λ 488 nm and GFP and FITC fluorescence was detected at λ 530 nm (FL-1 channel) and RPE fluorescence was detected at λ 588 nm (FL-2 channel). Direct detection of RFP was not possible as the available flow cytometer was not equipped a laser capable of exciting RFP. Therefore, L-selectin-RFP-expressing cells were analysed by labelling with mouse anti-L-selectin DREG56 and then anti-mouse-FITC conjugated secondary antibody. Data were acquired and analysed with CellQuest™Pro Version 4.0.2 (BD Biosciences) acquisition and analysis software.

2.13.2 Antibody labelling procedure

All cells were labelled on ice in 96-well plates. Primary and secondary antibody incubations were 30 and 15 minutes in duration, respectively. All centrifugation was performed at 4°C and at 1200 rpm (SORVALL® Legend RT, U.K.) for 1 minute. All washes were performed using 10% FCS in HBSS (GIBCO®, Invitrogen) or THP-1 media (RPMI-1640 medium supplemented with 10% FCS, 1% penicillin/streptomycin and 0.05 mM BME) supplemented with 25mM HEPES to ensure Fc receptors blockage by FCS. After approximately 100,000 cells per sample were harvested, the cells were centrifugated, supernatant discarded, and cells were washed. THP-1 cells were subsequently labelled with either primary antibodies or appropriate IgG isotype control antibodies, all at 1:80 dilution in 50 µL. The cells were then washed three times and incubated with anti-mouse-RPE/FITC-conjugated secondary antibodies at 1:20 dilution in a 50 µL volume. After incubation with secondary antibodies, cells were washed three times, each sample resuspended in 150 µL of washing buffer/media and then added to 200 µL of PBS that had been pre-added to glass FACS tubes (BD Falcon™). The samples prepared in this way were subsequently analysed by flow cytometry. Analysis of cells were performed exclusively on the “live gate”. These were determined based on their distinctive scatter pattern. A minimum of 10,000 cells were counted for each sample in every experiment and samples were performed in triplicate. Data from shedding experiments are represented as percentage of L-selectin surface expression relative to untreated cells after adjustment for background fluorescence with control isotype-matched antibody-stained cells.

2.14 PARALLEL PLATE FLOW CHAMBER ASSAY

All cells were resuspended in THP-1 media (RPMI-1640 medium with 10% FCS, 1% penicillin/streptomycin and 0.05 mM BME) supplemented with 25 nM HEPES buffer prior

to the perfusion assays, referred to as “perfusion media”. HEPES is a CO_2-independent buffering system and its addition ensured that media pH was maintained at physiological levels during the perfusion assays where no CO_2 supply was present.
When interaction of THP-1 cells with HUVEC was analysed, HUVEC monolayer was grown to confluency and stimulated with 10 ng/mL TNF-α overnight.

2.14.1 Technical equipment

All experiments were performed in 37°C, 5% CO_2 incubator (SolentScientific) and visualized using Olympus IX81 time-lapse inverted fluorescence microscope connected to a Hamamatsu C10600 ORCA-R2 digital video camera. A Harvard syringe pump (Harvard Apparatus®, U.S.A) was used to generate a flow rate of 0.25 mL/min (corresponding to 1.24 dyn/cm^2, which is a physiological shear stress of the blood flow). Images were acquired into a video file (Volocity® Imaging software, Perkin Eelmer). Schematic of the parallel plate flow chamber as well as a photograph of assembled chamber can be seen in **figure 2.2**.

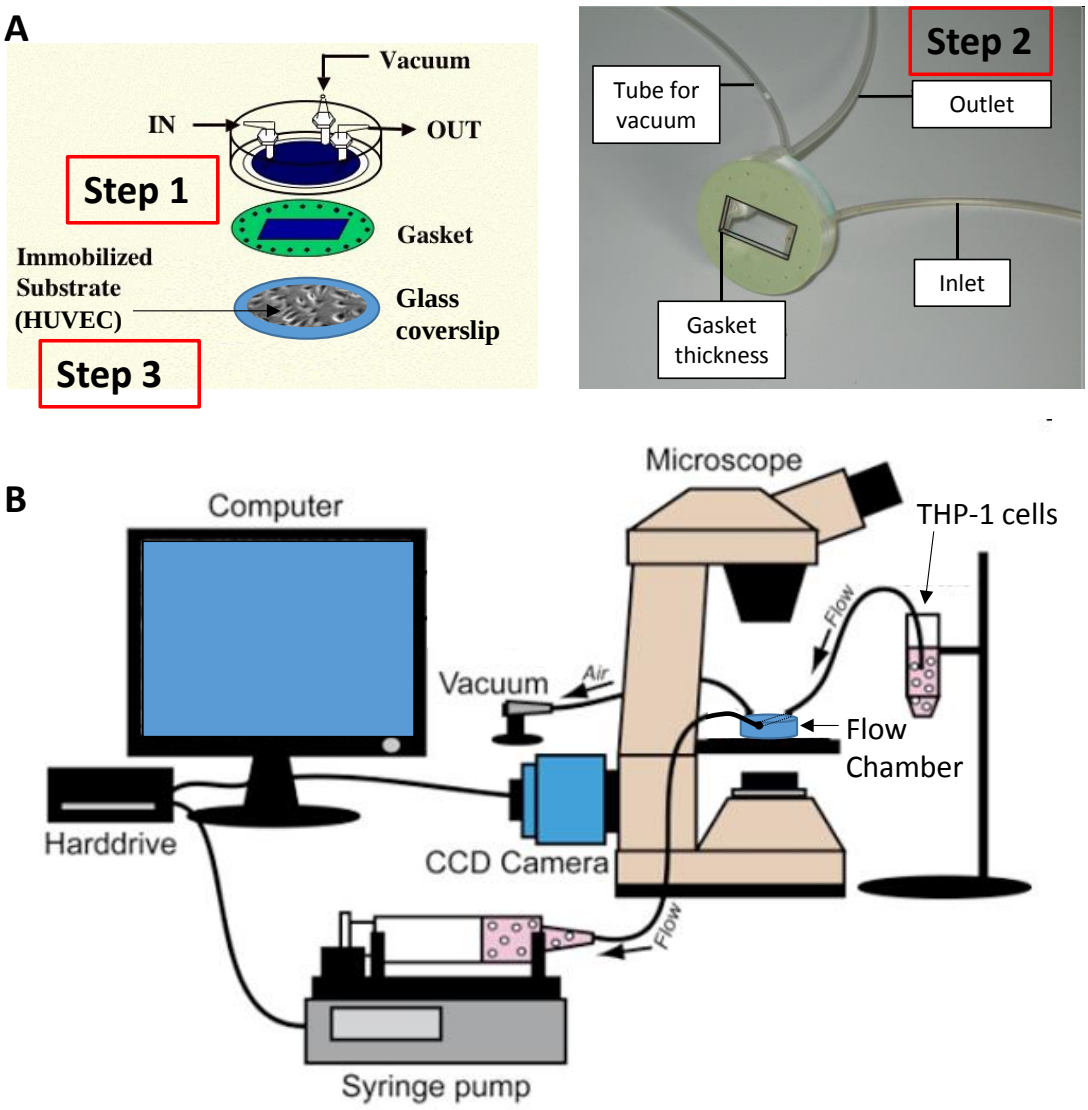

Figure 2.2 Parallel plate flow chamber system. A) Three steps of parallel plate flow assembly. *Step 1*: top part of the chamber containing inlet/outlet ports as well as a vacuum port was attached to the silicon gasket. *Step 2*: inlet, outlet and vacuum tubes were attached to their respective ports. *Step 3*: Vacuum force was applied and the apparatus was "sucked" onto a glass coverslip on which HUVEC cells were grown. **B)** Diagram illustrating the complete system used for the parallel plate flow chamber assay. In brief, the assembled chamber was placed over the objective of an inverted microscope in an environmental chamber heated to 37°C. A syringe pump applied suction force that drew the cell suspension through the chamber with a set flow rate (set by a syringe refill rate). The flow through waste was collected in the syringe. Video footage of the microscope image was recorded by a CCD (charge-coupled device) camera with video recorder connected to the computer acquired with Volocity visualisation and analysis software.

2.14.2 Cell co-perfusion experiments

Experiments were performed as co-perfusions where two THP-1 cell lines were co-perfused at 1:1 ratio. Prior to the flow chamber assays, one of the cell lines was labelled with 10 nM Cell Tracker® Green (Molecular Probes®, Invitrogen®, Paisley, U.K.) and the other with Cell Tracker® Orange (Molecular Probes®, Invitrogen®, Paisley, U.K.) in

HBSS (without serum) for 10 minutes in 37 °C. The cells were then harvested by centrifugation (SORVALL® Legend RT, U.K.), washed and resuspended in perfusion media at total density of 0.5 x 10^6 cells/mL. The cells were perfused over TNF-α activated HUVEC, grown in 6-well plastic dishes, for ten minutes. The footage was recorded from the moment the pump was switched on using a x4 objective, and four separate fields of view were acquired per experiment. Three frame-views per minute were acquired for the phase contrast, the GFP channel (to visualise Cell Tracker® Green) and the RFP channel (to visualise Cell Tracker® Orange). The footage was analysed using Volocity software (PerkinElemer, U.S.A). Number of recruited cells was counted manually.

2.14.3 Perfusion of cells for confocal microscopy, FLIM/FRET and pseudopod dynamics analysis

For these experiments HUVEC were grown on 35 mm diameter sterile glass coverslips (ThermoScientific, Germany) that were pre-coated with 10 µg/mL fibronectin. Cells in the perfusion media were perfused over TNF-α activated HUVEC at a density of 0.25 x 10^6 cells/mL and the footage was acquired for 15 minutes for three separate fields of view using x10 objective. Four frame-views per minute were acquired for the phase contrast and the GFP channel. In experiments where cells were pre-incubated with R0-31-9790 metalloprotease inhibitor, the inhibitor was added at a working concentration of 30 µM 30 minutes prior to the assay. After recording was completed, the coverslips were fixed with 4% paraformaldehyde (PFA) (w/v) for 20 minutes at room temperature, washed three times with PBS and processed either for analysis using confocal microscopy (**section 2.16)** or for FLIM analysis of FRET (**section 2.18**). The acquired footage was analysed using Volocity software (PerkinElemer, U.S.A). Analysis included manual counting of cells having one, two or multiple pseudopods. Additionally, still images were exported for the purpose of cell spreading area analysis using ImageJ® software (**section 2.15**).

2.15 CELL SPREADING AREA ANALYSIS

Video footage from time-lapse parallel-plate flow chamber experiments (**section 2.14.3**) was used to generate still images using Volocity software (PerkinElemer, U.S.A). Two stills were generated per field of view, corresponding to early and late time point of perfusion, respectively. Three fields of view were acquired per experiment and all experiments were repeated on three independent occasions. The images were loaded in to ImageJ® software (N.I.H., U.S.A.) and the scale was adjusted. At least 30 cells per one still image were analysed. Analysis was performed by outlining the cell shape with a drawing tool cursor, and the cell area measurements (in μm^2) were automatically generated by the ImageJ® software.

2.16 CONFOCAL MICROSCOPY

2.16.1 Technical equipment

Leica TCS SP5 confocal microscope (Leica Microsystems, Germany) was used to acquire all images. GFP was excited at λ = 488 nm with an Argon laser, whereas TRITC-phalloidin and Alexafluor®633 were excited with Helium-Neon lasers at λ = 543/568 and 633 nm, respectively. Images were acquired as single Z-planes or as series of Z-stacks.

2.16.2 Cell labelling procedure

For L-selectin-GFP visualisation, cells were perfused over TNF-α activated HUVEC as described in **section 2.14.3**. For biglycan visualisation HUVEC were grown to confluence and stimulated with TNF-α or left untreated. Cells were then fixed with 4% PFA in PBS (w/v) for 10 minutes at RT and washed 3 times with PBS. Nonident P-40 (NP40) (Fluka BioChemika) was then added at a concentration of 0.1% in PBS (v/v) for no more than 3 minutes in order to permeabilise the cells. Cells were subsequently washed three times in PBS and blocked with 5% BSA in PBS (v/v) for 40 minutes at room temperature. For early endosome antigen 1 (EEA1) and biglycan staining, samples were incubated with anti-EEA1 or anti-biglycan antibody in the blocking solution at 1:500 or 1:300 dilution, respectively, for 1 hour at room temperature. Samples were subsequently washed three times with PBS and TRITC-phalloidin (1:300 dilution) and appropriate Alexafluor®633-conjugated secondary antibodies (1:250 dilution) were added in a blocking solution. When no additional staining was performed, TRITC-phalloidin (1:300 in blocking solution) was added straight after the blocking step. Coverslips were stained at 4°C overnight. Following day, coverslips were washed three times with PBS and mounted on a microscopic slide with a use of fluorescent mounting media (DAKO).

2.16.3 Three-dimensional (3D) rendering

Z-stacks were acquired with Leica TCS SP5 confocal microscope with the scan speed of 200 Hz and 3 line averages per scan. Acquired z-stacks were saved as series of TIFF files and imported into Imaris imaging software (Bitplane AG, Switzerland). Three-dimensional (3D) reconstruction was performed manually using “Volume rendering” task for both green and red channels, which corresponded to L-selectin-GFP and TRITC-phalloidin-stained actin, respectively. Snapshot of the generated 3D image was taken and saved as a JPG photograph.

2.16.4 Analysis of L-selectin-GFP “spots”, “spikes” and “clusters”

THP-1 cells expressing either wild type or mutant L-selectin-GFP were perfused over TNF-α activated HUVEC as described in **section 2.14.3**. TRITC-phalloidin labelling

enabled visualisation of HUVEC actin cables and THP-1 cell protrusions positioned underneath the endothelial cells could therefore be identified. Single z-plane images were acquired with Leica TCS SP5 confocal microscope. To improve image quality, clarity, and accuracy and to reduce noise for single z-plane scans, the scan speed was reduced to 100 Hz and line averages were increased to 4 as compared to microscope settings used for z-stacks acquisition (**section 2.16.3**). One image per cell was acquired in order to obtain maximal possible magnification. Darkfield images of the GFP channel were loaded in to Volocity imaging software and only the protrusions were selected for analysis. Analysis was performed using "Find Spots" task, where manual adjustment of local fluorescence intensity minima were applied for each image. Clusters were identified as large bright L-selectin-GFP agglomerations. Spikes were counted manually. Fifteen cells were analysed per experiment and experiments were repeated three times for each cell line.

2.17 L-SELECTIN SHEDDING ASSAYS

2.17.1 Shedding in response to PMA and TNF-α stimulation

Cell stimulation with either PMA or TNF-α was followed by analysis of cell surface expression of L-selectin. In each case, approximately 100,000 cells were treated in 200 µL of medium. The medium used was either 10% FCS (v/v) in HBSS or the THP-1 media (RPMI-1640 medium supplemented with 10% FCS, 1% penicillin/streptomycin and 0.05 mM BME), and medium was supplemented with 25 mM HEPES. The stimulation was performed at 37ºC and 5% CO_2 for 30 minutes (PMA) or 1 hour (TNF-α). Levels of cell surface L-selectin were subsequently determined by flow cytometry as described in **section 2.13**. Experiments were performed in triplicate on at least three independent occasions.

2.17.2 Shedding during static transmigration assay

HUVEC monolayers were grown to confluence in 6-well plastic dishes and stimulated with 10 ng/mL TNF-α overnight. (2×10^5) were added in 1 mL of media per one well of HUVEC and incubated for 0, 5, 10, 20, 30 or 60 minutes. The supernatant (unbound THP-1 fraction) and HUVEC fraction (bound THP-1 fraction) were then harvested, washed once with PBS and lysed in appropriate volume of Cytobuster™ Protein Extraction Reagent supplemented with protease inhibitors cocktail (Sigma-Aldrich®, Germany). After x4 protein loading buffer addition and sample boiling at 95 °C (5 minutes), the samples were resolved on polyacrylamide gels as described in **section 2.8.1** and L-selectin-GFP was detected by Western blotting using anti–GFP antibody as described in **section 2.8.3**.

2.18 FLIM ANALYSIS OF FRET

2.18.1 Preparation and labelling of cells

In order to study clustering of L-selectin, THP-1 cells were double transduced with lentivirus carrying WT or mutant L-selectin-GFP followed by the lentivirus carrying WT or corresponding mutant L-selectin-RFP. These cells were referred to as GFP/RFP. GFP is an excellent donor molecule for FLIM is it exhibits mono-exponential decay kinetics. RFP acts as suitable acceptor for GFP as the excitation spectra overlaps with the emission spectra of GFP. When investigating clustering of L-selectin during TEM, HUVEC were seeded on to 35 mm diameter fibronectin-coated glass coverslips (ThermoScientific, Germany) and grown to confluency. Once confluent HUVEC were stimulated with 10 ng/mL TNF-α overnight. The GFP/RFP "double expressors" were perfused over TNF-α activated HUVECs for 15 minutes (for parallel flow chamber assays protocol see **section 2.14.3**) and then fixed with 4% PFA for 20 minutes at RT. For antibody-mediated "Inside-out" L-selectin clustering assays (see **section 2.19**), poly-L-lysine (PLL)-coated coverslips were prepared by applying neat PLL to the coverslip (100 µL) for 20 minutes at room temperature. Excess PLL was aspirated and the coverslips were left to dry overnight at room temperature. After antibody labelling, GFP/RFP cells were resuspended in PBS and plated on PLL-coated glass coverslips. Binding of cells to PLL were performed at RT for 5 minutes. Cells were then fixed with 4% PFA for 20 minutes at RT. After PFA fixation, the cells were washed 3 times with PBS. Subsequent permeabilisation of cells was perfomed with 0.1% NP40 in PBS (v/v) for no more than 3 minutes the cells were then washed three times with PBS. Sample was subsequently treated with 1 mg/mL of sodium boryhydride for 10 minutes. Sodium boryhydride is a reducing agent that decreases the background fluorescence, minimising "noise" during detection. Samples were subsequently blocked with 5% BSA (v/v) in PBS for 40 minutes at room temperature. For experiments investigating L-selectin clustering during TEM, Alexafluor®633-phalloidin in at 1:300 dilution in the blocking solution was added. Actin staining with Alexafluor®633-phalloidin enabled visualisation of HUVEC actin cables. This allowed identification of the z-planes at which THP-1 cells were positioned in respect to the endothelial cells (i.e. on top or underneath the HUVEC monolayer). For experiments investigating "Inside-out" L-selectin clustering, donkey anti-goat Alexafluor®633-conjugated tertiary antibody was added in blocking solution at 1:100 dilution. Samples were stained at 4°C overnight. The glass coverslips were washed three times with PBS and then mounted on the microscopic slides (ThermoScientific, Germany) with a use of fluorescent mounting medium (DAKO). Mounted slides were dried at 37°C for one hour and then placed in a dark box and stored at +4ºC until analysis of protein interactions by fluorescence lifetime imaging microscopy (FLIM) measurement

of FRET was performed. All image collection and data analysis were performed by Dr Maddy Parsons (Randall Division of Cell and Molecular Biophysics, King's College London).

2.18.2 Technical equipment and data analysis

FLIM measurement of FRET was performed with a multi photon microscope system as described previously [153, 402]. A Nikon TE2000E inverted microscope combined with an in-house scanner and Chameleon Ti:Sapphire ultrafast pulsed multiphoton laser (Coherent) was used for excitation of GFP (at 890nm). Fluorescence lifetime imaging capability was provided by time-correlated single photon counting electronics (Becker & Hickl, SPC 700). A 40x objective was used throughout (Nikon, CFI60 Plan Fluor N.A. 1.3) and data were acquired at 500 ± 20 nm through a bandpass filter (Coherent Inc. 35-5040). Acquisition times of the order of 300 s at low excitation power were used to achieve sufficient photon statistics for fitting, while avoiding either pulse pile-up or significant photobleaching. Data were analysed as previously described [153, 402]. The FRET efficiency is related to the molecular separation of donor and acceptor and the fluorescence lifetime of the interacting fraction by:

$$\eta_{FRET} = (R_0^6/(R_0^6 + r^6)) = 1 - \frac{\tau FRET}{\tau d}$$

Where η_{FRET} is the FRET efficiency, R_0 is the Förster radius, r the molecular separation, $\tau FRET$ is the lifetime of the interacting fraction and τd the lifetime of the donor in the absence of acceptor. The donor only control is used as the reference against which all other lifetimes are calculated in each experiment. $\tau FRET$ and τd can also be taken to be the lifetime of the interacting fraction and non-interacting fraction, respectively. Quantification was made from all pixels within each cell was analysed. All image collection and data analysis was performed by Dr Maddy Parsons (Randall Division of Cell and Molecular Biophysics, King's College London) using TRI2 software (developed by Dr Paul Barber, Gray Cancer Institute, London, U.K.). Cell line generation, staining and slide preparation was performed by me, Karolina Rzeniewicz. FLIM data presented in this thesis is shown as histograms showing mean FRET efficiency from the stated n number of cells from 3 independent experiments, +/- standard error of the mean (S.E.M). Statistical differences between various populations were calculated by One-way ANOVA.

2.19 ANTIBODY-MEDIATED CROSS-LINKING ASSAYS

For investigation of "inside-out" signalling leading to L-selectin clustering, THP-1 cells (1 x 10^5) double expressing wild type or mutant forms of L-selectin-GFP/RFP were used. For analysis of Rho GTPase biosensor activity 1 x 10^5 THP-1 cells expressing WT or ΔM-N L-selectin-RFP and/or CFP/YFP RhoA, Rac1 or Cdc42 biosensors were used. Cells washed once with wash media (THP-1 media – RPMI-1640 medium with 10% FCS, 1% penicillin/streptomycin and 0.05 mM BME – supplemented with 25 nM HEPES) and incubated with antibodies against extracellular epitopes of L-selectin, PSGL-1, JAM-1, CD43, CD44 or PECAM-1 (1:50 dilutions in THP-1 media (v/v) supplemented with 25mM HEPES). All antibodies were of the same stock concentration (**table 2.2**). Alternatively, the cells were incubated with just THP-1 media. After 30 minutes at 4°C, the cells were washed three times with wash media and incubated with appropriate secondary antibodies conjugated to Alexafluor®633. After further 30 minutes incubation at 4°C, the cells were resuspended in 100 µL PBS and added on to glass coverslips (diameter of 13 mm, thickness No. 0, VWR International, U.K.) pre-coated with poly-L-Lysine (PLL). PLL-coated coverslips were prepared by applying neat PLL to the coverslip (100 µL) for 20 minutes at room temperature. Excess PLL was aspirated and the coverslips were left to dry overnight at room temperature. After 5 minutes of incubation at room temperature, the excess cells were aspirated off the coverslips and coverslips were fixed with 4% PFA (w/v) and labelled for FLIM analysis of FRET as described in **section 2.18.1**.

2.20 TRANSWELL MIGRATION ASSAYS

Transwell chambers (6.5 mm with 5.0µm Pore Polycarbonate Membrane Insert, Corning) were used in all assays. When investigating transmigration through HUVEC, the filters were coated with 10 µg/mL fibronectin (FN) for 1 hour at 37°C, then excess FN was aspirated and 2.5 x 10^4 HUVEC cells were seeded per filter. HUVEC were grown to confluence and stimulated with 10 ng/mL TNF-α on an evening prior to the experiment. Appropriate concentrations of chemoattractants were prepared in 0.1% BSA in RPMI (v/v). Either 0.1% BSA in RPMI (v/v), 50 ng/mL MCP-1 or increasing (0,1, 3 ,50 ,100) ng/mL CXCL-1 chemoattractants (600 µm) were added to the lower compartments of the transwell. THP-1 cells were harvested and resuspended in 0.1% BSA in RPMI (v/v) at 1 x 10^6 cells/mL. When investigating migration towards MCP-1, in some experiments the cells were resuspended in 0.1% BSA in RPMI (v/v) supplemented with 50 ng/mL MCP-1. This created environment each in MCP-1 but devoid of gradient and was used to investigate if cell migration was due to cell chemokinesis (directional movement) or chemotaxis (random movement). This technique is known as checkboard analysis. Prepared cell suspension (300 µL) was mixed with 300 µL of THP-1 media (RPMI-1640

medium supplemented with 10% FCS, 1% penicillin/streptomycin and 0.05 mM BME) and kept in 37°C, 5% CO_2 until the migration assay was completed. These were referred to as “input”. Next, the rest of the prepared cell suspension was added to the upper compartments (300 µL per each well) of the transwell chamber and allowed to transmigrate for 2 hours and 15 minutes at 37°C, 5% CO_2, and were subsequently analysed by flow cytometry. Briefly, 600 µL of 0.1% BSA in RPMI (v/v) (with or without chemoattractant), containing transmigrated cells were harvested from each lower compartment. Number of events was recorded for one minute and the acquired value divided by the value obtained for “input”. This allowed determination of the percentage of transmigrated cells. All the experiments were performed in triplicates on three independent occasions.

2.21 STATISTICAL EVALUATION

All quantified data were collected and processed in Microsoft® EXCEL 2007 (or higher) (Microsoft Corporation, U.S.A). Statistical evaluation was performed using GraphPad Prism® version 5.02b (or higher) for Windows (GraphPad Software, U.S.A.) with which bar and line graph plots were also generated. Statistical tests used to determine significant differences were unpaired, two-tailed t-tests and one-way ANOVA (followed by Dunnett’s or Tukey’s post-tests), where mentioned in text. Differences were considered significant when $p < 0.05$.

CHAPTER 3. GENERATION AND CHARACTERISATION OF A MONOCYTE CELL LINE STABLY EXPRESSING L-SELECTIN TAGGED TO GREEN FLUORESCENT PROTEIN (GFP)

3.1 INTRODUCTION

Monocytes are cells of crucial importance in the outcome of both acute and chronic inflammation (**section 1.6**). L-selectin has been reported to play a role in monocyte recruitment to the inflamed venules at the site of infection [631], to the HEV of secondary lymphoid organs during an inflammatory response [56], to the activated endothelium *in vitro* [410, 460] and to atherosclerotic lesions *in vivo* [299]. However, the molecular mechanisms by which L-selectin exerts its function(s) during the adhesion cascade, particularly in respect of signalling, remain poorly understood. The fact that L-selectin expression has been observed in emigrated monocytes, but not neutrophils, in a thioglycollate-induced model of peritonitis, strobly suggests that this cell adhesion molecule retains the capacity to function and signal during TEM [527].

As described in **section 1.7.5.2**, the current methods used to visualise the cellular distribution of L-selectin rely on labelling of L-selectin with fluorescently conjugated mAbs. This approach poses a serious risk to proper data interpretation as engagement of L-selectin with mAbs has been shown to trigger L-selectin signalling and lead to various cellular responses (**section 1.11** and **table 1.3**). It was therefore decided that tagging L-selectin with green fluorescent protein would help address the aforementioned issue. In other words, it would provide a “non-invasive” method to monitor the spatio-temporal distribution of L-selectin during the adhesion cascade.

Two monocytic cell lines were considered for this study: THP-1 and U937. Both cell lines are immortalized human monocyte cell lines that are commonly utilised in leukocyte research. Interestingly, U937 cells have been previously used to stably express L-selectin but the study was limited to investigating the adhesion to endothelial monolayers under flow conditions and transendothelial migration was not investigated [410]. It could be suggested that, more importantly, the U937 cell line is a monoblast leukemia cell line and as a result exhibits a less mature monocytic phenotype than the THP-1 cell line, which is a monocytic leukemia cell line [632]. As a result THP-1 cells were chosen to serve as a model cell line for the studies presented in this thesis. In order to express fluorescently tagged L-selectin in THP-1 cells, a lentiviral transgene delivery system was chosen and stable cell lines were generated.

The cytoplasmic tail of L-selectin is only 17 amino acid long, and green fluorescent protein (GFP) is relatively large having 238 amino acids [633]. It was therefore of high importance to establish if GFP-tagging of L-selectin tail caused any adverse effects on

L-selectin expression, form and function. Hence, the hypothetical influence of the GFP tag on the behaviour of L-selectin was rigorously tested.

This chapter describes the successful generation of monocyte THP-1 cell lines stably expressing GFP-tagged to the C-terminus of L-selectin and control THP-1 cell line expressing GFP alone. The results outlined in the latter sections of this chapter show that L-selectin-GFP chimera stably expressed by THP-1 monocytes exhibited correct localisation, and no overt alterations in physiological characteristics as compared with wild type L-selectin.

3.2 EXPERIMENTAL DESIGN

As described in **section 3.1**, in order to analyse the subcellular distribution of L-selectin in monocytes during the leukocyte adhesion cascade, it was decided that the THP-1 monocyte cell line would be used to express fluorescently tagged L-selectin. THP-1 cells were purchased from the American Type Culture Collection (ATCC) to guarantee the true identity of the cell line. When choosing tags to be linked to the protein of interest, two options are available: C- and N-terminal tags. L-selectin is a type I transmembrane protein, which means N-terminal tagging would ligate GFP to the extracellular domain and C-terminal tagging would ligate GFP to the cytosolic tail. As described in **section 1.7.1**, the very N-terminal part of L-selectin comprises the ligand-binding lectin domain and thus fusing a tag on this side would likely interfere with L-selectin functionality, as well as appropriate delivery to the plasma membrane (as the very N-terminus contains the pro-domain and leader sequence for membrane targeting). In conclusion, the favoured position for tagging L-selectin with a fluorescent tag was at the C-terminal cytoplasmic tail.

Two ways of protein expression can be achieved in cells: transient and stable. The obvious advantage of the latter method is a long-term protein expression. The stable expression also prevents any adverse effects that might be caused by transiently transfecting cells. In addition, transient transfection is highly ‘stressful” for the cell and requires subjection to high voltage. Stressed cells often shed their L-selectin. Therefore it was decided to achieve stable expression of fluorescently tagged L-selectin in THP-1 monocytes.

Lentiviruses are known to infect leukocytic cell lines with high efficiency and were chosen as a transgene delivery method for stable cell line generation. Human L-selectin cDNA was cloned into the lentiviral backbone plasmid carrying open reading frames (ORF) of enhanced GFP (eGFP, hereafter referred to as GFP) or red fluorescent protein (RFP), and lentiviral particles were produced in HEK 293T cells. Transduction and subsequent fluorescence-associated cell sorting (FACS) of THP-1 cells were used to generate uniform monocytic cell lines stably expressing fluorescently-tagged L-selectin.

In order to test the potential influence of the GFP tag on L-selectin expression and biological activity, a series of experiments was designed. L-selectin-GFP expression and cellular localisation were tested by fluorescence microscopy, flow cytometry analysis, scanning electron microscopy and Western blotting. Upon cell activation, L-selectin undergoes proteolytic ectodomain cleavage (commonly termed "shedding", **section 1.9.2**) [326, 419, 495, 496, 515, 521, 529], and this property was tested using a number of known shedding activators, both artificial and physiological. The sheddase inhibitor was also used to assess basal L-selectin-GFP turnover that is known to occur physiologically under resting conditions [521, 544]. Furthermore, the interaction of the L-selectin cytoplasmic tail with its binding partner calmodulin was analysed in "pull-down" assays. Finally, the ability of L-selectin-GFP to mediate interaction with its ligands under flow was tested in parallel-plate flow chamber assays. The tetrasaccharide, slialyl Lewis X (sLe^x), is a physiological L-selectin ligand and therefore the ability of THP-1 cells stably expressing L-selectin-GFP to interact with immobilised sLe^x under flow was examined. Importantly, U937 monocytic cell line and human primary monocytes are known to interact with cytokine-activated human umbilical endothelial cells (HUVEC) in L-selectin-dependent manner [410]. HUVEC are used routinely in the Ivetic laboratory as a model to study primary vascular endothelial cells. Hence, the interaction of THP-1 cells expressing L-selectin-GFP with cytokine-activated HUVEC was also analysed. Overall, the experimental design ensured that the functionality of L-selectin-GFP fusion protein was thoroughly analysed.

3.3 RESULTS

3.3.1 Generation of cell lines stably expressing wild type L-selectin-GFP

3.3.1.1 Cloning of human L-selectin cDNA into pHR´SIN-SEW lentiviral backbone vector

Human wild type (WT) L-selectin cDNA was amplified by PCR from pCMV6-AC-GFP vector (OriGene) (**figure 3.1 A**). PCR primers were designed with BamHI and XhoI restriction sites engineered at 5´ and 3´ ends, respectively. Insertion of the WT L-selectin cDNA was obtained with pHR´SIN-SEW-GFP or pHR´SIN-SEW-RFP lentiviral vectors that were acquired as a kind gift from Professor Adrian Thrasher (Institute of Child's Health, UCL) (**figure 3.1 B**). The ORFs of generated pHR´SIN-SEW-L-selectin-GFP and pHR´SIN-SEW-L-selectin-RFP lentiviral vectors were subsequently sequenced (**figure 3.1 C**) and the vectors were named pHR´SIN-SEW-L-selectin^{WT}-GFP and pHR´SIN-SEW-L-selectin^{WT}-RFP, respectively (for the details of the cloning procedure see **section 2.3**). At this stage pHR´SIN-SEW-L-selectin^{WT}-RFP plasmid was frozen for future

experiments and pHR´SIN-SEW-L-selectin^{WT}-GFP plasmid was used to generate the lentiviruses.

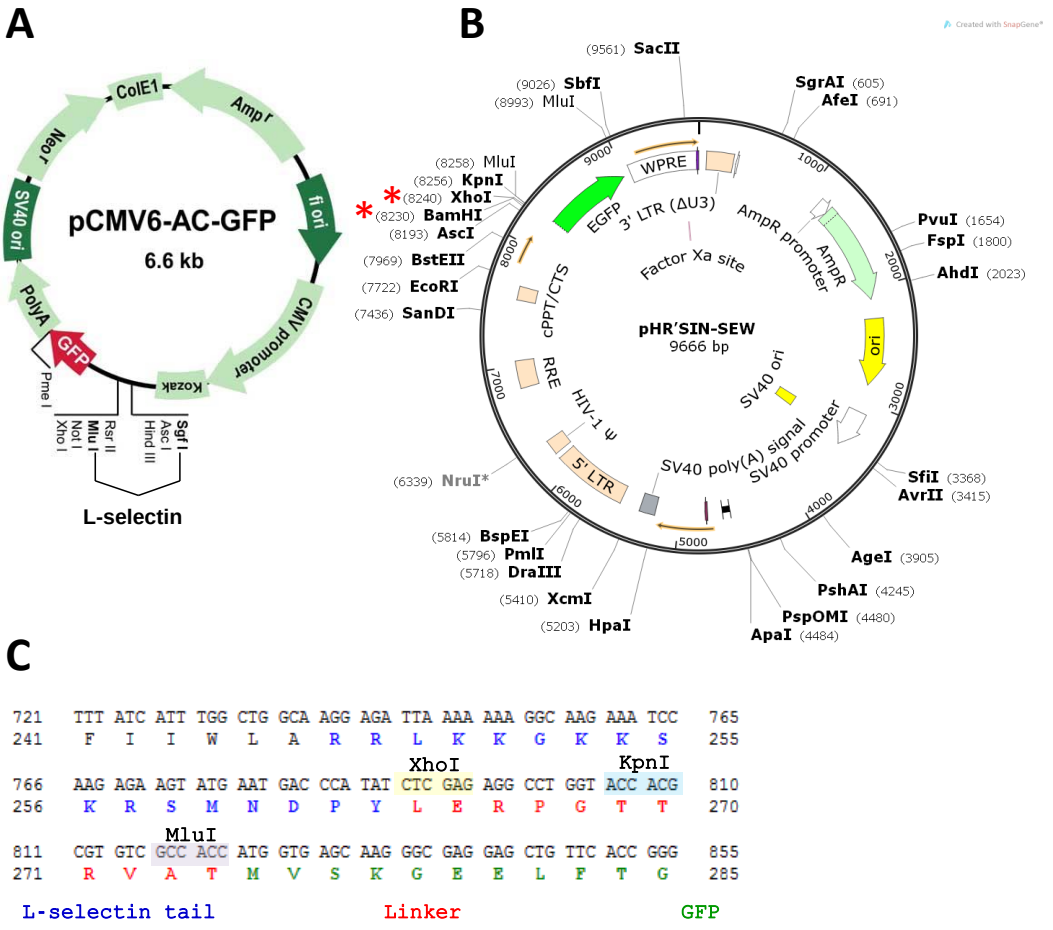

Figure 3.1 Cloning of L-selectin cDNA into lentiviral expression vector. A) Plasmid map of pCMV6-AC-GFP vector, supplied by OriGene. L-selectin ORF (ORF size: 1119 bp) is present between SgfI and MluI cloning sites. L-selectin cDNA was amplified from pCMV6-AC-GFP vector using PCR primers designed with BamHI and XhoI restriction sites engineered at 5´ and 3´ends, respectively. Image taken from from OriGene (OriGene Technologies, I. pCMV6-AC-GFP. Vol. 2010./ http://www.origene.com/destination_vector/PS100010.aspx). **B)** Map of pHR´SIN-SEW lentiviral vector carrying GFP C-terminal tag (pHR´SIN-SEW-GFP). Vector was double digested with BamHI and XhoI restriction enzymes (cleavage sites shown by red stars) and ligated with the PCR product amplified as described in A). Vector map was created using SnapGene® software on the basis of the sequence provided by Professor Adrian Thrasher (Institute of Child's Health, UCL). **C)** Multiple cloning site of pHR´SIN-SEW vector carrying WT L-selectin-GFP. The sequence shows wild type L-selectin (17 amino acid C-terminal tail of L-selectin is shown in blue) successfully cloned into the pHR´SIN-SEW-GFP vector (termed pHR´SIN-SEW-L-selectin^{WT}-GFP). Sequence shown in red represents the linker between L-selectin and GFP. Sequence shown in green represents GFP. XhoI restriction site used for cloning is highlighted in yellow and KpnI and MluI restriction sites present within the linker are highlighted in blue and purple, respectively. An identical cloning strategy was used to insert L-selectin gene into the pHR´SIN-SEW-RFP vector yielding pHR´SIN-SEW-L-selectin-RFP construct.

3.3.1.2 Lentiviral particle generation using HEK 293T packaging cell line

The lentiviral transgene delivery system is well known for producing stable cell lines with high efficiency of transduction. The main advantages of this system are long-term transgene expression that results from stable integration to the host genome, and little or no toxicity. Long-term expression enables re-using of generated cell lines and therefore ensures reproducibility between experiments. As a comparison, transient transfections of cells have generally low reproducibility and could also cause adverse effects. When deciding on lentiviral transgene delivery system, one needs to be aware of the associated risks. These are the potential of production of replication-competent viruses and oncogenesis. To address those health and safety issues, multiple plasmids are commonly used when generating lentiviruses. The very packaging system used in this thesis is known as a second generation packaging system. In this system the "transfer" vector carries the gene of interest and contains the sequences that will incorporate into the host genome. Viral genes necessary for assembly of functional viruses are split between two "helper plasmids". The viral particles assembled in this way carry only the sequences encoded by the transfer plasmid and are incapable of replication. This ensures that, upon transduction, the host cells are unable to produce functional viruses as the genes encoded by the helper plasmids are no longer present. Although this approach greatly improves the safety of lentivirus generation, critical care should still be taken when working with these vectors. A simple schematic, describing the steps of lentivirus generation, is shown in **figure 3.2**, and the method is described in detail in **section 2.11.1** of this thesis. In brief, HEK 293T packaging cells were transfected with transfer pHR'SIN-SEW-L-selectin^{WT}-GFP lentivirus backbone vector and two helper plasmids: "envelope" pMD2.G (carrying genes encoding envelope protein VSV G) and "packaging" psPAX2 (carrying HIV gag, pol, rev, and tat genes) (**figure 3.2** *step 1*). The assembled lentiviral particles released in to the supernatant of 293T HEK cells were harvested 48 hours and then again 72 hours post-transfection (**figure 3.2** *step 2*), pooled, and the concentrated lentivirus of a known titre was used to transduce target THP-1 cells (**figure 3.2** *step 3*). A detailed protocol describing lentivirus concentration can be found in **section 2.11.2** of this thesis.

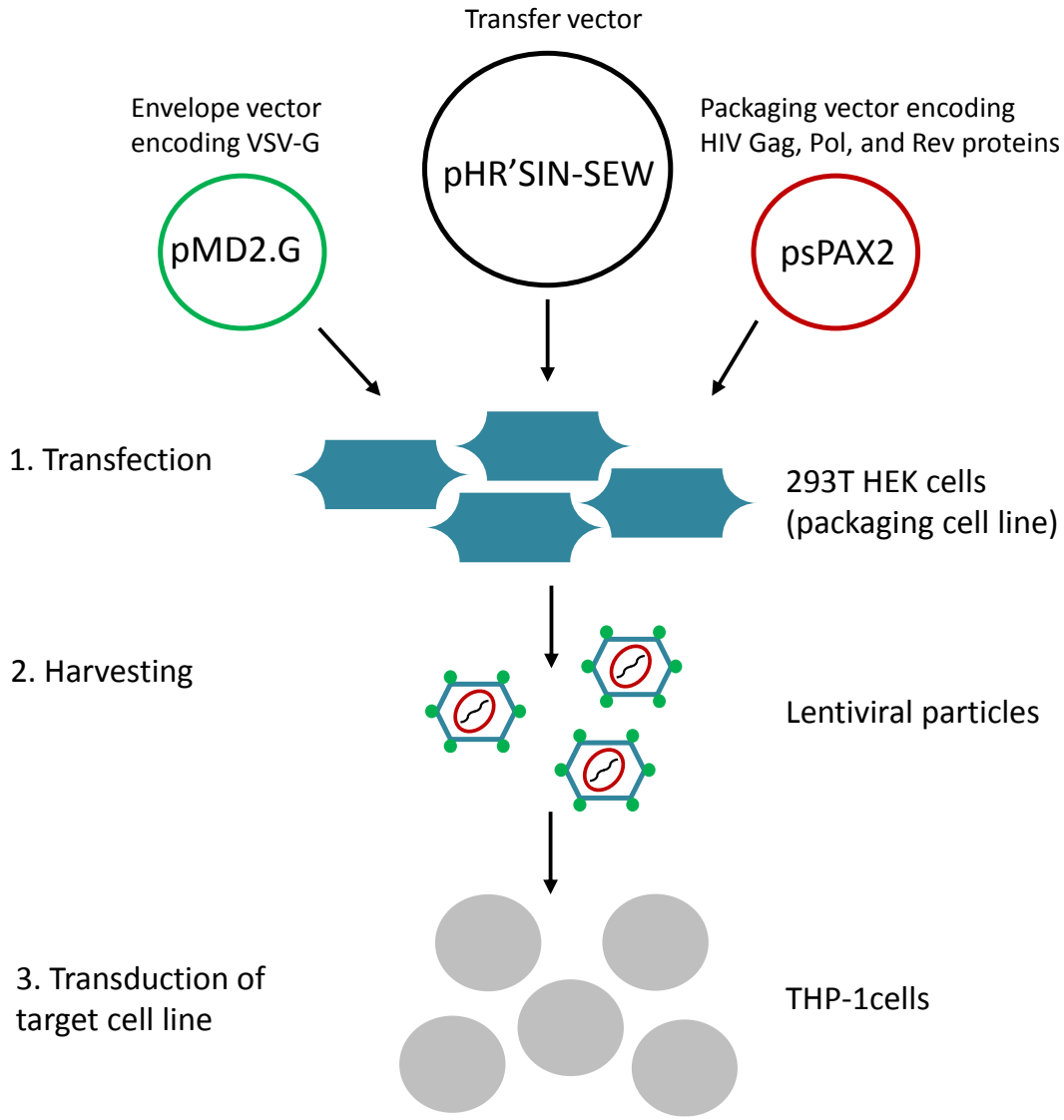

Figure 3.2 Lentiviral transgene delivery system. Lentiviral vectors were generated by cotransfection of a packaging cell line (HEK 293T) with the pHR´SIN-SEW transfer plasmid carrying L-selectin-GFP or –RFP transgene, and two helper plasmids **(1)**. Helper plasmids psPAX2 and pMD2.G encode structural and envelope proteins, respectively. Genome of a lentiviral particle produced by HEK 293T cells encoded sequences from the pHR´SIN-SEW transfer plasmid only. After the incubation period (48 and 72 hours), the lentiviral particles released into HEK 293T cells supernatant were harvested **(2)**, concentrated by ultracetrifugation and used to transduce target THP-1 cells **(3)**. VSV-G, the vesicular stomatitis virus G protein; HIV, human immunodeficiency virus, Gag, gene encoding group specific antigen; Pol, viral polymerase; Rev, regulator of expression of virion proteins.

The lentivirus titre, defined as the number of infectious units per mL (i.u./mL), was established by serial dilution (0, 10^{-6}, $10^{-5,}$ $10^{-4,}$ $10^{-3,}$ $10^{-2,}$ 10^{-1}) of the concentrated lentivirus stock to infect a given number of HEK 293T cells. The titre was determined by analysis of GFP-tag expression by flow cytometry. **Figure 3.3** shows the steps that were undertaken to calculate the lentivirus titre and the titration method is described in more detail in **section 2.11.3**. Firstly, the percentage of GFP positive (GFP+) cells versus the

dilution of the lentivirus stock was plotted (**figure 3.3** *i*). This was then used to determine the dilutions resulting in no more than 30% of transduction efficiency, and those dilutions were further used to determine the linear range of transduction (**figure 3.3** *ii*). Using the dilutions placed within the linear range assured that multiple lentiviral integrations were avoided when calculating the titre. Equation 1 (**figure 3.3** *iii*) was used to calculate the titre of the lentivirus carrying WT L-selectin-GFP transgene, which was established to be 2.128 x 10^8 i.u./mL.

i. Serial dilution.

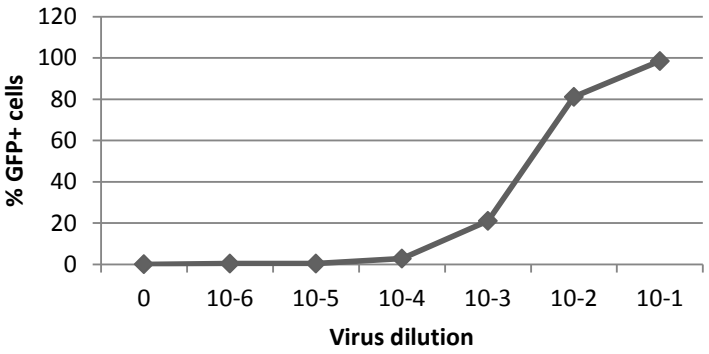

Dilution	%GFP+ cells
0	0
10^{-6}	0.435
10^{-5}	0.415
10^{-4}	2.8
10^{-3}	21.065
10^{-2}	81.08
10^{-1}	98.445

ii. Linear range.

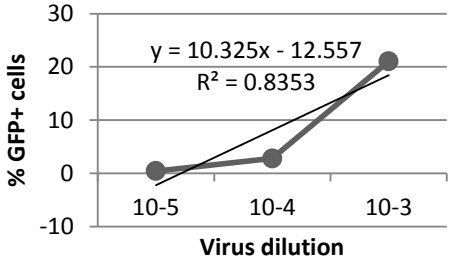

Dilution	%GFP+ cells
10^{-5}	0.415
10^{-4}	2.8
10^{-3}	21.065

iii. Titer calculation.

Equation 1

$$T = \frac{PN}{DV}$$

- **T** Titer (infection units per millilitre, i.u./mL)
- **P** Per-cent of transduced cells
- **N** Number of cells at the day of transduction
- **D** Lentivirus dilution
- **V** Volume of lentivirus added (mL)

Dilution	Titer
10^{-5}	292575000
10^{-4}	197400000
10^{-3}	148508250

Average titer:
2.128 x 10^8 i.u./mL

Figure 3.3 Titration of lentiviral particles containing pHR´SIN-SEW vector carrying WT L-selectin-GFP construct. (i) HEK 293T cells were transduced with serial dilutions (0, 10^{-6}, 10^{-5}, 10^{-4}, 10^{-3}, 10^{-2}, 10^{-1}) of the concentrated lentivirus suspension and the percentage of GFP positive (GFP+) cells was established by flow cytometry. **(ii)** Lower-end dilutions were used to determine linear range in order to avoid multiple integrations. **(iii)** Lentiviral titre was calculated using the Equation 1 for all the linear range dilutions.

3.3.1.3 Lentivirus mediated transduction of THP-1 cells

In order to achieve reproducible levels of protein expression, the "multiplicity of infection" (MOI) is used as a quantitative unit of measure when transducing cells with lentiviral particles. MOI defines the number of infectious units (lentiviral particles) delivered per target cell. It was decided that 5 and 20 would be used to represent low and high, respectively, MOIs when transducing THP-1 cells with lentiviral particles carrying the WT L-selectin-GFP transgene.

To achieve MOI of 5 and MOI of 20, volumes of lentivirus stock were calculated according to the Equation 2 (**figure 3.4**) where 1 x 10^6 THP-1 cells were inoculated with the lentivirus stock of a titre of 2.128 x 10^8 i.u./mL (as calculated in **section 3.3.1.2.**). The detailed method of THP-1 cell transduction is described in **section 2.11.4**.

Transduced THP-1 cells were termed low expressor "THP-1 WT L-selectin-GFP MOI 5" and high expressor "THP-1 WT L-selectin-GFP MOI 20". Generated cell lines were maintained in culture until a sufficient number had expanded which allowed sorting of the cells into uniform-expressing populations. This was performed to enrich the cell populations expressing the transgene, and also to ensure consistency and reproducibility of future experiments. Unsorted parental cell populations would exhibit variations in the percentage of L-selectin positive cells and unmatched expression levels. This could severely impair interpretation of any future results as L-selectin expression levels is an important factor for its adhesiveness [634]. Thus, unsorted low and high expressors were taken to a core-funded FACS sorting facility, and were sorted in to uniform populations termed THP-1 WT L-selectin-GFP Lo5 and THP-1 WT L-selectin-GFP Hi20, respectively. Four cell lines: low expressors: unsorted THP-1 WT L-selectin-GFP MOI 5 and sorted THP-1 WT L-selectin-GFP Lo5, and high expressors: unsorted THP-1 WT L-selectin-GFP MOI 20 and sorted THP-1 WT L-selectin-GFP Hi20, were then examined by fluorescence microscopy to assess L-selectin-GFP expression. Images of both phase contrast and GFP channel were acquired and representative images of each cell type are shown in **figure 3.4**. No GFP signal could be detected in control untransduced THP-1 cells (**figure 3.4 A**), suggesting THP-1 cells have negligible autofluorescence in the FL1 channel (that detects GFP). In transduced cells, the average percentage of green cells per field of view was determined by analysing images acquired for five different fields of view per cell line. As expected, transduction with MOI of 20 resulted in higher average percentage (67%) of green cells (**figure 3.4 D**) than transduction with MOI of 5 (38%) (**figure 3.4 B**).

Equation 2

$$MOI = \frac{VT}{N}$$

MOI Multiplicity of infection
T Titer (infection units/mililiter; i.u./mL)
N Number of cells to be transduced
V Volume of lentivirus to be added (mL)

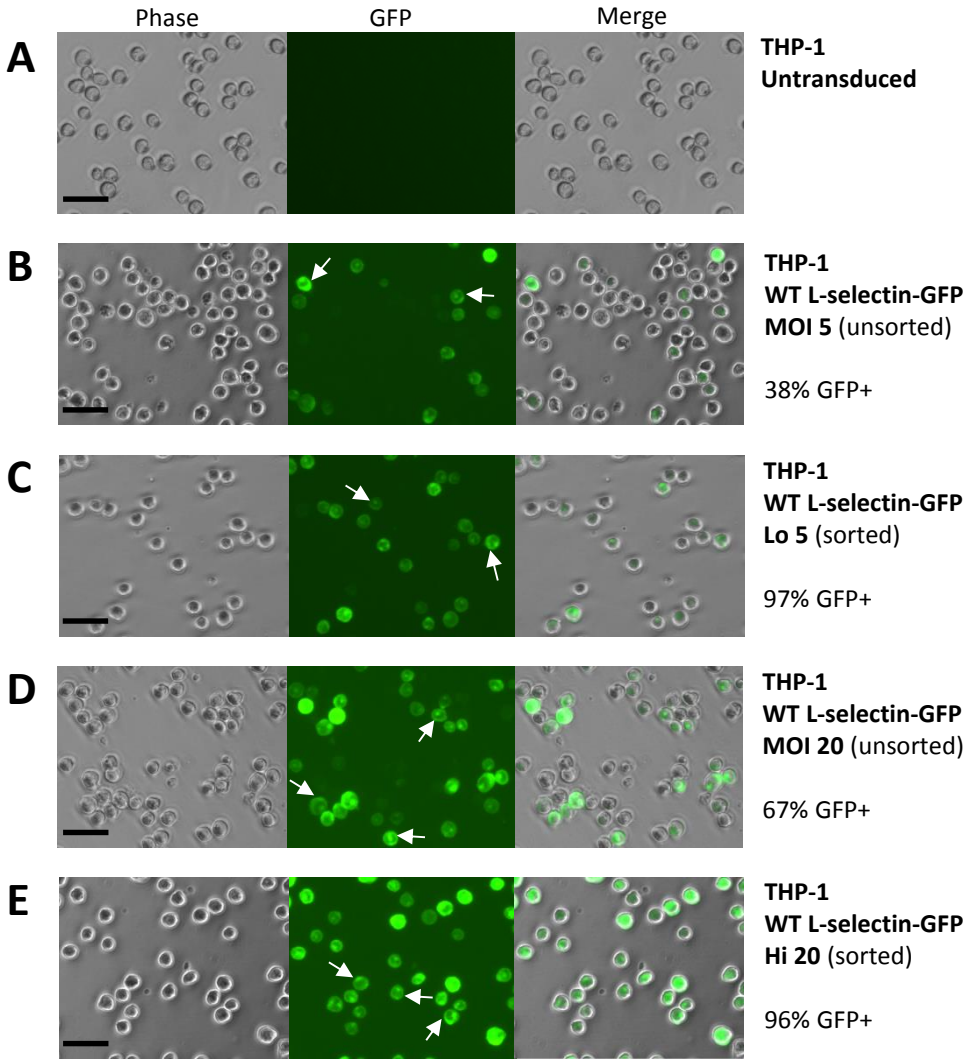

Figure 3.4 Generation of THP-1 cell lines expressing L-selectin-GFP. Equation 2 was used to calculate volume of lentivirus suspension that would transduce 1 x 10^6 THP-1 cells. Low and high multiplicities of infection (MOI), MOI 5 and MOI 20, respectively, were used to transduce THP-1 cells with lentiviral particles carrying pHR´SIN-SEW-L-selectin^{WT}-GFP. THP-1 WT L-selectin-GFP MOI 5 and THP-1 WT L-selectin GFP MOI 20 cell lines were obtained as low and high L-selectin-GFP expressors, and FACS was used to sort them into uniform populations termed THP-1 WT L-selectin-GFP Lo5 and THP-1 WT L-selectin-GFP Hi20 , respectively. Fluorescence microscopy was used to detect GFP and establish the extent of transduction as a percentage of GFP positive (GFP+) cells. **A)** No GFP signal in untransduced THP-1 cells. **B)** Unsorted low expressor cell line where average 38% GFP+ cells were detected. **C)** Sorted, uniform low expressor cell line having average 97% GFP+ cells. **D)** Unsorted high expressor cell line with average 67% GFP+ cells. **E)** Sorted, uniform high expressor cell line where average 96% GFP+ cells were detected. Percentage of GFP+ cells was calculated as an average obtained from five different fields of view. Arrows in B-E show localisation of L-selectin to the plasma membrane. Scale bar 30 µm.

Enrichment in the green cell populations was seen in sorted cell populations to average 97% for THP-1 WT L-selectin-GFP Lo5 (**figure 3.4 C**) and 96% for WT L-selectin-GFP Hi20 (**figure 3.4 E**).

Furthermore, fluorescence microscopy also revealed peripheral localisation of L-selectin-GFP (**figure 3.4 B-E** *arrows*), which served as the initial indication that GFP tagging of L-selectin was not interfering with its traffic through the "secretory pathway" towards the plasma membrane.

To further determine L-selectin-GFP expression levels, the generated THP-1 cell lines were subjected to flow cytometry analysis. This approach enabled examination of many more cells (approximately 10,000) than fluorescence microscopy. Five cell lines were analysed: control untransduced THP-1 cells, low expressors: unsorted THP-1 WT L-selectin-GFP MOI 5 and sorted, uniform THP-1 WT L-selectin-GFP Lo5 and high expressors: unsorted THP-1 WT L-selectin-GFP MOI 20 and sorted, uniform THP-1 WT L-selectin-GFP Hi 20. Two methods of analysis were employed: analysis of GFP levels and analysis of surface L-selectin levels. GFP levels were analysed by simply measuring the GFP fluorescence and analysis of surface L-selectin levels was by labelling THP-1 cells with mouse anti-L-selectin DREG56 antibody, followed by anti-mouse secondary antibody conjugated to fluorescent dye R-phycoerythrin (RPE). DREG56 is an antibody that recognises an extracellular N-terminal epitope of L-selectin [635], and as a result all the RPE signal specifically corresponded to surface-expressed L-selectin. Viable and single cell population was selected for analysis (**figure 3.5 A**, Gate R1). Histograms were generated for GFP (**figure 3.5 B** and **C**, *left panels*) and RPE fluorescence intensities (**figure 3.5 B** and **C**, *right panels*) and the percentage of GFP or RPE positive cells within fluorescent positive gate M1 (shown on the histograms) was determined. Sorting of THP-1 WT L-selectin-GFP MOI 5 cells into THP-1 WT L-selectin-GFP Lo5 uniform cell population resulted in the enrichment of GFP positive cells from 42.04% to 95.89% (**figure 3.5 B**, *left panel*) and in the enrichment of surface L-selectin positive cells (as measured by RPE signal) from 47.8% to 94.78% (**figure 3.5 B**, *right panel*). This was also true when analysing GFP and RPE levels of THP-1 WT L-selectin-GFP MOI 20 and THP-1 WT L-selectin-GFP Hi 20 cells, where the percentage of GFP positive cells rose from 77.84% to 98%, respectively, (**figure 3.5 C**, *left panel*) and the percentage of RPE positive cells increased from 80.85% to 96.6%, respectively (**figure 3.5 C**, *right panel*). These values were in line with those obtained by utilisation of the fluorescence microscopy (**figure 3.4**), and DREG56/RPE labelling confirmed that L-selectin was expressed at the cell surface.

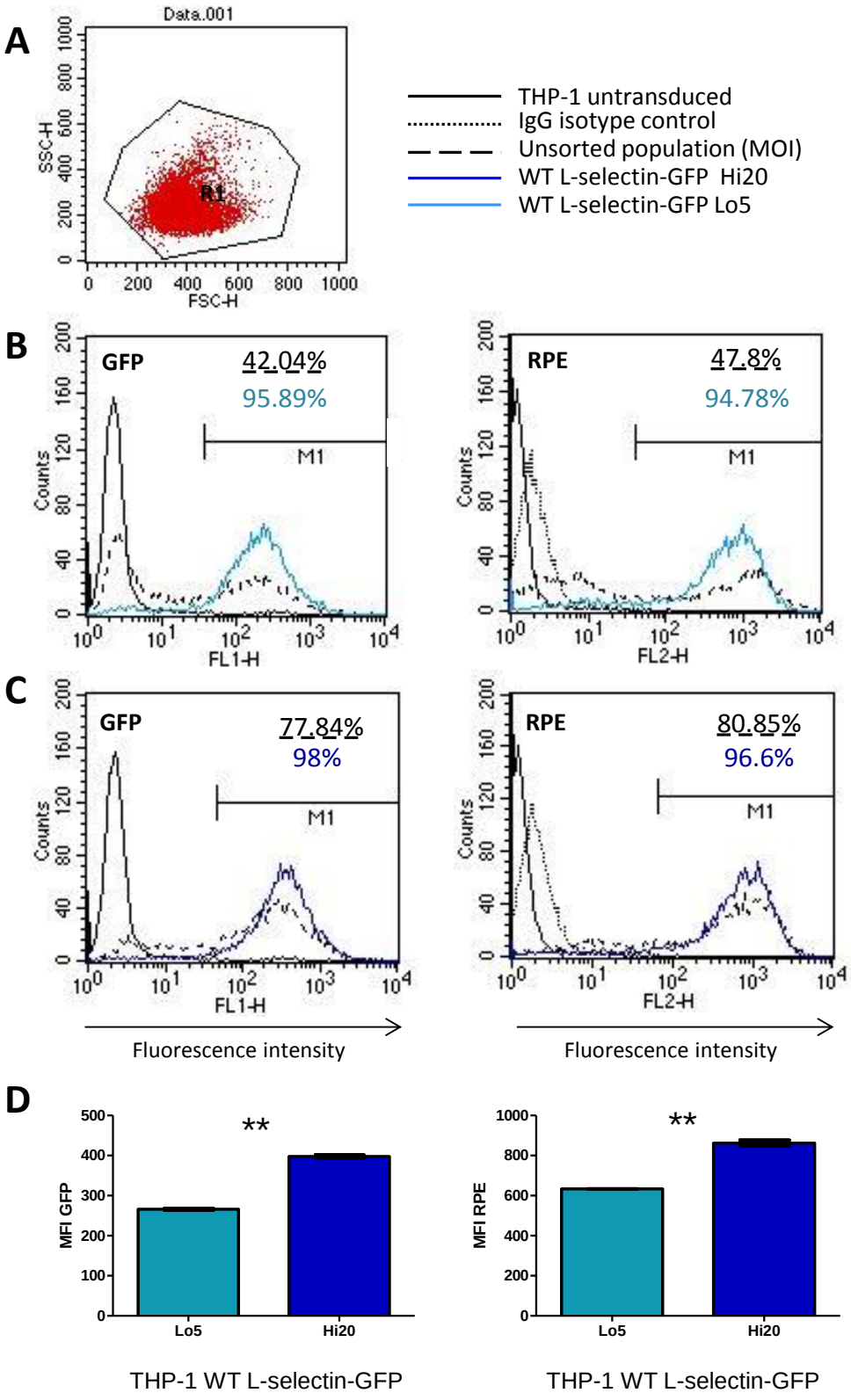

Figure 3.5 Flow cytometry analysis of L-selectin expression in THP-1 cells expressing low or high levels of L-selectin-GFP. THP-1 cells were transduced with pHR'SIN-SEW-L-selectin^{WT}-GFP carrying lentivirus and sorted into uniform populations of low (Lo5) and high expressors (Hi20) as described in **figure 3.4**. Cells were stained with either mouse anti-L-selectin DREG56 or mouse IgG isotype control antibodies followed by α-mouse secondary antibody conjugated to RPE fluorescent dye and compared to their unsorted parental cell lines. The DREG56 antibody recognises the extracellular epitope of L-selectin and is an indicator of surface L-selectin expression. Dot plot **(A)** shows the gate used to analyse singe and viable cells only. In

case of both Lo5 **(B)** and Hi20 **(C)** cell lines, enrichment in both GFP (left histograms) and RPE (right histograms) gated cells (gate M1) was observed within sorted populations as compared to unsorted populations (Lo5:MOI5 = 95.89%:42.04% for GFP signal and 94.78 %:47.8% for RPE signal; Hi20:MOI20 = 98%:77.84% for GFP signal and 96.6%:80.85% for RPE signal). Bar graphs in **D)** show significantly higher mean fluorescence intensities (MFIs) of both GFP (left graph) and RPE (right graph) of Hi20 cell line as compared to Lo5 cell line. Analysis was performed in duplicates on three independent occasions. Data represent mean ± S.E.M. Statistical analysis: two tailed unpaired t-test. **= $p<0.01$. MFI, mean fluorescence intensity.

Importantly, flow cytometry analysis additionally showed that THP-1 cells did not express endogenous L-selectin (figu**re 3.5 B** and **D**, *right panel*, compare dotted line – IgG isotype control and black line - untransduced cells stained with Dreg56). This would mean that any potential L-selectin-dependent effects would be a direct result of the ectopic L-selectin-GFP chimera expression, which would be most useful should any mutated L-selectin-GFP was to be introduced to the THP-1 cells in the further studies. Of note, ATCC-obtained THP-1 cells have been shown previously not to express endogenous L-selectin [636], however L-selectin-positive THP-1 cells have also been reported [637]. This discrepancy highlights the importance of accurate cell line characterisation before any experiments are commenced.

At this stage the parental unsorted THP-1 WT L-selectin-GFP MOI 5 cells and THP-1 WT L-selectin-GFP MOI 20 cells were excluded from any further analysis and experiments, and only sorted, uniform populations of THP-1 WT L-selectin-GFP Lo5 and THP-1 WT L-selectin-GFP Hi20 cells were taken forward. Bar graphs of the mean fluorescence intensities (MFIs) shown in **figure 3.5 D** depict the increase in surface L-selectin levels and a corresponding increase in GFP levels of THP-1 WT L-selectin-GFP Hi20 cells as compared to THP-1 WT L-selectin-GFP Lo5 cells. Due to their high levels of both GFP and surface L-selectin, the THP-1 WT L-selectin-GFP Hi20 cells were chosen for further characterisation and experimentation. If the high L-selectin-GFP expression levels proved to cause adverse effects on THP-1 monocyte cell biology, low expressors would be tested.

Having generated THP-1 cells stably expressing L-selectin tagged to GFP protein, it was deemed necessary to generate a control THP-1 cell line expressing just GFP alone. Since THP-1 WT L-selectin-GFP Hi20 cells were chosen for further studies, it was considered appropriate to generate THP-1 cells expressing matching levels of GFP. To this end, lentiviral particles were generated as described in **section 3.3.1.2**, using original pHR´SIN-SEW-GFP lentiviral backbone vector. The titre of this virus was established as described in **section 3.3.1.2**, and was calculated to be of 2.56×10^8 i.u./mL. THP-1 cells were transduced with MOI 20 and seven days post-infection, GFP expression in those cells, termed THP-1 GFP MOI 20, was monitored by fluorescence

microscopy and compared to untransduced cells (**figure 3.6 A** and **B**). Scoring of GFP positive cells per field of view (five fields of view analysed) was used to establish the average number of cells expressing GFP, which was 62%. To obtain uniform GFP-expressing cell lines, THP-1 GFP MOI 20 cells were sorted with a use of FACS sorting facility, and the uniform cell population was termed THP-1 GFP Hi20 (**figure 3.6 C**). WT L-selectin-GFP Hi20 cells were used as a reference population to set the GFP gate during cell sorting. This allowed GFP levels to be a close match to L-selectin-GFP levels. As analysed by flow cytometry, the sorting enriched the GFP positive cells from 57,92% in THP-1 GFP MOI 20 to 96,87% in THP-1 GFP Hi20 (**figure 3.6 D**).

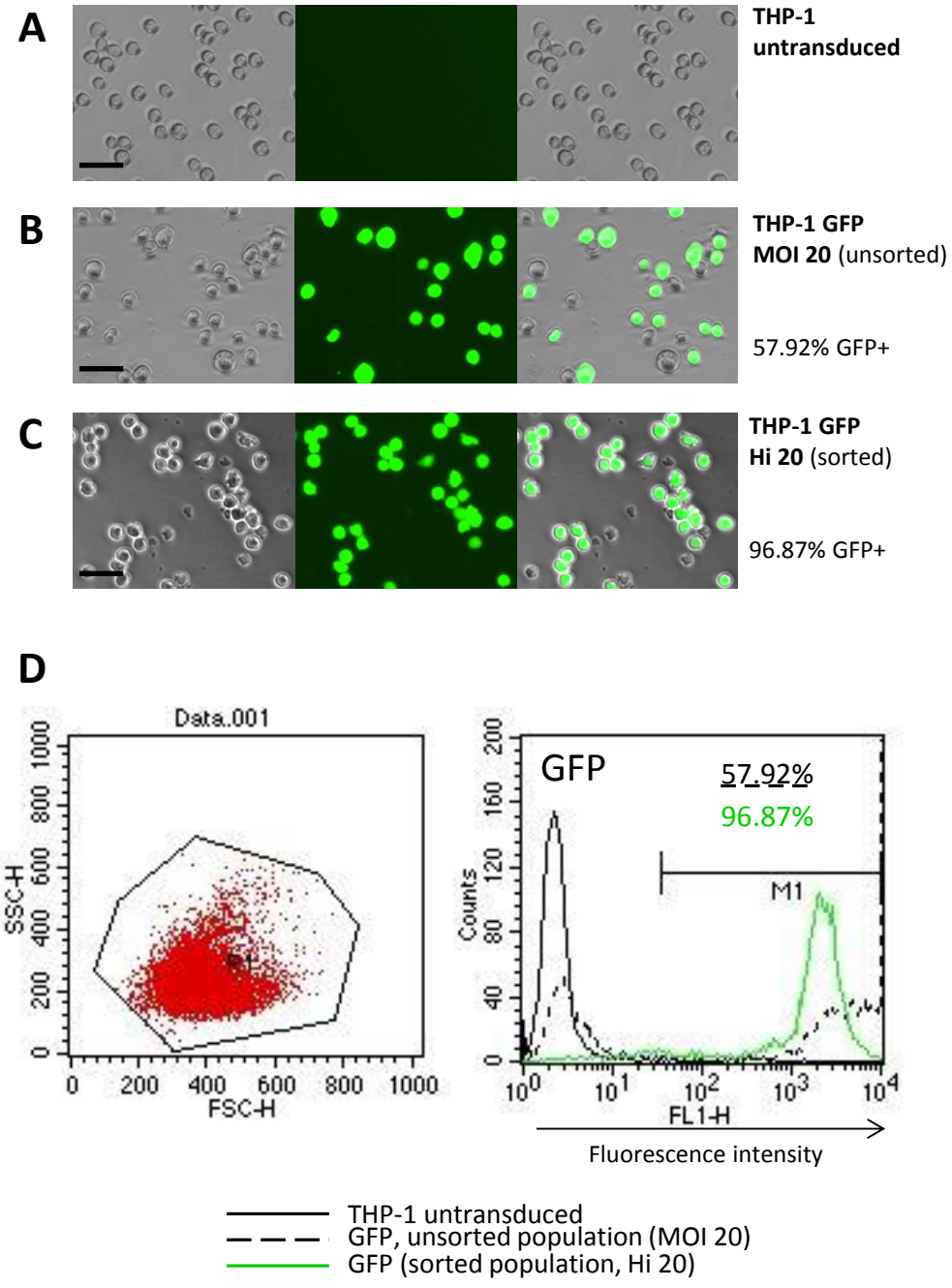

Figure 3.6 Generation of THP-1 cell line expressing uniform levels of GFP. THP-1 cells **(A)** were transduced with lentivirus carrying GFP protein transgene using a MOI of 20 **(B)** and

subsequently sorted into a uniform population termed THP-1 GFP Hi20 **(C)**. **D)** Sorting led to an increase in the percentage of GFP positive cells from 57.92% to 96.87% (right histogram) as analysed by flow cytometry. Dot plot on the left shows gate used to analyse singe and viable cells only. Scale bar in A, B and C: 30 µm.

3.3.2 Monitoring L-selectin-GFP expression levels during THP-1 cell line maintenance in tissue culture

Previous work in the Ivetic laboratory, performed by David Killock (a then PhD student in the Ivetic lab), revealed a strong correlation between cell density and L-selectin shedding in the 300.19 murine pre-B cell line. This has also been reported by others in the field [638, 639]. Therefore, THP-1 WT L-selectin-GFP Hi20 cells were monitored over a period of days to establish any potential changes in L-selectin expression. As presented in **figure 3.7**, L-selectin surface expression was inversely proportional to the cell culture density as measured by flow cytometry. On day one, cell culture density and both GFP and surface L-selectin levels of a 3-day culture were noted and cells were split to 0.4 x 10^6 cells/mL. On the following day (day two) levels of both surface L-selectin and GFP were recorded and those were treated as 100% expression. This allowed for back-calculation that the levels of GFP and surface L-selectin were 83% and 89%, respectively in the initial 3-day culture. On day three a decrease in GFP and surface L-selectin levels to 87% and 88%, respectively, was seen. On day four L-selectin surface levels further decreased to 86%, whereas GFP-tag levels started to climb up reaching 90% of the levels observed on day two. When the cells were left unpassaged on the day 1, the levels of GFP and surface L-selectin reached 58% and 50%, respectively, on day four of the experiment. This corresponded to an overgrown 7-day culture. Having established a significant effect of cell culture density on L-selectin-GFP levels it was considered necessary to maintain stable cell densities during cell culture. Therefore, the cells were split every two or three days when in culture, and seeded overnight at a density of 0.4 x 10^6 cells/mL before each experiment. This was thought to ensure that cells had matched L-selectin-GFP levels between experiments.

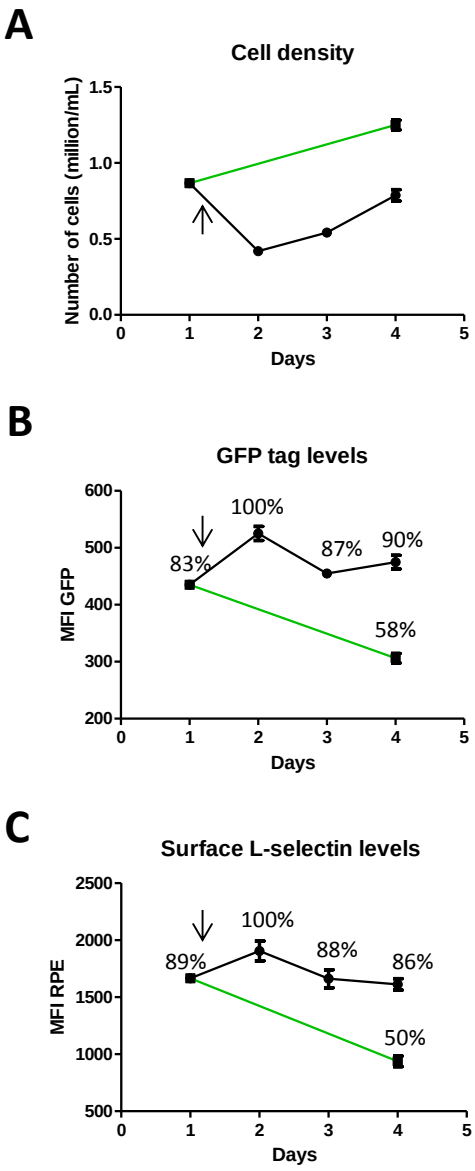

Figure 3.7 Maintanance of THP-1 cells expressing L-selectin-GFP in tissue culture. THP-1 cells expressing WT L-selectin-GFP Hi20 were monitored for their surface L-selectin expression and GFP levels across 4 days, with respect to cell culture density. Cells were split (arrow) on day one to 0.4 x 10^6 cells/mL (black line) or were left unpassaged (green line). **A)** Graph showing cell culture density on the monitored days. Flow cytometry was used to assess GFP **(B)** and surface L-selectin **(C)** expression. Acquired MFI values were used to calculate average percentages of expression. GFP and surface L-selectin levels on day two (first measurement after splitting) were treated as 100%. Experiment was performed on three independent occasions. Error bars represent standard error. MFI, mean fluorescence intensity.

3.3.3 Characterisation of THP-1 L-selectin-GFP Hi20 stable cell line

As explained in **sections 3.1.** and **3.2.**, it was considered crucial to establish whether tagging of the short cytoplasmic tail of L-selectin with a bulky GFP protein of a molecular weight of 27 kDa had any effect on L-selectin expression and L-selectin function. A

number of experiments were performed in order to establish that fluorescently tagged L-selectin is correctly localised and functions properly in THP-1 monocytes. The experiments were performed on THP-1 WT L-selectin-GFP Hi20 cells and included monitoring of L-selectin expression at the plasma membrane, its localisation to microvilli, ability to undergo proteolytic cleavage, its interaction with endogenous calmodulin, its ability to recognise its physiological ligand under flow and to tether and adhere to endothelial cells under flow.

3.3.3.1 L-selectin expression

L-selectin is a single-pass type I transmembrane protein and is known to localise to the tips of leukocyte microvilli [16]. Labelling of cells with DREG56, and subsequent flow cytometry used when generating stable cell lines revealed that L-selectin-GFP was expressed at the plasma membrane (**figure 3.5**). This proved that addition of the GFP-tag was not affecting L-selectin traffic from the endoplasmic reticulum to the plasma membrane. Additionally, L-selectin-GFP localisation to the plasma membrane of THP-1 monocytes was confirmed by fluorescence microscopy. Initial peripheral localisation of L-selectin-GFP was noted during cell line generation (**figure 3.4 B-E**). This was now further confirmed using an objective of higher magnification and THP-1 cells expressing GFP alone as a control. A distinct membrane staining could be seen in THP-1 WT L-selectin-GFP Hi20, but not in THP-1 GFP Hi20 cells (**figure 3.8 A** *arrows*). Additionally, in each cell a high-intensity GFP fluorescence signal was seen, which was likely to represent the Golgi apparatus, where L-selectin-GFP expression was also expected to be high due to the ongoing glycosylation of newly translated proteins (**figure 3.8 A** *stars*). Next, immunogold labelling of DREG56-decorated THP-1 cells, performed by Dr Aleksandar Ivetic, and scanning electron microscopy (SEM) revealed that L-selectin-GFP was localised to the microvilli of the THP-1 cells (**figure 3.8 B**).

Commercially available anti-GFP antibody was then used to examine L-selectin-GFP expression by Western blotting. The results presented in **figure 3.8 C** show that the antibody was indeed GFP specific as it recognised 27 kDa protein derived from THP-1 GFP Hi20 cells (*middle lane*) but did not detect any signal in the lane corresponding to untransduced THP-1 cells (*first lane*). Furthermore, three different bands were detected that were L-selectin-specific (*last lane*), as they did not appear in the lanes corresponding to the untransduced THP-1 cells and THP-1 GFP Hi20 cells. The heaviest form, migrating at 90-110 kDa was considered to be the full-length surface form of L-selectin. After subtraction of 27 kDa (the MW of GFP) the obtained MW for L-selectin would be 60-90 kDa, which is in accordance with the reported molecular weights. The predicted molecular weight (MW) of L-selectin is approximately 30 kDa, but the actual MW varies between 74 kDa in lymphocytes [402] and 90-120 kDa in neutrophils [381]. This is

thought to be the result of extensive glygosylation modifications [313]. In keeping with this, the fuzzy appearance of the band suggested that the protein was highly glycosylated, which is seen in primary leukocytes.

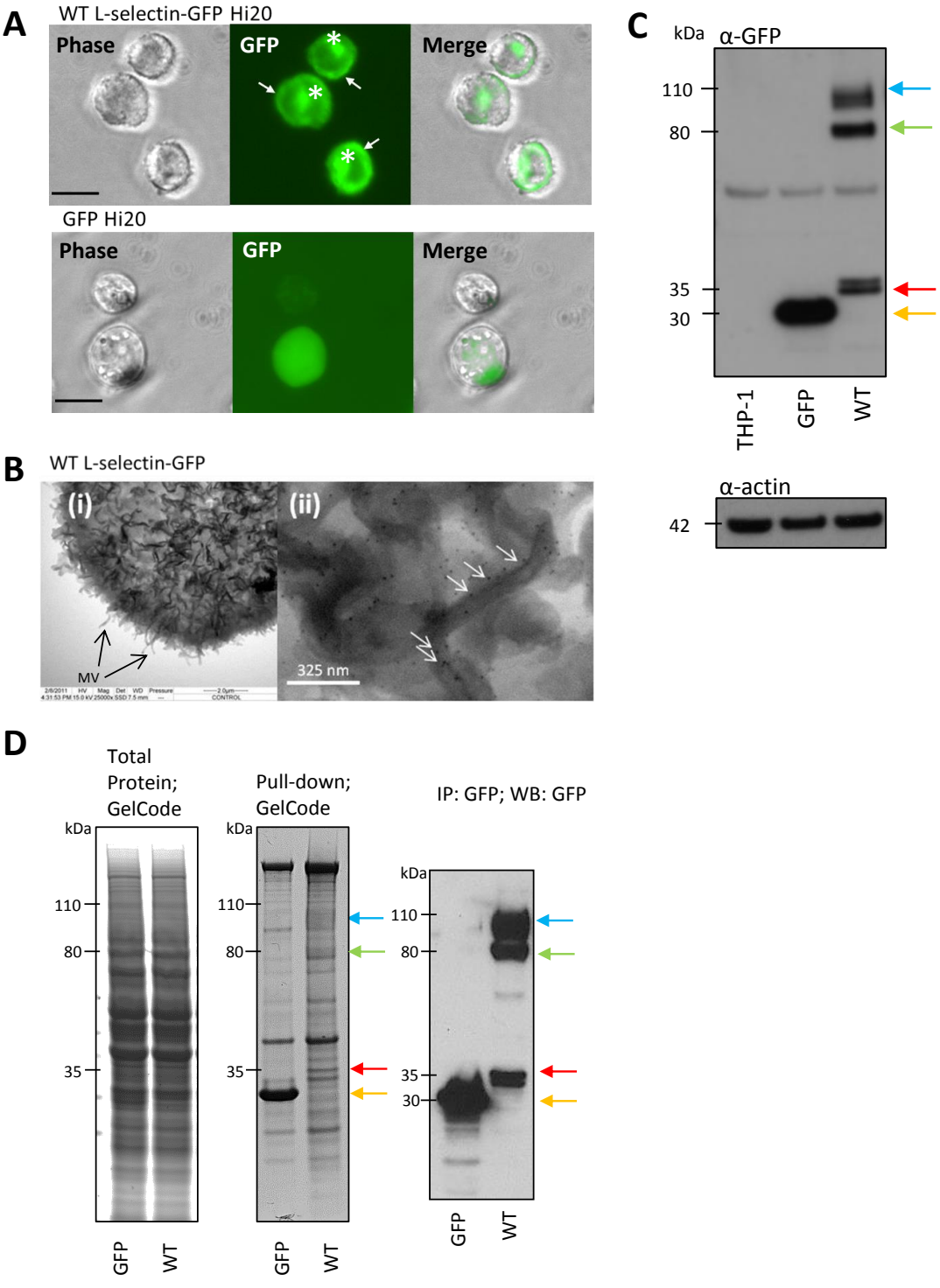

Figure 3.8 GFP-tagging does not influence expression of L-selectin by THP-1 cells. A) *Upper panel:* L-selectin-GFP is successfully localised to the plasma membrane (arrows) of THP-1 cells. Distinctive high-intensity fluorescence signal (stars) is thought to represent Golgi apparatus compartment where L-selectin-GFP undergoes glycosylation. *Bottom panel:* Diffused distribution and lack of distinctive membrane localisation of the GFP protein in control THP-1 cells. Scale bar: 10 µm. **B)** Scanning electron microscopy (SEM) images of THP-1 cells expressing L-

selectin-GFP show that microvilli (MV, arrows) were formed in THP-1 monocytes expressing L-selectin-GFP (i). Scale bar: 2 µm. Immunogold staining of L-selectin further demonstrated that L-selectin-GFP (white arrows) was mainly localised to the microvilli (appearing as phase dark) and not to the cell body (appearing as phase light) (ii). Scale bar: 325 nm. **C)** Biochemical characterisation of L-selectin-GFP expression in stably transduced THP-1 cells. THP-1 cells were grown under resting conditions, harvested prior to the experiment and analysed by Western blotting as described in **section 2.8.3**. Representative Western blotting showing three forms of L-selectin-GFP present in the lysates of THP-1 cells expressing wild type L-selectin-GFP Hi 20. Anti-GFP antibody was used to detect GFP-tag in the lysates from cells expressing L-selectin-GFP (WT) and GFP protein in control cells expressing GFP alone (GFP). Fuzzy 90-110 kilo Dalton (kDa) band (blue arrow) corresponds to the surface fully-glycosylated L-selectin-GFP, 80 kDa band is thought to be the non-glycosylated intracellular form of L-selectin-GFP (associated with Golgi apparatus and endoplasmic reticulum, green arrow) and the two bands detected at around 35 kDa are thought to be forms of L-selectin-GFP cleavage product ("stump", yellow arrow), which is formed upon L-selectin extracellular domain cleavage. Specificity of the anti-GFP antibody is shown when analysing lysates from untransduced THP-1 cells (THP-1), where no bands can be detected. **D)** Further characterisation of L-selectin-GFP and GFP expression. Lysates from THP-1 cells expressing GFP Hi20 alone (GFP) or wild type L-selectin-GFP Hi20 (WT) were used to perform GFP-Trap® immunoprecipitation (IP) as described in **section 2.8.4**. Left panel shows representative GelCode staining of the total protein present in the cell lysates. Surface (blue arrow), intracellular (green arrow) and "stump" (red arrow) forms of L-selectin-GFP as well as GFP protein (yellow arrow) can be seen in the GelCode staining of the pull-down fraction (middle panel). Representative anti-GFP Western blotting (WB) performed on the pulled-down protein shows expression of all of the proteins (right panel). Note: Immunogold labelling of L-selectin-GFP shown in B was performed by Dr Aleksandar Ivetic.

The second largest molecular weight species of L-selectin, migrating at 80 kDa was thought to be an intracellular L-selectin-GFP form, localised to the trans Golgi network. This form of L-selectin was thought not to have undergone the full complement of glycosylation events, hence the lack of fuzzy band appearance. Partial glycosylation was thought to occur as the form was still larger than the predicted MW of the non-glycosylated L-selectin-GFP. Third and the smallest form migrated at approximately 33-35 kDa in the form of two bands. Subtraction of the molecular weight of GFP left MW that corresponded to the L-selectin cleavage product ("stump") that is generated upon L-selectin ectodomain cleavage and has been reported to migrate at around 6 kDa [326, 515]. Further confirmation of L-selectin-GFP expression was performed using GFP-Trap® immunoprecipitation beads (**figure 3.8 D**). GFP-Trap® is a commercially available pull-down system, where a GFP-binding protein (which is also able to detect eGFP) is covalently linked to the sepharose beads and is therefore a very useful method for detecting GFP-fused proteins. The beads were incubated with cell lysates from THP-1 cells expressing either GFP Hi20 or WT L-selectin-GFP Hi20, which allowed for pull-down of either GFP or the L-selectin-GFP chimera. The three L-selectin-GFP forms could already be seen in the pull-down fractions of the protein gels stained with GelCode protein gel stain, and were even more prominent when Western blotting using an anti-GFP antibody was performed on the pulled-down protein. This additionally confirmed

that L-selectin-GFP was successfully expressed in THP-1 cells, and also formulated a ground for future co-precipitation experiments as an easy and clean method for L-selectin-GFP pull-down was established.

3.3.3.2 Shedding of L-selectin-GFP in THP-1 cells

Numerous stimuli have been used to promote the rapid endoproteolytic cleavage of L-selectin, or L-selectin shedding, which results in production of soluble L-selectin (sL-selectin) and a cleavage product ("stump") (**section 1.9.2**) [326, 515]. Examples of cell-activating stimuli include the potent leukocyte activator phorbol 12-myristate 13-acetate (PMA) [495, 496, 529, 640], TNF-α [496] and the phosphatase inhibitor Calyculin A [496]. Sequences within the tail of L-selectin are known to influence L-selectin shedding [323, 558], and therefore it was crucial to establish whether the fusion of GFP protein to the tail of L-selectin had any adverse effects on L-selectin shedding. THP-1 WT L-selectin-GFP Hi20 cells were stimulated with Calyculin A, TNF-α or PMA and processing of L-selectin-GFP was analysed by Western blotting of whole cell lysates. As shown in **figure 3.9**, treatment with all three stimuli resulted in a significant loss of full-length surface-expressed L-selectin-GFP, and Calyculin A and PMA triggered ectodomain shedding to a much higher extent than TNF-α (**figure 3.9 A** and **B**). Moreover, the L-selectin "stump" was detected in the extracts from non-stimulated cells (**figure 3.9 A** *control lane*), suggesting that constitutive L-selectin-GFP shedding was occurring in the THP-1 WT L-selectin-GFP Hi20 cell line. Although no statistical difference could be seen when analysing changes in the levels of L-selectin cleavage product, a clear trend could be seen, where the "stump" levels increased following stimulation with all three stimuli (**figure 3.9 A** and **C**). This indicated that GFP-tagging of the cytoplasmic tail of L-selectin did not hinder the ability of the ectodomain to undergo proteolytic cleavage. Additionally, no loss of the 80 kDa form of L-selectin-GFP was observed upon cell activation (**figure 3.9 A**), which further confirmed this form was an intracellular L-selectin-GFP form.

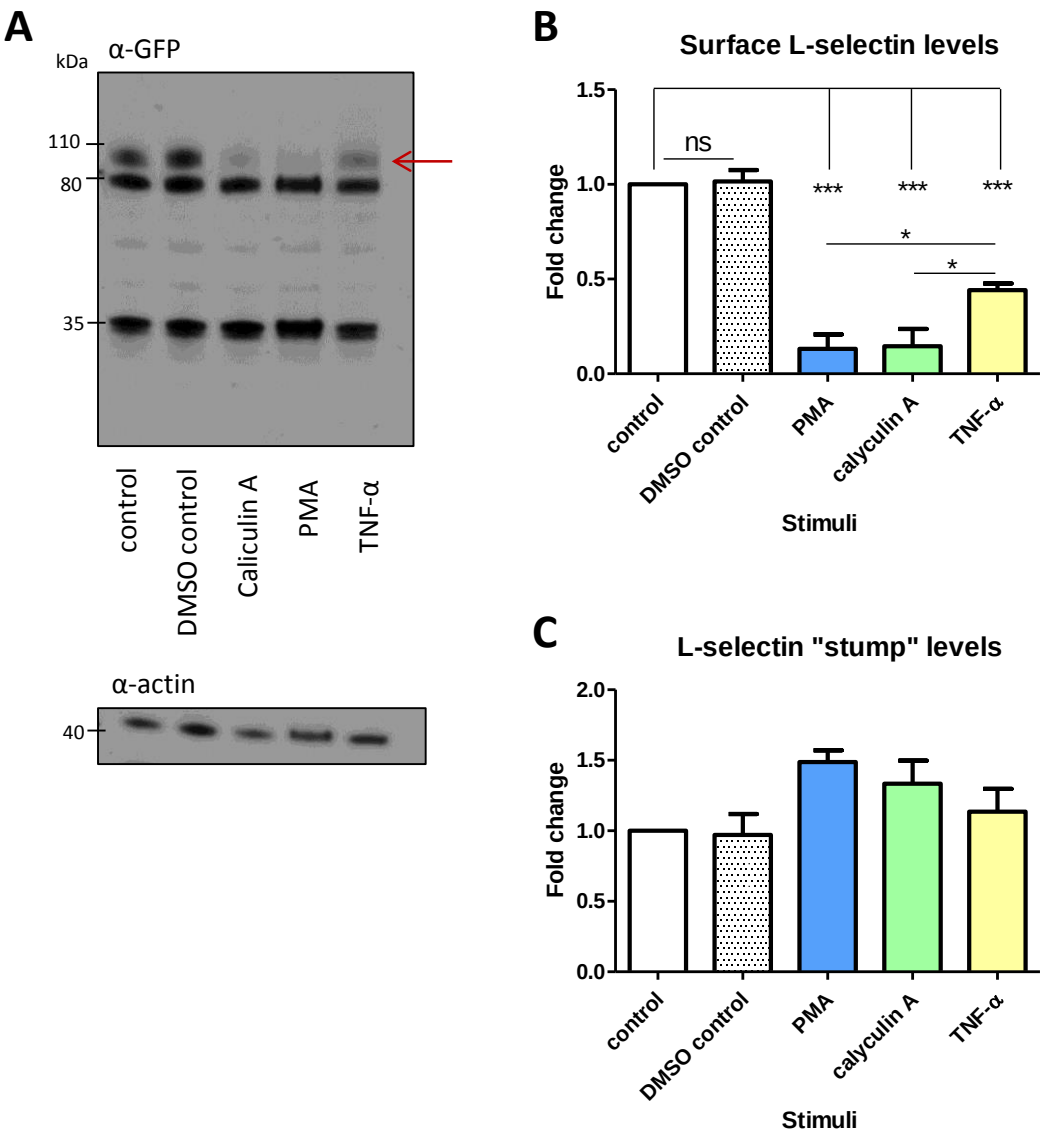

Figure 3.9 The GFP-tag does not interfere with L-selectin's ability to undergo proteolytic cleavage. THP-1 cells expressing WT L-selectin-GFP Hi20 were stimulated with PMA, caliculin A, TNF-α, left untreated (control) or treated with vehicle control (DMSO control), and subjected to Western blotting analysis as described in **section 2.8.3**. **A)** Representative Western blotting showing that loss of the fully-glycosylated surface L-selectin-GFP (red arrow) can be seen with all three stimuli. **B)** Fold-change in the surface L-selectin expression following all three treatments, where TNF-α-caused downregulation of surface L-selectin was not as severe as with the other two stimuli. **C)** Fold-change in the "stump" L-selectin levels following cell-activation. No significant changes were found by statistical analysis however, a trend can be seen, where cell activation leads to upregulation of the L-selectin cleavage product. No influence of DMSO control was seen on L-selectin shedding. Fold-change data was obtained by densitometric analysis (**section 2.8.5**) of the bands corresponding to full length L-selectin or L-selectin "stump", and normalised against actin. The experiment was repeated on three independent occasions. Data represent mean ± standard error. Statistical analysis: One-way ANOVA followed by Tukey's post-test. * = $p < 0.05$, *** = $p < 0.001$.

The ADAM17 metalloprotease is known to cleave L-selectin from the leukocyte surface upon cell activation (**section 1.9.2**) and can be inhibited by Ro-31-9790 compound. Ro-

31-9790 is a hydroxamate-based broad-spectrum zinc-metalloprotease inhibitor and has been shown to inhibit L-selectin shedding under various cell-activating conditions [520, 641]. Flow cytometry analysis revealed that the profound loss of surface L-selectin-GFP seen following PMA stimulation was blocked by pre-incubating the cells with Ro-31-9790 (**figure 3.10 A**). Additionally, incubation of the cells with Ro-31-9790 alone resulted in the upregulation of surface L-selectin-GFP levels above the levels exhibited by non-treated cells (**figure 3.10 A**), suggesting that metalloproteases are involved in basal turnover of L-selectin-GFP that occurs under resting conditions. This further confirmed that GFP did not influence normal L-selectin function as basal turnover of L-selectin is known to occur physiologically and is dependent on metalloprotease activity [521, 544]. Interestingly, although not statistically significant, a trend could be seen in the GFP levels, which followed that of surface L-selectin levels (**figure 3.10 B**). A slight decrease in GFP-tag expression was seen following PMA stimulation and this was rescued when unstimulated cells were pre-incubated with Ro-31-9790. Treatment with Ro-31-9790 alone resulted in slight increase in GFP-tag levels, which again paralleled with changes to surface L-selectin. These results suggest a very dynamic turnover of WT L-selectin-GFP chimera at the plasma membrane of unstimulated THP-1 cells, and this process is greatly potentiated by PMA-mediated cell activation.

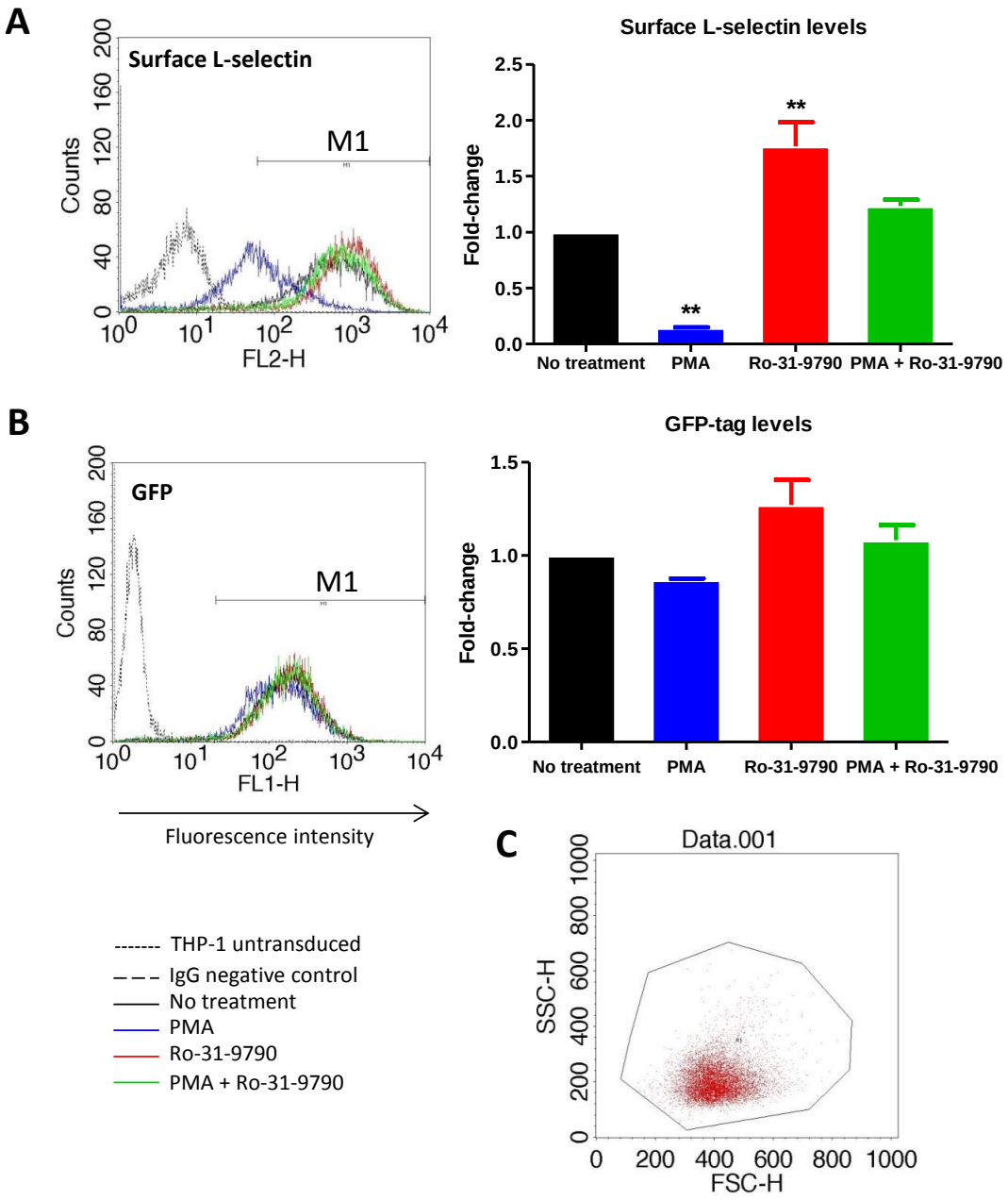

Figure 3.10 L-selectin-GFP is subjected to basal shedding. THP-1 WT L-selectin-GFP Hi20 cells were stimulated with PMA, ADAM17 inhibitor Ro-31-9790 or both and analysed for both GFP-tag and surface L-selectin levels by flow cytometry (**section 2.13**). **A)** Surface L-selectin levels measured by using mouse anti-L-selectin DREG56 antibody and following anti-mouse-RPE conjugated secondary antibody. L-selectin expression was downregulated following PMA stimulation, which could be prevented by pre-incubation with Ro-31-9790. Inhibition of basal metalloprotease activity by Ro-31-9790 treatment led to increased surface L-selectin expression. M1 on the histogram shows gate for RPE positive THP-1 cell population. **B)** GFP-tag levels, where M1 (histogram) shows gate for GFP positive cells, followed pattern observed with surface L-selectin but changes in MFI values were not significant. **C)** Gate R1 in the dot plot contains population of viable THP-1 cells and was applied to all samples. Histograms in A, B and C represent the changes seen in a typical experiment and fold-changes of L-selectin surface levels shown on corresponding graphs were established on the basis of MFI values acquired in triplicates for 3 independent experiments. Data represent mean ± S.E.M. and significance was determined by One-way ANOVA and Dunnett's post-test against "No treatment", ** = $p < 0.01$.

3.3.3.3 Interaction of endogenous calmodulin with L-selectin-GFP

The cytoplasmic calcium-sensing protein calmodulin (CaM) is known to interact with the L-selectin tail (**section 1.10.4**). Importantly, calmodulin is known to negatively regulate L-selectin shedding [559]. *In vitro*, calmodulin inhibitors severely decrease binding of lymphocytes to HEV and rolling of neutrophils on MECA-79 antigen, a physiological L-selectin ligand [515]. Thus, it was important to establish whether tagging of GFP to the cytoplasmic tail of L-selectin had any detrimental effects on CaM binding. Immunoprecipitation has been used in the past to detect L-selectin-CaM interaction [515]. GFP-Trap® was successfully used to pull-down L-selectin-GFP (**figure 3.8 D**), and it was now employed to test whether CaM co-precipitated with L-selectin-GFP. To this end, resting THP-1 WT L-selectin-GFP Hi20 cells and control THP-1 GFP Hi20 cells were harvested and lysates were added to GFP-Trap® beads slurry. The data presented in **figure 3.11 A** and **C** show significant increase of pulled-down CaM when L-selectin-GFP interacted with the GFP-Trap® as compared to just GFP. Binding of CaM to GFP alone was thought to be a result of non-specific binding caused by a great abundance of GFP (**figure 3.11 B**). This suggested that L-selectin indeed had the ability to interact with endogenous calmodulin, eliminating the possibility of detrimental effects of the GFP-tag on L-selectin/CaM interaction.

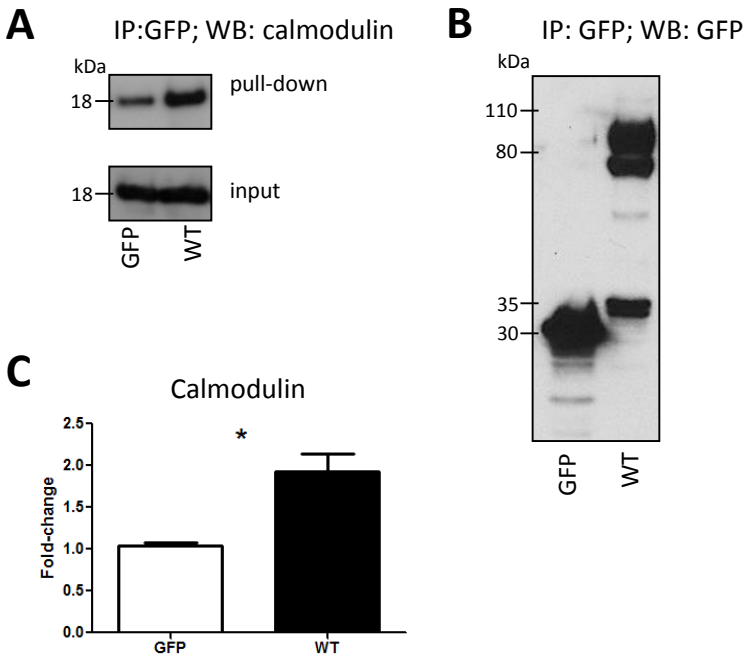

Figure 3.11 WT L-selectin-GFP associates with endogenous calmodulin (CaM). GFP-Trap® (**section 2.8.4**)/Western blotting (WB, **section 2.8.3**) analysis of interaction between L-selectin-GFP and CaM in resting THP-1 WT L-selectin-GFP Hi20 cells. **A)** Representative Western blotting showing CaM signal detected upon GFP-Trap® IP. Enrichment of CaM protein

in the pull-down fraction can be seen when L-selectin-GFP is used as compared to just GFP. Protein input lysate is shown on the bottom blot. **B)** Representative anti-GFP Western blotting showing immunoprecipitating L-selectin-GFP and GFP proteins. **C)** Densitometric analysis of three independent Western blottings shown in A. Mean values ± standard error are shown. Statistical analysis: two-tailed, unpaired Student's t-test. *= P<0.05.

L-selectin tail is also known to interact with ezrin/radixin/moesin (ERM) proteins (**section 1.10.3**) and the attempts were made to investigate this interaction in THP-1 cells expressing WT L-selectin-GFP. Unfortunately however, attempts to immunoprecipitate ERM proteins using GFP-Trap® proved unsuccessful.

3.3.3.4 Interaction of L-selectin-GFP on THP-1 cells with physiological ligands under flow conditions

3.3.3.4.1 L-selectin recognises sialyl Lewis X (sLe^x)

In order to determine whether L-selectin-GFP expressing THP-1 cells were capable of rolling on L-selectin ligands, THP-1 WT L-selectin-GFP Hi20 cells were perfused over immobilised sialyl Lewis X (sLe^x). Sialyl Lewis X tetrasaccharide was chosen as it is a known physiological L-selectin ligand (**section 1.7.2**) and has been reported to mediate L-selectin-dependent rolling of leukocytes under flow in the parallel plate flow chamber assays [642].

The experiments were performed by Dr Aleksandar Ivetic and Mr Ahmed Ahmed (during his MSc research project in the Ivetic lab), using the aforementioned THP-1 WT L-selectin-GFP Hi20 cells. Briefly, excess sLe^x-biotin (1 µg/mL) was added to increasing amounts of immobilised neutravidin, which approach achieved increasing concentration of sLe^x available for L-selectin binding (**figure 3.12 A**). The cells were subsequently perfused over the immobilised ligand under a shear stress parallel to the physiological stress of a blood flow (shear stress defined as a force imparted by the flow parallel to the vessel wall), and analysed for rolling. The mean rolling velocity of cells perfused over 2 µg/mL of neutravidin co-immobilised with sLe^x was 43.6 µm/s (**figure 3.12 B**). This velocity decreased to 34.9 µm/s when 3 µg/mL of neutravidin was used, and no further decrease was seen with 4 µg/mL (mean cell velocity was recorded as 35.2 µm/s) (**figure 3.12 B**), suggesting that the L-selectin/sLe^x interaction per monocyte reached saturation. Analysis of the rolling flux (**figure 3.12 C**) revealed that the flux was directly proportional to the concentration of neutravidin immobilised, and therefore to the amount of sLe^x available for L-selectin binding. These results indicate that transgenic L-selectin-GFP chimera was able to recognise its ligand and mediate cell rolling, and that the rolling flux increased in a dose-dependent manner.

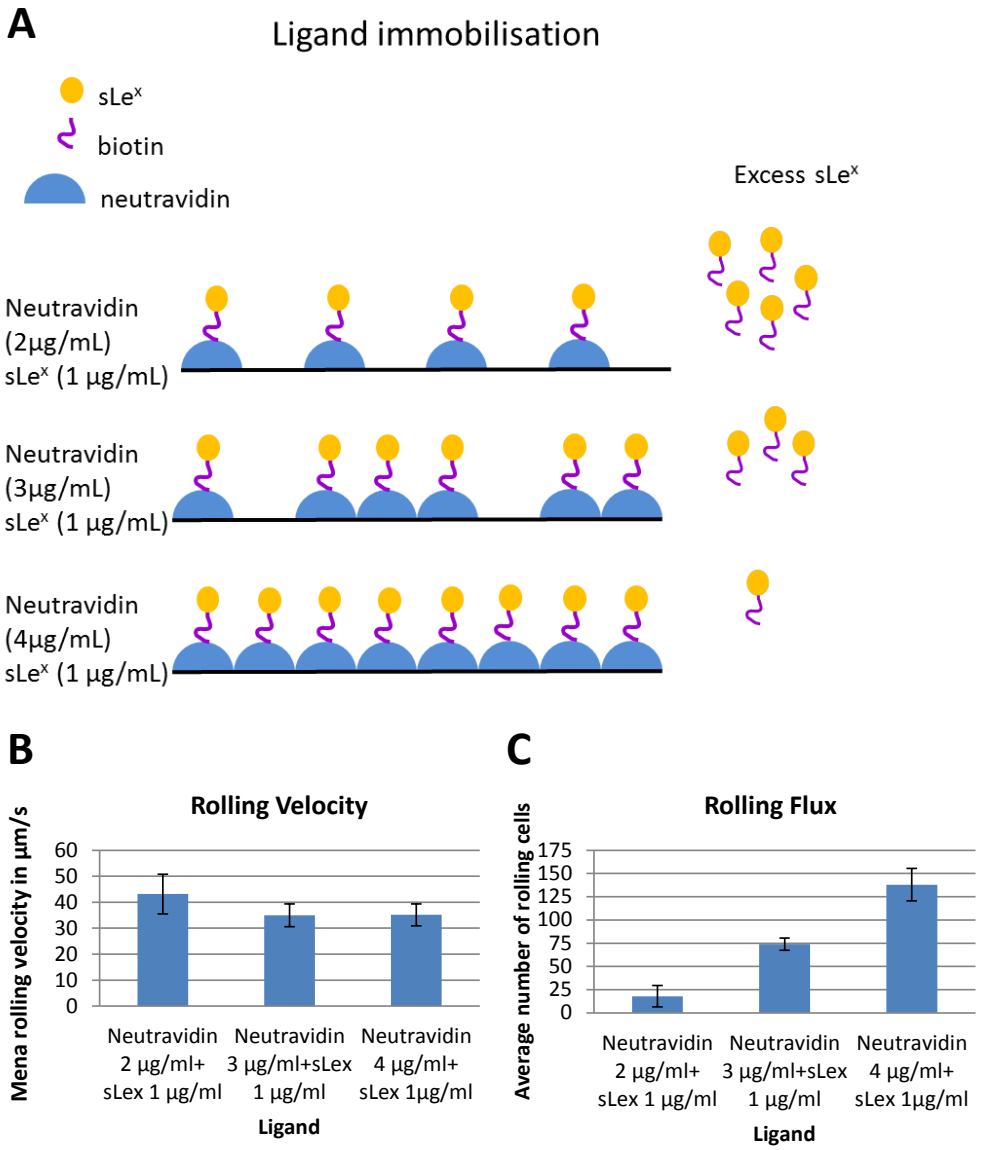

Figure 3.12 Interaction of THP-1 cells expressing WT L-selectin-GFP with sialyl Lewis X (sLe^x) ligand under conditions of flow. THP-1 cells expressing L-selectin-GFP were subjected to a parallel-plate flow chamber assay where the interaction with L-selectin physiological ligand, sLe^x tetrasaccharide was monitored. **A)** Schematic describing immobilisation of sLe^x ligand. Surface of the plastic well dishes was coated with poly-L-lysine and then increasing amounts of neutravidin were immobilised on to plastic wells. This was followed by the addition of an excess amount of biotinylated sLe^x. Binding of biotin on sLe^x to neutravidin achieved an increasing surface density of sLe^x. **B)** Slight decrease in the mean rolling velocity was observed with 3 µg/mL and 4 µg/mL neutravidin concentration. **C)** Increased rolling flux was observed to be directly proportional to the amount of neutravidin immobilised. Error bars represent S.E.M. All flow assays were performed at a shear stress of 2.5 dynes per cm^2.Unpublished data obtained by Dr Aleksandar Ivetic and Mr Ahmend Ahmed, an MSc student in the Ivetic laboratory.

3.3.3.4.2 L-selectin mediates interactions of THP-1 cells with TNF-α-activated endothelium

Initial attachment of primary human monocytes to interleukin 4 (IL-4) or TNF-α activated HUVEC was shown to be dependent on L-selectin [410, 575]. In addition, stable expression of L-selectin in the U937 monocytic cell line grants the ability to roll on and attach to IL-4 activated HUVEC under flow, which is thought to be a result of direct binding of L-selectin to its endothelial-expressed ligands [410]. To establish whether expression of L-selectin-GFP by THP-1 monocytic cells conferred the ability to attach to TNF-α activated HUVEC, a set of co-perfusion experiments was performed using the parallel plate flow chamber assay. The chamber that was used throughout this thesis is described in **section 2.14.1**, and the detailed method of the co-perfusion experiments is outlined in **section 2.14.2**. Firstly, THP-1 WT L-selectin-GFP Hi20 cells were compared against untransduced THP-1 cells to analyse the effect the ectopic expression of L-selectin-GFP on the interactions between the THP-1 monocytes and the HUVEC monolayer (**figure 3.13 A**). Next, THP-1 WT L-selectin-GFP Hi20 were compared against THP-1 GFP Hi 20 cells to examine the influence of the GFP expression on THP-1 cell recruitment in the absence of L-selectin (**figure 3.13 B**). Finally, untransduced THP-1 cells and THP-1 GFP Hi 20 cells were compared against each other to assess the influence of the lentiviral gene delivery on THP-1 cell recruitment (**figure 3.13 C**). All the perfusions were performed as co-perfusions, comparing one cell line directly against another, over a 10 minute period. Orange and Green Cell Tracker® dyes were used to differentially label each cell line under investigation. Additionally, the dyes were swapped between the experiments to exclude any effects the dyes could have had on the behaviour of the cells. Panels **A** and **B** in **figure 3.13** show that an average of 10% increase in the number of recruited cells occurred when THP-1 cells were expressing L-selectin-GFP as compared to control (L-selectin negative) cells. No difference in the recruitment numbers was found between untransduced THP-1 cells and cells expressing GFP alone (**figure 3.13 C**), further confirming that the augmented recruitment was a result of L-selectin expression and not an unspecific effect of lentiviral transduction or GFP expression.

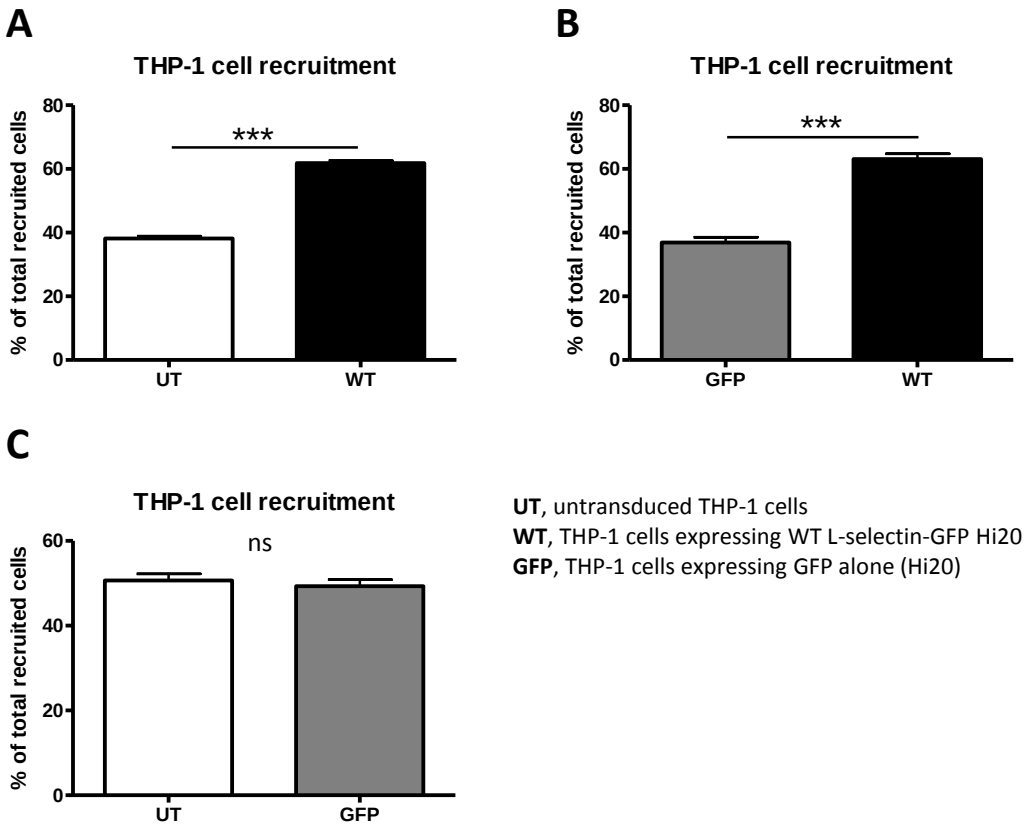

Figure 3.13 Expression of L-selectin augments recruitment of THP-1 monocytes to TNF-α-activated HUVEC. Confluent HUVEC monolayers were stimulated overnight with 10 ng/mL TNF-α and THP-1 cells expressing WT L-selectin-GFP (WT), GFP alone (GFP) or THP-1 cells that had not been transduced (UT, untransduced) were perfused over the monolayer in the parallel-plate flow chamber as described in **section 2.14.2**. The experiments were performed as co-perfusions, where two types of cells at ratio 1:1 were perfused at the same time for 10 minutes. Prior to perfusion, cells were labelled with cell tracker dyes (one cell line with Cell Tracker® Green and one with Cell Tracker® Orange). The dyes were swapped between the experiments to ensure the results were not influenced by the dyes themselves. **A)** Significantly more WT THP-1 cells bound to TNF-α activated HUVEC than UT THP-1 cells. **B)** Significantly more WT THP-1 cells bound to TNF-α activated HUVEC than GFP THP-1 cells. **C)** No difference in recruitment numbers was seen when UT and GFP THP-1 cells were co-perfused. Three independent co-perfusions were performed for each pair of cell lines. Error bars represent S.E.M. Statistical analysis: two-tailed, unpaired Student's t-test. ***= $p<0.001$.

3.4 DISCUSSION

3.4.1 Stable expression of L-selectin-GFP in THP-1 cells using lentiviral vectors

The ultimate aim of the studies presented in this thesis is to gain new insights into the role of monocyte L-selectin during the leukocyte adhesion cascade and particularly its contribution to TEM. Using cell lines is generally considered advantageous due to the convenient supply of a large number of cells without dependency on a donor [643]. What is more, cell lines provide a simplified model of the biology of a certain cell type, which

is extremely important when studying novel cellular processes. Furthermore, cell lines are in principle uniform and immortal, which again provides a simple and convenient model for the study of basic cellular processes. Additionally, a recent review suggests that THP-1 monocytic cell line is specifically well suited for studying function of monocytes in the vascular system, as the interaction between THP-1 cells and endothelial cells is comparable to that of human primary monocytes and endothelial cells [644].

Lentiviral vectors are commonly employed tools for gene delivery and have successfully been used to express proteins of interest in various cell types of hematopoietic origin [645-650]. More specifically, human monocytic cell lines, including THP-1 cells, have been reported to become stably transduced using lentiviral vectors [651-654]. It was therefore decided to create lentiviral particles carrying the L-selectin transgene fused to fluorescent tags and use the viruses to transduce THP-1 cells. Human L-selectin cDNA was successfully cloned into C-terminal GFP- and RFP-tagging lentiviral backbone vectors, pHR´SIN-SEW-GFP and pHR´SIN-SEW-RFP, respectively (**section 3.3.1.1**, **figure 3.1**). At this stage pHR´SIN-SEW-L-selectin^{WT}-RFP vector was frozen for future experiments and pHR´SIN-SEW-L-selectin^{WT}-GFP was used to generate the lentiviral particles (**figure 3.2**). Two MOIs were used to overexpress L-selectin in THP-1 cells: low (MOI 5) and high (MOI 20). Obtaining high levels of L-selectin-GFP expression would be more desirable, however it could potentially have some adverse effects on cell function. If this was the case, it was hoped that the low expressors could be used to overcome this issue. Both MOIs were able to transduce THP-1 cells as confirmed by fluorescence microscopy of GFP channel and flow cytometry analysis of both GFP-tag and surface L-selectin expression; however, as expected, a MOI of 20 resulted in higher transduction efficiency than a MOI of 5 (**figure 3.4** and **figure 3.5**). The THP-1 WT L-selectin-GFP MOI 5 and THP-1 WT L-selectin-GFP MOI 20 were then FACS sorted into uniform populations, low expressor THP-1 WT L-selectin-GFP Lo5 and high expressor THP-1 WT L-selectin-GFP Hi20, respectively. In sorted, uniform populations, each cell within a population was expressing matched levels of L-selectin-GFP. This was an important to ensure consistency and repeatability for future experiments as the parental unsorted cell populations included L-selectin-negative cells and cells of variable L-selectin expression levels. Flow cytometric analysis of uniform cell lines showed that THP-1 WT L-selectin-GFP Hi20 cells had significantly higher levels of both GFP-tag and surface L-selectin levels than THP-1 WT L-selectin-GFP Lo5 cells as determined by MFI values (**figure 3.5**), and this cell line was chosen for further characterisation. If any adverse effects of high L-selectin-GFP expression were found, low expressor THP-1 WT L-selectin-GFP Lo5 cells would be then tested.

In order to control for any effects lentiviral transduction might have had on the THP-1 cells, a cell line was generated, where GFP protein was expressed on its own. To this end, the original pHR´SIN-SEW-SEW-GFP vector was used to produce lentiviral particles that were subsequently employed to transduce THP-1 cells with the MOI of 20. The THP-1 GFP MOI 20 cell line was subjected to FACS sorting in order to achieve uniform cell population (**figure 3.6**), where GFP levels would resemble those of GFP tag levels in THP-1 WT L-selectin-GFP Hi20 cells as closely as possible.

Additionally, it was established that the levels of L-selectin-GFP expression in the THP-1 cells was highly dependent on the cell culture density (**figure 3.7**), and it was decided that prior to the experiments, the cells would be seeded overnight at a strictly defined density of 0.4 x 10^6 cells/mL. This would ensure that the L-selectin-GFP levels would be matched between experiments.

In conclusion, lentiviral gene delivery was successfully used to stably express L-selectin-GFP in THP-1 monocytic cells. Two sorted, uniformly-expressing cell lines, low and high L-selectin-GFP expressors were created. High L-selectin expressor THP-1 WT L-selectin-GFP Hi20 was chosen for further characterisation alongside control high GFP expressor THP-1 GFP Hi20.

3.4.2 Tagging of the L-selectin cytoplasmic tail with GFP does not influence L-selectin expression, localisation and function

Fusing of proteins of interest to fluorescent tags is a well-known method used in cellular biology that enables non-invasive monitoring of protein localisation over time. Although generally considered useful, this approach has been reported to cause some adverse effects on the biology of the target protein under investigation [655, 656]. In this particular study, where a relatively large, 27 kDa protein (GFP) was fused to a short 17 amino acid L-selectin cytoplasmic tail, the possibility of the tag negatively affecting L-selectin function had to be taken in to consideration. A set of experiments was therefore designed that would test for characteristic features of L-selectin, including its expression at the cell plasma membrane, its localisation to microvilli, its ability to undergo shedding in response to cell stimulation, its capacity to interact with endogenous cytosolic binding partners and its ability to recognise its ligands under flow.

Biochemical analysis of L-selectin expression revealed three separate protein forms of approximately 90-110, 80 and 35 kDa (**figure 3.8 C** and **D**). After substraction of 27 kDa belonging to the GFP, the obtained MWs (60-90, 53 and 5-8 kDa) correspond to those reported for endogenous L-selectin [381, 402, 515], suggesting that successful production of L-selectin-GFP chimera in the THP-1 cells had occurred. The fuzzy appearance of the heaviest band (90-110 kDa) suggested the full-length protein was heavily glycosylated, which was a further indicative of its mature form. The smallest form

(35 kDa) was identified as L-selectin cleavage product that is retained upon shedding ("stump"). The L-selectin-GFP "stump" appeared as a doublet, which was not entirely clear but it was thought that further cleavage might occur in the cell after L-selectin ectodomain was shed. The 80 kDa band was recognised as the intracellular form of L-selectin that was associated with endoplasmic reticulum and Golgi apparatus structures. The evidence for intracellular L-selectin-GFP was also found when analysing fluorescence microscopy data, where distinct high-fluorescence L-selectin-GFP signal was seen within each cell (**figure 3.8 A**). The abundance of such form was expected as the lentiviral gene delivery system is based on the constitutively active promoter, and hence constitutive protein production was understood to take place.

The initial evidence for L-selectin-GFP fusion protein expression at the cell surface was obtained by flow cytometry analysis during the cell line generation process (**figure 3.5**). Further investigation using fluorescence microscope revealed a distinct plasma membrane localisation of L-selectin-GFP chimera that could not be seen when only GFP was expressed in THP-1 cells (**figure 3.8 A**). More specifically, L-selectin is known to be localised to microvilli, and immunogold labelling followed by scanning electron microscopy (SEM) has been used before to assess this property in monocytes [18]. A study by Bruehl et al. [18] found that an average 72% of surface L-selectin is localised to the tips of monocyte microvilli and the rest of the protein is found on the cell body. Although quantification of the gold particles was not executed in the study performed in our laboratory, the SEM photographs clearly show that the majority of L-selectin-GFP was localised to the microvilli of the THP-1 monocytes (**figure 3.8 B**).

ADAM17 is known to be the main metalloprotease that cleaves L-selectin following cell activation (**section 1.9.2**), and it has been reported that two distinct ways of ADAM17 activation exist depending on the nature of the stimulus [496]. Killock and Ivetic (2010) showed that PKC-dependent L-selectin cleavage occurs upon stimulation with potent cell activator PMA, whereas p38-dependent shedding occurs after treatment with phosphatase inhibitors [496]. Examination of shedding in response to stimulation with PMA and protease inhibitor calyculin A would help to assess whether these two modes of L-selectin cleavage were functioning properly in the THP-1 WT L-selectin-GFP Hi20 cells. Additionally, TNF-α, which was reported to cause L-selectin shedding in monocytes in a mechanism similar to that of protease inhibitors [496], was also used as a physiological stimulus. All three stimuli caused shedding of L-selectin as examined by Western blotting (**figure 3.9**), and shedding in response to PMA stimulation was addiotionally confirmed by flow cytometry (**figure 3.10 A** *blue bar*). While analysing the Westrn blottings, an inversely proportional relationship between surface L-selectin and "stump" levels was observed (**figure 3.9 A and C**). This was expected, as it is known that cleavage of L-selectin ectodomain leads to accumulation of the "stump" [657]. The

fact that the increase in the “stump” levels was not statistically significant could be due to its rapid turnover following the cleavage. Furthermore, pre-treatment of the cells with metalloprotease inhibitor Ro-31-9790 prevented PMA-induced shedding of L-selectin, indicating that cleavage was mediated by a metalloprotease (**figure 3.10 A**).

Treatment with metalloprotease inhibitor on its own (in the absence of shedding stimulus) resulted in increased surface L-selectin expression (**figure 3.10 A**). This suggested that L-selectin was being constitutively cleaved in resting THP-1 WT L-selectin-GFP Hi20 cells, a phenomenon known as basal L-selectin shedding (**section 1.9.2**). In keeping with this, Western blotting analysis revealed that L-selectin-GFP “stump” could be detected under resting conditions (**figure 3.9 A** *control lane* and **figure 3.8 C** and **D**). Little is currently known about the mechanism regulating basal shedding of L-selectin, but it has been reported that it occurs in both primary cells [521] and cell lines [544]. Although the same cleavage site seems to be involved as in the activation-induced shedding, the metalloprotease that cleaves L-selectin under resting conditions is not known [544]. ADAM17-dependent and ADAM17-independent basal L-selectin turnover has been shown [521, 544], and thus it appears that more than one mechanism regulating basal L-selectin shedding exists. It is possible that other metalloproteases like ADAM8 [524] or ADAM10 [525], which are known to have the ability to cleave L-selectin, can take part in basal L-selectin turnover. Since Ro-31-9790 is a broad-spectrum metalloprotease inhibitor, it is capable of inhibiting not only ADAM17, but also other metalloproteases. Therefore, it could not be discerned from this experiment which metalloprotease was responsible for basal L-selectin turnover in this particular system. Nevertheless, the ability of L-selectin-GFP to undergo cleavage under both cell-activating and basal conditions was confirmed.

Shedding of L-selectin is modified by calmodulin and ERM, which are cytosolic proteins that bind to the L-selectin tail (**sections 1.10.3** and **1.10.4**) [496, 558, 559]. Interactions between cytosolic proteins and the L-selectin tail have also been shown to be important for L-selectin adhesiveness and surface expression [515, 557, 558], as well as in the signalling induced downstream of L-selectin clustering [245, 562]. Even though no issues with L-selectin-GFP shedding were found in the THP-1 cells, this data did not provide any direct evidence as to L-selectin/CaM or L-selectin/ERM interaction. Direct proof for L-selectin/CaM interaction was obtained using GFP-Trap®/Western blotting analysis (**figure 3.11**), and this suggested that the GFP-tag did not impair the ability of the L-selectin tail to bind CaM. GFP-Trap® was also used to attempt co-precipitation of L-selectin-GFP and ERM proteins, unfortunately however, this proved unsuccessful. This is not thought to be a result of a lack of actual interaction, since ERM-dependent localisation of L-selectin-GFP to the microvilli [558] has been confirmed for these cells (**figure 3.8 B**). Furthermore, L-selectin, CaM and ERM were proposed to exist as a 1:1:1

ternary complex [572], and a very recent research performed by Deng et al. (2013) suggests sequential ERM and CaM binding to L-selectin tail [573]. In this model, moesin desorbs L-selectin from the anionic lipids within the inner leaflet of the plasma membrane, which is a prerequisite for subsequent CaM association (**section 1.10.4** and **figure 1.11**) [573]. Since L-selectin-CaM interaction was detected for THP-1 WT L-selectin-GFP Hi20 cells (**figure 3.11**), it strongly implies that ERM interaction had also occurred. Additionally, no apparent cell shape alterations could be observed, which would most probably be the case if the ERM proteins failed to link L-selectin-GFP cytoplasmic tail to the cytoskeletal network. Previous work in the Ivetic laboratory came across similar ERM immunoprecipitation problems, however L-selectin-ERM interaction has been seen using other approaches (Dr Aleksandar Ivetic and Dr Maddy Parsons, King's College London, personal communication).

Functional L-selectin mediates leukocyte rolling (**sections 1.2.2** and **1.7.5.1**) [11, 52, 365, 407], and so rolling of the THP-1 WT L-selectin-GFP Hi20 cells on immobilised sLe^x was examined (Dr Aleksandar Ivetic and Mr Ahmed Ahmed during his MSc research project in the Ivetic laboratory). An increase in the amount of immobilised sLe^x caused a reduction in the mean rolling velocity of L-selectin-GFP expressing cells (**figure 3.12 B**), suggesting that the cells started to roll slower when more tethers between L-selectin and sLe^x were formed. This was thought to be an indication of L-selectin-GFP successfully recognising its ligand. The increase of rolling flux that was directly proportional to the increase in the immobilised sLe^x (**figure 3.12 C**), further served to prove that L-selectin-GFP mediated rolling of the THP-1 monocytes. In order to fully control for the L-selectin-GFP interaction with sLe^x, these experiments should be complimented with appropriate controls. For example, analysis of mean rolling velocities and rolling flux of untransduced THP-1 cells or cells expressing GFP alone could be performed. Nevertheless, changes in the rolling behaviour of the cells that corresponded directly to the amount of sLe^x available, suggested that tagging of the L-selectin cytoplasmic tail with GFP did not hamper the functionality of the ligand-binding lectin domain of L-selectin. Finally, expression of L-selectin-GFP in THP-1 cells increased the recruitment of these cells to TNF-α-activated HUVEC as compared to untransduced THP-1 cells and THP-1 monocytes expressing GFP alone by an average 10% (**figure 3.13**). L-selectin stably expressed by U937 monocytic cells (U937-LAM1) was also found to mediate attachment of those cells to IL-4 activated HUVEC; however, in this study attachment of L-selectin null U937 cells or U937-LAM1 cells pre-treated with anti-L-selectin antibodies was completely abolished [410]. The difference in the extent of L-selectin contribution between the study presented in this thesis (around 10%) and the study by Luscinskas et al (1994) (100%) [410], may lie in the monocytic cell type. Alternatively, the difference could be caused by the cytokine used to activate HUVEC (i.e. IL-4 versus TNF-α). Unlike

TNF-α, IL-4 does not induce E-selectin expression [658], and thus the observed contribution to recruitment in U937 cells could have been caused by L-selectin-dependent secondary tethering and rolling (**section 1.2.3**). Additionally, the authors suggest that the inducible L-selectin ligand is present on the IL-4 activated HUVEC [410], and it is not known whether the same ligand is induced by TNF-α. On the other hand TNF-α has been shown to induce yet unidentified ligands for L-selectin on various ECs *in vitro* (**section 1.8.2**, summarised in **table 1.2**) [457-459], opening up a possibility that ligands for L-selectin (other than E-selectin) exist also on the TNF-α stimulated HUVEC. Thus, the observed L-selectin-GFP-dependent increase in recruitment of THP-1 cells to the TNF-α-stimulated HUVEC monolayers could be a result of secondary L-selectin tethering, direct L-selectin endothelial ligand binding or both. Analysis of leukocyte strings – formation of which is thought to be indicative of secondary leukocyte capture (**section 1.2.3**) – could prove useful in identification of L-selectin-depedent secondary capture, however such analysis was not formally performed in this study.

Taken together, data presented in this section indicate that generated THP-1 WT L-selectin GFP Hi20 cells expressed functional L-selectin-GFP chimera that exhibited correct localisation to plasma membrane and monocyte microvilli. High expression levels of L-selectin were not found to have any adverse effects and, therefore, it was concluded that those cells could be effectively used in further studies designed to investigate the fate of monocyte L-selectin during leukocyte adhesion cascade.

CHAPTER 4. MONITORING THE SHEDDING OF L-SELECTIN-GFP IN THP-1 CELLS

4.1 INTRODUCTION

The physiological significance of L-selectin shedding has been studied using two main approaches, the synthetic inhibitors of L-selectin shedding or mice expressing "sheddase-resistant" L-selectin. Certain studies showed that shedding of L-selectin regulate leukocyte rolling and suggested that shedding might limit leukocyte accumulation at sites of inflammation [519, 551, 552]. Importantly, reduced transendothelial migration of naive lymphocytes across PLN HEV was seen when shedding of L-selectin was blocked [22, 518]. Shedding was also shown to prevent activated T cells from re-entering the lymph nodes [22, 419]. Furthermore, impaired chemotaxis at sites of inflammation was observed amongst leukocytes expressing sheddase-resistant L-selectin [419]. These reports establish the importance of L-selectin shedding for the successful recruitment of leukocytes. However, just when and where during the leukocyte adhesion cascade the shedding occurs remains elusive. Transmigrated leukocytes have lost the majority of their surface L-selectin [520, 554-556], suggesting that shedding occurs during the transendothelial migration step of the cascade. However, in the examples listed, studies were performed as end-point analysis assays. In other words, the studies monitored L-selectin expression after the transmigration had already occurred. For example L-selectin expression was analysed on neutrophils recovered from the bottom compartment of a transwell chamber [520], or transmigrated monocytes recovered from the abluminal side of HUVEC monolayers [554]. Another report measured L-selectin levels on emigrated leukocytes isolated from cantharidin-induced skin blisters [555, 556]. In all of these end-point assays, no information could be gleaned with respect to understanding the spatio-temporal distribution of L-selectin shedding during TEM.

The cytoplasmic tail of L-selectin has been shown to control L-selectin shedding [323]. Specifically, the serine residues within the L-selectin tail were found to affect shedding in response to cell activating stimuli [496]. It is currently unknown whether these residues are also involved in L-selectin shedding during the leukocyte adhesion cascade, namely TEM. It is possible that those serines can modify the extent and/or timing of L-selectin shedding, thereby affecting leukocyte TEM.

This chapter addresses the question of the spatio-temporal distribution of L-selectin shedding during monocyte TEM. The biochemistry and cell biology experiments performed in this chapter suggest that L-selectin shedding occurs during the early stages

of monocyte TEM, and that the serine residues within the L-selectin cytoplasmic tail are involved in regulating of this process.

4.2 EXPERIMENTAL DESIGN

Both full-length and cleaved (occasionally referred to as the "stump") forms of L-selectin-GFP can be detected on Western blots using anti-GFP antibody with high specificity (**figures 3.8** and **3.9**). This property allowed us to design a simple and reproducible method to detect L-selectin shedding over-time. The L-selectin-GFP expressing THP-1 cells and activated HUVEC monolayers were co-cultured over increasing periods of time. Changes in full-length L-selectin and "stump" levels were assessed by Western blotting. The rationale behind this approach was to pin-point the time at which shedding was occurring during TEM. The assay was carried out under static conditions, as performing biochemistry studies on flowing cells is experimentally challenging, if not impossible.

Serine residues within the cytoplasmic tail of L-selectin are important for L-selectin shedding [496]. This was established by generating murine pre-B 300.19 cells stably expressing non-phosphorylatable mutants of L-selectin [496]. Analogically, THP-1 cells were now used to create cell lines stably expressing serine-to-alanine cytoplasmic mutants of L-selectin-GFP. A lentiviral gene delivery system described in **Chapter 3** was used to achieve mutant L-selectin expression in THP-1 monocytes. Flow cytometry was used to examine the surface expression to ensure that all generated cells expressed equivalent levels of L-selectin-GFP as compared to the THP-1 WT L-selectin-GFP Hi20 cells described in **Chapter 3**. Shedding of WT and non-phosphorylatable mutants of L-selectin in response to PMA and TNF-α was assessed by FACS. Any cells that showed an interesting phenotype were further analysed in co-culture assays as described in **section 2.17.2**. This would allow insights in to the role of the cytoplasmic serines in L-selectin shedding during TEM.

Once the static transmigration assays to monitor shedding were completed, *in vitro* parallel plate flow chamber assays were then employed. The results of the static transmigration assays were used to decide on the perfusion length. This was to ensure the cells were being monitored over a time at which shedding of L-selectin-GFP was occurring. THP-1 cells stably expressing "sheddase-resistant" L-selectin-GFP were generated to investigate whether the lack of shedding influenced the sub-cellular distribution of L-selectin-GFP during TEM. The cells were generated using the lentiviral transgene delivery system presented throughout this thesis. Flow cytometric analysis ensured that expression of the sheddase-resistant L-selectin-GFP matched that of WT L-selectin-GFP. Confocal microscopy was used to analyse L-selectin-GFP spatio-temporal distribution in the various cell lines that were fixed at the end of the flow assays.

4.3 RESULTS

4.3.1 Shedding of L-selectin-GFP peaks at 20 minutes in THP-1 cells undergoing TEM

As described in **section 4.1**, transmigrated leukocytes are known to have shed L-selectin from the cell surface, but the exact point in time at which this occurs is not known. It is practically not possible to perform biochemistry on flowing cells, therefore a "static" transmigration assay was designed that allowed examination of L-selectin-GFP shedding in THP-1 cells when co-cultured with activated HUVEC (**section 2.17.2**). THP-1 WT L-selectin-GFP Hi20 cells were added to TNF-α stimulated HUVEC grown on fibronectin-coated 6-well plastic dishes for 1, 5, 10, 20, 30 and 60 minutes. Unbound (supernatant) and HUVEC-bound fractions were collected, cells were lysed and analysed by Western blotting. Anti-GFP antibody was used to detect full-length and cleaved forms of L-selectin-GFP at each time point for both supernatant and HUVEC-bound fractions. The antibody does not recognise any epitopes derived from TNF-α-activated HUVEC (**figure 4.1 A**), which allows for the detection of L-selectin with great specificity. **Figure 4.1 B** shows that almost all THP-1 cells firmly bound to HUVEC by 5 minutes as no L-selectin-GFP can be detected in the supernatant fraction at later time-points. It was thus assumed that the 5 minute time-point represented 100% of surface L-selectin. A decrease in surface L-selectin-GFP was seen in 10, 20, 30 and 60 minute time-points as compared to the 5 minute time-point. The reduction in surface L-selectin-GFP was accompanied by an increase in cleaved L-selectin-GFP ("stump"), which suggested that shedding was occurring. Densitometric analysis of surface L-selectin-GFP revealed that maximum shedding occurred at 20 minute time-point, where 44.08% of surface L-selectin was retained (**figure 4.2 C**). Although less dramatic, a further decrease was observed at later time points, namely 39.5% of surface L-selectin was present at 30 minutes and 32.12% was retained at 60 minutes (**figure 4.2 C**). This suggested that the first 20 minutes of rapid shedding was likely to be a result of THP-1 cell activation by contact with activated HUVEC. A subsequent and gradual decline in the levels, seen at 30 and 60 minute time-points, could represent the ongoing basal L-selectin shedding that continued beyond the first 20 minutes of activation induced shedding. The level of L-selectin-GFP "stump" increased almost two-fold at 10 minutes and persisted up to the 30 minute time-point (**figure 4.2 D**). Due to the variations between the experiments the changes were not significantly different. However, it could be suggested that the observed increase in the "stump" levels reflected its generation during the proteolytic cleavage of the L-selectin-GFP ectodomain. Interestingly, at the 60 minute-time point, the "stump" levels matched the levels observed at the 5 minute time-point (**figure 4.2 D**). This suggested that between 30 and 60 minute time-points the

"stump" had been cleared from the cell membrane and degraded. Furthermore, it can be speculated that it takes around one hour for the "stump" to be turned-over after shedding is initiated when THP-1 cells are co-cultured with HUVEC. Overall, this data suggests that when THP-1 monocytes interact with TNF-α activated HUVEC under static conditions, L-selectin shedding starts to occur at 10 minutes (as indicated by "stump" generation) and peaks at 20 minutes.

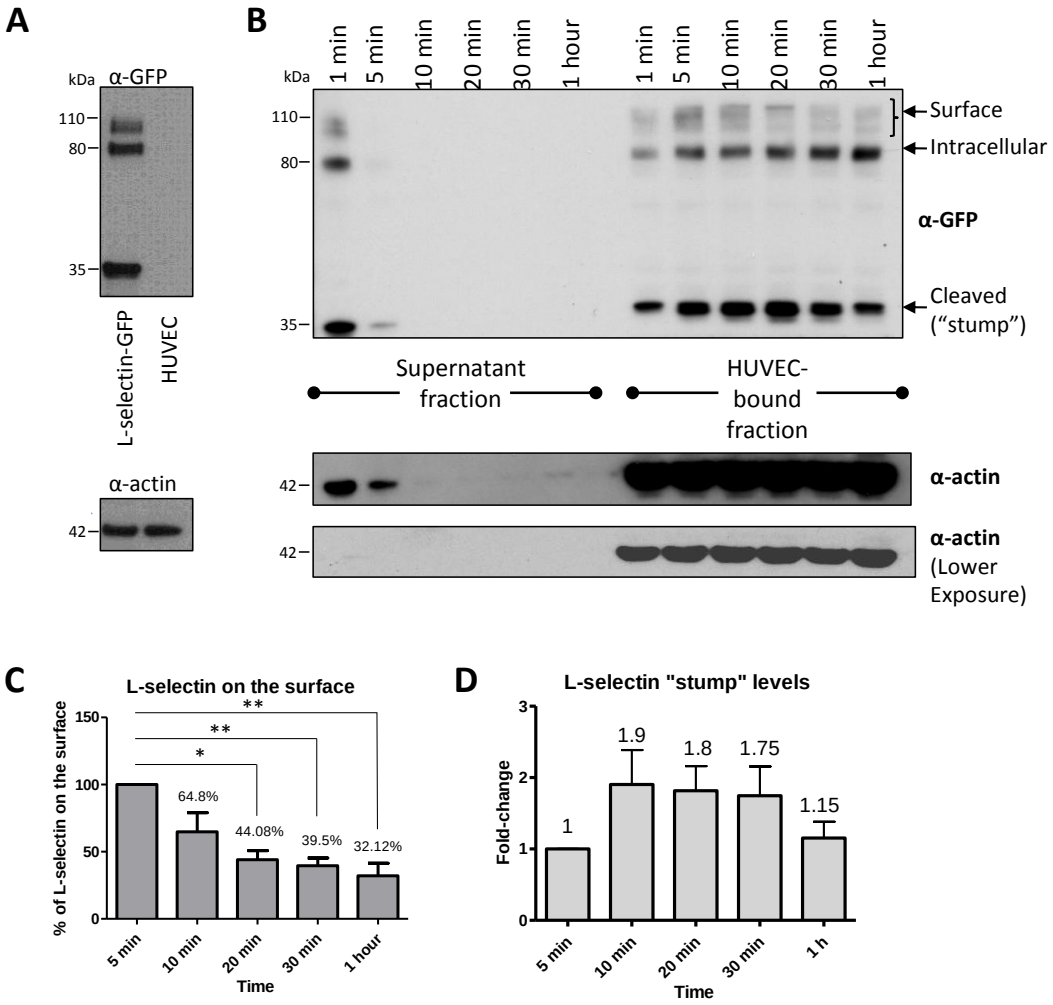

Figure 4.1 Time-course of WT L-selectin shedding when THP-1 cells interact with TNF-α activated HUVEC. A) Specificity of the anti-GFP antibody. Cell lysates of TNF-α stimulated THP-1 WT L-selectin-GFP Hi20 (left lane) and HUVEC cells (right lane) were analysed by Western blotting using anti-GFP antibody. No unspecific bands can be seen in the HUVEC lane. **B)** Representative Western blotting showing L-selectin-GFP shedding in response to THP-1 cells interacting with TNF-α-activated HUVEC. THP-1 WT L-selectin-GFP Hi20 cells were added on top of activated HUVECs for 1, 5, 10, 20, 30 and 60 minutes. Supernatant and HUVEC-bound fractions were then collected, lysed and analysed for L-selectin protein by Western blotting using anti-GFP antibody. **C)** Densitometric analysis of surface L-selectin protein derived from three independent Western blots shown in B. Data is represented as a percentage of L-selectin remaining on the surface. As depicted by the graph, shedding of the 110 kDa form of surface L-selectin peaks at 20 minutes, after which only a minor decrease can be observed. **D)** Densitometric analysis of L-selectin-GFP "stump" derived from three independent Western blots shown in B. Data is represented as a fold-change of the levels observed at 5 minute time-point. The error bars represent standard error. Statistical analysis: One-way ANOVA followed by

Tukey's post-test. No differences were detected in D due to the variability between the experiments. *=p < 0.05, **=p < 0.01.

4.3.2. Generation of cell lines expressing non-phosphorylatable serine-to-alanine mutants of L-selectin-GFP

By mutating the two serine residues within the cytoplasmic tail of human L-selectin into non-phosphorylatable alanines, Killock and Ivetic (2010) had previously shown that those amino acids regulate L-selectin shedding in lymphocytes. To investigate whether the cytoplasmic serines also affect L-selectin shedding in monocytes during TEM, it was decided to generate THP-1 cells expressing serine-to-alanine mutant forms of L-selectin-GFP. THP-1 cell line is L-selectin negative (**figure 3.5**), hence the lack of endogenous L-selectin would allow direct comparisons with WT and mutant cell lines.

The lentiviral vector pHR´SIN-SEW-L-selectin^{WT}-GFP was used to generate various mutant L-selectin-GFP constructs by site-directed *in vitro* PCR mutagenesis as described in **section 2.5**. This allowed the generation of mutant L-selectin constructs with serine-364 and/or serine-367 mutated to alanine (**figure 4.2 A)**, termed S364A, S367A and SSAA. All constructs were sequenced to ensure that the desired mutations had been achieved and no spontaneous mutations had occurred in L-selectin-GFP ORF. The lentivirus backbone vectors carrying mutant forms of L-selectin were then used to generate lentiviral particles as described in **section 3.3.1.2** and **section 2.12**. The titres of the obtained concentrated lentivirus suspensions are presented in **table 2.5**.

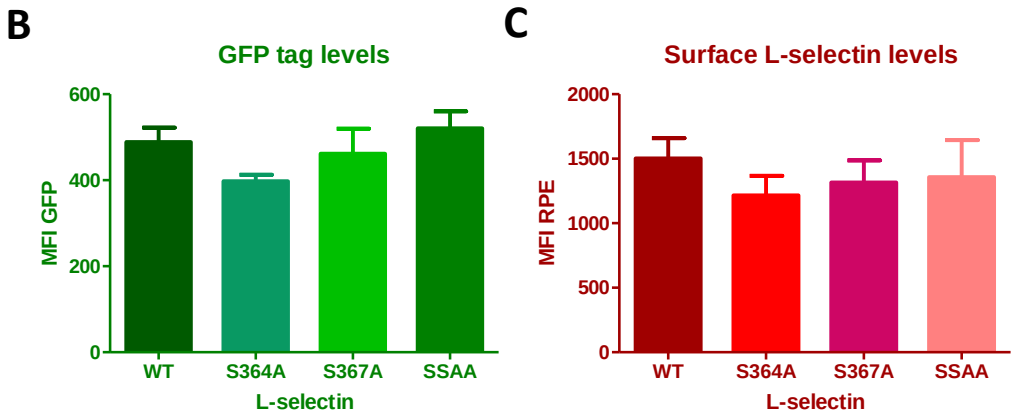

Figure 4.2 Generation and stable expression of L-selectin cytoplasmic tail mutants in THP-1 cells. **A)** Site directed PCR mutagenesis was performed to substitute serines at position 364 or 367 of human WT L-selectin with non-phosphorylatable alanines. Constructs were also made in which both serines were replaced with alanines. THP-1 cells expressing matched levels of: WT-, S364A-, S367A- or SSAA-GFP L-selectin Hi20 were subjected to flow cytometry analysis (**section 2.13**) of both GFP tag levels **(B)** and surface L-selectin levels **(C)** on four different dates across a period of two months. MFI values show closely matched expression levels of WT and all mutant forms of L-selectin as One-way ANOVA detected no significant differences in the L-selectin or GFP expression between the cell lines. Error bars represent S.E.M.

Following the described method of THP-1 cell transduction outlined in **section 3.3.1.3**, THP-1 cells were transduced with lentiviruses at MOI 5 or MOI 20. As soon as a large enough polyclonal population of cells were established, the cells were then sorted by FACS into uniform-expressing populations. **Table 4.1** shows all the serine-to-alanine mutant L-selectin-GFP expressing THP-1 cell lines that were generated in this process.

Mutation	Expressor	Unsorted /sorted (uniform)	Cell line name
S364A	low	unsorted	THP-1 S364A L-selectin-GFP MOI 5
S364A	low	sorted	THP-1 S364A L-selectin-GFP Lo5
S364A	high	unsorted	THP-1 S364A L-selectin-GFP MOI 20
S364A	high	sorted	THP-1 S364A L-selectin-GFP Hi20
S367A	low	unsorted	THP-1 S367A L-selectin-GFP MOI 5
S367A	low	sorted	THP-1 S367A L-selectin-GFP Lo5

S367A	high	unsorted	THP-1 S367A L-selectin-GFP MOI 20
S367A	high	sorted	THP-1 S367A L-selectin-GFP Hi20
SSAA	low	unsorted	THP-1 SSAA L-selectin-GFP MOI 5
SSAA	low	sorted	THP-1 SSAA L-selectin-GFP Lo5
SSAA	high	unsorted	THP-1 SSAA L-selectin-GFP MOI 20
SSAA	high	sorted	THP-1 SSAA L-selectin-GFP Hi20

Table 4.1 THP-1 cell lines expressing serine-to-alanine mutant forms of L-selectin-GFP. This table shows THP-1 cell lines expressing mutant forms of L-selectin-GFP where serine-364, serine-367 or both were substituted with non-phosphorylatable alanines rendering respective mutants: S364A, S367A and SSAA.

Once sorted, THP-1 cells expressing S364A, S367A and SSAA L-selectin-GFP Hi20 were monitored for surface L-selectin and GFP tag expression and compared to levels from WT L-selectin-GFP Hi20 cells. Comparable levels of both GFP tag (**figure 4.2 B**) and surface L-selectin (**figure 4.2 C**) were found between the cell lines as analysed by flow cytometry. Closely matched WT, S364A, S367A and SSAA L-selectin-GFP levels in THP-1 Hi20 cells ensured that any differences between the cell lines that could be identified during the shedding assays, would be a direct result of the introduced mutations and not differences in L-selectin expression.

4.3.3 Double serine mutant within the L-selectin tail reduces TNF-α induced shedding

Phosphorylation of serine residues in the L-selectin tail have been previously found to play a central role in regulating PMA- but not phosphatase inhibitor-induced shedding in murine pre-B 300.19 cells stably expressing human L-selectin [496]. Serine-to-alanine mutations of serine-364 (S364A) and serine-367 (S367A) resulted in decreased L-selectin shedding at 10 nM and higher concentrations of PMA [496]. Additionally, double serine mutation (SSAA) resulted in reduced shedding at 100 nM and higher PMA concentrations (David Killock, unpublished data). To test the effect of PMA-induced shedding of L-selectin-GFP on THP-1 cells, WT and mutant cell lines were subjected to increasing doses of PMA, and surface L-selectin levels was monitored by flow cytometry. Treatment with 10 nM PMA resulted in almost complete loss of surface L-selectin, with an average of 5% of cell surface expression of WT or mutant forms of L-selectin-GFP (**figure 4.3 A**). This was rather unexpected as the study by Killock and Ivetic (2010) revealed that incubation with 10 nM PMA resulted in retention of 60% of surface WT L-selectin and 20% WT L-selectin was still present on the surface when 1000 nM PMA was used [496]. This could be simply due to the difference in cell type (i.e. comparing murine pre-B cells with a human monocyte cell line). To test whether lower concentrations of PMA would reveal any difference in L-selectin shedding between WT and the mutants,

5 and 7 nM concentrations of PMA were used. Again, no differences were observed the cell expressing WT or mutant forms of L-selectin-GFP (**figure 4.3 A**). Having found no effect of serine phosphorylation on PMA induced shedding of L-selectin-GFP, the effect of TNF-α on the shedding of WT and mutant L-selectin was next explored. Killock and Ivetic (2010) found that, unlike PKC-driven (i.e. PMA-induced) shedding, TNF-α- and phosphatase inhibitor-induced shedding are both mediated by p38 MAPK [496]. This means that PMA- and TNF-α-induced shedding of L-selectin are mechanistically different [496]. Thus, perhaps the serine residues were important for TNF-α induced L-selectin shedding from THP-1 monocytes. THP-1 WT, S364A, S367A or SSAA L-selectin-GFP Hi20 cells were therefore subjected to increasing amounts of TNF-α, and surface L-selectin levels was again monitored by flow cytometry. As shown in **figure 4.3 B**, a decrease in shedding was seen with the double serine-to-alanine mutant SSAA at 10 and 20 ng/mL of TNF-α. A similar trend in the loss of S364A and S367A L-selectin-GFP expression in response to 10 and 20 ng/mL concentration of TNF-α was observed, but this was not statistically significant. This suggests that both serine residues could play a role in TNF-α induced L-selectin-GFP shedding. No significant differences between WT and mutant L-selectin-GFP expressing cell lines were observed at 50 ng/mL TNF-α.

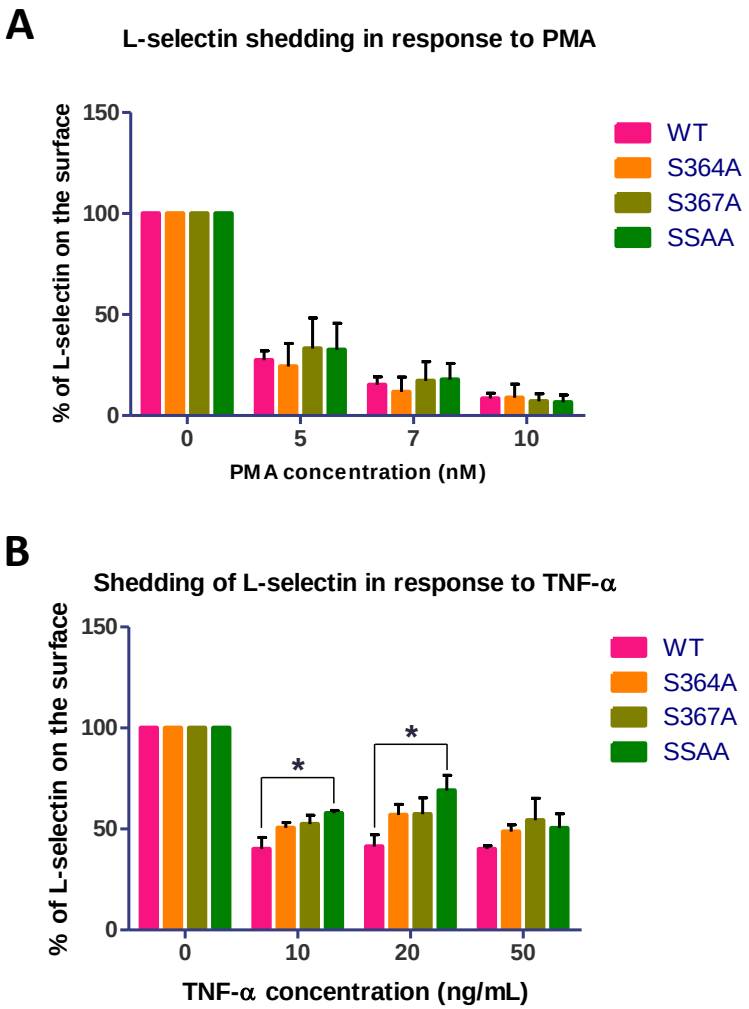

Figure 4.3 Both S364 and S367 are required for TNF-α induced shedding. THP-1 WT, S364A, S367A or SSAA L-selectin-GFP Hi20 were challenged with increasing doses of either PMA **(A)** or TNF-α **(B)** for 30 or 60 minutes, respectively, at 37º C. L-selectin surface levels were subsequently monitored by flow cytometry. PMA concentrations used were 0, 5, 7 and 10 nM and TNF-α concentrations used were 0, 10, 20 or 50 ng/mL. All the experiments were performed at least three times in triplicate. Data represent mean values ± SEM. Statistical difference was calculated for each concentration using One-way ANOVA followed by Dunnet's test against WT. *=$p < 0.05$.

Although the results seem to contradict those of Killock and Ivetic (2010), this could potentially be explained by the fact that different cell lines were used for the studies. Cells used by Killock and Ivetic (2010) were murine pre-B lymphocytes that were stably expressing human L-selectin and the cells used in this study were human monocytes expressing human L-selectin. The fact that 10nM PMA concentration caused around 95% loss of surface L-selectin in THP-1 cells but only 40% loss in 300.19 cells suggests that monocytes are much more sensitive to this stimulus than lymphocytes. As a result, it cannot be excluded that at concentrations lower that 5 nM, differences in PMA-shedding could be seen between WT and mutant forms of L-selectin-GFP. Nevertheless,

these results show that phosphorylation of both serine-364 and serine-367 within the cytoplasmic tail of L-selectin is important for TNF-α induced shedding of L-selectin-GFP from THP-1 monocytes.

4.3.4 SSAA mutation delays L-selectin shedding when THP-1 cells interact with activated HUVEC under static conditions

Western blotting of static transmigration assays showed that WT L-selectin-GFP is shed when THP-1 cells are added on to activated HUVEC (**figure 4.1**). The data presented in **figure 4.3** shows a reduction in TNF-α induced shedding of L-selectin-GFP when both cytoplasmic serine residues are mutated to non phosphorylatable alanines when cells are in suspension. To test whether the SSAA mutation also had an effect on L-selectin shedding during the static transmigration assays, THP-1 SSAA L-selectin-GFP Hi20 cells were subjected to the assays and Western blotting analysis of the bound fraction as described in **section 4.3.3**. Western blotting showed that a loss of surface SSAA L-selectin-GFP peaked at 30 minutes, where 44.6% of SSAA L-selectin-GFP remained cell associated (**figure 4.4 A** and **B**). No further decrease was seen at later time-points (**figure 4.4 A** and **B**). The L-selectin-GFP "stump" was first generated at the 10 minute time-point as seen by a 1.7 fold-increase as compared to the 5 minute time-point (**figure 4.4 A** and **C**). The elevated "stump" levels persisted for up to 30 minutes into the assay, and then decreased to levels slightly above those observed at 5 minutes (1.18 fold change) (**figure 4.4 A** and **C**). Results were quantified and compared to the corresponding values obtained for WT L-selectin-GFP (presented earlier in **figure 4.1**). Statistical analysis showed that significantly more full-length SSAA L-selectin was found at the 20 minute time-point than WT L-selectin (74.36% versus 44.08%, respectively) (**figure 4.4 D**). Additionally, more full-length L-selectin-GFP was detected in the SSAA mutant (91.02%) than WT (64.8%) at 10 minutes, although this was not statistically significant. No differences in full-length L-selectin levels were detected at 30 minute and 60 minute time-points, suggesting that SSAA mutation did not affect shedding at later time-points. Thus, it could be proposed that abrogating phosphorylation of L-selectin cytoplasmic serine residues leads to an approximately 10 minute delay in shedding of L-selectin during the initial stages of monocyte TEM under static conditions. Additionally, analysis of the SSAA L-selectin-GFP "stump" levels showed an increase in the fold-change at 20 minutes when compared to the WT L-selectin-GFP "stump" levels. A lack of statistical significance was likely due to variability between the experiments.

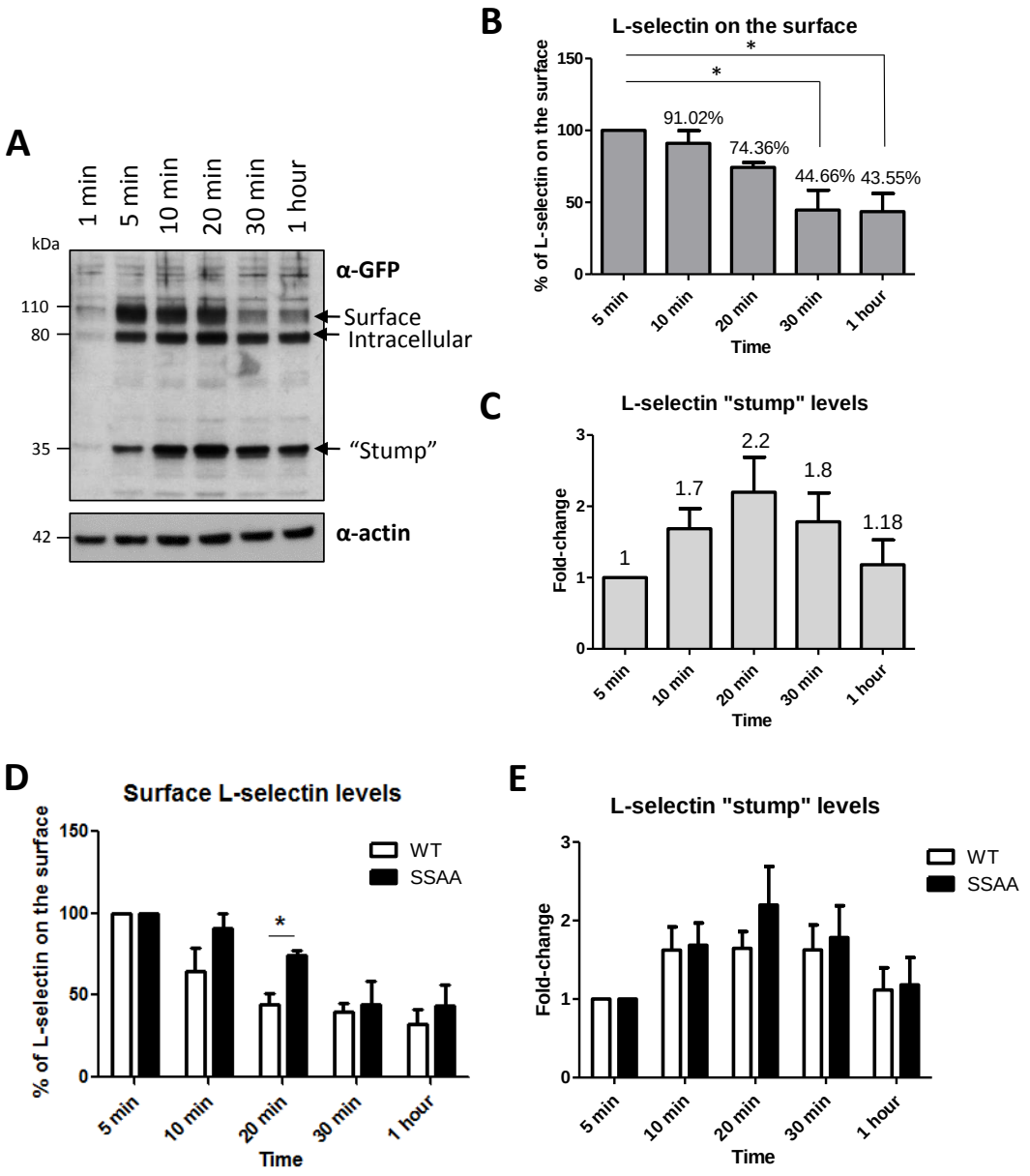

Figure 4.4 Serine-to-alanine mutation of the L-selectin tail delays shedding when THP-1 cells are incubated with activated HUVEC under static conditions. THP-1 cells expressing SSAA L-selectin-GFP Hi20 were added on top of activated HUVEC for 1 to 60 minutes. Bound fractions were then collected, lysed and analysed for L-selectin protein by Western blotting using anti-GFP antibody. **A)** Representative Western blotting showing shedding of surface SSAA-L-selectin-GFP when THP-1 cells interact with TNF-α-activated HUVEC over one hour period of time. Three independent Western blots were used to perform densitometric analysis of surface SSAA L-selectin-GFP (**B**) and L-selectin-GFP "stump" (**C**). **D)** Comparison of densitometric results of full-length WT- and SSAA-L-selectin-GFP levels on THP-1 cells interacting with TNF-α-activated HUVEC monolayers. Significantly more surface L-selectin was found at 20 minute time-point for SSAA mutant as compared to WT L-selectin-GFP expressing THP-1 cells. **E)** Comparison of changes in L-selectin-GFP "stump" levels between WT and SSAA mutant. Statistical analysis in B and C: One-way ANOVA followed by Tukey's post-test. No differences were detected in C. Statistical analysis in D and E: Two-tailed, unpaired Student's t-test for each time point. Error bars represent standard error. *=$p<0.05$.

4.3.5 Characterisation of interactions between THP-1 cells and TNF-α activated HUVEC under flow

The results shown above indicate that, when subjected to the static transmigration assay, THP-1 cells bind to TNF-α-activated HUVEC within the first 5 minutes and L-selectin shedding peaks at 20 minutes (**figure 4.1**). During the optimisation phase of the *in vitro* parallel plate flow chamber experiments, it was noticed that it took two minutes for the first THP-1 cells to arrive from the cells reservoir, and the cells were rapidly attaching to the activated HUVEC monolayer. A parallel plate flow chamber assay was hence designed, where cells were perfused over a monolayer of TNF-α activated HUVEC over a 15 minute period of time. This was thought to represent the time at which L-selectin shedding was occurring, and it was hence important to establish what type of interactions were formed between THP-1 cells and activated HUVEC cells during this period. A detailed method of the *in vitro* parallel plate flow chamber assay used in these experiments is described in **section 2.14**. Few cells could be identified as "fully transmigrated" when the experiment was stopped after 15 minutes of flow. Transmigrated leukocytes can be easily identified by their phase-dark appearance [659-662], and extremely rarely such cells could be seen (approximately 1 cell per experiment where three fields of view were acquired). However, the cells appeared to have commenced transmigration by forming membrane extensions, termed pseudopods, which were thought to extend beneath the HUVEC monolayer. Still images from a recorded movie clearly show that the cells started to form pseudopods as early as 3 minutes after attachment, and that these pseudopods were very dynamic (**figure 4.5**, compare minute 3 to minute 9).

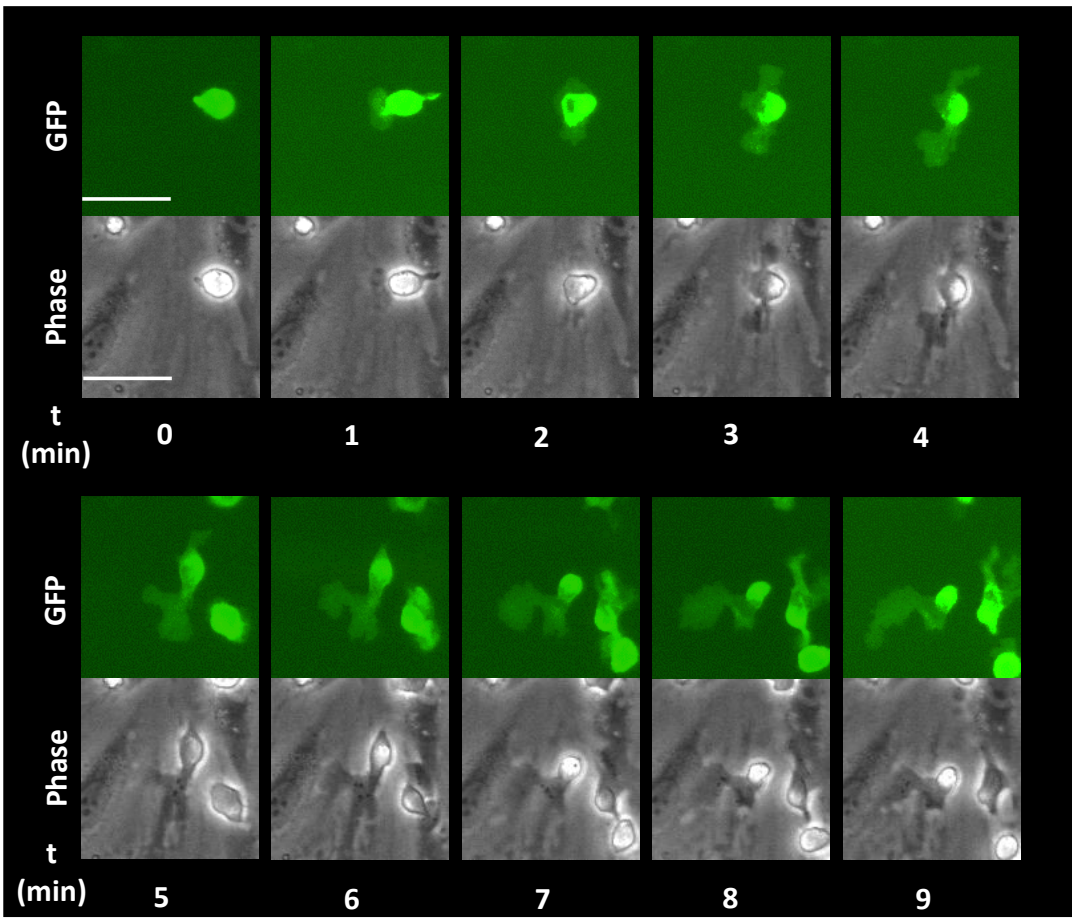

Figure 4.5 THP-1 cells form pseudopods just a few minutes after adhesion. THP-1 WT L-selectin-GFP Hi20 cells were perfused over TNF-α activated HUVEC monolayer (see **section 2.14.3**) and the acquired footage was used to generate time-lapse stills. Just a few minutes after adhesion (time point=0 min), THP-1 cells send processes (pseudopods) underneath the HUVEC monolayer. Scale bar: 30 µm.

Although the phase dark appearance of the pseudopods suggested their subendothelial localisation, this had to be validated to ensure that THP-1 cells were indeed undergoing transmigration. In order to analyse this, the experiment was repeated, flow was stopped after 7 minutes and the cells were fixed with 4% PFA. The seven minute perfusion meant that the cells had been interacting with HUVEC for 5 minutes after attachment and as a result the fixed sample was a representative of 5 minutes, as shown in **figure 4.5**. Fixed cells were permeabilised and stained with TRITC-phalloidin and prepared for confocal microscopy as described in **section 2.16.2**. TRITC-phalloidin staining enabled visualisation of actin cables belonging to HUVEC and hence it was possible to identify the z-positions of THP-1 cells. The monocyte cell body was attached to the apical HUVEC surface (**figure 4.6 A** *"Top"*), and this z-plane is hereafter referred to as "Top". The pseudopods were positioned underneath the HUVEC monolayer (**figure 4.6 A** *"Bottom"*) and this z-plane is hereafter referred to as "Bottom". Z-stacks of the cells were acquired and used to generate 3D images of the THP-1 and HUVEC cells (**section**

2.16.3). Phalloidin staining of the actin-based cytoskeleton was used as a guide to what was above and beneath the endothelium. Three-dimensional reconstruction of thin optical sections (0.75 μm) obtained from laser scanning confocal microscopy revealed that the pseudopods of THP-1 cells were positioned underneath the actin cables belonging to HUVEC cells (**figure 4.6 B**). To test whether the pseudopods remained underneath the endothelium at the end of the flow experiments, 3D reconstruction was repeated with cells fixed after 15 minutes of perfusion. Again, it was discovered that the pseudopods were positioned underneath the HUVEC monolayer (**figure 4.6 C**). These results demonstrated that THP-1 WT L-selectin-GFP Hi20 cells initiated transmigration through TNF-α activated HUVEC by extending dynamic membrane pseudopods underneath the endothelial cells, and such cells are hereafter referred to as "transmigrating cells". Unfortunately, the cells did not fully transmigrate underneath the endothelium. This was thought to be a result of the sheer size of the cell, or its nucleus; THP-1 cells are large and are physically unable to undergo full TEM. The drawback of this is that the process of complete TEM cannot be studied in our model. However, the advantage of this is that we can more closely interrogate the initial phases of TEM.

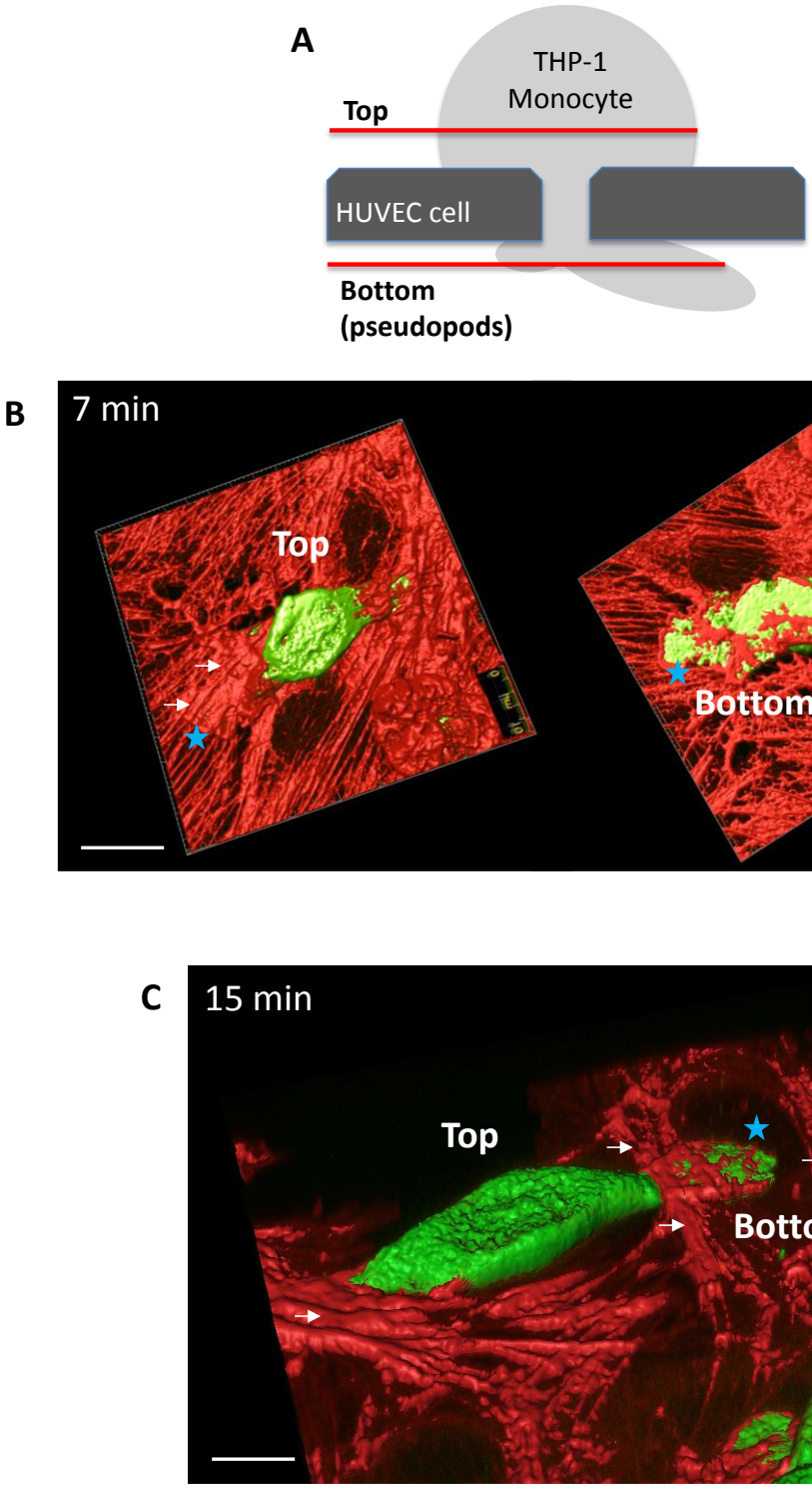

Figure 4.6 THP-1 monocytes expressing L-selectin-GFP initiate transmigration through HUVEC by extending pseudopods underneath the endothelial cells. THP-1 WT L-selectin-GFP Hi20 cells were perfused over TNF-α activated HUVEC for 7 or 15 minutes (**section 2.14.3**), fixed with 4% PFA and stained with TRITC-phalloidin (**section 2.16.2**). Series of z-stacks were acquired by confocal microscope and Imaris software was used to compile the stacks, followed by "volume rendering" (**section 2.16.3**). The GFP channel was used to render THP-1 cells volume (shown in green) and TRITC-phalloidin was used to render actin volume (shown in red). **A)** Schematic showing typical appearance of a THP-1 monocyte interacting with HUVEC under flow. Cell body is attached to the apical surface of the endothelial cells ("Top") and the pseudopods extend beneath the HUVEC monolayer ("Bottom"). **B)** Top and Bottom view showing a representative 3D reconstruction of a THP-1 cell transmigrating through a monolayer of HUVEC

at 7 minute time-point. Pseudopods (blue stars) extend underneath the actin cables of endothelial cells (arrows). Scale bar: 10 µm. **C)** Representative 3D reconstruction of THP-1 cell transmigration at 15 minutes. In this particular example, the monocyte pseudopod (blue star) is positioned directly underneath the nucleus of the endothelial cell. The endothelial cell can be identified by characteristic actin cables (arrows). The nucleus can be detected by typical oval shape where phalloidin staining is absent. The large gap where the nucleus is positioned, and neither GFP nor actin volume is present, allows a "see-through" mode, and thus both Top and Bottom views can be seen in a single view. Scale bar: 5 µm.

4.3.6 WT L-selectin-GFP is enriched in "spots" in the protruding pseudopods of transmigrating THP-1 cells under flow

Data presented in the section above show that during 15 minute perfusion over activated HUVEC, THP-1 cells form dynamic pseudopods that protrude underneath the endothelial monolayer. This represents early transmigration stage of the leukocyte adhesion cascade. Additionally, based on the results obtained during static transmigration assays (**figure 4.1**), shedding of L-selectin is understood to occur during this time. It was hoped that detailed, high magnification images of transmigrating THP-1 monocytes could provide information as to the spatial distribution of L-selectin-GFP during the 15 minutes of perfusion. This in turn could provide clues as to where L-selectin shedding was occurring in any given cell. To this end, flow experiments were stopped after 7 or 15 minutes of perfusion and the cells were fixed with 4% PFA. The seven minute time-point was thought to represent the time of minimal L-selectin-GFP shedding, and the 15 minute time-point was thought to be a representative of the time at which shedding was nearly at its maximum. Fixed cells were prepared for confocal microscopy (**section 2.16.2**), and confocal images were acquired of single z-planes representing Top and Bottom views (Top and Bottom views were as shown in **figure 4.7 A**). Control THP-1 GFP Hi20 cells exhibited a uniform, diffuse GFP distribution at 7 minutes, which did not change over time (**figure 4.7 A**). Although not abundant, high intensity GFP "spots" were found to be localised in the pseudopods of transmigrating THP-1 WT L-selectin-GFP Hi20 cells at 7 minute time-point (**figure 4.7 B**). Interestingly, these GFP-positive spots appeared to accumulate more with time as seen in the images from the 15 minute time-point (**figure 4.7 C**). A lack of GFP-positive spots in the control cells suggested that there were specific accumulations of L-selectin-GFP, and not GFP protein alone. For quantification of L-selectin-GFP spots, only the pseudopods were selected. This was because L-selectin-GFP was previously found to be abundant in the intracellular compartments (**figure 3.8**). It was hence assumed that the L-selectin-GFP spots present in the cell body could be easily confused for protein localised to the endoplasmic reticulum or the trans Golgi network. By excluding the cell body from the analysis one could ensure that only L-selectin-GFP spots present in protruding and transmigrated regions of the cell were

being assessed. The method for analysing L-selectin-GFP spots is described in more detail in **section 2.16.4**. As shown in **figure 4.8**, an average 26 L-selectin-GFP spots per cell were seen in the pseudopods at the 7 minute time-point, and average of 62 spots per cell were present in the pseudopods after 15 minutes. This indicated a time-dependent increase in the formation of these spots. No spots were seen in the pseudopods of the control THP-1 GFP Hi20 cells across the two time-points analysed, further suggesting that the spots represented L-selectin-GFP.

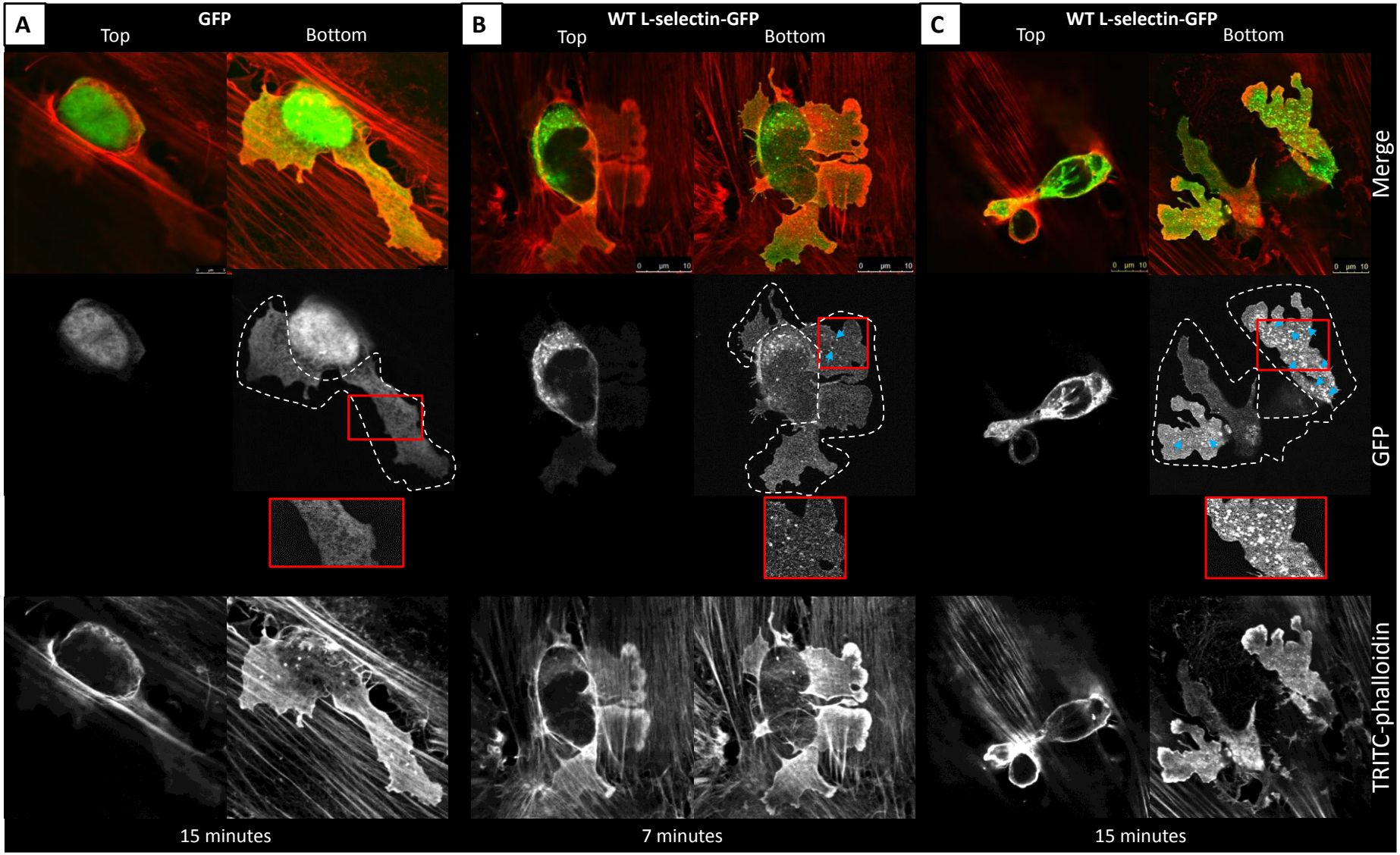
A
GFP
Top
Bottom
B
WT L-selectin-GFP
Top
Bottom
C
WT L-selectin-GFP
Top
Bottom
Merge
GFP
TRITC-phalloidin
15 minutes
7 minutes
15 minutes

Figure 4.7 A time-dependent accumulation of WT L-selectin-GFP "spots" in the pseudopods of THP-1 cells. GFP or WT L-selectin-GFP expressing THP-1 cells were perfused over TNF-α activated HUVEC monolayer for 7 or 15 minutes, fixed with 4% PFA and stained with TRITC-phalloidin. Figures A-C show representative single z-plane (0.75 μm thickness) confocal images of the fixed cells, where the pseudopods are outlined with dashed lines. Top and Bottom z-planes are as shown in **figure 4.6 A**. Images of the GFP channel include magnified sections of the areas outlined in red. For perfusion of cells in the parallel plate flow chamber assay see **section 2.14.3**. Preparation of cells for confocal microscopy and z-stack acquisition are described in **sections 2.16.2** and **2.16.3**, respectively. **A)** A diffuse distribution of GFP in the control THP-1 GFP Hi20 cells at 15 minutes. Similar images for the 7 minute time-point exist, but are not shown in the figure. Scale bar: 5 μm. **B)** Low numbers of WT L-selectin-GFP spots (blue arrows) in the pseudopods of THP-1 WT L-selectin-GFP Hi20 cells at 7 minute time-point. Scale bar: 10 μm. **C)** At the 15 minute time-point, WT L-selectin-GFP "spots" (blue arrows) can be seen in the pseudopods of THP-1 WT L-selectin-GFP Hi20 cells. Scale bar: 10 μm.

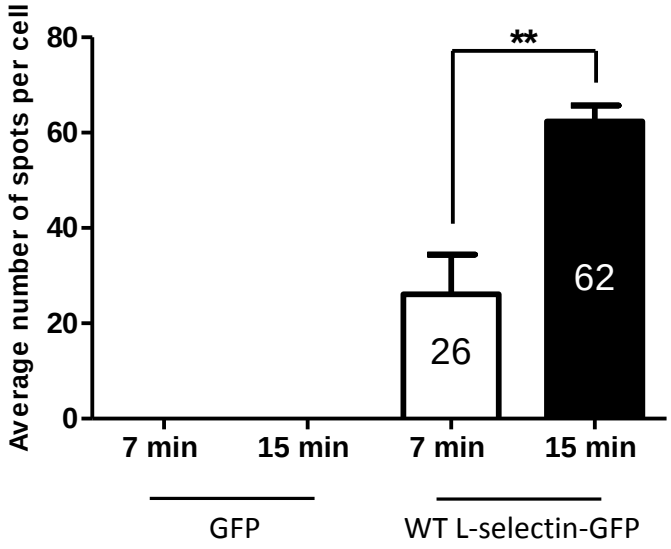

Figure 4.8 Quantitative analysis of L-selectin-GFP spots accumulating in the pseudopods of THP-1 cells over time. The GFP-positive spots shown in **figure 4.3** were scored using the "Find spots" feature on Volocity image analysis software (**section 2.16.4**). The graph shows the average number of spots per cell. No spots can be seen accumulating in THP-1 GFP Hi20 cells. At 7 minutes, an average of 26 spots are present in THP WT L-selectin-GFP Hi20 cells (WT L-selectin-GFP), which increases to an average of 62 spots at 15 minute time-point. Fifteen cells were analysed per experiment and experiments were repeated three times for each cell line. Mean values are shown for each bar. Error bars represent S.E.M. Statistical analysis: Two-tailed, unpaired Student's t-test. **=$p<0.01$.

The results demonstrated that when THP-1 cells initiated TEM by sending pseudopods underneath the HUVEC monolayer, L-selectin-GFP accumulated in those pseudopods over-time. Yet, the nature of the L-selectin-GFP spots was unclear at this point. Since the scoring was performed on the GFP-tag, the spots could represent full-length L-selectin-GFP, L-selectin-GFP "stump" or a mix of the two. It was hypothesised that, if the spots represented L-selectin "stump", their accumulation could indicate L-selectin

shedding. On the other hand, accumulation of full-length L-selectin-GFP could mean that the spots represented clustered L-selectin.

4.3.7 Generation of THP-1 cell lines expressing the sheddase-resistant (ΔM-N) form of L-selectin-GFP

A sheddase-resistant form of L-selectin has been used in the past to study the role of shedding [22, 419, 529]. It was thus decided to generate THP-1 cell line expressing sheddase resistant L-selectin-GFP to further investigate the role of L-selectin shedding during the initial stages of TEM. L-selectin is cleaved in the extracellular region between lysine-321 and serine-322, which is close to the plasma membrane [326], and deletions within this region are known to abrogate L-selectin shedding [528]. A two-step site-directed *in vitro* PCR mutagenesis was performed on wild type L-selectin cDNA in the lentivirus backbone vector pHR´SIN-SEW-L-selectin^{WT}-GFP (**section 2.5)**. Deletion of an 8 amino acid sequence (MIKEGDYN) within the membrane proximal site rendered L-selectin sheddase- resistant, and this form from hereon will be termed ΔM-N L-selectin (**figure 4.9**). The ΔM-N mutant has been characterized previously and was demonstrated to effectively inhibit PMA-induced shedding [522]. The resulting construct, termed pHR´SIN-SEW-L-selectin$^{\Delta M\text{-}N}$-GFP was sequenced to ensure that the desired deletion had been achieved and no spontaneous mutations had occurred within the L-selectin ORF. The lentiviral backbone vector carrying ΔM-N L-selectin-GFP was then used to generate lentiviral particles as described in **section 3.3.1.2** and **section 2.11**. The titre of the concentrated lentivirus suspension is presented in **table 2.5**.

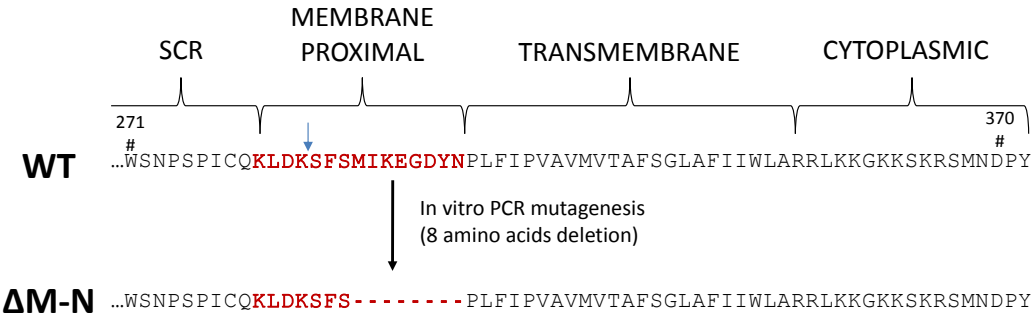

Figure 4.9 Construction of sheddase resistant (ΔM-N) L-selectin mutant. Amino acid sequence of the C-terminal portion of human L-selectin, including the entire cytoplasmic, transmembrane and membrane proximal (shown in red) sites. A two-step site-directed *in vitro* PCR mutagenesis (**section 2.5**) was used to delete sequence of eight amino acids within membrane proximal site to render L-selectin shedding resistant (ΔM-N). The cleavage site is shown with the blue arrow. SCR, sequence consensus repeats.

Following the established method of THP-1 cell transduction, originally outlined in **section 3.3.1.3,** THP-1 cells were infected with MOI or 5 and 20 with lentivirus carrying the ΔM-N L-selectin-GFP transgene. A detailed method of THP-1 cell transduction is described in **section 2.11.4**. The resultant polyclonal cell lines, termed THP-1 ΔM-N L-selectin-GFP MOI 5 (indicating a low expressor cell line) and ΔM-N L-selectin-GFP MOI 20 (indicating a high expressor cell line), were FACS-sorted into uniform cell populations expressing matched levels of L-selectin. The sorted cell lines were named THP-1 ΔM-N L-selectin-GFP Lo5 (low expressor) and THP-1 ΔM-N L-selectin-GFP Hi20 (high expressor).

4.3.8 Characterisation of THP-1 cell lines expressing ΔM-N L-selectin-GFP

4.3.8.1 Analysis of ΔM-N L-selectin-GFP expression levels in THP-1 cells

The expression levels of WT and serine-to-alanine mutant forms of L-selectin-GFP have so far all been matched. Matched L-selectin expression was seen with high expressor cell lines (Hi20) (**figure 4.6**). However, it was the low expressor THP-1 ΔM-N L-selectin-GFP Lo5 cells that had matched L-selectin expression levels to those of THP-1 WT L-selectin-GFP Hi20 cells (**figure 3.10 A** and **B**). THP-1 ΔM-N L-selectin-GFP Hi20 had significantly higher levels of both GFP-tag and surface L-selectin than THP-1 WT L-selectin-GFP Hi20 (**figure 4.10 A** and **B**). This was hypothesised to be due to the lack of basal shedding in ΔM-N L-selectin-GFP. When Ro-31-9790 is used to inhibit basal shedding in THP-1 WT L-selectin-GFP Hi20 cells, surface L-selectin levels increase significantly (**figure 3.10**). Therefore L-selectin expression on THP-1 ΔM-N L-selectin-GFP Hi20 cells could mimic an outcome seen in Ro-31-9790-treated WT L-selectin-GFP Hi20cells. As a result, in order to ensure matched L-selectin levels between the cell lines, THP-1 ΔM-N L-selectin-GFP Lo5 cell line was chosen for further studies. It was noticed that, even though RPE MFI values, representing surface L-selectin levels, between THP-1 WT L-selectin-GFP Hi20 and THP-1 ΔM-N L-selectin-GFP Lo5 were matched, the flow cytometric profiles showed slightly different distribution of the cell populations (**figure 4.10 C**). The ΔM-N histogram appeared as a sharp peak at the higher end of the fluorescence intensity scale, whereas the WT histogram was shorter and broader suggesting a much broader distribution of surface L-selectin expression between the cells within the population (**figure 4.10 C** *right histogram*). No differences were seen in the histograms representing GFP-tag levels (**figure 4.10 C** *left histogram*). The reason for this was not clear but it was hypothesised that a lack of basal shedding in THP-1 ΔM-N L-selectin-GFP Lo5 cells resulted in an accumulation of L-selectin at the plasma membrane. As such, there would be little variability in the surface L-selectin expression between the cells within the population. Conversely, WT L-selectin-GFP was subjected

to constitutive turnover (**figure 3.10**), and hence a slight variability in surface L-selectin expression within the population was likely to occur. As expected, Western blotting analysis revealed that THP-1 ΔM-N L-selectin-GFP Lo5 cells did not produce a L-selectin "stump", suggesting that basal shedding was abolished in this cell line. This is explored further in the **section 4.3.8.2** below. Furthermore, the intracellular (~80 kDa) band in the lysates from THP-1 ΔM-N L-selectin-GFP Lo5 cells was less abundant than in the lysates derived from the THP-1 WT L-selectin-GFP Hi20 cells (**figure 4.10 D**). This made sense given the different MOIs used (5 versus 20).

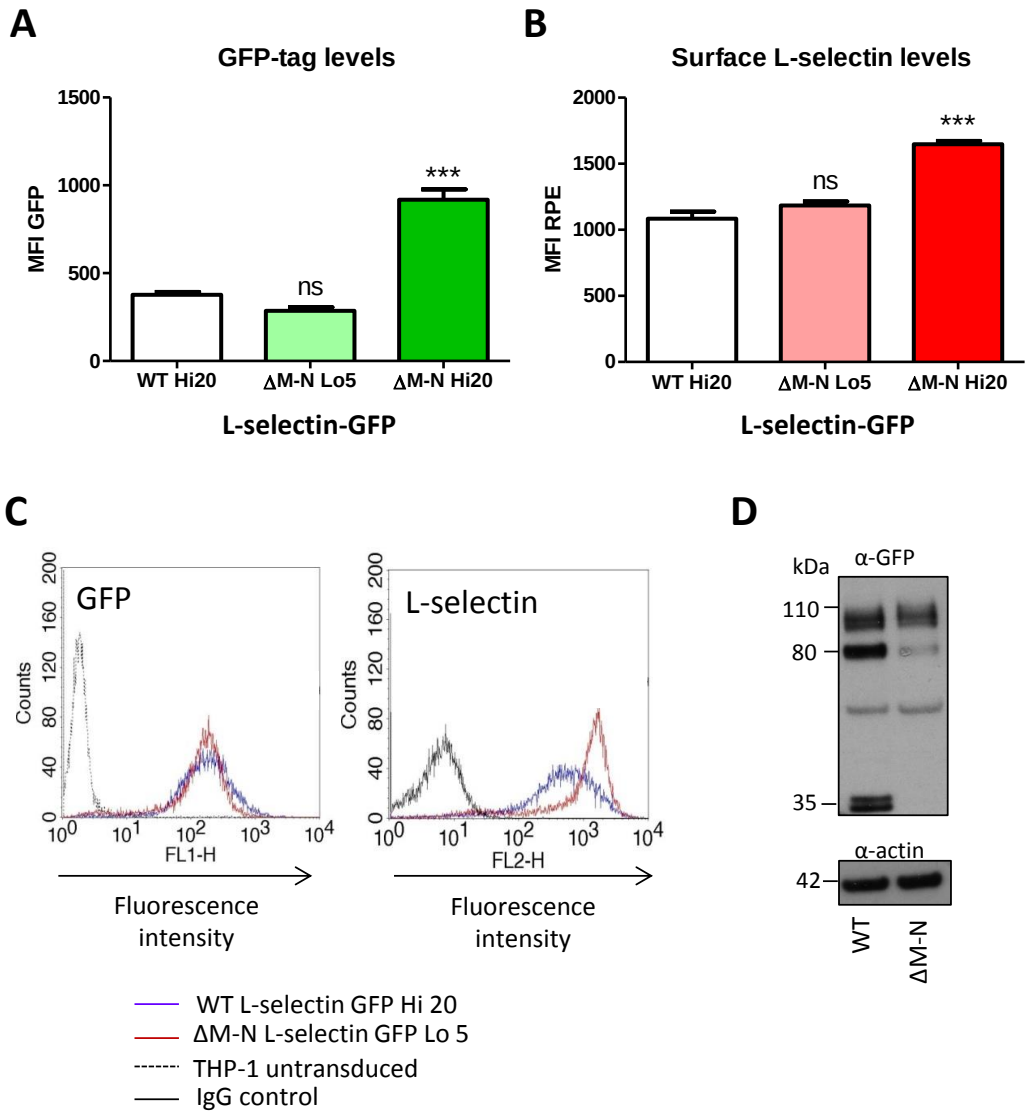

Figure 4.10 Expression of ΔM-N L-selectin-GFP in THP-1 cells. THP-1 cells expressing low (Lo5) or high (Hi20) levels of ΔM-N L-selectin-GFP were compared to THP-1 cells expressing WT L-selectin-GFP Hi20. Flow cytometry analysis (**section 2.13**) was performed to compare MFI values of both GFP-tag **(A)** and surface L-selectin **(B)**. Experiments were performed in triplicates on three independent occasions. Error bars represent S.E.M. **C)** Representative histograms comparing GFP-tag (left histogram) and surface L-selectin (right histogram) levels of THP-1 WT L-selectin-GFP Hi20 and ΔM-N L-selectin-GFP Lo5. **D**) Representative Western blotting showing lack of L-selectin-GFP "stump" and decrease in L-selectin-GFP intracellular form in the extracts

from THP-1 ΔM-N L-selectin-GFP Lo5 cells as compared to the THP-1 WT L-selectin-GFP Hi20 cells. Statistical analysis in A and B: One-way ANOVA and Dunnett's post-test against "WT Hi20". ***=p<0.001. MFI, Mean Fluorescence Intensity.

4.3.8.2 Basal and activated L-selectin shedding is abrogated in THP-1 cells expressing ΔM-N L-selectin-GFP

To formally test the hypothesis that ΔM-N L-selectin-GFP could not be turned over in THP-1 cells, the cells were treated with Ro-31-9790 metalloprotease inhibitor that can inhibit ADAM17 enzyme. The metalloprotease inhibitor Ro-31-9790 did not cause any additional increase in the surface expression of ΔM-N L-selectin-GFP (**figure 4.11 A** red bar), confirming that ΔM-N mutation abrogates basal shedding of L-selectin in THP-1 cells. As expected, PMA stimulation did not promote shedding in this cell line (**figure 4.11 A** blue bar). Interestingly, surface levels of ΔM-N L-selectin increased slightly upon PMA stimulation, although this was not statistically significant. Whether this finding was a coincidence or whether there was an actual influence of PMA stimulation on surface ΔM-N L-selectin levels was not clear. It may be that PMA stimulation increased trafficking of ΔM-N L-selectin-GFP to the plasma membrane via activation of the secretory pathway. PMA has been shown previously to stimulate secretory pathways [663] and elevate cell surface protein levels [664]. No change in GFP-tag levels upon PMA stimulation (**figure 4.11 B** blue bar) would support this hypothesis. The GFP-tag would provide the same flow cytometric read-out irrespective of its intracellular or surface localisation.

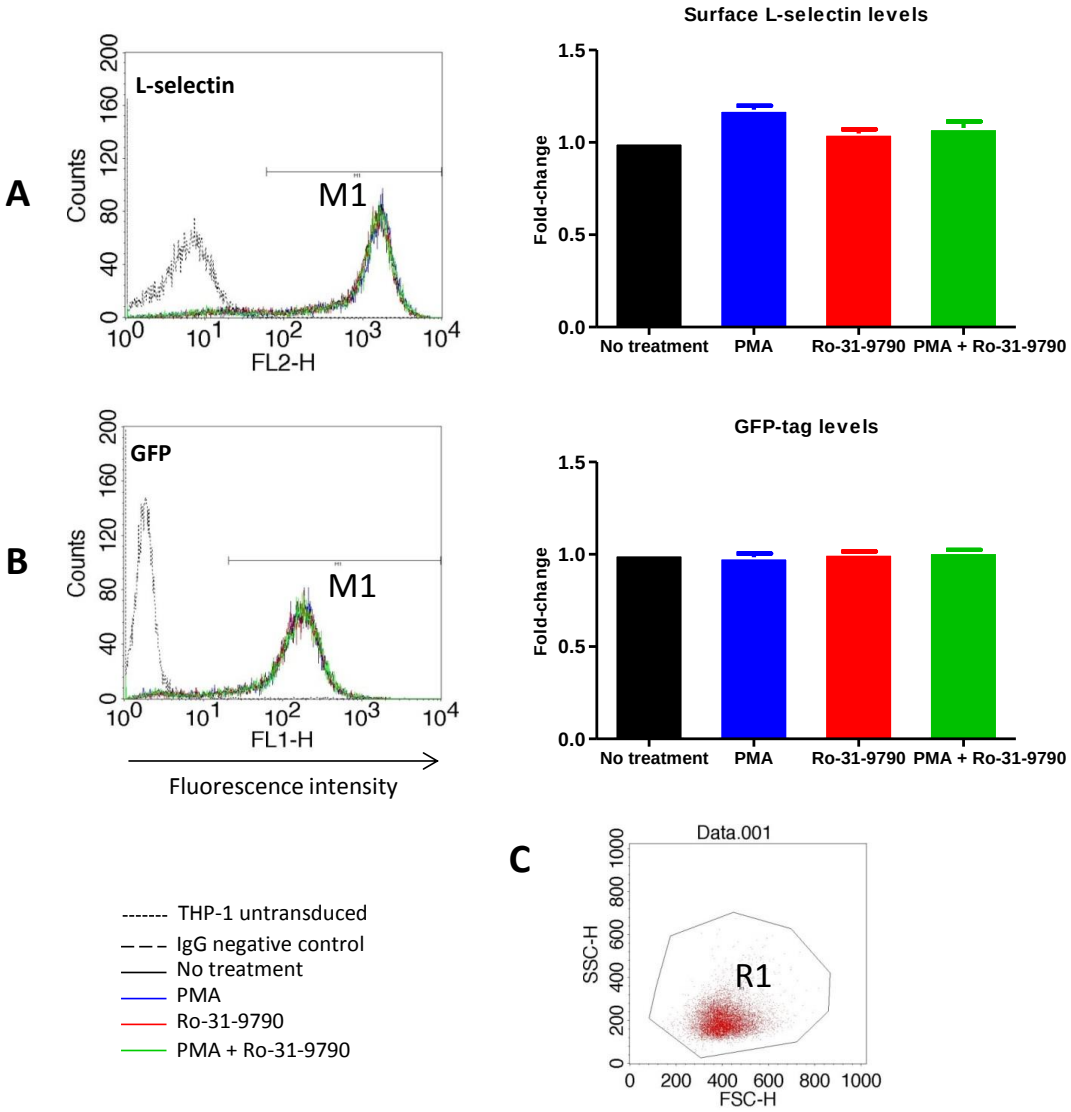

Figure 4.11 No shedding occurs in THP-1 cells expressing ΔM-N L-selectin. THP-1 cells expressing ΔM-N L-selectin-GFP Lo 5 were stimulated with PMA, ADAM17 inhibitor Ro-31-9790 or both and analysed for both GFP-tag and surface L-selectin levels as described in **figure 3.10**. **A)** Surface L-selectin expression was not modified by any of the stimuli used. Slight increase in the expression was seen in MFI values upon PMA stimulation but this was not statistically significant. M1 on the histogram shows gate for RPE positive THP-1 cell population. **B)** GFP-tag levels, where M1 (histogram) shows gate for GFP positive cells did not change upon treatment with any of the stimuli. **C)** Gate R1 in the scatter profile contains population of viable THP-1 cells and was applied to all samples. Histograms in A, B and C represent the changes seen in a typical experiment and fold-changes of L-selectin surface levels shown on corresponding graphs were established on the basis of MFI values acquired for 3 independent experiments. Data represent mean ± SEM and no significance were found by One-way ANOVA.

4.3.9. Shedding of L-selectin-GFP directly correlates with an accumulation of GFP-positive "spots" in the transmigrating pseudopods of THP-1 cells

As described in **section 4.3.5** and **4.3.6**, mutating both serines in the L-selectin tail to alanines would decrease the extent of shedding in response to TNF-α (**figure 4.3 B**). In

addition, a corresponding delay in shedding of L-selectin-GFP was observed in the static transmigration assays **(figure 4.4**). Following the hypothesis that accumulation of WT L-selectin-GFP spots in the pseudopods of transmigrating THP-1 cells could indicate shedding (**section 4.3.2**), it would be of interest to determine if the accumulation of SSAA L-selectin-GFP spots was also decreased. Additionally, analysis of the ΔM-N L-selectin-GFP accumulation could directly answer the question whether shedding and GFP-positive spots accumulation were linked. Flow cytometric analysis revealed that THP-1 SSAA L-selectin-GFP Hi20 and ΔM-N L-selectin-GFP Lo5 cells had matched L-selectin-GFP expression to that of THP-1 WT L-selectin-GFP Hi20 cells (**figure 4.2** and **figure 4.10**). These cell lines were therefore employed in this study. Accumulation of WT L-selectin-GFP spots was observed after 15 minutes of flow (**figure 4.8**), and this time-point corresponds to the period just before the peak of shedding is seen in the static transmigration assays (**figure 4.1**). It was hence anticipated that if any differences were to be seen between WT, SSAA and ΔM-N L-selectin-GFP accumulation, this would be most prominent after 15 minutes of perfusion. The cells were therefore subjected to a 15 minute-long flow assay and then numbers of spots were compared to THP-1 WT L-selectin-GFP Hi20 cells. **Figure 4.12** shows that after 15 minute perfusion, both SSAA L-selectin-GFP and ΔM-N L-selectin-GFP appeared to accumulate less spots than WT L-selectin-GFP. Additionally, very prominent long and thin membrane extensions, termed spikes, were seen extending from some of the cells. To analyse possible differences between the cell lines against WT L-selectin-GFP, spots were analysed as described earlier in **section 4.3.2**. Spikes were manually counted for each cell, and average number per cell was calculated (see **section 2.16.4**). As shown in **figure 4.13 A**, the average number of SSAA L-selectin-GFP spots was significantly lower than that observed for WT L-selectin-GFP (35 versus 62). The ΔM-N L-selectin-GFP spots accumulated even less, as the average number of spots per cell was calculated to be only 17. This was below the number of WT L-selectin-GFP spots seen accumulating at 7 minutes (average 26 spots per cell) (**figure 4.8**). Hence, it appeared that ΔM-N L-selectin-GFP spots did not accumulate at all. Although an increase in spikes was seen in THP-1 cells expressing SSAA L-selectin-GFP, it was not considered to be statistically significant (**figure 4.13 B**). Additionally, a great variability of number of spikes was seen between cells within any given cell line.

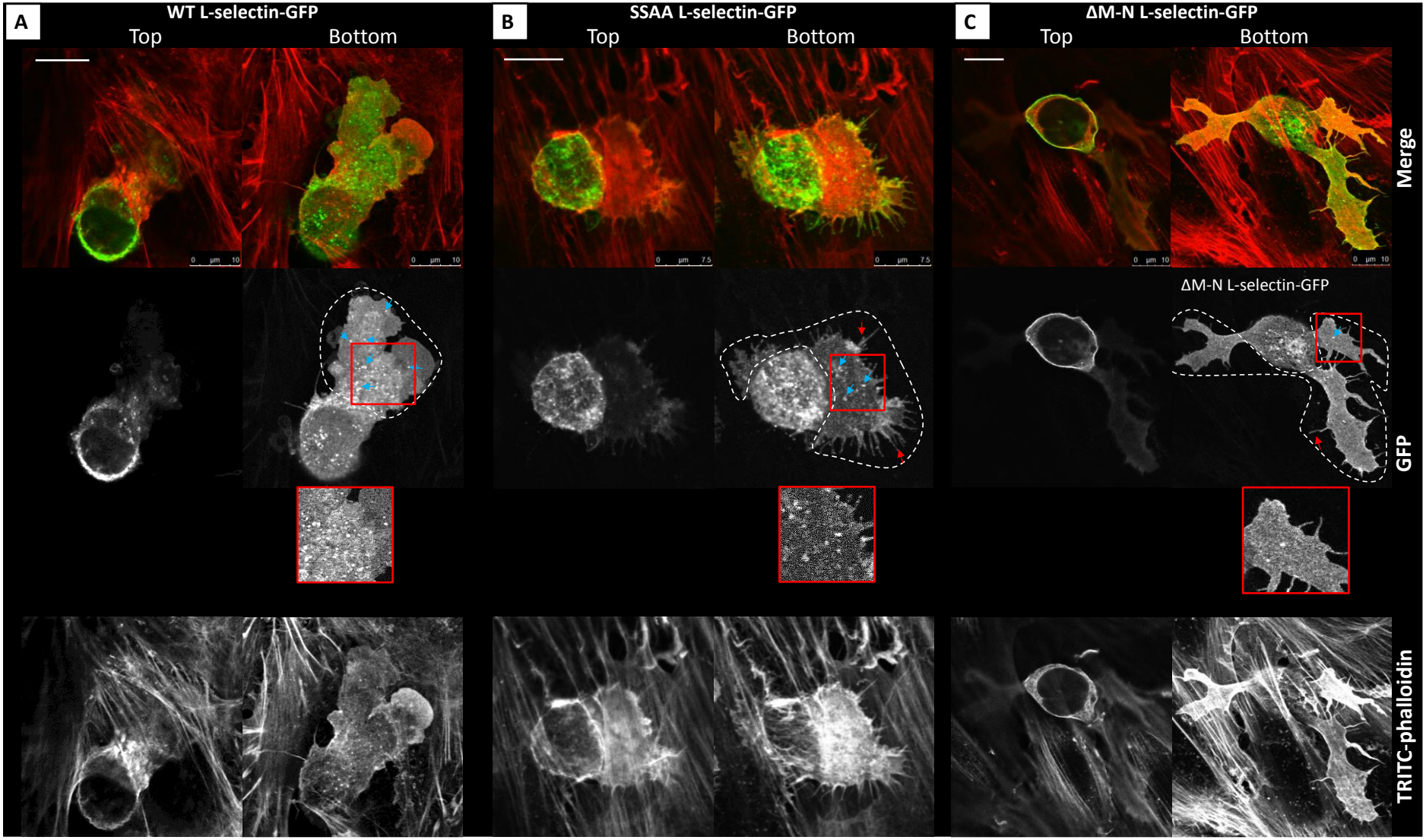
A
WT L-selectin-GFP
Top
Bottom
B
SSAA L-selectin-GFP
Top
Bottom
C
ΔM-N L-selectin-GFP
Top
Bottom
Merge
ΔM-N L-selectin-GFP
GFP
TRITC-phalloidin

Figure 4.12 Relationship between shedding and accumulation of L-selectin-GFP spots in the protruding pseudopods of THP-1 cells. THP-1 cells expressing SSAA or ΔM-N L-selectin were perfused over TNF-α activated HUVEC for 15 minutes, fixed with 4% PFA, stained with TRITC-phalloidin and analysed by confocal microscopy. For detailed methods describing parallel plate flow chamber assay and the confocal microscopy analysis see **sections 2.14.3** and **2.16**, respectively. Representative single z-plane confocal images of Top and Bottom views (see **figure 4.6 A**) of transmigrating THP-1 cells at a 15 minute time-point are shown. L-selectin-GFP spots are shown with blue arrows. Magnified sections of selected areas are shown in red. Spikes extending from the pseudopods are indicated with red arrows. The dashed lines encircle the protruded areas that were analysed to measure spots. **A)** WT L-selectin-GFP accumulates in the pseudopods of THP-1 cells. This particular cell does not have any spikes. Scale bar: 10 μm. **B)** SSAA L-selectin-GFP accumulates in the pseudopods, although less spots seem to be formed. This particular cell presents with a high number of spikes. Scale bar: 7.5 μm. **C)** ΔM-N L-selectin-GFP spots does not accumulate in the pseudopods. A few spikes can be seen in this example cell. Scale bar: 10 μm.

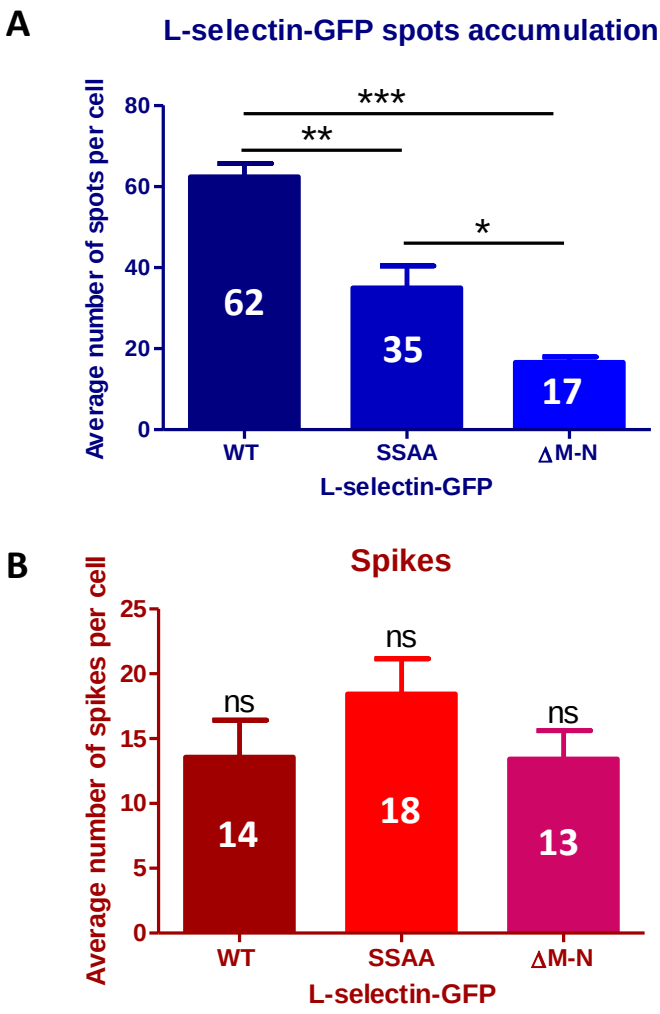

Figure 4.13 Monitoring the accumulation of spots and spikes in the protruding pseudopods of transmigrating THP-1 cells expressing WT, SSAA or ΔM-N L-selectin-GFP. L-selectin-GFP spots and spikes shown in the representative images in **figure 4.12** were quantified. Each bar in the histogram shows the average number of GFP-positive spots per cell. **A)** Spots were

analysed as described in **figure 4.8**. Accumulation of ΔM-N L-selectin-GFP spots did not occur and accumulation of SSAA L-selectin-GFP spots was less than that of WT L-selectin-GFP. **B)** Spikes were counted manually. Fifteen cells were analysed per experiment and experiments were repeated three times for each cell line. Mean values are shown for each bar. Error bars represent S.E.M. Statistical analysis: One-way ANOVA followed by Tukey's post-test. *=p<0.05 **=p<0.01, ***=p<0.001.

Since ΔM-N L-selectin-GFP does not undergo shedding and SSAA L-selectin-GFP sheds much slower that WT L-selectin-GFP in the static transmigration assays **(figure 4.4**), these results suggested a correlation existed between L-selectin shedding and the accumulation of spots. Although this work has not fully concluded that the spots signify shed L-selectin, it remains a strong possibility.

4.3.10 Investigating the fate of the L-selectin "stump" following shedding during transendothelial migration of THP-1 cells

Examination of the L-selectin-GFP spots in the pseudopods of transmigrating THP-1 monocytes suggested that WT L-selectin-GFP might be shed and accumulation of "stump" might occur in the pseudopods (**section 4.3.6** and **4.3.9**). When analysing L-selectin-GFP by confocal microscopy, it is not possible to distinguish between full-length L-selectin-GFP and L-selectin-GFP "stump" as both of the forms are attached to GFP. One way to address this issue would be to stain the fixed cells with DREG56 antibody and perform co-localisation analysis between GFP and DREG56. Unfortunately, DREG56 antibody does not recognise L-selectin from fixed specimens and this approach was not feasible.

The fate of the cleaved L-selectin is currently not known. It has been proposed that once the L-selectin ectodomain is shed, the "stump" is internalised and degraded [563]. When lymphocytes are stimulated with PMA over 60 minute period of time, Western blotting analysis shows that "stump" levels peak at 15 minutes and then gradually decrease [323]. Static transmigration assay used in this study showed that WT L-selectin-GFP "stump" is rapidly generated at 10 minutes and the levels persist up to 30 minutes after which "stump" is also being cleared (**figure 4.1 D**). Cells internalise membrane proteins by endocytosis and hence the observed clearance of the "stump" could be a result of endosomal uptake. If this was the case, L-selectin-GFP spots observed in the pseudopods after 15 minutes of flow could represent L-selectin-GFP "stump"-loaded endosomes. Two endosomal markers, early endosomal antigen 1 (EEA1) and late endosomal-lysosomal marker CD63 antigen are commonly used to detect early and late endosomes, respectively [665, 666]. Early endosomes can recycle back to the plasma membrane or mature into late endosomes [667]. Late endosomes proceed down the lysosomal route of protein degradation [667]. To test whether L-selectin-GFP spots co-

localised with any of the endosomal markers, THP-1 WT L-selectin-GFP cells were subjected to a 15 minute-long parallel plate flow chamber assay, fixed with 4% PFA and prepared for confocal microscopy as described in **section 2.16.2**. No co-localisation of WT L-selectin-GFP with CD63 was found (Dr A. Ivetic, unpublished data) suggesting that L-selectin-GFP "stump" did not undergo degradation through this pathway. Similarly, no co-localisation was found between WT L-selectin-GFP spots and EEA1 (**figure 4.14**). However, this result is hard to interpret as the EEA1 staining was clearly seen in the HUVEC cells suggesting that antibody did not recognise its antigen in THP-1 cells. Although EEA1 has been used previously to detect early endosomes in THP-1 cells, the staining was performed after three days of PMA treatment [665]. It is thus possible that undifferentiated THP-1 cells have a relatively low capacity to phagocytose and on that basis, it is possible that they express low levels of EEA1. It has also been observed that primary smooth muscle cells lose EEA1 expression upon immortalisation (Aleksander Kapustin, King's College London, personal communication) and perhaps THP-1 cell line does not express EEA1 antigen.

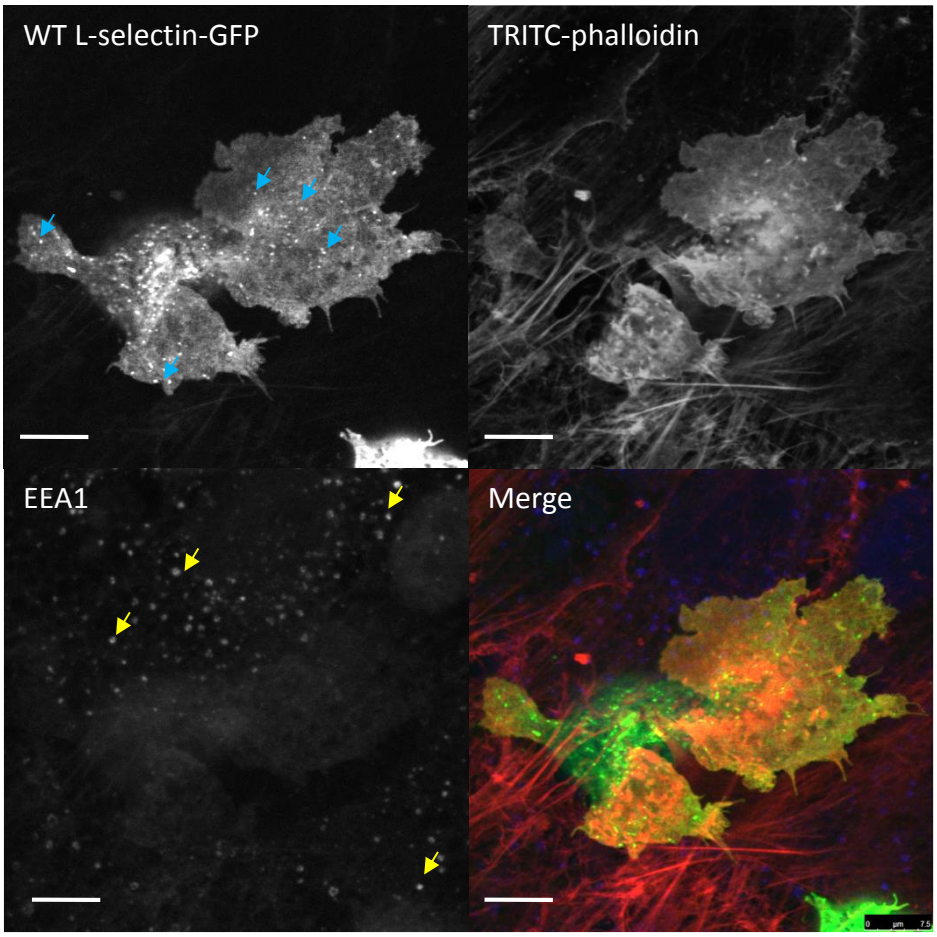

Figure 4.14 WT L-selectin-GFP in the pseudopods of transmigrating THP-1 cells does not co-localise with early endosome marker. THP-1 cells expressing WT L-selectin-GFP Hi20 were perfused over TNF-α activated HUVEC for 15 minutes (**section 2.14.3**), fixed with 4% PFA, stained with TRITC-phalloidin and early endosomes marker EEA1 and analysed by confocal microscopy (**section 2.16**). Images were acquired in the "Bottom" z-planes as shown in **figure**

4.6 A. Representative image shows L-selectin-GFP spots (blue arrows) in THP-1 cells and EEA1 staining (yellow arrows) in the HUVEC cells. No co-localisation between the two could be detected. Scale bar: 7.5 µm.

4.4 DISCUSSION

Leukocytes have been observed to shed their L-selectin during transendothelial migration [554-556], and blocking shedding results in abnormal emigration in to the surrounding tissue [22, 419, 518, 668]. This chapter attempts to determine the spatio-temporal resolution of L-selectin shedding during TEM and whether the serine residues in the cytoplasmic tail are involved in this regulation. Finally, this chapter embarked on experiments that were set out to explore the fate of the L-selectin "stump" following shedding.

4.4.1 L-selectin shedding is likely to occur during the early stages of TEM and is dependent on cytoplasmic serine residues

The results presented in this chapter demonstrate that when THP-1 cells are perfused over TNF-α activated HUVEC, the cells form dynamic pseudopods (**figure 4.5**). The pseudopods extend underneath the endothelial monolayer as early as 7 minutes in to the flow experiment and remain underneath the endothelium for the duration of the 15 minute-long flow assay (**figure 4.6**). However, THP-1 cells never fully complete transmigration across the HUVEC monolayer, which has been described by others [153, 643]. As a result this model of transendothelial migration is used to monitor L-selectin as cells are undergoing transmigration – in other words the early stages of TEM (see diagram in **figure 4.6 A**). Western blotting analysis of surface L-selectin revealed that shedding peaks at 20 minutes in the static transmigration assays (**figure 4.1**). Although this data did not provide any information as to the part of the cell at which shedding occurred, it clearly demonstrated that interaction of THP-1 cells with TNF-α activated HUVEC triggers L-selectin ectodomain shedding. This, alongside the results discussed above, suggests that L-selectin shedding and pseudopods extension could occur concomitantly. However, it is difficult to directly relate these events as the timing of TEM in static assays might not be an exact match of the timing seen under flow conditions. It should be noted that the static assay is devoid of flow and this may in itself influence the outcome of the observations.

To test the function played by L-selectin tail serine phosphorylation, non-phosphorylatable mutants of L-selectin were created. Stable cell lines expressing each serine mutant were generated successfully in THP-1 cells. The fact that all serine mutant constructs could be expressed to similar levels in these cells suggests that tail

phosphorylation is neither required for nor detrimental to, L-selectin-GFP expression and does not affect basal L-selectin shedding as assessed by flow cytometry (**figure 4.2**). However, it can be hypothesised that phosphorylation of the serines plays a role in TNF-α induced shedding of L-selectin from THP-1 monocytes, as introduction of the SSAA mutation resulted in reduced shedding (**figure 4.3**). Thus it could be suggested that the above described shedding of L-selectin-GFP induced by interaction of THP-1 monocytes with TNF-α activated HUVEC monolayers, could also be influenced by the phosphorylation of the serine residues. To test this possibility, THP-1 SSAA L-selectin-GFP Hi20 cells were subjected to the static transmigration assays and the changes in surface L-selectin-GFP occurring over time were compared to that of WT L-selectin-GFP. **Figure 4.4** shows that significantly more SSAA than WT L-selectin-GFP was retained at the cell surface at 20 minutes, and a similar trend was observed at a 10 minute time-point. No changes were seen at later time-points, suggesting that the SSAA mutation caused a delay in L-selectin ectodomain cleavage during the static transmigration assay. Hence, it is tempting to speculate that phosphorylation of the tail serines plays a role in L-selectin shedding during THP-1 monocyte TEM. Interestingly, Tsubota et al. (2013) showed that treatment of monocytes with a broad spectrum metalloprotease inhibitor GM6001 caused a delay in their transmigration through HUVEC monolayers under both static and flow conditions [669]. Although the authors attributed this result to inhibition of Mac-1 integrin cleavage, GM6001 – within the concentration range employed by Tsubota et al., 2013 [669] – is also used to prevent L-selectin shedding [670-673], and thus it seems that the contribution of L-selectin to the observed effect cannot be formally excluded. Surprisingly, however, this was not at all investigated in this study [669]. Since THP-1 cells do not fully transmigrate in the system used in this thesis, it was not possible to compare the number of transmigrated cells between THP-1 WT and SSAA L-selectin-GFP Hi20 cell lines. A modified system is currently being developed in the Ivetic laboratory, where HUVEC monolayers are grown on a mixture of collagen/matrigel substrates, and it is hoped that this will generate sufficient subendothelial space for THP-1 cells to undergo full transmigration under both static and flow conditions. In light of the results discussed above, it would be interesting to see whether delayed shedding of the SSAA mutant will also delay THP-1 transmigration. If this was the case, additional studies could be designed to analyse relative contribution of Mac-1 – which is expressed by THP-1 cell line [674] – and L-selectin cleavage to monocyte TEM.

4.4.2 Accumulation of GFP-positive "spots" occurs in the protruding pseudopods of transmigrating THP-1 cells and correlates directly with L-selectin shedding

The main reason for tagging L-selectin with GFP was to "non-invasively" monitor its spatio-temporal distribution during transendothelial migration. The results presented in

section 4.3.6 show that WT L-selectin-GFP accumulate over time in the pseudopods of transmigrating THP-1 cells. This is seen as the appearance of characteristic GFP-positive "spots" that are not observed in control cells expressing matched levels of GFP protein (**figure 4.7**). However, the caveat of this analysis lies in the fact that by following the GFP-tag it is not possible to distinguish between full-length surface L-selectin-GFP and L-selectin-GFP "stump". It was hoped that by analysing the mutant forms of L-selectin-GFP some insights could be gained pertaining to the nature of the spots. As discussed above SSAA mutation results in delayed shedding of L-selectin-GFP when THP-1 cells interact with TNF-α activated HUVEC. Additionally, a "severe" shedding mutant, namely ΔM-N L-selectin-GFP, was generated and stably expressed in THP-1 cells (**section 4.3.7**). Apart from activation-induced, basal shedding is also abrogated in the ΔM-N L-selectin mutant (**figure 4.11**). A lack of basal shedding was thought to be a reason behind the extremely high surface L-selectin-GFP levels in THP-1 ΔM-N L-selectin-GFP Hi20 cells that were exceeding those of THP-1 WT L-selectin-GFP Hi20 cells (**figure 4.10**). As a result, low expressor THP-1 ΔM-N L-selectin-GFP Lo5 was a closer match to the THP-1 WT L-selectin-GFP Hi20 cells and was employed in all further studies. Examination of WT SSAA and ΔM-N L-selectin-GFP spots formed in the pseudopods of the respective cell lines after 15 minutes of flow revealed interesting differences. Both SSAA and ΔM-N L-selectin-GFP presented fewer GFP-positive spots when compared to WT L-selectin-GFP (**figure 4.13**). These results demonstrate a strong correlation with the extent of shedding and the formation of the GFP-positive spots in transmigrating monocytes. It is tempting to speculate that the GFP-positive spots represent the L-selectin-GFP "stump" accumulating in the pseudopods of THP-1 cells during TEM. However, the nature of the spots still remains unclear and accumulation of full length L-selectin-GFP cannot be formally excluded. For example, spots could represent aggregates of full-length L-selectin that form as pre-requisite for shedding. Additionally, L-selectin is known to cluster upon ligand binding and extracellular matrix L-selectin ligands have been identified (**section 1.8.3**). Therefore, it is possible that full length L-selectin-GFP clusters in the pseudopods of transmigrating THP-1 cells upon binding of ECM ligand(s) deposited by TNF-α activated HUVEC. Pre-treating THP-1 cells expressing WT L-selectin-GFP with Ro31-9790 may result in a reduction of spots, lending further weight to the possibility that the spots are due to shedding.

4.4.3 Investigating the fate of L-selectin-GFP "stump"

The fate of the L-selectin "stump" is currently unknown. Zhao et al. (2001) showed that a gradual decrease in the L-selectin cleavage product generated upon PMA treatment starts 15 minutes after stimulation, and it is entirely cleared from the membrane by 60 minutes [323]. Likewise, results showed in this chapter demonstrate that WT L-selectin-

GFP “stump” generated during static transmigration assays is turned-over within a 1 hour period (**figure 4.1**). When investigating the influence of cytoplasmic serine residues on shedding of L-selectin-GFP during TEM, it was noticed that the SSAA L-selectin-GFP “stump” was more abundant than WT L-selectin-GFP “stump” at 20 minutes (**figure 4.4**). A statistical test did not find this change significant and this result could just be a coincidence. However, it can be speculated that rapid protein turnover is hard to measure by Western blotting where time-points are at least 5 minutes apart and saturation of the bands can be an issue when quantifying the results. Perhaps using antibodies directly labelled with near-infrared dyes that do not reach saturation upon development would prove more informative in future.

The clearance of the L-selectin-GFP “stump” from the membrane could be a result of its internalisation. It was proposed that L-selectin-GFP spots accumulating in the pseudopods of transmigrating THP-1 cells could represent vesicles containing the internalised “stump”. Attempts were made to investigate whether the L-selectin-GFP spots co-localised with the endosomal markers CD63 and EEA1. No co-localisation between the GFP-positive spots and CD63 was seen (Dr A. Ivetic, unpublished data), suggesting that the “stump” was not targeted for degradation through the endosomal/lysosomal pathway. Investigation of co-localisation of the GFP-positive spots and EEA1 staining proved unsuccessful. Further optimisation of the method would be needed to analyse possible association of L-selectin-GFP spots with the early endosome compartments. Alternatively, the small GTPase Rab5 is another known early endosome marker [675], and it would be of interest to determine if Rab5 can be detected in THP-1 cells, and if so, if it would co-localise with the L-selectin-GFP spots.

It has been suggested that L-selectin “stump” can be further cleaved by a gamma-secretase complex (Ann Ager, Cardiff University, personal communication). Indeed, membrane secretases have been proposed to have the ability to cleave any surface protein that lack a bulky membrane-proximal globular domain [676]. Two bands migrating at the molecular weight of the L-selectin-GFP “stump” have been detected in Western blots (**figure 3.8**), suggesting that further cleavage of “stump” might indeed occur in THP-1 WT L-selectin-GFP Hi20 cells. Interestingly, the ADAM17 substrate, Notch receptor, is known to be internalised and further cleaved by gamma-secretase complex [677]. Gamma-secretase dependent cleavage depends on monoubiquitination and clathrin-dependent endocytosis of cleaved Notch product [677]. Additionally, is was suggested that Notch receptor monoubiquitination occurs on a juxtamembrane lysine residue [677]. L-selectin tail contains five lysine residues (K359, K360, K362, K363 and K365) and therefore it is highly likely that ubiquitination could occur on one of them. It is hence possible that ADAM17 induced L-selectin cleavage is followed by endocytosis and

further cleavage in a manner similar to that of the Notch receptor. Finally, clathrin-mediated internalisation of the stump would be interesting to explore in future studies.

CHAPTER 5. CLUSTERING OF L-SELECTIN DURING TRANSENDOTHELIAL MIGRATION

5.1 INTRODUCTION

Previous studies have suggested that L-selectin might play a role beyond the vasculature [221, 354, 398, 416, 419, 420, 465, 479]. Specifically, L-selectin null leukocytes have been shown to have reduced infiltration into the tissue interstitium at various sites of inflammation [11, 392, 398, 420], and impaired locomotion away from the venule and towards the inflammatory source [398, 416]. Additionally, aberrant chemotaxis *in vivo* has also been reported for leukocytes expressing the sheddase-resistant L-selectin [419]. However, this area has never been researched at the molecular level, and no mechanism for L-selectin-dependent TEM or interstitial migration has been suggested. It is likely that L-selectin-dependent emigration may vary between the leukocyte subsets, as it has been shown that L-selectin levels on murine neutrophils and monocytes are regulated differently upon emigration into the inflamed peritoneum [527]. The results presented in **Chapter 4** of this thesis show that L-selectin-GFP spots accumulate in the pseudopods of transmigrating THP-1 monocytes (**figure 4.4**), and this appears to be dependent on cytoplasmic serine residues as well as L-selectin's ability to be shed (**figure 4.13**). In the previous chapter, the spots of L-selectin-GFP were hypothesised to be internalised vesicles containing the "stump" of L-selectin-GFP but this was never formally addressed. However, biochemical assessment using anti-GFP Western blotting of the whole cell lysates derived from THP-1 cells stably expressing either WT or ΔM-N-L-selectin, revealed the only difference between these cell lines to be the stump. This would strongly support the theory that the observed GFP-positive spots were the "stump". One other possibility is that the accumulation of L-selectin-GFP spots could represent clusters of full-length L-selectin-GFP that form as pre-requisite to shedding. Indeed, a recent paper has shown that high-density sulphated ligands (such as those derived from the ECM) can drive L-selectin clustering and subsequent shedding [678]. Additionally, a number of ECM ligands for L-selectin have now been described (**section 1.8.3**, summarised in **table 1.2**), and binding of L-selectin with a subendothelial ligand could serve to drive L-selectin clustering.

When considering clustering, there are two types of clustering that can occur: "outside-in" and "inside-out". Outside-in refers to direct clustering of L-selectin as a consequence of ligand binding, and inside-out refers to a mechanism that is driven by a pathway independent of L-selectin. L-selectin clustering has been reported to coincide with L-selectin dependent signalling (**section 1.11**). It is possible that L-selectin clustering occurs during TEM, which plays a role in leukocyte exit from the vasculature.

This chapter explores the theory that L-selectin is clustered in the pseudopods of transmigrating THP-1 cells.

5.2 EXPERIMENTAL DESIGN

Clustering is a term that describes a situation where a given set of receptors localise together at high densities. Adjacent receptors are brought so close together that they can physically interact. Physical protein-protein interactions *in vivo* can be detected by fluorescence lifetime measurement (FLIM) of fluorescence resonance energy transfer (FRET) efficiency between GFP- and RFP-tags that are attached to the proteins of interest. This technique measures the fluorescence lifetime of a donor fluorophore, in this case GFP, after excitation. The donor fluorophore's lifetime is decreased when it is located within 10 nm (100 Å) of an acceptor fluorophore, such as RFP, due to absorption of energy by this acceptor, hence the term fluorescence resonance energy transfer (or FRET). Data presented in **Chapter 3** describe the generation of THP-1 cell lines stably expressing WT L-selectin-GFP. Co-expression of WT L-selectin-RFP in the same cell line would allow detection of an interaction between adjacent L-selectin molecules by measuring FLIM of FRET between GFP and RFP tags. This would allow detection of L-selectin clustering during TEM. When generating biosystems for FLIM measurement of FRET, the acceptor is commonly present in excess to saturate donor binding. It was therefore decided that low expressor THP-1 WT L-selectin-GFP Lo5 would be used so that lentivirus particles carrying L-selectin-RFP could be transduced at a higher MOI. This resulted in the generation of a "double expressor" THP-1 cell line, termed THP-1 WT L-selectin-GFP/RFP. Once the cell line was generated, clustering of L-selectin during TEM was measured by FLIM analysis and the extent of clustering was expressed as the FRET efficiency. Briefly, THP-1 cells were perfused over TNF-α activated HUVEC for 15 minutes, after which time the cells were fixed with 4% PFA and prepared for FLIM/FRET analysis. The fifteen minute time-point was chosen as this was the period at which L-selectin-GFP spots were seen accumulating in the pseudopods of transmigrating THP-1 cells (**figures 4.7** and **4.8**). The FLIM analysis and FRET efficiencies were performed and calculated by Dr Maddy Parsons of the Randall Division of Cell and Molecular Biophysics at King's College London.

Extracellular matrix proteoglycans are known to bind L-selectin [221, 354, 463-466], and could potentially cause L-selectin clustering in THP-1 monocyte pseudopods that protrude underneath the HUVEC monolayer. Initial data suggesting expression of biglycan (dermatan sulphate proteoglycan) by activated HUVEC cells was obtained by Dr Aleksandar Ivetic. To further analyse the subcellular distribution of biglycan, immunofluorescence experiments were performed. This was to assess whether biglycan expression could be specifically detected beneath the HUVEC monolayer.

Extracellular and intracellular mutants of L-selectin were also used to address the individual and combined roles of the cleavage domain and cytoplasmic serines in regulating L-selectin clustering. All newly generated mutant double expressor cell lines were FACS sorted to match their total GFP- and RFP-tagged L-selectin levels to that of THP-1 WT L-selectin-GFP/RFP cells. Once matched L-selectin expression was ensured, all the double expressor cell lines were subjected to 15 minute-long parallel plate flow chamber assay and FLIM/FRET analysis of L-selectin clustering during TEM was performed.

The double expressor cell lines were further used to test whether ligation of other endogenous CAMs could promote L-selectin clustering in the manner of "inside-out" signalling. To this end, an assay was designed where antibodies against extracellular domains of PSGL-1, JAM-A, CD43, CD44 and PECAM-1 – which are all known to be expressed by THP-1 cells [153, 679-682] – were used to cross-link those CAMs on the surface of WT or mutant L-selectin-GFP/RFP expressing THP-1 cells. L-selectin clustering was subsequently tested by FLIM measurement of FRET.

5.3 RESULTS

5.3.1 Generation of a THP-1 cell line stably expressing GFP- and RFP-tagged WT L-selectin

The pHR´SIN-SEW-L-selectin^{WT}-RFP vector was used to generate lentiviral particles carrying WT L-selectin-RFP and is described in more detail in **section 3.3.1.1**. Lentiviruses were generated and titrated as described in **sections 3.3.1.2** and **2.11**, and the obtained titre was 12.56 x 10^8 i.u./mL (**table 2.5**). For reasons explained in **section 5.2**, low expressor THP-1 WT L-selectin-GFP Lo5 cells were used for transduction. In **Chapter 3**, rigorous biochemical and cell biological testing of THP-1 L-selectin-GFP Hi20 cells presented with no obvious defects. Although the THP-1 L-selectin-GFP Lo5 were not subjected to similar testing, it was reasoned that as they expressed fewer L-selectin molecules on the surface, it was unlikely that they would present with any defective phenotype. To achieve excess acceptor (RFP-tag) to donor (GFP-tag) ratio, an MOI of 10 was used to transduce THP-1 L-selectin-GFP Lo5 cells with lentivirus carrying the L-selectin-RFP transgene. The THP-1 cell transduction method is described in more detail in **section 2.11.4**. The resultant double expressors were subjected to FACS sorting to obtain uniform surface expression levels. Fluorescence of both GFP- and RFP-tags was used to select cells of low uniform GFP and high uniform RFP expression (**figure 5.1**). As before, the cells displayed characteristic L-selectin membrane localisation seen in both GFP and RFP channels. Membrane localisation of L-selectin-RFP suggested that

the RFP-tag did not affect L-selectin expression and trafficking to the membrane. Hence, the cells were deemed suitable for FLIM/FRET experiments.

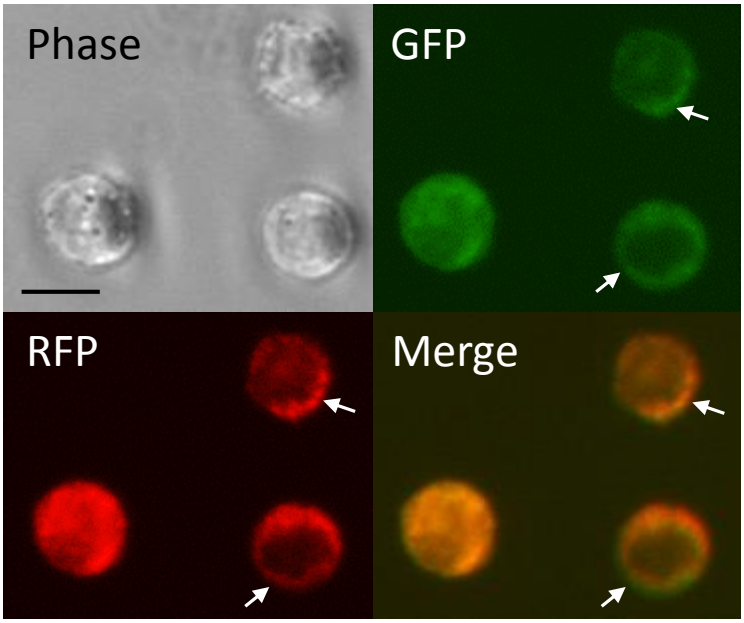

Figure 5.1 THP-1 cell line expressing WT L-selectin-GFP and -RFP (THP-1 WT L-selectin GFP/RFP). Representative image showing THP-1 WT L-selectin GFP/RFP cells. Both L-selectin-GFP and -RFP localise to the cell membrane (arrows). Scale bar: 10 µm.

5.3.2 L-selectin clusters in the pseudopods of transmigrating THP-1 cells

To investigate if L-selectin clustered during monocyte transendothelial migration, THP-1 WT L-selectin-GFP/RFP cells were perfused over the TNF-α activated HUVEC monolayer in a parallel-plate flow chamber assay (**section 2.14.3**). Data presented in **Chapter 4** shows that this type of experiment captures cells in the initial stages of TEM, where THP-1 cells extend pseudopods underneath the endothelium (**figure 4.6**). After 15 minutes of flow, when L-selectin-GFP spots are known to accumulate (**figures 4.7** and **4.8**), the cells were fixed and samples were prepared for FLIM/FRET analysis as described in **section 2.18.1**. The experiment was repeated with THP-1 cells expressing L-selectin-GFP only to measure lifetime of the donor in the absence of acceptor. This was required to calculate FRET efficiency (Π_{FRET}). A detailed method of FLIM/FRET data analysis is described in **section 2.18** of this thesis. Staining with phalloidin-Alexa633 enabled visualisation of HUVEC actin cables and allowed recognition of non-transmigrated and transmigrated parts of the same cell, referred to as Top and Bottom z-planes, respectively (**figure 5.2 A**). Analysis revealed that the FRET efficiency was highest in the pseudopods of transmigrating THP-1 cells and very little FRET was detected in the non-transmigrated parts of the cells (**figure 5.2 B**). The areas in which FRET occurs, as determined by a decreased fluorescence lifetime of GFP, are shown

using a pseudo-colour scale with green through yellow to red, indicating areas of progressively shorter lifetime and, therefore, increasing FRET (**figure 5.2 B**). Blue areas represent long lifetimes and no FRET. Calculation of FRET efficiency showed that average 4.033% η_{FRET} was present in the non-transmigrated parts of the cells, whereas η_{FRET} in the pseudopods totalled average 9.873% (**figure 5.2 C**). This suggested that L-selectin clustered in the pseudopods of transmigrating THP-1 monocytes, and not in the non-transmigrated parts.

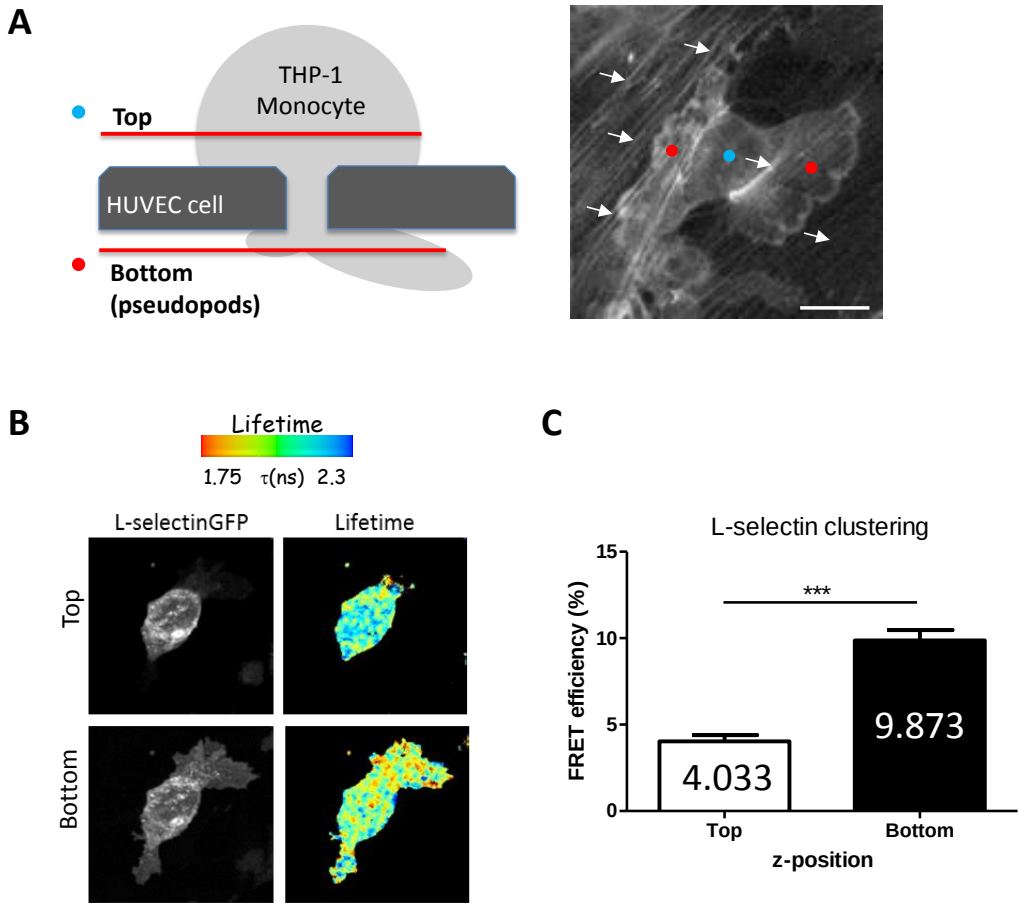

Figure 5.2 Clustering of L-selecting during transendothelial migration. THP-1 cells were perfused over TNF-α activated HUVEC for 15 minutes (**section 2.14.3**), fixed with 4% PFA and prepared for FLIM/FRET analysis as described in **section 2.18.1**. FLIM measurement of FRET was used to assess the interaction between adjacent L-selectin molecules to determine if L-selectin clustering had occurred. **A)** *Left panel*: schematic showing typical appearance of a THP-1 monocyte interacting with HUVEC under flow. Non-transmigrated and transmigrated parts of the cells are shown as Top (blue dot) and Bottom (pseudopods, red dots) z-planes, respectively. *Right panel*: Representative wide-field CCD camera image of phalloidin-Alexa633 staining. Arrows point out HUVEC actin cables. Blue and red dots indicate z-planes as shown in the schematic on the left. Scale bar: 10 µm. **B)** Representative images showing Top and Bottom z-planes of a transmigrating THP-1 monocyte. Left panels show images of L-selectin-GFP and the right panels show corresponding GFP multi-photon intensity images. Lifetime of fluorescence is shown as a pseudo-colour scale of blue (high lifetime) to red (low lifetime). The lower the lifetime of fluorescence, the closer the association between the two tagged proteins (more detailed explanation of FLIM/FRET measurement and analysis is described in **section 2.18**). **C)** Quantitation of FRET efficiency between L-selectin-GFP and L-selectin-RFP. Analysis was

performed on a total of 15 cells derived from three independent experiments. Mean values are shown for each bar. Error bars represent S.E.M. Statistical analysis: Two-tailed, unpaired Student's t-test. ***=p<0.001.

5.3.3. TNF-α activated HUVEC express the L-selectin ligand biglycan

The above presented results show that L-selectin clusters in the pseudopods of transmigrating THP-1 monocytes. L-selectin is known to cluster upon ligand binding (**section 1.11**) and it was hypothesised that discovered L-selectin clustering during TEM might be indicative of subendothelial ligand binding. A number of ECM ligands for L-selectin have now been recognised (**section 1.8.3**, see summary in **table 1.2**). The majority of such ECM ligands are highly sulphated proteoglycans, and collagen XVIII, versican and biglycan are most frequently reported [221, 354, 463, 465, 466]. Proteoglycans are commonly produced by endothelial cells, suggesting that the observed clustering of L-selectin during TEM could be the result of a proteoglycan binding event. Additionally, both collagen XVIII and biglycan have been reported to be expressed by the HUVEC monolayer [663, 683]. To investigate whether proteoglycans were present in our model, and to assess the effect of TNF-α stimulation on their potential expression, Western blotting analysis was performed by Dr Aleksandar Ivetic. The results showed that both collagen XVIII and biglycan can be detected in the extracts from unstimulated HUVEC (**figure 5.3**). Collagen XVIII has a molecular weight (MW) of 180-200 kDa and a faint band was detected migrating at this weight, whereas an abundant 45 kDa band was detected for biglycan core protein (**figure 5.3**). Interestingly, upon 10 ng/mL TNF-α stimulation – which was a concentration used to stimulate HUVEC for parallel-plate flow chamber experiments – collagen XVIII could no longer be detected and biglycan expression decreased (**figure 5.3**).

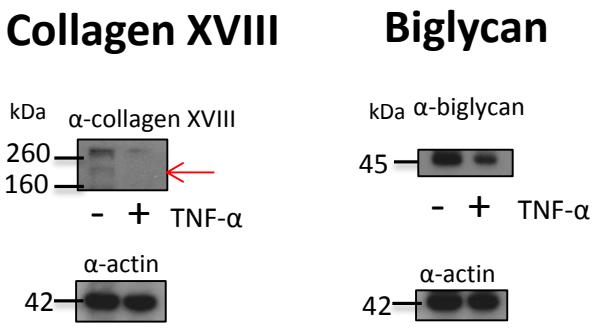

Figure 5.3 Effect of TNF-α stimulation on HUVEC proteoglycan expression. Confluent HUVEC monolayers were stimulated overnight with 10 ng/mL TNF-α or were left untreated. Representative Western blots of proteoglycans detected with anti-collagen XVIII and anti-biglycan antibodies. Collagen XVIII migrated at its predicted molecular weight of 180-200 (red arrow), and could no longer be detected upon 10 ng/mL TNF-α stimulation. Biglycan core protein migrating at

45 kDa was detected in extracts from both stimulated and non-stimulated HUVEC, however TNF-α treatment decreased its expression. The experiment was performed by Dr Aleksandar Ivetic.

As detection of biglycan core protein was still visible after TNF-α stimulation, it was likely that its glycosylated form was secreted by HUVEC and could still have the capacity to cluster L-selectin during TEM. A recent report by Yin et al (2013) found that biglycan is constitutively secreted by HUVEC, and secretion is greatly potentiated by PMA stimulation [663]. Secretion was assumed to take place into the ECM deposited by HUVEC but to formally investigate what effect TNF-α stimulation had on the sub-cellular distribution of biglycan in HUVEC culture, immunofluorescence analysis was performed. Confluent HUVEC cells were stimulated with 10 ng/mL TNF-α overnight or were left untreated. Upon fixation with 4% PFA, cells were prepared for confocal microscopy as described in **section 2.16.2**. After z-stack acquisition, Top and Bottom z-planes, as shown on a diagram in **figure 5.4 A**, were compared. Control staining with fluorescently-conjugated secondary antibody and no anti-biglycan antibody showed minimal background staining (**figure 5.4** *Bottom panel*). It has to be noted though that in order to fully control for this experiment, additional control, where isotype-matched control primary antibody was used, should be performed. Unstimulated cells presented with disseminated biglycan staining as well as areas of intense fluorescent signal (**figure 5.4 B** *Top panel*). The areas where the fluorescent signal was most concentrated could represent intracellular stores, although this was not formally tested. The majority of biglycan was seen as diffuse staining in the Bottom z-plane suggesting that biglycan was likely deposited in subendothelial regions (i.e. between the basal surface of the HUVEC monolayer and the glass coverslip). After TNF-α stimulation the intense fluorescent signal areas were no longer seen (**figure 5.4 B** *Middle panel*). If the concentrated signal was indeed representing biglycan intracellular stores, it is possible that TNF-α caused biglycan secretion, much like what had previously been observed with PMA stimulation [663]. The biglycan staining in the Bottom z-plane persisted after TNF-α stimulation, however, it was difficult to assess whether the amount of subendothelial biglycan decreased, increased or was maintained at the same levels as without treatment. The overall biglycan expression was likely to be decreased by TNF-α stimulation as seen by Western blotting and lack of the areas of the intense fluorescent signal. Nonetheless, the confocal microscopy results indicated that after TNF-α stimulation, biglycan was still present in the Bottom z-plane. Altogether the Western blotting and immunostaining results suggest that biglycan could be present underneath the HUVEC monolayer during the parallel-plate flow chamber experiments. This in turn open the possibility that L-selectin/biglycan binding could occur during TEM, which could lead to L-selectin

clustering in the pseudopods of transmigrating THP-1 cells. Given time, it would have been interesting to perform similar Western blotting and immunofluorescence analysis for versican expression.

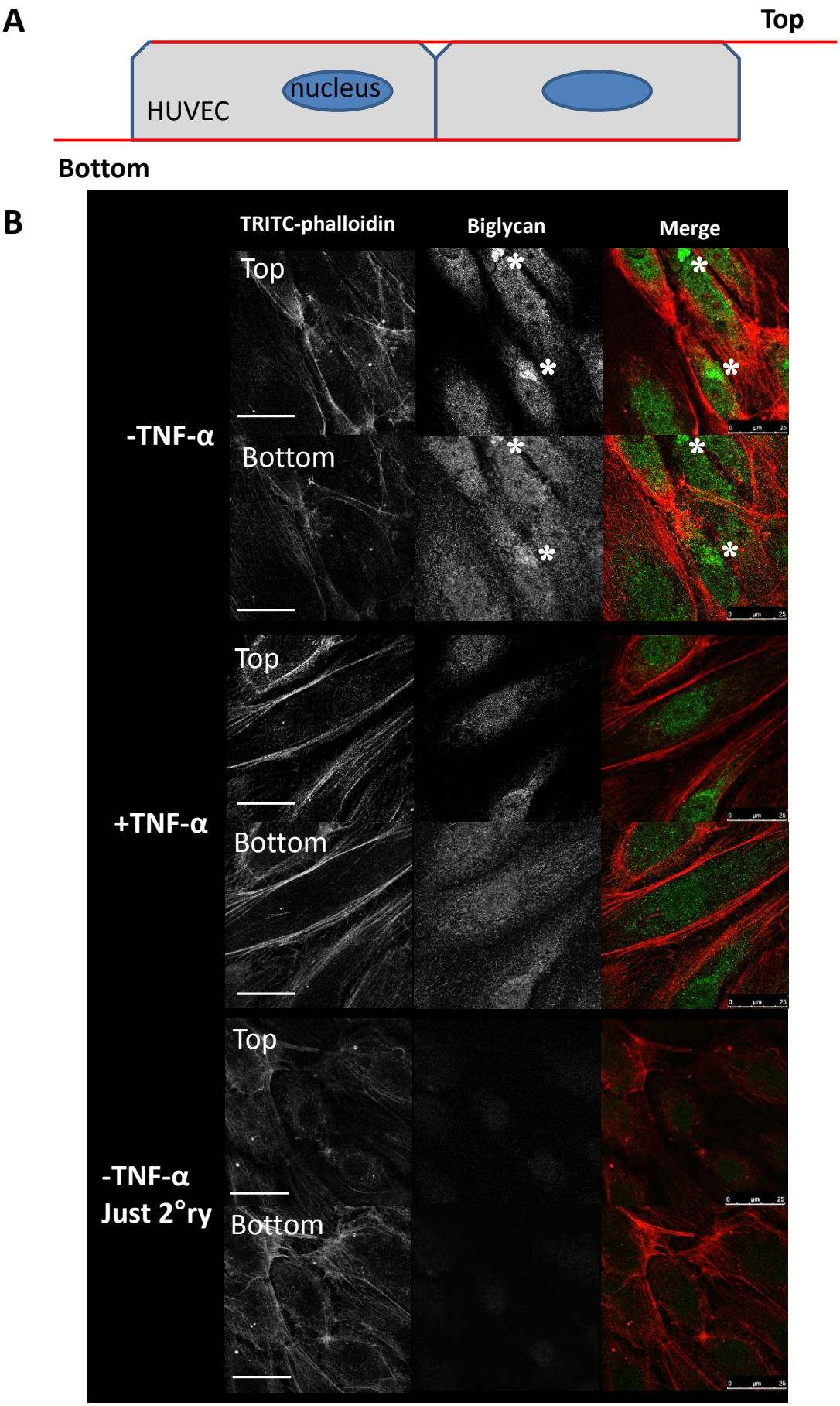
A
Top
HUVEC
nucleus
Bottom
B
TRITC-phalloidin
Biglycan
Merge
Top
-TNF-α
Bottom
Top
+TNF-α
Bottom
Top
-TNF-α
Just 2°ry
Bottom

Figure 5.4 Biglycan expression pre- and post-TNF-α stimulation of HUVEC monolayers. HUVEC were grown to confluence and stimulated with 10 ng/mL TNF-α overnight or left untreated. Cells were then fixed with 4% PFA and prepared for confocal microscopy as described in **section 2.16.2**. **A)** Schematic showing z-planes in which biglycan expression was analysed. **B)** Representative images of biglycan expression in Top and Bottom z-planes of unstimulated HUVEC (*Top panel*), TNF-α stimulated HUVEC (*Middle panel*), and unstimulated HUVEC stained with secondary antibody (2°ry) only (*Bottom panel*). Stars indicate areas of concentrated fluorescent signal (potential intracellular biglycan "stores"). Scale bar: 25 μm.

5.3.4 Generation of THP-1 cell lines stably expressing GFP- and RFP-tagged ΔM-N L-selectin

THP-1 cells expressing shedding resistant (ΔM-N) L-selectin-GFP presented with a strikingly different phenotype to WT L-selectin, in that little to no GFP-positive spots were observed in the pseudopods of transmigrating cells (**figure 4.13**). To determine if the absence of subendothelial spots in ΔM-N L-selectin could be correlated with a lack of subendothelial clustering, a suitable THP-1 cell line, expressing both GFP- and RFP-tagged forms of ΔM-N L-selectin, was generated. A two-step *in vitro* site-directed mutagenesis – described in **section 4.3.7** for pHR´SIN-SEW-L-selectin^{WT}-GFP vector – was performed on the pHR´SIN-SEW-L-selectin^{WT}-RFP template vector (for WT L-selectin cloning into the pHR´SIN-SEW-RFP vector see **sections 3.3.1.1** and **2.3**). Refer to **section 2.5** for a detailed method of the site-directed PCR mutagenesis protocol. The resultant vector, termed pHR´SIN-SEW-L-selectin$^{\Delta M\text{-}N}$-RFP, was used to generate lentiviral particles as described in **sections 3.3.1.2** and **2.11**. The lentiviral titre was calculated to be 1.87 x 10^8 i.u./mL (**table 2.5**). A MOI of 10 was used to transduce THP-1 ΔM-N L-selectin-GFP Lo5 cell line (described in **section 4.3.8**) with newly generated lentiviral particles carrying the ΔM-N L-selectin-RFP transgene. Double expressors were subsequently FACS sorted in to a uniform cell line, named THP-1 ΔM-N L-selectin-GFP/RFP. When sorting the cells, THP-1 WT L-selectin-GFP/RFP cells were taken to the sorting facility and used as a reference population to set both GFP and RFP gates. This was to select matching lower-end ΔM-N L-selectin-GFP/RFP expressors, as it had been established that transduction with the same MOIs results in higher ΔM-N L-selectin than WT L-selectin surface expression (see **section 4.3.8.1**). In order to measure the total surface L-selectin levels upon sorting, cells were labelled with DREG56 anti-L-selectin antibody followed by RPE-conjugated secondary antibody. The flow cytometer used was not equipped to excite or detect fluorescence emitted from RFP, and therefore RPE fluorescence intensity was an indication of total (both GFP- and RFP-tagged) L-selectin levels. **Figure 5.5** shows that surface L-selectin expression profiles of THP-1 WT- and ΔM-N L-selectin-GFP/RFP cells were a close match. A slight shift to the right can be seen in the ΔM-N L-selectin histogram as compared to WT L-selectin histogram.

This was most probably a result of basal shedding occurring in WT, but not in ΔM-N L-selectin.

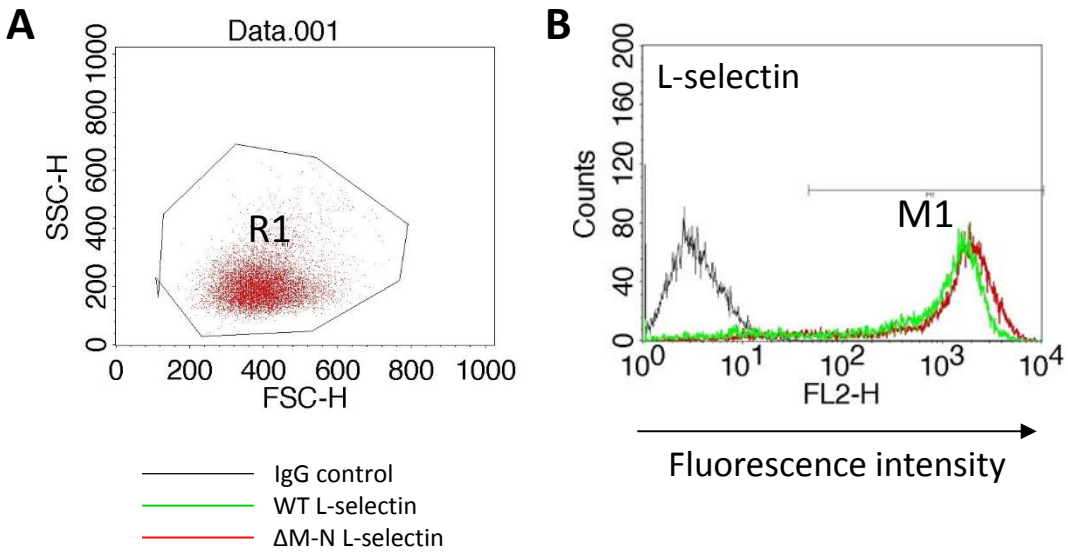

Figure 5.5 Surface WT- and ΔM-N L-selectin-GFP/RFP expression in THP-1 cells. Flow cytometry analysis (**section 2.13**) of L-selectin expression. THP-1 WT L-selectin-GFP/RFP and THP-1 ΔM-N L-selectin-GFP/RFP cells were labelled with anti-L-selectin DREG56 antibody and then secondary antibody conjugated to RPE. Representative histograms are shown. **A)** Dot plot showing the population of viable and single THP-1 cells analysed (gate R1). **B)** The histogram depicting total (GFP- and RFP-tagged) surface L-selectin expression in THP-1 cells as measured by RPE fluorescence. Gate M1 indicates L-selectin positive cells.

5.3.5 Inhibition of L-selectin shedding completely reverses the subcellular distribution of clustered L-selectin in transmigrating cells

THP-1 ΔM-N L-selectin-GFP/RFP cells were subjected to 15 minute-long parallel plate flow chamber assay, fixed and prepared for FLIM/FRET analysis as described in **section 5.3.2**. Interestingly, ΔM-N L-selectin clustered in a spatially opposite way to WT L-selectin. A shown in **figure 5.6 A**, no appreciable FRET efficiency was detected in the pseudopods of transmigrating THP-1monocytes. In contrast, “hot-spots” of FRET were seen it the Top z-plane (Top and Bottom z-planes as shown in **figure 5.2 A**), corresponding to the non-transmigrated part of the cells. To further investigate whether this reversed phenotype was a result of a lack of L-selectin shedding, THP-1 WT L-selectin-GFP/RFP cells were pre-incubated with the sheddase inhibitor, Ro-30-9790. This inhibitor was previously shown to abrogate

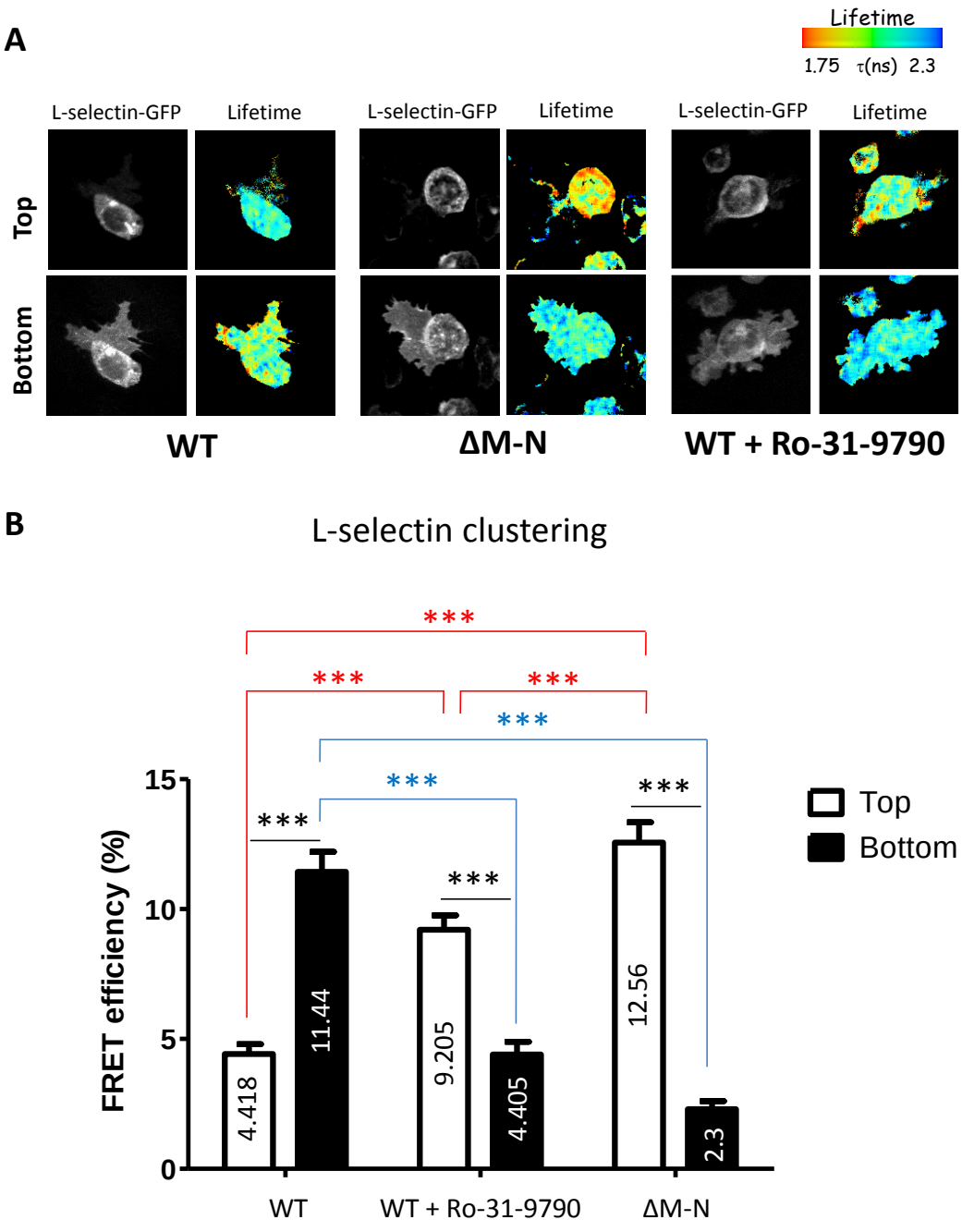

Figure 5.6 Inhibition of L-selectin shedding reverses the subcellular distribution of L-selectin clustering during TEM of THP-1 monocytes. THP-1 cells stably expressing WT or ΔM-N L-selectin-GFP/RFP were pretreated with or without Ro-31-9790 (30 minutes at 37°C and 5% CO_2) and perfused over TNF-α activated HUVEC for 15 minutes as described in **section 2.14.3**. Specimens were subsequently fixed in 4% PFA and prepared for FLIM/FRET analysis as described in **section 2.18.1**. Relative positions of the Top and Bottom z-planes shown previously in a schematic, represented in **figure 5.2 A**. **A)** Representative images showing Top and Bottom z-planes of transmigrating THP-1 cells. Images show L-selectin-GFP and the corresponding GFP multi-photon intensity images. Pseudo-colour scale of blue (high lifetime) to red (low lifetime) is used to show lifetime fluorescence. L-selectin clustering occurs where low lifetimes are seen (orange to red), whereas high lifetimes indicate areas free of L-selectin clustering (blue). **B)** Quantitation of FRET efficiency between L-selectin-GFP and L-selectin-RFP. Analysis was performed on a following number of THP-1 cells: 22 of WT L-selectin-GFP/RFP, 22 of WT L-selectin-GFP/RFP + Ro-31-9790 and 15 ΔM-N L-selectin-GFP/RFP. Cells were derived from three independent experiments. Mean values are shown for each bar. Error bars represent S.E.M.

Statistical analysis: Two-tailed unpaired Student's t-test was used to calculate differences between Top and Bottom for each cell line. ***=p<0.001. One-way ANOVA followed by Tukey's post-test was used to calculate differences between cell lines in Top (coloured red) and Bottom (coloured blue) z -planes. ***=p<0.001

shedding of WT L-selectin from THP-1 cells (**figure 3.10**). As anticipated, no FRET was found in THP-1 cell pseudopods, but L-selectin clustering occurred in the non-transmigrated parts of the cells (**figure 5.6 A**). Analysis of FRET efficiency showed that significant differences between Top and Bottom z-planes occurred in all cells (**figure 5.6 B**). However, when FRET efficiency of WT L-selectin was low at the Top (4.418%) and high at the Bottom (11.44%), the FRET efficiency of ΔM-N L-selectin and L-selectin from monocytes treated with Ro-30-9790 inhibitor was high at the Top (9.205% and 12.56%, respectively) and low at the Bottom (4.405% and 2.3% respectively) (**figure 5.6 B**). This suggested that spatial regulation of L-selectin clustering during TEM was dictated by the ability of the ectodomain to undergo shedding. Although ΔM-N L-selectin and WT L-selectin from THP-1 cells treated with Ro-30-9790 showed the same clustering phenotype (high FRET efficiency on Top and low FRET efficiency at the Bottom), ΔM-N L-selectin exhibited a more severe phenotype as shown by significantly higher FRET efficiency at the Top (**figure 5.6 B**). This could represent short- versus long-term outcome of inhibiting L-selectin shedding (i.e. more ΔM-N L-selectin molecules have accumulated at the cell surface than WT L-selectin from monocytes pre-treated with the sheddase inhibitor).

From these results, the most plausible conclusion would be that ectodomain shedding regulates the sub-cellular distribution of clustered L-selectin. However, one cannot formally exclude the possibility that the intracellular domain plays an active role in this process. For example, it is also highly likely that the prolonged presence of L-selectin at the cell surface could lead to post-translational modification of the serine residues on the L-selectin tail. The next section explores this issue in more detail.

5.3.6 Serine-to-alanine mutagenesis of the L-selectin tail dramatically alters the sub-cellular distribution of clustered ΔM-N L-selectin, but not WT L-selectin, during TEM

As suggested at the end of the section above, it was possible that persistent presence of ΔM-N L-selectin at the cell surface could induce modifications to the serine residues within the L-selectin tail. Cell activating stimuli are known to cause phosphorylation of the L-selectin tail [495, 567] as well as L-selectin shedding [495, 496, 529]. Therefore, the link between tail phosphorylation and L-selectin shedding is well recognised, but whether phosphorylation occurs before, during or just after shedding is currently not

known. If phosphorylation was to occur first, interaction of THP-1 monocytes with TNF-α activated HUVEC would be likely to cause cell activation and phosphorylation of ΔM-N L-selectin tail. Hence, it is possible that lack of shedding would maintain this state and more ΔM-N L-selectin molecules would become serine-phosphorylated with time. This could potentially result in overall "hyperphosphorylation" of L-selectin tail. It could be speculated that the movement of clustered L-selectin from the non-transmigrated part of the cell to the pseudopods requires linkage to the actin cytoskeleton, for example through the ERM proteins that are known to bind to the L-selectin tail [563, 572]. If this was the case, perhaps this interaction could become disrupted in the ΔM-N mutant due to the hyperphosphorylation. As a result ΔM-N L-selectin clustering in the transmigrated pseudopods would be abolished, and clustering would be seen only in the Top z-plane. If this was the case, mutating the serines in the cytoplasmic tail of ΔM-N L-selectin into non-phosphorylatable alanines could reverse ΔM-N L-selectin clustering phenotype back to that seen in WT L-selectin.

To test this hypothesis constructs were generated, where *in vitro* PCR site-directed mutagenesis was used to introduce two alanine residues in the place of the serine residues of the ΔM-N L-selectin cDNA in both pHR´SIN-SEW-L-selectin$^{\Delta M\text{-}N}$-GFP and pHR´SIN-SEW-L-selectin$^{\Delta M\text{-}N}$-RFP lentiviral vectors. The obtained constructs were named pHR´SIN-SEW-L-selectin$^{\Delta M\text{-}NSSAA}$-GFP and pHR´SIN-SEW-L-selectin$^{\Delta M\text{-}NSSAA}$-RFP, respectively. Additionally, to test L-selectin clustering of the SSAA mutant, both serine residues in pHR´SIN-SEW-L-selectin^{WT}-RFP construct were replaced with alanines, and the construct was termed pHR´SIN-SEW-L-selectin^{SSAA}-RFP. For a detailed method describing *in vitro* PCR site-directed mutagenesis see **section 2.5**. Lentiviruses carrying ΔM-N SSAA L-selectin-GFP or -RFP or SSAA L-selectin-RFP were generated and titrated as described in **sections 3.3.1.2** and **2.11**, and the obtained titres are shown in **table 2.5**. To create double expressor ΔM-N SSAA L-selectin-GFP/RFP or SSAA L-selectin-GFP/RFP cells, the same transduction procedure was used as before for the WT L-selectin-GFP/RFP cells (**section 5.3.1**). For detailed method of THP-1 cell transduction see **section 2.11.4**. Once large numbers of newly generated cells were obtained, the cells were sorted into uniform populations with the aid of FACS sorter. Once again, THP-1 WT L-selectin-GFP/RFP cells were used as a reference population on which both GFP and RFP gates were set. Once sorted, the uniform cell lines were named THP-1 ΔM-N SSAA L-selectin-GFP/RFP and THP-1 SSAA L-selectin-GFP/RFP. Surface expression of both GFP- and RFP-tagged L-selectin was analysed by flow cytometry on all newly generated cells. DREG56 staining was used to label all surface L-selectin and expression was compared to that of THP-1 WT- and ΔM-N L-selectin-GFP/RFP cells. As expected, a slight shift towards higher fluorescence was seen in cells expressing sheddase resistant forms of L-selectin (ΔM-N and ΔM-N SSAA L-selectin).

Additionally, the peak corresponding to SSAA L-selectin was marginally shorter than that for WT L-selectin, indicating that there could be slightly less SSAA L-selectin molecules at the cell surface. Overall, however, all cell lines were considered to have matched surface L-selectin levels (**figure 5.7**).

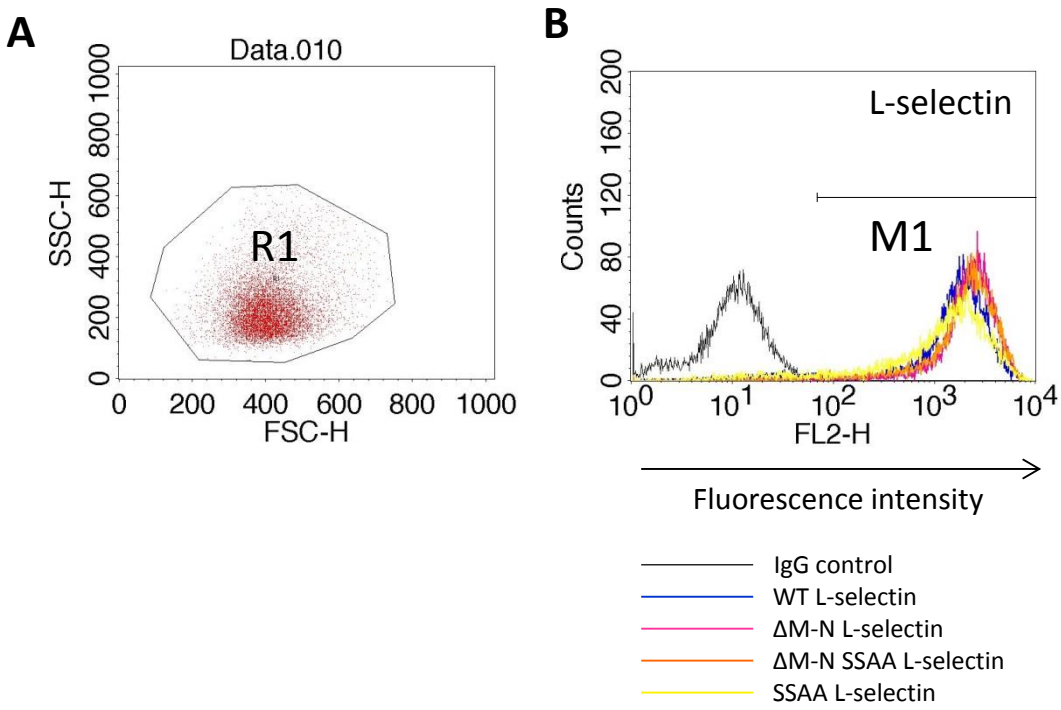

Figure 5.7 Surface WT and mutant L-selectin-GFP/RFP expression in THP-1 cells. Flow cytometry analysis of L-selectin expression. THP-1 WT and mutant (ΔM-N, ΔM-N SSAA or SSAA) L-selectin-GFP/RFP cells were labelled with anti-L-selectin DREG56 antibody and then secondary antibody conjugated to RPE. Representative histograms are shown. **A)** Dot plot depicting the population of viable, single THP-1 cells analysed (gate R1). **B)** Histogram showing total (GFP- and RFP-tagged) surface L-selectin expression in THP-1 cells as measured by RPE fluorescence. Gate M1 indicates L-selectin positive cells.

Newly generated double expressor cells were subjected to 15 minute-long parallel plate flow chamber assay, fixed and prepared for FLIM/FRET analysis as described in **section 5.3.2**. FRET results were compared to those obtained earlier for WT L-selectin, ΔM-N L-selectin and WT L-selectin from THP-1 monocytes pre-treated with Ro-31-9790 (hereafter referred to as WT Ro-31-9790 L-selectin). **Figures 5.8** and **5.9** consolidate all the FRET data acquired for all the cell lines. SSAA L-selectin clustering phenotype resembled that of WT L-selectin with high FRET seen at the Bottom and low FRET at the Top **(figure 5.8 A),** but with lower FRET efficiencies **(figure 5.8 B)**. Interestingly, ΔM-N SSAA L-selectin FRET was seen both at the Top and Bottom suggesting that this

mutant did not entirely reverse the clustering phenotype to WT as anticipated, but rather served as an “intermediate” mutant **(figure 5.8 A)**. Analysis of FRET efficiencies showed that in all the cell lines significant differences between Top and Bottom occurred, but the least difference was found for ΔM-N SSAA L-selectin. This again suggested that the clustering phenotype of this mutant placed it half way between two extremes: WT and ΔM-N L-selectin **(figure 5.8 B)**.

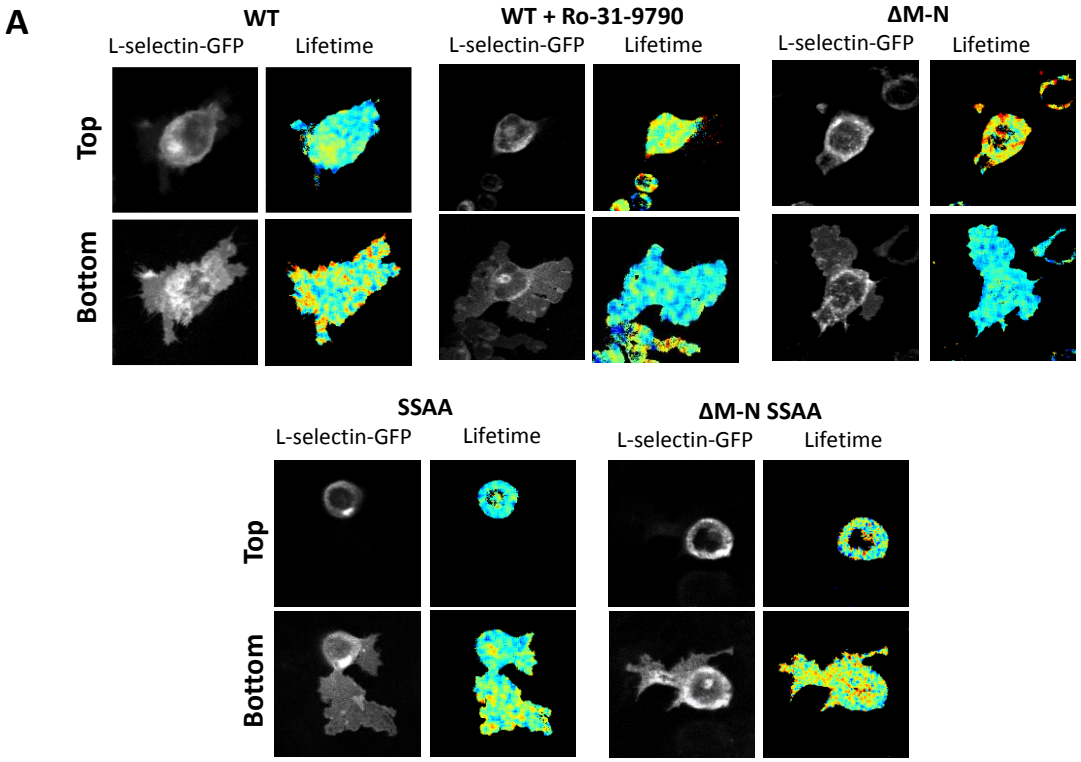

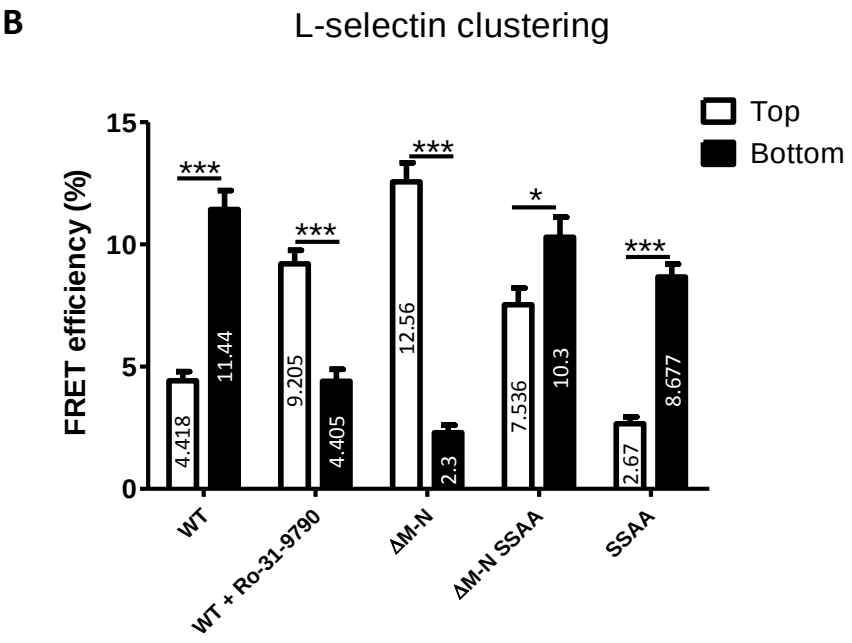

Figure 5.8 Differences in the subcellular distribution of clustered WT and mutant forms of L-selectin. Summary of L-selectin clustering phenotypes observed during transmigration of THP-1 cells expressing WT and mutant (ΔM-N, ΔM-N SSAA or SSAA) forms of L-selectin-GFP/RFP. THP-1 WT L-selectin-GFP/RFP cells were either untreated or pre-treated with Ro-31-9790 metalloprotease inhibitor. All cell lines were perfused over TNF-α activated HUVEC in a 15 minute-long parallel plate flow chamber assy as described in **section 2.14.3**. The cells were then fixed and prepared for FLIM/FRET analysis (see **section 2.18.1**). Top and Bottom z-planes correspond to the planes indicated in schematic in **figure 5.2 A**. **A)** Representative images showing Top and Bottom z-planes of transmigrating THP-1 cells. Images of L-selectin GFP and corresponding GFP multi-photon intensity images are shown in all panels. GFP lifetime is shown as a pseudocolour scale of blue (high lifetime) to red (low lifetime). L-selectin clustering occurs where low lifetimes are seen (orange to red), whereas no clustering occur where high lifetimes are seen (blue). **B)** Quantitation of FRET efficiency between L-selectin-GFP and L-selectin-RFP. Analysis was performed on a following number of THP-1 cells: 22 of WT L-selectin-GFP/RFP, 22 of WT Ro-31-9790 L-selectin-GFP/RFP, 15 ΔM-N L-selectin-GFP/RFP, 18 ΔM-N SSAA L-selectin-GFP/RFP and 15 SSAA L-selectin-GFP/RFP. Three independent experiments were performed for each cell line. Mean values are shown for each bar. Error bars represent S.E.M. Statistical analysis: Two-tailed, unpaired Student's t-test was used to calculate differences between Top and Bottom for each cell line. *=p<0.05, ***=p<0.001.

In order to analyse more closely the impact that the various mutations had on L-selectin clustering, the FRET efficiencies at the Top (**figure 5.9 A**) and Bottom (**figure 5.9 B**) of transmigrating cells were collectively subjected to statistical analysis. Analysis of FRET efficiencies in the Top z-plane (**figure 5.9 A**) revealed low η_{FRET} values for WT and SSAA L-selectin. Since these were the only cell lines where shedding could occur, it suggested that L-selectin clustering at the Top, as seen by high η_{FRET} of ΔM-N, ΔM-N SSAA and WT Ro-31-9790 L-selectin could be a result of lack of shedding. Because η_{FRET} of ΔM-N L-selectin was 12.56% and η_{FRET} of ΔM-N SSAA L-selectin was 7.536%, it could be speculated that it was the SSAA mutation that decreased ΔM-N L-selectin clustering at the Top. Although not statistically significant, slightly lower η_{FRET} value of SSAA L-selectin (2.67%) than WT L-selectin (4.418%) could correspond to a minor difference in the peak height seen on the flow cytometry histogram of L-selectin surface expression (**figure 5.7**).

Analysis of the FRET efficiencies in the pseudopods of transmigrating THP-1 cells (Bottom z-plane) (**figure 5.9 B**) showed that ΔM-N L-selectin and WT Ro-31-9790 L-selectin had significantly lower η_{FRET} values that those calculated for WT, ΔM-N SSAA and SSAA L-selectin. Interestingly, the FRET efficiency of ΔM-N SSAA L-selectin – a form that also could not undergo shedding – was high and no different to WT L-selectin η_{FRET}. This suggested that lack of clustering in the pseudopods seen with ΔM-N L-selectin and WT Ro-31-9790 L-selectin could not be due to lack of shedding. In fact, a vast difference in η_{FRET} values between ΔM-N and ΔM-N SSAA L-selectin (2.3% versus 10.3%, respectively), strongly suggests that clustering in the pseudopods is negatively regulated by serine phosphorylation. Data from Dr Angela Rey Gallardo (a postdoctoral

scientist in Dr Ivetic's lab) reveals that mutating both serines in the L-selectin tail to phospho-mimicking aspartates results in the accumulation of clustered L-selectin exclusively to the non-transmigrated part of the cell. This would further support the hypothesis that the cytoplasmic serine residues in ΔM-N L-selectin are hyperphosphorylated. Interestingly η_{FRET} of ΔM-N SSAA L-selectin was not different to neither WT nor SSAA L-selectin, but statistical analysis detected difference between WT and SSAA L-selectin. One explanation for this could be a delay in FRET of SSAA L-selectin that would correspond to delay in shedding seen in static transmigration assays (**figure 4.4**). Aleternatively, the difference could be a result of slightly lower surface expression of SSAA L-selectin as compared to WT L-selectin (**figure 5.7**).

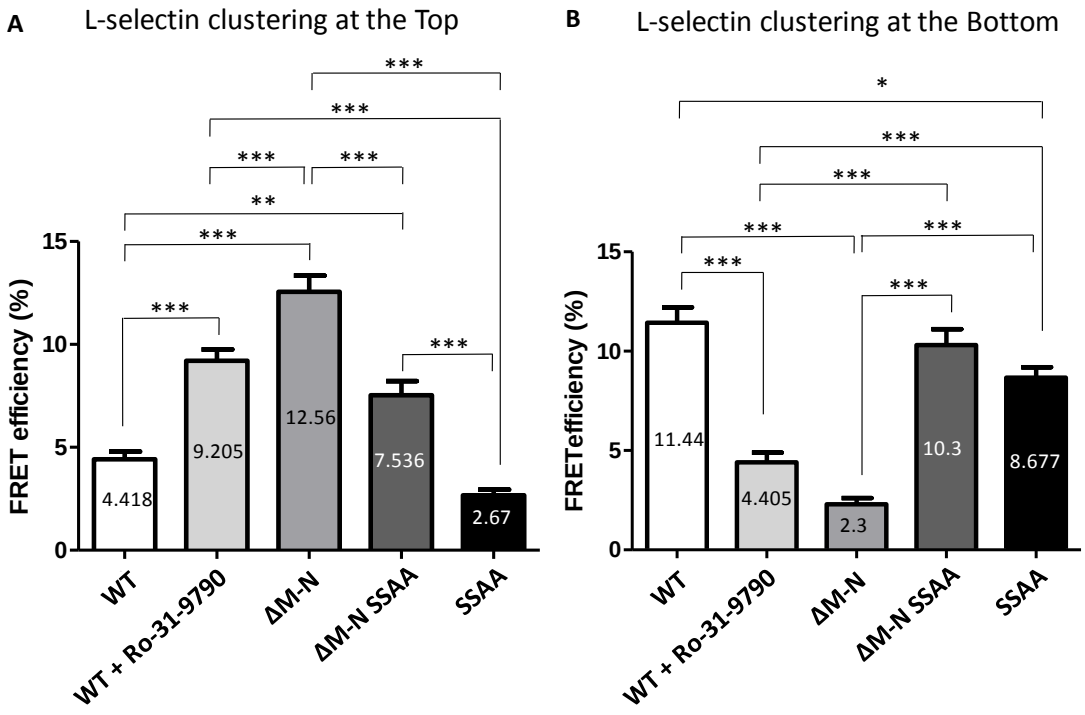

Figure 5.9 Statistical analysis of differences between clustering of WT and mutant forms of L-selectin during THP-1 cell transmigration. The graphs display FRET efficiencies as shown in **figure 5.9 B**, but data for Top (**A**) and Bottom (**B**) z-planes are dissected into two separate panels. Mean values are shown for each bar. Error bars represent S.E.M. Statistical analysis: One-way ANOVA followed by Tukey's post-test was used to calculate differences between cell lines in each graph (z-plane). *=p<0.05, **=p<0.001, ***=p<0.0001

5.3.7 ΔM-N SSAA L-selectin appears in large "aggregates" in the pseudopods of transmigrating THP-1 cells

Taken together, it appears that there is a correlation with the spots that are seen in the protruding pseudopods and the increase in FRET efficiency (**figures 4.12**, **4.13**, **5.8** and

5.9). For example, both WT L-selectin-GFP spots (as observed using laser scanning confocal microscopy) and WT L-selectin-GFP/RFP clusters (as seen with FRET/FLIM analysis) accumulate in the pseudopods of transmigrating THP-1 cells. Similarly, the subcellular distribution of SSAA L-selectin-GFP was also seen to accumulate in the protruding pseudopods, however, the number of GFP-positive spots counted and the relative FRET efficiency are both less than the values obtained for WT L-selectin-GFP. As shown before, neither GFP spots nor clustering was seen in the protruding pseudopods of THP-1 cells stably expressing ΔM-N L-selectin-GFP. The previous section revealed that the SSAA ΔM-N L-selectin clustered both in the transmigrated and non-transmigrated parts of the cell. Laser scanning confocal microscopy was used to further understand whether ΔM-N SSAA L-selectin-GFP also accumulated in the protruding pseudopod. THP-1 ΔM-N SSAA L-selectin-GFP/RFP cells were perfused over TNF-α activated HUVEC for 15 minutes, fixed and prepared for confocal microscopy as described in **sections 2.14.3 and 2.16.2**, respectively. Single images of Top and Bottom z-planes were acquired for GFP and TRITC-phalloidin channels as described in **section 2.16.4**. THP-1 ΔM-N SSAA L-selectin-GFP/RFP cells appeared to have a high number of spikes, and hence both spots and spikes were scored as described in **sections 4.3.9** and **2.16.4**. Quantified spots and spikes were compared to corresponding values obtained earlier for THP-1 WT, SSAA and ΔM-N-GFP cells (**section 4.3.9**). Cumulative results are presented in **figure 5.10**. Analysis revealed that ΔM-N SSAA L-selectin-GFP spots did not accumulate in the pseudopods of transmigrating THP-1 cells as average number of spots did not exceed that observed for ΔM-N L-selectin (**figure 5.10 A**). Additionally, no significant differences were seen in spikes formation between the cell lines, although trend was seen where cells expressing L-selectin whose serines were mutated to alanines had slightly more spikes (**figure 5.10 B**). Interestingly, a new form of L-selectin-GFP accumulation was identified in the pseudopods of THP-1 ΔM-N SSAA L-selectin-GFP/RFP cells, termed “aggregates”, which were much larger than spots (**figure 5.11**). At this point images of transmigrating THP-1 WT, SSAA and ΔM-N L-selectin-GFP cells were re-analysed for the presence of the aggregates. Interestingly, very rarely aggregates could be seen in those cells, which explains why they were not spotted before. Scoring of the aggregates revealed that, on average, 7 out of 10 cells would present with a ΔM-N SSAA L-selectin-GFP aggregate in the pseudopods. On average, only 1 out of 10 cells would present with WT, SSAA or ΔM-N L-selectin-GFP aggregate (**figure 5.10 C**), suggesting that relationship between the aggregates and FRET is not likely.

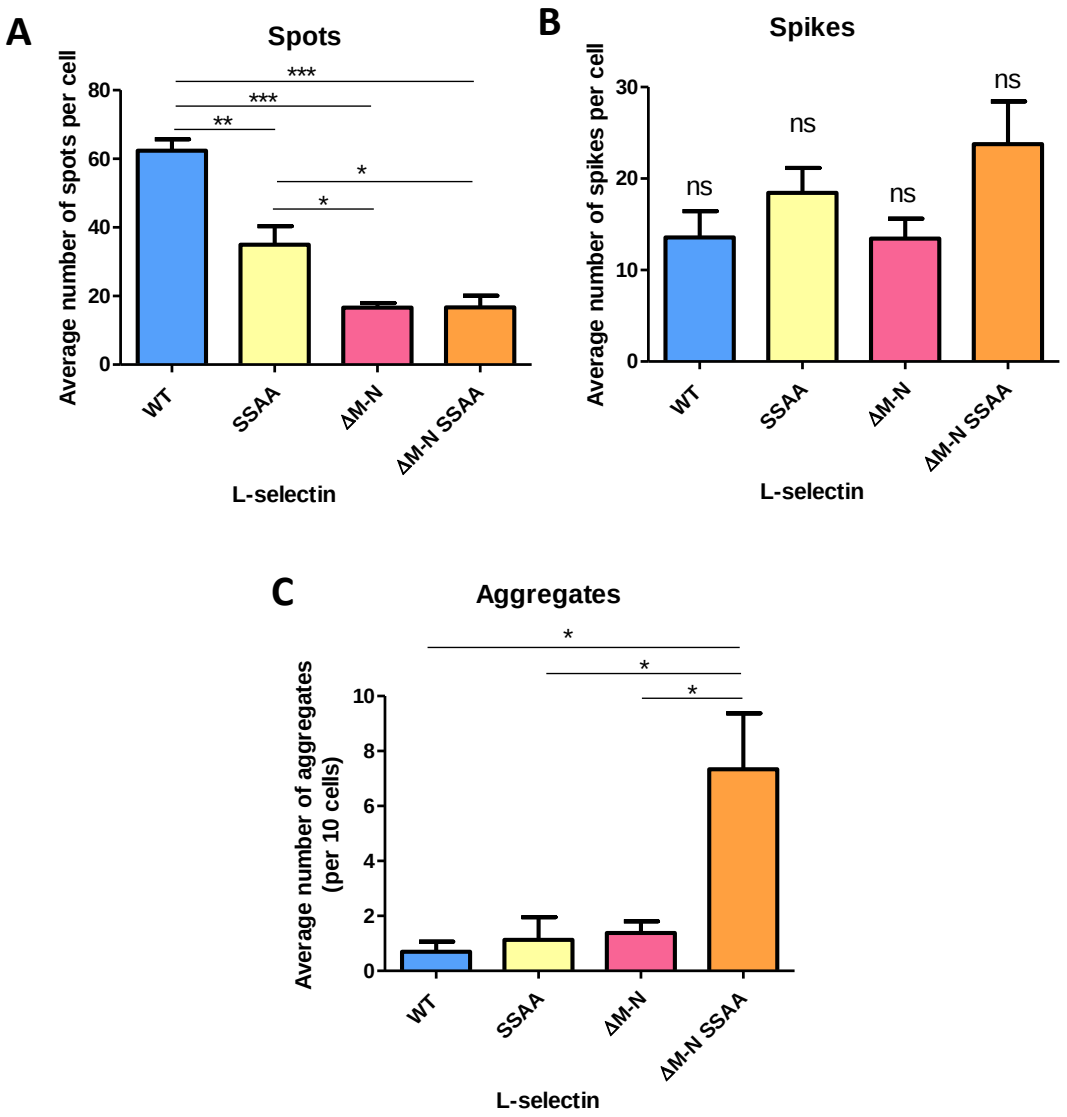

Figure 5.10 Quantitation of spots, spikes and "aggregates" of WT, SSAA, ΔM-N and ΔM-N SSAA L-selectin-GFP. THP-1 ΔM-N SSAA L-selectin-GFP/RFP cells were perfused over TNF-α activated HUVEC for 15 minutes, fixed with 4% PFA and prepared for confocal analysis (**sections 2.14.3** and **2.16.2**). Spots and aggregates of L-selectin-GFP were analysed in the pseudopods of transmigrating THP-1 cells. Spikes were quantified using Volocity software and aggregates were counted manually. Spikes were counted manually. Analysis of spots and spikes of THP-1 WT, SSAA and ΔM-N L-selectin-GFP was performed earlier (**figure 4.13**) and the images were now re-analysed for the presence of aggregates. Graphs presented in this figure show consolidated data of spots (**A**), spikes (**B**) and aggregates (**C**) quantitation. For detailed method of spots, spikes and aggregates analysis see **section 2.16.4**. Error bars represent S.E.M. Statistical analysis: One-way ANOVA followed by Tukey's post-test. *=p<0.05 **=p<0.01, ***=p<0.001.

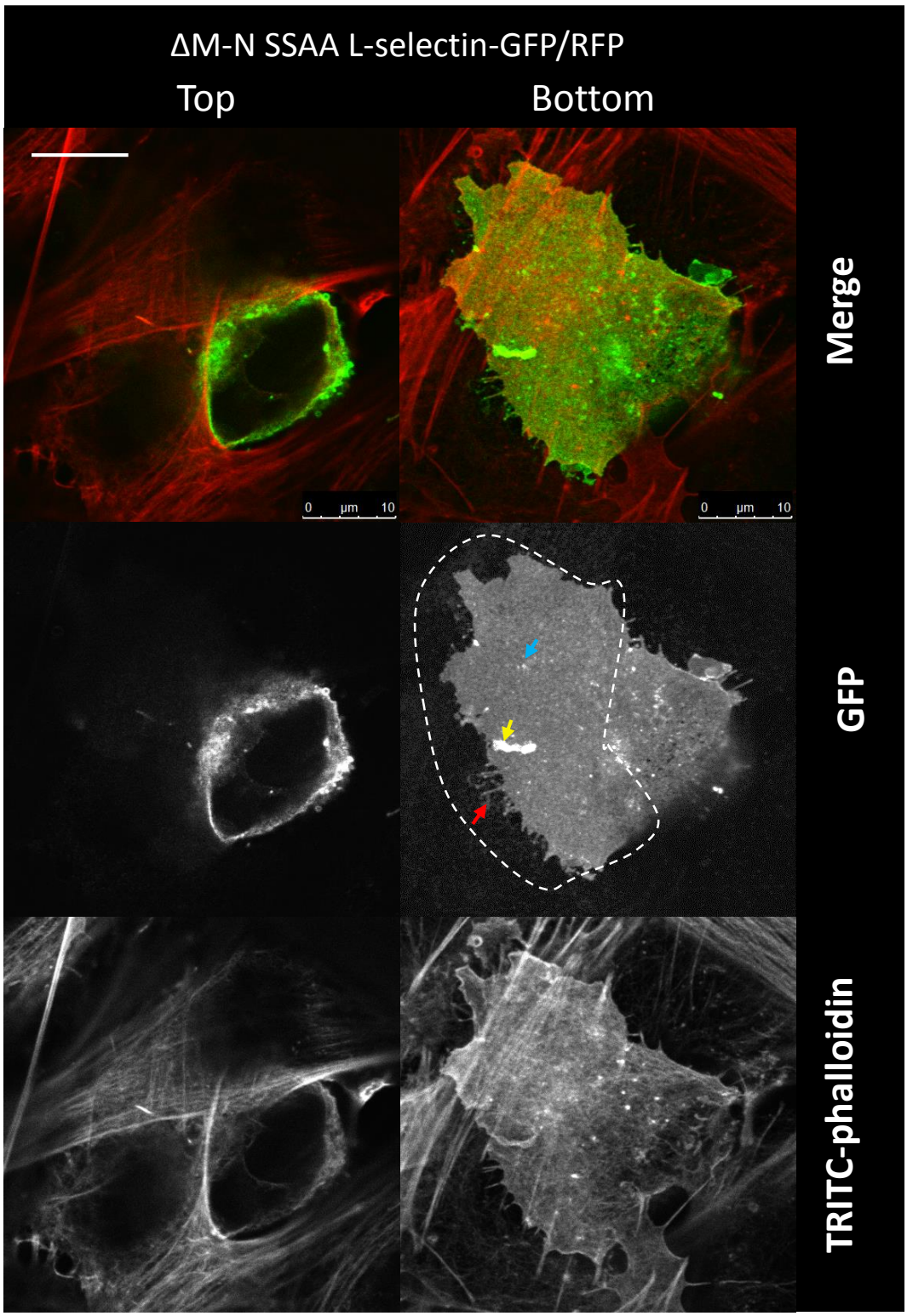

Figure 5.11 Large ΔM-N SSAA L-selectin-GFP aggregates accumulate in the pseudopods of transmigrating THP-1 cells. THP-1 cells expressing ΔM-N SSAA L-selectin-GFP/RFP were perfused over TNF-α activated HUVEC for 15 minutes, fixed with 4% PFA, stained with TRITC-phalloidin and analysed by confocal microscopy (**sections 2.14.3** and **2.16**). Representative single z-plane confocal images of Top and Bottom z-planes (Top and Bottom as depicted in schematic in **figure 4.2 A**) are shown. L-selectin-GFP spots and aggregates are shown with blue and yellow arrows, respectively. Spikes extending from the pseudopods are indicated with red arrows. The dashed lines encircle the protruded areas that were analysed. Scale bar: 10 µm.

This data shows that even though the ΔM-N SSAA L-selectin-GFP did not accumulate in the form of spots, another form of accumulation – big L-selectin-GFP formations termed aggregates – were seen in the pseudopods of transmigrating THP-1 cells. The nature of these aggregates is not known. Since little aggregates were seen formed by WT and SSAA L-selectin that cluster in the transmigrating pseudopods (**figure 5.8**), it is not likely that they correspond to ΔM-N SSAA L-selectin-GFP/RFP clustering that was detected in the pseudopods by FRET (**figure 5.8**). It has to be acknowledged that whilst analysis of WT, SSAA and ΔM-N L-selectin-GFP accumulation in the pseudopods of transmigrating THP-1 monocytes was performed on cells expressing only GFP-tagged L-selectin, accumulation of ΔM-N SSAA L-selectin was performed in the double expressor (GFP/RFP) THP-1 cells. As a result it was possible that total levels of ΔM-N SSAA L-selectin were not an exact match to the corresponding "single expressors". However, L-selectin-GFP spots and aggregates were analysed using images of the GFP channel only. MOI of 5 was used to transduce THP-1 cells with lentiviral particles carrying ΔM-N SSAA L-selectin-GFP transgene. Hence, levels of ΔM-N SSAA L-selectin-GFP were most probably similar to those on THP-1 ΔM-N L-selectin-GFP Lo5 cells, and thus to all the other single expressor cell lines. Therefore, it is believed that analysis of spots and aggregates should not be influenced by the fact that additional ΔM-N SSAA L-selectin-RFP form was also present in the cells. As for examination of spikes, the possibly unmatched total ΔM-N SSAA L-selectin levels could skew the analysis. Although not statistically significant differences were found between the cell lines, THP-1 ΔM-N SSAA L-selectin-GFP/RFP cells showed a trend where more spikes were present. This could be a result of higher total ΔM-N SSAA L-selectin levels. Notably, a trend was also seen where THP-1 SSAA L-selectin-GFP Hi20 cells formed slightly more spikes that both THP-1 WT L-selectin-GFP Hi20 and ΔM-N L-selectin-GFP Lo5 cells. Thus, it is more likely that the trend was due to SSAA mutation rather than total L-selectin levels.

5.3.8 Clustering of L-selectin is promoted by antibody-mediated cross-linking of either CD43 or PECAM-1

Data presented in the sections above shows that L-selectin clustering occurs during the initial stages of TEM, when THP-1 monocytes send pseudopods underneath the HUVEC monolayer. L-selectin clustering in the pseudopods could be the result of ECM ligand binding, i.e. binding to HUVEC-expressed biglycan (**figures 5.3** and **5.4**). At the same time, other mechanisms of L-selectin clustering could also be in action. One possibility is that engagement of other CAMs that are present on the surface of THP-1 monocytes, generates intracellular signals that in turn result in clustering of L-selectin. Signals generated intracellularly are known to cause upregulation and increase in affinity of

leukocyte integrins, and this phenomenon is known as “inside-out” signalling (**section 1.2.4**). To test this hypothesis cell adhesion molecules were selected to represent proteins that were involved in various stages of the multi-step adhesion cascade: PSGL-1, JAM-A, CD43, CD44 and PECAM-1. All of these CAMs are known to be expressed in THP-1 cells [153, 679-682], and flow cytometry was used to analyse their endogenous expression on THP-1 WT L-selectin-GFP/RFP cells. **Figure 5.12** shows that although all the CAMs were expressed on the THP-1 cells, the expression levels varied between the CAMs tested. For example expression of CD43 and CD44 were in the same log scale range as L-selectin (around 10^4), but the expression levels of PSGL-1, PECAM-1 and JAM-A were much lower (around 10^2).

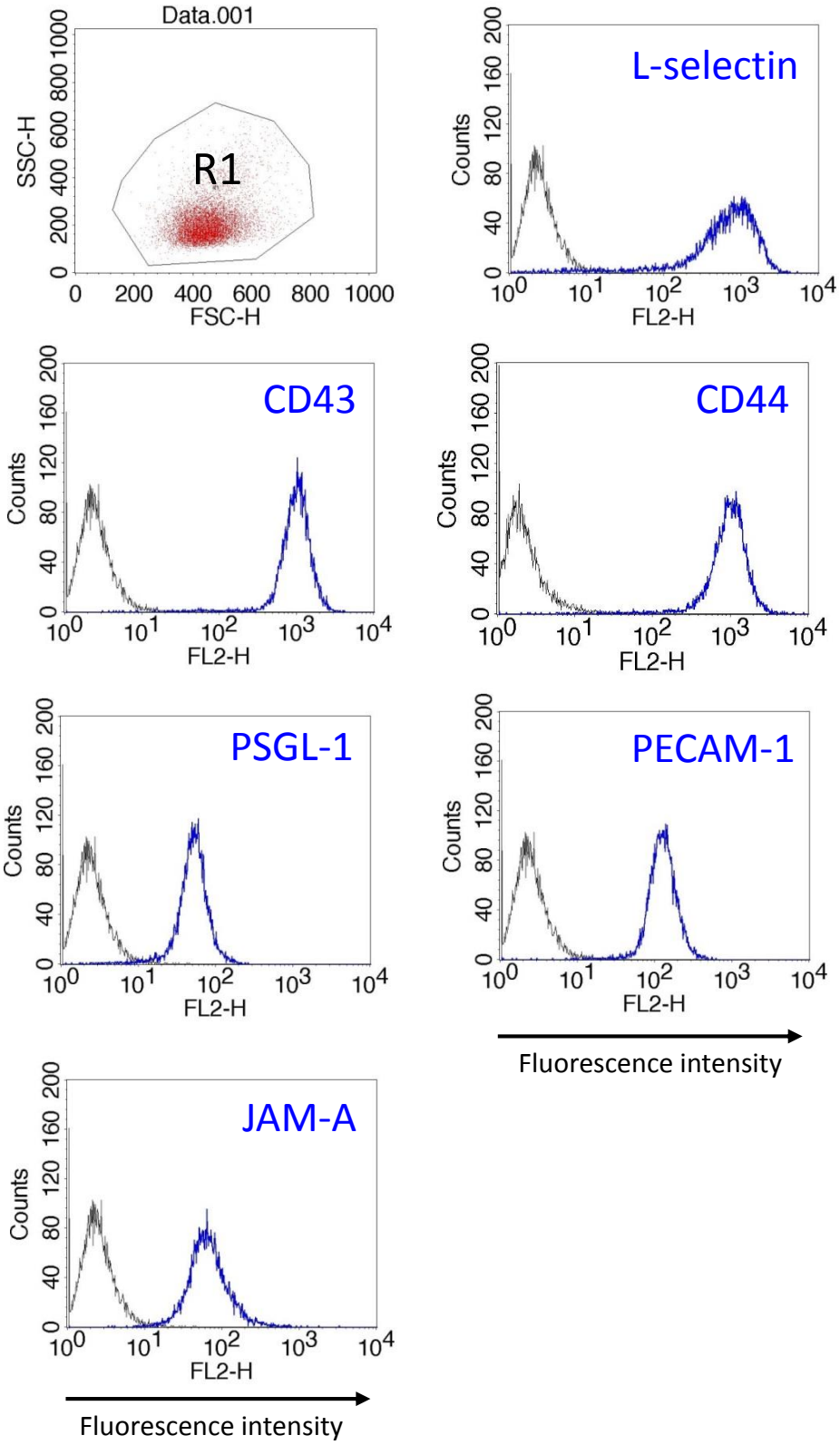

Figure 5.12 Expression levels of THP-1 CAMs. THP-1 WT L-selectin-GFP/RFP cells were labelled with anti-L-selectin, -CD43, -CD4, -PSGL-1, -PECAM-1, -JAM-A or appropriate IgG isotype control antibodies and then RPE-conjugated secondary antibodies, and analysed by flow cytometry as described in **section 2.13**. Dot plot in the upper left corner shows gate R1 that was used to select single and viable cells only. Histograms show expression levels of indicated CAMs. All used antibodies were of the same stock concentration and the same dilution was used for all samples.

To test whether clustering of any of the CAMs would in turn induce L-selectin clustering in a manner of inside-out signalling, the cells were subjected to the cross-linking assay described in **section 2.19**. Briefly, monoclonal antibody was used to specifically label PSGL-1, JAM-A, CD43, CD44 or PECAM-1 on the surface of WT L-selectin-GFP/RFP, the molecules were cross-linked with relevant secondary antibodies and cells were seeded on to ploy-L-lysine (PLL)-coated coverslips. The extent of L-selectin clustering was measured by FLIM/FRET. In the control experiments L-selectin was labelled with or without DREG56 and cross-linking was promoted with a secondary antibody. All stock concentrations of the primary antibodies were matched (**table 2.2**) and 1:50 dilution was used to treat all cells. As expected, cross-linking L-selectin resulted in a dramatic increase in FRET efficiency, whereas no FRET was detected in untreated cells (**figure 5.13 A**). Remarkably, whilst no FRET was seen when PSGL-1, JAM-A and CD44 were cross-linked, cross-linking CD43 or PECAM-1 caused significant clustering of L-selectin (**figure 5.13 A**). Analysis of FRET efficiencies showed that direct L-selectin cross-liking resulted in maximal L-selectin clustering. As expected, no clustering was seen in the control cells where cross-linking was not performed, implying that the action of seeding cells on to PLL did not influence the clustering of L-selectin. Cross-linking of CD43 and PECAM-1 caused the same extent of L-selectin clustering as no statistically significant differences in η_{FRET} values were seen between the two (**figure 5.13 B**). Interestingly, localisation of L-selectin FRET signal and PECAM-1 staining appeared as an exact match. CD43 staining was seen in the same areas as L-selectin FRET, but also in other areas where L-selectin did not cluster (**figure 5.13 A**). This could suggest possible differences in the way PECAM-1 and CD43 relay their signals to cluster L-selectin.

The fact that cross-linking CD43 or PECAM-1 did and PSGL-1, CD44 and JAM-A did not cause L-selectin clustering, suggested that the potential of these molecules to cluster L-selectin was not necessarily dependent on their relative abundance (**figure 5.12**). On the other hand it had to be appreciated that the relative affinities of the antibodies for their ligands were not known. It is possible that this could also have an effect on downstream signalling and L-selectin clustering. Although this does not question the fact that CD43 and PECAM-1 caused L-selectin clustering, it does not formally exclude the possibility that CD44, JAM-A and PSGL-1 could also cluster L-selectin under different experimental conditions.

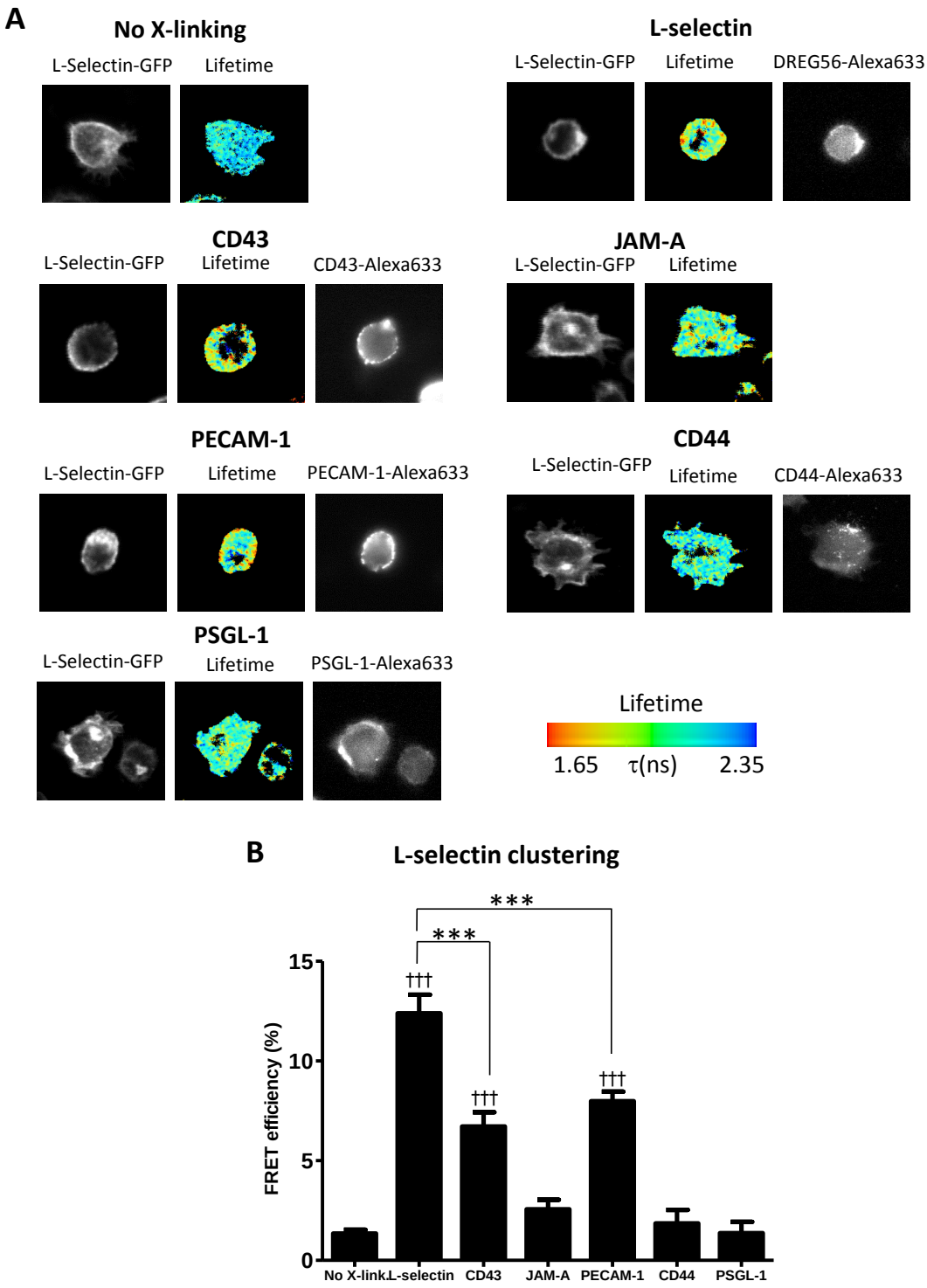

Figure 5.13 Clustering of L-selectin in response to CD43 and PECAM-1 cross-linking. THP-1 WT L-selectin-GFP/RFP cells were labelled with primary antibodies against indicated CAMs and, and subsequently cross-linked with relevant Alexa633-conjugated secondary antibodies. Alternatively, the cells were incubated with just media ("No X-linking"), and cells were seeded on to PLL pre-coated coverslips (for method details see **section 2.19**). After 5 minutes of binding, cells were fixed with 4% PFA and prepared for FLIM/FRET analysis as described in **section 2.18.1**. **A)** In all panels images show L-selectin-GFP (left columns), the GFP multi-photon intensity (middle columns) and relevant Alexa633 fluorescent images (right columns). Lifetime of GFP fluorescence is shown as a pseudocolour scale of blue (high lifetime) to red (low lifetime = FRET).

No Alexa633 image corresponding to JAM-A staining was available. **B**) Quantified data showing FRET efficiency between L-selectin-GFP and L-selectin-RFP. Average 15 cells were analysed for each condition per cell line and cells were derived from 3 independent experiments. Error bars represent S.E.M. Statistical analysis: One-way ANOVA followed by Tukey's post-test. "†" represent difference against "No X-link.", "*" represent indicated differences between cross-linked samples. † † †=p<0.001, ***=p<0.001.

5.3.9 Alanine-to-serine mutation of the L-selectin tail is sufficient to block PECAM-1, but not CD43, mediated clustering of L-selectin

As described in **section 5.3.9** above, cross-linking of both CD43 and PECAM-1 resulted in L-selectin clustering. To investigate whether this was dependent on cytoplasmic serines and/or L-selectin extracellular cleavage site, it was decided that that THP-1 ΔM-N, ΔM-N SSAA and SSAA L-selectin-GFP/RFP cells were to be subjected to the same cross-linking assay. Expression levels of CD43 and PECAM-1 in WT and mutant L-selectin double expressing cells were first analysed by flow cytometry. No detectable changes in the expression levels of CD43 or PECAM-1 expression were found in any of the cell lines tested (**figure 5.14**).

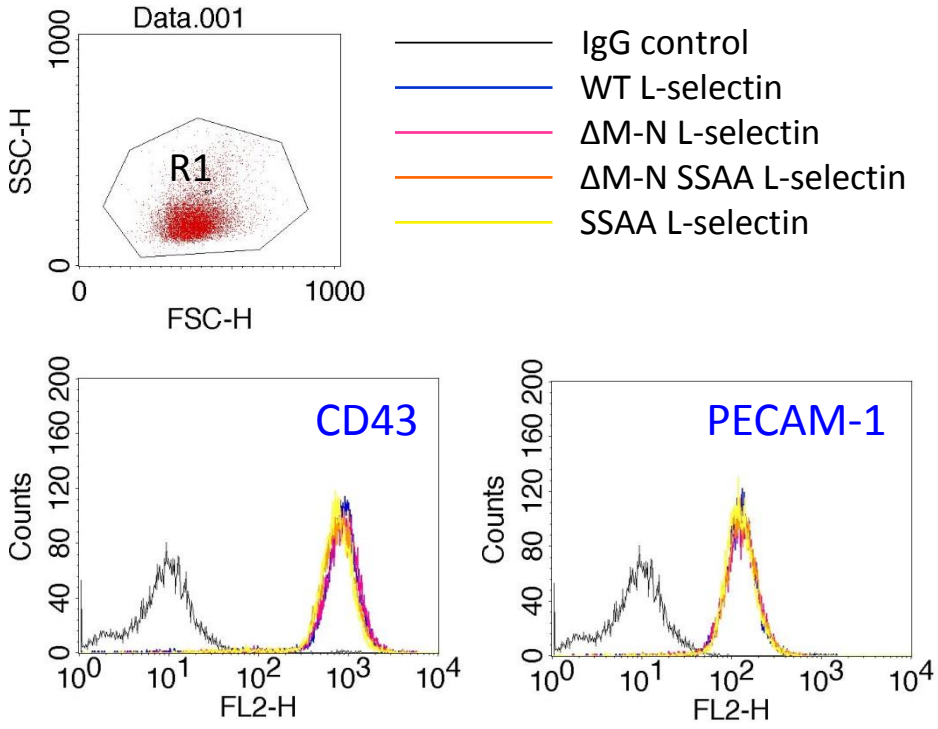

Figure 5.14 CD43 and PECAM-1 levels are matched in THP-1 cells expressing WT or mutant forms of L-selectin-GFP/RFP. THP-1 cells expressing WT, ΔM-N, ΔM-N SSAA or SSAA L-selectin-GFP/RFP were labelled with anti-CD43, anti-PECAM-1 or IgG isotype control antibodies. Cells were subsequently labelled with RPE-conjugated secondary antibody and analysed by flow cytometry (**section 2.13**). Dot plot in the top panel shows single and viable THP-1 cells (Gate R1) selected for analysis. Histograms in the bottom panel show CD43 (left histogram) and PECAM-1 (right histogram) expression.

CD43 or PECAM-1 molecules on THP-1 ΔM-N, ΔM-N SSAA or SSAA L-selectin-GFP/RFP cells were cross-linked as described in **section 5.3.8** (for detailed description of the assay see **section 2.19**), and the cells were prepared for FLIM/FRET analysis (**section 2.18.1**). All results were compared to the previous results obtained for WT L-selectin (**figure 5.12**) and cumulative data is represented in **figure 5.15**. FRET analysis showed that all mutants clustered in response to cross-linking with DREG56 antibody. Interestingly, the only L-selectin mutant that did not undergo clustering in response to either PECAM-1 or CD43 cross-linking was ΔM-N L-selectin. This could be due to the possibility that the cytoplasmic tail of ΔM-N is modified in some way (such as hyperphosphorylation). In support of this, both ΔM-N SSAA and SSAA L-selectin underwent clustering in response to CD43 cross-linking, suggesting that hyperphosphorylation of the L-selectin tail may well be the reason for blocking the response in ΔM-N L-selectin. The fact that rendering serine residues of ΔM-N L-selectin non-phosphorylatable restored L-selectin clustering, would suggest that blocking serine phosphorylation is indeed an important requirement for CD43-mediated L-selectin clustering. None of the L-selectin mutants clustered in response to PECAM-1 cross-linking. This result was surprising because of the data obtained for CD43-mediated L-selectin clustering. Yet, as suggested at the end of **section 5.3.8**, it is possible that CD43 and PECAM-1 employ distinct signalling pathways to trigger L-selectin clustering. Perhaps PECAM-1-mediated pathway requires both intact L-selectin extracellular cleavage site as well as wild type serine residues that can undergo dynamic phosphorylation/dephosphorylation events.

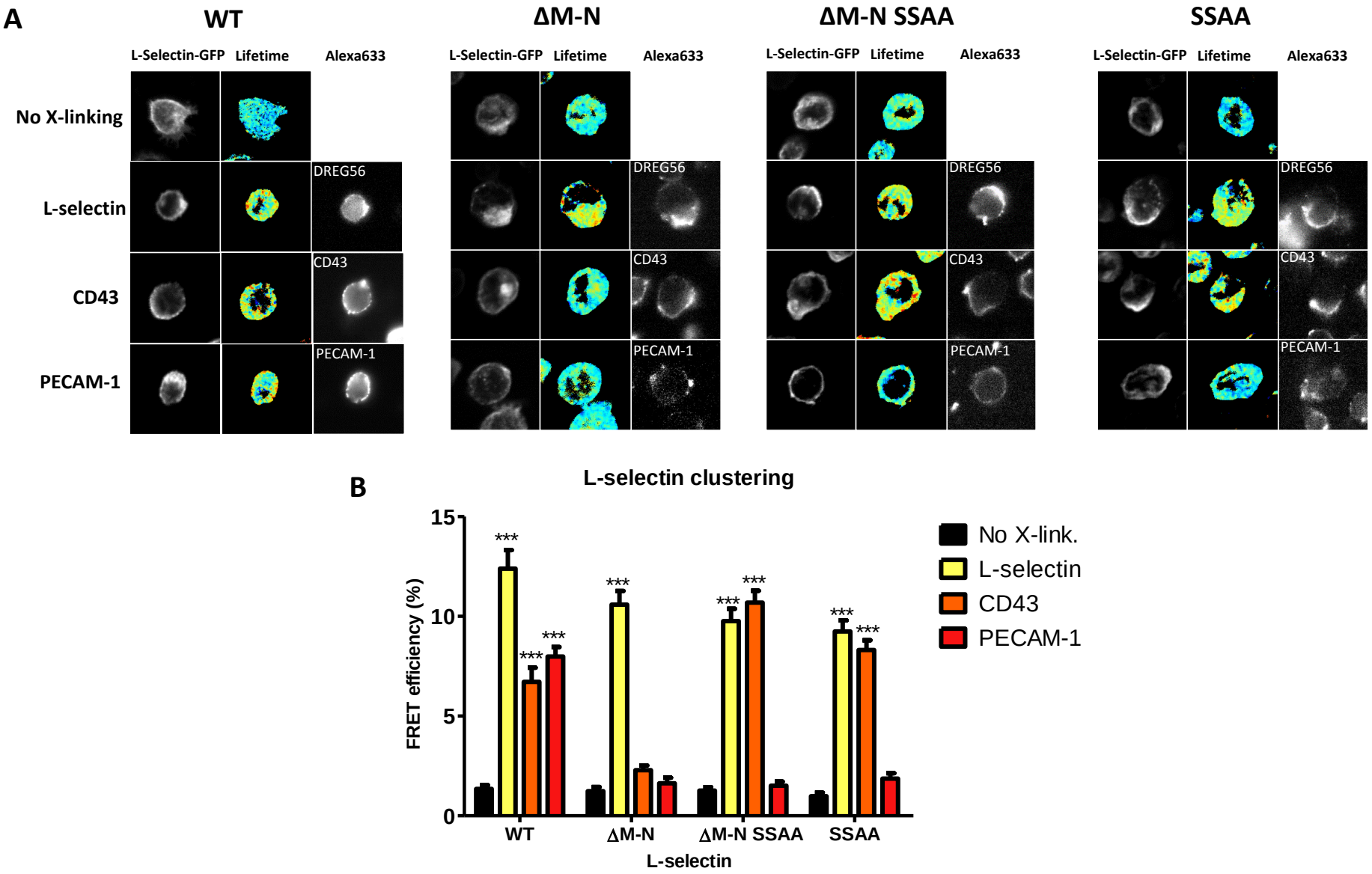
A
WT
ΔM-N
ΔM-N SSAA
SSAA
L-Selectin-GFP
Lifetime
Alexa633
No X-linking
L-selectin
CD43
PECAM-1
DREG56
CD43
PECAM-1
B
L-selectin clustering
FRET efficiency (%)
15
10
5
0
***
WT
ΔM-N
ΔM-N SSAA
SSAA
L-selectin
No X-link.
L-selectin
CD43
PECAM-1

Figure 5.15 Clustering of mutant L-selectin in response to CD43 and PECAM1-cross-linking. L-selectin, CD43 or PECAM-1 on THP-1 ΔM-N, ΔM-N SSAA or SSAA L-selectin-GFP/RFP were cross-liked or cells were left untreated, and cells were allowed to bind to PLL-coated coverslips for 5 minutes at RT (**section 2.19**). After 4% PFA fixation, cells were prepared for FLIM/FRET analysis as described in **section 2.18.1**. **A)** In all panels images show L-selectin-GFP (left columns), the GFP multi-photon intensity (middle columns) and relevant Alexa633 fluorescent images (right columns). Pseudo-colour scale of blue (high lifetime) to red (low lifetime) is used to show lifetime fluorescence. **B**) Quantified data showing FRET efficiency between L-selectin-GFP and L-selectin-RFP. Average 15 cells were analysed for each condition per cell line and cells were derived from 3 independent experiments. Error bars represent S.E.M. Statistical analysis: One-way ANOVA followed by Dunnett's post-test against "No X-link." was performed for each cell line. ***=p<0.001.

5.4 DISCUSSION

5.4.1 Two putative models to explain L-selectin clustering during the leukocyte adhesion cascade

The results presented in this chapter show two major findings: (i) WT L-selectin clusters in the pseudopods of transmigrating THP-1 cells (**figure 5.2**), and (ii) L-selectin clusters following antibody-mediated cross-linking of either CD43 or PECAM-1 (**figure 5.13**). Whether there is a relationship between these two events is currently unknown. However, given the current knowledge about the role of CD43 and PECAM-1 in the leukocyte adhesion cascade, two models for L-selectin clustering can be proposed. The first model postulates that engagement of CD43 during rolling drives L-selectin clustering and enhances leukocyte recruitment. The second model proposes that PECAM-1 plays a role in L-selectin clustering during TEM, which could facilitate binding of ECM ligand and/or L-selectin shedding. A schematic summary of the two models is shown in **figure 5.16**, and each model is discussed in more detail below.

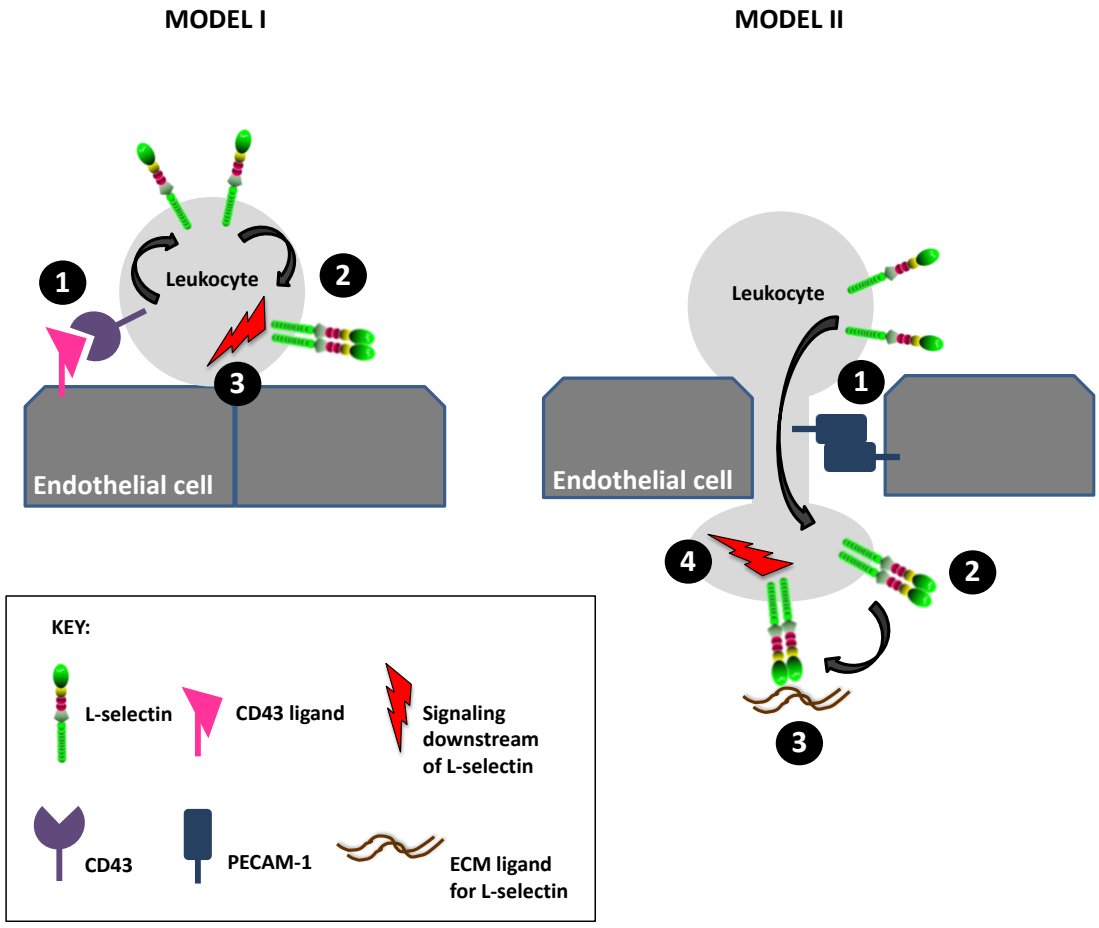

Figure 5.16 Schematic of two possible models of L-selectin clustering. The findings described in this chapter have been used to create two putative models for L-selectin clustering during the leukocyte adhesion cascade. **I)** Engagement of CD43 with endothelial ligand (e.g. E-selectin) (1) leads to L-selectin clustering (2). This initiates signalling downstream of L-selectin tail (3), which promotes leukocyte recruitment. **II)** Leukocyte PECAM-1 engages with its endothelial counterpart (1). This causes or enhances L-selectin clustering and serves to translocate clustered L-selectin to the transmigrated pseudopods (2). Clustered L-selectin has high affinity for the ECM ligand(s) and binding occurs (3). This triggers signalling downstream of L-selectin tail (4), one possible outcome being L-selectin shedding.

Model I

The role of CD43 during the adhesion cascade is somewhat controversial. It has been reported that CD43 is a negative regulator of monocyte, neutrophil and *ex vivo* (naïve) lymphocyte rolling due to its highly negative charge that forms a functional barrier in an electrochemically repulsive manner [684, 685]. On the other hand, Mody et al. (2007) reported that CD43 has a positive effect on the trafficking of central memory, but not naïve, T cells to the LNs [686]. Homing of lymphocytes to LNs is exclusively dependent on L-selectin [11, 389-392, 687], and it was possible that CD43 deficiency negatively regulated L-selectin expression in the central memory T cells. However, the group did not find any changes in L-selectin expression on CD43 null T cells, yet the cells showed

marked reduction in their ability to home to the LNs [686]. In the light of results presented in this chapter (**figure 5.13**), it can be hence proposed that during lymphocyte rolling on HEV, CD43 acts upstream of L-selectin to enhance recruitment. Since no positive effect of CD43 on naïve T cell recruitment has been reported [684, 686], this mechanism might be employed solely by the central memory T cells. Upon activation naïve T cells lose their L-selectin [386], which prevents them from re-entering the LNs and prompt them to home to the sites of inflammation. Upon resolution of the inflammatory response, majority of activated T cells undergo apoptosis [688], but some develop into effector memory T cells and some into central memory T cells [498]. It is the central memory T cells that re-express L-selectin and can home to LNs, where they can rapidly respond to re-stimulation with antigen [387, 498]. Notably, it has been reported that ligation of L-selectin leads to increased adhesion through β1 and β2 integrins in naïve, but not memory T cells [86, 88]. Perhaps central memory T cells acquire different to naïve T cells functional requirements, where engagement of CD43 is firstly needed to cluster L-selectin and initiate signals that promote recruitment to the LNs. It would be of interest to perform adoptive transfer experiments *in vivo*, where the influence of CD43 cross-linking could be evaluated on naïve versus central memory T cell trafficking.

Interestingly, it has also been reported that neutrophil and monocyte infiltration into the inflamed peritoneum and transmigration across platelet activating factor (PAF)-perfused venules of the cremasteric muscle was significantly impaired in CD43 deficient mice [685]. This suggests that CD43 might also play a role in leukocyte recruitment to sites of inflammation. CD43 is known to bind E-selectin during leukocyte rolling [689-691], and hence it is likely that engagement of CD43 clusters L-selectin to increase avidity, reduce rolling velocity and aid better recruitment. This could be particularly true in mouse, where, unlike in humans, neutrophil L-selectin cannot bind to E-selectin [381]. In such case, where direct activation of L-selectin by E-selectin is not possible, CD43 might play a role to transduce signalling from E-selectin to L-selectin. For example, it has been shown that rolling of human neutrophils on E-selectin and ICAM-1 causes co-clustering of L-selectin and PSGL-1, which leads to β2 integrin activation and transition from rolling to arrest [413]. Perhaps in mouse it is the binding of CD43 to E-selectin that clusters L-selectin, which in turns leads to integrin activation.

Model II

Leukocyte PECAM-1 is known to mediate transendothelial migration [692], and hence it is easy to envisage a mechanism, where engagement of PECAM-1 triggers intracellular signals resulting in L-selectin clustering. Leukocyte PECAM-1 is known to rapidly redistribute to detergent resistant membranes (DRM) during transmigration [155]. GlyCAM-1 binding and antibody-mediated cross-linking of L-selectin have also been

shown to drive translocation to DRM [560, 587]. Through casual observations, it seems as though PECAM-1 clustering was super-imposed with L-selectin clustering (**figure 5.13**). During TEM, leukocyte PECAM-1 makes like-for-like interactions with endothelial PECAM-1. As this process ensues, one can imagine that clustering of leukocyte/endothelial PECAM-1 at endothelial junctions could potentially serve to translocate L-selectin from the non-transmigrated part of the cell to the transmigrating pseudopod (**figure 5.2**). It is therefore possible that once monocyte initiates transmigration, PECAM-1 and L-selectin co-localise in cholesterol-rich membrane domains, e.g. lipid rafts, where PECAM-1 mediated signalling cause L-selectin clustering. Additionally, clustering of L-selectin via PECAM-1 could bring about a conformational change that aids binding of multiple sulphated polysaccharide chains belonging to an ECM ligand. Clustering of membrane receptors has been proposed as a mechanism that modulate the affinity of these receptors for their ligands [693], and lipid rafts are known platforms mediating immune cells signalling [588]. Extracellular matrix proteoglycans bearing long sulphated polysaccharide chains, i.e. collagen XVIII, biglycan and versican, have been shown to bind to L-selectin [221, 354, 463-466]. As shown in **figures 5.3** and **5.4**, biglycan is expressed by TNF-α activated HUVEC and is a likely candidate for a subendothelial L-selectin ligand. Remarkably, no research has been devoted to investigate the potential signalling triggered by binding of L-selectin to sulphated proteoglycans and/or glycolipids. It is likely that this signalling would be of a completely different nature to the one evoked by "classic" sLe^x-epitope bearing ligands. Multiple long polysaccharide chains that exhibit a high degree of sulfation could bind L-selectin in a structurally different way to that of the relatively small sLe^x moieties. This could in turn result in activation of a distinct signalling pathway downstream of L-selectin tail. Notably, Liu and Kiick (2011) analysed the influence of ligand architecture and sulphation on L-selectin binding and shedding, and the authors state that sulphation and certain ligand density – or spacing between the ligands – needs to be present for the binding to induce shedding [678]. It is interesting to note that amid the multitude of cellular responses triggered by L-selectin cross-linking, shedding has been reported the most frequently [91, 529, 533-536]. Perhaps very densely spaced ligands, such as sulphated polysaccharide chains, induce L-selectin clustering in a specific conformation, which over time results in L-selectin shedding. It is noteworthy that engagement of PECAM-1 on human neutrophils has been shown to induce shedding of L-selectin [694]. Additionally, ADAM17, a protease that cleaves L-selectin upon cell activation, has been reported to cleave its substrates in lipid rafts [695, 696]. Perhaps a certain membrane lipid raft environment, where PECAM-1, L-selectin and ADAM-17 co-cluster is formed during TEM, which – upon ECM ligand binding – results in L-selectin shedding exclusively in the transmigrating pseudopods. Understanding the timing of pseudopod

protrusion, its influence from L-selectin-dependent adhesion (with ECM-derived ligands) and signalling, and shedding of L-selectin will be important areas of research to explore.

5.4.2 Cytoplasmic serine residues regulate L-selectin clustering

Based on long (over 30 minutes to 1 hour) end-point assays, emigrated leukocytes are known to have shed their L-selectin [520, 554-556]. Data presented in **Chapter 4** shows that L-selectin-GFP shedding occurs in the first 20 minutes of TEM under static conditions (**figure 4.1**), which is delayed when the cytoplasmic serine residues are mutated into non-phosphorylatable alanines (**figure 4.4**). Additionally, a correlation was identified between L-selectin shedding and accumulation of L-selectin-GFP spots in the pseudopods of transmigrating THP-1 cells after 15 minutes of flow (**section 4.3.9**, **figure 4.13**). The results presented within this chapter show that L-selectin clusters in the pseudopods of transmigrating THP-1 monocytes after 15 minutes of perfusion (**figure 5.2**). A question therefore arose as to a possible relationship between cytoplasmic serine phosphorylation, L-selectin shedding and L-selectin clustering during TEM. Interestingly, both WT and SSAA L-selectin clustered in protruding pseudopods (**figure 5.8**), suggesting that rendering of the cytoplasmic serine residues non-phosphorylatable does not affect L-selectin clustering during monocyte TEM. A decrease in FRET efficiency was seen in the SSAA mutant as compared to WT L-selectin, which could correspond to the observed delay in shedding seen in the static transmigration assay (**figure 4.4**). Most interestingly, ΔM-N L-selectin as well as L-selectin from monocytes treated with Ro-31-9790 metalloprotease inhibitor did not cluster in the pseudopods of transmigrating THP-1 monocytes (**figure 5.6**). In fact, a reverse subcellular distribution of clustered L-selectin was seen, where L-selectin clustered exclusively in the non-transmigrated parts of the cells (Top z-plane) (**figure 5.6**). This could be interpreted in one of two ways. One explanation would be that shedding is required for clustering, and the clustered form is L-selectin cleavage product (“stump”). However, this hypothesis does not explain why ΔM-N L-selectin clustering was seen in the Top z-plane of the transmigrating cells. Cell activating stimuli are known to cause phosphorylation of L-selectin tail as well as induce L-selectin shedding [495, 496, 567], but whether those events occur simultaneously or one precedes the other is unclear. If tail phosphorylation precedes shedding, both ΔM-N L-selectin and L-selectin from monocytes treated with Ro-31-9790 might become hyperphosphorylated when the cells become activated upon contact with the TNF-α activated HUVEC monolayer. Attempts were made to detect phosphorylated serines on immunoprecipitated ΔM-N L-selectin, however the antibody used proved unsuccessful. Further optimisation of the technique would be needed to address this question. However, a hypothesis was formulated where hyperphosphorylation of ΔM-N L-selectin uncoupled it from cytoskeleton – perhaps via abrogating interaction with ERM proteins –

and caused physical aggregation of L-selectin molecules in the non-transmigrated parts of the cells, seen as clustering in the Top z-plane. To test the hypothesis that excessive tail phosphorylation prevents L-selectin clustering in monocyte pseudopods during TEM, ΔM-N SSAA L-selectin mutant was generated. As expected ΔM-N SSAA clustered in the pseudopods of transmigrating THP-1 cells (**figure 5.8**), suggesting that rendering the cytoplasmic serines of ΔM-N L-selectin non-phosphorylatable can restore L-selectin clustering in the pseudopods to that seen with WT L-selectin. This also suggests that FRET in the pseudopods is a result of full-length, and not "stump" L-selectin clustering. Furthermore, it could be proposed that for L-selectin to cluster in the transmigrated pseudopods of THP-1 cells, the cytoplasmic serine residues must not be phosphorylated. Supportive of this data are results of experiments conducted in the Ivetic laboratory with ΔM-N L-selectin mutant whose serine residues were mutated to phospho-mimicking aspartates (ΔM-N SSDD). This mutant presented with the same clustering phenotype as ΔM-N L-selectin, where no L-selectin clustering was observed in the transmigrated pseudopods of THP-1 cells, yet L-selectin FRET was detected in the Top z-plane (Dr Angela Rey-Gallardo, unpublished data). Additionally, it can be proposed that the clustering in the non-transmigrated parts of the cell, as seen with the sheddase-resistant L-selectin mutants, namely ΔM-N, ΔM-N SSAA and ΔM-N SSDD, is non-specific (i.e. independent of the serine residues), and could be a result of random interactions between L-selectin molecules that are forced to accumulate together at the plasma membrane due to lack of shedding.

WT, SSAA and ΔM-N SSAA L-selectin, but not ΔM-N L-selectin, underwent clustering in response to CD43 cross-linking. This suggests that blocking L-selectin phosphorylation is needed for CD43-mediated clustering of L-selectin (**figure 5.15**). Both CD43 and L-selectin are known to bind ERM proteins [563, 572, 697, 698]. Interestingly, it has been shown that mutating serine-76 within cytoplasmic domain of CD43 into a phospho-mimicking aspartate abolishes binding of CD43 to ezrin [698]. Phosphorylation of the same serine residue is thought to mediate CD43 signalling [698]. Perhaps phosphorylation of serine-76 on CD43 uncouples the ERM proteins, which can then bind to adjacent non-phosphorylated L-selectin tail, and this in turn induces L-selectin clustering. This could represent a potential mechanism by which CD43 regulates L-selectin-mediated trafficking of central memory T cells to the LNs. Further experimentation would be required to formally test this hypothesis.

That none of the L-selectin mutants underwent clustering in response to PECAM-1 cross-linking is puzzling (**figure 5.15**). However, it can be speculated that both extracellular cleavage site and intact cytoplasmic serines are required for successful L-selectin clustering in response to PECAM-1 cross-linking.

CHAPTER 6. MONITORING CELLULAR RESPONSES TO L-SELECTIN CLUSTERING AND SHEDDING DURING TEM

6.1 INTRODUCTION

The leukocyte adhesion cascade is a sequence of highly co-ordinated adhesion and activation events that lead to extravasation of the leukocytes into the inflamed tissue (**section 1.2**) [6]. During this process the spherical shape of a circulating leukocyte undergoes a series of dramatic changes. Through changes in F-actin reorganisation, activated leukocyte acquires anterior-posterior polarity with an extended leading edge (the front of the cell) and a rounded back (uropod) [699, 700]. The importance of this process is emphasised by the fact that loss of cell polarity abolishes successful locomotion of the leukocytes [234, 240, 701]. During the TEM event, leukocytes extend their leading edge (i.e. the pseudopods) underneath the endothelium [702, 703]. Leukocytes project multiple pseudopods that dynamically protrude and retract [36]. This is thought to be a way of "path finding" and exploring of the subendothelial environment. Once emigrated, leukocytes migrate through the interstitial ECM, and towards the source of inflammation [6, 398, 419, 704]. This process is known as directed cell migration or chemotaxis. Chemotaxis is highly dependent on cell polarity, and numerous chemokines regulate polarisation [705, 706]. Interestingly, it has been reported that L-selectin null as well as "sheddase-resistant" L-selectin murine leukocytes are both able to exit inflamed venules but are incapable to migrate through the interstitium towards the chemoattractant source [398, 419]. This paradoxical observation suggests that L-selectin may have to be shed and then re-expressed on the cell surface for correct chemotaxis in to the surrounding tissue. Alternatively the L-selectin "stump" generated upon L-selectin cleavage may be important for downstream signal propagation resulting in successful chemotaxis (as the stump is both absent in the L-selectin knock-out model and the sheddase-resistant model). Whether the observed L-selectin-dependent chemotaxis defect was due to the compromised leukocyte polarity is not known.

The Rho family of small GTPases are highly conserved molecular switches that control actin cytoskeleton dynamics, thereby affecting cell shape and motility. The Rho GTPases are involved in a number of cellular responses during the leukocyte adhesion cascade (**section 1.5**, see summary in **table 1.1**). The most widely studied members of the family are RhoA, Rac1/2 and Cdc42. Expression of dominant active or inactive forms of those Rho GTPases, or inhibition of their downstream effectors, severely impair leukocyte TEM, polarisation and chemotaxis [118, 234-238, 240, 241, 704]. The Rho GTPases are, therefore, the "first suspects" where an altered cell shape is observed. The Rho GTPase proteins cycle between an inactive GDP-bound and an active GTP-bound forms, and

various methods have been developed to detect the active form. For example, Rho GTPase “pull-down assays” are commonly used to quantify the activation of the Rho GTPases in cell extracts [707-710]. Additionally, FRET based probes (i.e. the Rho GTPase biosensors or the Raichu probes) can be used to monitor the spatio-temporal activation of the Rho GTPases in living cells [118, 711-713].

The data presented in **Chapters 4** and **5** of this thesis describes the results of the experiments designed to investigate shedding and clustering of L-selectin during TEM. The aim of the work contributing to this chapter is to establish whether L-selectin regulates THP-1 monocyte morphology during TEM and if it plays a role in chemotaxis. By studying THP-1 cell shape, it is believed that L-selectin plays a role in monocyte polarisation during TEM. Additionally, the serine residues within the L-selectin tail are shown to be involved in directing THP-1 cell morphology during TEM. The role of the serines is still not clear in this process, however the results presented in this chapter suggest that preventing their phosphorylation could render the cells less “invasive” during TEM.

6.2 EXPERIMENTAL DESIGN

Chapter 5 describes the parallel plate flow chamber assays that were used to investigate WT and mutant L-selectin clustering during TEM. L-selectin mutants were either sheddase-resistant (ΔM-N), had non-phosphorylatable cytoplasmic serines (SSAA), or both (ΔM-N SSAA). Those mutants were generated to help understand what role the extracellular cleavage site and the cytoplasmic serine residues play in L-selectin shedding and clustering during TEM. The assays lasted 15 minutes, which captured cells at a moment before L-selectin shedding had reached its peak. All the perfusions were recorded with the use of the time-lapse inverted fluorescence microscope, where images of the phase contrast and the GFP channel (representing GFP or L-selectin-GFP) were acquired into digital video file. The video footages were now re-analysed to examine THP-1 cell morphology during the perfusion. The aim of this task was to overlay data for THP-1 cell shape change with the existing data acquired for L-selectin shedding and clustering during TEM. Pseudopod formation and cell spreading area of THP-1 monocytes were thus analysed to evaluate the impact of L-selectin expression (and its mutants) on cell shape changes during TEM.

Analysis of the video footage showed striking differences in the cell morphology between the cells expressing WT and ΔM-N L-selectin. The Rho family of the small GTPase proteins control cytoskeletal dynamics and hence regulate cell shape to aid migration. It was shown previously that ligation of L-selectin can activate Rac1 and Rac2 proteins [245, 246, 603]. This suggests that morphology of the THP-1 cells during TEM could be driven by L-selectin-mediated activation of Rho GTPases. Our laboratory has reported

an efficient method for monitoring of the Rho GTPase activation in leukocytes [714].This method was employed to investigate the basal levels of Rho GTPases activation in resting THP-1 monocytes. This was to investigate whether expression of L-selectin or its shedding altered the basal activity of the Rho GTPases.

FRET-based probes that can visualize local changes in Rho GTPase activity in living cells can be used for investigation of the spatio-temporal regulation of these proteins. The Rho GTPase biosensors were first reported by Pertz et al. (2006), and were designed to monitor RhoA activity during fibroblast migration [711]. The Rho GTPase biosensors are built of four domains: the FRET donor (CFP), the FRET acceptor (YFP), a Rho GTPase and its "affinity reagent" (binding partner) (**figure 6.1**). In a non-active state, the separation between YFP and CFP results in low FRET efficiency. Upon activation, binding of Rho GTPase to its affinity reagent brings CFP into a close proximity (<10 nm) of YFP, which increases FRET efficiency. For an explanation of FRET phenomenon and FLIM measurement of FRET efficiency see **sections 2.18** and **5.2**.

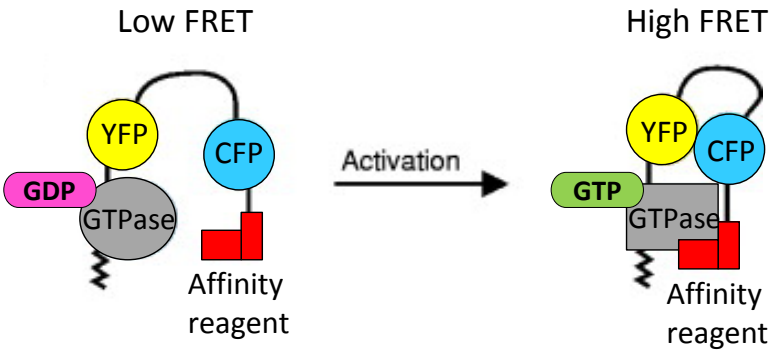

Figure 6.1 Schematic of CFP/YFP FRET-based Rho GTPase biosensor. The Rho GTPase biosensor contains the YFP and CFP fluorescent proteins inserted between the Rho GTPase and the Rho GTPase "affinity reagent". When inactive, the probe is in its relaxed form (left diagram), where CFP and YFP are wide apart and low FRET efficiency is seen. On stimulation, the GDP on Rho GTPase is exchanged for GTP, the active Rho GTPase binds the affinity reagent, and high FRET efficiency is detected (right diagram). Image adapted from Hodgson et al., *Methods in Cell Biology*, 2008 [715].

RhoA, Rac1 and Cdc42 biosensors in lentiviral vectors were constructed and kindly provided by Oliver Pertz (University of Basel, Switzerland). The lentiviral gene delivery system that has been used throughout this thesis was again employed to introduce the biosensors in to the THP-1 monocytes. Excitation wavelength (λ_{ex}) of CFP is 433 nm and its emission wavelength (λ_{em}) is 475 nm. For YFP, λ_{ex} and λ_{em} are 525 nm and 573 nm, respectively. Since λ_{ex} and λ_{em} of GFP are 488 and 507, the CFP/YFP biosensors could not be introduced in to the described in **Chapters 3** and **4** L-selectin-GFP expressing cell lines. This was because the GFP-tag would interfere with the FRET signal due to a

spectral overlap. The probes had to be therefore co-expressed with RFP-tagged L-selectin. RFP has λ_{ex} of 584 nm and λ_{em} of 607 nm, and hence would not interfere with CFP/YFP FRET detection. Generated in **Chapter 5** lentiviral particles carrying RFP-tagged WT or ΔM-N L-selectin were used for transduction. THP-1 cell lines expressing CFP/YFP Rho GTPase biosensors and L-selectin-RFP were subjected to the parallel plate flow chamber assays. Additionally, grounds were set for a new static assay, where WT or ΔM-N L-selectin-RFP was cross-linked and RhoGTPase activation was measured. FLIM analysis of FRET between CFP and YFP was performed with the collaboration of Dr Maddy Parsons (Randall Division of Cell and Molecular Biophysics, King's College London).

Analysis of the video footage showed that WT and ΔM-N L-selectin expressing cells had different morphology during TEM. A polarisation defect was hypothesised to occur in the cells expressing ΔM-N L-selectin. A theory was formed that this could lead to defects in subsequent directed cell migration (chemotaxis) of the cells towards a chemoattractant source. Transwell assays are commonly used to evaluate chemotaxis of cells, and so the transwell chambers were used to monitor THP-1 cell migration. Migration of cells across porous filters as well as activated HUVEC monolayers was assessed.

6.3 RESULTS

6.3.1 Analysis of pseudopod behaviour during THP-1 monocyte transmigration across activated HUVEC under conditions of flow

6.3.1.1 L-selectin expression promotes pseudopod formation during early phases of TEM

Analysis of the time-lapse video recordings (GFP channel) of THP-1 WT L-selectin-GFP/RFP cells perfused over TNF-α activated HUVEC showed that the protruding cells presented with one, two or multiple (three or more) pseudopods (**figure 6.2 A**). To assess whether the number of protruding pseudopods increased over time, the cells were scored half-way through the flow assay (7 minutes), and at the end of the assay (15 minutes). The behaviour of the pseudopods over-time is hereafter referred to as "pseudopod dynamics". The scoring assessed the percentage of cells presenting with a certain number of pseudopods (one, two or multiple) at the given time-points. The percentage was calculated from the total number of cells recruited at any given time-point (both protruding and non-protruding). The same analysis was performed on THP-1 GFP Hi20 cells that were subjected to the same 15 minute-long parallel-plate flow chamber assay. This was to investigate whether differences existed in pseudopods formation between cells expressing fluorescently tagged L-selectin and cells expressing GFP protein alone. Using high GFP expressor cell line (Hi20) ensured that any possible

differences could be interpreted as resulting from L-selectin expression and not from any effects that could be caused by lentiviral gene delivery. The results presented in **figure 6.2 B** show that at 7 minutes 41% of L-selectin expressing cells were protruding, compared to only 28% for THP-1 cells expressing GFP alone. This analysis broadly assessed the total number of protruding cells, irrespective of the number of pseudopods they had. When the total numbers of protruding cells were analysed at 15 minutes, no differences were seen between the cell lines. Interestingly, the number of the total protruding L-selectin expressors did not increase, remaining at 40%, but rather the GFP expressing cells reached a similar level of 42% (**figure 6.2 B**). Next, the number of pseudopods the cells were making was analysed. At 7 minutes, the percentages of cells having two or multiple pseudopods were significantly increased amongst L-selectin expressing cells compared to GFP-expressing cells (**figure 6.2 C**). This difference diminished with time as similar percentages of cells expressing L-selectin and cells expressing GFP presented with one, two or multiple pseudopods at 15 minutes (**figure 6.2 D**). The pseudopod dynamics was found to be different between the two cell lines. The percentage of cells having only one pseudopod increased significantly with time in both of the cell lines (13% to 20% for WT L-selectin and 14% to 24% for GFP) (**figure 6.2 E** and **F**). The percentage of cells having two pseudopods did not change much with time in either cell line, however, the percentage of L-selectin expressing cells that initially had multiple pseudopods decreased significantly with time from 12% to 7% (**figure 6.2 E** and **F**). The fraction of GFP-expressing cells that had multiple pseudopods did not change over time. These results suggest that L-selectin overexpression initially renders THP-1 monocytes more “invasive”, which manifested in increased percentage of total protruding cells and a greater number of cells having more than one pseudopod. This effect reduced over time, which presented as a decrease in the number of cells having multiple pseudopods and a corresponding increase in the number of cells having a single pseudopod at 15 minutes.

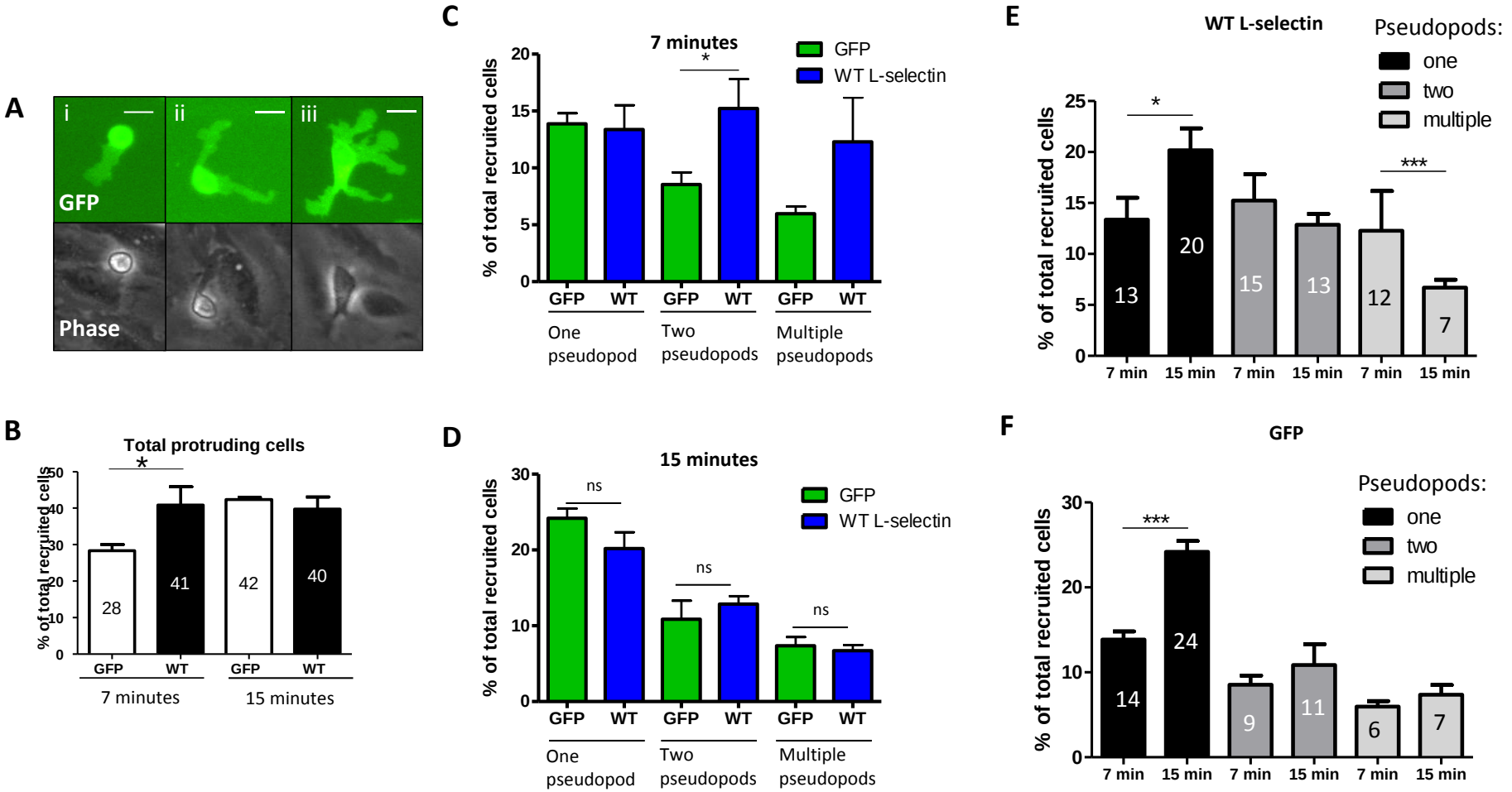
A
i
ii
iii
GFP
Phase
B
Total protruding cells
% of total recruited cells
*
28
41
42
40
GFP
WT
GFP
WT
7 minutes
15 minutes
C
7 minutes
*
GFP
WT L-selectin
% of total recruited cells
GFP
WT
GFP
WT
GFP
WT
One pseudopod
Two pseudopods
Multiple pseudopods
D
15 minutes
ns
ns
ns
GFP
WT L-selectin
% of total recruited cells
GFP
WT
GFP
WT
GFP
WT
One pseudopod
Two pseudopods
Multiple pseudopods
E
WT L-selectin
Pseudopods:
one
two
multiple
*
***
% of total recruited cells
13
20
15
13
12
7
7 min
15 min
7 min
15 min
7 min
15 min
F
GFP
Pseudopods:
one
two
multiple
***
% of total recruited cells
14
24
9
11
6
7
7 min
15 min
7 min
15 min
7 min
15 min

Figure 6.2 Pseudopod behaviour in THP-1 cells transmigrating across activated HUVEC. THP-1 cells expressing wild type L-selectin-GFP/RFP (WT) or GFP alone (GFP) were perfused over TNF-α activated HUVEC for 15 minutes (**section 2.14.3**). The video of the GFP channel was used to score the number of pseudopods the cells were making at two different time-points (7 and 15 minutes). Percentages of cells with a specific number of pseudopods were calculated against the total number of cells (protruding and non-protruding) recruited at that given time-point. **A)** Representative images of cells having one (i), two (ii) or multiple (iii) pseudopods. Scale bar: 10 µm. **B)** Total number of protruding cells (irrespective of pseudopod number) were scored at the 7 and 15 minutes. **C)** Percentage of cells with one, two or multiple pseudopods at the 7 minutes. **D)** Percentage of cells with one, two or multiple pseudopods at the 15 minutes. **E)** Time-dependent change (dynamics) in the number of THP-1 WT L-selectin-GFP/RFP cells forming one, two or multiple pseudopods. **F)** Pseudopod dynamics of THP-1 GFP Hi20 cells. The video footage was derived from three independent experiments. Each experiment was performed in triplicate and three separate fields of view were analysed for each replicate. Total 672 THP-1 GFP Hi20 and 1368 THP-1 WT L-selectin-GFP/RFP cells were analysed. Data represent mean ± S.E.M. Statistical analysis: two-tailed, unpaired Student's t-test. *=p<0.05, ***=p,0.001, ns, not statistically significant.

6.3.1.2 Effects of SSAA L-selectin expression on THP-1 cells pseudopod dynamics

Substitution of the cytoplasmic serines with alanines caused a delay in L-selectin shedding in static transmigration assays (**figure 4.4**), and resulted in decreased L-selectin clustering in pseudopods of transmigrating THP-1 cells (**figures 5.8** and **5.9**). Analysis of the time-lapse footage of THP-1 SSAA L-selectin-GFP/RFP cells transmigrating through TNF-activated HUVEC, showed that those cells had 31% of total protruding cells compared to 41% of THP-1 WT L-selectin-GFP/RFP cells (**figure 6.3 A**). This was, however, not statistically significant, most probably due to the variability in the number of protruding cells between the experiments. Unlike with the WT L-selectin-expressing cells (**figure 6.2 E**), the percentage of SSAA L-selectin-expressing monocytes with a given number of pseudopods did not change with time (**figure 6.3 B**). At 7 minutes, the highest number of cells with one pseudopod (16%), moderate number of cells with two pseudopods (10%) and low number of cells with one pseudopod (6%) were observed, which corresponded to 13%, 8% and 6% at 15 minutes, respectively (**figure 6.3 B**). No differences were detected in the pseudopod formation between SSAA L-selectin expressing cells and WT L-selectin expressing cells when the percentages of cells with any given pseudopod number was compared. However, a trend was seen where THP-1 SSAA L-selectin-GFP/RFP cells had fewer cells with multiple pseudopods at 7 minutes (6% versus 12% for WT L-selectin) (**figure 6.3 C**). Additionally lower fraction of SSAA L-selectin expressing cells with one pseudopod was seen at 15 minutes (13% versus 20% for WT L-selectin), which was just below statistical significance (p=0.052) (**figure 6.3 D**). This could be a result of a decreased trend in the number of total

protruding cells (**figure 6.3 A**). Overall, these results suggest that rendering of the cytoplasmic serines non-phosphorylatable does not have a significant effect on L-selectin-dependent protrusion dynamics. However, a subtle effect can be seen, where SSAA L-selectin expressing cells protrude less that WT L-selectin expressing cells. Additionally, the pseudopods seem less dynamic – as seen by lack of time-dependant change in the percentages of cells having one, two or multiple pseudopods.

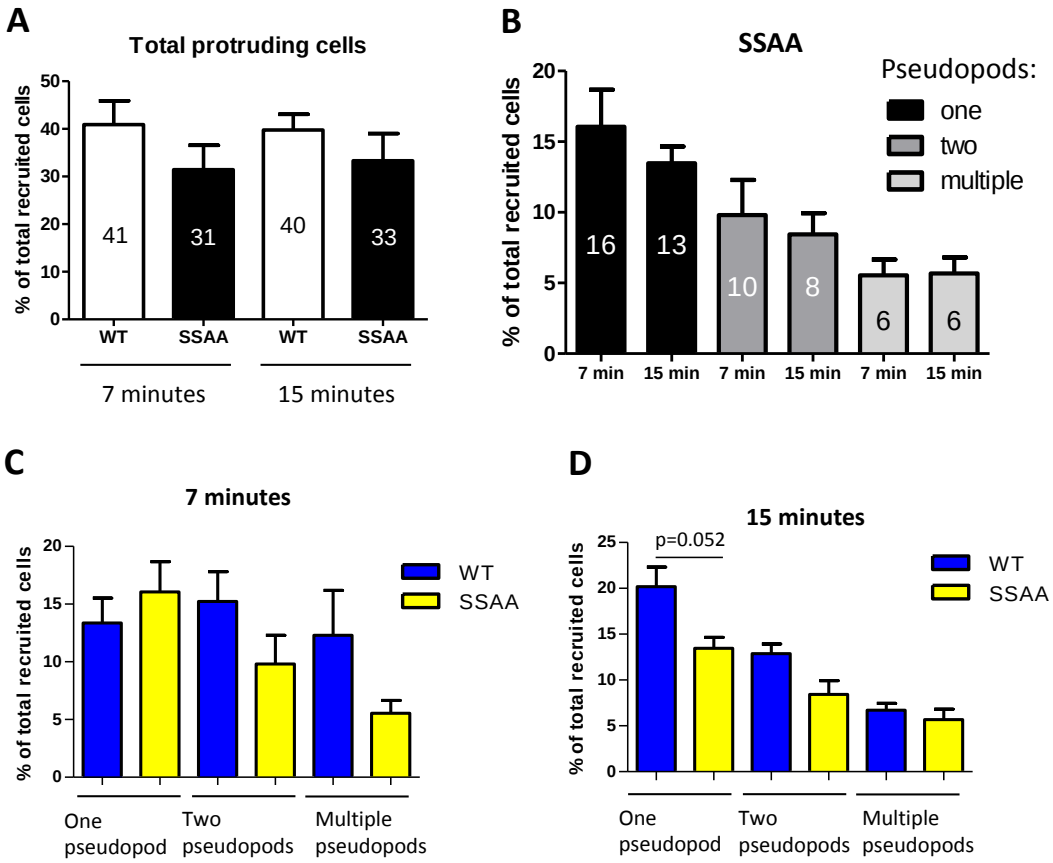

Figure 6.3 Pseudopod dynamics of SSAA L-selectin expressing THP-1 cells. Time-lapse videos of THP-1 SSAA L-selectin-GFP/RFP cells perfused over TNF- activated HUVEC were analysed for pseudopod formation as described in **figure 6.1**. Pseudopod formation was compared to that of THP-1 WT L-selectin-GFP/RFP cells. **A)** Total number of protruding cells at 7 and 15 minutes. **B)** Pseudopod dynamics of THP-1 SSAA L-selectin-GFP/RFP cells. Percentage of cells having one, two or multiple pseudopods were compared across the two time-points. **C)** Comparison of pseudopod formation between WT and SSAA L-selectin expressing cells at 7 minutes. **D)** Corresponding comparison at 15 minutes. The video footage was derived from three independent experiments and three separate fields of view were analysed for each experiment. Total 2200 THP-1 SSAA L-selectin-GFP/RFP and 1368 THP-1 WT L-selectin-GFP/RFP cells were analysed. Data represent mean ± S.E.M. Statistical analysis: two-tailed, unpaired Student's t-test.

6.3.1.3 Blocking L-selectin shedding promotes the formation of multiple pseudopods during TEM that persist over-time

Blocking L-selectin shedding by rendering the extracellular cleavage site "sheddase-resistant" (ΔM-N L-selectin), or by treating WT L-selectin expressing cells with Ro-31-9790 metalloprotease inhibitor abolished L-selectin clustering in the pseudopods of transmigrating THP-1 monocytes (**figure 5.6**). It was hence of interest to investigate whether the lack of L-selectin clustering had any effects on THP-1 cells pseudopod dynamics. Time-lapse video recordings of the 15 minute-long parallel plate flow chamber assays were analysed as described in the sections above. At 7 minutes, the percentage of total protruding cells was 33% for the cells expressing ΔM-N L-selectin and 34% for the cells expressing WT L-selectin treated with Ro-31-9790 inhibitor, referred to as WT Ro-31-9790 L-selectin, which was slightly less compared to to the cells expressing WT L-selectin (41%) (**figure 6.4 A**). This disappeared with time as equal numbers of WT, ΔM-N and WT Ro-31-9790 L-selectin expressing cells protruded at 15 minutes (**figure 6.4 A**). Strikingly, at 7 minutes not many ΔM-N L-selectin expressing cells formed one (7%) or two (6%) pseudopods, but a large number of cells sent multiple pseudopods instead (18%) (**figure 6.4 B**). This phenotype become more severe with time, as at 15 minutes only 5% and 4% of cells had one and two pseudopods, respectively, whereas 35% of the cells had multiple pseudopods (**figure 6.4 B**). Ro-31-9790 treated WT L-selectin-expressing cells presented with the same pseudopod dynamics, where cells with multiple pseudopods prevailed at both 7 and 15 minutes (**figure 6.4 C**).

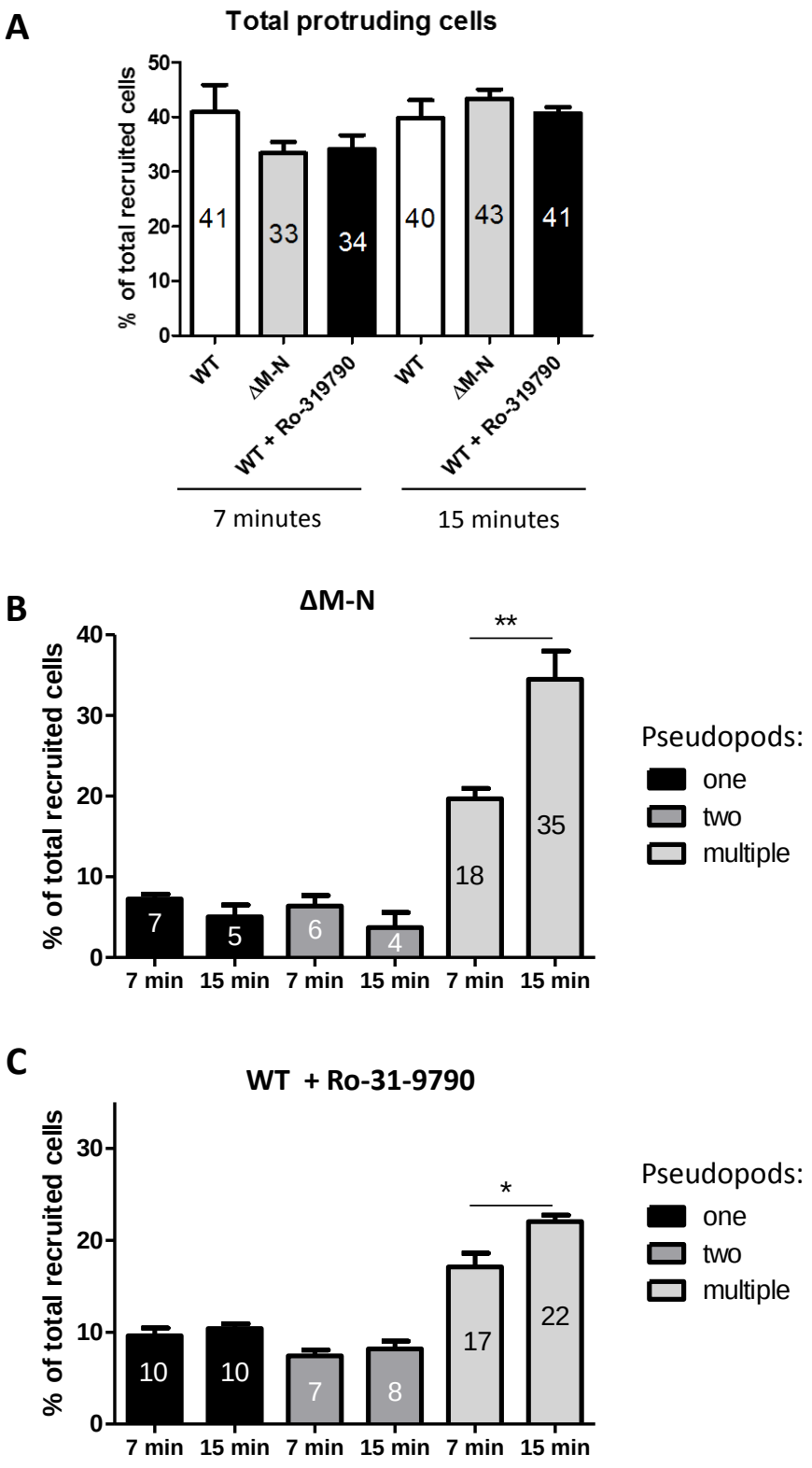

Figure 6.4 Pseudopod formation of cells expressing ΔM-N L-selectin or WT L-selectin treated with Ro-31-9790 inhibitor. Time-lapse videos of THP-1 ΔM-N L-selectin-GFP/RFP cells or THP-1 WT L-selectin-GFP/RFP cells pre-treated with Ro-31-9790 metalloprotease inhibitor (WT + Ro-31-9790) perfused over TNF-α activated HUVEC were scored for pseudopod formation as described in **figure 6.1**. **A)** Total number of protruding cells at 7 and 15 minutes. The percentage is calculated from the total number of cells recruited to the endothelium at given time-point (protruding and non-protruding). Total number of protruding THP-1 WT L-selectin-GFP/RFP

cells is shown for comparison. **B)** Pseudopod dynamics of THP-1 ΔM-N L-selectin-GFP/RFP cells. The graph shows percentage of cells with one, two or multiple pseudopods at 7 and 15 minutes. **C)** Corresponding analysis as in B, but performed on THP-1 WT L-selectin-GFP/RFP cells treated with Ro-3197-90. The video footage was derived from three independent experiments and three separate fields of view were analysed for each experiment. Total 1826 THP-1 ΔM-N L-selectin-GFP/RFP cells, 1368 THP-1 WT L-selectin-GFP/RFP cells and 2515 THP-1 WT L-selectin-GFP/RFP cells pre-treated with Ro-31-9790 were analysed. Data represent mean ± S.E.M. Statistical analysis in A: One-way ANOVA followed by Tukey's post-test. No differences were detected. Statistical analysis in B and C: two-tailed, unpaired Student's t-test for each pair of the time-points.

To more thoroughly analyse the effects of blocking L-selectin shedding on pseudopod dynamics, each cell morphotype – morphotype defined by a number of pseudopods – was analysed separately at both 7 and 15 minutes. The analysis included cells expressing WT, ΔM-N and WT Ro-31-9790 L-selectin and the cumulative data is presented in **figure 6.5**. At 7 minutes, the percentages of WT L-selectin expressing cells having one (**figure 6.5 A**) or two (**figure 6.5 B**) pseudopods were significantly higher than the corresponding percentages of ΔM-N and WT Ro-31-9790 L-selectin expressing cells. As for cells having multiple pseudopods, ΔM-N and WT Ro-31-9790 L-selectin expressing cells had slightly higher percentages than those cells as compared to WT L-selectin-expressing cells, but no statistical significant differences were found (**figure 6.5 C**). At 15 minutes a high percentage of cells with one pseudopod was found amongst WT L-selectin expressing cells, whereas low percentages of such cells were seen for both ΔM-N and WT Ro-31-9790 L-selectin expressing cells (**figure 6.5 D**). When cells with two pseudopods were scored, the highest percentage of such cells was found amongst WT L-selectin expressing cells and lowest amongst ΔM-N L-selectin expressing cells (**figure 6.5 E**). WT Ro-31-9790 L-selectin-expressing cells had more two-pseudopod cells than ΔM-N L-selectin cells but less than WT L-selectin expressing cells (**figure 6.5 E**). At 15 minutes, cells sending multiple pseudopods were most abundant amongst ΔM-N L-selectin expressing cells, and the lowest percentage of such cells was found amongst WT L-selectin-expressing cells (**figure 6.5 F**). THP-1 monocytes expressing WT L-selectin that were pre-treated with Ro-31-9790 had also an increased percentage of cells with multiple pseudopods as compared to non-treated cells, but this number was not as high as that calculated for cells expressing ΔM-N L-selectin (**figure 6.5 F**).

These results show that, over-time, cells expressing WT L-selectin minimise the fraction of cells having multiple pseudopods and maximise the number of cells that have one pseudopod. Conversely, the percentage of cells with multiple pseudopods increased profoundly with time amongst ΔM-N L-selectin expressing cells and WT Ro-31-9790 L-selectin cells. Overall, these data suggest that blocking L-selectin shedding promotes

multiple pseudopod formation during TEM of THP-1 cells. It is possible that shedding of L-selectin is required to retract multiple pseudopods to ultimately consolidate them in to a single (or fewer) pseudopod(s).

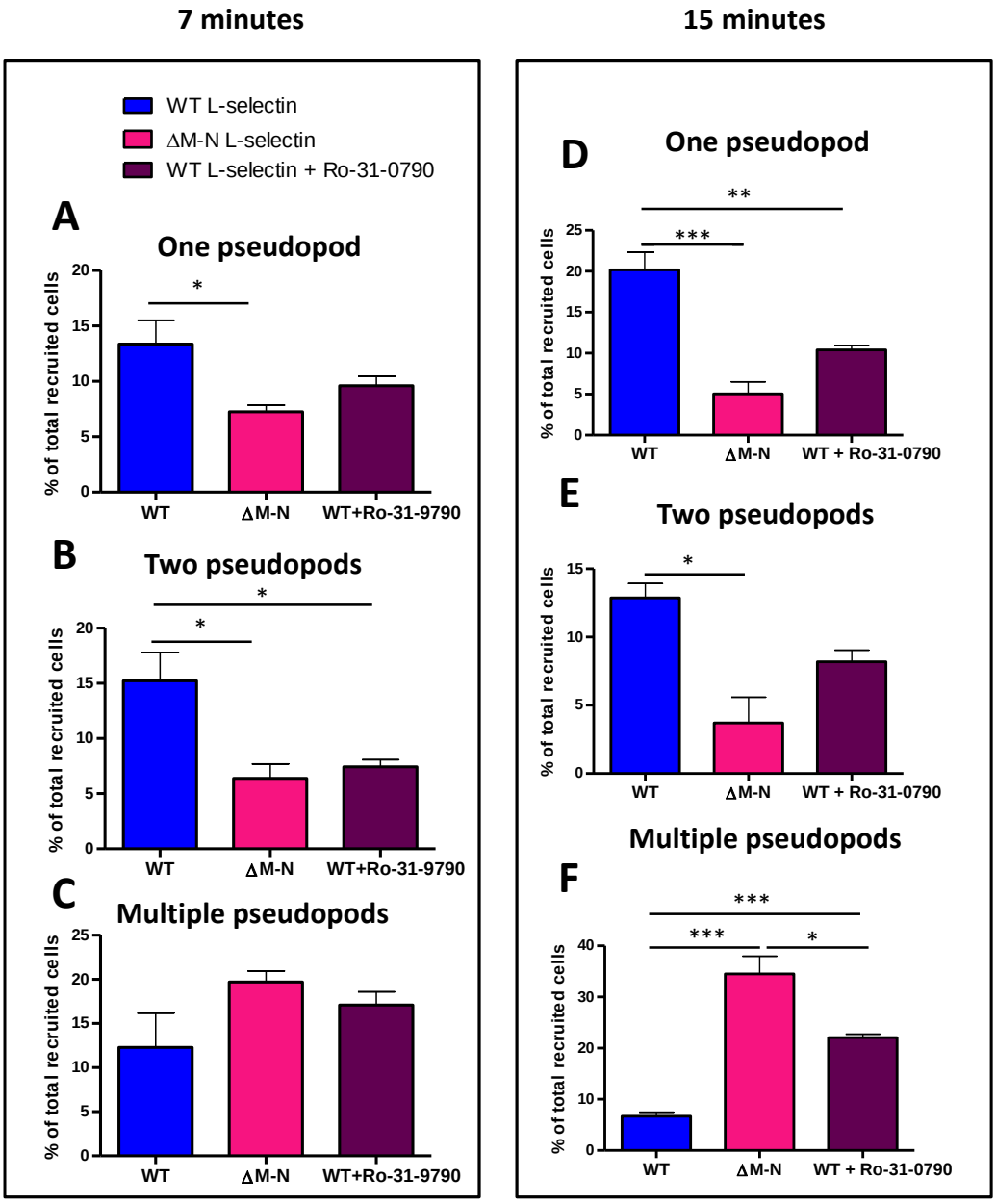

Figure 6.5 Effects of blocking L-selectin shedding on THP-1 monocyte pseudopod behaviour. THP-1 WT L-selectin-GFP/RFP cells pre-treated with (WT + Ro-31-9790) or without Ro-31-9790 metalloprotease inhibitor (WT) or THP-1 ΔM-N L-selectin-GFP/RFP cells were perfused over TNF-α activated HUVEC and video recordings of the microscope images were analysed for pseudopod formation as described in **figure 6.1**. Pseudopod formation at 7 minutes (**A-C**) and 15 minutes (**D-F**) was analysed. Comparison of the number of cells having one pseudopod is shown in **A** and **D**, two pseudopods in **B** and **E**, and multiple pseudopods in **C** and **F**. The video footage was derived from three independent experiments and three separate fields of view were analysed for each experiment. Total 1826 THP-1 ΔM-N L-selectin-GFP/RFP cells, 1368 THP-1 WT L-selectin-GFP/RFP cells and 2515 THP-1 WT L-selectin-GFP/RFP cells pre-

treated with Ro-31-9790 were analysed. Data represent mean ± S.E.M. Statistical analysis: One-way ANOVA followed by Tukey's post-test for each graph. *=p<0.05, **=p<0.01, ***=p<0.001.

6.3.1.4 Monitoring the effect of Ro-31-9790 treatment on pseudopod formation by THP-1 cells expressing GFP alone

THP-1 monocytes expressing ΔM-N L-selectin and WT Ro-31-9790 L-selectin presented with the same pseudopod dynamics. This suggests that WT Ro-31-9790 L-selectin cells formed multiple pseudopods as a result of lack of L-selectin shedding. However, Ro-31-9790 is a broad spectrum metalloprotease inhibitor, and thus it could not be formally excluded that blocking of other molecules present on the surface of THP-1 monocytes contributed to the observed effect. For example, cleavage of integrins is also known to occur during monocyte TEM, which can be blocked by pre-incubation of cells with broad-spectrum metalloprotease inhibitors [669], such as Ro-31-9790. To investigate whether Ro-31-9790 treatment affected pseudopod formation in the absence of L-selectin, THP-1 GFP Hi20 cells were pre-treaded with Ro-31-9790 and subjected to the 15 minute-long parallel plate flow chamber assay. Pseudopods were scored as described above and compared to the corresponding values obtained earlier for THP-1 GFP Hi20 cells. **Figure 6.6** shows that no effect of Ro-31-9790 treatment was found on THP-1 cells that were expressing just GFP protein. Ro-31-9790 treated and non-treated cells had the same number of total protruding cells at 7 minutes (30±2%), and in both cases this number increased with time to 42.5±0.5% (**figure 6.6 A**). Both types of cells presented with the same percentage of cells having one, two or multiple pseudopods at both 7 minutes and at 15 minutes (**figure 6.6 B**). This data shows that formation of multiple pseudopods by THP-1 WT L-selectin-GFP/RFP cells pre-treated with Ro-31-9790 metalloprotease inhibitor is highly likely due to the blockade of L-selectin shedding.

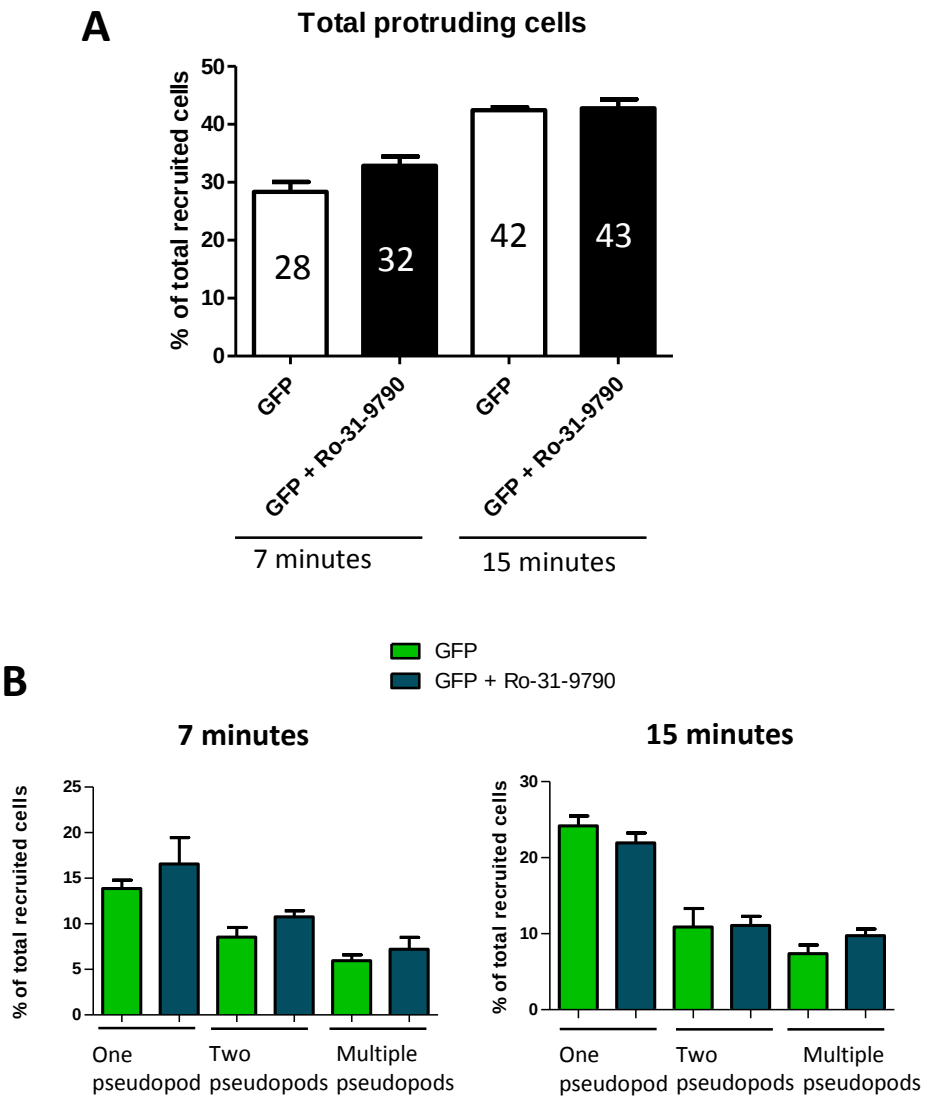

Figure 6.6 Pseudopod formation of THP-1 GFP Hi20 cells pre-treated with Ro-31-9790. Time-lapse movies of Ro-31-9790 treated THP-1 GFP Hi20 cells (GFP + Ro-31-9790) perfused over TNF-α activated HUVEC were analysed for pseudopod formation as described in **figure 6.1**. Obtained percentages were compared to the corresponding ones calculated earlier for THP-1 GFP Hi20 cells that were perfused without inhibitor. **A)** Total number of protruding cells at 7 and 15 minutes. **B)** Percentage of cells with one, two or multiple pseudopods at 7 minutes (left panel) and 15 minutes (right panel). The video footage was derived from three independent experiments and three separate fields of view were analysed for each experiment. Total 672 THP-1 GFP Hi20 and 830 THP-1 GFP Hi20 cells pre-treated with Ro-31-9790 were analysed. Data represent mean ± S.E.M. Statistical analysis: two-tailed, unpaired Student's t-test detected no differences.

6.3.1.5 Effects of ΔM-N SSAA L-selectin expression on THP-1 monocyte pseudopod dynamics

Rendering cytoplasmic serines of ΔM-N L-selectin non-phosphorylatable (ΔM-N SSAA L-selectin), promoted L-selectin clustering in the pseudopods of transmigrating THP-1, which was not seen in the ΔM-N L-selectin cells (**figure 5.8**). Analysis of time-lapse

videos was now performed to investigate whether introducing the SSAA mutation in to ΔM-N L-selectin altered pseudopod dynamics. Interestingly, at 7 minutes, THP-1 monocytes expressing ΔM-N SSAA L-selectin had a similar percentage of total protruding cells to that of cells expressing WT L-selectin (43% and 41%, respectively), which was slightly higher but not statistically significant than that of cells expressing ΔM-N L-selectin (33%) (**figure 6.7 A**). This slight difference was no longer seen at 15 minutes, where all cell lines had 42.5±2.5% of total protruding cells (**figure 6.7 A**). At 7 minutes, amongst the cells expressing ΔM-N SSAA L-selectin, high percentages of cells with one pseudopod (16%) and multiple pseudopods (19%) were seen, and a relatively low number of cells having two pseudopods was present (8%) (**figure 6.7 B**). This did not change much with time, as the calculated percentages were 19%, 10% and 16% for cells having one, two or multiple pseudopods, respectively (**figure 6.7 B**).

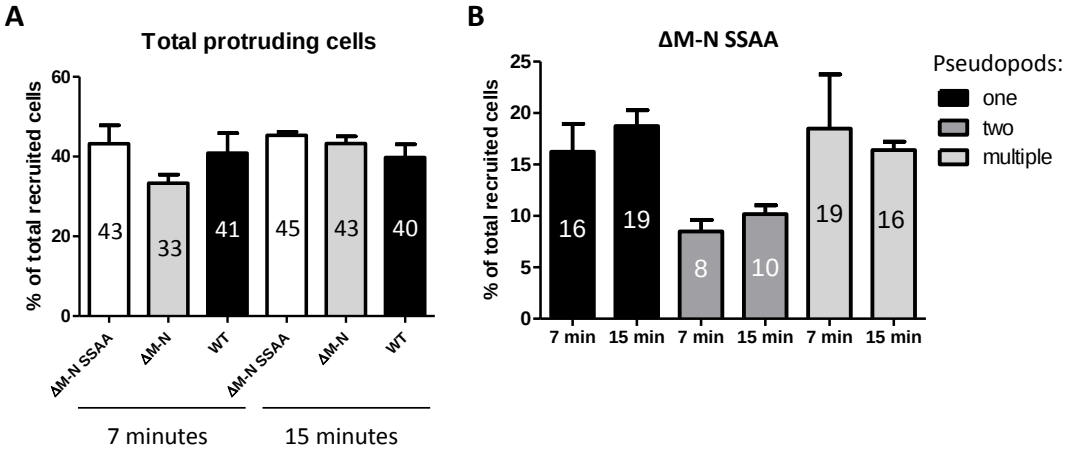

Figure 6.7 Pseudopod formation by THP-1 cells expressing ΔM-N SSAA L-selectin. Time-lapse videos of THP-1 ΔM-N SSAA L-selectin-GFP/RFP cells perfused over TNF-α activated HUVEC were analysed for pseudopod formation as described in **figure 6.1**. **A)** Total number of protruding cells at 7 and 15 minutes. Total numbers of protruding cells expressing WT L-selectin or ΔM-N L-selectin are shown for comparison. **B)** Pseudopod dynamics of THP-1 ΔM-N SSAA L-selectin-GFP/RFP cells. The video footage was derived from three independent experiments and three separate fields of view were analysed for each experiment. Total 1826 THP-1 ΔM-N L-selectin-GFP/RFP cells, 1368 THP-1 WT L-selectin-GFP/RFP cells and 1422 THP-1 ΔM-N SSAA L-selectin-GFP/RFP cells were analysed. Data represent mean ± S.E.M. Statistical analysis in A: One-way ANOVA followed by Tukey's post-test. No differences were detected. Statistical analysis in B and C: two-tailed, unpaired Student's t-test for each pair of time-points. No differences were detected.

Cells expressing ΔM-N SSAA L-selectin had a relatively high percentage of cells with one pseudopod, but also relatively high percentage of cells with multiple pseudopods. This suggested that this cell line had pseudopod dynamics that was intermediate between those displayed by THP-1 WT L-selectin-GFP/RFP (**figure 6.1**) and THP-1 ΔM-N L-selectin-GFP/RFP cells (**figure 6.3**). To verify this hypothesis, the percentage of

cells having one, two or multiple pseudopods were analysed separately at each time-point. Analysis included cells expressing WT L-selectin, and cells expressing ΔM-N L-selectin. At 7 minutes there were more cells with one pseudopod amongst cells expressing ΔM-N SSAA or WT L-selectin as compared to the cells expressing ΔM-N L-selectin (**figure 6.8 A**). Surprisingly, the percentage of cells having two pseudopods was similar between cells expressing ΔM-N SSAA (8%) and ΔM-N L-selectin (6%), and this was lower than the corresponding percentage calculated for cells expressing WT L-selectin (15%) (**figure 6.8 B**). Similar percentage of cells with multiple pseudopods was seen amongst all the cell lines at 7 minutes, however cells expressing "sheddase-resistant" (ΔM-N or ΔM-N SSAA) L-selectin forms had a slightly higher fraction of those cells than cells expressing WT L-selectin (18% for ΔM-N, 16% for ΔM-N SSAA and 13% for WT L-selectin) (**figure 6.8 C**). At 15 minutes, cells expressing ΔM-N SSAA L-selectin or WT L-selectin a had much higher proportion of cells with one pseudopod than the cells expressing ΔM-N L-selectin (**figure 6.8 D**). The same was true when cells having two pseudopods were analysed (**figure 6.8 E**). When cells with multiple pseudopods were scored, the highest percentage of such cells was found amongst ΔM-N expressing cells, and the lowest amongst WT L-selectin expressing cells (**figure 6.8 F**). Percentage of multiple pseudopod-cells amongst cells expressing ΔM-N SSAA L-selectin was higher than those amongst WT L-selectin expressing cells but lower than those amongst ΔM-N L-selectin expressing cells (**figure 6.8 F**). These results suggest that rendering cytoplasmic serines of ΔM-N L-selectin non-phosphorylatable has a profound effect on the number of pseudopods THP-1 cells make during early TEM. The typical multiple pseudopod phenotype caused by ΔM-N L-selectin is no longer seen. THP-1 cells expressing ΔM-N SSAA L-selectin do have higher fraction of cells with multiple pseudopods than the cells expressing WT L-selectin. However, they also have a similar number of cells presenting a single pseudopod as cells expressing WT L-selectin. This suggests that rendering cytoplasmic serines of ΔM-N L-selectin non-phosphorylatable can partially revert the ΔM-N phenotype towards something that resembles a WT phenotype.

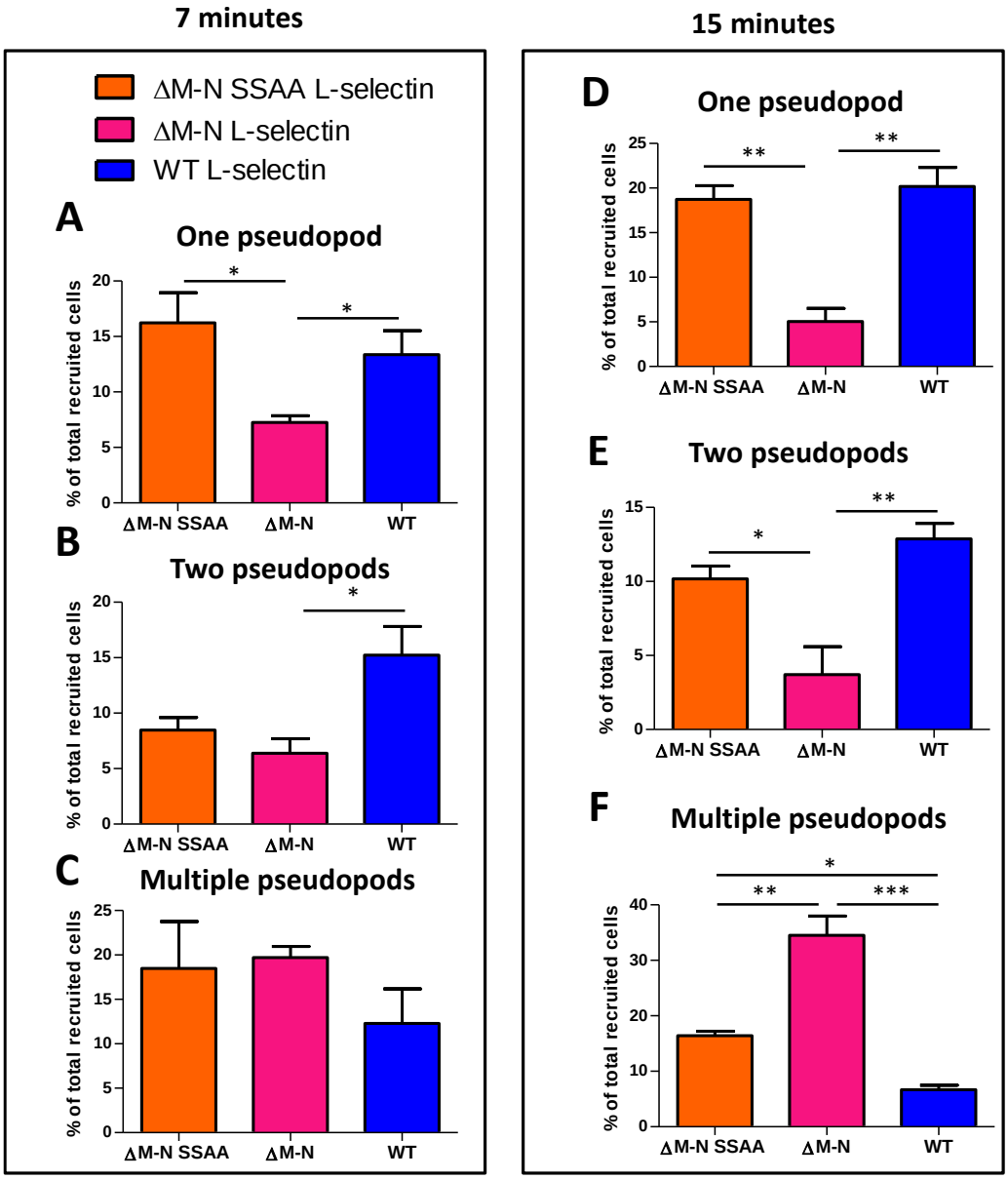

Figure 6.8 Effects of ΔM-N SSAA L-selectin expression on THP-1 monocyte pseudopod dynamics. THP-1 ΔM-N SAA L-selectin-GFP/RFP cells were perfused over TNF-α activated HUVEC and video recordings of the microscope images were analysed for pseudopod formation as described in **figure 6.1**. Calculated values were compared for corresponding ones acquired earlier for cells expressing WT L-selectin and cells expressing ΔM-N L-selectin. Pseudopod formation at 7 minutes (**A-C**) and 15 minutes (**D-F**) is shown. Comparison of number of cells having one pseudopod is shown in **A** and **D**, two pseudopods in **B** and **E**, and multiple pseudopods in **C** and **F**. The video footage was derived from three independent experiments and three separate fields of view were analysed for each experiment. Total 1826 THP-1 ΔM-N L-selectin-GFP/RFP cells, 1368 THP-1 WT L-selectin-GFP/RFP cells and 1422 THP-1 ΔM-N SSAA L-selectin-GFP/RFP cells were analysed. Data represent mean ± S.E.M. Statistical analysis: One-way ANOVA followed by Tukey's post-test for each graph. *=p<0.05, **=p<0.01, ***=p<0.001.

6.3.2 Analysis of cell spreading during THP-1 transmigration across activated HUVEC under conditions of flow

Time-lapse video recordings analysed in **section 6.3.1** for pseudopod formation, were also used to determine the cell spreading area of transmigrating THP-1 monocytes. Still images of 7 minutes and then 15 minutes of perfusion were loaded in to ImageJ software and cell spreading area was measured as described in **section 2.15**. As shown in **figure 6.9 A**, expression of L-selectin did not influence the cell spreading area as compared to overexpression of GFP only. However, cells expressing SSAA L-selectin had a smaller spread area than the cells expressing WT L-selectin, which was consistent at both time-points (**figure 6.9 B**). This suggested that the SSAA mutation limited cell spreading, but whether this was a direct or an indirect effect of L-selectin was not determined. Blocking L-selectin shedding increased THP-1 cell spreading area as compared to WT L-selectin expressing cells (**figure 6.9 C**). A larger spread area was seen in cells expressing ΔM-N L-selectin at both early (7 minutes) and late (15 minutes) time-points, whereas treatment of WT L-selectin expressing cells with Ro-31-9790 resulted in increased cell spreading area only at 15 minutes (**figure 6.9 C**). The increased spread area promoted by Ro-31-9790 treatment appeared to be because of a direct effect on blocking L-selectin shedding, as no effect on cell spreading was seen when THP-1 GFP Hi20 cells were pre-incubated with this inhibitor (**figure 6.9 D**). Interestingly, when serine residues within ΔM-N L-selectin tail were rendered non-phosphorylatable, the cells decreased their spreading area to that seen with WT L-selectin expressing cells (**figure 6.9 E**). These results suggested that blocking L-selectin shedding prompted the cells to increase their spread area, whilst substituting the cytoplasmic serine residues with non-phosphorylatable alanines had an opposite effect. The fact that there is a small spreading area (**figure 6.9 B**) as well as decreased shedding in the SSAA L-selectin expressing cells (**figures 4.3** and **4.4**) suggests that the serine residues might play a dominant role in regulating cell spreading area.

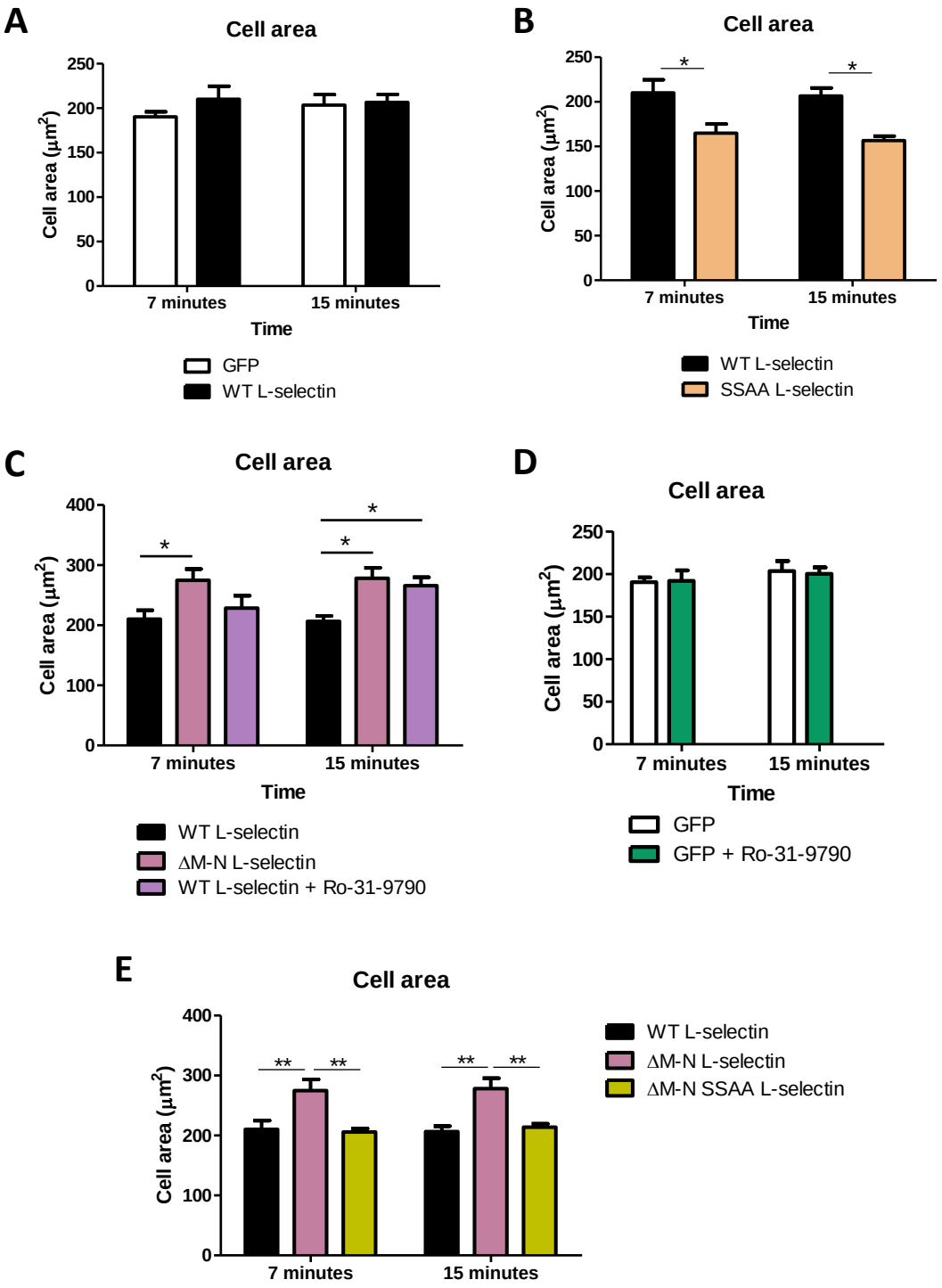

Figure 6.9 Measuring the cell spreading area of THP-1 monocytes at early and late phases of TEM. Cell spreading areas of THP-1 cells perfused over TNF-α activated HUVEC were analysed as described in **section 2.15**. Analysis was performed at early time-point (7 minutes) and late time-point (15 minutes). Following THP-1 cells were analysed: WT L-selectin-GFP/RFP expressors pre-treated with or without Ro-319790 metalloprotease inhibitor; GFP Hi20 expressors pre-treated with or without Ro-319790 metalloprotease inhibitor; SSAA L-selectin-GFP/RFP expressors, ΔM-N L-selectin-GFP/RFP expressors, ΔM-N SSAA L-selectin-GFP/RFP expressors. **A)** Comparison of cell spreading areas between GFP expressors and WT L-selectin expressors. **B)** The influence of SSAA mutation on the cell spreading area of L-selectin expressing cells. **C)** Effect of blocking L-selectin shedding on cell spreading area. Blocking of L-selectin shedding was analysed by using "sheddase resistant" (ΔM-N) L-selectin or by treating

WT L-selectin expressing cells with Ro-31-9790 metalloprotease inhibitor. **D)** The effect of Ro-31-9790 metalloprotease inhibitor on spreading area of GFP expressing cells. **E)** Comparison of cell spreading areas between cells expressing WT, ΔM-N and ΔM-N SSAA L-selectin. At least 270 cells per time-point were analysed for each cell line/condition. Analysed cells were derived from three independent experiments. Data represent mean ± S.E.M. Statistical analysis: Two-way ANOVA followed by Bonferroni post-test. *=p<0.05, **=p<0.01.

6.3.3 THP-1 monocytes expressing GFP, WT L-selectin-GFP or ΔM-N L-selectin-GFP have comparable levels of RhoGTPase activity when in suspension culture

The canonical Rho family of small GTPases; RhoA, Rac1 and Cdc42 play a critical role in driving leukocyte polarity and motility during various stages of the leukocyte adhesion cascade (**section 1.5**) [118, 234, 237, 238, 240, 241]. The results presented in the sections above show that during early phases of TEM, THP-1 monocytes expressing WT L-selectin and those expressing ΔM-N L-selectin present with strikingly different phenotypes. Whilst cells expressing WT L-selectin tend to polarise with time, as seen by majority of cells projecting one or two pseudopods at 15 minutes, ΔM-N L-selectin expressing cells project multiple pseudopods that do not retract with time (**figures 6.2** and **6.4** and **6.5**). The difference between the two cell lines is further demonstrated by an enlarged spread area promoted by ΔM-N L-selectin (**figure 6.9 C**). These results would strongly suggest that the activity of RhoGTPases – the main drivers of cell shape change – could be different between the two cell lines. It was possible that expression of ΔM-N L-selectin altered the basal activity of Rho GTPases, which could explain, in part, the pseudopod retraction defect. To test this hypothesis the activity of RhoA, Rac1 and Cdc42 was monitored in resting THP-1 WT L-selectin-GFP Hi20 and THP-1 ΔM-N L-selectin Lo5 cells using classic pull-down assays. It is noteworthy to mention that all cell lines had matched L-selectin expression levels (**figure 4.10**). To control for the L-selectin-expressing cell lines, RhoA, Rac1 and Cdc42 activity was monitored in THP-1 GFP Hi20 cells. This was particularly important as analysis of pseudopod dynamics during parallel plate flow chamber assays showed that cells expressing WT L-selectin were more “invasive” than cells expressing GFP protein during the first half of the assay (7 minutes) (**figure 6.1**). To analyse the activity of RhoGTPases in resting THP-1 cells, glutathione-S-transferase (GST)-fusion GTPase bait proteins were conjugated to glutathione sepharose beads, and beads were used in pull-down assays. The bait proteins used were of Rho GTPase effector domains and were kindly provided by John G. Collard (Netherlands Cancer Institute, Amsterdam, the Netherlands). The following bait proteins were used: for RhoA – the Rho-binding domain of Rhotekin (Rhotekin-C21), for Rac1 – p21-binding domain of PAK (PAK-PBD) and for Cdc42 – the Cdc42/Rac interacting domain (cassette) of the Wiskott-Aldrich syndrome protein (WASP-CRIB-C).

The detailed methods of GST-fusion proteins purification and Rho GTPase activation assays are described in **sections 2.9** and **2.10** of this thesis. As shown in **figure 6.10**, no differences in RhoGTPase activity were found between the tested cell lines. This suggested that changes seen in THP-1 monocyte morphology during TEM were not pre-disposed by altered basal Rho GTPase activity. It was hypothesised that Rho GTPases in GFP, WT L-selectin or ΔM-N L-selectin expressing cells could become regulated differently upon monocyte activation during parallel plate flow chamber assays.

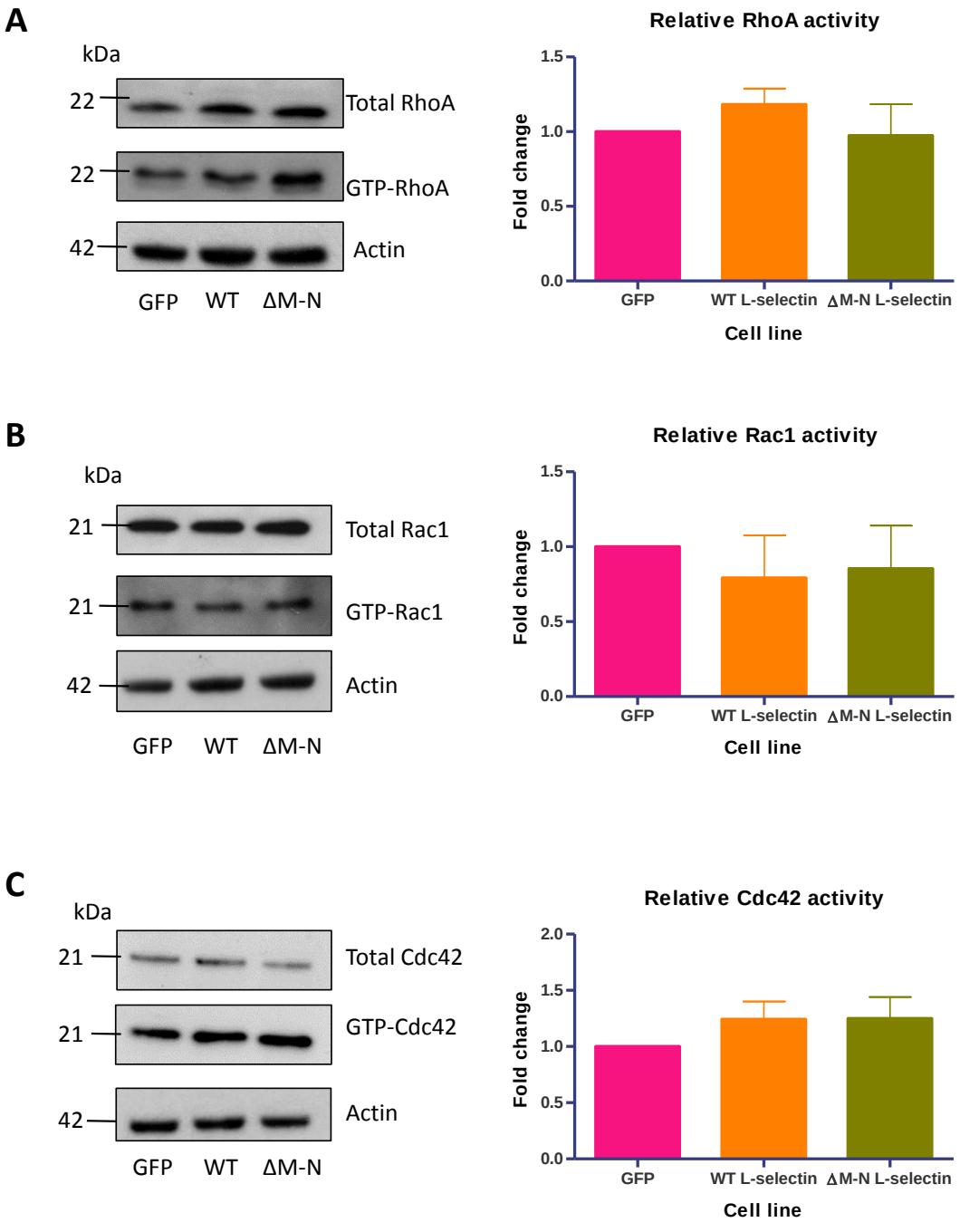

Figure 6.10 Monitoring Rho GTPase activity in THP-1 cells expressing GFP, WT L-selectin-GFP or ΔM-N L-selectin-GFP. Activity of RhoA, Rac1 and Cdc42 in the cells expressing GFP,

WT L-selectin-GFP or ΔM-N L-selectin-GFP was assessed by the pull down assays using the Rhotekin-C21 binding domain for RhoA, the PAK-PBD binding domain for Rac1 or the WASP-CRIB-C binding domain for Cdc42. The method is described in detail in **section 2.10**. Representative Western blots of RhoA (**A**), Rac1 (**B**) and Cdc42 (**C**) are shown. In each panel, the diagrams on the right illustrate the corresponding densitometric analysis of the relative activities of RhoA, Rac1, and Cdc42. This is shown as a ratio of GTP-bound GTPase (active) to total Rho GTPase protein. Total RhoGTPase levels were normalised against actin. Densitometric analysis was performed on Western blottings from three independent experiments. Data represent mean ± standard error. One-way ANOVA did not detect any differences in Rho GTPAse activity between the cell lines.

6.3.4 Generation of THP-1 cell lines expressing Rho GTPase biosensors

The Rho GTPase biosensors (**figure 6.1**) are used to monitor the spatio-temporal activity of Rho GTPases in living cells (**section 6.2**). It was hoped that utilizing such biosensors would allow insights in to Rho GTPase activity in THP-1 monocytes undergoing TEM. Lentiviral vectors (pLenti CMV Puro DEST (w118-1)) carrying CFP/YFP-based RhoA, Rac1 and Cdc42 biosensor constructs were kindly provided by Oliver Pertz (Universty of Basel, Switzerland). The vectors were used to produce lentiviral particles as described in **section 2.11**. The titres of generated lentiviruses are presented in **table 2.5** of this thesis. Moderate MOI of 7 was used to transduce THP-1 cells with lentiviruses carrying RhoA, Rac1 or Cdc42 biosensors, yielding polyclonal cell lines, named THP-1 RhoA, THP-1 Rac1 or THP-1 Cdc42, respectively. These cell lines were left in culture or were further used for transduction with lentiviruses carrying WT L-selectin-RFP or ΔM-N L-selectin-RFP described in **sections 5.3.1** and **5.3.4**, respectively. MOI of 20 was used for lentiviruses carrying WT L-selectin-RFP and MOI of 5 for lentiviruses carrying ΔM-N L-selectin-RFP. These MOIs were previously found to produce matching L-selectin levels between the two cell lines (**section 4.10**). The method of THP-1 cell transduction is described in **section 2.11.4**. In total, nine polyclonal cell lines were generated. The cell lines are outlined in **table 6.1**.

CFP/YFP Rho GTPase biosensor	L-selectin-RFP	Cell line name
RhoA	-	THP-1 RhoA
RhoA	WT	THP-1 WT L-selectin-RFP RhoA
RhoA	ΔM-N	THP-1 ΔM-N L-selectin-RFP RhoA
Rac1	-	THP-1 Rac1
Rac1	WT	THP-1 WT L-selectin-RFP Rac1
Rac1	ΔM-N	THP-1 ΔM-N L-selectin-RFP Rac1
Cdc42	-	THP-1 Cdc42
Cdc42	WT	THP-1 WT L-selectin-RFP Cdc42

Cdc42	ΔM-N	THP-1 ΔM-N L-selectin-RFP Cdc42

Table 6.1 Polyclonal THP-1 cell lines expressing Rho GTPase Raichu probes. THP-1 cells were transduced with lentiviruses carrying RhoA, Rac1 or Cdc42 CFP/YFP biosensors. Those cell lines were further infected with lentiviruses carrying WT L-selectin-RFP or ΔM-N L-selectin-RFP. Overall, nine different cell lines were generated and are displayed in this table.

Once generated, the cell lines were analysed by fluorescence microscopy for YFP and RFP expression that were indicative of Rho GTPase biosensor and L-selectin expression, respectively. All cell lines showed uniform YFP distribution and peripheral RFP localisation. This suggested the transgenes were expressed correctly as Rho GTPases display general diffuse distribution pattern [716], and L-selectin localises to the plasma membrane. Varied expression levels of L-selectin and Rho GTPase biosensors were readily observed, which was expected for a polyclonal stable cell lines. Representative images of THP-1 WT L-selectin-RFP RhoA cells are shown in **figure 6.11 A**. Unfortunately, preliminary parallel-plate flow chamber experiments showed that none of the nine cell lines had undergone TEM across activated HUVEC during the 15 minute period of parallel plate flow chamber assay (data not shown). In other words, the adhered cells did not extend pseudopods that were seen to protrude underneath the HUVEC. Occasionally, very small pseudopods were formed, that were extending on top of the endothelium (as seen by phase-bright appearance). Lentiviruses carrying pHR´SIN-SEW-GFP/RFP constructs had been used successfully to deliver transgenes throughout this thesis. It was hence hypothesised that it was the pLenti CMV Puro DEST (w118-1) construct that had adverse effects, seen as loss of THP-1 transmigratory capacity. Alternatively, it was possible that simultaneous expression of the Rho GTPase biosensors and the RFP-tagged L-selectin resulted in an overall negative effect on THP-1 cell behaviour. It is possible that expression of three fluorescent proteins (CFP, YFP and RFP) at once was stressful to THP-1 cell function. An attempt was made to select for low Rho GTPase biosensor expressors amongst the cell lines, in the hope that the low expressors would not be affected by such adverse effects. All nine cell lines were subjected to FACS sorting in order to eliminate cells with high Rho GTPase biosensor expression. On this occasion, L-selectin expression between cells expressing WT L-selectin-RFP and cells expressing ΔM-N L-selectin-RFP was monitored to ensure continued matched expression. Untransduced THP-1 cells and cells expressing L-selectin-RFP were used as control populations on which both the YFP and RFP gates were set. Representative histograms in figure **6.11 B** show THP-1 RhoA cell line pre- and post-sorting. The same levels of Rho GTPase biosensor expression was achieved in the remaining eight cell lines.

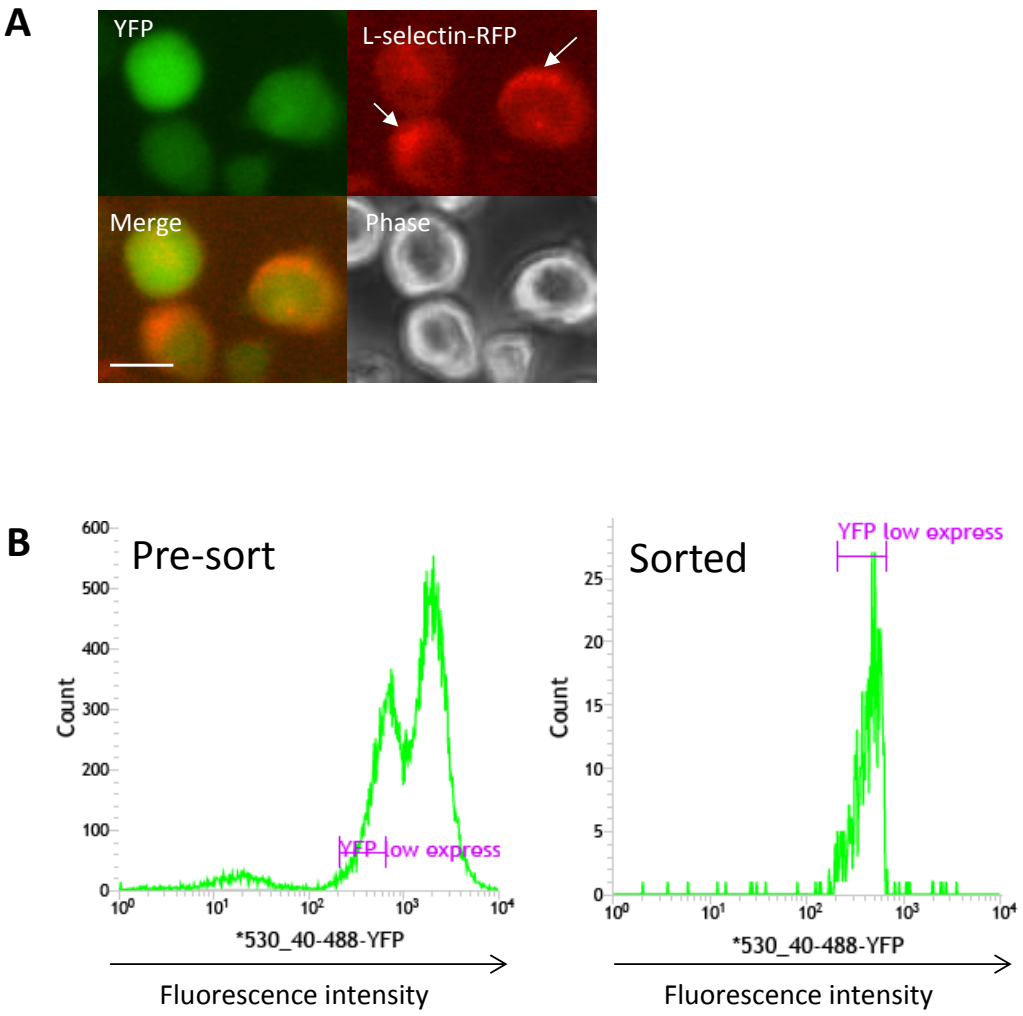

Figure 6.11 Expression of Rho GTPase biosensors and L-selectin-RFP in THP-1 monocytes. A) Representative images of THP-1 L-selectin-RFP RhoA cells. YFP image shows diffuse distribution of RhoA biosensor. The RFP channel shows L-selectin-RFP that localises to the plasma membrane (arrows). Scale bar: 10 µm. **B)** Flow cytometry profiles of unsorted (left histogram) and sorted low RhoA biosensor expressors (right histogram) THP-1 RhoA cells. Similar histograms exist for THP-1 Rac1, Cdc42, WT L-selectin-RFP RhoA, WT L-selectin-RFP Rac1, WT L-selectin-RFP Cdc42, ΔM-N L-selectin-RFP RhoA, ΔM-N L-selectin-RFP Rac1 and ΔM-N L-selectin-RFP Cdc42 cells.

Sorted cell lines were subjected to the parallel plate flow chamber assays in the hope that the reduced Rho GTPase expression would allow the THP-1 monocytes to form pseudopods. Unfortunately, no transmigrating cells were seen after 15 minutes of flow in any of the nine sorted cell lines. It was postulated that the cells might be delayed in their transmigration ability and so the experiments were repeated where flow was applied for 30 minutes. As shown on the representative still images of sorted THP-1 RhoA, THP-1 WT L-selectin-RFP RhoA or THP-1 ΔM-N L-selectin-RFP RhoA cells, no cells were seen undergoing TEM after 30 minutes of flow (**figure 6.12 A**-**C**). Again small protrusions were sometimes generated, but none of them were transmigrating (**figure 6.12 C** red

stars). **Figure 6.12 D** shows typical appearance of transmigrating THP-1 cells, where large pseudopods can be seen for comparison. This was also true for sorted cell lines expressing Rac1 or Cdc42 biosensors. These results show that, unfortunately, the stable cell lines were not suitable for investigating of RhoGTPase activity in THP-1 cells undergoing TEM.

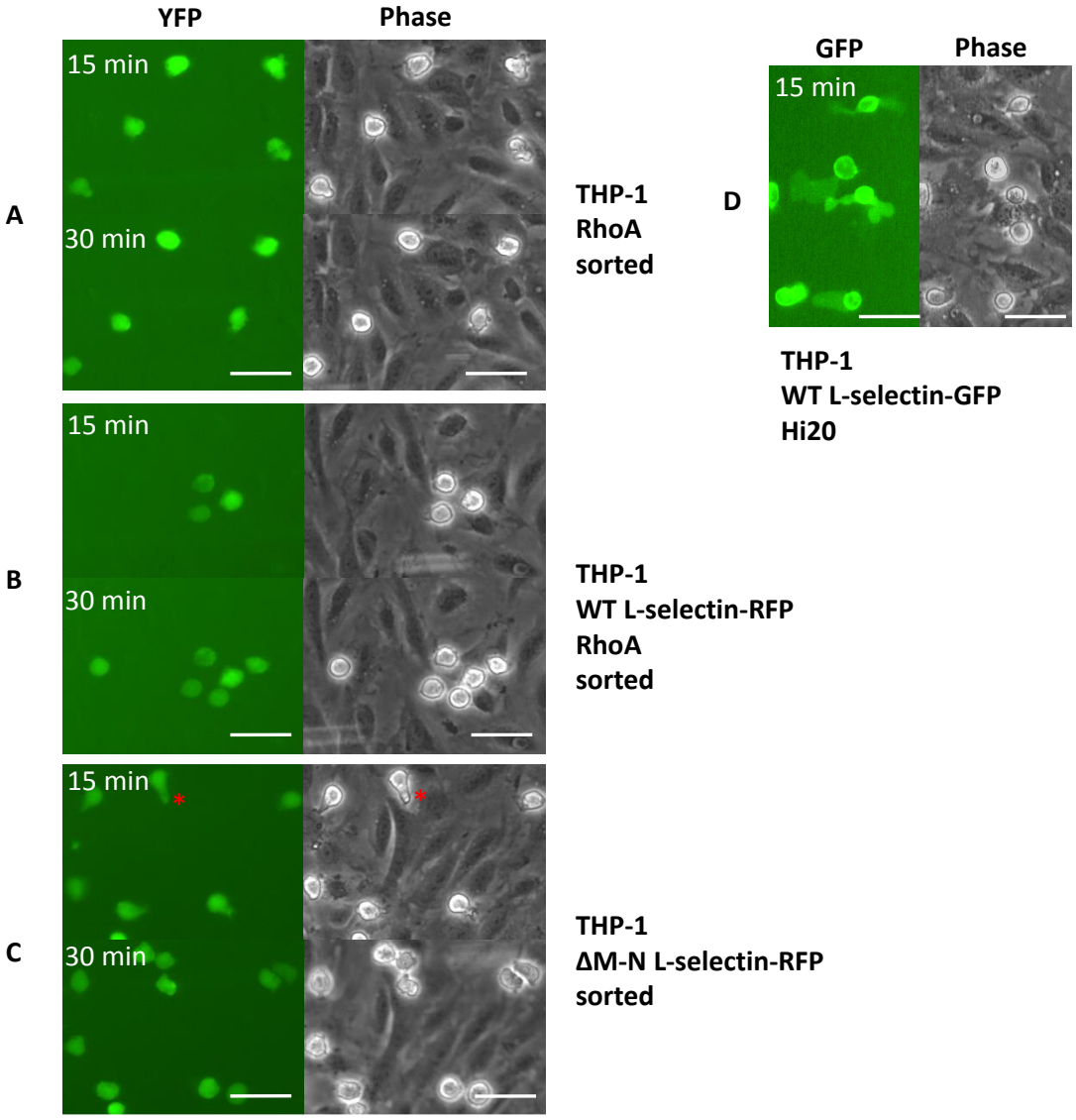

Figure 6.12 Transmigration defect in THP-1 cells expressing RhoGTPase biosensors. Sorted populations of THP-1 RhoA (**A**) THP-1 WT L-selectin-RFP Rho A (**B**) or THP-1 ΔM-N L-selectin-RFP RhoA (**C**) cells were perfused over TNF-α activated HUVEC for 30 minutes. Time-lapse footage of the YFP channel and phase contrast was used to generate still images corresponding to 15 and 30 minutes of flow. All the cells bound to the endothelial monolayer but no protruding pseudopods were formed. Very small pseudopods could be seen forming, but none were actually protruding beneath the endothelial monolayer (red stars). Corresponding footage exists for the sorted cell lines expressing Rac1 or Cdc42 biosensors, where also no transmigrating cells can be seen. **D)** Transmigrating THP-1 WT L-selectin-GFP Hi20 cells are shown for comparison. Prominent pseudopods can be seen extending from the cell bodies. Scale bar: 30μm.

6.3.5 Monitoring Rho GTPase activity in THP-1 cells following antibody-mediated cross-linking of L-selectin

As described above, the THP-1 cell lines could not be used to monitor the spatio-temporal distribution of Rho GTPase activity as the cells failed to undergo TEM. As a final attempt, the Rho GTPase activity in cells expressing WT and ΔM-N L-selectin could be monitored following cross-linking of L-selectin with monoclonal antibody. If signalling downstream of the L-selectin tail regulates Rho GTPases differently between WT and ΔM-N L-selectin, this was likely to be seen upon cross-linking. Previous FRET/FLIM experiments have clearly shown that L-selectin is monomeric in the plasma membrane and can be clustered following cross-linking with the DREG56 monoclonal antibody (**figure 5.13**).L-selectin null cells were left untreated (incubation with media alone) and L-selectin on THP-1 cells expressing WT or ΔM-N L-selectin-RFP and RhoA, Rac1 or Cdc42 biosensors were labelled with DREG56 antibody and then cross-linked with secondary antibody. Alternatively the cells were incubated with just media. The cells were subsequently plated on to poly-L-lysine (PLL) coated coverslips, fixed and prepared for FRET/FLIM analysis. A detailed description of the assay can be found in **section 2.19** of this thesis. The basal levels of RhoA activity (no antibodies used) seemed comparable between the cells, although cells expressing WT L-selectin had slightly more active RhoA than the other two cell lines (**figure 6.13 A** *Upper panel* and **B**). Interestingly, a decrease in RhoA biosensor FRET efficiency could be seen following WT but not ΔM-N L-selectin cross-linking (**figure 6.13 B**). The basal activity of Rac1 appeared lowest in THP-1 cells lacking L-selectin, moderate in THP-1 cells expressing WT L-selectin and highest in cells expressing ΔM-N L-selectin (**figure 6.13 A** *Middle panel* and **B**). The same pattern was seen in basal Cdc42 activity (**figure 6.13 A** *Lower panel* and **B**). Notably, whilst L-selectin cross-linking did not alter Cdc42 activity, decreased Rac1 biosensor FRET efficiency was seen upon clustering of ΔM-N but not WT L-selectin (**figure 6.13 B**). Due to the time constraints of this PhD project, the experiment was performed only once. This however can serve as a foundation for future investigations of the RhoGTPase activity in L-selectin expressing cells in our laboratory. At this point however, it has to be appreciated that the Rho GTPase biosensor expressing cell lines used in this study were shown to fail to extend pseudopods underneath the HUVEC under flow (**figure 6.12**). To what extent the cells were compromised is unknown, and hence the relevance of the results obtained in the cross-linking experiments is questionable. It is interesting though that previous work in the Ivetic laboratory showed that cross-linking of WT L-selectin on 300.19 pre-B cells had no effect on Rac1 activity, but led to the downregulation of RhoA activity, as measured by active RhoA pull-down assays (Marouan Zarrouk, unpublished data). This would suggest that the decreased FRET of RhoA biosensor and no change

in FRET of Rac1 biosensor seen upon WT L-selectin cross-linking could be a meaningful result, as the Rho GTPase activation pattern followed that seen previously in the pull-down assays. Perhaps, despite their transmigration defect, the generated cell lines are still suitable for monitoring of Rho GTPase activity in simple antibody-mediated cross-linking assays.

.

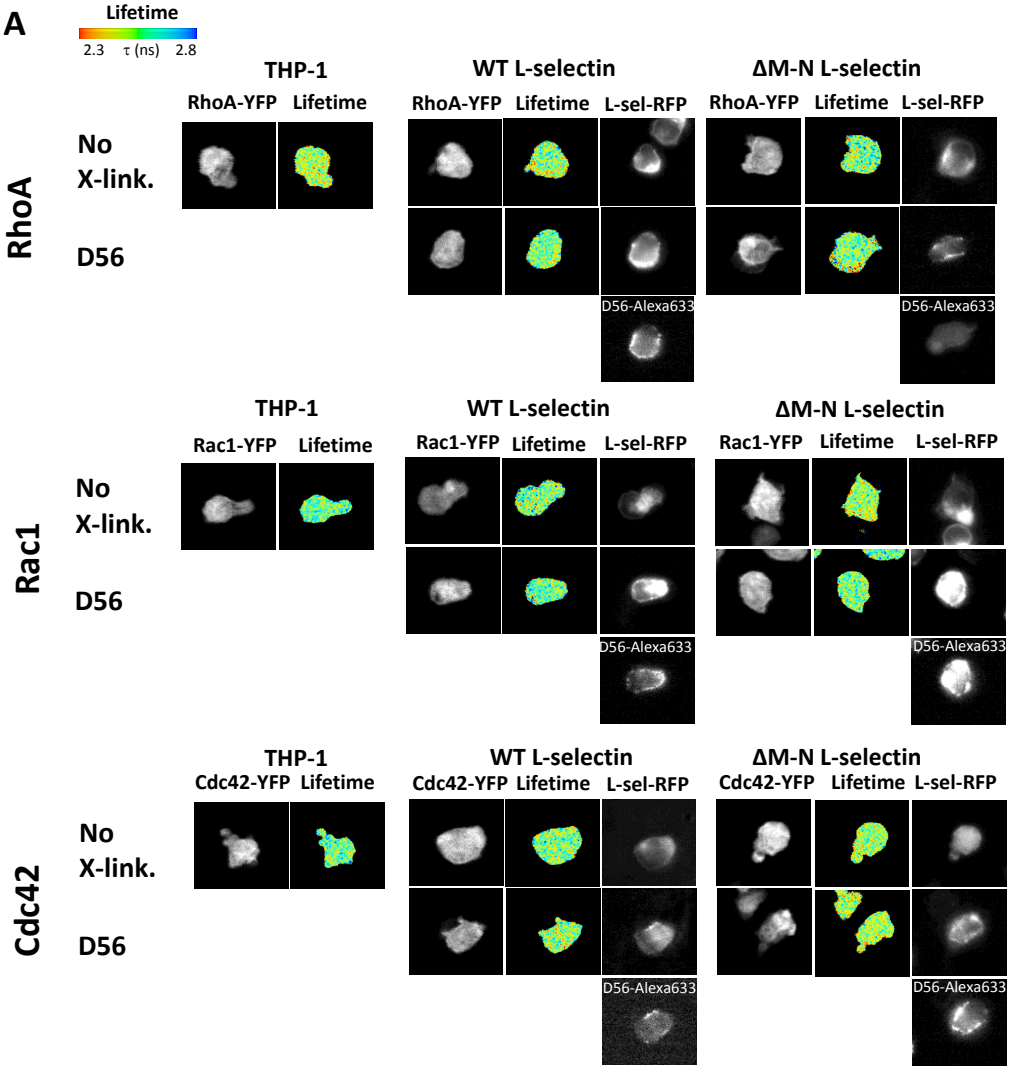
A
Lifetime
2.3 τ (ns) 2.8
THP-1
WT L-selectin
ΔM-N L-selectin
RhoA-YFP Lifetime
RhoA-YFP Lifetime L-sel-RFP
RhoA-YFP Lifetime L-sel-RFP
RhoA
No X-link.
D56
D56-Alexa633
Rac1-YFP Lifetime
Rac1-YFP Lifetime L-sel-RFP
Rac1-YFP Lifetime L-sel-RFP
Rac1
Cdc42-YFP Lifetime
Cdc42-YFP Lifetime L-sel-RFP
Cdc42-YFP Lifetime L-sel-RFP
Cdc42

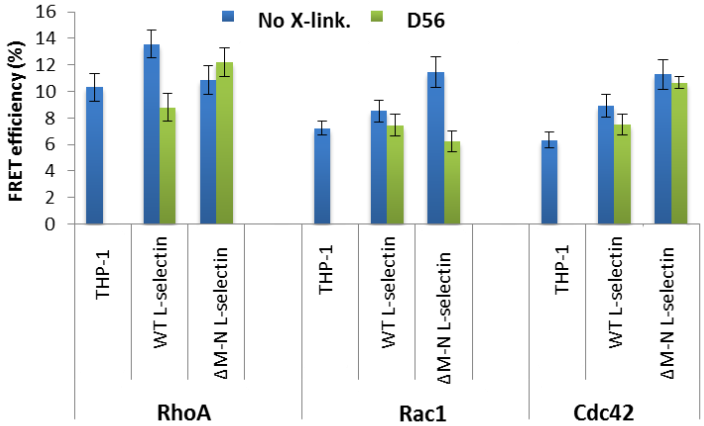
B
FRET efficiency (%)
No X-link.
D56
THP-1
WT L-selectin
ΔM-N L-selectin
RhoA
Rac1
Cdc42

Figure 6.13 L-selectin-dependent signalling to Rho GTPases in THP-1 cells. THP-1 cells expressing WT or ΔM-N L-selectin-RFP and/or RhoA, Rac1 or Cdc42 biosensors were labelled with DREG56 antibody (D56) and cross-liked with secondary antibody. Alternatively, the cells were incubated with just media (No. X-link.). For assay details see **section 2.19**. Cells were plated on PLL for 5 minutes before fixation and then prepared for FLIM/FRET analysis as described in **section 2.18.1**. **A**) The panels show YFP images corresponding to the Rho GTPase biosensors (left columns), multiphoton FLIM images of the FRET between CFP and YFP in the Rho GTPase biosensor (middle columns) and RFP images corresponding to L-selectin (right columns). Additionally Alexa633 images of DREG56 antibody staining are shown where relevant. Pseudo-colour scale of blue (high lifetime,) to red (low lifetime,) is used to show lifetime fluorescence. High lifetime indicates no FRET and non-active Rho GTPase biosensors. Low lifetime indicates FRET and the active biosensors. *Upper panel*: Activity of RhoA, *Middle panel*: activity of Rac1, *Lower panel*: activity of Cdc42. **B)** Quantified data showing FRET efficiency between CFP and YFP. Average 5 cells were analysed for each condition and the cells were derived from one experiment only.

6.3.6 Analysis of THP-1 cell chemotaxis

L-selectin null leukocytes as well as leukocytes expressing "sheddase-resistant" L-selectin have been shown to have impaired chemotaxis *in vivo* [398, 419]. The data presented in **section 6.3.1** of this chapter show that, during TEM, cells expressing WT L-selectin promote a reduction in pseudopods over-time, whereas cells expressing ΔM-N L-selectin seemed to sustain a multi-pseudopod phenotype (**figures 6.2**, **6.4** and **6.5**). It was hence hypothesised that this multi-pseudopod phenotype could result in defective chemotaxis. To investigate chemotaxis of L-selectin expressing cells versus L-selectin null cells, untransduced THP-1 cells and THP-1 GFP Hi20 cells were chosen. By comparing GFP-expressing cells and untransduced cells, one could assess the effect of lentiviral transduction and ectopic protein expression on THP-1 cell directed migration. Transwell assays are used commonly for studying chemotaxis. Transwell chambers are composed of upper and lower compartments that are separated by a porous filter. Chemoattractant is added to a lower compartment and the cells are placed in the upper compartment, from where they migrate towards the chemotactic source. Monocyte chemoattractant protein-1 (MCP-1) is a potent chemotaxis mediator of mononuclear cells, capable of causing migration of THP-1 cells in transwell assays [717, 718]. MCP-1 binds to the C-C chemokine receptor type 2 (CCR2) on the surface of the leukocytes. Before transwell assays were perforemed, it was first analysed whether ectopic expression of WT or ΔM-N L-selectin had any effects on CCR2 receptor levels. As shown in figure **6.14**, no such effects were found as all cells had the same levels of CCR2 expression.

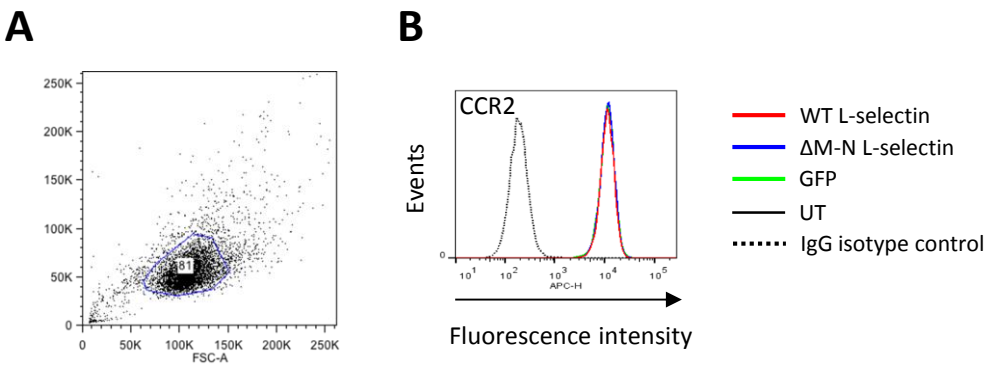

Figure 6.14 CCR2 expression on THP-1 cells. Expression of CCR2 on untransduced THP-1 cells (UT), THP-1 GFP Hi20 (GFP), THP-1 WT L-selectin-GFP Hi20 (WT L-selectin) and THP-1 ΔM-N L-selectin Lo5 (ΔM-N L-selectin) cells was monitored by flow cytometry as described in **section 2.13**. Representative histograms are shown. **A)** Dot plot showing the population of single and viable cells that were analysed (gate is shown with the blue line). **B)** Histogram showing CCR2 expression on tested THP-1 cells.

Before transmigration of the cells towards the MCP-1 could be assessed, a technique called "checkboard analysis" was used to prove that cell migration is a result of chemotaxis and not chemokinesis. Unlike directional chemotaxis, chemokinesis is a random, non-directional movement of cells that results from the presence of a stimulant in the surrounding environment. Checkboard analysis was performed by adding MCP-1 (50 ng/mL) to either the bottom compartment, or to both the top and the bottom compartments. The first creates a gradient of MCP-1, whereas the second generates uniform MCP-1 distribution and hence tests for chemokinesis. For a detailed description of the transwell assays see **section 2.20**. Checkerboard analysis revealed that THP-1 cell migration depended on the presence of a MCP-1 gradient across the filter, suggesting MCP-1 induced chemotaxis and not chemokinesis (**figure 6.15 A**). However, no differences in the transmigration across the filter was seen between the tested cell lines (**figure 6.15 A**). This suggested that transduction of THP-1 cells with lentiviral particles does not influence directed cell migration of those cells. This has also suggested that overexpression of L-selectin does not influence THP-1 chemotaxis across the filter up the MCP-1 gradient. Furthermore, shedding of L-selectin did not play a role in this process either as the same percentage of cells expressing ΔM-N L-selectin and cells expressing WT L-selectin had transmigrated. This was rather surprising as impaired polarisation of ΔM-N L-selectin expressing cells during TEM (**section 6.3.1.3**) implied that chemotaxis of those cells could be affected. However, a single time point was analysed in these studies and it cannot be excluded that any differences in transmigration could have been overlooked. Preliminary experiments where 100 or 200 ng/mL MCP-1 were used resulted in similar percentages of transmigrated THP-1 cells

(data not shown) suggesting that no differences in chemotaxis were likely to occur using a higher MCP-1 concentration. However, it could be argued that migration across the "naked" filter of the transwell chamber was not representative of transmigration of leukocytes crossing an activated endothelial monolayer. The work outlined in this thesis so far would postulated that it is the interaction of the THP-1 monocytes with the activated HUVECs that triggered L-selectin-dependent pseudopod formation. If this was the case, differences in chemotaxis across the activated HUVEC monolayer could be seen between WT and ΔM-N L-selectin expressing cells. To test this hypothesis confluent HUVEC monolayers were grown on top of the fibronectin-coated transwell filters and were activated with TNF-α. Transmigration of untransduced THP-1 cells and cells expressing GFP, WT L-selectin-GFP or ΔM-N L-selectin-GFP was analysed. As shown in figure **6.15 B**, again no differences in the number of transmigrated cells were seen. This was unexpected but a possible explanation of this result could be proposed. First of all, it was possible that differences could be seen at other time-points that were not tested in this study. Secondly, following the rationale that transmigration across the naked filter does not resemble TEM across HUVEC, emigrated leukocytes in the lower compartment of the transwell assay would not be representative of leukocytes emigrating into the interstitial space *in vivo*. In the transwell chamber, transmigrated leukocytes simply "free fall" in the medium of the lower compartment, whereas *in vivo* they found themselves in the thick 3D ECM matrix, which they have to move through to reach the chemoattractant source. Therefore, polarity would not play any role in case of the cells that had transmigrated into the media, but would be crucial for the cells that emigrated into the thick and complex ECM. It is therefore possible that differences could be seen in the directed cell migration of GFP, WT and ΔM-N L-selectin expressing cells under different experimental conditions. Generation of collagen/matrigel composites is currently being optimised in the Ivetic laboratory. Those composites mimic ECM environment and could be used to develop more suited chemotaxis assays. For example, an interesting assay for studying THP-1 directed cell migration was reported by Cain et al. (2010) [719]. In brief, collagen gels were polymerized in transwell filters and HUVEC were grown on top of the gels. MCP-1 was added to the lower compartment and THP-1 cells were added on top of the activated HUVEC monolayer [719]. After indicated amounts of time the samples were fixed and processed by confocal microscopy [719]. Acquired z-stacks showed leukocytes migrating in the thick collagen block before reaching the pores of the filter and the lower transwell compartment [719].

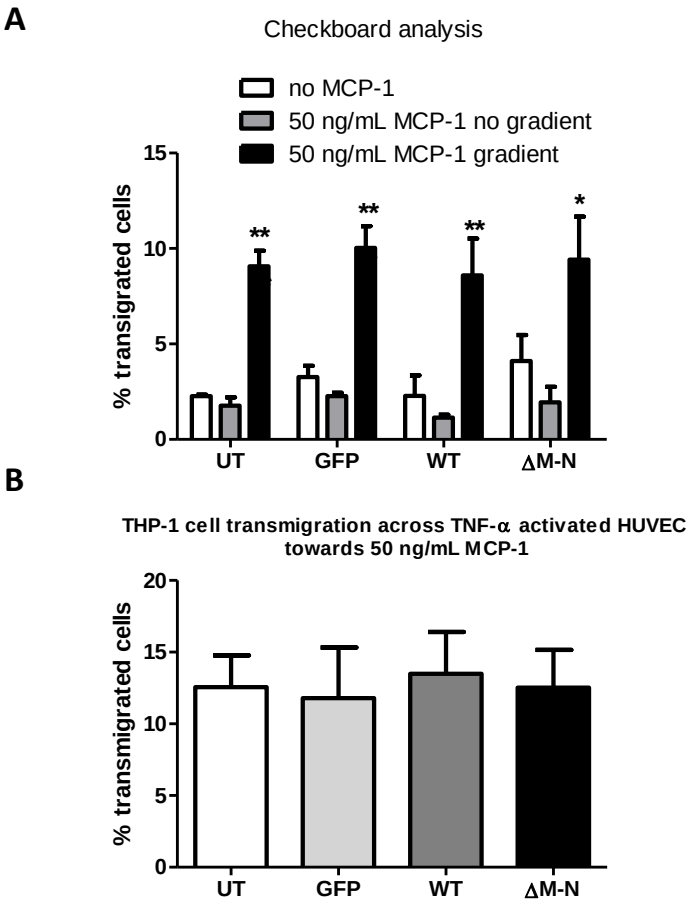

Figure 6.15 Chemotaxis of THP-1 cells towards MCP-1. Untransduced THP-1 cells (UT) and cells expressing GFP (GFP), WT L-selectin-GFP (WT) or ΔM-N L-selectin-GFP (ΔM-N) were subjected to the transwell assays. All cells were added to the upper compartment. At the end of the assay (2 hours and 15 minutes), the transmigrated cells in the bottom compartment were collected and the percentage of transmigrated cells was calculated against the input number as described in **section 2.20**. **A)** Checkboard analysis of THP-1 migration. No MCP-1 was added to neither of the compartments in the control experiments (no MCP-1). For analysis of chemokinesis MCP-1 (50 ng/mL) was added to both upper and lower compartments (no gradient). For chemotaxis analysis MCP-1 was added to the bottom compartment only (gradient). **B)** Chemotaxis of THP-1 cells across TNF-α activated HUVEC monolayer and towards 50 ng/mL MCP-1. Experiments were repeated in triplicates on three independent occasions. Data represent mean ± S.E.M. Statistical analysis in A: One-way ANOVA followed by Dunnett's post-test against "No MCP-1" for each cell line and One-way ANOVA followed by Tukey's post-test for "MCP-1 gradient" across all cell lines (no difference detected) *=p<0.05, **=p<0.01. Statistical analysis in B: One-way ANOVA followed by Tukey's post-test (no differences detected).

A possibility also existed that effect of MCP-1 could override any effects seen by L-selectin. In other words that changes in polarity seen between WT and ΔM-N L-selectin expressing cells were overridden by the MCP-1 induced chemotaxis. It was possible that differences between WT and ΔM-N L-selectin expressing cells could be seen when other chemoattractants were used. The *in vivo* research that identified that L-selectin

expression as well as its shedding is important for leukocyte directed migration utilised murine keratinocyte chemoattractant (KC) chemokine [398, 419]. Thus, it was possible that chemotaxis towards KC could reveal differences in migration of GFP, WT L-selectin and ΔM-N L-selectin expressing cells. Although KC is generally considered to be a neutrophil chemoattractant, migration of monocytes towards KC, or its human equivalent CXCL-1, has been reported [720]. Chemotaxis towards increasing concentration of CXCL-1 was thus analysed using the transwell assays. Unfortunately, none of the THP-1 cell lines responded to CXCL-1 (**figure 6.16**).

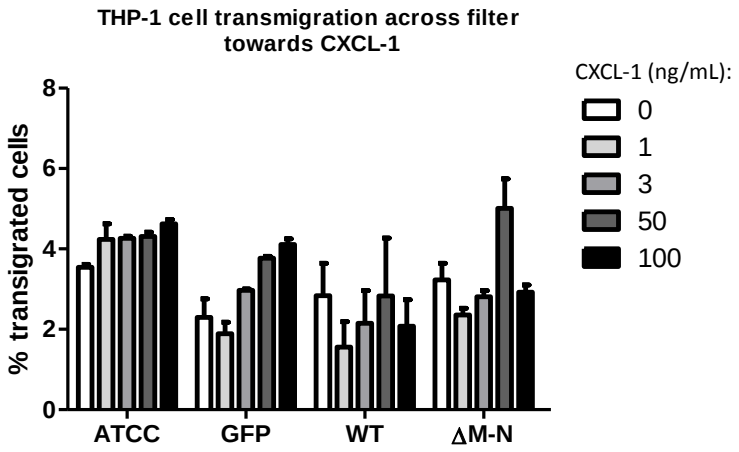

Figure 6.16 THP-1 monocytes do not migrate towards CXCL-1. Untransduced THP-1 cells (UT) and cells expressing GFP (GFP), WT L-selectin-GFP (WT) or ΔM-N L-selectin-GFP (ΔM-N) were subjected to the transwell assays as described in **section 2.20**. Indicated concentrations of CXCL-1 were used. After a 3-hour long assay, cells that migrated from the upper to lower compartments were collected and analysed against the input cells by flow cytometry. Experiments were repeated in triplicates on three independent occasions. Data represent mean ± S.E.M.

6.4 DISCUSSION

6.4.1 L-selectin shedding regulates THP-1 monocyte polarisation during TEM

The results presented in this chapter show that ectopic expression of L-selectin primes the THP-1 cells to be more “invasive” during the first 7 min of flow. When compared to cells expressing GFP alone, WT L-selectin-expressing THP-1 cells have a higher fraction of total protruding cells, and higher fractions of cells with two or multiple pseudopods (**figure 6.2**). This clearly changes at 15 min, when the pseudopod numbers become similar between GFP- and WT L-selectin-expressing cells (**figure 6.2**). The transition from multiple pseudopods to single could be an indicator that shedding of WT L-selectin has occurred. Indeed, it is known that blocking L-selectin shedding (either with Ro-31-9790, or through mutating the cleavage site) dramatically increases pseudopod number by the 15 min time point (**figure 6.4** and **6.5**). It is noteworthy that the peak activity of L-

selectin shedding during TEM was observed to be 20 min in static TEM assays (**figure 4.1**), so, although not formally tested, shedding of L-selectin may be hastened under flow conditions. Perhaps a role for L-selectin during monocyte TEM could be to augment the initial invasion across the endothelial monolayer. In fact, a role for L-selectin in regulating the invasion of trophoblasts during embryo implantation has been speculated before [721].

Interestingly, the spread area of the WT L-selectin-expressing THP-1 cells does not decrease over time, but is in fact sustained (**figure 6.9**). This suggests that multiple pseudopods are retracting, but not to an extent that would cause the cells to "round-up". Instead, it would appear that the cells are consolidating their multiple protrusions in to one or two pseudopods with a continued commitment towards establishing polarity. Again, as suggested above, this may be driven by the actual event of L-selectin shedding. When L-selectin shedding is blocked, THP-1 cells form multiple pseudopods that do not retract with time (**figure 6.4**). Additionally, the spread area in THP-1 cells expressing ΔM-N L-selectin is much larger than in those cells with an intact cleavage site (**figure 6.9**). This is thought to reflect the area gained by continuous pseudopod extension and a lack of multi-pseudopod retraction. These results suggest that L-selectin shedding must occur for the THP-1 monocyte to establish polarity during TEM. These observations may help understand why ΔM-N L-selectin clusters at the non-transmigrated part of the cell, which is the total opposite to the WT L-selectin (**figure 5.6**). In **section 5.3.6** it was hypothesised that the cytoplasmic tail of ΔM-N L-selectin could be hyperphosphorylated and that this could block its movement from the non-transmigrated part of the cell to the transmigrated pseudopod. As ΔM-N L-selectin is seen to cluster at the top of the cell (**figure 5.6**), it is possible that as the pseudopods expand beneath the monolayer, more membrane is dedicated to the transmigrated part of the cell than the non-transmigrated part. This would create a very limited membrane microenvironment for ΔM-N L-selectin to move around in. Furthermore, if indeed ΔM-N L-selectin is hyperphosphorylated, it could increase random interactions with other L-selectin molecules (as they may not be "tethered" to the cortical actin cytoskeleton by the interaction with the ERM proteins). This hypothesis is also supported by the observations made through mutating the serines to non-phosphorylatable alanines (see **section 6.4.2**)

The establishment and maintenance of cell polarity is important for successful migration of cells, including leukocytes. Leukocytes that have lost their polarity present with impaired chemotaxis [234, 237, 238, 243, 247, 710, 722]. Furthermore, leukocytes expressing a "sheddase-resistant" form of L-selectin cannot undergo chemotaxis *in vivo* [419]. It was hence hypothesised that the loss of polarity in the THP-1 monocytes expressing ΔM-N L-selectin could lead to a defect in chemotaxis. Transwell chambers

were used where transmigration of THP-1 cells across HUVEC monolayers towards a gradient of MCP-1 was assessed. The assays revealed no differences in transmigration between WT and ΔM-N L-selectin expressing cells (**figure 6.15**). This challenged our hypothesis, however it is possible that differences in chemotaxis could be seen at different time-points. Additionally, it could be argued that a modified experimental system is needed to study the contribution of L-selectin and its shedding to chemotaxis of THP-1 monocytes. An alternative experiment that was not executed during the course of this PhD (due to lack of time) would include a relatively thick ECM-mimicking composite (i.e. matrigel and/or collagen block) in which cells could migrate upon transmigration. Perhaps L-selectin-driven polarity does not influence transmigration of leukocytes per-se, but rather prime the cells for subsequent directed cell migration through the ECM. Furthermore, it is possible that for L-selectin-dependent chemotaxis to occur, leukocytes must be first recruited from flow. L-selectin mediates leukocyte tethering and rolling and its outside-in signalling contributes to leukocyte arrest (**sections 1.2.4**, **1.7.5.1.1** and **1.11.2**). Perhaps it is these early interactions of L-selectin with the endothelium that are required for L-selectin to then drive chemotaxis. In support of this theory, transwell experiments have shown that L-selectin enhances lymphocyte chemotaxis across activated HUVEC only if L-selectin is cross-linked prior to the assay [85, 91].

Cell motility and polarity is affected by the family of Rho GTPases that regulate cytoskeletal dynamics (**section 1.5**). The initial idea for Rho GTPase-mediated polarisation of leukocytes was that the activity of Rac1 and Cdc42 at the leading edge promote the formation of the protrusions, whereas protrusions at the back are suppressed by high RhoA activity in this area [237, 238, 240, 241]. However, with an advent of FRET-based probes that monitor spatio-temporal distribution of Rho GTPase activity in real-time, this “black-and-white” model of Rho GTPase function has been revised. For example, it has been reported that RhoA is also active at the front of transmigrating lymphocytes, where it governs both membrane protrusion and retraction, which allows for successful formation of the leading edge [118]. RhoA activity was also detected in lymphocyte filopodia extending beneath the HUVEC monolayer [118]. Similarly, in migrating epithelial cells and fibroblasts RhoA undergoes cyclic activation and deactivation at the leading edge [712, 713]. Specifically, highly localised RhoA activation increases and decreases in synchrony with protrusion and retraction, respectively [712, 713]. The data regarding L-selectin clustering and Rho GTPase activity was obtained in the closing phases of this PhD project and as n=1 only. Therefore, only a purely hypothetical model incorporating Rho GTPases and L-selectin-dependant polarity during TEM can be proposed. According to this model, it could be speculated that clustering of L-selectin in the transmigrated pseudopods (**figure 5.2**) could lead to a localised decrease in RhoA activity (**figure 6.13**), resulting in the possible

retraction of some of the projecting pseudopods. The result of this is the extension of a single pseudopod (**figure 6.2**), and correct establishment of a leading edge. The lack of such clustering in the pseudopods of cells expressing ΔM-N L-selectin (**figure 5.6**) leads to uncontrolled protrusion of multiple pseudopods (**figure 6.4**) and loss of polarity. Interestingly, the ΔM-N L-selectin only clusters in the non-transmigrated part of the cell, so its effects on pseudopod dynamics are likely to be very indirect. The decrease in Rac1 activity following ΔM-N clustering would suggest that perhaps another Rho GTPase is active downstream of ΔM-N L-selectin clustering to promote extensive pseudopod formation following clustering of ΔM-N L-selectin (**figure 6.13**). In short, the results are too preliminary to draw any major conclusions and clearly an alternative biosensor is required to assess the spatio-temporal resolution of Rho GTPases during TEM.

The results presented in this chapter and in **figures 5.2** and **5.6** (**Chapter 5**) were used to generate a theoretical model that proposes how L-selectin might regulate monocyte TEM (**figure 6.16**). Many migrating cells extend and collapse protrusions at the leading edge, which is a way of "path finding" [713]. It is proposed that L-selectin may take part in this process. According to this model L-selectin clusters at the leading edge (pseudopods) of the transmigrating cells, which results in local deactivation of RhoA. The combined effect of many local RhoA inactivity points results in retraction of some of the pseudopods. The overall effect is a transmigrated monocyte that is polarised and is able to migrate through the extracellular matrix and towards a chemoattractant source. When shedding is blocked, clustering of L-selectin occurs in the non-transmigrated parts and no clustering in the pseudopods occurs. As a result, high local RhoA activity at the leading edge persists and retraction of the excess pseudopods fails to occur. The emigrated monocyte loses its polarity. Such "confused" monocytes are then unable to proceed through the ECM and up the chemoattractant gradient. When involvement of L-selectin shedding in driving monocyte polarity during TEM seems highly likely, the proposed involvement of RhoA is purely hypothetical and further experiments would be required to verify this working model.

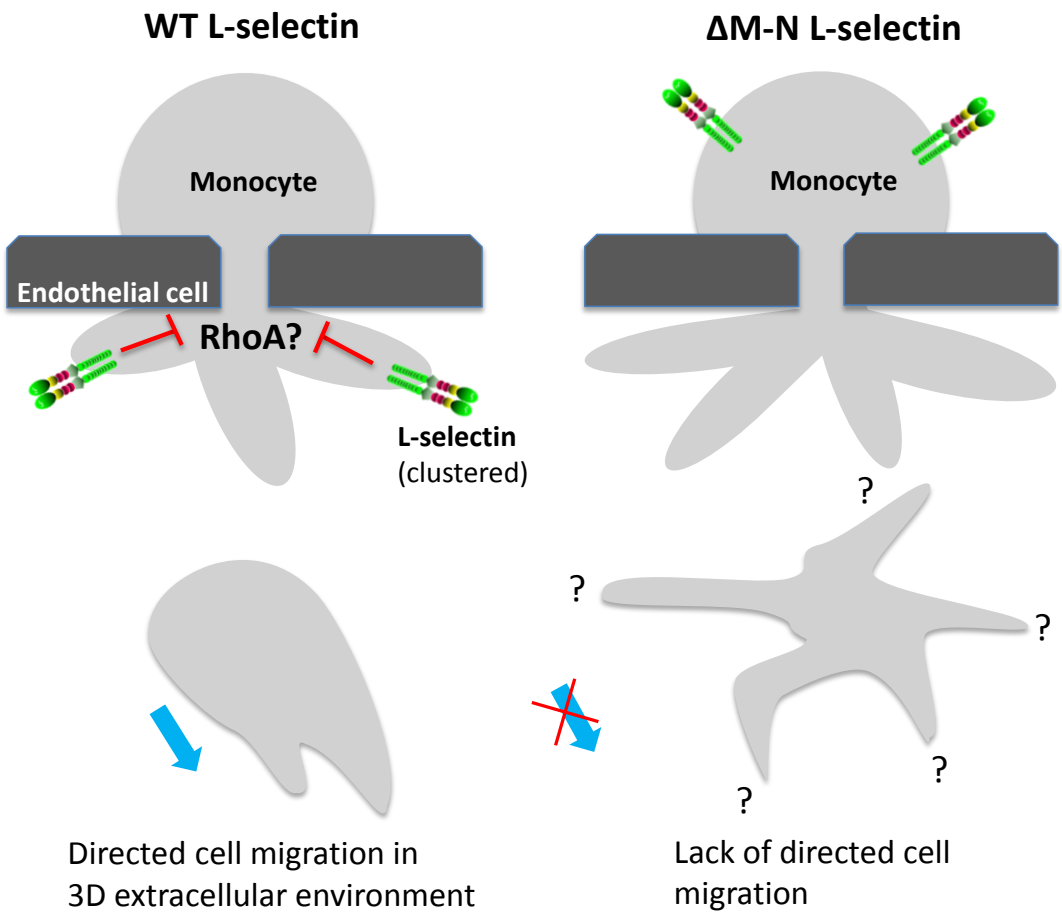

Figure 6.17 Model of L-selectin dependent migration. Clustering of WT L-selectin occurs at the leading edge (pseudopods) of the transmigrating cells, which results in local deactivation of RhoA. This leads to retraction of excess pseudopods and contributes to cell polarity. Upon transmigration, the polarised monocyte successfully migrates through the extracellular matrix and towards the chemoattractant source. "Sheddase-resistant" L-selectin (ΔM-N L-selectin), clusters in the non-transmigrated parts of the monocyte, and not in the transmigrating pseudopods. As a result RhoA activity and extension of multiple pseudopods is maintained and the emigrated monocyte loses its polarity. Lack of polarity prevents the monocyte to successfully respond to the chemoattractant gradient and directed migration through the ECM is abolished.

6.4.2 Serine residues within the L-selectin tail regulate THP-1 cell pseudopod dynamics

Mutation of the cytoplasmic serine residues within the L-selectin tail into non-phosphorylatable alanines (SSAA L-selectin) resulted in a slight decrease in the percentage of total protruding cells when compared to the WT L-selectin expressing cells (**figure 6.3**). This was accompanied by decreased dynamics of the pseudopods (**figure 6.3**) and reduced cell spreading area (**figure 6.9**). Therefore, it appears that rendering of the L-selectin cytoplasmic serines non-phosphorylatable results in decreased

"invasiveness" of the THP-1 monocytes. Perhaps phosphorylation of the tail serines is needed for initial dynamic pseudopod extension. This would support the hypothesis that the tail of ΔM-N L-selectin might be hyperphosphorylated. The hypothesis, initially produced in **Chapter 5**, assumes that when THP-1 cells become activated upon contact with the activated HUVEC monolayer, the L-selectin tail becomes phosphorylated. Lack of shedding prevents any further tail modifications and as a result ΔM-N L-selectin remains in a hyperphosphorylated state. If tail phosphorylation was driving initial pseudopod extension, cells expressing hyperphosphorylated ΔM-N L-selectin would become "locked" in this initial phase. This could be seen as increased cell spreading area and formation of multiple pseudopods that do not retract with time (**figure 6.4** and **6.9**). Future experiments using SSDD mutants may best serve to further unfold this mystery.

The cells that express ΔM-N SSAA L-selectin have the same cell spreading area to that of the cells expressing WT L-selectin (**figure 6.9**). However, the pseudopod dynamics of ΔM-N SSAA L-selectin expressing cells lie in between those found in the cells expressing WT L-selectin and those found in the cells expressing ΔM-N L-selectin (**figure 6.8**). On one side, the percentage of the polarised cells that form one pseudopod only is similar to that amongst the WT L-selectin expressing cells. On the other hand though, the percentage of cells with multiple pseudopods does not decrease with time and overall more cells with multiple pseudopods are seen at the end of the assay as compared to the WT L-selectin expressing cells. The fact that the ΔM-N SSAA L-selectin expressing cells show similarities to either WT L-selectin or to the ΔM-N L-selectin expressing cells, but not to SSAA L-selectin expressing cells, questions the fact that tail serine phosphorylation is important for the initial pseudopod extension. The difference between cells expressing SSAA L-selectin and those expressing ΔM-N SSAA L-selectin is that the former accumulate L-selectin cleavage product ("stump") during shedding. Perhaps it is the presence of the non-phosphorylatable "stump" at the plasma membrane of SSAA L-selectin expressing cells that limits the "invasiveness" of these cells. It is possible that a negative feedback loop exists where the dephosphorylated "stump" – that would normally be generated later on during the transmigration – affects the extension and the dynamics of the pseudopods. Possible future experiments may rest with engineering AD and DA mutants to specifically pseudophosphorylate one serine residue and not the other. This may help determine the contribution of each serine when phosphorylated. The outcome of these results will heavily depend of whether the mutations will radically affect the overall structure of the L-selectin tail.

Although it is difficult to propose the complete theory on how the cytoplasmic serine residues within the L-selectin tail influence THP-1 pseudopod dynamics, it can be speculated that modification of the L-selectin tail by cyclic

phosphotylation/dephosphorylation events are likely to occur. Those modifications are proposed to regulate L-selectin ectodomain shedding and L-selectin clustering. This in turn regulates signalling downstream of L-selectin and affects formation and dynamics of the pseudopods during transendothelial migration.

CHAPTER 7. GENERAL DISCUSSION

The experiments described in the **Chapters 3-6** of this thesis were designed to investigate the role that L-selectin and its shedding may play during monocyte TEM. To this end, THP-1 monocytic cell lines were generated that were expressing WT or cytoplasmic/extracellular domain mutants of L-selectin tagged to GFP and/or RFP. The first set of experiments to be performed was a rigorous analysis of the expression, localisation and function of the GFP-tagged L-selectin, which showed that the fluorescent tag did not have any adverse effects on the L-selectin protein behaviour (**Chapter 3**). Thus, a powerful tool was gained that allowed the investigation of the spatio-temporal distribution of the L-selectin localisation, shedding and clustering during TEM. More importantly, this approach required no monoclonal antibody to visualise L-selectin, which could potentially interfere with its function and particularly with respect to clustering. Utilisation of such cell lines in a number of carefully designed assays yielded 4 major findings: (i) that shedding of L-selectin peaks at 20 minutes when THP-1 monocytes are co-cultured with activated HUVEC (**Chapter 4**); (ii) that prior to the peak of shedding activity, L-selectin clusters in the pseudopods of transmigrating monocytes (**Chapter 5**); (iii) that engagement of either endogenous CD43 or PECAM-1 on THP-1 cells may serve to drive L-selectin clustering – either independently or in concert with ligand-induced clustering (**Chapter 5**); and (iv) that shedding of L-selectin regulates monocyte cell spreading area and polarisation during TEM (**Chapter 6**). Furthermore, in all of the findings described (i-iv), the L-selectin extracellular cleavage site, the cytoplasmic serine residues (S364 and S367), or both, have been identified to play a prominent role in the regulation of L-selectin function.

L-selectin plays a pivotal role during leukocyte tethering, rolling and β1/2 integrin-mediated adhesion. There is a mounting body of evidence that defines a novel role for L-selectin, which is the interstitial locomotion of the emigrated leukocytes (chemotaxis) [398, 415-417]. Chemotaxis *in vivo* has been shown to be dependent on L-selectin shedding [419], and emigrated leukocytes have been reported to have shed the majority of their L-selectin both *in vitro* and *in vivo* [520, 554-556]. Therefore it appears that the intraluminal and interstitial activity of L-selectin may be linked through the ectodomain shedding that occurs during the TEM event. Due to the limitations of the transmigration system used in this study, only the early transmigration stage was examined, whereby THP-1 cells extend probing pseudopods underneath the HUVEC monolayer but never fully transmigrate. In this experimental system it was found that shedding of L-selectin peaks at 20 minutes into the assay (**figure 4.1**). Monocytes take 10-20 minutes to complete transmigration *in vitro* [56, 669, 723], suggesting that L-selectin shedding is likely to occur throughout the whole TEM event. This implies that L-selectin shedding

might play a regulatory function during TEM. Additionally, this thesis is the first to show that shedding of L-selectin during TEM is dependent on the cytoplasmic serine residues, the phosphorylation of which is likely to promote/accelerate shedding (**figure 4.4**).

7.1 WHAT IS CURRENTLY KNOWN ABOUT THE SUBCELLULAR DISTRIBUTION OF L-SELECTIN?

The experiments undertaken in this thesis were designed to explore two main aspects concerning the subcellular distribution of L-selectin during TEM. The first one is the GFP-signal, throughout this thesis referred to as the "L-selectin GFP-positive spots", which could be detected using the confocal microscopy. The second one is the distribution of L-selectin clustering, which could be seen through FLIM analysis of FRET between L-selectin-GFP and L-selectin-RFP.

7.1.1 The subcellular distribution of the L-selectin-GFP spots

Analysis of the spatio-temporal distribution of the L-selectin-GFP spots during TEM revealed that the spots accumulate with time in the transmigrating pseudopods. This is reduced in the SSAA L-selectin mutant and is abolished when ΔM-N L-selectin is expressed (**figures 4.12 and 4.13**), suggesting that the observed L-selectin-GFP spots accumulation is the L-selectin-GFP "stump" generated during shedding. However, to formally test this hypothesis it would be crucial to perform further experiments that could verify that the spots lacked the extracellular domain. Simple examination of the GFP localisation is not conclusive enough as the GFP-signal could correspond to both full-length and cleaved L-selectin-GFP. One approach would be to stain the fixed samples with LAM1-14 mAb that has now arrived in our laboratory and, unlike DREG56, has the ability to recognise L-selectin extracellular domain on fixed samples. Furthermore, it is possible that the GFP-positive spots represent internalised L-selectin, whether full-length or the "stump". Unfortunately the approach undertaken in this thesis (EEA1 endosomal marker staining) did not prove successful in answering of this question, however other experiments can be envisioned for the future. For example, P-selectin is known to cluster in clathrin-coated pits before it is internalised [724], and so it would be interesting to perform co-localisation studies between L-selectin-GFP and clathrin. Additional staining with LAM1-14 could serve to further distinguish between the full-length versus the L-selectin "stump".

Accumulation of the L-selectin-GFP "stump" would mean that shedding of L-selectin occurs in the transmigrating pseudopods. This hypothesis is in line with data obtained by Miss Abigail Newe, a PhD student in the Ivetic laboratory, who discovered that L-selectin/CaM interaction can be detected in the pseudopods of transmigrating THP-1 cells after 7 minutes of perfusion, but the interaction no longer exists after 25 minutes,

suggesting that CaM disassociates from L-selectin over time (A. Newe, unpublished data, **figure 7.1**). At the same time, L-selectin/CaM interaction in the non-transmigrated parts of the THP-1 monocytes was readily detected at both 7 and 25 minute time-points (A. Newe, unpublished data, **figure 7.1**). As CaM negatively regulates L-selectin shedding [559], this could indicate that shedding of L-selectin occurs exclusively in the transmigrating pseudopods. The implications of such localised shedding could be numerous. For example full-length and cleaved L-selectin could bind different cytosolic proteins and could support the assembly of distinct signalling platforms at the L-selectin tail. L-selectin is known to mediate intracellular signalling and several different signalling complexes have been reported/hypothesised to be associated with the L-selectin tail upon stimulation through the extracellular domain [245, 572, 602]. Perhaps the change-over of the binding partners that occurs just before, during, or shortly after shedding could trigger signalling downstream of the L-selectin tail that would be spatially limited to the transmigrating pseudopods. On the other hand, L-selectin/CaM interaction and the lack of shedding in the non-transmigrated parts of the cell could serve to preserve full-length L-selectin at the uropod to support secondary capture of the flowing leukocytes, or for any other role it may later play during chemotaxis.

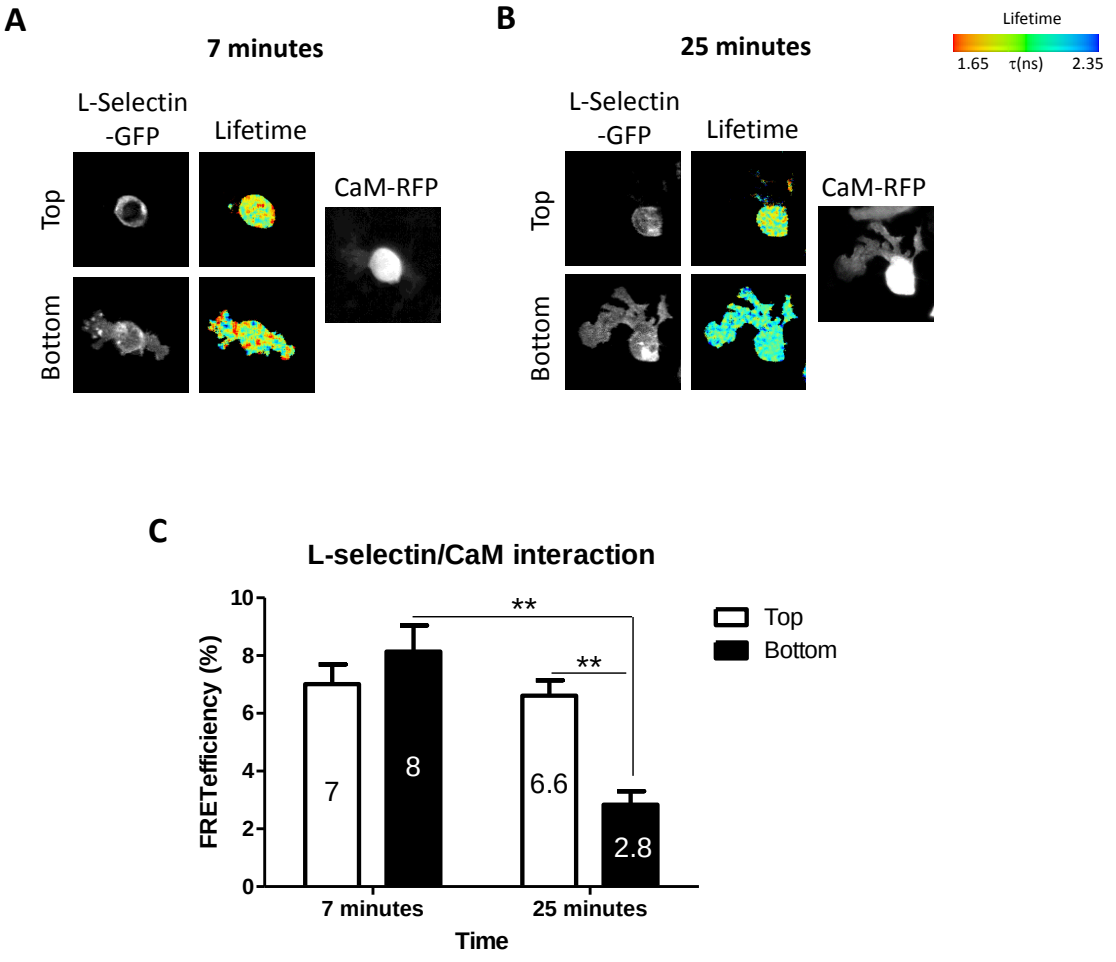

Figure 7.1 Interaction between L-selectin and calmodulin during THP-1 cell transmigration.

Wild type RFP-tagged calmodulin (CaM-RFP) was introduced into THP-1 WT L-selectin-GFP Lo5 cell line and cells were perfused over TNF-α activated HUVEC monolayer (for the method of the parallel plate flow chamber experiments see **section 2.14.3**). The samples were fixed and prepared for FLIM/FRET analysis as described in **section 2.18.1**. FLIM measurement of FRET was used to assess the interaction between L-selectin-GFP and CaM-RFP in the Top and Bottom z-planes (Top and Bottom are as shown in **figure 5.2 A**). The figure shows representative images of a transmigrating THP-1 monocytes after 7 (**A**) or 25 (**B**) minutes of perfusion. *Left panels*: images of L-selectin-GFP. *Middle panels*: corresponding GFP multi-photon intensity images. Lifetime of fluorescence is shown as a pseudo-colour scale of blue (high lifetime) to red (low lifetime). The lower the lifetime of fluorescence, the closer the association between L-selectin-GFP and CaM-RFP. *Right panels*: Representative wide-field CCD camera image of CaM-RFP. **C)** Quantitation of FRET efficiency between L-selectin-GFP and CaM-RFP. Analysis was performed on a total of 15 cells derived from three independent experiments. Mean values are shown for each bar. Error bars represent S.E.M. Statistical analysis: Two-tailed unpaired Student's t-test. **=p<0.01. These unpublished experiments were conducted by Miss Abigail Newe (Cardiovascular Division, KCL) and FLIM/FRET analysis was performed by Dr Maddy Parsons (the Randall Division of Cell and Molecular Biophysics, KCL).

7.1.2 The subcellular distribution of the L-selectin clustering

In keeping with the hypothesis that L-selectin signalling could be triggered in the pseudopods of transmigrating THP-1 cells, this thesis is the first to show that L-selectin clusters in the monocyte pseudopods during TEM (**figure 5.2**). L-selectin is monomeric in membranes [579, 580], and clustering is associated with ligand binding and signalling downstream of the tail and subsequent cellular responses (**table 1.3**). Clustering of L-selectin in the transmigrating pseudopods is abolished when shedding cannot occur (**figure 5.6**), highlighting the importance of shedding for L-selectin-dependent signalling during TEM. Interestingly, modification of the cytoplasmic serine residues into non-phosphorylatable alanines can restore clustering of the sheddase-resistant L-selectin in the transmigrating pseudopods (**figure 5.8**). This suggests that the cytoplasmic serine residues have a dominant role over the extracellular cleavage site as far as the clustering is concerned. It also implies that the serine residues are likely to be hyperphosphorylated in the ΔM-N L-selectin, which in turn prevents clustering. Interestingly, clustering of N-formyl peptide receptor (FPR) occurs in the absence of receptor phosphorylation, which is a pre-requisite for subsequent phosphorylation and FPR internalisation [725]. Although FPR and L-selectin are functionally distinct, it is possible that they might share a similar clustering mechanism, whereby clustering in the absence of phosphorylation is a requirement for subsequent phosphorylation-dependent signalling processes.

7.2 WHAT COULD BE THE RELATIONSHIP BETWEEN L-SELECTIN CLUSTERING AND SHEDDING IN THE TRANSMIGRATING PSEUDOPODS?

One possibility is that shedding and clustering of L-selectin in the pseudopods are two independent events. Perhaps a population of L-selectin molecules clusters in response

to the ECM ligand binding, and another population undergoes shedding as a result of cellular activation. Proceeding down one of the routes could depend on the membrane microenvironment a given L-selectin molecule would be surrounded by. In support of this theory, the membrane environment has been shown to regulate L-selectin/CaM/ERM interaction [573, 576], and 51±7% of the neutrophil surface L-selectin has been reported to reside in lipid rafts under resting conditions, suggesting a pre-existing dichotomy in L-selectin plasma membrane distribution [726]. Another possibility is that clustering and shedding are two consequent stages of the same event. There are several lines of evidence to support this hypothesis. First of all, L-selectin cross-linking, and thus clustering, has been repeatedly shown to cause L-selectin shedding [529, 533-536]. Furthermore, densely-spaced sulfated ligands, the nature of which resembles those of the ECM sulfated proteoglycans that bind to L-selectin, have been shown to cause L-selectin clustering and, ultimately, shedding (**figure 7.2**) [678, 727]. Expression of biglycan (L-selectin ECM ligand) by the TNF-α activated HUVEC monolayers has been detected in the experimental set-up employed throughout this study (**figures 5.3** and **5.4**). This hypothesis can potentially explain why the ΔM-N SSAA mutant clusters in the transmigrating pseudopods, however no accumulation of GFP-positive spots can be seen (**figures 5.9** and **5.11**). If clustering is a pre-requisite for shedding and is dependent on the lack of the serine phosphorylation, the ΔM-N SSAA L-selectin can therefore be effectively clustered. A lack of the extracellular cleavage site prevents shedding, and hence no GFP-positive spots can be seen accumulating. To test whether ECM components have the ability to cause L-selectin shedding, THP-1 cells expressing GFP-tagged L-selectin could be incubated with purified biglycan, versican or collagen XVIII and the cell supernatants could be tested for sL-selectin using ELISA. Utilisation of the serine mutants in such assays would provide clues as to the role of serine phosphorylation in ligand-induced L-selectin shedding. Additionally, cross-linking of CD43 or PECAM-1 prior to the assays could help to understand if these molecules play a role in the modulation of the extent of the L-selectin shedding. Other experiments to consider would be to seed the L-selectin-GFP/RFP double expressor THP-1 cells on to purified immobilised ECM ligands (such as biglycan) and determine if L-selectin clustering is directly influenced, as assessed by FRET and compared to cells plated on to PLL.

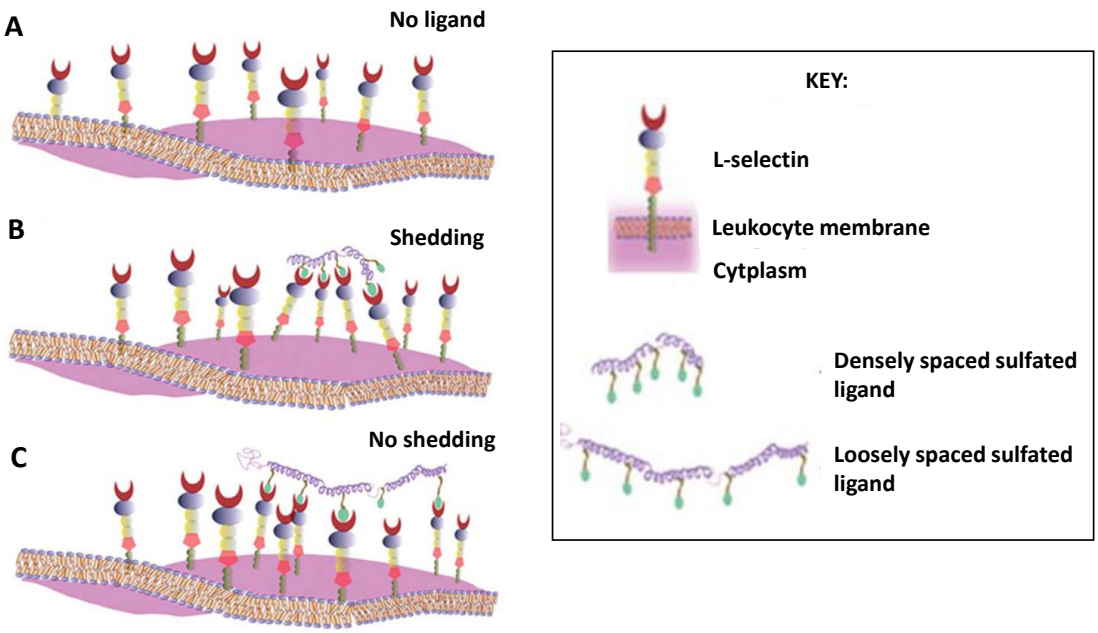

Figure 7.2 Relationship between the ligand type and L-selectin clustering and shedding. **A**) Distribution of L-selectin at the plasma membrane when no ligand is bound. **B**) Engagement with densely spaced sulfated ligand causes clustering, conformational changes and shedding of L-selectin. **C**) Engagement with loosely spaced sulfated ligands does not induce conformational changes in L-selectin, and as a result shedding does not occur. Image adapted from Liu and Kiick, *Polym. Chem.,* 2011 [678].

7.3 HOW IMPORTANT IS INSIDE-OUT SIGNALLING FOR CLUSTERING OF L-SELECTIN?

This thesis is the first to report that the engagement of endogenous CD43 or PECAM-1 causes L-selectin clustering. This discovery sets the foundations for a novel avenue of investigation, which would involve: (1) dissecting the signalling pathways between CD43/PECAM-1 and L-selectin and (2) analysing the physiological relevance of these interactions for leukocyte recruitment. The current study identified that CD43-mediated L-selectin clustering occurs in the absence of cytoplasmic tail serine phosphorylation, whereas it is hypothesised that PECAM-1-mediated clustering is likely to require dynamic phosphorylation/dephosphorylation events on the L-selectin serine residues. This in turn suggests that CD43 and PECAM-1 signal to L-selectin at distinct stages during the recruitment, which makes sense, given the spatio-temporal difference in the engagement of CD43 and PECAM-1 during the leukocyte adhesion cascade (the putative models explaining CD43 or PECAM-1-mediated L-selectin clustering during the leukocyte adhesion cascade were discussed in more detail in **section 5.4.1**). As mentioned above, a role of CD43/PECAM-1-induced L-selectin clustering in L-selectin shedding could be explored, however it would be also interesting to investigate what proteins bind to the L-selectin tail in response to CD43/PECAM-1 signalling. A possible experiment could involve cross-linking of CD43/PECAM-1 and subjecting the cell lysates to the affinity

chromatography, using the 17 C-terminal amino acids of the L-selectin tail as “bait”. Such column has been successfully used in the past for the identification of the L-selectin binding partners in the lysates from the PMA-stimulated lymphocytes [563]. Once identified, the binding partners could be tagged to RFP and introduced to the L-selectin-GFP expressing THP-1 cell lines and FRET between the two could be measured during TEM over a series of time points.

7.4 WHAT IS THE BIOLOGICAL SIGNIFICANCE OF L-SELECTIN’S ACTIVITY DURING TEM?

Chapter 6 of this thesis is the first to demonstrate that L-selectin influences monocyte morphology and pseudopod dynamics during TEM. The data presented suggest that expression of L-selectin renders the cells more invasive in the very early stages of TEM as compared to monocytes expressing GFP alone (**figure 6.1**). This finding could have potentially important therapeutic implications, given the prominent role of monocyte recruitment in chronic inflammatory diseases such as atherosclerosis. With time this pro-invasive advantage is lost, a phenomenon that could be potentially explained by L-selectin shedding occurring in the pseudopods. In keeping with this, transmigrating monocytes expressing WT L-selectin consolidate their multiple “invasive” pseudopods into one or two as the time progresses, which is thought to occur by “channelling” of the available membrane area into the dominant pseudopods without overall reduction in the cell spreading area (**figure 6.9**). This allows the monocytes to acquire a polarised phenotype. In the absence of L-selectin shedding no pseudopod rearrangement seems to occur, multiple pseudopods are maintained and the cell loses polarity (**figures 6.4** and **6.5**). Interestingly, pseudopod dynamics and polarity appears to be also regulated by the cytoplasmic serine residues, as the SSAA mutation of the ΔM-N L-selectin tail can partially restore the dynamics seen with WT L-selectin (**figure 6.8**). This highlights the importance of the non-phosphorylated state of the serines required for L-selectin clustering in the pseudopods (**Chapter 5**), and suggests a link between clustering, shedding and monocyte polarisation. If the two-step model of L-selectin shedding in the pseudopods is true, then it is possible that the serine residues regulate L-selectin clustering and induce signalling necessary for the shedding response.

Although the morphology of fully transmigrated cells could not be analysed in this study, it is tempting to speculate that emigrated monocytes would present with a polarised appearance, where the cell front would be devoid of full-length L-selectin. In support of this theory, preliminary experiments from the Ivetic laboratory show that when PBMCs are labelled with fluorescently tagged LAM1-14 mAb and subsequently perfused over activated endothelial cells, around 30-50% of them retain L-selectin expression at the uropod following TEM (Dr A. Ivetic, unpublished data). Why the remaining population

lose their L-selectin is unknown, and also it is not known whether the THP-1 cells studied in this project truly represent the monocytes that retain their L-selectin expression following TEM. One way to investigate this question in the THP-1 cell model would be to grow HUVEC on the thick collagen/matrigel substrates, allow the monocytes to transmigrate fully and monitor their fate beyond the endothelial barrier and in to the ECM. Yet again, the non-function blocking anti-L-selectin antibody LAM1-14 would prove useful, to label L-selectin prior to the assay or in the fixed samples. Such experiments are currently underway in the Ivetic laboratory in a new PhD project.

7.5 A PUTATIVE MODEL FOR THE ROLE OF L-SELECTIN DURING TEM AND BEYOND

The above has described four major findings of this PhD project were used to generate a hypothetical model explaining the involvement and implications of L-selectin's activity during TEM. The graphical summary of the model is presented in **figure 7.3**, and the model is discussed in more detail below. It is proposed that during the resting state and the early stages of the leukocyte adhesion cascade, the tail of L-selectin is cyclically phosphorylated/dephosphorylated. This might involve stages, where only one of the serines (S364 or S367) is phosphorylated, two serines are phosphorylated or none is phosphorylated. Such regulation is likely to be very dynamic and allow for regulation of L-selectin function, e.g. modulation of the tail interaction with CaM, ERM and the inner leaflet of the plasma membrane, regulation of basal L-selectin shedding, ligand binding during tethering and rolling or clustering in response to CD43 engagement. Based on the data presented in this thesis, it is likely that the serines may play a redundant role, which is why mutating both serines will lead to an observed phenotype. During transmigration, L-selectin is exposed to the ECM environment, where it can bind to its sulfated ligands. It is proposed that the cytoplasmic serine residues must not be phosphorylated for ligand-induced clustering to occur. Furthermore, the binding could be facilitated by the CD43/PECAM-1-mediated L-selectin clustering. CD43/PECAM-1-induced clustering of L-selectin could bring about a conformational change that would increase the avidity of L-selectin for the ECM ligand. Inside-out signalling evoked by stimulation of leukocytes with lineage specific stimuli has been reported to improve the affinity of L-selectin for PPME ligand mimetic before [728]. Additionally, due to its prominent role in TEM and leukocyte/EC junction interaction, PECAM-1 could serve to translocate clustered L-selectin from the non-transmigrated to transmigrated (pseudopod) part of the cell. Alternatively, L-selectin/ligand binding could occur first, and CD43/PECAM-1-induced inside-out signalling could modulate the avidity of this complex. It is further hypothesised that specific conformation of clustered L-selectin, induced by ECM ligand binding and/or inside-out CD43/PECAM-1-mediated signalling triggers

shedding of L-selectin. This event is thought to be limited to the transmigrating pseudopods only. Shedding of L-selectin has been reported to be mediated by p38 MAPK [496, 531], and activation of p38 MAPK downstream of L-selectin clustering has been reported [589]. This opens up a possibility that engagement of L-selectin ectodomain could lead to L-selectin shedding in a p38 MAPK-dependent manner. Interestingly, p38 MAPK inhibitors have been shown to have no influence on leukocyte rolling or adhesion but caused chemotaxis defects parallel to those seen in L-selectin deficient mice [729]. This could imply a role for p38 MAPK-mediated shedding of L-selectin during TEM as a pre-requisite for chemotaxis. It is further postulated that clustering and shedding of L-selectin are important for the establishment of cell polarity during TEM. It is proposed that signalling downstream of clustered or cleaved (“stump”) L-selectin could drive the retraction of competing pseudopods and could stimulate extension of the dominant pseudopod. It is tempting to speculate that the signalling pathway involves activation/deactivation of certain Rho GTPases, although the data presented in this thesis is currently too preliminary to draw any meaningful conclusions. It is hypothesised that due to L-selectin clustering and shedding, emigrated leukocytes would have an established polarity and would therefore be primed for directional migration in the extravascular space. It is also possible that the L-selectin “stump” could play a further role in the chemotaxis event itself.

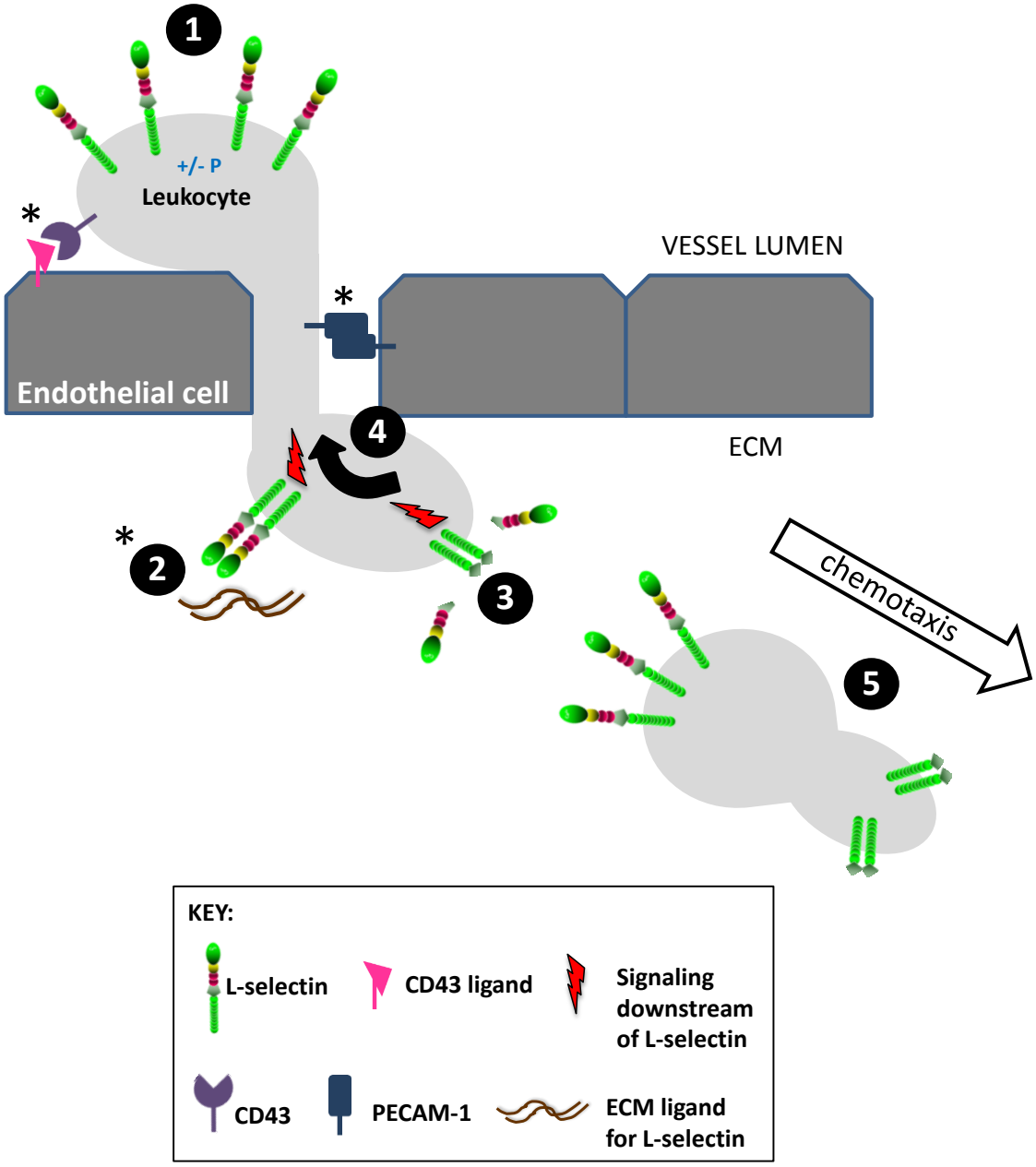

Figure 7.3 Schematic model representing the possible role of L-selectin clustering and shedding in TEM and chemotaxis. This model was produced based on the four major findings of this PhD thesis and currently available literature. It is proposed that the L-selectin tail is cyclically modified by phosphorylation/dephosphorylation events that regulate basal shedding, ligand binding during tethering and rolling, as well as the interaction of L-selectin with CaM, ERM and the plasma membrane (**1**). During TEM, L-selectin clusters upon ECM ligand binding, which could be modulated by CD43/PECAM-1-mediated inside-out signaling (**2**). Clustering is likely to involve CaM/ERM interaction in *cis*, binding of K-Ras to SOS (not shown on the schematic, see text below and **figure 7.4**) (**2**). Clustering results in L-selectin shedding (**3**). Pseudopod-specific clustering and shedding of L-selectin leads to retraction of multiple pseudopods, dedication of the plasma membrane towards one or two dominant pseudopods and leukocyte polarisation (**4**). Transmigrated leukocyte is polarised with full-length L-selectin at the uropod and L-selectin "stump" localised to the leading edge (**5**). Polarisation of the cell results in successful chemotaxis (**5**).

7.6 HOW DOES THIS WORK FIT WITH THE PREVIOUS OBSERVATIONS MADE IN THE IVETIC LABORATORY?

Not much is currently known about the molecular players that could be involved in the initiation of the signalling postulated in this thesis. However, Killock et al. (2009) has proposed that under resting conditions each L-selectin molecule forms an independent 1:1:1 heterotrimeric complex with CaM and ERM, where CaM associates with K-Ras and ERM associates with SOS (son of sevenless, GEF for Ras) (**figure 7.4**) [572]. Clustering of L-selectin was proposed to bring CaM, ERM, as well as their respective binding partners, from the adjacent L-selectin tails close together, which allows K-Ras to SOS binding (**figure 7.4**) [572]. This in turn could create a signalling platform capable of signal initiation downstream of the L-selectin tail [572]. Interestingly both K-Ras and SOS have been shown to activate p38 MAPK [730, 731], and engagement of L-selectin ectodomain stimulates the Ras pathway through SOS [245]. Additionally, Ras has been shown to mediate lamellipodia extension during cancer cell migration [732] and SOS has been seen accumulating at the leading edge of the migrating fibroblasts and COS cells [733]. It is hence possible that L-selectin clustering in the pseudopods results in CaM/ERM interaction in *cis*, association of K-Ras and SOS and recruitment of p38 MAPK to the complex. The SOS/K-Ras interaction could drive membrane extension, which could be subsequently modulated by p38 MAPK-induced shedding of L-selectin. It would be interesting to generate cell lines where L-selectin-GFP would be complimented with SOS-RFP or Ras-RFP and FRET could be measured between these molecules during TEM. Alternatively, as a more simple approach, L-selectin could be cross-linked and techniques like immunoprecipitation or affinity chromatography could be used to investigate proteins that associate with clustered L-selectin. Additionally, mutations of the serine residues within the L-selectin tail could help to understand if these amino acids are also involved in regulating the assembly of the putative signalling platforms upon clustering.

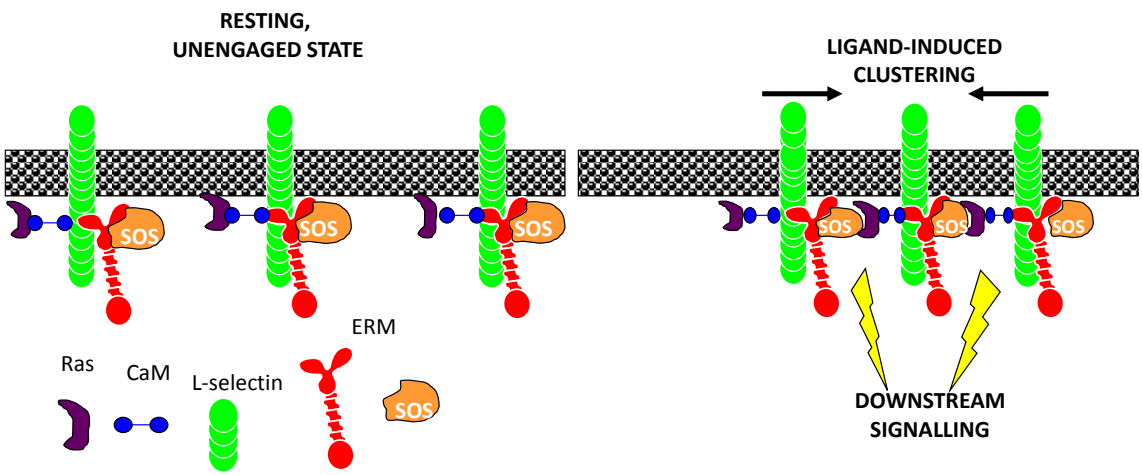

Figure 7.4 Clustering of L-selectin prompts interaction between CaM and ERM in *cis*. In resting cells, L-selectin, ERM and CaM form a heterotrimeric complex. Within the complex, ERM and CaM hold proteins involved in initiation of signalling, such as SOS and K-Ras, sufficiently far apart to prevent signal propagation. Clustering of L-selectin (as might occur in the transmigrating pseudopods) brings ERM and CaM together in *cis*, leading to binding of SOS to K-Ras, and subsequent signalling. Image was generated by Dr D. Killock as an adaptation from Killock et al., *J. Biol. Chem.*, 2009 [572].

7.7 ARE THERE ANY OTHER POTENTIAL PLAYERS THAT COULD BE INVOLVED IN L-SELECTIN-DEPENDENT SIGNALLING DURING TEM OR CHEMOTAXIS?

L-selectin clustering through ligand binding has been shown to upregulate CXCR4 chemokine receptor and maintain receptor expression at the cell surface [85, 90]. This was dependent on the activation of the Src kinases [90], and another report has shown that the Src kinase family member $p56^{lck}$ becomes activated downstream of L-selectin clustering in lymphocytes [245, 602]. It would be interesting to establish whether Src kinases are activated downstream of L-selectin in THP-1 cells, as the Src kinases have been reported to play a role in monocyte chemotaxis [734]. It would be especially interesting to investigate whether the Src kinases could bind to the full-length L-selectin or to the L-selectin "stump" generated during shedding.

Interestingly, infiltration of monocytes to the synovium of patients with rheumatoid arthritis was found to be dependent on Src/Ras/p38 MAPK pathway [734]. Even more interestingly, the chemoattractant in this case was found to be the soluble E-selectin [734], which is an L-selectin ligand for human neutrophils [381]. This highlights the importance of the signalling through Src kinases, p38 MAPK and Ras for monocyte chemotaxis, and further supports the hypothesis that these signalling molecules could be involved in the regulation of L-selectin-dependent signalling pathways during TEM and chemotaxis. It would be of interest to investigate if L-selectin from human monocytes can bind E-selectin, or if CD43/E-selectin binding on would lead to L-selectin clustering and/or shedding.

Although the work presented in this thesis goes some way to advance our understanding of the role of L-selectin in the leukocyte recruitment, a number of questions still remains to be answered and also new questions arise, what with the discoveries made in this thesis. It will be important to understand where L-selectin fits between other CAMs that can also be clustered, can transmit signalling and can be shed. It is now clear that L-selectin functions not only during leukocyte tethering and rolling, but also plays a role in leukocyte polarisation during TEM (this thesis) and mediates chemotaxis (**sections 1.7.5.1.2** and **1.11.3**). To understand how L-selectin can perform its multiple functions would be crucial in the design of novel anti-inflammatory drugs and therapies. It is plausible that interference with L-selectin shedding, modulation of the L-selectin tail

phosphorylation by specific kinase inhibitors or blocking of upstream or downstream L-selectin effectors could prove to be effective strategies for treatment of some of the chronic inflammatory diseases. Understanding what signalling platforms are being assembled at the L-selectin tail and how and when shifts in L-selectin signalling occur, would prove useful to interfere with specific stages of the leukocyte adhesion cascade without disruption of the others.

7.8 CONCLUDING REMARKS

In summary, this research project has identified a possible role for L-selectin during monocyte TEM. The results presented in this thesis suggest that L-selectin clusters and is most probably shed exclusively in the transmigrating pseudopods. This in turn results in the establishment of cell polarity, which is understood to play a crucial role in the interstitial migration of leukocytes. Hence, this thesis contributes to the current understanding of L-selectin's function by possibly bridging the gap between the role of L-selectin inside the vasculature and the role of L-selectin outside the vasculature. This could have potentially powerful therapeutic implications, especially with regard to chronic inflammatory diseases that are mediated by monocytes. However, more research is needed to fully understand the mechanisms involved in the clustering, shedding and signalling of L-selectin during TEM as well as L-selectin's relationship with other CAMs involved in the leukocyte adhesion cascade. Further assessment of full length versus cleaved L-selectin with respect to interstitial migration would be of great importance in the near future. Finally, this work has been entirely dedicated to monocytes. An important future aim would be to determine if these observations are specific to monocytes, or common to all leukocytes expressing L-selectin.

REFERENCES

1. Schulz C, Perdiguero EG, Chorro L, Szabo-Rogers H, Cagnard N, Kierdorf K, Prinz M, Wu B, Jacobsen SEW, Pollard JW, et al: **A Lineage of Myeloid Cells Independent of Myb and Hematopoietic Stem Cells.** *Science* 2012, **336:**86-90.
2. Li S, Ballou LR, Morham SG, Blatteis CM: **Cyclooxygenase-2 mediates the febrile response of mice to interleukin-1beta.** *Brain Res* 2001, **910:**163-173.
3. Portanova JP, Zhang Y, Anderson GD, Hauser SD, Masferrer JL, Seibert K, Gregory SA, Isakson PC: **Selective neutralization of prostaglandin E2 blocks inflammation, hyperalgesia, and interleukin 6 production in vivo.** *J Exp Med* 1996, **184:**883-891.
4. Freire J, Ajona D, de Biurrun G, Agorreta J, Segura V, Guruceaga E, Bleau AM, Pio R, Blanco D, Montuenga LM: **Silica-induced Chronic Inflammation Promotes Lung Carcinogenesis in the Context of an Immunosuppressive Microenvironment.** *Neoplasia* 2013, **15:**913-924.
5. Matsuzaki H, Maeda M, Lee S, Nishimura Y, Kumagai-Takei N, Hayashi H, Yamamoto S, Hatayama T, Kojima Y, Tabata R, et al: **Asbestos-induced cellular and molecular alteration of immunocompetent cells and their relationship with chronic inflammation and carcinogenesis.** *J Biomed Biotechnol* 2012, **2012:**492608.
6. Ley K, Laudanna C, Cybulsky MI, Nourshargh S: **Getting to the site of inflammation: the leukocyte adhesion cascade updated.** *Nat Rev Immunol* 2007, **7:**678-689.
7. Schmid-Schonbein GW, Usami S, Skalak R, Chien S: **The interaction of leukocytes and erythrocytes in capillary and postcapillary vessels.** *Microvasc Res* 1980, **19:**45-70.
8. Nobis U, Pries AR, Cokelet GR, Gaehtgens P: **Radial distribution of white cells during blood flow in small tubes.** *Microvascular Research* 1985, **29:**295-304.
9. Shao JY, Ting-Beall HP, Hochmuth RM: **Static and dynamic lengths of neutrophil microvilli.** *Proc Natl Acad Sci U S A* 1998, **95:**6797-6802.
10. Sundd P, Gutierrez E, Pospieszalska MK, Zhang H, Groisman A, Ley K: **Quantitative dynamic footprinting microscopy reveals mechanisms of neutrophil rolling.** *Nat Methods* 2010, **7:**821-824.
11. Arbones ML, Ord DC, Ley K, Ratech H, Maynard-Curry C, Otten G, Capon DJ, Tedder TF: **Lymphocyte homing and leukocyte rolling and migration are impaired in L-selectin-deficient mice.** *Immunity* 1994, **1:**247-260.
12. Gallatin WM, Weissman IL, Butcher EC: **A cell-surface molecule involved in organ-specific homing of lymphocytes.** *Nature* 1983, **304:**30-34.
13. Grailer JJ, Kodera M, Steeber DA: **L-selectin: role in regulating homeostasis and cutaneous inflammation.** *J Dermatol Sci* 2009, **56:**141-147.
14. Alon R, Kassner PD, Carr MW, Finger EB, Hemler ME, Springer TA: **The integrin VLA-4 supports tethering and rolling in flow on VCAM-1.** *J Cell Biol* 1995, **128:**1243-1253.
15. Berlin C, Bargatze RF, Campbell JJ, von Andrian UH, Szabo MC, Hasslen SR, Nelson RD, Berg EL, Erlandsen SL, Butcher EC: **alpha 4 integrins mediate lymphocyte attachment and rolling under physiologic flow.** *Cell* 1995, **80:**413-422.
16. Kansas GS: **Selectins and their ligands: current concepts and controversies.** *Blood* 1996, **88:**3259-3287.
17. Moore KL, Patel KD, Bruehl RE, Li F, Johnson DA, Lichenstein HS, Cummings RD, Bainton DF, McEver RP: **P-selectin glycoprotein ligand-1 mediates rolling of human neutrophils on P-selectin.** *J Cell Biol* 1995, **128:**661-671.
18. Bruehl RE, Springer TA, Bainton DF: **Quantitation of L-selectin distribution on human leukocyte microvilli by immunogold labeling and electron microscopy.** *Journal of Histochemistry & Cytochemistry* 1996, **44:**835-844.
19. Stein JV, Cheng G, Stockton BM, Fors BP, Butcher EC, von Andrian UH: **L-selectin-mediated leukocyte adhesion in vivo: microvillous distribution determines tethering efficiency, but not rolling velocity.** *J Exp Med* 1999, **189:**37-50.

20. Eriksson EE, Xie X, Werr J, Thoren P, Lindbom L: **Importance of primary capture and L-selectin-dependent secondary capture in leukocyte accumulation in inflammation and atherosclerosis in vivo.** *J Exp Med* 2001, **194:**205-218.
21. Warnock RA, Askari S, Butcher EC, von Andrian UH: **Molecular mechanisms of lymphocyte homing to peripheral lymph nodes.** *J Exp Med* 1998, **187:**205-216.
22. Galkina E, Tanousis K, Preece G, Tolaini M, Kioussis D, Florey O, Haskard DO, Tedder TF, Ager A: **L-selectin shedding does not regulate constitutive T cell trafficking but controls the migration pathways of antigen-activated T lymphocytes.** *J Exp Med* 2003, **198:**1323-1335.
23. Bullard DC, Kunkel EJ, Kubo H, Hicks MJ, Lorenzo I, Doyle NA, Doerschuk CM, Ley K, Beaudet AL: **Infectious susceptibility and severe deficiency of leukocyte rolling and recruitment in E-selectin and P-selectin double mutant mice.** *J Exp Med* 1996, **183:**2329-2336.
24. Jung U, Ley K: **Mice lacking two or all three selectins demonstrate overlapping and distinct functions for each selectin.** *J Immunol* 1999, **162:**6755-6762.
25. Mayadas TN, Johnson RC, Rayburn H, Hynes RO, Wagner DD: **Leukocyte rolling and extravasation are severely compromised in P selectin-deficient mice.** *Cell* 1993, **74:**541-554.
26. Abbassi O, Kishimoto TK, McIntire LV, Smith CW: **Neutrophil adhesion to endothelial cells.** *Blood Cells* 1993, **19:**245-259; discussion 259-260.
27. Lawrence MB, Springer TA: **Leukocytes roll on a selectin at physiologic flow rates: distinction from and prerequisite for adhesion through integrins.** *Cell* 1991, **65:**859-873.
28. Ley K, Gaehtgens P, Fennie C, Singer MS, Lasky LA, Rosen SD: **Lectin-like cell adhesion molecule 1 mediates leukocyte rolling in mesenteric venules in vivo.** *Blood* 1991, **77:**2553-2555.
29. von Andrian UH, Chambers JD, McEvoy LM, Bargatze RF, Arfors KE, Butcher EC: **Two-step model of leukocyte-endothelial cell interaction in inflammation: distinct roles for LECAM-1 and the leukocyte beta 2 integrins in vivo.** *Proc Natl Acad Sci U S A* 1991, **88:**7538-7542.
30. Olofsson AM, Arfors KE, Ramezani L, Wolitzky BA, Butcher EC, von Andrian UH: **E-selectin mediates leukocyte rolling in interleukin-1-treated rabbit mesentery venules.** *Blood* 1994, **84:**2749-2758.
31. Dore M, Korthuis RJ, Granger DN, Entman ML, Smith CW: **P-selectin mediates spontaneous leukocyte rolling in vivo.** *Blood* 1993, **82:**1308-1316.
32. Sriramarao P, von Andrian UH, Butcher EC, Bourdon MA, Broide DH: **L-selectin and very late antigen-4 integrin promote eosinophil rolling at physiological shear rates in vivo.** *J Immunol* 1994, **153:**4238-4246.
33. Sigal A, Bleijs DA, Grabovsky V, van Vliet SJ, Dwir O, Figdor CG, van Kooyk Y, Alon R: **The LFA-1 integrin supports rolling adhesions on ICAM-1 under physiological shear flow in a permissive cellular environment.** *J Immunol* 2000, **165:**442-452.
34. Chesnutt BC, Smith DF, Raffler NA, Smith ML, White EJ, Ley K: **Induction of LFA-1-dependent neutrophil rolling on ICAM-1 by engagement of E-selectin.** *Microcirculation* 2006, **13:**99-109.
35. Dunne JL, Collins RG, Beaudet AL, Ballantyne CM, Ley K: **Mac-1, but not LFA-1, uses intercellular adhesion molecule-1 to mediate slow leukocyte rolling in TNF-alpha-induced inflammation.** *J Immunol* 2003, **171:**6105-6111.
36. Green CE, Schaff UY, Sarantos MR, Lum AF, Staunton DE, Simon SI: **Dynamic shifts in LFA-1 affinity regulate neutrophil rolling, arrest, and transmigration on inflamed endothelium.** *Blood* 2006, **107:**2101-2111.
37. Chen J, Salas A, Springer TA: **Bistable regulation of integrin adhesiveness by a bipolar metal ion cluster.** *Nat Struct Biol* 2003, **10:**995-1001.

38. Kunkel EJ, Dunne JL, Ley K: **Leukocyte arrest during cytokine-dependent inflammation in vivo.** *J Immunol* 2000, **164:**3301-3308.
39. Grabovsky V, Feigelson S, Chen C, Bleijs DA, Peled A, Cinamon G, Baleux F, Arenzana-Seisdedos F, Lapidot T, van Kooyk Y, et al: **Subsecond induction of alpha4 integrin clustering by immobilized chemokines stimulates leukocyte tethering and rolling on endothelial vascular cell adhesion molecule 1 under flow conditions.** *J Exp Med* 2000, **192:**495-506.
40. Ley K, Baker JB, Cybulsky MI, Gimbrone MA, Jr., Luscinskas FW: **Intravenous interleukin-8 inhibits granulocyte emigration from rabbit mesenteric venules without altering L-selectin expression or leukocyte rolling.** *J Immunol* 1993, **151:**6347-6357.
41. Sundd P, Pospieszalska MK, Ley K: **Neutrophil rolling at high shear: Flattening, catch bond behavior, tethers and slings.** *Molecular Immunology* 2013, **55:**59-69.
42. Sundd P, Pospieszalska MK, Cheung LS, Konstantopoulos K, Ley K: **Biomechanics of leukocyte rolling.** *Biorheology* 2011, **48:**1-35.
43. Pospieszalska MK, Zarbock A, Pickard JE, Ley K: **Event-tracking model of adhesion identifies load-bearing bonds in rolling leukocytes.** *Microcirculation* 2009, **16:**115-130.
44. Lawrence MB, Kansas GS, Kunkel EJ, Ley K: **Threshold Levels of Fluid Shear Promote Leukocyte Adhesion through Selectins (CD62L,P,E).** *The Journal of Cell Biology* 1997, **136:**717-727.
45. McEver RP, Zhu C: **Rolling cell adhesion.** *Annu Rev Cell Dev Biol* 2010, **26:**363-396.
46. Yago T, Wu J, Wey CD, Klopocki AG, Zhu C, McEver RP: **Catch bonds govern adhesion through L-selectin at threshold shear.** *J Cell Biol* 2004, **166:**913-923.
47. Lou J, Yago T, Klopocki AG, Mehta P, Chen W, Zarnitsyna VI, Bovin NV, Zhu C, McEver RP: **Flow-enhanced adhesion regulated by a selectin interdomain hinge.** *J Cell Biol* 2006, **174:**1107-1117.
48. Zhu C, Yago T, Lou J, Zarnitsyna VI, McEver RP: **Mechanisms for flow-enhanced cell adhesion.** *Ann Biomed Eng* 2008, **36:**604-621.
49. Marshall BT, Long M, Piper JW, Yago T, McEver RP, Zhu C: **Direct observation of catch bonds involving cell-adhesion molecules.** *Nature* 2003, **423:**190-193.
50. Sarangapani KK, Yago T, Klopocki AG, Lawrence MB, Fieger CB, Rosen SD, McEver RP, Zhu C: **Low force decelerates L-selectin dissociation from P-selectin glycoprotein ligand-1 and endoglycan.** *J Biol Chem* 2004, **279:**2291-2298.
51. Kunkel EJ, Ley K: **Distinct phenotype of E-selectin-deficient mice. E-selectin is required for slow leukocyte rolling in vivo.** *Circ Res* 1996, **79:**1196-1204.
52. Jung U, Bullard DC, Tedder TF, Ley K: **Velocity differences between L- and P-selectin-dependent neutrophil rolling in venules of mouse cremaster muscle in vivo.** *Am J Physiol* 1996, **271:**H2740-2747.
53. Lawrence MB, Bainton DF, Springer TA: **Neutrophil tethering to and rolling on E-selectin are separable by requirement for L-selectin.** *Immunity* 1994, **1:**137-145.
54. Alon R, Fuhlbrigge RC, Finger EB, Springer TA: **Interactions through L-selectin between leukocytes and adherent leukocytes nucleate rolling adhesions on selectins and VCAM-1 in shear flow.** *The Journal of Cell Biology* 1996, **135:**849-865.
55. Jung S, Swinney HL: **Velocity difference statistics in turbulence.** *Phys Rev E Stat Nonlin Soft Matter Phys* 2005, **72:**026304.
56. Luscinskas FW, Ding H, Tan P, Cumming D, Tedder TF, Gerritsen ME: **L- and P-selectins, but not CD49d (VLA-4) integrins, mediate monocyte initial attachment to TNF-alpha-activated vascular endothelium under flow in vitro.** *J Immunol* 1996, **157:**326-335.
57. Jung U, Norman KE, Scharffetter-Kochanek K, Beaudet AL, Ley K: **Transit time of leukocytes rolling through venules controls cytokine-induced inflammatory cell recruitment in vivo.** *J Clin Invest* 1998, **102:**1526-1533.

58. Lawrence MB, Springer TA: **Leukocytes roll on a selectin at physiologic flow rates: Distinction from and prerequisite for adhesion through integrins.** *Cell* 1991, **65:**859-873.
59. Campbell JJ, Hedrick J, Zlotnik A, Siani MA, Thompson DA, Butcher EC: **Chemokines and the Arrest of Lymphocytes Rolling Under Flow Conditions.** *Science* 1998, **279:**381-384.
60. Bargatze RF, Kurk S, Butcher EC, Jutila MA: **Neutrophils roll on adherent neutrophils bound to cytokine-induced endothelial cells via L-selectin on the rolling cells.** *The Journal of Experimental Medicine* 1994, **180:**1785-1792.
61. Walcheck B, Moore KL, McEver RP, Kishimoto TK: **Neutrophil-neutrophil interactions under hydrodynamic shear stress involve L-selectin and PSGL-1. A mechanism that amplifies initial leukocyte accumulation of P-selectin in vitro.** *J Clin Invest* 1996, **98:**1081-1087.
62. Sperandio M, Smith ML, Forlow SB, Olson TS, Xia L, McEver RP, Ley K: **P-selectin glycoprotein ligand-1 mediates L-selectin-dependent leukocyte rolling in venules.** *J Exp Med* 2003, **197:**1355-1363.
63. Kadash KE, Lawrence MB, Diamond SL: **Neutrophil string formation: hydrodynamic thresholding and cellular deformation during cell collisions.** *Biophys J* 2004, **86:**4030-4039.
64. Paschall CD, Lawrence MB: **L-selectin shear thresholding modulates leukocyte secondary capture.** *Ann Biomed Eng* 2008, **36:**622-631.
65. Kunkel EJ, Chomas JE, Ley K: **Role of primary and secondary capture for leukocyte accumulation in vivo.** *Circ Res* 1998, **82:**30-38.
66. King MR, Hammer DA: **Multiparticle adhesive dynamics: hydrodynamic recruitment of rolling leukocytes.** *Proc Natl Acad Sci U S A* 2001, **98:**14919-14924.
67. Rainger GE, Fisher AC, Nash GB: **Endothelial-borne platelet-activating factor and interleukin-8 rapidly immobilize rolling neutrophils.** *Am J Physiol* 1997, **272:**H114-122.
68. Chan JR, Hyduk SJ, Cybulsky MI: **Chemoattractants Induce a Rapid and Transient Upregulation of Monocyte α4 Integrin Affinity for Vascular Cell Adhesion Molecule 1 Which Mediates Arrest.** *The Journal of Experimental Medicine* 2001, **193:**1149-1158.
69. Gerszten RE, Garcia-Zepeda EA, Lim YC, Yoshida M, Ding HA, Gimbrone MA, Jr., Luster AD, Luscinskas FW, Rosenzweig A: **MCP-1 and IL-8 trigger firm adhesion of monocytes to vascular endothelium under flow conditions.** *Nature* 1999, **398:**718-723.
70. Carveth HJ, Bohnsack JF, McIntyre TM, Baggiolini M, Prescott SM, Zimmerman GA: **Neutrophil activating factor (NAF) induces polymorphonuclear leukocyte adherence to endothelial cells and to subendothelial matrix proteins.** *Biochem Biophys Res Commun* 1989, **162:**387-393.
71. Weber C, Kitayama J, Springer TA: **Differential regulation of beta 1 and beta 2 integrin avidity by chemoattractants in eosinophils.** *Proc Natl Acad Sci U S A* 1996, **93:**10939-10944.
72. Jiang Y, Zhu JF, Luscinskas FW, Graves DT: **MCP-1-stimulated monocyte attachment to laminin is mediated by beta 2-integrins.** *Am J Physiol* 1994, **267:**C1112-1118.
73. Szabo MC, Butcher EC, McIntyre BW, Schall TJ, Bacon KB: **RANTES stimulation of T lymphocyte adhesion and activation: role for LFA-1 and ICAM-3.** *Eur J Immunol* 1997, **27:**1061-1068.
74. Luscinskas FW, Gerszten RE, Garcia-Zepeda EA, Lim Y-C, Yoshida M, Ding HA, Gimbrone MA, Luster AD, Rosenzweig A: **C-C and C-X-C Chemokines Trigger Firm Adhesion of Monocytes to Vascular Endothelium under Flow Conditionsa.** *Annals of the New York Academy of Sciences* 2000, **902:**288-293.
75. Shamri R, Grabovsky V, Gauguet JM, Feigelson S, Manevich E, Kolanus W, Robinson MK, Staunton DE, von Andrian UH, Alon R: **Lymphocyte arrest requires instantaneous induction of an extended LFA-1 conformation mediated by endothelium-bound chemokines.** *Nat Immunol* 2005, **6:**497-506.

76. Weber C, Alon R, Moser B, Springer TA: **Sequential regulation of alpha 4 beta 1 and alpha 5 beta 1 integrin avidity by CC chemokines in monocytes: implications for transendothelial chemotaxis.** *J Cell Biol* 1996, **134:**1063-1073.
77. Takagi J, Petre BM, Walz T, Springer TA: **Global conformational rearrangements in integrin extracellular domains in outside-in and inside-out signaling.** *Cell* 2002, **110:**599-511.
78. Salas A, Shimaoka M, Chen S, Carman CV, Springer T: **Transition from rolling to firm adhesion is regulated by the conformation of the I domain of the integrin lymphocyte function-associated antigen-1.** *J Biol Chem* 2002, **277:**50255-50262.
79. Chen C, Mobley JL, Dwir O, Shimron F, Grabovsky V, Lobb RR, Shimizu Y, Alon R: **High affinity very late antigen-4 subsets expressed on T cells are mandatory for spontaneous adhesion strengthening but not for rolling on VCAM-1 in shear flow.** *J Immunol* 1999, **162:**1084-1095.
80. Constantin G, Majeed M, Giagulli C, Piccio L, Kim JY, Butcher EC, Laudanna C: **Chemokines Trigger Immediate β2 Integrin Affinity and Mobility Changes: Differential Regulation and Roles in Lymphocyte Arrest under Flow.** *Immunity* 2000, **13:**759-769.
81. Nijhara R, van Hennik PB, Gignac ML, Kruhlak MJ, Hordijk PL, Delon J, Shaw S: **Rac1 Mediates Collapse of Microvilli on Chemokine-Activated T Lymphocytes.** *The Journal of Immunology* 2004, **173:**4985-4993.
82. Simon SI, Hu Y, Vestweber D, Smith CW: **Neutrophil Tethering on E-Selectin Activates {beta}2 Integrin Binding to ICAM-1 Through a Mitogen-Activated Protein Kinase Signal Transduction Pathway.** *J Immunol* 2000, **164:**4348-4358.
83. Evangelista V, Manarini S, Sideri R, Rotondo S, Martelli N, Piccoli A, Totani L, Piccardoni P, Vestweber D, de Gaetano G, Cerletti C: **Platelet/polymorphonuclear leukocyte interaction: P-selectin triggers protein-tyrosine phosphorylation-dependent CD11b/CD18 adhesion: role of PSGL-1 as a signaling molecule.** *Blood* 1999, **93:**876-885.
84. Blanks JE, Moll T, Eytner R, Vestweber D: **Stimulation of P-selectin glycoprotein ligand-1 on mouse neutrophils activates beta 2-integrin mediated cell attachment to ICAM-1.** *Eur J Immunol* 1998, **28:**433-443.
85. Ding Z, Issekutz TB, Downey GP, Waddell TK: **L-selectin stimulation enhances functional expression of surface CXCR4 in lymphocytes: implications for cellular activation during adhesion and migration.** *Blood* 2003, **101:**4245-4252.
86. Hwang ST, Singer MS, Giblin PA, Yednock TA, Bacon KB, Simon SI, Rosen SD: **GlyCAM-1, a physiologic ligand for L-selectin, activates beta 2 integrins on naive peripheral lymphocytes.** *The Journal of Experimental Medicine* 1996, **184:**1343-1348.
87. Green CE, Pearson DN, Christensen NB, Simon SI: **Topographic requirements and dynamics of signaling via L-selectin on neutrophils.** *American Journal of Physiology - Cell Physiology* 2003, **284:**C705-C717.
88. Giblin P, Hwang S, Katsumoto T, Rosen S: **Ligation of L-selectin on T lymphocytes activates beta1 integrins and promotes adhesion to fibronectin.** *J Immunol* 1997, **159:**3498-3507.
89. Crockett-Torabi E, Sulenbarger B, Smith CW, Fantone JC: **Activation of human neutrophils through L-selectin and Mac-1 molecules.** *J Immunol* 1995, **154:**2291-2302.
90. Duchesneau P, Gallagher E, Walcheck B, Waddell TK: **Up-regulation of leukocyte CXCR4 expression by sulfatide: an L-selectin-dependent pathway on CD4+ T cells.** *Eur J Immunol* 2007, **37:**2949-2960.
91. Tsang YT, Neelamegham S, Hu Y, Berg EL, Burns AR, Smith CW, Simon SI: **Synergy between L-selectin signaling and chemotactic activation during neutrophil adhesion and transmigration.** *The Journal of Immunology* 1997, **159:**4566-4577.

92. Spertini O, Kansas GS, Munro JM, Griffin JD, Tedder TF: **Regulation of leukocyte migration by activation of the leukocyte adhesion molecule-1 (LAM-1) selectin.** *Nature* 1991, **349:**691-694.
93. Totani L, Evangelista V: **Platelet-leukocyte interactions in cardiovascular disease and beyond.** *Arterioscler Thromb Vasc Biol* 2010, **30:**2357-2361.
94. Beglova N, Blacklow SC, Takagi J, Springer TA: **Cysteine-rich module structure reveals a fulcrum for integrin rearrangement upon activation.** *Nat Struct Biol* 2002, **9:**282-287.
95. Moser M, Bauer M, Schmid S, Ruppert R, Schmidt S, Sixt M, Wang HV, Sperandio M, Fassler R: **Kindlin-3 is required for beta2 integrin-mediated leukocyte adhesion to endothelial cells.** *Nat Med* 2009, **15:**300-305.
96. Malinin NL, Zhang L, Choi J, Ciocea A, Razorenova O, Ma YQ, Podrez EA, Tosi M, Lennon DP, Caplan AI, et al: **A point mutation in KINDLIN3 ablates activation of three integrin subfamilies in humans.** *Nat Med* 2009, **15:**313-318.
97. Hyduk SJ, Rullo J, Cano AP, Xiao H, Chen M, Moser M, Cybulsky MI: **Talin-1 and kindlin-3 regulate alpha4beta1 integrin-mediated adhesion stabilization, but not G protein-coupled receptor-induced affinity upregulation.** *J Immunol* 2011, **187:**4360-4368.
98. Bouaouina M, Lad Y, Calderwood DA: **The N-terminal domains of talin cooperate with the phosphotyrosine binding-like domain to activate beta1 and beta3 integrins.** *J Biol Chem* 2008, **283:**6118-6125.
99. Calderwood DA, Zent R, Grant R, Rees DJ, Hynes RO, Ginsberg MH: **The Talin head domain binds to integrin beta subunit cytoplasmic tails and regulates integrin activation.** *J Biol Chem* 1999, **274:**28071-28074.
100. Svensson L, Howarth K, McDowall A, Patzak I, Evans R, Ussar S, Moser M, Metin A, Fried M, Tomlinson I, Hogg N: **Leukocyte adhesion deficiency-III is caused by mutations in KINDLIN3 affecting integrin activation.** *Nat Med* 2009, **15:**306-312.
101. McDowall A, Svensson L, Stanley P, Patzak I, Chakravarty P, Howarth K, Sabnis H, Briones M, Hogg N: **Two mutations in the KINDLIN3 gene of a new leukocyte adhesion deficiency III patient reveal distinct effects on leukocyte function in vitro.** *Blood* 2010, **115:**4834-4842.
102. Rantala JK, Pouwels J, Pellinen T, Veltel S, Laasola P, Mattila E, Potter CS, Duffy T, Sundberg JP, Kallioniemi O, et al: **SHARPIN is an endogenous inhibitor of beta1-integrin activation.** *Nat Cell Biol* 2011, **13:**1315-1324.
103. Kempf T, Zarbock A, Widera C, Butz S, Stadtmann A, Rossaint J, Bolomini-Vittori M, Korf-Klingebiel M, Napp LC, Hansen B, et al: **GDF-15 is an inhibitor of leukocyte integrin activation required for survival after myocardial infarction in mice.** *Nat Med* 2011, **17:**581-588.
104. Marlin SD, Springer TA: **Purified intercellular adhesion molecule-1 (ICAM-1) is a ligand for lymphocyte function-associated antigen 1 (LFA-1).** *Cell* 1987, **51:**813-819.
105. Rothlein R, Dustin ML, Marlin SD, Springer TA: **A human intercellular adhesion molecule (ICAM-1) distinct from LFA-1.** *J Immunol* 1986, **137:**1270-1274.
106. Makgoba MW, Sanders ME, Ginther Luce GE, Dustin ML, Springer TA, Clark EA, Mannoni P, Shaw S: **ICAM-1 a ligand for LFA-1-dependent adhesion of B, T and myeloid cells.** *Nature* 1988, **331:**86-88.
107. Staunton DE, Dustin ML, Springer TA: **Functional cloning of ICAM-2, a cell adhesion ligand for LFA-1 homologous to ICAM-1.** *Nature* 1989, **339:**61-64.
108. Diamond MS, Staunton DE, de Fougerolles AR, Stacker SA, Garcia-Aguilar J, Hibbs ML, Springer TA: **ICAM-1 (CD54): a counter-receptor for Mac-1 (CD11b/CD18).** *J Cell Biol* 1990, **111:**3129-3139.
109. Chavakis T, Bierhaus A, Al-Fakhri N, Schneider D, Witte S, Linn T, Nagashima M, Morser J, Arnold B, Preissner KT, Nawroth PP: **The Pattern Recognition Receptor (RAGE) Is a Counterreceptor for Leukocyte Integrins.** *The Journal of Experimental Medicine* 2003, **198:**1507-1515.

110. Hyduk SJ, Cybulsky MI: **Role of alpha4beta1 integrins in chemokine-induced monocyte arrest under conditions of shear stress.** *Microcirculation* 2009, **16:**17-30.
111. Berlin C, Berg EL, Briskin MJ, Andrew DP, Kilshaw PJ, Holzmann B, Weissman IL, Hamann A, Butcher EC: **Alpha 4 beta 7 integrin mediates lymphocyte binding to the mucosal vascular addressin MAdCAM-1.** *Cell* 1993, **74:**185-195.
112. Giagulli C, Ottoboni L, Caveggion E, Rossi B, Lowell C, Constantin G, Laudanna C, Berton G: **The Src family kinases Hck and Fgr are dispensable for inside-out, chemoattractant-induced signaling regulating beta 2 integrin affinity and valency in neutrophils, but are required for beta 2 integrin-mediated outside-in signaling involved in sustained adhesion.** *J Immunol* 2006, **177:**604-611.
113. Gakidis MAM, Cullere X, Olson T, Wilsbacher JL, Zhang B, Moores SL, Ley K, Swat W, Mayadas T, Brugge JS: **Vav GEFs are required for β2 integrin-dependent functions of neutrophils.** *The Journal of Cell Biology* 2004, **166:**273-282.
114. Phillipson M, Heit B, Colarusso P, Liu L, Ballantyne CM, Kubes P: **Intraluminal crawling of neutrophils to emigration sites: a molecularly distinct process from adhesion in the recruitment cascade.** *J Exp Med* 2006, **203:**2569-2575.
115. Bartholomaus I, Kawakami N, Odoardi F, Schlager C, Miljkovic D, Ellwart JW, Klinkert WE, Flugel-Koch C, Issekutz TB, Wekerle H, Flugel A: **Effector T cell interactions with meningeal vascular structures in nascent autoimmune CNS lesions.** *Nature* 2009, **462:**94-98.
116. Frommhold D, Kamphues A, Hepper I, Pruenster M, Lukic IK, Socher I, Zablotskaya V, Buschmann K, Lange-Sperandio B, Schymeinsky J, et al: **RAGE and ICAM-1 cooperate in mediating leukocyte recruitment during acute inflammation in vivo.** *Blood* 2010.
117. Schenkel AR, Mamdouh Z, Muller WA: **Locomotion of monocytes on endothelium is a critical step during extravasation.** *Nat Immunol* 2004, **5:**393-400.
118. Heasman SJ, Carlin LM, Cox S, Ng T, Ridley AJ: **Coordinated RhoA signaling at the leading edge and uropod is required for T cell transendothelial migration.** *J Cell Biol* 2010, **190:**553-563.
119. Alstergren P, Zhu B, Glougauer M, Mak TW, Ellen RP, Sodek J: **Polarization and directed migration of murine neutrophils is dependent on cell surface expression of CD44.** *Cellular Immunology*, **231:**146-157.
120. Alstergren P, Zhu B, Glogauer M, Mak TW, Ellen RP, Sodek J: **Polarization and directed migration of murine neutrophils is dependent on cell surface expression of CD44.** *Cell Immunol* 2004, **231:**146-157.
121. Sasawatari S, Yoshizaki M, Taya C, Tazawa A, Furuyama-Tanaka K, Yonekawa H, Dohi T, Makrigiannis AP, Sasazuki T, Inaba K, Toyama-Sorimachi N: **The Ly49Q receptor plays a crucial role in neutrophil polarization and migration by regulating raft trafficking.** *Immunity* 2010, **32:**200-213.
122. Barreiro O, Zamai M, Yanez-Mo M, Tejera E, Lopez-Romero P, Monk PN, Gratton E, Caiolfa VR, Sanchez-Madrid F: **Endothelial adhesion receptors are recruited to adherent leukocytes by inclusion in preformed tetraspanin nanoplatforms.** *J Cell Biol* 2008, **183:**527-542.
123. Rohlena J, Volger OL, van Buul JD, Hekking LH, van Gils JM, Bonta PI, Fontijn RD, Post JA, Hordijk PL, Horrevoets AJ: **Endothelial CD81 is a marker of early human atherosclerotic plaques and facilitates monocyte adhesion.** *Cardiovasc Res* 2009, **81:**187-196.
124. Barreiro O, de la Fuente H, Mittelbrunn M, Sanchez-Madrid F: **Functional insights on the polarized redistribution of leukocyte integrins and their ligands during leukocyte migration and immune interactions.** *Immunol Rev* 2007, **218:**147-164.
125. Carman CV, Springer TA: **A transmigratory cup in leukocyte diapedesis both through individual vascular endothelial cells and between them.** *J Cell Biol* 2004, **167:**377-388.

126. Yang L, Froio RM, Sciuto TE, Dvorak AM, Alon R, Luscinskas FW: **ICAM-1 regulates neutrophil adhesion and transcellular migration of TNF-alpha-activated vascular endothelium under flow.** *Blood* 2005, **106:**584-592.
127. Barreiro O, Yanez-Mo M, Serrador JM, Montoya MC, Vicente-Manzanares M, Tejedor R, Furthmayr H, Sanchez-Madrid F: **Dynamic interaction of VCAM-1 and ICAM-1 with moesin and ezrin in a novel endothelial docking structure for adherent leukocytes.** *J Cell Biol* 2002, **157:**1233-1245.
128. Phillipson M, Kaur J, Colarusso P, Ballantyne CM, Kubes P: **Endothelial domes encapsulate adherent neutrophils and minimize increases in vascular permeability in paracellular and transcellular emigration.** *PLoS One* 2008, **3:**e1649.
129. Millan J, Hewlett L, Glyn M, Toomre D, Clark P, Ridley AJ: **Lymphocyte transcellular migration occurs through recruitment of endothelial ICAM-1 to caveola- and F-actin-rich domains.** *Nat Cell Biol* 2006, **8:**113-123.
130. Shaw SK, Ma S, Kim MB, Rao RM, Hartman CU, Froio RM, Yang L, Jones T, Liu Y, Nusrat A, et al: **Coordinated redistribution of leukocyte LFA-1 and endothelial cell ICAM-1 accompany neutrophil transmigration.** *J Exp Med* 2004, **200:**1571-1580.
131. Muller WA: **Mechanisms of leukocyte transendothelial migration.** *Annu Rev Pathol* 2011, **6:**323-344.
132. Marchesi VT: **The site of leucocyte emigration during inflammation.** *Q J Exp Physiol Cogn Med Sci* 1961, **46:**115-118.
133. Schoefl GI: **The migration of lymphocytes across the vascular endothelium in lymphoid tissue. A reexamination.** *J Exp Med* 1972, **136:**568-588.
134. Anderson AO, Anderson ND: **Lymphocyte emigration from high endothelial venules in rat lymph nodes.** *Immunology* 1976, **31:**731-748.
135. Marchesi VT, Gowans JL: **The Migration of Lymphocytes through the Endothelium of Venules in Lymph Nodes: An Electron Microscope Study.** *Proc R Soc Lond B Biol Sci* 1964, **159:**283-290.
136. Farr AG, De Bruyn PP: **The mode of lymphocyte migration through postcapillary venule endothelium in lymph node.** *Am J Anat* 1975, **143:**59-92.
137. Feng D, Nagy JA, Pyne K, Dvorak HF, Dvorak AM: **Neutrophils emigrate from venules by a transendothelial cell pathway in response to FMLP.** *J Exp Med* 1998, **187:**903-915.
138. Hoshi O, Ushiki T: **Scanning electron microscopic studies on the route of neutrophil extravasation in the mouse after exposure to the chemotactic peptide N-formyl-methionyl-leucyl-phenylalanine (fMLP).** *Arch Histol Cytol* 1999, **62:**253-260.
139. Mamdouh Z, Mikhailov A, Muller WA: **Transcellular migration of leukocytes is mediated by the endothelial lateral border recycling compartment.** *J Exp Med* 2009, **206:**2795-2808.
140. Carman CV, Sage PT, Sciuto TE, de la Fuente MA, Geha RS, Ochs HD, Dvorak HF, Dvorak AM, Springer TA: **Transcellular diapedesis is initiated by invasive podosomes.** *Immunity* 2007, **26:**784-797.
141. Carman CV, Springer TA: **Trans-cellular migration: cell-cell contacts get intimate.** *Curr Opin Cell Biol* 2008, **20:**533-540.
142. Lossinsky AS, Shivers RR: **Structural pathways for macromolecular and cellular transport across the blood-brain barrier during inflammatory conditions. Review.** *Histol Histopathol* 2004, **19:**535-564.
143. Wolburg H, Wolburg-Buchholz K, Engelhardt B: **Diapedesis of mononuclear cells across cerebral venules during experimental autoimmune encephalomyelitis leaves tight junctions intact.** *Acta Neuropathol* 2005, **109:**181-190.
144. Gerard A, van der Kammen RA, Janssen H, Ellenbroek SI, Collard JG: **The Rac activator Tiam1 controls efficient T-cell trafficking and route of transendothelial migration.** *Blood* 2009, **113:**6138-6147.

145. Schulte D, Kuppers V, Dartsch N, Broermann A, Li H, Zarbock A, Kamenyeva O, Kiefer F, Khandoga A, Massberg S, Vestweber D: **Stabilizing the VE-cadherin-catenin complex blocks leukocyte extravasation and vascular permeability.** *EMBO J* 2011, **30:**4157-4170.
146. Alcaide P, Newton G, Auerbach S, Sehrawat S, Mayadas TN, Golan DE, Yacono P, Vincent P, Kowalczyk A, Luscinskas FW: **p120-Catenin regulates leukocyte transmigration through an effect on VE-cadherin phosphorylation.** *Blood* 2008, **112:**2770-2779.
147. Allingham MJ, van Buul JD, Burridge K: **ICAM-1-mediated, Src- and Pyk2-dependent vascular endothelial cadherin tyrosine phosphorylation is required for leukocyte transendothelial migration.** *J Immunol* 2007, **179:**4053-4064.
148. Imhof BA, Aurrand-Lions M: **Adhesion mechanisms regulating the migration of monocytes.** *Nat Rev Immunol* 2004, **4:**432-444.
149. Wegmann F, Petri B, Khandoga AG, Moser C, Khandoga A, Volkery S, Li H, Nasdala I, Brandau O, Fassler R, et al: **ESAM supports neutrophil extravasation, activation of Rho, and VEGF-induced vascular permeability.** *J Exp Med* 2006, **203:**1671-1677.
150. Schenkel AR, Mamdouh Z, Chen X, Liebman RM, Muller WA: **CD99 plays a major role in the migration of monocytes through endothelial junctions.** *Nat Immunol* 2002, **3:**143-150.
151. Lou O, Alcaide P, Luscinskas FW, Muller WA: **CD99 is a key mediator of the transendothelial migration of neutrophils.** *J Immunol* 2007, **178:**1136-1143.
152. Sans E, Delachanal E, Duperray A: **Analysis of the roles of ICAM-1 in neutrophil transmigration using a reconstituted mammalian cell expression model: implication of ICAM-1 cytoplasmic domain and Rho-dependent signaling pathway.** *J Immunol* 2001, **166:**544-551.
153. Mamdouh Z, Chen X, Pierini LM, Maxfield FR, Muller WA: **Targeted recycling of PECAM from endothelial surface-connected compartments during diapedesis.** *Nature* 2003, **421:**748-753.
154. Mamdouh Z, Kreitzer GE, Muller WA: **Leukocyte transmigration requires kinesin-mediated microtubule-dependent membrane trafficking from the lateral border recycling compartment.** *J Exp Med* 2008, **205:**951-966.
155. Florey O, Durgan J, Muller W: **Phosphorylation of leukocyte PECAM and its association with detergent-resistant membranes regulate transendothelial migration.** *J Immunol* 2010, **185:**1878-1886.
156. Woodfin A, Voisin MB, Imhof BA, Dejana E, Engelhardt B, Nourshargh S: **Endothelial cell activation leads to neutrophil transmigration as supported by the sequential roles of ICAM-2, JAM-A, and PECAM-1.** *Blood* 2009, **113:**6246-6257.
157. Woodfin A, Reichel CA, Khandoga A, Corada M, Voisin MB, Scheiermann C, Haskard DO, Dejana E, Krombach F, Nourshargh S: **JAM-A mediates neutrophil transmigration in a stimulus-specific manner in vivo: evidence for sequential roles for JAM-A and PECAM-1 in neutrophil transmigration.** *Blood* 2007, **110:**1848-1856.
158. Woodfin A, Voisin MB, Nourshargh S: **PECAM-1: a multi-functional molecule in inflammation and vascular biology.** *Arterioscler Thromb Vasc Biol* 2007, **27:**2514-2523.
159. Ostermann G, Weber KS, Zernecke A, Schroder A, Weber C: **JAM-1 is a ligand of the beta(2) integrin LFA-1 involved in transendothelial migration of leukocytes.** *Nat Immunol* 2002, **3:**151-158.
160. Dangerfield J, Larbi KY, Huang MT, Dewar A, Nourshargh S: **PECAM-1 (CD31) homophilic interaction up-regulates alpha6beta1 on transmigrated neutrophils in vivo and plays a functional role in the ability of alpha6 integrins to mediate leukocyte migration through the perivascular basement membrane.** *J Exp Med* 2002, **196:**1201-1211.
161. Woodfin A, Voisin MB, Beyrau M, Colom B, Caille D, Diapouli FM, Nash GB, Chavakis T, Albelda SM, Rainger GE, et al: **The junctional adhesion molecule JAM-C regulates**

polarized transendothelial migration of neutrophils in vivo. *Nat Immunol* 2011, **12:**761-769.
162. Nourshargh S, Hordijk PL, Sixt M: **Breaching multiple barriers: leukocyte motility through venular walls and the interstitium.** *Nat Rev Mol Cell Biol* 2010, **11:**366-378.
163. Hanna S, Etzioni A: **Leukocyte adhesion deficiencies.** *Annals of the New York Academy of Sciences* 2012, **1250:**50-55.
164. Etzioni A, Frydman M, Pollack S, Avidor I, Phillips ML, Paulson JC, Gershoni-Baruch R: **Brief report: recurrent severe infections caused by a novel leukocyte adhesion deficiency.** *N Engl J Med* 1992, **327:**1789-1792.
165. Crowley CA, Curnutte JT, Rosin RE, Andre-Schwartz J, Gallin JI, Klempner M, Snyderman R, Southwick FS, Stossel TP, Babior BM: **An inherited abnormality of neutrophil adhesion. Its genetic transmission and its association with a missing protein.** *N Engl J Med* 1980, **302:**1163-1168.
166. Kuijpers TW, Van Lier RA, Hamann D, de Boer M, Thung LY, Weening RS, Verhoeven AJ, Roos D: **Leukocyte adhesion deficiency type 1 (LAD-1)/variant. A novel immunodeficiency syndrome characterized by dysfunctional beta2 integrins.** *J Clin Invest* 1997, **100:**1725-1733.
167. Schmidt S, Moser M, Sperandio M: **The molecular basis of leukocyte recruitment and its deficiencies.** *Mol Immunol* 2013, **55:**49-58.
168. Kishimoto TK, Hollander N, Roberts TM, Anderson DC, Springer TA: **Heterogeneous mutations in the beta subunit common to the LFA-1, Mac-1, and p150,95 glycoproteins cause leukocyte adhesion deficiency.** *Cell* 1987, **50:**193-202.
169. von Andrian UH, Berger EM, Ramezani L, Chambers JD, Ochs HD, Harlan JM, Paulson JC, Etzioni A, Arfors KE: **In vivo behavior of neutrophils from two patients with distinct inherited leukocyte adhesion deficiency syndromes.** *J Clin Invest* 1993, **91:**2893-2897.
170. Luhn K, Wild MK, Eckhardt M, Gerardy-Schahn R, Vestweber D: **The gene defective in leukocyte adhesion deficiency II encodes a putative GDP-fucose transporter.** *Nat Genet* 2001, **28:**69-72.
171. Lubke T, Marquardt T, Etzioni A, Hartmann E, von Figura K, Korner C: **Complementation cloning identifies CDG-IIc, a new type of congenital disorders of glycosylation, as a GDP-fucose transporter deficiency.** *Nat Genet* 2001, **28:**73-76.
172. Homeister JW, Thall AD, Petryniak B, Maly P, Rogers CE, Smith PL, Kelly RJ, Gersten KM, Askari SW, Cheng G, et al: **The alpha(1,3)fucosyltransferases FucT-IV and FucT-VII exert collaborative control over selectin-dependent leukocyte recruitment and lymphocyte homing.** *Immunity* 2001, **15:**115-126.
173. Pasvolsky R, Feigelson SW, Kilic SS, Simon AJ, Tal-Lapidot G, Grabovsky V, Crittenden JR, Amariglio N, Safran M, Graybiel AM, et al: **A LAD-III syndrome is associated with defective expression of the Rap-1 activator CalDAG-GEFI in lymphocytes, neutrophils, and platelets.** *J Exp Med* 2007, **204:**1571-1582.
174. Bergmeier W, Goerge T, Wang HW, Crittenden JR, Baldwin AC, Cifuni SM, Housman DE, Graybiel AM, Wagner DD: **Mice lacking the signaling molecule CalDAG-GEFI represent a model for leukocyte adhesion deficiency type III.** *J Clin Invest* 2007, **117:**1699-1707.
175. Limaye V, Vadas M: **The vascular endothelium: structure and function.** In *Mechanisms of Vascular Disease: A Textbook for Vascular Surgeons.* Edited by Thompson RFaM. Cambridge: Cambridge University Press 2007: 1-8
176. Millan J, Cain RJ, Reglero-Real N, Bigarella C, Marcos-Ramiro B, Fernandez-Martin L, Correas I, Ridley AJ: **Adherens junctions connect stress fibres between adjacent endothelial cells.** *BMC Biol* 2010, **8:**11.
177. Dejana E, Corada M, Lampugnani MG: **Endothelial cell-to-cell junctions.** *FASEB J* 1995, **9:**910-918.
178. Farquhar MG, Palade GE: **Junctional complexes in various epithelia.** *J Cell Biol* 1963, **17:**375-412.

179. Schneeberger EE, Lynch RD: **Structure, function, and regulation of cellular tight junctions.** *Am J Physiol* 1992, **262:**L647-661.
180. Furuse M, Fujita K, Hiiragi T, Fujimoto K, Tsukita S: **Claudin-1 and -2: novel integral membrane proteins localizing at tight junctions with no sequence similarity to occludin.** *J Cell Biol* 1998, **141:**1539-1550.
181. Sonoda N, Furuse M, Sasaki H, Yonemura S, Katahira J, Horiguchi Y, Tsukita S: **Clostridium perfringens enterotoxin fragment removes specific claudins from tight junction strands: Evidence for direct involvement of claudins in tight junction barrier.** *J Cell Biol* 1999, **147:**195-204.
182. Wilcox ER, Burton QL, Naz S, Riazuddin S, Smith TN, Ploplis B, Belyantseva I, Ben-Yosef T, Liburd NA, Morell RJ, et al: **Mutations in the gene encoding tight junction claudin-14 cause autosomal recessive deafness DFNB29.** *Cell* 2001, **104:**165-172.
183. Niimi T, Nagashima K, Ward JM, Minoo P, Zimonjic DB, Popescu NC, Kimura S: **claudin-18, a novel downstream target gene for the T/EBP/NKX2.1 homeodomain transcription factor, encodes lung- and stomach-specific isoforms through alternative splicing.** *Mol Cell Biol* 2001, **21:**7380-7390.
184. Furuse M, Sasaki H, Tsukita S: **Manner of interaction of heterogeneous claudin species within and between tight junction strands.** *J Cell Biol* 1999, **147:**891-903.
185. Inai T, Kobayashi J, Shibata Y: **Claudin-1 contributes to the epithelial barrier function in MDCK cells.** *Eur J Cell Biol* 1999, **78:**849-855.
186. McCarthy KM, Francis SA, McCormack JM, Lai J, Rogers RA, Skare IB, Lynch RD, Schneeberger EE: **Inducible expression of claudin-1-myc but not occludin-VSV-G results in aberrant tight junction strand formation in MDCK cells.** *J Cell Sci* 2000, **113 Pt 19:**3387-3398.
187. Colegio OR, Van Itallie CM, McCrea HJ, Rahner C, Anderson JM: **Claudins create charge-selective channels in the paracellular pathway between epithelial cells.** *Am J Physiol Cell Physiol* 2002, **283:**C142-147.
188. Furuse M, Hirase T, Itoh M, Nagafuchi A, Yonemura S, Tsukita S, Tsukita S: **Occludin: a novel integral membrane protein localizing at tight junctions.** *J Cell Biol* 1993, **123:**1777-1788.
189. Liu Y, Nusrat A, Schnell FJ, Reaves TA, Walsh S, Pochet M, Parkos CA: **Human junction adhesion molecule regulates tight junction resealing in epithelia.** *J Cell Sci* 2000, **113 (Pt 13):**2363-2374.
190. Nasdala I, Wolburg-Buchholz K, Wolburg H, Kuhn A, Ebnet K, Brachtendorf G, Samulowitz U, Kuster B, Engelhardt B, Vestweber D, Butz S: **A transmembrane tight junction protein selectively expressed on endothelial cells and platelets.** *J Biol Chem* 2002, **277:**16294-16303.
191. Cohen CJ, Shieh JT, Pickles RJ, Okegawa T, Hsieh JT, Bergelson JM: **The coxsackievirus and adenovirus receptor is a transmembrane component of the tight junction.** *Proc Natl Acad Sci U S A* 2001, **98:**15191-15196.
192. Martin-Padura I, Lostaglio S, Schneemann M, Williams L, Romano M, Fruscella P, Panzeri C, Stoppacciaro A, Ruco L, Villa A, et al: **Junctional adhesion molecule, a novel member of the immunoglobulin superfamily that distributes at intercellular junctions and modulates monocyte transmigration.** *J Cell Biol* 1998, **142:**117-127.
193. Scheiermann C, Colom B, Meda P, Patel NS, Voisin MB, Marrelli A, Woodfin A, Pitzalis C, Thiemermann C, Aurrand-Lions M, et al: **Junctional adhesion molecule-C mediates leukocyte infiltration in response to ischemia reperfusion injury.** *Arterioscler Thromb Vasc Biol* 2009, **29:**1509-1515.
194. van Kempen MJ, Jongsma HJ: **Distribution of connexin37, connexin40 and connexin43 in the aorta and coronary artery of several mammals.** *Histochem Cell Biol* 1999, **112:**479-486.

195. van Rijen HV, van Kempen MJ, Postma S, Jongsma HJ: **Tumour necrosis factor alpha alters the expression of connexin43, connexin40, and connexin37 in human umbilical vein endothelial cells.** *Cytokine* 1998, **10:**258-264.
196. Jara PI, Boric MP, Saez JC: **Leukocytes express connexin 43 after activation with lipopolysaccharide and appear to form gap junctions with endothelial cells after ischemia-reperfusion.** *Proc Natl Acad Sci U S A* 1995, **92:**7011-7015.
197. Vliagoftis H, Hutson AM, Mahmudi-Azer S, Kim H, Rumsaeng V, Oh CK, Moqbel R, Metcalfe DD: **Mast cells express connexins on their cytoplasmic membrane.** *J Allergy Clin Immunol* 1999, **103:**656-662.
198. Zahler S, Hoffmann A, Gloe T, Pohl U: **Gap-junctional coupling between neutrophils and endothelial cells: a novel modulator of transendothelial migration.** *Journal of Leukocyte Biology* 2003, **73:**118-126.
199. Falk MM: **Adherens junctions remain dynamic.** *BMC Biol* 2010, **8:**34.
200. Lampugnani MG: **Endothelial adherens junctions and the actin cytoskeleton: an 'infinity net'?** *J Biol* 2010, **9:**16.
201. Suzuki S, Sano K, Tanihara H: **Diversity of the cadherin family: evidence for eight new cadherins in nervous tissue.** *Cell Regul* 1991, **2:**261-270.
202. Lampugnani MG, Corada M, Caveda L, Breviario F, Ayalon O, Geiger B, Dejana E: **The molecular organization of endothelial cell to cell junctions: differential association of plakoglobin, beta-catenin, and alpha-catenin with vascular endothelial cadherin (VE-cadherin).** *J Cell Biol* 1995, **129:**203-217.
203. Dejana E: **Endothelial adherens junctions: implications in the control of vascular permeability and angiogenesis.** *J Clin Invest* 1996, **98:**1949-1953.
204. Del Maschio A, Zanetti A, Corada M, Rival Y, Ruco L, Lampugnani MG, Dejana E: **Polymorphonuclear leukocyte adhesion triggers the disorganization of endothelial cell-to-cell adherens junctions.** *J Cell Biol* 1996, **135:**497-510.
205. Burridge K, Chrzanowska-Wodnicka M: **Focal adhesions, contractility, and signaling.** *Annu Rev Cell Dev Biol* 1996, **12:**463-518.
206. Solomkin JS, Robinson CT, Cave CM, Umanskiy K, Matlin K, Williams MA, Lentsch AB: **Formation of Focal Adhesion-Like Structures in Circulating Human Neutrophils After Severe Injury: Triggering of A Tissue-Phase Response in the Vascular Space.** *Shock* 2006, **25:**440-445 410.1097/1001.shk.0000209559.0000277198.0000209591.
207. Parish CR: **The role of heparan sulphate in inflammation.** *Nat Rev Immunol* 2006, **6:**633-643.
208. Hirschi KK, D'Amore PA: **Pericytes in the microvasculature.** *Cardiovascular Research* 1996, **32:**687-698.
209. Nathan C, Srimal S, Farber C, Sanchez E, Kabbash L, Asch A, Gailit J, Wright SD: **Cytokine-induced respiratory burst of human neutrophils: dependence on extracellular matrix proteins and CD11/CD18 integrins.** *J Cell Biol* 1989, **109:**1341-1349.
210. Ferguson TA, Mizutani H, Kupper TS: **Two integrin-binding peptides abrogate T cell-mediated immune responses in vivo.** *Proc Natl Acad Sci U S A* 1991, **88:**8072-8076.
211. Bohnsack JF: **CD11/CD18-independent neutrophil adherence to laminin is mediated by the integrin VLA-6.** *Blood* 1992, **79:**1545-1552.
212. Rieu P, Lesavre P, Halbwachs-Mecarelli L: **Evidence for integrins other than beta 2 on polymorphonuclear neutrophils: expression of alpha 6 beta 1 heterodimer.** *J Leukoc Biol* 1993, **53:**576-582.
213. Heck LW, Blackburn WD, Irwin MH, Abrahamson DR: **Degradation of basement membrane laminin by human neutrophil elastase and cathepsin G.** *Am J Pathol* 1990, **136:**1267-1274.
214. Watanabe H, Hattori S, Katsuda S, Nakanishi I, Nagai Y: **Human neutrophil elastase: degradation of basement membrane components and immunolocalization in the tissue.** *J Biochem* 1990, **108:**753-759.

215. Cepinskas G, Sandig M, Kvietys PR: **PAF-induced elastase-dependent neutrophil transendothelial migration is associated with the mobilization of elastase to the neutrophil surface and localization to the migrating front.** *J Cell Sci* 1999, **112 (Pt 12):**1937-1945.
216. Leppert D, Waubant E, Galardy R, Bunnett NW, Hauser SL: **T cell gelatinases mediate basement membrane transmigration in vitro.** *J Immunol* 1995, **154:**4379-4389.
217. Wang S, Voisin MB, Larbi KY, Dangerfield J, Scheiermann C, Tran M, Maxwell PH, Sorokin L, Nourshargh S: **Venular basement membranes contain specific matrix protein low expression regions that act as exit points for emigrating neutrophils.** *J Exp Med* 2006, **203:**1519-1532.
218. Voisin MB, Woodfin A, Nourshargh S: **Monocytes and neutrophils exhibit both distinct and common mechanisms in penetrating the vascular basement membrane in vivo.** *Arterioscler Thromb Vasc Biol* 2009, **29:**1193-1199.
219. Proebstl D, Voisin MB, Woodfin A, Whiteford J, D'Acquisto F, Jones GE, Rowe D, Nourshargh S: **Pericytes support neutrophil subendothelial cell crawling and breaching of venular walls in vivo.** *J Exp Med* 2012, **209:**1219-1234.
220. Voisin MB, Probstl D, Nourshargh S: **Venular basement membranes ubiquitously express matrix protein low-expression regions: characterization in multiple tissues and remodeling during inflammation.** *Am J Pathol* 2010, **176:**482-495.
221. Kawashima H, Watanabe N, Hirose M, Sun X, Atarashi K, Kimura T, Shikata K, Matsuda M, Ogawa D, Heljasvaara R, et al: **Collagen XVIII, a basement membrane heparan sulfate proteoglycan, interacts with L-selectin and monocyte chemoattractant protein-1.** *J Biol Chem* 2003, **278:**13069-13076.
222. Yang B-G, Tanaka T, Jang MH, Bai Z, Hayasaka H, Miyasaka M: **Binding of Lymphoid Chemokines to Collagen IV That Accumulates in the Basal Lamina of High Endothelial Venules: Its Implications in Lymphocyte Trafficking.** *The Journal of Immunology* 2007, **179:**4376-4382.
223. Lammermann T, Bader BL, Monkley SJ, Worbs T, Wedlich-Soldner R, Hirsch K, Keller M, Forster R, Critchley DR, Fassler R, Sixt M: **Rapid leukocyte migration by integrin-independent flowing and squeezing.** *Nature* 2008, **453:**51-55.
224. Friedl P, Entschladen F, Conrad C, Niggemann B, Zanker KS: **CD4+ T lymphocytes migrating in three-dimensional collagen lattices lack focal adhesions and utilize beta1 integrin-independent strategies for polarization, interaction with collagen fibers and locomotion.** *Eur J Immunol* 1998, **28:**2331-2343.
225. Bhakta NR, Oh DY, Lewis RS: **Calcium oscillations regulate thymocyte motility during positive selection in the three-dimensional thymic environment.** *Nat Immunol* 2005, **6:**143-151.
226. Sarris M, Masson JB, Maurin D, Van der Aa LM, Boudinot P, Lortat-Jacob H, Herbomel P: **Inflammatory chemokines direct and restrict leukocyte migration within live tissues as glycan-bound gradients.** *Curr Biol* 2012, **22:**2375-2382.
227. Hall A: **Rho GTPases and the actin cytoskeleton.** *Science* 1998, **279:**509-514.
228. Ridley AJ: **Rho GTPases and cell migration.** *J Cell Sci* 2001, **114:**2713-2722.
229. Van Aelst L, D'Souza-Schorey C: **Rho GTPases and signaling networks.** *Genes Dev* 1997, **11:**2295-2322.
230. Schmidt A, Hall A: **Guanine nucleotide exchange factors for Rho GTPases: turning on the switch.** *Genes Dev* 2002, **16:**1587-1609.
231. Moon SY, Zheng Y: **Rho GTPase-activating proteins in cell regulation.** *Trends Cell Biol* 2003, **13:**13-22.
232. Olofsson B: **Rho guanine dissociation inhibitors: pivotal molecules in cellular signalling.** *Cell Signal* 1999, **11:**545-554.
233. Schmitz AA, Govek EE, Bottner B, Van Aelst L: **Rho GTPases: signaling, migration, and invasion.** *Exp Cell Res* 2000, **261:**1-12.

234. Allen WE, Zicha D, Ridley AJ, Jones GE: **A role for Cdc42 in macrophage chemotaxis.** *J Cell Biol* 1998, **141:**1147-1157.
235. Weber KS, Klickstein LB, Weber PC, Weber C: **Chemokine-induced monocyte transmigration requires cdc42-mediated cytoskeletal changes.** *Eur J Immunol* 1998, **28:**2245-2251.
236. Honing H, van den Berg TK, van der Pol SM, Dijkstra CD, van der Kammen RA, Collard JG, de Vries HE: **RhoA activation promotes transendothelial migration of monocytes via ROCK.** *J Leukoc Biol* 2004, **75:**523-528.
237. Srinivasan S, Wang F, Glavas S, Ott A, Hofmann F, Aktories K, Kalman D, Bourne HR: **Rac and Cdc42 play distinct roles in regulating PI(3,4,5)P3 and polarity during neutrophil chemotaxis.** *J Cell Biol* 2003, **160:**375-385.
238. Pestonjamasp KN, Forster C, Sun C, Gardiner EM, Bohl B, Weiner O, Bokoch GM, Glogauer M: **Rac1 links leading edge and uropod events through Rho and myosin activation during chemotaxis.** *Blood* 2006, **108:**2814-2820.
239. Miguel A, del P, Vicente-Manzanares M, Tejedor R, Serrador JM, Sánchez-Madrid F: **Rho GTPases control migration and polarization of adhesion molecules and cytoskeletal ERM components in T lymphocytes.** *European Journal of Immunology* 1999, **29:**3609-3620.
240. Worthylake RA, Burridge K: **RhoA and ROCK Promote Migration by Limiting Membrane Protrusions.** *Journal of Biological Chemistry* 2003, **278:**13578-13584.
241. Worthylake RA, Lemoine S, Watson JM, Burridge K: **RhoA is required for monocyte tail retraction during transendothelial migration.** *J Cell Biol* 2001, **154:**147-160.
242. Eddy RJ, Pierini LM, Matsumura F, Maxfield FR: **Ca2+-dependent myosin II activation is required for uropod retraction during neutrophil migration.** *Journal of Cell Science* 2000, **113:**1287-1298.
243. Roberts AW, Kim C, Zhen L, Lowe JB, Kapur R, Petryniak B, Spaetti A, Pollock JD, Borneo JB, Bradford GB, et al: **Deficiency of the Hematopoietic Cell-Specific Rho Family GTPase Rac2 Is Characterized by Abnormalities in Neutrophil Function and Host Defense.** *Immunity* 1999, **10:**183-196.
244. Croker BA, Handman E, Hayball JD, Baldwin TM, Voigt V, Cluse LA, Yang FC, Williams DA, Roberts AW: **Rac2-deficient mice display perturbed T-cell distribution and chemotaxis, but only minor abnormalities in T(H)1 responses.** *Immunol Cell Biol* 2002, **80:**231-240.
245. Brenner B, Gulbins E, Schlottmann K, Koppenhoefer U, Busch GL, Walzog B, Steinhausen M, Coggeshall KM, Linderkamp O, Lang F: **L-selectin activates the Ras pathway via the tyrosine kinase p56lck.** *Proc Natl Acad Sci U S A* 1996, **93:**15376-15381.
246. Brenner B, Gulbins E, Busch GL, Koppenhoefer U, Lang F, Linderkamp O: **L-Selectin Regulates Actin Polymerisation via Activation of the Small G-Protein Rac2.** *Biochemical and Biophysical Research Communications* 1997, **231:**802-807.
247. Szczur K, Zheng Y, Filippi M-D: **The small Rho GTPase Cdc42 regulates neutrophil polarity via CD11b integrin signaling.** *Blood* 2009, **114:**4527-4537.
248. Akashi K, Traver D, Miyamoto T, Weissman IL: **A clonogenic common myeloid progenitor that gives rise to all myeloid lineages.** *Nature* 2000, **404:**193-197.
249. van Furth R, Cohn ZA: **The origin and kinetics of mononuclear phagocytes.** *J Exp Med* 1968, **128:**415-435.
250. Liu K, Waskow C, Liu X, Yao K, Hoh J, Nussenzweig M: **Origin of dendritic cells in peripheral lymphoid organs of mice.** *Nat Immunol* 2007, **8:**578-583.
251. Warren MK, Vogel SN: **Bone marrow-derived macrophages: development and regulation of differentiation markers by colony-stimulating factor and interferons.** *J Immunol* 1985, **134:**982-989.
252. Zhou LJ, Tedder TF: **CD14+ blood monocytes can differentiate into functionally mature CD83+ dendritic cells.** *Proc Natl Acad Sci U S A* 1996, **93:**2588-2592.

253. Varol C, Landsman L, Fogg DK, Greenshtein L, Gildor B, Margalit R, Kalchenko V, Geissmann F, Jung S: **Monocytes give rise to mucosal, but not splenic, conventional dendritic cells.** *J Exp Med* 2007, **204:**171-180.
254. Geissmann F, Jung S, Littman DR: **Blood Monocytes Consist of Two Principal Subsets with Distinct Migratory Properties.** *Immunity* 2003, **19:**71-82.
255. Swirski FK, Nahrendorf M, Etzrodt M, Wildgruber M, Cortez-Retamozo V, Panizzi P, Figueiredo JL, Kohler RH, Chudnovskiy A, Waterman P, et al: **Identification of splenic reservoir monocytes and their deployment to inflammatory sites.** *Science* 2009, **325:**612-616.
256. Auffray C, Sieweke MH, Geissmann F: **Blood monocytes: development, heterogeneity, and relationship with dendritic cells.** *Annu Rev Immunol* 2009, **27:**669-692.
257. Gordon S, Taylor PR: **Monocyte and macrophage heterogeneity.** *Nat Rev Immunol* 2005, **5:**953-964.
258. Nahrendorf M, Swirski FK, Aikawa E, Stangenberg L, Wurdinger T, Figueiredo JL, Libby P, Weissleder R, Pittet MJ: **The healing myocardium sequentially mobilizes two monocyte subsets with divergent and complementary functions.** *J Exp Med* 2007, **204:**3037-3047.
259. Passlick B, Flieger D, Ziegler-Heitbrock HW: **Identification and characterization of a novel monocyte subpopulation in human peripheral blood.** *Blood* 1989, **74:**2527-2534.
260. Cros J, Cagnard N, Woollard K, Patey N, Zhang S-Y, Senechal B, Puel A, Biswas SK, Moshous D, Picard C, et al: **Human CD14dim Monocytes Patrol and Sense Nucleic Acids and Viruses via TLR7 and TLR8 Receptors.** *Immunity* 2010, **33:**375-386.
261. Murray EGD WR, Swann MBR: **A disease of rabbits characterized by a large mononuclear monocytosis, caused by a hitherto undescribed bacillus Bacterium monocytogenes.** *J Pathol Bacteriol* 1926, **29**.
262. Jia T, Serbina NV, Brandl K, Zhong MX, Leiner IM, Charo IF, Pamer EG: **Additive roles for MCP-1 and MCP-3 in CCR2-mediated recruitment of inflammatory monocytes during Listeria monocytogenes infection.** *J Immunol* 2008, **180:**6846-6853.
263. Serbina NV, Salazar-Mather TP, Biron CA, Kuziel WA, Pamer EG: **TNF/iNOS-producing dendritic cells mediate innate immune defense against bacterial infection.** *Immunity* 2003, **19:**59-70.
264. Kurihara T, Warr G, Loy J, Bravo R: **Defects in macrophage recruitment and host defense in mice lacking the CCR2 chemokine receptor.** *J Exp Med* 1997, **186:**1757-1762.
265. Serbina NV, Pamer EG: **Monocyte emigration from bone marrow during bacterial infection requires signals mediated by chemokine receptor CCR2.** *Nat Immunol* 2006, **7:**311-317.
266. Serbina NV, Hohl TM, Cherny M, Pamer EG: **Selective expansion of the monocytic lineage directed by bacterial infection.** *J Immunol* 2009, **183:**1900-1910.
267. Scott HM, Flynn JL: **Mycobacterium tuberculosis in chemokine receptor 2-deficient mice: influence of dose on disease progression.** *Infect Immun* 2002, **70:**5946-5954.
268. Kipnis A, Basaraba RJ, Orme IM, Cooper AM: **Role of chemokine ligand 2 in the protective response to early murine pulmonary tuberculosis.** *Immunology* 2003, **109:**547-551.
269. Dunay IR, Damatta RA, Fux B, Presti R, Greco S, Colonna M, Sibley LD: **Gr1(+) inflammatory monocytes are required for mucosal resistance to the pathogen Toxoplasma gondii.** *Immunity* 2008, **29:**306-317.
270. Li L, Huang L, Sung SS, Vergis AL, Rosin DL, Rose CE, Jr., Lobo PI, Okusa MD: **The chemokine receptors CCR2 and CX3CR1 mediate monocyte/macrophage trafficking in kidney ischemia-reperfusion injury.** *Kidney Int* 2008, **74:**1526-1537.
271. Chomarat P, Banchereau J, Davoust J, Palucka AK: **IL-6 switches the differentiation of monocytes from dendritic cells to macrophages.** *Nat Immunol* 2000, **1:**510-514.

272. Chomarat P, Dantin C, Bennett L, Banchereau J, Palucka AK: **TNF Skews Monocyte Differentiation from Macrophages to Dendritic Cells.** *The Journal of Immunology* 2003, **171:**2262-2269.
273. Randolph GJ, Inaba K, Robbiani DF, Steinman RM, Muller WA: **Differentiation of phagocytic monocytes into lymph node dendritic cells in vivo.** *Immunity* 1999, **11:**753-761.
274. Palframan RT, Jung S, Cheng G, Weninger W, Luo Y, Dorf M, Littman DR, Rollins BJ, Zweerink H, Rot A, von Andrian UH: **Inflammatory Chemokine Transport and Presentation in HEV: A Remote Control Mechanism for Monocyte Recruitment to Lymph Nodes in Inflamed Tissues.** *The Journal of Experimental Medicine* 2001, **194:**1361-1374.
275. Janatpour MJ, Hudak S, Sathe M, Sedgwick JD, McEvoy LM: **Tumor necrosis factor-dependent segmental control of MIG expression by high endothelial venules in inflamed lymph nodes regulates monocyte recruitment.** *J Exp Med* 2001, **194:**1375-1384.
276. Auffray C, Fogg D, Garfa M, Elain G, Join-Lambert O, Kayal S, Sarnacki S, Cumano A, Lauvau G, Geissmann F: **Monitoring of blood vessels and tissues by a population of monocytes with patrolling behavior.** *Science* 2007, **317:**666-670.
277. Audoy-Remus J, Richard JF, Soulet D, Zhou H, Kubes P, Vallieres L: **Rod-Shaped monocytes patrol the brain vasculature and give rise to perivascular macrophages under the influence of proinflammatory cytokines and angiopoietin-2.** *J Neurosci* 2008, **28:**10187-10199.
278. Jung K, Kim P, Leuschner F, Gorbatov R, Kim JK, Ueno T, Nahrendorf M, Yun SH: **Endoscopic Time-Lapse Imaging of Immune Cells in Infarcted Mouse Hearts.** *Circ Res* 2013.
279. Swirski FK, Libby P, Aikawa E, Alcaide P, Luscinskas FW, Weissleder R, Pittet MJ: **Ly-6Chi monocytes dominate hypercholesterolemia-associated monocytosis and give rise to macrophages in atheromata.** *J Clin Invest* 2007, **117:**195-205.
280. Tacke F, Alvarez D, Kaplan TJ, Jakubzick C, Spanbroek R, Llodra J, Garin A, Liu J, Mack M, van Rooijen N, et al: **Monocyte subsets differentially employ CCR2, CCR5, and CX3CR1 to accumulate within atherosclerotic plaques.** *J Clin Invest* 2007, **117:**185-194.
281. Combadiere C, Potteaux S, Rodero M, Simon T, Pezard A, Esposito B, Merval R, Proudfoot A, Tedgui A, Mallat Z: **Combined inhibition of CCL2, CX3CR1, and CCR5 abrogates Ly6C(hi) and Ly6C(lo) monocytosis and almost abolishes atherosclerosis in hypercholesterolemic mice.** *Circulation* 2008, **117:**1649-1657.
282. Zhang SH, Reddick RL, Piedrahita JA, Maeda N: **Spontaneous hypercholesterolemia and arterial lesions in mice lacking apolipoprotein E.** *Science* 1992, **258:**468-471.
283. Hahn C, Schwartz MA: **Mechanotransduction in vascular physiology and atherogenesis.** *Nat Rev Mol Cell Biol* 2009, **10:**53-62.
284. Zand T, Hoffman AH, Savilonis BJ, Underwood JM, Nunnari JJ, Majno G, Joris I: **Lipid deposition in rat aortas with intraluminal hemispherical plug stenosis. A morphological and biophysical study.** *Am J Pathol* 1999, **155:**85-92.
285. Mora R, Lupu F, Simionescu N: **Prelesional events in atherogenesis. Colocalization of apolipoprotein B, unesterified cholesterol and extracellular phospholipid liposomes in the aorta of hyperlipidemic rabbit.** *Atherosclerosis* 1987, **67:**143-154.
286. Steinberg D: **Low Density Lipoprotein Oxidation and Its Pathobiological Significance.** *Journal of Biological Chemistry* 1997, **272:**20963-20966.
287. Khaidakov M, Mitra S, Wang X, Ding Z, Bora N, Lyzogubov V, Romeo F, Schichman SA, Mehta JL: **Large impact of low concentration oxidized LDL on angiogenic potential of human endothelial cells: a microarray study.** *PLoS One* 2012, **7:**e47421.

288. Johnson RC, Chapman SM, Dong ZM, Ordovas JM, Mayadas TN, Herz J, Hynes RO, Schaefer EJ, Wagner DD: **Absence of P-selectin delays fatty streak formation in mice.** *J Clin Invest* 1997, **99:**1037-1043.
289. Collins RG, Velji R, Guevara NV, Hicks MJ, Chan L, Beaudet AL: **P-Selectin or Intercellular Adhesion Molecule (Icam)-1 Deficiency Substantially Protects against Atherosclerosis in Apolipoprotein E–Deficient Mice.** *The Journal of Experimental Medicine* 2000, **191:**189-194.
290. Dong ZM, Brown AA, Wagner DD: **Prominent Role of P-Selectin in the Development of Advanced Atherosclerosis in ApoE-Deficient Mice.** *Circulation* 2000, **101:**2290-2295.
291. Shih PT, Brennan ML, Vora DK, Territo MC, Strahl D, Elices MJ, Lusis AJ, Berliner JA: **Blocking very late antigen-4 integrin decreases leukocyte entry and fatty streak formation in mice fed an atherogenic diet.** *Circ Res* 1999, **84:**345-351.
292. Galkina E, Ley K: **Leukocyte influx in atherosclerosis.** *Curr Drug Targets* 2007, **8:**1239-1248.
293. Eriksson EE: **Mechanisms of leukocyte recruitment to atherosclerotic lesions: future prospects.** *Curr Opin Lipidol* 2004, **15:**553-558.
294. Gerrity RG: **The role of the monocyte in atherogenesis: I. Transition of blood-borne monocytes into foam cells in fatty lesions.** *Am J Pathol* 1981, **103:**181-190.
295. Ross R: **The pathogenesis of atherosclerosis: a perspective for the 1990s.** *Nature* 1993, **362:**801-809.
296. Bobryshev YV: **Dendritic cells in atherosclerosis: Current status of the problem and clinical relevance.** *European Heart Journal* 2005, **26:**1700-1704.
297. Libby P: **Inflammation in atherosclerosis.** *Nature* 2002, **420:**868-874.
298. Eriksson EE, Xie X, Werr J, Thoren P, Lindbom L: **Direct viewing of atherosclerosis in vivo: plaque invasion by leukocytes is initiated by the endothelial selectins.** *FASEB J* 2001, **15:**1149-1157.
299. Eriksson EE: **Intravital Microscopy on Atherosclerosis in Apolipoprotein E-Deficient Mice Establishes Microvessels as Major Entry Pathways for Leukocytes to Advanced Lesions.** *Circulation* 2011.
300. An G, Wang H, Tang R, Yago T, McDaniel JM, McGee S, Huo Y, Xia L: **P-selectin glycoprotein ligand-1 is highly expressed on Ly-6Chi monocytes and a major determinant for Ly-6Chi monocyte recruitment to sites of atherosclerosis in mice.** *Circulation* 2008, **117:**3227-3237.
301. Potteaux S, Gautier EL, Hutchison SB, van Rooijen N, Rader DJ, Thomas MJ, Sorci-Thomas MG, Randolph GJ: **Suppressed monocyte recruitment drives macrophage removal from atherosclerotic plaques of Apoe-/- mice during disease regression.** *J Clin Invest* 2011, **121:**2025-2036.
302. Ingersoll MA, Platt AM, Potteaux S, Randolph GJ: **Monocyte trafficking in acute and chronic inflammation.** *Trends Immunol* 2011, **32:**470-477.
303. Greaves DR, Gordon S: **The macrophage scavenger receptor at 30 years of age: current knowledge and future challenges.** *J Lipid Res* 2009, **50 Suppl:**S282-286.
304. Steinberg D, Parthasarathy S, Carew TE, Khoo JC, Witztum JL: **Beyond cholesterol. Modifications of low-density lipoprotein that increase its atherogenicity.** *N Engl J Med* 1989, **320:**915-924.
305. Kruth HS, Huang W, Ishii I, Zhang W-Y: **Macrophage Foam Cell Formation with Native Low Density Lipoprotein.** *Journal of Biological Chemistry* 2002, **277:**34573-34580.
306. Bobryshev YV: **Monocyte recruitment and foam cell formation in atherosclerosis.** *Micron* 2006, **37:**208-222.
307. Ohayon J, Finet G, Gharib AM, Herzka DA, Tracqui P, Heroux J, Rioufol G, Kotys MS, Elagha A, Pettigrew RI: **Necrotic core thickness and positive arterial remodeling index: emergent biomechanical factors for evaluating the risk of plaque rupture.** *Am J Physiol Heart Circ Physiol* 2008, **295:**H717-727.

308. Berman CL, Yeo EL, Wencel-Drake JD, Furie BC, Ginsberg MH, Furie B: **A platelet alpha granule membrane protein that is associated with the plasma membrane after activation. Characterization and subcellular localization of platelet activation-dependent granule-external membrane protein.** *J Clin Invest* 1986, **78:**130-137.
309. Isenberg WM, McEver RP, Shuman MA, Bainton DF: **Topographic distribution of a granule membrane protein (GMP-140) that is expressed on the platelet surface after activation: an immunogold-surface replica study.** *Blood Cells* 1986, **12:**191-204.
310. Bonfanti R, Furie BC, Furie B, Wagner DD: **PADGEM (GMP140) is a component of Weibel-Palade bodies of human endothelial cells.** *Blood* 1989, **73:**1109-1112.
311. Bevilacqua MP, Pober JS, Mendrick DL, Cotran RS, Gimbrone MA: **Identification of an inducible endothelial-leukocyte adhesion molecule.** *Proceedings of the National Academy of Sciences* 1987, **84:**9238-9242.
312. McEver RP: **Selectins: novel receptors that mediate leukocyte adhesion during inflammation.** *Thromb Haemost* 1991, **65:**223-228.
313. Ord DC, Ernst TJ, Zhou LJ, Rambaldi A, Spertini O, Griffin J, Tedder TF: **Structure of the gene encoding the human leukocyte adhesion molecule-1 (TQ1, Leu-8) of lymphocytes and neutrophils.** *J Biol Chem* 1990, **265:**7760-7767.
314. Drickamer K: **Two distinct classes of carbohydrate-recognition domains in animal lectins.** *J Biol Chem* 1988, **263:**9557-9560.
315. O'Connell D, Koenig A, Jennings S, Hicke B, Han HL, Fitzwater T, Chang YF, Varki N, Parma D, Varki A: **Calcium-dependent oligonucleotide antagonists specific for L-selectin.** *Proc Natl Acad Sci U S A* 1996, **93:**5883-5887.
316. Geng JG, Moore KL, Johnson AE, McEver RP: **Neutrophil recognition requires a Ca(2+)-induced conformational change in the lectin domain of GMP-140.** *J Biol Chem* 1991, **266:**22313-22318.
317. Gibson RM, Kansas GS, Tedder TF, Furie B, Furie BC: **Lectin and epidermal growth factor domains of P-selectin at physiologic density are the recognition unit for leukocyte binding.** *Blood* 1995, **85:**151-158.
318. Kansas GS, Saunders KB, Ley K, Zakrzewicz A, Gibson RM, Furie BC, Furie B, Tedder TF: **A role for the epidermal growth factor-like domain of P-selectin in ligand recognition and cell adhesion.** *J Cell Biol* 1994, **124:**609-618.
319. Bowen BR, Fennie C, Lasky LA: **The Mel 14 antibody binds to the lectin domain of the murine peripheral lymph node homing receptor.** *J Cell Biol* 1990, **110:**147-153.
320. Tu L, Chen A, Delahunty MD, Moore KL, Watson SR, McEver RP, Tedder TF: **L-selectin binds to P-selectin glycoprotein ligand-1 on leukocytes: interactions between the lectin, epidermal growth factor, and consensus repeat domains of the selectins determine ligand binding specificity.** *J Immunol* 1996, **157:**3995-4004.
321. Somers WS, Tang J, Shaw GD, Camphausen RT: **Insights into the Molecular Basis of Leukocyte Tethering and Rolling Revealed by Structures of P- and E-Selectin Bound to SLeX and PSGL-1.** *Cell* 2000, **103:**467-479.
322. Phan UT, Waldron TT, Springer TA: **Remodeling of the lectin-EGF-like domain interface in P- and L-selectin increases adhesiveness and shear resistance under hydrodynamic force.** *Nat Immunol* 2006, **7:**883-889.
323. Zhao L, Shey M, Farnsworth M, Dailey MO: **Regulation of membrane metalloproteolytic cleavage of L-selectin (CD62l) by the epidermal growth factor domain.** *J Biol Chem* 2001, **276:**30631-30640.
324. Johnston GI, Cook RG, McEver RP: **Cloning of GMP-140, a granule membrane protein of platelets and endothelium: sequence similarity to proteins involved in cell adhesion and inflammation.** *Cell* 1989, **56:**1033-1044.
325. Tedder TF, Isaacs CM, Ernst TJ, Demetri GD, Adler DA, Disteche CM: **Isolation and chromosomal localization of cDNAs encoding a novel human lymphocyte cell surface molecule, LAM-1. Homology with the mouse lymphocyte homing receptor and other human adhesion proteins.** *J Exp Med* 1989, **170:**123-133.

326. Kahn J, Ingraham RH, Shirley F, Migaki GI, Kishimoto TK: **Membrane proximal cleavage of L-selectin: identification of the cleavage site and a 6-kD transmembrane peptide fragment of L-selectin.** *J Cell Biol* 1994, **125:**461-470.
327. Kishimoto TK, Jutila MA, Berg EL, Butcher EC: **Neutrophil Mac-1 and MEL-14 adhesion proteins inversely regulated by chemotactic factors.** *Science* 1989, **245:**1238-1241.
328. Smalley DM, Ley K: **L-selectin: mechanisms and physiological significance of ectodomain cleavage.** *J Cell Mol Med* 2005, **9:**255-266.
329. Cervello M, Virruso L, Lipani G, Giannitrapani L, Soresi M, Carroccio A, Gambino R, Sanfililippo R, Marasà L, Montalto G: **Serum concentration of E-selectin in patients with chronic hepatitis, liver cirrhosis and hepatocellular carcinoma.** *Journal of Cancer Research and Clinical Oncology* 2000, **126:**345-351.
330. Turkoz Y, Evereklioglu C, Ozkiris A, Mistik S, Borlu M, Ozerol IH, Duygulu F, Ilhan O: **Serum levels of soluble P-selectin are increased and associated with disease activity in patients with Behcet's syndrome.** *Mediators Inflamm* 2005, **2005:**237-241.
331. True DD, Singer MS, Lasky LA, Rosen SD: **Requirement for sialic acid on the endothelial ligand of a lymphocyte homing receptor.** *J Cell Biol* 1990, **111:**2757-2764.
332. Moore KL, Varki A, McEver RP: **GMP-140 binds to a glycoprotein receptor on human neutrophils: evidence for a lectin-like interaction.** *J Cell Biol* 1991, **112:**491-499.
333. Tyrrell D, James P, Rao N, Foxall C, Abbas S, Dasgupta F, Nashed M, Hasegawa A, Kiso M, Asa D, et al.: **Structural requirements for the carbohydrate ligand of E-selectin.** *Proc Natl Acad Sci U S A* 1991, **88:**10372-10376.
334. Handa K, Nudelman ED, Stroud MR, Shiozawa T, Hakomori S: **Selectin GMP-140 (CD62; PADGEM) binds to sialosyl-Le(a) and sialosyl-Le(x), and sulfated glycans modulate this binding.** *Biochem Biophys Res Commun* 1991, **181:**1223-1230.
335. Berg EL, Robinson MK, Mansson O, Butcher EC, Magnani JL: **A carbohydrate domain common to both sialyl Le(a) and sialyl Le(X) is recognized by the endothelial cell leukocyte adhesion molecule ELAM-1.** *J Biol Chem* 1991, **266:**14869-14872.
336. Zhou Q, Moore KL, Smith DF, Varki A, McEver RP, Cummings RD: **The selectin GMP-140 binds to sialylated, fucosylated lactosaminoglycans on both myeloid and nonmyeloid cells.** *J Cell Biol* 1991, **115:**557-564.
337. Imai Y, Singer MS, Fennie C, Lasky LA, Rosen SD: **Identification of a carbohydrate-based endothelial ligand for a lymphocyte homing receptor.** *J Cell Biol* 1991, **113:**1213-1221.
338. Fukuda M, Spooncer E, Oates JE, Dell A, Klock JC: **Structure of sialylated fucosyl lactosaminoglycan isolated from human granulocytes.** *Journal of Biological Chemistry* 1984, **259:**10925-10935.
339. Maly P, Thall A, Petryniak B, Rogers CE, Smith PL, Marks RM, Kelly RJ, Gersten KM, Cheng G, Saunders TL, et al: **The alpha(1,3)fucosyltransferase Fuc-TVII controls leukocyte trafficking through an essential role in L-, E-, and P-selectin ligand biosynthesis.** *Cell* 1996, **86:**643-653.
340. Ellies LG, Sperandio M, Underhill GH, Yousif J, Smith M, Priatel JJ, Kansas GS, Ley K, Marth JD: **Sialyltransferase specificity in selectin ligand formation.** *Blood* 2002, **100:**3618-3625.
341. Sperandio M, Frommhold D, Babushkina I, Ellies LG, Olson TS, Smith ML, Fritzsching B, Pauly E, Smith DF, Nobiling R, et al: **Alpha 2,3-sialyltransferase-IV is essential for L-selectin ligand function in inflammation.** *Eur J Immunol* 2006, **36:**3207-3215.
342. Hemmerich S, Bistrup A, Singer MS, van Zante A, Lee JK, Tsay D, Peters M, Carminati JL, Brennan TJ, Carver-Moore K, et al: **Sulfation of L-selectin ligands by an HEV-restricted sulfotransferase regulates lymphocyte homing to lymph nodes.** *Immunity* 2001, **15:**237-247.
343. Uchimura K, Kadomatsu K, El-Fasakhany FM, Singer MS, Izawa M, Kannagi R, Takeda N, Rosen SD, Muramatsu T: **N-acetylglucosamine 6-O-sulfotransferase-1 regulates**

expression of L-selectin ligands and lymphocyte homing. *J Biol Chem* 2004, **279:**35001-35008.
344. Varki A: **Selectin ligands.** *Proc Natl Acad Sci U S A* 1994, **91:**7390-7397.
345. Hirakawa J, Tsuboi K, Sato K, Kobayashi M, Watanabe S, Takakura A, Imai Y, Ito Y, Fukuda M, Kawashima H: **Novel anti-carbohydrate antibodies reveal the cooperative function of sulfated N- and O-glycans in lymphocyte homing.** In *Journal of Biological Chemistry*2010.
346. Alon R, Rosen S: **Rolling on N-linked glycans: a new way to present L-selectin binding sites.** *Nat Immunol* 2007, **8:**339-341.
347. Mitoma J, Bao X, Petryanik B, Schaerli P, Gauguet JM, Yu SY, Kawashima H, Saito H, Ohtsubo K, Marth JD, et al: **Critical functions of N-glycans in L-selectin-mediated lymphocyte homing and recruitment.** *Nat Immunol* 2007, **8:**409-418.
348. Wilkins PP, Moore KL, McEver RP, Cummings RD: **Tyrosine sulfation of P-selectin glycoprotein ligand-1 is required for high affinity binding to P-selectin.** *J Biol Chem* 1995, **270:**22677-22680.
349. Stryer L: *Biochemistry.* New York: W. H. Freeman and Company; 1995.
350. McEver RP: **Selectins: lectins that initiate cell adhesion under flow.** *Curr Opin Cell Biol* 2002, **14:**581-586.
351. Moore KL, Eaton SF, Lyons DE, Lichenstein HS, Cummings RD, McEver RP: **The P-selectin glycoprotein ligand from human neutrophils displays sialylated, fucosylated, O-linked poly-N-acetyllactosamine.** *J Biol Chem* 1994, **269:**23318-23327.
352. Hanley WD, Napier SL, Burdick MM, Schnaar RL, Sackstein R, Konstantopoulos K: **Variant isoforms of CD44 are P- and L-selectin ligands on colon carcinoma cells.** *FASEB J* 2006, **20:**337-339.
353. Kerr SC, Fieger CB, Snapp KR, Rosen SD: **Endoglycan, a member of the CD34 family of sialomucins, is a ligand for the vascular selectins.** *J Immunol* 2008, **181:**1480-1490.
354. Kawashima H, Hirose M, Hirose J, Nagakubo D, Plaas AH, Miyasaka M: **Binding of a large chondroitin sulfate/dermatan sulfate proteoglycan, versican, to L-selectin, P-selectin, and CD44.** *J Biol Chem* 2000, **275:**35448-35456.
355. Picker LJ, Warnock RA, Burns AR, Doerschuk CM, Berg EL, Butcher EC: **The neutrophil selectin LECAM-1 presents carbohydrate ligands to the vascular selectins ELAM-1 and GMP-140.** *Cell* 1991, **66:**921-933.
356. Alcaide P, King SL, Dimitroff CJ, Lim YC, Fuhlbrigge RC, Luscinskas FW: **The 130-kDa glycoform of CD43 functions as an E-selectin ligand for activated Th1 cells in vitro and in delayed-type hypersensitivity reactions in vivo.** *J Invest Dermatol* 2007, **127:**1964-1972.
357. Fuhlbrigge RC, King SL, Sackstein R, Kupper TS: **CD43 is a ligand for E-selectin on CLA+ human T cells.** *Blood* 2006, **107:**1421-1426.
358. Hanley WD, Burdick MM, Konstantopoulos K, Sackstein R: **CD44 on LS174T colon carcinoma cells possesses E-selectin ligand activity.** *Cancer Res* 2005, **65:**5812-5817.
359. Katayama Y, Hidalgo A, Chang J, Peired A, Frenette PS: **CD44 is a physiological E-selectin ligand on neutrophils.** *J Exp Med* 2005, **201:**1183-1189.
360. Dimitroff CJ, Lee JY, Rafii S, Fuhlbrigge RC, Sackstein R: **CD44 is a major E-selectin ligand on human hematopoietic progenitor cells.** *J Cell Biol* 2001, **153:**1277-1286.
361. Thomas SN, Zhu F, Schnaar RL, Alves CS, Konstantopoulos K: **Carcinoembryonic antigen and CD44 variant isoforms cooperate to mediate colon carcinoma cell adhesion to E- and L-selectin in shear flow.** *J Biol Chem* 2008, **283:**15647-15655.
362. Levinovitz A, Muhlhoff J, Isenmann S, Vestweber D: **Identification of a glycoprotein ligand for E-selectin on mouse myeloid cells.** *J Cell Biol* 1993, **121:**449-459.
363. Steegmaier M, Levinovitz A, Isenmann S, Borges E, Lenter M, Kocher HP, Kleuser B, Vestweber D: **The E-selectin-ligand ESL-1 is a variant of a receptor for fibroblast growth factor.** *Nature* 1995, **373:**615-620.

364. Dallas MR, Chen SH, Streppel MM, Sharma S, Maitra A, Konstantopoulos K: **Sialofucosylated podocalyxin is a functional E- and L-selectin ligand expressed by metastatic pancreatic cancer cells.** *Am J Physiol Cell Physiol* 2012, **303:**C616-624.
365. Ley K, Bullard DC, Arbones ML, Bosse R, Vestweber D, Tedder TF, Beaudet AL: **Sequential contribution of L- and P-selectin to leukocyte rolling in vivo.** *J Exp Med* 1995, **181:**669-675.
366. Wang HB, Wang JT, Zhang L, Geng ZH, Xu WL, Xu T, Huo Y, Zhu X, Plow EF, Chen M, Geng JG: **P-selectin primes leukocyte integrin activation during inflammation.** *Nat Immunol* 2007, **8:**882-892.
367. Yang J, Hirata T, Croce K, Merrill-Skoloff G, Tchernychev B, Williams E, Flaumenhaft R, Furie BC, Furie B: **Targeted gene disruption demonstrates that P-selectin glycoprotein ligand 1 (PSGL-1) is required for P-selectin-mediated but not E-selectin-mediated neutrophil rolling and migration.** *J Exp Med* 1999, **190:**1769-1782.
368. Yao L, Setiadi H, Xia L, Laszik Z, Taylor FB, McEver RP: **Divergent inducible expression of P-selectin and E-selectin in mice and primates.** *Blood* 1999, **94:**3820-3828.
369. Johnson RC, Mayadas TN, Frenette PS, Mebius RE, Subramaniam M, Lacasce A, Hynes RO, Wagner DD: **Blood cell dynamics in P-selectin-deficient mice.** *Blood* 1995, **86:**1106-1114.
370. Larsen E, Celi A, Gilbert GE, Furie BC, Erban JK, Bonfanti R, Wagner DD, Furie B: **PADGEM protein: a receptor that mediates the interaction of activated platelets with neutrophils and monocytes.** *Cell* 1989, **59:**305-312.
371. McEver RP: **Adhesive interactions of leukocytes, platelets, and the vessel wall during hemostasis and inflammation.** *Thromb Haemost* 2001, **86:**746-756.
372. Furman MI, Benoit SE, Barnard MR, Valeri CR, Borbone ML, Becker RC, Hechtman HB, Michelson AD: **Increased platelet reactivity and circulating monocyte-platelet aggregates in patients with stable coronary artery disease.** *J Am Coll Cardiol* 1998, **31:**352-358.
373. Elizalde JI, Gomez J, Panes J, Lozano M, Casadevall M, Ramirez J, Pizcueta P, Marco F, Rojas FD, Granger DN, Pique JM: **Platelet activation In mice and human Helicobacter pylori infection.** *J Clin Invest* 1997, **100:**996-1005.
374. Huo Y, Schober A, Forlow SB, Smith DF, Hyman MC, Jung S, Littman DR, Weber C, Ley K: **Circulating activated platelets exacerbate atherosclerosis in mice deficient in apolipoprotein E.** *Nat Med* 2003, **9:**61-67.
375. Merten M, Thiagarajan P: **P-selectin expression on platelets determines size and stability of platelet aggregates.** *Circulation* 2000, **102:**1931-1936.
376. Huang RB, Eniola-Adefeso O: **Shear stress modulation of IL-1beta-induced E-selectin expression in human endothelial cells.** *PLoS One* 2012, **7:**e31874.
377. Huang K, Fishwild DM, Wu HM, Dedrick RL: **Lipopolysaccharide-induced E-selectin expression requires continuous presence of LPS and is inhibited by bactericidal/permeability-increasing protein.** *Inflammation* 1995, **19:**389-404.
378. Bevilacqua MP, Stengelin S, Gimbrone MA, Jr., Seed B: **Endothelial leukocyte adhesion molecule 1: an inducible receptor for neutrophils related to complement regulatory proteins and lectins.** *Science* 1989, **243:**1160-1165.
379. Hidalgo A, Peired AJ, Wild MK, Vestweber D, Frenette PS: **Complete identification of E-selectin ligands on neutrophils reveals distinct functions of PSGL-1, ESL-1, and CD44.** *Immunity* 2007, **26:**477-489.
380. Puri KD, Finger EB, Springer TA: **The faster kinetics of L-selectin than of E-selectin and P-selectin rolling at comparable binding strength.** *J Immunol* 1997, **158:**405-413.
381. Zollner O, Lenter MC, Blanks JE, Borges E, Steegmaier M, Zerwes HG, Vestweber D: **L-selectin from human, but not from mouse neutrophils binds directly to E-selectin.** *J Cell Biol* 1997, **136:**707-716.

382. Yago T, Shao B, Miner JJ, Yao L, Klopocki AG, Maeda K, Coggeshall KM, McEver RP: **E-selectin engages PSGL-1 and CD44 through a common signaling pathway to induce integrin {alpha}L{beta}2-mediated slow leukocyte rolling.** *Blood* 2010.
383. Mueller H, Stadtmann A, Van Aken H, Hirsch E, Wang D, Ley K, Zarbock A: **Tyrosine kinase Btk regulates E-selectin-mediated integrin activation and neutrophil recruitment by controlling phospholipase C (PLC){gamma}2 and PI3K{gamma} pathways.** *Blood* 2010.
384. Dailey MO, Gallatin WM, Weissman IL: **The in vivo behavior of T cell clones: altered migration due to loss of the lymphocyte surface homing receptor.** *J Mol Cell Immunol* 1985, **2:**27-36.
385. Reichert RA, Gallatin WM, Weissman IL, Butcher EC: **Germinal center B cells lack homing receptors necessary for normal lymphocyte recirculation.** *J Exp Med* 1983, **157:**813-827.
386. Chao CC, Jensen R, Dailey MO: **Mechanisms of L-selectin regulation by activated T cells.** *J Immunol* 1997, **159:**1686-1694.
387. Weninger W, Crowley MA, Manjunath N, von Andrian UH: **Migratory properties of naive, effector, and memory CD8(+) T cells.** *J Exp Med* 2001, **194:**953-966.
388. Kishimoto TK, Jutila MA, Butcher EC: **Identification of a human peripheral lymph node homing receptor: a rapidly down-regulated adhesion molecule.** *Proc Natl Acad Sci U S A* 1990, **87:**2244-2248.
389. Steeber DA, Green NE, Sato S, Tedder TF: **Lyphocyte migration in L-selectin-deficient mice. Altered subset migration and aging of the immune system.** *J Immunol* 1996, **157:**1096-1106.
390. Steeber DA, Green NE, Sato S, Tedder TF: **Humoral immune responses in L-selectin-deficient mice.** *J Immunol* 1996, **157:**4899-4907.
391. Tang ML, Hale LP, Steeber DA, Tedder TF: **L-selectin is involved in lymphocyte migration to sites of inflammation in the skin: delayed rejection of allografts in L-selectin-deficient mice.** *J Immunol* 1997, **158:**5191-5199.
392. Tedder TF, Steeber DA, Pizcueta P: **L-selectin-deficient mice have impaired leukocyte recruitment into inflammatory sites.** *The Journal of Experimental Medicine* 1995, **181:**2259-2264.
393. Wagner N, Löhler J, Tedder TF, Rajewsky K, Müller W, Steeber DA: **L-selectin and β7 integrin synergistically mediate lymphocyte migration to mesenteric lymph nodes.** *European Journal of Immunology* 1998, **28:**3832-3839.
394. Steeber DA, Tang ML, Zhang XQ, Muller W, Wagner N, Tedder TF: **Efficient lymphocyte migration across high endothelial venules of mouse Peyer's patches requires overlapping expression of L-selectin and beta7 integrin.** *J Immunol* 1998, **161:**6638-6647.
395. Venturi GM, Conway RM, Steeber DA, Tedder TF: **CD25+CD4+ regulatory T cell migration requires L-selectin expression: L-selectin transcriptional regulation balances constitutive receptor turnover.** *J Immunol* 2007, **178:**291-300.
396. Lasky LA, Singer MS, Yednock TA, Dowbenko D, Fennie C, Rodriguez H, Nguyen T, Stachel S, Rosen SD: **Cloning of a lymphocyte homing receptor reveals a lectin domain.** *Cell* 1989, **56:**1045-1055.
397. Jalkanen S, Bargatze RF, de los Toyos J, Butcher EC: **Lymphocyte recognition of high endothelium: antibodies to distinct epitopes of an 85-95-kD glycoprotein antigen differentially inhibit lymphocyte binding to lymph node, mucosal, or synovial endothelial cells.** *J Cell Biol* 1987, **105:**983-990.
398. Hickey MJ, Forster M, Mitchell D, Kaur J, De Caigny C, Kubes P: **L-selectin facilitates emigration and extravascular locomotion of leukocytes during acute inflammatory responses in vivo.** *J Immunol* 2000, **165:**7164-7170.

399. Steeber DA, Tang ML, Green NE, Zhang XQ, Sloane JE, Tedder TF: **Leukocyte entry into sites of inflammation requires overlapping interactions between the L-selectin and ICAM-1 pathways.** *J Immunol* 1999, **163:**2176-2186.
400. Shimada Y, Hasegawa M, Kaburagi Y, Hamaguchi Y, Komura K, Saito E, Takehara K, Steeber DA, Tedder TF, Sato S: **L-selectin or ICAM-1 deficiency reduces an immediate-type hypersensitivity response by preventing mast cell recruitment in repeated elicitation of contact hypersensitivity.** *J Immunol* 2003, **170:**4325-4334.
401. Kaburagi Y, Hasegawa M, Nagaoka T, Shimada Y, Hamaguchi Y, Komura K, Saito E, Yanaba K, Takehara K, Kadono T, et al: **The cutaneous reverse Arthus reaction requires intercellular adhesion molecule 1 and L-selectin expression.** *J Immunol* 2002, **168:**2970-2978.
402. Tedder TF, Matsuyama T, Rothstein D, Schlossman SF, Morimoto C: **Human antigen-specific memory T cells express the homing receptor (LAM-1) necessary for lymphocyte recirculation.** *Eur J Immunol* 1990, **20:**1351-1355.
403. Hasslen SR, von Andrian UH, Butcher EC, Nelson RD, Erlandsen SL: **Spatial distribution of L-selectin (CD62L) on human lymphocytes and transfected murine L1-2 cells.** *Histochem J* 1995, **27:**547-554.
404. Chen S, Alon R, Fuhlbrigge RC, Springer TA: **Rolling and transient tethering of leukocytes on antibodies reveal specializations of selectins.** *Proc Natl Acad Sci U S A* 1997, **94:**3172-3177.
405. Alon R, Chen S, Puri KD, Finger EB, Springer TA: **The kinetics of L-selectin tethers and the mechanics of selectin-mediated rolling.** *J Cell Biol* 1997, **138:**1169-1180.
406. Davenpeck KL, Steeber DA, Tedder TF, Bochner BS: **P- and L-selectin mediate distinct but overlapping functions in endotoxin-induced leukocyte-endothelial interactions in the rat mesenteric microcirculation.** *J Immunol* 1997, **159:**1977-1986.
407. von Andrian UH, Chambers JD, Berg EL, Michie SA, Brown DA, Karolak D, Ramezani L, Berger EM, Arfors KE, Butcher EC: **L-selectin mediates neutrophil rolling in inflamed venules through sialyl LewisX-dependent and -independent recognition pathways.** *Blood* 1993, **82:**182-191.
408. Xu J, Grewal IS, Geba GP, Flavell RA: **Impaired primary T cell responses in L-selectin-deficient mice.** *J Exp Med* 1996, **183:**589-598.
409. Ley K, Tedder TF, Kansas GS: **L-selectin can mediate leukocyte rolling in untreated mesenteric venules in vivo independent of E- or P-selectin.** *Blood* 1993, **82:**1632-1638.
410. Luscinskas FW, Kansas GS, Ding H, Pizcueta P, Schleiffenbaum BE, Tedder TF, Gimbrone MA, Jr.: **Monocyte rolling, arrest and spreading on IL-4-activated vascular endothelium under flow is mediated via sequential action of L-selectin, beta 1-integrins, and beta 2-integrins.** *J Cell Biol* 1994, **125:**1417-1427.
411. Johnston B, Walter UM, Issekutz AC, Issekutz TB, Anderson DC, Kubes P: **Differential roles of selectins and the alpha4-integrin in acute, subacute, and chronic leukocyte recruitment in vivo.** *J Immunol* 1997, **159:**4514-4523.
412. Ma XL, Weyrich AS, Lefer DJ, Buerke M, Albertine KH, Kishimoto TK, Lefer AM: **Monoclonal antibody to L-selectin attenuates neutrophil accumulation and protects ischemic reperfused cat myocardium.** *Circulation* 1993, **88:**649-658.
413. Green CE, Pearson DN, Camphausen RT, Staunton DE, Simon SI: **Shear-dependent capping of L-selectin and P-selectin glycoprotein ligand 1 by E-selectin signals activation of high-avidity beta2-integrin on neutrophils.** *J Immunol* 2004, **172:**7780-7790.
414. Gopalan PK, Smith CW, Lu H, Berg EL, McIntire LV, Simon SI: **Neutrophil CD18-dependent arrest on intercellular adhesion molecule 1 (ICAM-1) in shear flow can be activated through L-selectin.** *J Immunol* 1997, **158:**367-375.
415. Subramanian H, Grailer JJ, Ohlrich KC, Rymaszewski AL, Loppnow JJ, Kodera M, Conway RM, Steeber DA: **Signaling through L-Selectin Mediates Enhanced Chemotaxis of**

Lymphocyte Subsets to Secondary Lymphoid Tissue Chemokine. *The Journal of Immunology* 2012, **188:**3223-3236.
416. Kanwar S, Steeber DA, Tedder TF, Hickey MJ, Kubes P: **Overlapping Roles for L-Selectin and P-Selectin in Antigen-Induced Immune Responses in the Microvasculature.** *The Journal of Immunology* 1999, **162:**2709-2716.
417. Grewal IS, Foellmer HG, Grewal KD, Wang H, Lee WP, Tumas D, Janeway Jr CA, Flavell RA: **CD62L Is Required on Effector Cells for Local Interactions in the CNS to Cause Myelin Damage in Experimental Allergic Encephalomyelitis.** *Immunity* 2001, **14:**291-302.
418. Huang K, Kikuta A, Rosen SD: **Myelin localization of a central nervous system ligand for L-selectin.** *J Neuroimmunol* 1994, **53:**133-141.
419. Venturi GM, Tu L, Kadono T, Khan AI, Fujimoto Y, Oshel P, Bock CB, Miller AS, Albrecht RM, Kubes P, et al: **Leukocyte migration is regulated by L-selectin endoproteolytic release.** *Immunity* 2003, **19:**713-724.
420. Ogawa D, Shikata K, Honke K, Sato S, Matsuda M, Nagase R, Tone A, Okada S, Usui H, Wada J, et al: **Cerebroside sulfotransferase deficiency ameliorates L-selectin-dependent monocyte infiltration in the kidney after ureteral obstruction.** *J Biol Chem* 2004, **279:**2085-2090.
421. Schaff U, Mattila PE, Simon SI, Walcheck B: **Neutrophil adhesion to E-selectin under shear promotes the redistribution and co-clustering of ADAM17 and its proteolytic substrate L-selectin.** *J Leukoc Biol* 2008, **83:**99-105.
422. Stoolman LM, Rosen SD: **Possible role for cell-surface carbohydrate-binding molecules in lymphocyte recirculation.** *J Cell Biol* 1983, **96:**722-729.
423. Rosen SD, Singer MS, Yednock TA, Stoolman LM: **Involvement of sialic acid on endothelial cells in organ-specific lymphocyte recirculation.** *Science* 1985, **228:**1005-1007.
424. Yednock TA, Butcher EC, Stoolman LM, Rosen SD: **Receptors involved in lymphocyte homing: relationship between a carbohydrate-binding receptor and the MEL-14 antigen.** *J Cell Biol* 1987, **104:**725-731.
425. Rosen SD: **Ligands for L-selectin: homing, inflammation, and beyond.** *Annu Rev Immunol* 2004, **22:**129-156.
426. von Andrian UH: **Intravital microscopy of the peripheral lymph node microcirculation in mice.** *Microcirculation* 1996, **3:**287-300.
427. Hemmerich S, Butcher EC, Rosen SD: **Sulfation-dependent recognition of high endothelial venules (HEV)-ligands by L-selectin and MECA 79, and adhesion-blocking monoclonal antibody.** *The Journal of Experimental Medicine* 1994, **180:**2219-2226.
428. Rosen SD: **Endothelial ligands for L-selectin: from lymphocyte recirculation to allograft rejection.** *Am J Pathol* 1999, **155:**1013-1020.
429. Scudder PR, Shailubhai K, Duffin KL, Streeter PR, Jacob GS: **Enzymatic synthesis of a 6'-sulphated sialyl-Lewisx which is an inhibitor of L-selectin binding to peripheral addressin.** *Glycobiology* 1994, **4:**929-932.
430. Bistrup A, Bhakta S, Lee JK, Belov YY, Gunn MD, Zuo FR, Huang CC, Kannagi R, Rosen SD, Hemmerich S: **Sulfotransferases of two specificities function in the reconstitution of high endothelial cell ligands for L-selectin.** *J Cell Biol* 1999, **145:**899-910.
431. Kimura N, Mitsuoka C, Kanamori A, Hiraiwa N, Uchimura K, Muramatsu T, Tamatani T, Kansas GS, Kannagi R: **Reconstitution of functional L-selectin ligands on a cultured human endothelial cell line by cotransfection of alpha1-->3 fucosyltransferase VII and newly cloned GlcNAcbeta:6-sulfotransferase cDNA.** *Proc Natl Acad Sci U S A* 1999, **96:**4530-4535.
432. Lasky LA, Singer MS, Dowbenko D, Imai Y, Henzel WJ, Grimley C, Fennie C, Gillett N, Watson SR, Rosen SD: **An endothelial ligand for L-selectin is a novel mucin-like molecule.** *Cell* 1992, **69:**927-938.

433. Lasky LA, Singer MS, Dowbenko D, Imai Y, Henzel W, Fennie C, Watson S, Rosen SD: **Glycosylation-dependent cell adhesion molecule 1: a novel mucin-like adhesion ligand for L-selectin.** *Cold Spring Harb Symp Quant Biol* 1992, **57:**259-269.
434. Baumheter S, Singer M, Henzel W, Hemmerich S, Renz M, Rosen S, Lasky L: **Binding of L-selectin to the vascular sialomucin CD34.** *Science* 1993, **262:**436-438.
435. Puri KD, Finger EB, Gaudernack G, Springer TA: **Sialomucin CD34 is the major L-selectin ligand in human tonsil high endothelial venules.** *J Cell Biol* 1995, **131:**261-270.
436. Sassetti C, Tangemann K, Singer MS, Kershaw DB, Rosen SD: **Identification of podocalyxin-like protein as a high endothelial venule ligand for L-selectin: parallels to CD34.** *J Exp Med* 1998, **187:**1965-1975.
437. Samulowitz U, Kuhn A, Brachtendorf G, Nawroth R, Braun A, Bankfalvi A, Bocker W, Vestweber D: **Human endomucin: distribution pattern, expression on high endothelial venules, and decoration with the MECA-79 epitope.** *Am J Pathol* 2002, **160:**1669-1681.
438. Umemoto E, Tanaka T, Kanda H, Jin S, Tohya K, Otani K, Matsutani T, Matsumoto M, Ebisuno Y, Jang MH, et al: **Nepmucin, a novel HEV sialomucin, mediates L-selectin-dependent lymphocyte rolling and promotes lymphocyte adhesion under flow.** *J Exp Med* 2006, **203:**1603-1614.
439. Berg EL, McEvoy LM, Berlin C, Bargatze RF, Butcher EC: **L-selectin-mediated lymphocyte rolling on MAdCAM-1.** *Nature* 1993, **366:**695-698.
440. Suzuki A, Andrew DP, Gonzalo JA, Fukumoto M, Spellberg J, Hashiyama M, Takimoto H, Gerwin N, Webb I, Molineux G, et al: **CD34-deficient mice have reduced eosinophil accumulation after allergen exposure and show a novel crossreactive 90-kD protein.** *Blood* 1996, **87:**3550-3562.
441. Clark RA, Fuhlbrigge RC, Springer TA: **L-Selectin Ligands That Are O-glycoprotease Resistant and Distinct from MECA-79 Antigen are Sufficient for Tethering and Rolling of Lymphocytes on Human High Endothelial Venules.** *The Journal of Cell Biology* 1998, **140:**721-731.
442. Michie SA, Streeter PR, Bolt PA, Butcher EC, Picker LJ: **The human peripheral lymph node vascular addressin. An inducible endothelial antigen involved in lymphocyte homing.** *Am J Pathol* 1993, **143:**1688-1698.
443. Streeter PR, Rouse BT, Butcher EC: **Immunohistologic and functional characterization of a vascular addressin involved in lymphocyte homing into peripheral lymph nodes.** *J Cell Biol* 1988, **107:**1853-1862.
444. Mackay CR, Marston WL, Dudler L, Spertini O, Tedder TF, Hein WR: **Tissue-specific migration pathways by phenotypically distinct subpopulations of memory T cells.** *Eur J Immunol* 1992, **22:**887-895.
445. Ruddle NH: **Lymphoid neo-organogenesis: lymphotoxin's role in inflammation and development.** *Immunol Res* 1999, **19:**119-125.
446. Hjelmstrom P: **Lymphoid neogenesis: de novo formation of lymphoid tissue in chronic inflammation through expression of homing chemokines.** *J Leukoc Biol* 2001, **69:**331-339.
447. Baumhueter S, Dybdal N, Kyle C, Lasky L: **Global vascular expression of murine CD34, a sialomucin-like endothelial ligand for L-selectin.** *Blood* 1994, **84:**2554-2565.
448. Kobayashi M, Hoshino H, Masumoto J, Fukushima M, Suzawa K, Kageyama S, Suzuki M, Ohtani H, Fukuda M, Nakayama J: **GlcNAc6ST-1-mediated decoration of MAdCAM-1 protein with L-selectin ligand carbohydrates directs disease activity of ulcerative colitis.** *Inflamm Bowel Dis* 2009, **15:**697-706.
449. Kobayashi M, Mitoma J, Nakamura N, Katsuyama T, Nakayama J, Fukuda M: **Induction of peripheral lymph node addressin in human gastric mucosa infected by Helicobacter pylori.** *Proc Natl Acad Sci U S A* 2004, **101:**17807-17812.

450. Salmi M, Granfors K, MacDermott R, Jalkanen S: **Aberrant binding of lamina propria lymphocytes to vascular endothelium in inflammatory bowel diseases.** *Gastroenterology* 1994, **106:**596-605.
451. Toppila S, Paavonen T, Nieminen MS, Hayry P, Renkonen R: **Endothelial L-selectin ligands are likely to recruit lymphocytes into rejecting human heart transplants.** *Am J Pathol* 1999, **155:**1303-1310.
452. Faveeuw C, Gagnerault MC, Lepault F: **Expression of homing and adhesion molecules in infiltrated islets of Langerhans and salivary glands of nonobese diabetic mice.** *J Immunol* 1994, **152:**5969-5978.
453. Duijvestijn AM, Horst E, Pals ST, Rouse BN, Steere AC, Picker LJ, Meijer CJ, Butcher EC: **High endothelial differentiation in human lymphoid and inflammatory tissues defined by monoclonal antibody HECA-452.** *Am J Pathol* 1988, **130:**147-155.
454. Kobayashi M, Mitoma J, Hoshino H, Yu SY, Shimojo Y, Suzawa K, Khoo KH, Fukuda M, Nakayama J: **Prominent expression of sialyl Lewis X-capped core 2-branched O-glycans on high endothelial venule-like vessels in gastric MALT lymphoma.** *J Pathol* 2011, **224:**67-77.
455. Eriksson EE: **No detectable endothelial- or leukocyte-derived L-selectin ligand activity on the endothelium in inflamed cremaster muscle venules.** *J Leukoc Biol* 2008, **84:**93-103.
456. Shigeta A, Matsumoto M, Tedder TF, Lowe JB, Miyasaka M, Hirata T: **An L-selectin ligand distinct from P-selectin glycoprotein ligand-1 is expressed on endothelial cells and promotes neutrophil rolling in inflammation.** *Blood* 2008, **112:**4915-4923.
457. Kanda T, Yamawaki M, Ariga T, Yu RK: **Interleukin 1 beta up-regulates the expression of sulfoglucuronosyl paragloboside, a ligand for L-selectin, in brain microvascular endothelial cells.** *Proc Natl Acad Sci U S A* 1995, **92:**7897-7901.
458. Brady HR, Spertini O, Jimenez W, Brenner BM, Marsden PA, Tedder TF: **Neutrophils, monocytes, and lymphocytes bind to cytokine-activated kidney glomerular endothelial cells through L-selectin (LAM-1) in vitro.** *The Journal of Immunology* 1992, **149:**2437-2444.
459. Zakrzewicz A, Gräfe M, Terbeek D, Bongrazio M, Auch-Schwelk W, Walzog B, Graf K, Fleck E, Ley K, Gaehtgens P: **L-Selectin–Dependent Leukocyte Adhesion to Microvascular But Not to Macrovascular Endothelial Cells of the Human Coronary System.** *Blood* 1997, **89:**3228-3235.
460. Giuffrè L, Cordey A-S, Monai N, Tardy Y, Schapira M, Spertini O: **Monocyte Adhesion to Activated Aortic Endothelium: Role of L-Selectin and Heparan Sulfate Proteoglycans.** *The Journal of Cell Biology* 1997, **136:**945-956.
461. Li YF, Kawashima H, Watanabe N, Miyasaka M: **Identification and characterization of ligands for L-selectin in the kidney. II. Expression of chondroitin sulfate and heparan sulfate proteoglycans reactive with L-selectin.** *FEBS Lett* 1999, **444:**201-205.
462. Watanabe N, Kawashima H, Li YF, Miyasaka M: **Identification and characterization of ligands for L-selectin in the kidney. III. Characterization of L-selectin reactive heparan sulfate proteoglycans.** *J Biochem* 1999, **125:**826-831.
463. Celie JWAM, Keuning ED, Beelen RHJ, Dräger AM, Zweegman S, Kessler FL, Soininen R, van den Born J: **Identification of L-selectin Binding Heparan Sulfates Attached to Collagen Type XVIII.** *Journal of Biological Chemistry* 2005, **280:**26965-26973.
464. Kawashima H, Atarashi K, Hirose M, Hirose J, Yamada S, Sugahara K, Miyasaka M: **Oversulfated chondroitin/dermatan sulfates containing GlcAbeta1/IdoAalpha1-3GalNAc(4,6-O-disulfate) interact with L- and P-selectin and chemokines.** *J Biol Chem* 2002, **277:**12921-12930.
465. Kawashima H, Li YF, Watanabe N, Hirose J, Hirose M, Miyasaka M: **Identification and characterization of ligands for L-selectin in the kidney. I. Versican, a large chondroitin sulfate proteoglycan, is a ligand for L-selectin.** *Int Immunol* 1999, **11:**393-405.

466. Kitaya K, Yasuo T: **Dermatan sulfate proteoglycan biglycan as a potential selectin L/CD44 ligand involved in selective recruitment of peripheral blood CD16(-) natural killer cells into human endometrium.** *J Leukoc Biol* 2009, **85:**391-400.
467. Frey H, Schroeder N, Manon-Jensen T, Iozzo RV, Schaefer L: **Biological interplay between proteoglycans and their innate immune receptors in inflammation.** *FEBS Journal* 2013, **280:**2165-2179.
468. Tran P-K, Agardh HE, Tran-Lundmark K, Ekstrand J, Roy J, Henderson B, Gabrielsen A, Hansson GK, Swedenborg J, Paulsson-Berne G, Hedin U: **Reduced perlecan expression and accumulation in human carotid atherosclerotic lesions.** *Atherosclerosis* 2007, **190:**264-270.
469. Seidelmann SB, Kuo C, Pleskac N, Molina J, Sayers S, Li R, Zhou J, Johnson P, Braun K, Chan C, et al: **Athsq1 Is an Atherosclerosis Modifier Locus With Dramatic Effects on Lesion Area and Prominent Accumulation of Versican.** *Arteriosclerosis, Thrombosis, and Vascular Biology* 2008, **28:**2180-2186.
470. Angheloiu GO, Haka AS, Georgakoudi I, Arendt J, Müller MG, Scepanovic OR, Evanko SP, Wight TN, Mukherjee P, Waldeck DH, et al: **Detection of coronary atherosclerotic plaques with superficial proteoglycans and foam cells using real-time intrinsic fluorescence spectroscopy.** *Atherosclerosis* 2011, **215:**96-102.
471. Halpert I, Sires UI, Roby JD, Potter-Perigo S, Wight TN, Shapiro SD, Welgus HG, Wickline SA, Parks WC: **Matrilysin is expressed by lipid-laden macrophages at sites of potential rupture in atherosclerotic lesions and localizes to areas of versican deposition, a proteoglycan substrate for the enzyme.** *Proceedings of the National Academy of Sciences* 1996, **93:**9748-9753.
472. Gutierrez P, O'Brien KD, Ferguson M, Nikkari ST, Alpers CE, Wight TN: **Differences in the Distribution of Versican, Decorin, and Biglycan in Atherosclerotic Human Coronary Arteries.** *Cardiovascular Pathology* 1997, **6:**271-278.
473. Talusan P, Bedri S, Yang S, Kattapuram T, Silva N, Roughley PJ, Stone JR: **Analysis of Intimal Proteoglycans in Atherosclerosis-prone and Atherosclerosis-resistant Human Arteries by Mass Spectrometry.** *Molecular & Cellular Proteomics* 2005, **4:**1350-1357.
474. Zeng X, Chen J, Miller YI, Javaherian K, Moulton KS: **Endostatin binds biglycan and LDL and interferes with LDL retention to the subendothelial matrix during atherosclerosis.** *Journal of Lipid Research* 2005, **46:**1849-1859.
475. Kunjathoor VV, Chiu DS, O'Brien KD, LeBoeuf RC: **Accumulation of Biglycan and Perlecan, but Not Versican, in Lesions of Murine Models of Atherosclerosis.** *Arteriosclerosis, Thrombosis, and Vascular Biology* 2002, **22:**462-468.
476. Moulton KS, Olsen BR, Sonn S, Fukai N, Zurakowski D, Zeng X: **Loss of Collagen XVIII Enhances Neovascularization and Vascular Permeability in Atherosclerosis.** *Circulation* 2004, **110:**1330-1336.
477. Jin C, Ekwall A-KH, Bylund J, Bjorkman L, Estrella RP, Whitelock JM, Eisler T, Bokarewa M, Karlsson NG: **Human synovial lubricin expresses sialyl Lewis x determinant and has L-selectin ligand activity.** *Journal of Biological Chemistry* 2012.
478. Suzuki Y, Toda Y, Tamatani T, Watanabe T, Suzuki T, Nakao T, Murase K, Kiso M, Hasegawa A, Tadano-Aritomi K, et al.: **Sulfated glycolipids are ligands for a lymphocyte homing receptor, L-selectin (LECAM-1), Binding epitope in sulfated sugar chain.** *Biochem Biophys Res Commun* 1993, **190:**426-434.
479. Shikata K, Suzuki Y, Wada J, Hirata K, Matsuda M, Kawashima H, Suzuki T, Iizuka M, Makino H, Miyasaka M: **L-selectin and its ligands mediate infiltration of mononuclear cells into kidney interstitium after ureteric obstruction.** *J Pathol* 1999, **188:**93-99.
480. Takei T, Iida A, Nitta K, Tanaka T, Ohnishi Y, Yamada R, Maeda S, Tsunoda T, Takeoka S, Ito K, et al: **Association between Single-Nucleotide Polymorphisms in Selectin Genes and Immunoglobulin A Nephropathy.** *The American Journal of Human Genetics* 2002, **70:**781-786.

481. Bao X, Moseman EA, Saito H, Petryniak B, Thiriot A, Hatakeyama S, Ito Y, Kawashima H, Yamaguchi Y, Lowe JB, et al: **Endothelial heparan sulfate controls chemokine presentation in recruitment of lymphocytes and dendritic cells to lymph nodes.** *Immunity* 2010, **33:**817-829.
482. Solic N, Wilson J, Wilson SJ, Shute JK: **Endothelial Activation and Increased Heparan Sulfate Expression in Cystic Fibrosis.** *American Journal of Respiratory and Critical Care Medicine* 2005, **172:**892-898.
483. Hirose M, Matsumura R, Sato K, Murai T, Kawashima H: **Binding of L-selectin to its vascular and extravascular ligands is differentially regulated by pH.** *Biochem Biophys Res Commun* 2011.
484. Martinez P, Vergoten G, Colomb F, Bobowski M, Steenackers A, Carpentier M, Allain F, Delannoy P, Julien S: **Over-sulfated glycosaminoglycans are alternative selectin ligands: insights into molecular interactions and possible role in breast cancer metastasis.** *Clin Exp Metastasis* 2013.
485. Lardner A: **The effects of extracellular pH on immune function.** *J Leukoc Biol* 2001, **69:**522-530.
486. Karhausen J, Haase VH, Colgan SP: **Inflammatory hypoxia: role of hypoxia-inducible factor.** *Cell Cycle* 2005, **4:**256-258.
487. Fieger CB, Sassetti CM, Rosen SD: **Endoglycan, a Member of the CD34 Family, Functions as an L-selectin Ligand through Modification with Tyrosine Sulfation and Sialyl Lewis x.** *Journal of Biological Chemistry* 2003, **278:**27390-27398.
488. Thomas SN, Schnaar RL, Konstantopoulos K: **Podocalyxin-like protein is an E-/L-selectin ligand on colon carcinoma cells: comparative biochemical properties of selectin ligands in host and tumor cells.** *Am J Physiol Cell Physiol* 2009, **296:**C505-513.
489. Laubli H, Stevenson JL, Varki A, Varki NM, Borsig L: **L-selectin facilitation of metastasis involves temporal induction of Fut7-dependent ligands at sites of tumor cell arrest.** *Cancer Res* 2006, **66:**1536-1542.
490. Nejatbakhsh R, Kabir-Salmani M, Dimitriadis E, Hosseini A, Taheripanah R, Sadeghi Y, Akimoto Y, Iwashita M: **Subcellular localization of L-selectin ligand in the endometrium implies a novel function for pinopodes in endometrial receptivity.** *Reprod Biol Endocrinol* 2012, **10:**46.
491. Genbacev OD, Prakobphol A, Foulk RA, Krtolica AR, Ilic D, Singer MS, Yang ZQ, Kiessling LL, Rosen SD, Fisher SJ: **Trophoblast L-selectin-mediated adhesion at the maternal-fetal interface.** *Science* 2003, **299:**405-408.
492. Dimitroff CJ, Lee JY, Fuhlbrigge RC, Sackstein R: **A distinct glycoform of CD44 is an L-selectin ligand on human hematopoietic cells.** *Proc Natl Acad Sci U S A* 2000, **97:**13841-13846.
493. Malhotra R, Ward M, Sim RB, Bird MI: **Identification of human complement Factor H as a ligand for L-selectin.** *Biochem J* 1999, **341 (Pt 1):**61-69.
494. Harms G, Kraft R, Grelle G, Volz B, Dernedde J, Tauber R: **Identification of nucleolin as a new L-selectin ligand.** *Biochem J* 2001, **360:**531-538.
495. Haribabu B, Steeber DA, Ali H, Richardson RM, Snyderman R, Tedder TF: **Chemoattractant receptor-induced phosphorylation of L-selectin.** *J Biol Chem* 1997, **272:**13961-13965.
496. Killock DJ, Ivetic A: **The cytoplasmic domains of TNF-alpha converting enzyme (TACE/ADAM17) and L-selectin are regulated differently by p38 MAPK and PKC to promote ectodomain shedding.** *Biochem J* 2010.
497. Mascarell L, Truffa-Bachi P: **T lymphocyte activation initiates the degradation of the CD62L encoding mRNA and increases the transcription of the corresponding gene.** *Immunol Lett* 2004, **94:**115-122.
498. Sallusto F, Lenig D, Forster R, Lipp M, Lanzavecchia A: **Two subsets of memory T lymphocytes with distinct homing potentials and effector functions.** *Nature* 1999, **401:**708-712.

499. Tatewaki M, Yamaguchi K, Matsuoka M, Ishii T, Miyasaka M, Mori S, Takatsuki K, Watanabe T: **Constitutive overexpression of the L-selectin gene in fresh leukemic cells of adult T-cell leukemia that can be transactivated by human T- cell lymphotropic virus type 1 Tax.** *Blood* 1995, **86:**3109-3117.
500. Furukawa Y, Umemoto E, Jang MH, Tohya K, Miyasaka M, Hirata T: **Identification of novel isoforms of mouse L-selectin with different carboxyl-terminal tails.** *J Biol Chem* 2008, **283:**12112-12119.
501. Bai A, Hu H, Yeung M, Chen J: **Kruppel-like factor 2 controls T cell trafficking by activating L-selectin (CD62L) and sphingosine-1-phosphate receptor 1 transcription.** *J Immunol* 2007, **178:**7632-7639.
502. Dang X, Raffler NA, Ley K: **Transcriptional regulation of mouse L-selectin.** *Biochim Biophys Acta* 2009, **1789:**146-152.
503. Lou Y, Lu X, Dang X: **FOXO1 Up-Regulates Human L-selectin Expression Through Binding to a Consensus FOXO1 Motif.** *Gene Regul Syst Bio* 2012, **6:**139-149.
504. Takada K, Wang X, Hart GT, Odumade OA, Weinreich MA, Hogquist KA, Jameson SC: **Kruppel-like factor 2 is required for trafficking but not quiescence in postactivated T cells.** *J Immunol* 2011, **186:**775-783.
505. Kerdiles YM, Beisner DR, Tinoco R, Dejean AS, Castrillon DH, DePinho RA, Hedrick SM: **Foxo1 links homing and survival of naive T cells by regulating L-selectin, CCR7 and interleukin 7 receptor.** *Nat Immunol* 2009, **10:**176-184.
506. Fabre S, Carrette F, Chen J, Lang V, Semichon M, Denoyelle C, Lazar V, Cagnard N, Dubart-Kupperschmitt A, Mangeney M, et al: **FOXO1 regulates L-Selectin and a network of human T cell homing molecules downstream of phosphatidylinositol 3-kinase.** *J Immunol* 2008, **181:**2980-2989.
507. Yamada T, Park CS, Mamonkin M, Lacorazza HD: **Transcription factor ELF4 controls the proliferation and homing of CD8+ T cells via the Kruppel-like factors KLF4 and KLF2.** *Nat Immunol* 2009, **10:**618-626.
508. Weinreich MA, Takada K, Skon C, Reiner SL, Jameson SC, Hogquist KA: **KLF2 transcription-factor deficiency in T cells results in unrestrained cytokine production and upregulation of bystander chemokine receptors.** *Immunity* 2009, **31:**122-130.
509. Carlson CM, Endrizzi BT, Wu J, Ding X, Weinreich MA, Walsh ER, Wani MA, Lingrel JB, Hogquist KA, Jameson SC: **Kruppel-like factor 2 regulates thymocyte and T-cell migration.** *Nature* 2006, **442:**299-302.
510. Gubbels Bupp MR, Edwards B, Guo C, Wei D, Chen G, Wong B, Masteller E, Peng SL: **T cells require Foxo1 to populate the peripheral lymphoid organs.** *Eur J Immunol* 2009, **39:**2991-2999.
511. Sinclair LV, Finlay D, Feijoo C, Cornish GH, Gray A, Ager A, Okkenhaug K, Hagenbeek TJ, Spits H, Cantrell DA: **Phosphatidylinositol-3-OH kinase and nutrient-sensing mTOR pathways control T lymphocyte trafficking.** *Nat Immunol* 2008, **9:**513-521.
512. Ren X, Zhang Y, Snyder J, Cross ER, Shah TA, Kalin TV, Kalinichenko VV: **Forkhead box M1 transcription factor is required for macrophage recruitment during liver repair.** *Mol Cell Biol* 2010, **30:**5381-5393.
513. Chen HY, Cui B, Wang S, Zhao ZF, Sun H, Zhao YJ, Li XY, Ning G: **L-selectin gene polymorphisms in Graves' disease.** *Clin Endocrinol (Oxf)* 2007, **67:**145-151.
514. Takei T, Hiraoka M, Nitta K, Uchida K, Deushi M, Yu T, Nitta N, Tsuchiya K, Yumura W, Nihei H, et al: **Functional impact of IgA nephropathy-associated selectin gene haplotype on leukocyte-endothelial interaction.** *Immunogenetics* 2006, **58:**355-361.
515. Kahn J, Walcheck B, Migaki GI, Jutila MA, Kishimoto TK: **Calmodulin regulates L-selectin adhesion molecule expression and function through a protease-dependent mechanism.** *Cell* 1998, **92:**809-818.
516. Feehan C, Darlak K, Kahn J, Walcheck B, Spatola AF, Kishimoto TK: **Shedding of the lymphocyte L-selectin adhesion molecule is inhibited by a hydroxamic acid-based**

protease inhibitor. Identification with an L-selectin-alkaline phosphatase reporter. *J Biol Chem* 1996, **271:**7019-7024.
517. Preece G, Murphy G, Ager A: **Metalloproteinase-mediated regulation of L-selectin levels on leucocytes.** *J Biol Chem* 1996, **271:**11634-11640.
518. Faveeuw C, Preece G, Ager A: **Transendothelial migration of lymphocytes across high endothelial venules into lymph nodes is affected by metalloproteinases.** *Blood* 2001, **98:**688-695.
519. Walcheck B, Kahn J, Fisher JM, Wang BB, Fisk RS, Payan DG, Feehan C, Betageri R, Darlak K, Spatola AF, Kishimoto TK: **Neutrophil rolling altered by inhibition of L-selectin shedding in vitro.** *Nature* 1996, **380:**720-723.
520. Allport JR, Ding HT, Ager A, Steeber DA, Tedder TF, Luscinskas FW: **L-selectin shedding does not regulate human neutrophil attachment, rolling, or transmigration across human vascular endothelium in vitro.** *J Immunol* 1997, **158:**4365-4372.
521. Li Y, Brazzell J, Herrera A, Walcheck B: **ADAM17 deficiency by mature neutrophils has differential effects on L-selectin shedding.** *Blood* 2006, **108:**2275-2279.
522. Chen A, Engel P, Tedder TF: **Structural requirements regulate endoproteolytic release of the L-selectin (CD62L) adhesion receptor from the cell surface of leukocytes.** *J Exp Med* 1995, **182:**519-530.
523. Peschon JJ, Slack JL, Reddy P, Stocking KL, Sunnarborg SW, Lee DC, Russell WE, Castner BJ, Johnson RS, Fitzner JN, et al: **An essential role for ectodomain shedding in mammalian development.** *Science* 1998, **282:**1281-1284.
524. Gomez-Gaviro M, Dominguez-Luis M, Canchado J, Calafat J, Janssen H, Lara-Pezzi E, Fourie A, Tugores A, Valenzuela-Fernandez A, Mollinedo F, et al: **Expression and regulation of the metalloproteinase ADAM-8 during human neutrophil pathophysiological activation and its catalytic activity on L-selectin shedding.** *J Immunol* 2007, **178:**8053-8063.
525. Le Gall SM, Bobe P, Reiss K, Horiuchi K, Niu XD, Lundell D, Gibb DR, Conrad D, Saftig P, Blobel CP: **ADAMs 10 and 17 represent differentially regulated components of a general shedding machinery for membrane proteins such as transforming growth factor alpha, L-selectin, and tumor necrosis factor alpha.** *Mol Biol Cell* 2009, **20:**1785-1794.
526. Edwards DR, Handsley MM, Pennington CJ: **The ADAM metalloproteinases.** *Mol Aspects Med* 2008, **29:**258-289.
527. Tang J, Zarbock A, Gomez I, Wilson CL, Lefort CT, Stadtmann A, Bell B, Huang LC, Ley K, Raines EW: **Adam17-dependent shedding limits early neutrophil influx but does not alter early monocyte recruitment to inflammatory sites.** *Blood* 2011, **118:**786-794.
528. Migaki GI, Kahn J, Kishimoto TK: **Mutational analysis of the membrane-proximal cleavage site of L-selectin: relaxed sequence specificity surrounding the cleavage site.** *J Exp Med* 1995, **182:**549-557.
529. Stoddart JH, Jr., Jasuja RR, Sikorski MA, von Andrian UH, Mier JW: **Protease-resistant L-selectin mutants. Down-modulation by cross-linking but not cellular activation.** *J Immunol* 1996, **157:**5653-5659.
530. Wang Y, Herrera AH, Li Y, Belani KK, Walcheck B: **Regulation of mature ADAM17 by redox agents for L-selectin shedding.** *J Immunol* 2009, **182:**2449-2457.
531. Lee D, Schultz JB, Knauf PA, King MR: **Mechanical shedding of L-selectin from the neutrophil surface during rolling on sialyl Lewis x under flow.** *J Biol Chem* 2007, **282:**4812-4820.
532. Andonegui G, Bonder CS, Green F, Mullaly SC, Zbytnuik L, Raharjo E, Kubes P: **Endothelium-derived Toll-like receptor-4 is the key molecule in LPS-induced neutrophil sequestration into lungs.** *J Clin Invest* 2003, **111:**1011-1020.
533. Palecanda A, Walcheck B, Bishop DK, Jutila MA: **Rapid activation-independent shedding of leukocyte L-selectin induced by cross-linking of the surface antigen.** *European Journal of Immunology* 1992, **22:**1279-1286.

534. Frey M, Appenheimer MM, Evans SS: **Tyrosine kinase-dependent regulation of L-selectin expression through the Leu-13 signal transduction molecule: evidence for a protein kinase C-independent mechanism of L-selectin shedding.** *J Immunol* 1997, **158:**5424-5434.
535. Jasuja RR, Mier JW: **Differential effects of hydroxamate inhibitors on PMA and ligand-induced L-Selectin down-modulation: role of membrane proximal and cytoplasmic domains.** *Int J Immunopathol Pharmacol* 2000, **13:**1-12.
536. Phong MC, Gutwein P, Kadel S, Hexel K, Altevogt P, Linderkamp O, Brenner B: **Molecular mechanisms of L-selectin-induced co-localization in rafts and shedding [corrected].** *Biochem Biophys Res Commun* 2003, **300:**563-569.
537. Vlad A, Deglesne P-A, Letestu R, Saint-Georges S, Chevallier N, Baran-Marszak F, Varin-Blank N, Ajchenbaum-Cymbalista F, Ledoux D: **Down-regulation of CXCR4 and CD62L in Chronic Lymphocytic Leukemia Cells Is Triggered by B-Cell Receptor Ligation and Associated with Progressive Disease.** *Cancer Research* 2009, **69:**6387-6395.
538. Jung TM, Gallatin WM, Weissman IL, Dailey MO: **Down-regulation of homing receptors after T cell activation.** *J Immunol* 1988, **141:**4110-4117.
539. Kaba NK, Schultz J, Law FY, Lefort CT, Martel-Gallegos G, Kim M, Waugh RE, Arreola J, Knauf PA: **Inhibition of Na+/H+ exchanger enhances low pH-induced L-selectin shedding and beta2-integrin surface expression in human neutrophils.** *Am J Physiol Cell Physiol* 2008, **295:**C1454-1463.
540. Fan H, Derynck R: **Ectodomain shedding of TGF-alpha and other transmembrane proteins is induced by receptor tyrosine kinase activation and MAP kinase signaling cascades.** *EMBO J* 1999, **18:**6962-6972.
541. Rizoli SB, Rotstein OD, Kapus A: **Cell volume-dependent regulation of L-selectin shedding in neutrophils. A role for p38 mitogen-activated protein kinase.** *J Biol Chem* 1999, **274:**22072-22080.
542. Schleiffenbaum B, Spertini O, Tedder TF: **Soluble L-selectin is present in human plasma at high levels and retains functional activity.** *J Cell Biol* 1992, **119:**229-238.
543. Tu L, Poe JC, Kadono T, Venturi GM, Bullard DC, Tedder TF, Steeber DA: **A functional role for circulating mouse L-selectin in regulating leukocyte/endothelial cell interactions in vivo.** *J Immunol* 2002, **169:**2034-2043.
544. Walcheck B, Alexander SR, St. Hill CA, Matala E: **ADAM-17-independent shedding of L-selectin.** *Journal of Leukocyte Biology* 2003, **74:**389-394.
545. Spertini O, Schleiffenbaum B, White-Owen C, Ruiz P, Jr., Tedder TF: **ELISA for quantitation of L-selectin shed from leukocytes in vivo.** *J Immunol Methods* 1992, **156:**115-123.
546. Font J, Pizcueta P, Ramos-Casals M, Cervera R, Garcia-Carrasco M, Navarro M, Ingelmo M, Engel P: **Increased serum levels of soluble L-selectin (CD62L) in patients with active systemic lupus erythematosus (SLE).** *Clin Exp Immunol* 2000, **119:**169-174.
547. Russell AI, Cunninghame Graham DS, Chadha S, Roberton C, Fernandez-Hart T, Griffiths B, D'Cruz D, Nitsch D, Whittaker JC, Vyse TJ: **No association between E- and L-selectin genes and SLE: soluble L-selectin levels do correlate with genotype and a subset in SLE.** *Genes Immun* 2005, **6:**422-429.
548. Kretowski A, Gillespie KM, Bingley PJ, Kinalska I: **Soluble L-selectin levels in type I diabetes mellitus: a surrogate marker for disease activity?** *Immunology* 2000, **99:**320-325.
549. Donnelly SC, Haslett C, Dransfield I, Robertson CE, Carter DC, Ross JA, Grant IS, Tedder TF: **Role of selectins in development of adult respiratory distress syndrome.** *Lancet* 1994, **344:**215-219.
550. Wang Y, Zhang AC, Ni Z, Herrera A, Walcheck B: **ADAM17 activity and other mechanisms of soluble L-selectin production during death receptor-induced leukocyte apoptosis.** *J Immunol* 2010, **184:**4447-4454.

551. Hafezi-Moghadam A, Ley K: **Relevance of L-selectin shedding for leukocyte rolling in vivo.** *J Exp Med* 1999, **189:**939-948.
552. Hafezi-Moghadam A, Thomas KL, Prorock AJ, Huo Y, Ley K: **L-selectin shedding regulates leukocyte recruitment.** *J Exp Med* 2001, **193:**863-872.
553. Klinger A, Gebert A, Bieber K, Kalies K, Ager A, Bell EB, Westermann J: **Cyclical expression of L-selectin (CD62L) by recirculating T cells.** *Int Immunol* 2009, **21:**443-455.
554. Bradfield PF, Scheiermann C, Nourshargh S, Ody C, Luscinskas FW, Rainger GE, Nash GB, Miljkovic-Licina M, Aurrand-Lions M, Imhof BA: **JAM-C regulates unidirectional monocyte transendothelial migration in inflammation.** *Blood* 2007, **110:**2545-2555.
555. Evans BJ, McDowall A, Taylor PC, Hogg N, Haskard DO, Landis RC: **Shedding of lymphocyte function-associated antigen-1 (LFA-1) in a human inflammatory response.** *Blood* 2006, **107:**3593-3599.
556. Dadfar E, Lundahl J, Fernvik E, Nopp A, Hylander B, Jacobson S: **Leukocyte CD11b and CD62l expression in response to interstitial inflammation in CAPD patients.** *Perit Dial Int* 2004, **24:**28-36.
557. Kansas GS, Ley K, Munro JM, Tedder TF: **Regulation of leukocyte rolling and adhesion to high endothelial venules through the cytoplasmic domain of L-selectin.** *J Exp Med* 1993, **177:**833-838.
558. Ivetic A, Florey O, Deka J, Haskard DO, Ager A, Ridley AJ: **Mutagenesis of the ezrin-radixin-moesin binding domain of L-selectin tail affects shedding, microvillar positioning, and leukocyte tethering.** *J Biol Chem* 2004, **279:**33263-33272.
559. Matala E, Alexander SR, Kishimoto TK, Walcheck B: **The cytoplasmic domain of L-selectin participates in regulating L-selectin endoproteolysis.** *J Immunol* 2001, **167:**1617-1623.
560. Evans SS, Schleider DM, Bowman LA, Francis ML, Kansas GS, Black JD: **Dynamic association of L-selectin with the lymphocyte cytoskeletal matrix.** *J Immunol* 1999, **162:**3615-3624.
561. Dwir O, Kansas GS, Alon R: **Cytoplasmic anchorage of L-selectin controls leukocyte capture and rolling by increasing the mechanical stability of the selectin tether.** *J Cell Biol* 2001, **155:**145-156.
562. Chen C, Ba X, Xu T, Cui L, Hao S, Zeng X: **c-Abl is involved in the F-actin assembly triggered by L-selectin crosslinking.** *J Biochem* 2006, **140:**229-235.
563. Ivetic A, Deka J, Ridley A, Ager A: **The cytoplasmic tail of L-selectin interacts with members of the Ezrin-Radixin-Moesin (ERM) family of proteins: cell activation-dependent binding of Moesin but not Ezrin.** *J Biol Chem* 2002, **277:**2321-2329.
564. Ivetic A, Ridley AJ: **The telling tail of L-selectin.** *Biochem Soc Trans* 2004, **32:**1118-1121.
565. Pavalko FM, Walker DM, Graham L, Goheen M, Doerschuk CM, Kansas GS: **The cytoplasmic domain of L-selectin interacts with cytoskeletal proteins via alpha-actinin: receptor positioning in microvilli does not require interaction with alpha-actinin.** *J Cell Biol* 1995, **129:**1155-1164.
566. Freeman EA, Jani P, Millette CE: **Expression and potential function of Rho family small G proteins in cells of the mammalian seminiferous epithelium.** *Cell Commun Adhes* 2002, **9:**189-204.
567. Kilian K, Dernedde J, Mueller E-C, Bahr I, Tauber R: **The Interaction of Protein Kinase C Isozymes α, ι, and θ with the Cytoplasmic Domain of L-selectin Is Modulated by Phosphorylation of the Receptor.** *Journal of Biological Chemistry* 2004, **279:**34472-34480.
568. Gary R, Bretscher A: **Ezrin self-association involves binding of an N-terminal domain to a normally masked C-terminal domain that includes the F-actin binding site.** *Mol Biol Cell* 1995, **6:**1061-1075.

569. Turunen O, Wahlstrom T, Vaheri A: **Ezrin has a COOH-terminal actin-binding site that is conserved in the ezrin protein family.** *J Cell Biol* 1994, **126:**1445-1453.
570. Tsukita S, Yonemura S: **Cortical actin organization: lessons from ERM (ezrin/radixin/moesin) proteins.** *J Biol Chem* 1999, **274:**34507-34510.
571. Ivetic A, Ridley AJ: **Ezrin/radixin/moesin proteins and Rho GTPase signalling in leucocytes.** *Immunology* 2004, **112:**165-176.
572. Killock DJ, Parsons M, Zarrouk M, Ameer-Beg SM, Ridley AJ, Haskard DO, Zvelebil M, Ivetic A: **In Vitro and in Vivo Characterization of Molecular Interactions between Calmodulin, Ezrin/Radixin/Moesin, and L-selectin.** *J Biol Chem* 2009, **284:**8833-8845.
573. Deng W, Cho S, Li R: **FERM domain of moesin desorbs the basic-rich cytoplasmic domain of L-selectin from the anionic membrane surface.** *Journal of Molecular Biology*.
574. Deng W, Putkey JA, Li R: **Calmodulin adopts an extended conformation when interacting with L-selectin in membranes.** *PLoS One* 2013, **8:**e62861.
575. Gifford JL, Ishida H, Vogel HJ: **Structural Insights into Calmodulin-regulated L-selectin Ectodomain Shedding.** *Journal of Biological Chemistry* 2012, **287:**26513-26527.
576. Deng W, Srinivasan S, Zheng X, Putkey JA, Li R: **Interaction of Calmodulin with l-Selectin at the Membrane Interface: Implication on the Regulation of l-Selectin Shedding.** *Journal of Molecular Biology* 2011, **411:**220-233.
577. Takasaki A, Hayashi N, Matsubara M, Yamauchi E, Taniguchi H: **Identification of the Calmodulin-binding Domain of Neuron-specific Protein Kinase C Substrate Protein CAP-22/NAP-22: DIRECT INVOLVEMENT OF PROTEIN MYRISTOYLATION IN CALMODULIN-TARGET PROTEIN INTERACTION.** *Journal of Biological Chemistry* 1999, **274:**11848-11853.
578. Krasel C, Dammeier S, Winstel R, Brockmann J, Mischak H, Lohse MJ: **Phosphorylation of GRK2 by Protein Kinase C Abolishes Its Inhibition by Calmodulin.** *Journal of Biological Chemistry* 2001, **276:**1911-1915.
579. Srinivasan S, Deng W, Li R: **L-selectin transmembrane and cytoplasmic domains are monomeric in membranes.** *Biochim Biophys Acta* 2011, **1808:**1709-1715.
580. Zhang Y, Jiang N, Zarnitsyna VI, Klopocki AG, McEver RP, Zhu C: **P-selectin glycoprotein ligand-1 forms dimeric interactions with E-selectin but monomeric interactions with L-selectin on cell surfaces.** *PLoS One* 2013, **8:**e57202.
581. Barkalow FJ, Barkalow KL, Mayadas TN: **Dimerization of P-selectin in platelets and endothelial cells.** *Blood* 2000, **96:**3070-3077.
582. Moore KL, Stults NL, Diaz S, Smith DF, Cummings RD, Varki A, McEver RP: **Identification of a specific glycoprotein ligand for P-selectin (CD62) on myeloid cells.** *J Cell Biol* 1992, **118:**445-456.
583. Ramachandran V, Yago T, Epperson TK, Kobzdej MMA, Nollert MU, Cummings RD, Zhu C, McEver RP: **Dimerization of a selectin and its ligand stabilizes cell rolling and enhances tether strength in shear flow.** *Proceedings of the National Academy of Sciences* 2001, **98:**10166-10171.
584. Dwir O, Steeber DA, Schwarz US, Camphausen RT, Kansas GS, Tedder TF, Alon R: **L-selectin dimerization enhances tether formation to properly spaced ligand.** *J Biol Chem* 2002, **277:**21130-21139.
585. Li X, Steeber DA, Tang MLK, Farrar MA, Perlmutter RM, Tedder TF: **Regulation of L-Selectin–mediated Rolling through Receptor Dimerization.** *The Journal of Experimental Medicine* 1998, **188:**1385-1390.
586. Mattila PE, Green CE, Schaff U, Simon SI, Walcheck B: **Cytoskeletal interactions regulate inducible L-selectin clustering.** *American Journal of Physiology - Cell Physiology* 2005, **289:**C323-C332.
587. Leid JG, Steeber DA, Tedder TF, Jutila MA: **Antibody Binding to a Conformation-Dependent Epitope Induces L-Selectin Association with the Detergent-Resistant Cytoskeleton.** *The Journal of Immunology* 2001, **166:**4899-4907.

588. Dykstra M, Cherukuri A, Sohn HW, Tzeng SJ, Pierce SK: **Location is everything: lipid rafts and immune cell signaling.** *Annu Rev Immunol* 2003, **21:**457-481.
589. Smolen JE, Petersen TK, Koch C, O'Keefe SJ, Hanlon WA, Seo S, Pearson D, Fossett MC, Simon SI: **L-Selectin Signaling of Neutrophil Adhesion and Degranulation Involves p38 Mitogen-activated Protein Kinase.** *Journal of Biological Chemistry* 2000, **275:**15876-15884.
590. Simon SI, Hu Y, Vestweber D, Smith CW: **Neutrophil tethering on E-selectin activates beta 2 integrin binding to ICAM-1 through a mitogen-activated protein kinase signal transduction pathway.** *J Immunol* 2000, **164:**4348-4358.
591. Steeber DA, Engel P, Miller AS, Sheetz MP, Tedder TF: **Ligation of L-selectin through conserved regions within the lectin domain activates signal transduction pathways and integrin function in human, mouse, and rat leukocytes.** *J Immunol* 1997, **159:**952-963.
592. Phillips R, Ager A: **Activation of pertussis toxin-sensitive CXCL12 (SDF-1) receptors mediates transendothelial migration of T lymphocytes across lymph node high endothelial cells.** *Eur J Immunol* 2002, **32:**837-847.
593. Eitner F, Cui Y, Hudkins KL, Alpers CE: **Chemokine receptor (CXCR4) mRNA-expressing leukocytes are increased in human renal allograft rejection.** *Transplantation* 1998, **66:**1551-1557.
594. Buckley CD, Amft N, Bradfield PF, Pilling D, Ross E, Arenzana-Seisdedos F, Amara A, Curnow SJ, Lord JM, Scheel-Toellner D, Salmon M: **Persistent induction of the chemokine receptor CXCR4 by TGF-beta 1 on synovial T cells contributes to their accumulation within the rheumatoid synovium.** *J Immunol* 2000, **165:**3423-3429.
595. Gonzalo JA, Lloyd CM, Peled A, Delaney T, Coyle AJ, Gutierrez-Ramos JC: **Critical involvement of the chemotactic axis CXCR4/stromal cell-derived factor-1 alpha in the inflammatory component of allergic airway disease.** *J Immunol* 2000, **165:**499-508.
596. Manning G, Whyte DB, Martinez R, Hunter T, Sudarsanam S: **The Protein Kinase Complement of the Human Genome.** *Science* 2002, **298:**1912-1934.
597. WIDMANN C, GIBSON S, JARPE MB, JOHNSON GL: **Mitogen-Activated Protein Kinase: Conservation of a Three-Kinase Module From Yeast to Human.** *Physiological Reviews* 1999, **79:**143-180.
598. Chen RE, Thorner J: **Function and regulation in MAPK signaling pathways: lessons learned from the yeast Saccharomyces cerevisiae.** *Biochim Biophys Acta* 2007, **1773:**1311-1340.
599. Ingley E: **Src family kinases: Regulation of their activities, levels and identification of new pathways.** *Biochimica et Biophysica Acta (BBA) - Proteins and Proteomics* 2008, **1784:**56-65.
600. Colicelli J: **ABL Tyrosine Kinases: Evolution of Function, Regulation, and Specificity.** *Sci Signal* 2010, **3:**re6-.
601. Waddell TK, Fialkow L, Chan CK, Kishimoto TK, Downey GP: **Signaling Functions of L-selectin.** *Journal of Biological Chemistry* 1995, **270:**15403-15411.
602. Xu T, Chen L, Shang X, Cui L, Luo J, Chen C, Ba X, Zeng X: **Critical role of Lck in L-selectin signaling induced by sulfatides engagement.** *Journal of Leukocyte Biology* 2008, **84:**1192-1201.
603. Brenner B, Weinmann S, Grassme H, Lang F, Linderkamp O, Gulbins E: **L-selectin activates JNK via src-like tyrosine kinases and the small G-protein Rac.** *Immunology* 1997, **92:**214-219.
604. Waddell TK, Fialkow L, Chan CK, Kishimoto TK, Downey GP: **Potentiation of the oxidative burst of human neutrophils. A signaling role for L-selectin.** *Journal of Biological Chemistry* 1994, **269:**18485-18491.
605. Brenner B, Grassme HU, Muller C, Lang F, Speer CP, Gulbins E: **L-selectin stimulates the neutral sphingomyelinase and induces release of ceramide.** *Exp Cell Res* 1998, **243:**123-128.

606. Kolesnick R, Golde DW: **The sphingomyelin pathway in tumor necrosis factor and interleukin-1 signaling.** *Cell* 1994, **77:**325-328.
607. Hannun YA: **The sphingomyelin cycle and the second messenger function of ceramide.** *J Biol Chem* 1994, **269:**3125-3128.
608. Chen C, Shang X, Cui L, Xu T, Luo J, Ba X, Zeng X: **L-selectin ligation-induced CSF-1 gene transcription is regulated by AP-1 in a c-Abl kinase-dependent manner.** *Human Immunology* 2008, **69:**501-509.
609. Laudanna C, Constantin G, Baron P, Scarpini E, Scarlato G, Cabrini G, Dechecchi C, Rossi F, Cassatella MA, Berton G: **Sulfatides trigger increase of cytosolic free calcium and enhanced expression of tumor necrosis factor-alpha and interleukin-8 mRNA in human neutrophils. Evidence for a role of L-selectin as a signaling molecule.** *Journal of Biological Chemistry* 1994, **269:**4021-4026.
610. Wang WC, Goldman LM, Schleider DM, Appenheimer MM, Subjeck JR, Repasky EA, Evans SS: **Fever-range hyperthermia enhances L-selectin-dependent adhesion of lymphocytes to vascular endothelium.** *J Immunol* 1998, **160:**961-969.
611. Leyko W, Bartosz G: **Membrane effects of ionizing radiation and hyperthermia.** *Int J Radiat Biol Relat Stud Phys Chem Med* 1986, **49:**743-770.
612. Khazen D, Jendoubi-Ayed S, Aleya WB, Sfar I, Mouelhi L, Matri S, Najjar T, Filali A, Gorgi Y, Abdallah TB, Ayed K: **Polymorphism in ICAM-1, PECAM-1, E-selectin, and L-selectin genes in Tunisian patients with inflammatory bowel disease.** *Eur J Gastroenterol Hepatol* 2009, **21:**167-175.
613. Rafiei A, Hajilooi M, Shakib RJ, Shams S, Sheikh N: **Association between the Phe206Leu polymorphism of L-selectin and brucellosis.** *J Med Microbiol* 2006, **55:**511-516.
614. Kretowski A, Kinalska I: **L-selectin gene T668C mutation in type 1 diabetes patients and their first degree relatives.** *Immunol Lett* 2000, **74:**225-228.
615. Liu J, Liu J-x, Xu S-n, Quan J-x, Tian L-m, Guo Q, Liu J, Wang Y-f, Shi Z-y: **Association of P213S polymorphism of the L-selectin gene with type 2 diabetes and insulin resistance in Chinese population.** *Gene* 2012, **509:**286-290.
616. Xia ZE, Li Y, Ming KH, Xiong XQ: **[Association of L-selectin gene polymorphism with susceptibility to coronary heart disease].** *Zhonghua Yi Xue Yi Chuan Xue Za Zhi* 2007, **24:**173-176.
617. Wei YS, Lan Y, Meng LQ, Nong LG: **The association of L-selectin polymorphisms with L-selectin serum levels and risk of ischemic stroke.** *J Thromb Thrombolysis* 2011, **32:**110-115.
618. Kamiuchi K, Hasegawa G, Obayashi H, Kitamura A, Ishii M, Yano M, Kanatsuna T, Yoshikawa T, Nakamura N: **Leukocyte-endothelial cell adhesion molecule 1 (LECAM-1) polymorphism is associated with diabetic nephropathy in type 2 diabetes mellitus.** *J Diabetes Complications* 2002, **16:**333-337.
619. Stavarachi M, Panduru NM, Serafinceanu C, Mota E, Mota M, Cimponeriu D, Ion DA: **Investigation of P213S SELL gene polymorphism in type 2 diabetes mellitus and related end stage renal disease. A case-control study.** *Rom J Morphol Embryol* 2011, **52:**995-998.
620. Heinold A, Opelz G, Dohler B, Scherer S, Ruhenstroth A, Tran TH: **Genetic polymorphisms of adhesion molecules and kidney transplant survival.** *Transplantation* 2010, **89:**1079-1087.
621. Ensembl: **Gene: SELL ENSG00000188404.**
622. Galkina E, Kadl A, Sanders J, Varughese D, Sarembock IJ, Ley K: **Lymphocyte recruitment into the aortic wall before and during development of atherosclerosis is partially L-selectin dependent.** *The Journal of Experimental Medicine* 2006, **203:**1273-1282.
623. Rozenberg I, Sluka SH, Mocharla P, Hallenberg A, Rotzius P, Boren J, Krankel N, Landmesser U, Borsig L, Luscher TF, et al: **Deletion of L-selectin increases atherosclerosis development in ApoE-/- mice.** *PLoS One* 2011, **6:**e21675.

624. Dominguez-Luis M, Herrera-Garcia A, Arce-Franco M, Armas-Gonzalez E, Rodriguez-Pardo M, Lorenzo-Diaz F, Feria M, Cadenas S, Sanchez-Madrid F, Diaz-Gonzalez F: **Superoxide anion mediates the L-selectin down-regulation induced by non-steroidal anti-inflammatory drugs in human neutrophils.** *Biochem Pharmacol* 2013, **85:**245-256.
625. Diaz-Gonzalez F, Gonzalez-Alvaro I, Campanero MR, Mollinedo F, del Pozo MA, Munoz C, Pivel JP, Sanchez-Madrid F: **Prevention of in vitro neutrophil-endothelial attachment through shedding of L-selectin by nonsteroidal antiinflammatory drugs.** *J Clin Invest* 1995, **95:**1756-1765.
626. Herrera-Garcia A, Dominguez-Luis M, Arce-Franco M, Lopez-Fernandez J, Feria M, Barreiro O, Sanchez-Madrid F, Diaz-Gonzalez F: **In vivo modulation of the inflammatory response by nonsteroidal antiinflammatory drug-related compounds that trigger L-selectin shedding.** *Eur J Immunol* 2013, **43:**55-64.
627. Seekamp A, van Griensven M, Rusu C, König J, Khan-Boluki J, Redl H: **The Effect of Anti-L-Selectin (Aselizumab) on the Posttraumatic Inflammatory Response in Multiply Traumatized Patients.** *European Journal of Trauma* 2005, **31:**557-567.
628. Gaber AO, Mulgaonkar S, Kahan BD, Woodle ES, Alloway R, Bajjoka I, Jensik S, Klintmalm GB, Patton PR, Wiseman A, et al: **YSPSL (rPSGL-Ig) for improvement of early renal allograft function: a double-blind, placebo-controlled, multi-center Phase IIa study.** *Clin Transplant* 2011, **25:**523-533.
629. Bernal A, San Martin N, Fernandez M, Covarello D, Molla F, Soldo A, Latini R, Cossu G, Galvez BG: **L-selectin and SDF-1 enhance the migration of mouse and human cardiac mesoangioblasts.** *Cell Death Differ* 2012, **19:**345-355.
630. Galvez BG, Sampaolesi M, Barbuti A, Crespi A, Covarello D, Brunelli S, Dellavalle A, Crippa S, Balconi G, Cuccovillo I, et al: **Cardiac mesoangioblasts are committed, self-renewable progenitors, associated with small vessels of juvenile mouse ventricle.** *Cell Death Differ* 2008, **15:**1417-1428.
631. León B, Ardavín C: **Monocyte migration to inflamed skin and lymph nodes is differentially controlled by L-selectin and PSGL-1.** *Blood* 2008, **111:**3126-3130.
632. Altieri DC, Edgington TS: **The saturable high affinity association of factor X to ADP-stimulated monocytes defines a novel function of the Mac-1 receptor.** *J Biol Chem* 1988, **263:**7007-7015.
633. Prasher DC, Eckenrode VK, Ward WW, Prendergast FG, Cormier MJ: **Primary structure of the Aequorea victoria green-fluorescent protein.** *Gene* 1992, **111:**229-233.
634. Galkina E, Florey O, Zarbock A, Smith BR, Preece G, Lawrence MB, Haskard DO, Ager A: **T lymphocyte rolling and recruitment into peripheral lymph nodes is regulated by a saturable density of L-selectin (CD62L).** *Eur J Immunol* 2007, **37:**1243-1253.
635. Prakobphol A, Genbacev O, Gormley M, Kapidzic M, Fisher SJ: **A role for the L-selectin adhesion system in mediating cytotrophoblast emigration from the placenta.** *Developmental Biology* 2006, **298:**107-117.
636. Burdick MM, Konstantopoulos K: **Platelet-induced enhancement of LS174T colon carcinoma and THP-1 monocytoid cell adhesion to vascular endothelium under flow.** *Am J Physiol Cell Physiol* 2004, **287:**C539-547.
637. Zhang J-z, McBride JW, Yu X-j: **L-selectin and E-selectin expressed on monocytes mediating Ehrlichia chaffeensis attachment onto host cells.** *FEMS Microbiology Letters* 2003, **227:**303-309.
638. Waters WR, Rahner TE, Palmer MV, Cheng D, Nonnecke BJ, Whipple DL: **Expression of L-Selectin (CD62L), CD44, and CD25 on activated bovine T cells.** *Infect Immun* 2003, **71:**317-326.
639. Tedder TF, Penta AC, Levine HB, Freedman AS: **Expression of the human leukocyte adhesion molecule, LAM1. Identity with the TQ1 and Leu-8 differentiation antigens.** *J Immunol* 1990, **144:**532-540.

640. Venturi GM, Tu L, Kadono T, Khan AI, Fujimoto Y, Oshel P, Bock CB, Miller AS, Albrecht RM, Kubes P, et al: **Leukocyte Migration Is Regulated by L-Selectin Endoproteolytic Release.** *Immunity* 2003, **19:**713-724.
641. Ord DC, Ernst TJ, Zhou LJ, Rambaldi A, Spertini O, Griffin J, Tedder TF: **Structure of the gene encoding the human leukocyte adhesion molecule-1 (TQ1, Leu-8) of lymphocytes and neutrophils.** *Journal of Biological Chemistry* 1990, **265:**7760-7767.
642. Alon R, Feizi T, Yuen CT, Fuhlbrigge RC, Springer TA: **Glycolipid ligands for selectins support leukocyte tethering and rolling under physiologic flow conditions.** *The Journal of Immunology* 1995, **154:**5356-5366.
643. Hashimoto K, Kataoka N, Nakamura E, Hagihara K, Okamoto T, Kanouchi H, Mohri S, Tsujioka K, Kajiya F: **Live-cell visualization of the trans-cellular mode of monocyte transmigration across the vascular endothelium, and its relationship with endothelial PECAM-1.** *The Journal of Physiological Sciences* 2012, **62:**63-69.
644. Qin Z: **The use of THP-1 cells as a model for mimicking the function and regulation of monocytes and macrophages in the vasculature.** *Atherosclerosis* 2012, **221:**2-11.
645. Gatlin J, Douglas J, Evans JT, Collins RH, Wendel GD, Garcia JV: **In vitro selection of lentivirus vector-transduced human CD34+ cells.** *Hum Gene Ther* 2000, **11:**1949-1957.
646. An DS, Kung SKP, Bonifacino A, Wersto RP, Metzger ME, Agricola BA, Mao SH, Chen ISY, Donahue RE: **Lentivirus Vector-Mediated Hematopoietic Stem Cell Gene Transfer of Common Gamma-Chain Cytokine Receptor in Rhesus Macaques.** *Journal of Virology* 2001, **75:**3547-3555.
647. Dyall J, Latouche J-B, Schnell S, Sadelain M: **Lentivirus-transduced human monocyte-derived dendritic cells efficiently stimulate antigen-specific cytotoxic T lymphocytes.** *Blood* 2001, **97:**114-121.
648. Cavalieri S, Cazzaniga S, Geuna M, Magnani Z, Bordignon C, Naldini L, Bonini C: **Human T lymphocytes transduced by lentiviral vectors in the absence of TCR activation maintain an intact immune competence.** *Blood* 2003, **102:**497-505.
649. Li M-J, Rossi JJ: **Lentivirus Transduction of Hematopoietic Cells.** *Cold Spring Harbor Protocols* 2007, **2007:**pdb.prot4755.
650. Stripecke R: **Lentiviral Vector-Mediated Genetic Programming of Mouse and Human Dendritic Cells.** In *Genetic Modification of Hematopoietic Stem Cells. Volume* 506. Edited by Baum C: Humana Press; 2009: 139-158: *Methods In Molecular Biology™*].
651. Lee J, Reiner N: **Stable Lentiviral Vector-Mediated Gene Silencing in Human Monocytic Cell Lines.** In *Macrophages and Dendritic Cells. Volume* 531. Edited by Reiner NE: Humana Press; 2009: 287-300: *Methods in Molecular Biology™*].
652. Zhang L, Liu H-j, Li T-j, Yang Y, Guo X-l, Wu M-c, Rui Y-c, Wei L-x: **Lentiviral vector-mediated siRNA knockdown of SR-PSOX inhibits foam cell formation in vitro.** *Acta Pharmacol Sin* 2008, **29:**847-852.
653. Qiu G, Hill JS: **Endothelial lipase enhances low density lipoprotein binding and cell association in THP-1 macrophages.** *Cardiovasc Res* 2007, **76:**528-538.
654. Reeves MB, Breidenstein A, Compton T: **Human cytomegalovirus activation of ERK and myeloid cell leukemia-1 protein correlates with survival of latently infected cells.** *Proc Natl Acad Sci U S A* 2012, **109:**588-593.
655. German-Retana S, Candresse T, Alias E, Delbos R-P, Le Gall O: **Effects of Green Fluorescent Protein or β-Glucuronidase Tagging on the Accumulation and Pathogenicity of a Resistance-Breaking Lettuce mosaic virus Isolate in Susceptible and Resistant Lettuce Cultivars.** *Molecular Plant-Microbe Interactions* 2000, **13:**316-324.
656. Feng Z, Ning Chen W, Vee Sin Lee P, Liao K, Chan V: **The influence of GFP-actin expression on the adhesion dynamics of HepG2 cells on a model extracellular matrix.** *Biomaterials* 2005, **26:**5348-5358.
657. Zhao LC, Edgar JB, Dailey MO: **Characterization of the rapid proteolytic shedding of murine L-selectin.** *Dev Immunol* 2001, **8:**267-277.

658. Thornhill MH, Haskard DO: **IL-4 regulates endothelial cell activation by IL-1, tumor necrosis factor, or IFN-gamma.** *The Journal of Immunology* 1990, **145:**865-872.
659. Salmi M, Koskinen K, Henttinen T, Elima K, Jalkanen S: **CLEVER-1 mediates lymphocyte transmigration through vascular and lymphatic endothelium.** *Blood* 2004, **104:**3849-3857.
660. Koskinen K, Vainio PJ, Smith DJ, Pihlavisto M, Ylä-Herttuala S, Jalkanen S, Salmi M: **Granulocyte transmigration through the endothelium is regulated by the oxidase activity of vascular adhesion protein-1 (VAP-1).** *Blood* 2004, **103:**3388-3395.
661. Cuvelier SL, Patel KD: **Shear-dependent Eosinophil Transmigration on Interleukin 4–stimulated Endothelial Cells: A Role for Endothelium-associated Eotaxin-3.** *The Journal of Experimental Medicine* 2001, **194:**1699-1709.
662. Aspinall AI, Curbishley SM, Lalor PF, Weston CJ, Miroslava B, Liaskou E, Adams RM, Holt AP, Adams DH: **CX3CR1 and vascular adhesion protein-1-dependent recruitment of CD16+ monocytes across human liver sinusoidal endothelium.** *Hepatology* 2010, **51:**2030-2039.
663. Yin X, Bern M, Xing Q, Ho J, Viner R, Mayr M: **Glycoproteomic Analysis of the Secretome of Human Endothelial Cells.** *Molecular & Cellular Proteomics* 2013, **12:**956-978.
664. Crnich R, Amberg GC, Leo MD, Gonzales AL, Tamkun MM, Jaggar JH, Earley S: **Vasoconstriction resulting from dynamic membrane trafficking of TRPM4 in vascular smooth muscle cells.** *American Journal of Physiology - Cell Physiology* 2010, **299:**C682-C694.
665. Clemens DL, Lee B-Y, Horwitz MA: **Virulent and Avirulent Strains of Francisella tularensis Prevent Acidification and Maturation of Their Phagosomes and Escape into the Cytoplasm in Human Macrophages.** *Infection and Immunity* 2004, **72:**3204-3217.
666. Kobayashi T, Beuchat M-H, Lindsay M, Frias S, Palmiter RD, Sakuraba H, Parton RG, Gruenberg J: **Late endosomal membranes rich in lysobisphosphatidic acid regulate cholesterol transport.** *Nat Cell Biol* 1999, **1:**113-118.
667. Grant BD, Donaldson JG: **Pathways and mechanisms of endocytic recycling.** *Nat Rev Mol Cell Biol* 2009, **10:**597-608.
668. Long C, Wang Y, Herrera AH, Horiuchi Dagger K, Walcheck B: **In vivo role of leukocyte ADAM17 in the inflammatory and host responses during E. coli-mediated peritonitis.** *J Leukoc Biol* 2010.
669. Tsubota Y, Frey JM, Tai PW, Welikson RE, Raines EW: **Monocyte ADAM17 Promotes Diapedesis during Transendothelial Migration: Identification of Steps and Substrates Targeted by Metalloproteinases.** *J Immunol* 2013.
670. Sina C, Gavrilova O, Förster M, Till A, Derer S, Hildebrand F, Raabe B, Chalaris A, Scheller J, Rehmann A, et al: **G Protein-Coupled Receptor 43 Is Essential for Neutrophil Recruitment during Intestinal Inflammation.** *The Journal of Immunology* 2009, **183:**7514-7522.
671. Ahrens I, Ellwanger C, Smith BK, Bassler N, Chen YC, Neudorfer I, Ludwig A, Bode C, Peter K: **Selenium supplementation induces metalloproteinase-dependent L-selectin shedding from monocytes.** *Journal of Leukocyte Biology* 2008, **83:**1388-1395.
672. Badr G, Borhis G, Treton D, Moog C, Garraud O, Richard Y: **HIV type 1 glycoprotein 120 inhibits human B cell chemotaxis to CXC chemokine ligand (CXCL) 12, CC chemokine ligand (CCL)20, and CCL21.** *J Immunol* 2005, **175:**302-310.
673. Mackarel AJ, Cottell DC, Russell KJ, FitzGerald MX, O'Connor CM: **Migration of neutrophils across human pulmonary endothelial cells is not blocked by matrix metalloproteinase or serine protease inhibitors.** *Am J Respir Cell Mol Biol* 1999, **20:**1209-1219.

674. Altieri DC, Bader R, Mannucci PM, Edgington TS: **Oligospecificity of the cellular adhesion receptor Mac-1 encompasses an inducible recognition specificity for fibrinogen.** *J Cell Biol* 1988, **107:**1893-1900.
675. Gorvel JP, Chavrier P, Zerial M, Gruenberg J: **rab5 controls early endosome fusion in vitro.** *Cell* 1991, **64:**915-925.
676. Brown MS, Ye J, Rawson RB, Goldstein JL: **Regulated Intramembrane Proteolysis: A Control Mechanism Conserved from Bacteria to Humans.** *Cell* 2000, **100:**391-398.
677. Gupta-Rossi N, Six E, LeBail O, Logeat F, Chastagner P, Olry A, Israël A, Brou C: **Monoubiquitination and endocytosis direct γ-secretase cleavage of activated Notch receptor.** *The Journal of Cell Biology* 2004, **166:**73-83.
678. Liu S, Kiick K: **Architecture effects on L-selectin shedding induced by polypeptide-based multivalent ligands.** *Polymer Chemistry* 2011, **2:**1513-1522.
679. Alves CS, Burdick MM, Thomas SN, Pawar P, Konstantopoulos K: **The dual role of CD44 as a functional P-selectin ligand and fibrin receptor in colon carcinoma cell adhesion.** *American Journal of Physiology - Cell Physiology* 2008, **294:**C907-C916.
680. Ogasawara N, Kojima T, Go M, Fuchimoto J, Kamekura R, Koizumi J-i, Ohkuni T, Masaki T, Murata M, Tanaka S, et al: **Induction of JAM-A during differentiation of human THP-1 dendritic cells.** *Biochemical and Biophysical Research Communications* 2009, **389:**543-549.
681. Pierres A, Benoliel A-M, Touchard D, Bongrand P: **How Cells Tiptoe on Adhesive Surfaces before Sticking.** *Biophysical Journal* 2008, **94:**4114-4122.
682. Charrad R-S, Gadhoum Z, Qi J, Glachant A, Allouche M, Jasmin C, Chomienne C, Smadja-Joffe F: **Effects of anti-CD44 monoclonal antibodies on differentiation and apoptosis of human myeloid leukemia cell lines.** *Blood* 2002, **99:**290-299.
683. Nasu K, Fujisawa K, Nishida Y, Kai S, Sugano T, Miyakawa I, Tateishi Y: **Expression of collagen XVIII mRNA and protein in human umbilical vein and placenta.** *Reprod Fertil Dev* 2003, **15:**107-114.
684. Stockton BM, Cheng G, Manjunath N, Ardman B, von Andrian UH: **Negative Regulation of T Cell Homing by CD43.** *Immunity* 1998, **8:**373-381.
685. Woodman RC, Johnston B, Hickey MJ, Teoh D, Reinhardt P, Poon BY, Kubes P: **The Functional Paradox of CD43 in Leukocyte Recruitment: A Study Using CD43-deficient Mice.** *The Journal of Experimental Medicine* 1998, **188:**2181-2186.
686. Mody PD, Cannon JL, Bandukwala HS, Blaine KM, Schilling AB, Swier K, Sperling AI: **Signaling through CD43 regulates CD4 T-cell trafficking.** *Blood* 2007, **110:**2974-2982.
687. Butcher EC, Picker LJ: **Lymphocyte homing and homeostasis.** *Science* 1996, **272:**60-66.
688. Kawabe Y, Ochi A: **Programmed cell death and extrathymic reduction of Vbeta8+ CD4+ T cells in mice tolerant to Staphylococcus aureus enterotoxin B.** *Nature* 1991, **349:**245-248.
689. Matsumoto M, Atarashi K, Umemoto E, Furukawa Y, Shigeta A, Miyasaka M, Hirata T: **CD43 functions as a ligand for E-Selectin on activated T cells.** *J Immunol* 2005, **175:**8042-8050.
690. Norman MU, Kubes P: **CD43, a novel lymphocyte ligand for E-selectin.** *Blood* 2006, **107:**1252.
691. Matsumoto M, Shigeta A, Miyasaka M, Hirata T: **CD43 Plays Both Antiadhesive and Proadhesive Roles in Neutrophil Rolling in a Context-Dependent Manner.** *The Journal of Immunology* 2008, **181:**3628-3635.
692. Muller WA, Weigl SA, Deng X, Phillips DM: **PECAM-1 is required for transendothelial migration of leukocytes.** *J Exp Med* 1993, **178:**449-460.
693. Care BR, Soula HA: **Impact of receptor clustering on ligand binding.** *BMC Syst Biol* 2011, **5:**48.
694. Elias CG, 3rd, Spellberg JP, Karan-Tamir B, Lin CH, Wang YJ, McKenna PJ, Muller WA, Zukowski MM, Andrew DP: **Ligation of CD31/PECAM-1 modulates the function of lymphocytes, monocytes and neutrophils.** *Eur J Immunol* 1998, **28:**1948-1958.

695. Tellier E, Canault M, Rebsomen L, Bonardo B, Juhan-Vague I, Nalbone G, Peiretti F: **The shedding activity of ADAM17 is sequestered in lipid rafts.** *Experimental Cell Research* 2006, **312:**3969-3980.
696. Boutet P, Agüera-González S, Atkinson S, Pennington CJ, Edwards DR, Murphy G, Reyburn HT, Valés-Gómez M: **Cutting Edge: The Metalloproteinase ADAM17/TNF-α-Converting Enzyme Regulates Proteolytic Shedding of the MHC Class I-Related Chain B Protein.** *The Journal of Immunology* 2009, **182:**49-53.
697. Yonemura S, Hirao M, Doi Y, Takahashi N, Kondo T, Tsukita S, Tsukita S: **Ezrin/Radixin/Moesin (ERM) Proteins Bind to a Positively Charged Amino Acid Cluster in the Juxta-Membrane Cytoplasmic Domain of CD44, CD43, and ICAM-2.** *The Journal of Cell Biology* 1998, **140:**885-895.
698. Cannon JL, Mody PD, Blaine KM, Chen EJ, Nelson AD, Sayles LJ, Moore TV, Clay BS, Dulin NO, Shilling RA, et al: **CD43 interaction with ezrin-radixin-moesin (ERM) proteins regulates T-cell trafficking and CD43 phosphorylation.** *Mol Biol Cell* 2011, **22:**954-963.
699. Ridley AJ, Schwartz MA, Burridge K, Firtel RA, Ginsberg MH, Borisy G, Parsons JT, Horwitz AR: **Cell Migration: Integrating Signals from Front to Back.** *Science* 2003, **302:**1704-1709.
700. Coates TD, Watts RG, Hartman R, Howard TH: **Relationship of F-actin distribution to development of polar shape in human polymorphonuclear neutrophils.** *J Cell Biol* 1992, **117:**765-774.
701. Park YM, Drazba JA, Vasanji A, Egelhoff T, Febbraio M, Silverstein RL: **Oxidized LDL/CD36 interaction induces loss of cell polarity and inhibits macrophage locomotion.** *Mol Biol Cell* 2012, **23:**3057-3068.
702. Marchesi VT, Florey HW: **Electron micrographic observations on the emigration of leucocytes.** *Q J Exp Physiol Cogn Med Sci* 1960, **45:**343-348.
703. Kawai T, Seki M, Hiromatsu K, Eastcott JW, Watts GFM, Sugai M, Smith DJ, Porcelli SA, Taubman MA: **Selective Diapedesis of Th1 Cells Induced by Endothelial Cell RANTES.** *The Journal of Immunology* 1999, **163:**3269-3278.
704. Khandoga AG, Khandoga A, Reichel CA, Bihari P, Rehberg M, Krombach F: **In vivo imaging and quantitative analysis of leukocyte directional migration and polarization in inflamed tissue.** *PLoS One* 2009, **4:**e4693.
705. Weiner OD, Servant G, Welch MD, Mitchison TJ, Sedat JW, Bourne HR: **Spatial control of actin polymerization during neutrophil chemotaxis.** *Nat Cell Biol* 1999, **1:**75-81.
706. del Pozo MA, Sánchez-Mateos P, Nieto M, Sánchez-Madrid F: **Chemokines regulate cellular polarization and adhesion receptor redistribution during lymphocyte interaction with endothelium and extracellular matrix. Involvement of cAMP signaling pathway.** *The Journal of Cell Biology* 1995, **131:**495-508.
707. Besson A, Gurian-West M, Schmidt A, Hall A, Roberts JM: **p27Kip1 modulates cell migration through the regulation of RhoA activation.** *Genes Dev* 2004, **18:**862-876.
708. Lim S, Ryu J, Shin JA, Shin MJ, Ahn YK, Kim JJ, Han KH: **Tumor necrosis factor-alpha potentiates RhoA-mediated monocyte transmigratory activity in vivo at a picomolar level.** *Arterioscler Thromb Vasc Biol* 2009, **29:**2138-2145.
709. Shi Y, Zhang J, Mullin M, Dong B, Alberts AS, Siminovitch KA: **The mDial formin is required for neutrophil polarization, migration, and activation of the LARG/RhoA/ROCK signaling axis during chemotaxis.** *J Immunol* 2009, **182:**3837-3845.
710. Takesono A, Heasman SJ, Wojciak-Stothard B, Garg R, Ridley AJ: **Microtubules regulate migratory polarity through Rho/ROCK signaling in T cells.** *PLoS One* 2010, **5:**e8774.
711. Pertz O, Hodgson L, Klemke RL, Hahn KM: **Spatiotemporal dynamics of RhoA activity in migrating cells.** *Nature* 2006, **440:**1069-1072.
712. Machacek M, Hodgson L, Welch C, Elliott H, Pertz O, Nalbant P, Abell A, Johnson GL, Hahn KM, Danuser G: **Coordination of Rho GTPase activities during cell protrusion.** *Nature* 2009, **461:**99-103.

713. Tkachenko E, Sabouri-Ghomi M, Pertz O, Kim C, Gutierrez E, Machacek M, Groisman A, Danuser G, Ginsberg MH: **Protein kinase A governs a RhoA-RhoGDI protrusion-retraction pacemaker in migrating cells.** *Nat Cell Biol* 2011, **13:**660-667.
714. Zarrouk M, Killock D, Ivetic A: **Monitoring RhoGTPase activity in lymphocytes.** *Methods Mol Biol* 2010, **616:**83-95.
715. Hodgson L, Pertz O, Hahn KM: **Design and Optimization of Genetically Encoded Fluorescent Biosensors: GTPase Biosensors.** In *Methods in Cell Biology. Volume* Volume 85. Edited by Kevin FS: Academic Press; 2008: 63-81
716. Spiering D, Hodgson L: **Dynamics of the Rho-family small GTPases in actin regulation and motility.** *Cell Adh Migr* 2011, **5:**170-180.
717. Ryu J-W, Hong KH, Maeng JH, Kim J-B, Ko J, Park JY, Lee K-U, Hong MK, Park SW, Kim YH, Han KH: **Overexpression of Uncoupling Protein 2 in THP1 Monocytes Inhibits β2 Integrin-Mediated Firm Adhesion and Transendothelial Migration.** *Arteriosclerosis, Thrombosis, and Vascular Biology* 2004, **24:**864-870.
718. Chuang S-Y, Yang S-H, Pang J-HS: **Cilostazol reduces MCP-1-induced chemotaxis and adhesion of THP-1 monocytes by inhibiting CCR2 gene expression.** *Biochemical and Biophysical Research Communications* 2011, **411:**402-408.
719. Cain RJ, Vanhaesebroeck B, Ridley AJ: **The PI3K p110α isoform regulates endothelial adherens junctions via Pyk2 and Rac1.** *The Journal of Cell Biology* 2010, **188:**863-876.
720. Zhou Z, Subramanian P, Sevilmis G, Globke B, Soehnlein O, Karshovska E, Megens R, Heyll K, Chun J, Saulnier-Blache Jean S, et al: **Lipoprotein-Derived Lysophosphatidic Acid Promotes Atherosclerosis by Releasing CXCL1 from the Endothelium.** *Cell Metabolism* 2011, **13:**592-600.
721. LaMarca HL, Ott CM, Höner zu Bentrup K, LeBlanc CL, Pierson DL, Nelson AB, Scandurro AB, Whitley GSJ, Nickerson CA, Morris CA: **Three-dimensional growth of extravillous cytotrophoblasts promotes differentiation and invasion.** *Placenta* 2005, **26:**709-720.
722. Kunisaki Y, Nishikimi A, Tanaka Y, Takii R, Noda M, Inayoshi A, Watanabe K-i, Sanematsu F, Sasazuki T, Sasaki T, Fukui Y: **DOCK2 is a Rac activator that regulates motility and polarity during neutrophil chemotaxis.** *The Journal of Cell Biology* 2006, **174:**647-652.
723. Kataoka N, Hashimoto K, Nakamura E, Hagihara K, Tsujioka K, Kajiya F: **Local Dynamic Recruitment of Endothelial PECAM-1 to Transmigrating Monocytes.** In *13th International Conference on Biomedical Engineering. Volume* 23. Edited by Lim C, Goh JH: Springer Berlin Heidelberg; 2009: 1941-1944: *IFMBE Proceedings*].
724. Setiadi H, Disdier M, Green SA, Canfield WM, McEver RP: **Residues throughout the cytoplasmic domain affect the internalization efficiency of P-selectin.** *J Biol Chem* 1995, **270:**26818-26826.
725. Xue M, Vines CM, Buranda T, Cimino DF, Bennett TA, Prossnitz ER: **N-formyl peptide receptors cluster in an active raft-associated state prior to phosphorylation.** *J Biol Chem* 2004, **279:**45175-45184.
726. Abbal C, Lambelet M, Bertaggia D, Gerbex C, Martinez M, Arcaro A, Schapira M, Spertini O: **Lipid raft adhesion receptors and Syk regulate selectin-dependent rolling under flow conditions.** *Blood* 2006, **108:**3352-3359.
727. Gordon EJ, Strong LE, Kiessling LL: **Glycoprotein-inspired materials promote the proteolytic release of cell surface l-Selectin.** *Bioorganic & Medicinal Chemistry* 1998, **6:**1293-1299.
728. Spertini O, Kansas GS, Munro JM, Griffin JD, Tedder TF: **Regulation of leukocyte migration by activation of the leukocyte adhesion molecule-1 (LAM-1) selectin.** *Nature* 1991, **349:**691-694.
729. Cara DC, Kaur J, Forster M, McCafferty DM, Kubes P: **Role of p38 mitogen-activated protein kinase in chemokine-induced emigration and chemotaxis in vivo.** *J Immunol* 2001, **167:**6552-6558.

730. Campbell SL, Khosravi-Far R, Rossman KL, Clark GJ, Der CJ: **Increasing complexity of Ras signaling.** *Oncogene* 1998, **17:**1395-1413.
731. Jun JE, Yang M, Chen H, Chakraborty AK, Roose JP: **Activation of extracellular signal-regulated kinase but not of p38 mitogen-activated protein kinase pathways in lymphocytes requires allosteric activation of SOS.** *Mol Cell Biol* 2013, **33:**2470-2484.
732. Yip SC, El-Sibai M, Coniglio SJ, Mouneimne G, Eddy RJ, Drees BE, Neilsen PO, Goswami S, Symons M, Condeelis JS, Backer JM: **The distinct roles of Ras and Rac in PI 3-kinase-dependent protrusion during EGF-stimulated cell migration.** *J Cell Sci* 2007, **120:**3138-3146.
733. Chen RH, Corbalan-Garcia S, Bar-Sagi D: **The role of the PH domain in the signal-dependent membrane targeting of Sos.** *EMBO J* 1997, **16:**1351-1359.
734. Kumar P, Hosaka S, Koch AE: **Soluble E-selectin induces monocyte chemotaxis through Src family tyrosine kinases.** *J Biol Chem* 2001, **276:**21039-21045.